# Paleogene Larger Benthic Foraminiferal Stratigraphy and Facies distribution: Implications for Tectono-stratigraphic Evolution of the Kohat Basin, Potwar Basin and the Trans Indus Ranges (TIR) northwest Pakistan

**Sajjad Ahmad**


**Thesis submitted for the degree of**

**Doctor of Philosophy**

**The University of Edinburgh**

**2010**

## Declaration

I declare that this thesis has been composed by myself unless explicitly stated, and that all other contributions have been acknowledged.

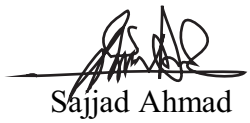

Sajjad Ahmad
2010

Recite: In the name of thy Lord who created man from a clot. Recite: And thy Lord is the Most Generous Who taught by the pen, taught man that which he knew not."
**(Al. Quran, 96:1-5)**

"To listen to the words of the learned and to instill unto others the lessons of science is better than religious exercises."
**(Prophet Muhammad PBUH)**

"Seek knowledge and wisdom, or whatever the vessel from which it flows, you will never be the loser."
(**Prophet Muhammad PBUH)**

## Abstract

Thick Paleogene sequences occur in the southern deformed fold and thrust belt of the Himalayas. In this thesis I describe detailed litho- and biostratigraphy from ten key stratigraphic sections in the Kohat Basin, the Potwar Basin and the Trans Indus Ranges (TIR). These stratigraphies combined with microfacies analysis resulted in a new interpretation of the tectono-stratigraphic history of the area, which is dominated by India-Asia collision but where eustatatic effects can also be identified. Of particular interest is documenting the timing of the final closure of the northern rim of the Tethys caused by this collision. The Kohat and Potwar Basins represent foreland basins within the collision zone. Their stratigraphies document effects of local tectonics and eustatic sea level.

The biostratigraphy is based on occurrences of larger benthic foraminifera. Taxonomy of the species is included in the thesis. The Paleogene rocks of the study area are divided into local larger benthic forminiferal biozones: BFZK 1- BFZK 6 in the Kohat Basin and BFZP 1-BFZP 3 in the Potwar Basin and the TIR. These local biozones are correlated to the global standard biozonation schemes of Höttinger (1960), Schaub (1981), and Serra Kiel et al. (1998). The ages of the sequences are Late Paleocene (Thanitian) to Middle Eocene (Upper Lutetian) in the Kohat Basin, and Late Paleocene (Thanitian) to Early Eocene (Middle Cuisian) in the Potwar Basin and the TIR. The sediments were deposited along a carbonate ramp platform in both areas (*sensu* Read, 1982, 1985).

The sequence stratigraphic histories of the two basins are described as follows. In the Kohat Basin, Thanitian to Middle Cuisian strata record the first Transgressive-Regressive cycle (TRK 1). The first sequence boundary (SBK 1) is followed by Middle Cuisian-Upper Cuisian lowstand progradational deposition that marks the end of TRK 1 cycle. Middle Lutetian 1-Upper Lutetian strata represent the second Transgressive-Regressive cycle (TRK 2). The second sequence boundary (SBK 2) ends TRK 2 deposition, after which no more deposition took place. In the Potwar Basin and the TIR, Thanitian strata comprise the first Transgressive-Regressive cycle (TRP 1), whilst Lower Lllerdian-Middle Lllerdian 1 strata constitute the second Transgressive-Regressive cycle (TRP 2). Middle Lllerdian 2 to Middle Cuisian strata mark the third Transgressive-Regressive cycle (TRP 3). Three sequence boundaries (the SBP 1, the SBP 2 and the SBP 3), marked by exposure surfaces, separate the three depositional cycles.

The SBP 1 and SBP 2 sequence boundaries are controlled by local tectonics. In contrast the SBP 3 and SBK 1 sequence boundaries are synchronous at 49.5 Ma, and represent a phase of significant relative sea level fall, possibly driven by the combined effect of uplift (collision tectonics) and eustatic sea level fall (e.g. Haq et al., 1987). This implies that proto-closure of the northern rim of the Tethys occurred around 49.5 Ma. Reestablishment of marine conditions in the Kohat Basin occurred in the Middle Lutetian 1 around 45.8 Ma, possibly caused by a combination of flexural loading of the Indian plate (Pivinik & Wells, 1996) and eustatic sea-level rise (e.g. Haq et al., 1987). The final closure of the Tethys, marked by the end of marine sedimentation in the Kohat Basin, occurred in the Upper Lutetian (41.2 Ma). Finally, Himalayan foreland molasses sedimentation occurred during Miocene to Pliocene.

## Acknowledgments

Almighty God deserves all the praises whose help at every step made it possible for me to accomplish this wok in due time. This thesis is dedicated to my parents whose love and affection has been a source of inspiration for me in every walk of life. My family has been my biggest support throughout my life. Anything I achieve is shared with them: my father, mother, brothers, sister and wife, Afsheen. They all got me through tough times and helped me throughout this study especially in the process of writing this dissertation. The kindness, love and support of my wife and kids Rehan and Suleman made my stay in Edinburgh, a memorable experience of life.

My PHD study was supported by the Higher Education Commission (HEC) of Pakistan who nominated me for the award of scholarship offered by the Commonwealth Scholarship Commission (CSC), UK. I am grateful to the CSC and British Council for all the administrative support that I received during this study.

I am very thankful to Dr. Susan Rigby who helped and encouraged me from the day I sent her the first draft of my research proposal for PHD studies. Her constant contribution in refinement of this study is worth mentioning and without her support this study was not possible.

I am very grateful to Prof Dick Kroon who supervised this study. His ideas, discussions and encouragement paved way for the successful completion of this work.

I am grateful to my friends/students at the Department of Geology, University of Peshawar who helped me in the collection of field data in very remote parts of the study area, they are Khalid Latif, Suleman Khan, Hamad, Rasheed (Lab Assistant), Syed Wajid, Ibrahim Afridi, Hasaam, Waheed and Saad.

All colleagues and office staff at the Department of Geology, University of Peshawar are thanked for their encouragement and support.

The names of Dr. Rachel Wood is of particular mention here whose-discussions and guidelines in the field of sedimentology and genetic stratigraphy helped me a lot in finalizing the project proposal for this study. Dr. Nicola Krazer is thanked for helping me in using SEM facility. Dr. Jhon Craven is thanked for helping in the using the petrographic microscope facilities. Mike Hall took all the pain in preparation of hundreds of rock thin sections and he deserves my special thanks. Dr. Kate Darling is thanked for her guidance in the study of smaller benthic foraminifera.

My colleagues Mathew, Romain, Rhian, Margaret, Mike, Anna, Samona and Katty are thanked for providing lovely and peaceful working atmosphere. All office staff that provided support at the School of Geosciences, Grant Institute of Earth Sciences deserves my sincere thanks.

# Table of contents

## Chapter 5

## 5: Larger benthic foraminiferal biostratigraphy of the Potwar Basin and the Trans Indus Ranges 138



## Chapter 6

## 6: Paleogene facies analysis of the Kohat Basin with implications for paleoenvironments 156

## Chapter 8

## 8: Tectono-stratigraphic evolution of the Kohat Basin, Potwar Basin and the Trans Indus Ranges (TIR)_____ 282

# Chapter 1 Introduction

## 1.1 Project rationale

The Paleogene rocks of the Kohat Basin, the Potwar Basin and the Trans Indus Ranges (TIR) in northwest Pakistan host well preserved foraminifera in carbonate-clastic mixed sequences (Eames, 1950; Meissner et al., 1974; Wells, 1984). Early foraminiferal stratigraphic investigations (Blanford, 1876; Noetling, 1903; Vredenburg, 1906; Nuttal, 1926; Davies, 1940; Eames, 1950; Naggapa, 1959; Pascoe, 1963; Meissner et al., 1968; 1974, Weiss, 1988, 1993; Afzal J, 1997; Sameeni, 1998) were hampered by a lack of detailed outcrop studies and biostratigraphic correlation. Existing nomenclature of the larger benthic foraminifera (*Nummulites/Assilina*) requires updating with the aim of refining the local biostratigraphic zonation, and improving correlation with the global benthic foraminiferal biozonation schemes (Höttinger, 1960; Schaub, 1981, Serra Kiel et al., 1998).

The integrated use of biostratigraphy, microfacies analysis and lithological data provides insights in the evolution of depositional sequences (e.g. Molina et al., 2006, Serra Kiel et al., 2003; Malcolm, 2000; Luterbacher, 1998). In this project I aim to use such an approach to the Paleogene sequences in the Himalayan foreland basins. The result will be understanding of the tectono-stratigraphic evolution of these basins (Kohat Basin, Potwar Basin and TIR). This evolution is critical for documenting the closure history of the northern Tethys Ocean within the India-Asia collision regime.

## 1.2 Objectives

The main objectives of the thesis are:

- To describe the litho-facies of stratigraphic units in selected key stratigraphic sections in the basins.
- To describe the larger benthic foraminifera with the aim to improve existing nomenclature of species.
- To identify age-diagnostic species for establishing local biozones.

- To correlate local biozones with global biozonation schemes, which leads to assignment of ages, and thus chronostratigraphy of stratigraphic units.
- To carry out a detailed facies analysis of stratigraphic units in all studied sections to document stratigraphic evolution of paleoenvironments in the basin.
- To identify depositional sequences within the sections in the basins.
- To describe the paleontological and sedimentological characterization of the depositional sequences.
- To identify key parts of the sequences: maximum flooding surfaces, condensed sections and sequence boundaries.
- To correlate depositional sequences with the global sea level charts of Haq et al., 1987) for identifying potential eustatic sea level influence on these sequences.
- To study the tectono-stratigraphic evolution of the sequences to finesse our understanding of the timing of the closure of the Tethys Ocean.

## 1.3 Stratigraphic sections

The lithostratigraphy (Chapter 2), foraminiferal paleontology (Chapter 3), biostratigraphy (Chapters 4-5) and facies analysis (Chapters 6 and 7) are based on the detailed logging and sampling of ten Paleogene stratigraphic sections exposed in different parts of the Kohat Basin, Potwar Basin and TIR, northwest Pakistan. In the Kohat Basin four key stratigraphic sections are described including 1) the Panoba Nala Section 2) the Tarkhobi Nala Section and 3) the Sheikhan Nala Section which lie in the northeast while 4) the Bahurkhel Salt Tunnel Section is located in the south-western part of the Kohat Basin (figure 1.1). From the Potwar Basin selected stratigraphic sections (figure 1.2) include 5) the Gharibwal Cement Factory Section and 6) the Sikki Village Section in the Eastern Salt Range 7) the Nammal Gorge Section in the Central Salt Range and 8) the Ziarat Thatti Sharif Section in the Western Salt Range. Two key stratigraphic sections from the Trans Indus Ranges include 9) the Kalabagh Hills Section and 10) the Chichali Nala Section in the Surghar Range (figure 1.2). An introduction of the studied sections is given here while detailed description are given in Chapter 2.

### 1.3.1 The Panoba Nala Section

The Panoba Nala Section is located about half a mile southeast of the village of Panoba in the Kohat district (figure 1.1). The area lies between latitude 71° 25′ 50″N to 71° 25′ 53″E and longitude 33° 35′ 41″ to 33° 35′ 50″N, within the Survey of Pakistan map number 36 O/8. This section is easily accessible from a metalled road that diverges from the Kohat - Rawalpindi road towards the Nizampur area.

Today, the Panoba Nala Section is exposed in a regional anticline, known as the Panoba Anticlinorium in the northeastern corner of the Kohat Plateau. It has an east-west orientation and it is flanked by Eocene and Miocene molasses sequences on either side. The Panoba fault, a south verging fore thrust, truncates the anticline with Eocene rocks occupying its hanging wall.

The oldest stratigraphic unit is exposed in the Panoba Nala Section. This unit belongs to the Late Paleocene-Early Eocene Patala Formation, which is successively overlain by the Early Eocene Panoba and Sheikhan Formations. These formations comprise marine sediments. The Kuldana Formation overlies the Sheikhan Formation and its sediments represent a phase of fluvial sediment deposition. Marine sedimention returned, however, in the Middle Eocene. These sediments of the Kohat Formation represent the last episode of marine sedimentation in the region. Finally, Miocene molasses sediments disconformably overly the Kohat Formation.

### 1.3.2 The Tarkhobi Nala Section

The Tarkhobi Nala Section is located near the Tarkhobi village in the north - eastern part of the Kohat Plateau (figure 1.1). The area lies between latitude 33° 35′ 30″ N and longitude 71° 35′ E within the Survey of Pakistan map number 36 O/8. The rock units exposed in this section include the Patala Formation which in turn is overlain by the Panoba and the Sheikhan Formations, respectively.

### 1.3.3 The Sheikhan Nala Section

The Sheikhan Nala Section is located in the Sheikhan Village which is situated 6km ENE of the Kohat City (figure 1.1). The area lies between latitude 33° 35′ 20″N to 33°36′50″N and longitude 71°22′30″N to 33°36′50″N within the -

Survey of Pakistan map number 36 O/8. This section is easily accessible from a metalled road that leads Hangu City to the south-west of Kohat. In this section the Panoba, Sheikhan, Kuldana and the Kohat Formations are exposed in the core of a regional syncline.

### 1.3.4 The Bahadur Khel Salt Tunnel Section

The Bahadur Khel Salt Tunnel Section is located between latitude 33° 10′ 30″N longitude 71° 15′ 30″E near the village of Bahadur Khel in the southwestern part of the Kohat Plateau (figure 1.1). The section starts with the Bahadur Khel Salt deposits, exposed in the core of a tight anticline. These salts occupy the same chrono-stratigraphic position as of the Panoba Formation to the northeast. The Jatta gypsum Facies overlies the Bahadur Khel Salt and occupies the same chrono-stratigraphic level as of the Sheikhan Formation to the northeast. The overlying Kuldana Formation fluvial-marine deposits are well exposed, which are in turn conformably overlain by marine carbonates of the Kohat Formation.

### 1.3.5 The Gharibwal Cement Factory Section

The Gharibwal Cement Factor Section is located near the Gharibwal Cement Factory, situated 25 miles north-east of the Choa Saidan Shah Town between latitude 32° 43′ 30″ N to longitude 72° 59′ 50″E on Survey of Pakistan map number 43 D/14, in the Eastern Salt Range, Potwar Basin (figure 1.2). A metalled road leads to the section where a very thick exposure of the Chorgali Formation is studied along the road.

### 1.3.6 The Sikki Village Section

The Sikki Village Section lies between latitude 32° 41′ 50″N to longitude 72° 45′ 50″E on Survey of Pakistan map number D/14 along a road in the Sikki Village near Choa Saidan Shah town in the Eastern Salt Range, Potwar Basin (figure 1.2). This section is selected for the stratigraphic analysis of the Chorgali Formation, which comprises grey coloured monotonous nodular limestone. It is 50m thick unit and has a thrusted lower contact with the Pre-Eocene rocks.

### 1.3.7 The Nammal Gorge Section

In the Nammal Gorge Section of the Central Salt Range area, the Patala Formation is overlain by the Nammal and Sakessar Formations of Early Eocene age. This section is located between latitude 20° 39′ 81″ N to longitude 71° 48′ 05″ E, (figure 1.2) on Survey of Pakistan map number 38 P/14.

### 1.3.8 The Ziarat Thatti Sharif Section

This section is located near Ziarat Thatti Sharif in Western Salt Range area of the Potwar Basin (figure 1.2). This section is situated at the right hand side of the Railway bridge, approximately 27 km from Mianwali city on the Mianwali-Bannu road between latitude 32° 50′ 20″ N to longitude 71° 40′ 10″ E. Paleocene Lockhart and Patala Formations are well exposed in this section.

### 1.3.9 The Kalabagh Hills Section

The Kalabagh Hills Section is located in a steep gorge, approximately at 42km distance from the Shakardara village along the Daud Khel-Kalabagh road (figure 1.2). In this section the Lockhart and Patala Formations are well exposed in the core of a broad regional anticline. The section lies between latitude 30° 15′ 30″ N to longitude 71° 10′ 25″ E on Survey of Pakistan map number 38 O/8.

### 1.3.10 The Chichali Nala Section

This section is located in the Chichali Nala (figure 1.2). Approximate location of the base of the section is latitude 33° 00′ 30″ N, longitude 71° 24′ 25″ E on Survey of Pakistan map number 38 O/8. The Paleocene-Early Eocene Patala Formation is overlain by the Early Eocene Nammal and Sakessar Formations respectively.

## 1.4 Methodology

### 1.4.1 Fieldwork

Detailed field excursions in the Kohat-Potwar Basins and TIR were carried out in three different periods, using geological maps from the Department of Geology, University of Peshawar. First fieldwork data were collected in the period November 2007 to January 2008. During this period four sections across the Kohat Basin were sampled (for details see table 1.1). The second field season was in the period October-December 2008. Four stratigraphic sections in the Potwar Basin and

| | Stratigraphic Sections | Total number of samples | Sampling rate | Biostratigraphic samples | | Facies analysis samples | | References |
|---|---|---|---|---|---|---|---|---|
| KOHAT BASIN | Panoba Nala Section | 200 | Variable (from 1-15m) | 305 | 98 | 317 | 102 | Details are in figures 2.4. 4.3 & 6.28. |
| | Tarkhobi Nala Section | 106 | Variable (from 1-12m) | | 53 | | 53 | Details are in figures 2.4, 4.4 & 6.29. |
| | Sheikhan Nala Section | 265 | Variable (from 1-13m) | | 131 | | 134 | Details are in figures 2.5, 4.5 & 6.30. |
| | Bahadur Khel Salt Tunnel Section | 51 | Variable (from 2-13m) | | 23 | | 28 | Details are in figures 2.5,4.6 & 6.31. |
| POTWAR BASIN | Gharibwal Cement Factory Sectin | 64 | Variable (from 1-2m) | 336 | 32 | 336 | 32 | Detalis are in figures 2.6, 5.1 & 7.27. |
| | Sikki Village Sectin | 68 | Variable (from 1-1.2m) | | 34 | | 34 | Details are in figures 2.6, 5.2 & 7.28. |
| | Nammal Gorge Section | 224 | Variable (from 10cm-26m) | | 112 | | 112 | Details are in figures 2.7,5.3 & 7.29. |
| | Ziarat Thatti Sharif Section | 66 | Variable (from 5-10m) | | 33 | | 33 | Details are in figures 2.7,5.4 & 7.30. |
| TIR | Kalabagh Hills Section | 74 | Variable (from 5m-10m) | | 37 | | 37 | Details are in figures 2.8, 5.5 & 7.31. |
| | Chichali Nala Section | 176 | Variable (from 10cm-23m) | | 88 | | 88 | Details are in figure 2.8, 5.6 & 7.32. |
| **Grand total** | | 1294 | | 641 | | 653 | | Details are in figures 2.4-2.8 4.3-4.6,5.1-5.6, 6.28-6.31, 7.27-7.32. |

**Table 1.1** Details of the of the rock sampling carried out for the Paleogene biostratigraphic and facies analysis in the study sections of the Kohat Basin, the Potwar Basin and the Trans Indus Ranges (TIR), northwest Pakistan.

two sections in the Trans Indus Ranges (TIR) were studied and sampled (see details in Table 1.1). The final field work was performed in the period December 2009 to January 2010, when several sections were revisited to enhance sample resolution (from 1m to 10cm sampling interval) in key parts of the stratigraphic sequences.

### 1.4.2 Laboratory work

Most of the laboratory work was performed in the School of GeoSciences, University of Edinburgh, but also some petrographic thin sections were prepared at the rock thin section laboratory in the Department of Geology, University of Peshawar, Pakistan.

#### *1.4.2.1 Sieving and picking*

All outcrop samples were weighed to obtain an aliquot of 300 grams for sieving. The 125 and 63 micron mesh size sieves were used to separate smaller benthic foraminifera from the rock sample. All rock samples with a high siliceous content were treated with 30 % aqueous solution of hydrogen peroxide until most of the siliceous material is dissolved and smaller benthic foraminifera are separated (see details in chapter 3 and 4). Using a binocular microscope smaller benthic foraminifera were picked with a zero size paint brush from the picking tray.

#### *1.4.2.2 Scanning Electron Microscopy (SEM)*

Specimens of smaller benthic foraminiferal species were photographed on the Philips XL30CP Scanning Electron Microscope. The acceleration voltage was 15 kV; the current was adjusted from 0.03 to 0.1 n A according to magnification.

#### *1.4.2.3 Thin sections*

Petrographic thin sections were made for microfacies analysis, and were studied under a polarizing microscope fitted with a digital camera (for details see Chapters 6 and 7). Oriented thin sections for the study of larger benthic foraminifera were also made for identification of species.

## 1.5 Graphic software

The Corel Draw X14 graphic software was used for the construction of biostratigraphic charts, rock correlation charts, and facies model diagrams.

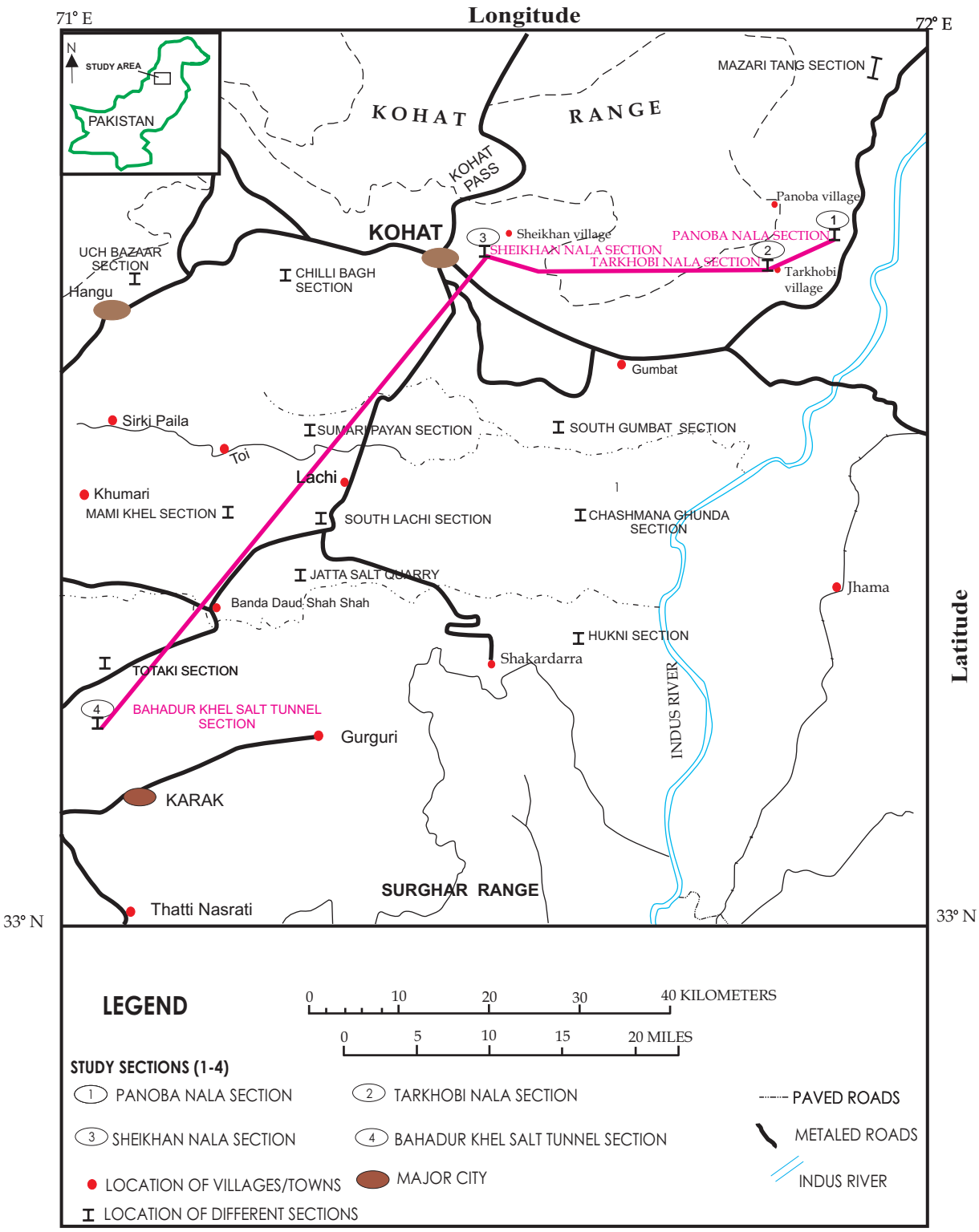


**Figure 1.1.** Location map of the studied sections in the Kohat Basin, northwest Pakistan.

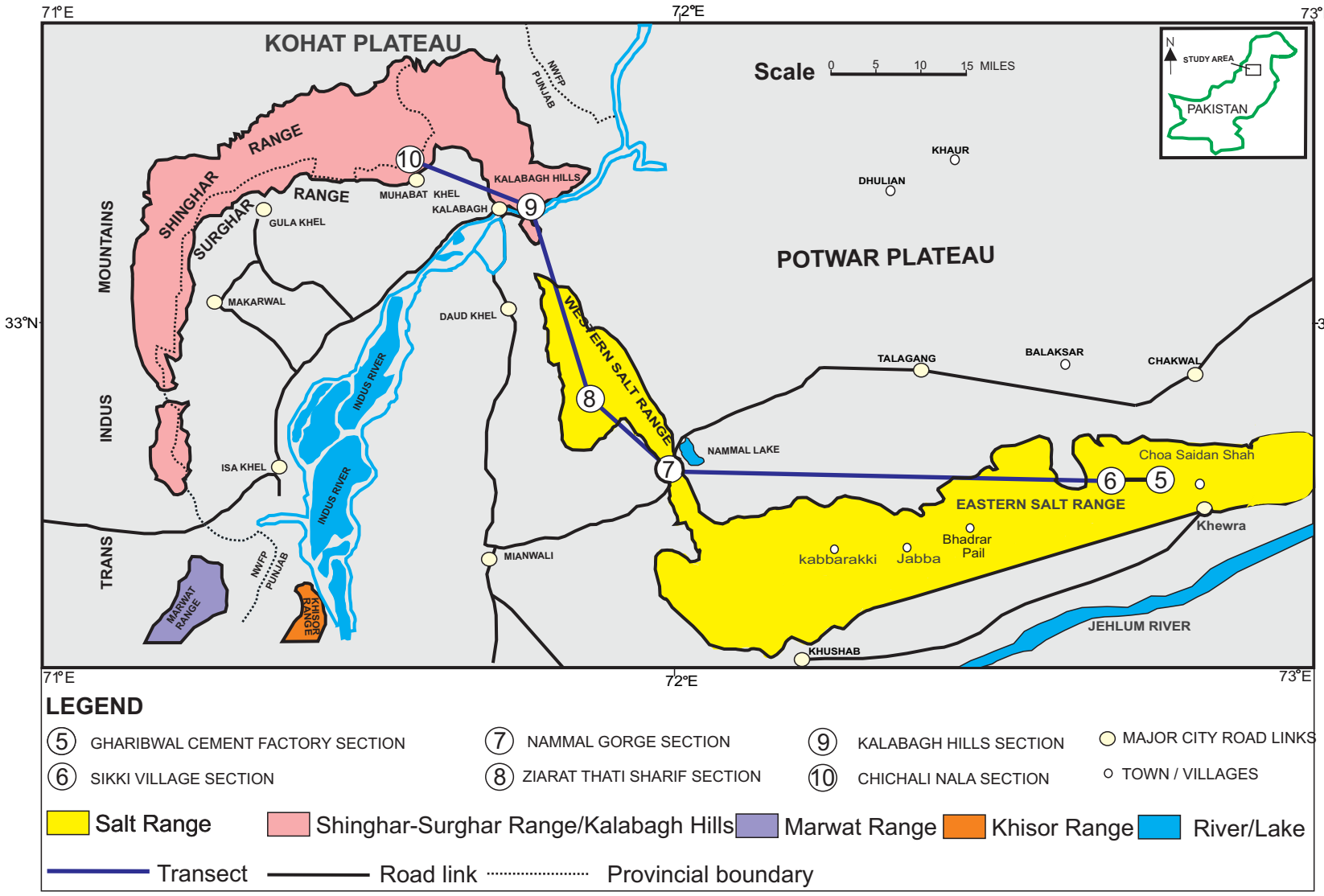


**Figure 1.2.** Location map of the studied sections in the Potwar Basin and the Trans Indus Ranges (TIR), northwest Pakistan.

# Chapter 2

# 2. Paleogene stratigraphy

## 2.1 Regional Geology

The Kohat and Potwar Basins forms plateaux in a structurally defined foreland fold and thrust belt also known as Kohat-Potwar fold and thrust belt. The major structural divisions of the Kohat-Potwar fold and thrust belt are the Kohat Plateau, the Bannu Sub-basin, the North Potwar Deformed Zone (NPDZ), the Soan Syncline, the Salt Range and the Trans-Indus Ranges (Meissner et al, 1975; Treloar and Izzat, 1993; Pivinik and Wells, 1996) (figure 2.1). The Kohat plateau, an approximately 10,000 $km^2$ area of rugged, unvegetated hills is bounded to the north by the Main Boundary Thrust fault system (MBT) (Pivinik and Wells, 1996) (figure 2.1) which contains highly deformed, Pre-Cambrian-Cenozoic sedimentary rocks (Yeast and Hussain, 1987). The southern boundary is the Trans-Indus Ranges and undeformed Bannu plain (figure 2.1) which is the equivalent of the Salt Range and southern Potwar Plateau in eastern Pakistan (Pivinik and Wells, 1996). The rocks that crop out west of the Kurram Fault, which is the western boundary of the Kohat Plateau, are highly deformed Mesozoic sedimentary rocks and minor amount of ultramafic igneous rocks comprising ophiolites and accreted volcanic arcs (Beck et al., 1995; 1996; Meissner et al, 1975; Treloar and Izzat, 1993; Pivinik and Wells, 1996). The Indus River forms the eastern boundary, separating the Kohat Plateau from the topographically subdued Potwar Plateau (Khan et al., 1990).

The structural geology of the Kohat Plateau is a series of north-dipping, low angle imbricate thrust faults underneath a blind roof thrust (Abassi & McElroy, 1991; McDougal & Hussain, 1991). The surface structural geology is dominated by east-west trending anticlines having both limbs overturned and steep down plunged ends. The anticlines are separated by broad synclinal valleys in which the Neogene fluvial foreland basin deposit crops out. These anticlines are formed as detachment folds and pressure ridges above complex, positive flower structures that represent north to south shortening (figure 2.2) (Pivinik and Wells, 1996; Sercombe et al., 1998).

(Kazmi and Rana, 1982). It is bounded to the south by the Salt Range Thrust and to the north by the Kalachitta-Margalla Hill Ranges, the River Indus to the west and the Jhelum River to the east.

It is mostly deformed in its northern part, which is called as the Northern Potwar Deformed Zone (NPDZ) (Baker et al., 1988; Abbasi and McElroy, 1991). The NPDZ forms a narrow zone between the Main Boundary Thrust (MBT) and the Soan Syncline (figure 2.1). It is characterized by east-west tight folds, overturned to the south and sheared by steep angle faults, pop-up style structures and triangle zones (Kazmi & Rana, 1982; Bannert, 1986).

The Salt Range Thrust (SRT) is the southernmost thrust zone along the foothills of the Salt Range and Trans-Indus Himalayan Range (figure 2.1) (Nakata et al., 1989; Gee, 1945). This thrust is largely covered by Quaternary alluvium and fanglomerates (Kazmi & Jan, 1997). However, in places the thrust is exposed and shows the Palaeozoic rocks overlying Neogene or Quaternary deposits of the Jehlum plain (Gee, 1945). Along the SRT there is a southward transport of the Salt Range and Potwar Plateau in the form of a large slab over the Jhelum plain. Thus the SRT is the surface expression of the leading edge of a decollment thrust (Lillie et al., 1987).

The South Potwar Basin is limited by the Salt Range in the south and by the Soan backthrust (also called the Dhurnal Fault) in the north. Developed first as an autochthonous part of the Himalayas foreland basin, the South Potwar subsequently became a piggy-back basin when its basal decollement was activated (Baker et al., 1988; Lilliet et al., 1987).

The Trans Indus Range (TIR) defines a sinuous fold-and-thrust belt and includes the Kalabagh Hills, the Surghar-Shinghar Range, the Marwat-Khisor Range, Sheikh Budin Hills and the Manzai Range. The Himalayan deformation in the Kohat foreland basin and associated Trans-Indus Salt Range is interpreted to be represented by an early phase of pre-molasses deformation followed by synmolasse and post-molasses deformation that is still active (Ahmad et al., 2010).

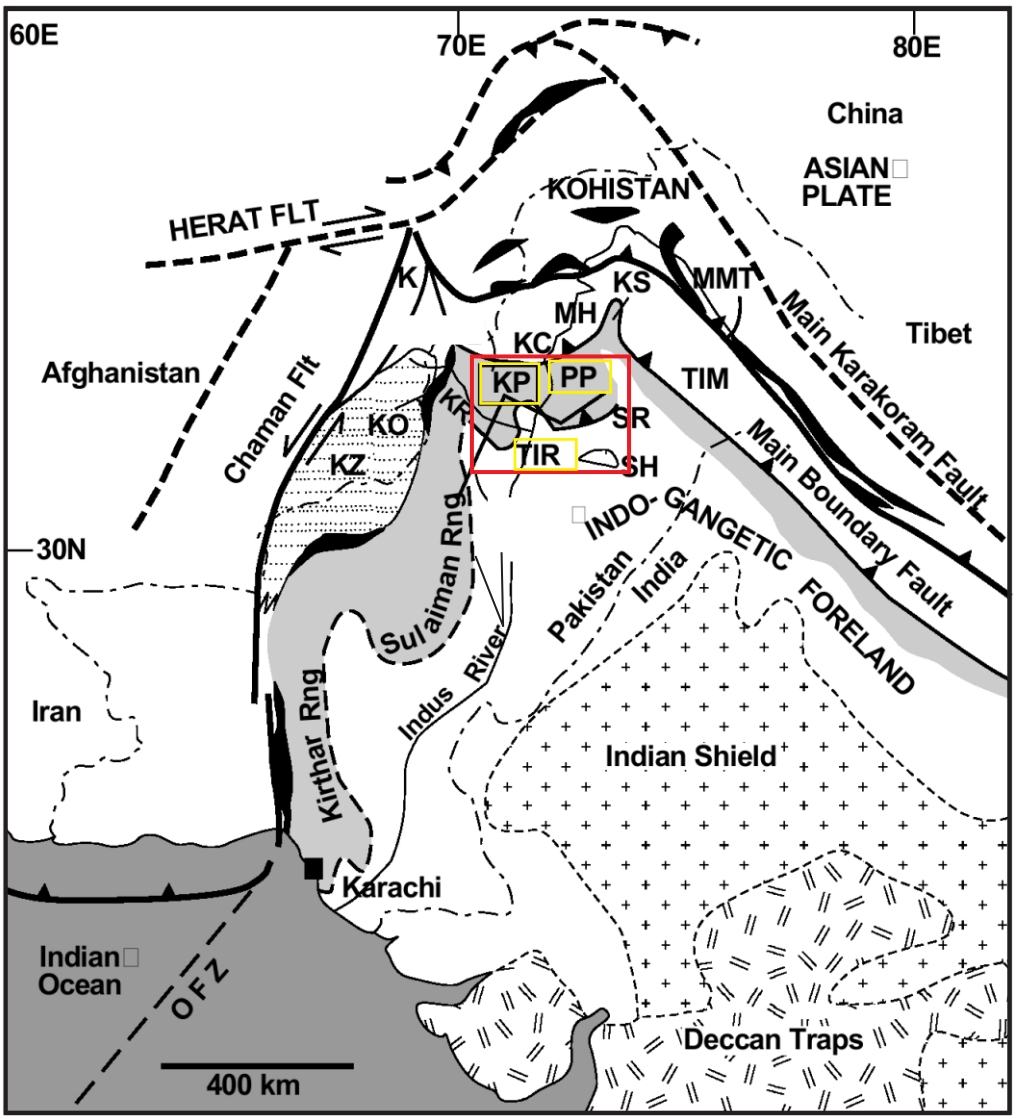


**Figure 2.1.** Tectonic map of northern Pakistan (inset showing location of the study area) and positions of the Asian plate, the Kohistan Island arc, the telescoped northern Indian continental margin **(TIM)**, major ophiolites (black), the deformed foreland basin (light shaded), the undeformed Indo-gangtic foreland and Indian Shield. Abbreviations are: K- Kabul Block; **KC**- Kala Chatta Range; **KO**- Khost Block; **KP**- Kohat Plateau; **KR**- Kurram River; **KS**- Kashmir Syntaxis; **KZ**- Katawaz Flysch Basin; **MH**- Margalla Hills; **MMT**- Main Mantle Thrust; **OFZ**- Owen Fracture Zone; **PP**- Potwar Plateau; **SH**- Sargodhah Hills; **SR**- Salt Range; **TIR**- Trans Indus Ranges (modified from Treloar and Izzat 1993 and Pivinik and Wells, 1996).

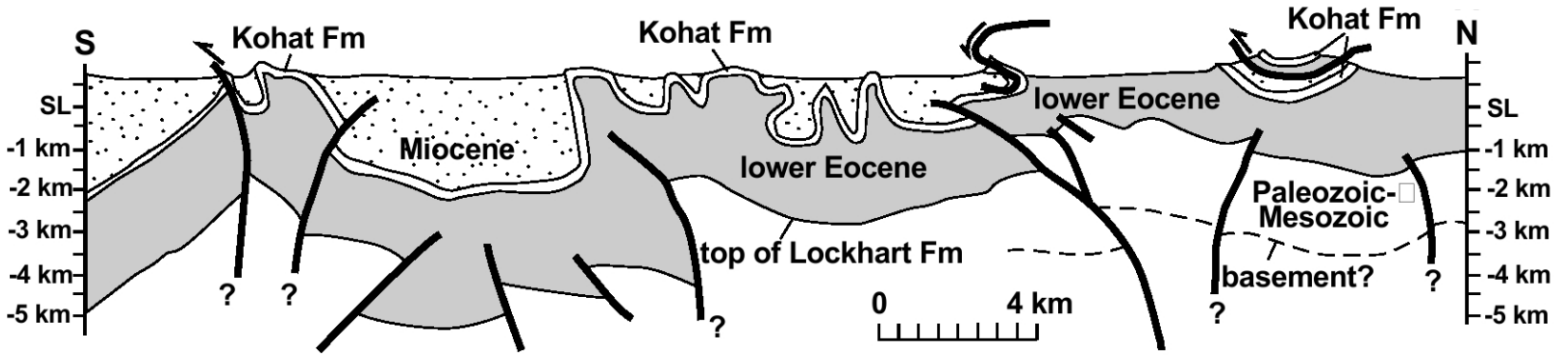


**Figure 2.2.** Structural cross section across the Kohat Plateau. The anticlines in the Kohat plateau are cored by high angle, oblique reverse faults. An earlier system of thrust faults has been folded above the reverse faults (modified from Pivinik and Wells, 1996).

## Paleogene stratigraphy of the Kohat Basin

During Late Palaeocene – Early Eocene time the Kohat basin was separated from the open sea resulting in deposition of pelagic clays interbedded with shallow marine limestone of the Patala Formation, thick clays of the Panoba Formation and platform carbonates of the Sheikhan Formation in the north while the Bahadur Khel Salt and Jatta Gypsum were deposited in the south. Clastic input from north and west in the Middle Eocene formed the sediments of the Kuldana Formation. The Middle Eocene transgression resulted in deposition of thick carbonates of the Kohat Formation in Kohat Basin and part of the Potwar and Kalachitta area. Most of these areas became part of the peneplain in Middle Eocene time until molasses sedimentation commenced (Kazmi and Abbassi, 2008).

A summary of the field stratigraphic logs of the studied section in the Kohat Basin is presented in figures 2.5-2.6 while a detailed description of stratigraphic units (Table 2.1) is given below.

### 2.2.1 The Patala Formation

The name Patala Formation was formalized by the Stratigraphic Committee of Pakistan for the "Patala Shale" of Davies and Pinfold (1937). The section exposed in Patala Nala in the Salt Range has been designated as type Section.

In the Panoba Nala Section the Patala Formation has a total measured thickness of 55m (figures 1.1 and 2.5). A basal 25m thick unit consists of thinly bedded dark grey to black, hard, calcareous shales with interbeds of yellowish grey coloured nodular limestone and is exposed in a major stream cut. Hard and splintery calcareous shales containing planktonic foraminifera constitute the major part of this unit. Alternate limestone and shale interbeds are also common. The middle part of the Patala Formation hosts a 18m thick grey coloured massive limestone which is full of larger benthic foraminifera (*Nummulites, Assilina, Operculina* and *Alveolina*), bivalves, small brachiopods and few gastropods. The upper 9m thick unit is a thick bedded, fossiliferous limestone with interbeds of

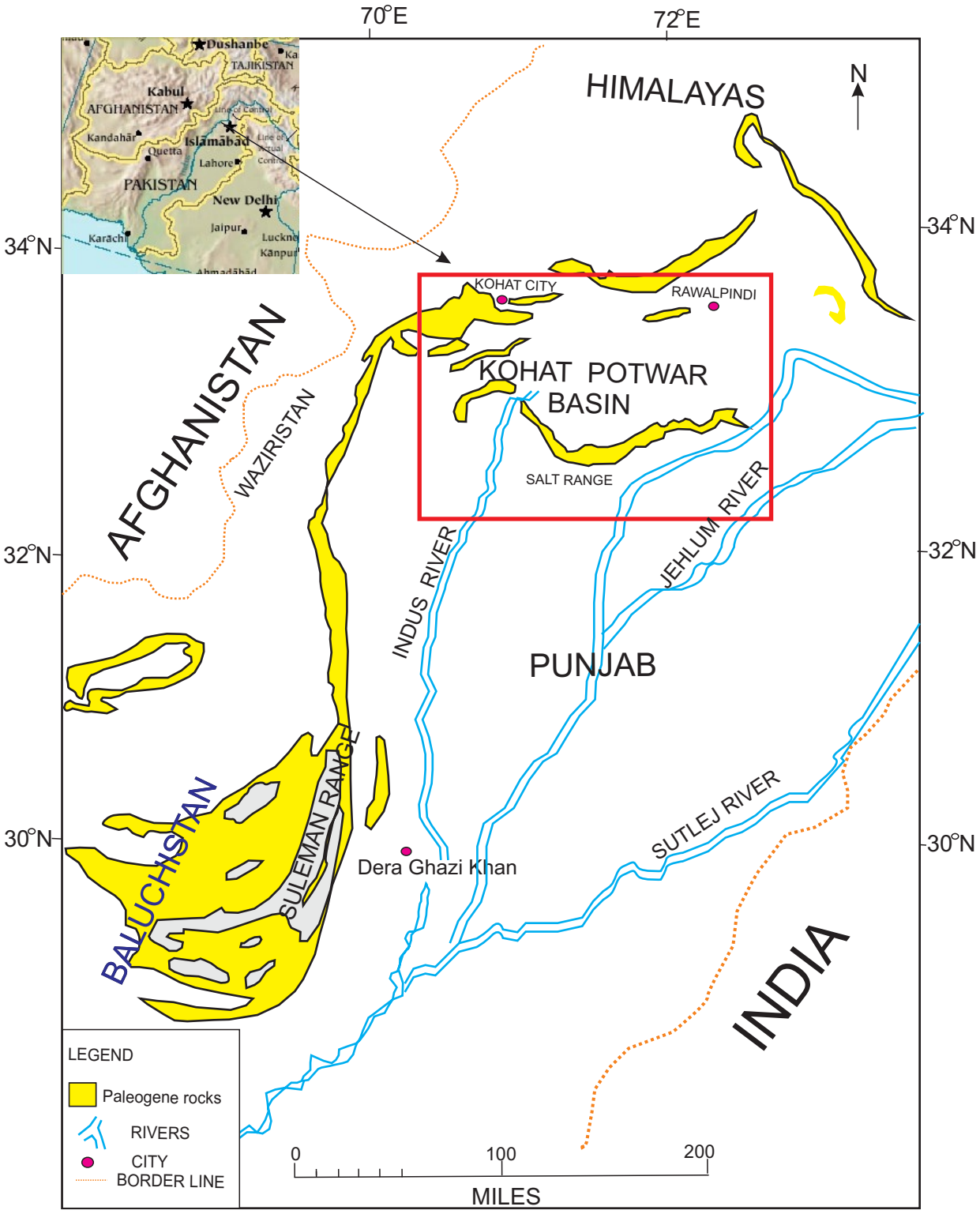


**Figure 2.3.** The figure shows the geographic distribution of the Paleogene rocks in the study area.

| SECTIONS / FORMATIONS | NE ← KOHAT BASIN → SW | | | | Measured stratigraphic thickness |
|---|---|---|---|---|---|
| | PANOBA NALA SECTION | TARKHOBI NALA SECTION | SHEIKHAN NALA SECTION | BAAHDUR KHEL SALT TUNNEL SECTION | |
| PATALA FORMATION | 55m | 152m | Not exposed | Not exposed | |
| PANOBA FORMATION | 100m | 70m | 25m | Not exposed | |
| SHEIKHAN FORMATION | 75m | 73m | 34m | Not exposed | |
| KULDNAN FORMATION | 30m | Not exposed | 25m | 38m | |
| KOHAT FORMATION | 40m | Not exposed | 67m | 42m | |

**Table 2.1.** Measured stratigraphic thicknesses of the Paleogene rocks exposesd in different study sections of the Kohat Basin, northwest Pakistan.

dark grey to black shales. Micro-stylotities and hairline calcite veins are common.

The Patala Formation is well exposed in the Tarkhobi Nala Section (figures 1.1 and 2.3). It is measured as 152m thick unit that comprised of 112m thick black shale and thinly bedded (8-60cm) thick argillaceous, nodular, grey coloured limestone in its lower part. The limestone beds within the lower part contain pyrite and discrete dolomite rhombs and are fossiliferous and contain abundant planktonic foraminifera. The upper part (40m thick) of the Patala Formation shows grey to brownish grey shale, which is ferruginous, limonitic, calcareous, laminated and interbedded with grey limestone that starts with the Irregularis Bed of Eames 1952 (A brownish grey coloured limestone with a grainstone depositional texture, full of larger benthic foraminifera dominated by *Nummulites irregularis* and *Assilina granulosa*). The faunal composition suggests Late Paleocene age Early Eocene age for the Patala Formation.

### 2.2.2 The Panoba Formation

This formation was named by Eames (1952) after Panoba village. It is also well exposed in the Sheikhan Nala Section (Wells, 1983). The Panoba Formation mainly consists of pelagic shales with some sandstone beds. Its lower contact with the Patala Formation and upper contact with the Sheikhan Formation are conformable.

In the Panoba Nala Section (figure 1.1), the Panoba Formation is measured as 100m thick unit comprised of green coloured clays and minor sandstone (figure 2.5). Few larger foraminifera (*Nummulites*) are found in yellowish grey argillaceous nodular limestone beds exposed in the middle of the formation.

In the Tarkhobi Nala Sectionb (figure 1.1) the Panoba Formation is a recessive outcrop which is 70m thick, dominated by greenish grey to yellowish grey coloured shale with limonitic concretions at the top (figure 2.5). A distinct greenish

coloured lithological character of the Panoba Formation makes it an easily identifiable unit in the field.

In the Sheikhan Nala Section (figure 1.1) the Panoba Formation is comprised of 25m thick greenish grey to light olive grey laminated shales intercalated with silty, sandy beds (figure 2.6). The upper 5m of the Panaba Formation is yellowish grey nodular limestone interbedded with greenish clays. Rare *Nummulites* and *Assilina* tests are present in upper marl / limestone beds.

The Panoba Formation is correlated with the Bahadurkhel Salt of the central and southern Kohat Plateau and has Eearly Eocene foraminifers including *Globorotalia* sp., *Assilina pustulosa, Orbitolites complanata, Nummulites sp.* and *Eponides sp.,* and an Early Eocene age is assigned to the formation (Meissner et al., 1974; Shah, 1977).

### 2.2.3 The Sheikhan Formation

The Stratigraphic Committee of Pakistan has formalized the Sheikhan Formation (Fatmi, 1973) to represent the "Gypsiferous Beds" "Upper Sheikhan Limestone", "Middle Sheikhan Limestone" and "Lower Sheikhan Limestone" of Eames (1952) in the Kohat area. The type section is located in the Sheikhan Nala Section, north-east of Kohat City.

The Sheikhan Formation mainly consists of limestone, dolomite and gypsiferous shale. The limestone is grey, thin bedded to massive and nodular. The shale is gypsiferous. In its lower portion shale is dominant while in the upper portion limestone and shale are prominently interbedded.

In the Panoba Nala Section (figure 1.1), the Sheikhan Formation is measured as a 75m thick unit which consists of nodular limestone, dolomite and gypsiferous shale (figure 2.5). The basal 10 m is comprised of yellowish grey to grey coloured nodular limestone which is thin to medium bedded, hard to friable on weathered surface. It contains numerous foraminifera (*Nummulites, Assilina, Operculina, Discocyclina* and *Alveolina*), bivalves, small gastropods, echinoids, algae and ostracodes. This unit is followed by 20m thick, thin beds (ranges from 20cm to 40cm in thickness) of yellowish grey claystone interbedded with thin nodular yellowish grey limestone. A shallowing upward facies trend is seen in this unit. The

limestone beds show a mudstone-wackestone depositional texture. Common sedimentary features found in this unit are bioturbation, burrows, stylolites, limonite patches and planar bedding. The upper part of the Sheikhan Formation is a cream - coloured dolomitize limestone with a mudstone-wackestone depositional texture, thin to medium bedded, aphanitic, highly fractured, internally shows plannar lamination and rare fossils. In the middle-upper part (at 50m height from the base) a significant 1m thick bed of dolomitic limestone with evidence of bioturbation, boring and iron crust. A very significant 13m thick green coloured gypsiferous bituminous shale facies with oil seepage is observed at the top of Sheikhan limestone.

In the Tarkhobi Nala Section (figure 1.1), the Sheikhan Formation is a 73m thick (figure 2.5) alternating sequence of greenish coloured splintery shales and yellowish grey coloured limestone interbeds, dominated (up to 70 %) by shale in the lower part. Limestone beds are thin and nodular with shale partings, ferruginous in part with rusty coatings as bedding surfaces. The limestone shows wackestone depositional texture, is highly fossiliferous with larger benthic foraminifera, echinoids, bivalves, ostracodes and algae and shows a shallowing upward facies trend.

In the Sheikhan Nala Section (figure 1.1) the Sheikhan Formation is 34m thick (figure 2.6) and consists of thin bedded nodular limestone, arenaceous limestone and gypsiferous shales. In the lower 8m the formation is characterized by thin-bedded, nodular, yellowish to yellowish grey limestone. It is highly bioturbated, fossiliferous, and vertical burrows are present. Larger benthic foraminifera (*Nummulites, Assilina* and *Alveolina*), ostracodes, bivalves, brachiopods, echinoids, fresh water algae and small gastropods are common. In the overlying 10m of the formation, thin-bedded nodular limestones, yellowish- to yellowish- grey in colour alternate with yellowish marls and calcareous shales. The upper 16m of the formation is comprised of thin to medium bedded, brownish grey arenaceous limestone with alternations of gypsiferouos clays.

Pascoe (1963) have reported Early Eocene species of foraminifers, which include *Alveolina oblonga*, *Assilina daviesi, Assilina laminosa, Nummulites atacicus* and *Orbitolites complanata*.

### 2.2.4 The Bahadur Khel Salt Facies

Meissner et al. (1968) introduced the term Bahadur Khel Salt for the "Kohat Saline Series" of Gee (1935). The salt is white, mostly thick bedded to massive, and at places contains black stringers. In the Bahadur Khel Salt Tunnel Section of the Kohat area, it is white with black stringers, in places dark grey to black in the upper part, bedded to massive (figure 2.6). The salt outcrops over a length of about 13 kilometres and width of about half kilometre. The salt has a variable thickness due to diapirism. The grey colouration of the salt is attributed to the presence of iron in the salt (Kazmi and Abassi, 2008). The Bahadur Khel Salt Facies occupies the same chronostratigraphic position as that of the Panoaba Formation in the southwestern Kohat Basin.

### 2.2.5 The Jatta Gypsum Facies

Meissner et al. (1968) introduced the term Jatta Gypsum for the upper part of the "Kohat Series" of Gee (1935) in the Kohat area. The Jatta Gypsum facies is comprised of gypsum and gypsiferous clays. The gypsum is greenish white in colour, massive to bedded and hard. Thin clay partings of red, purple and green colour occur at different intervals.

The outcrops of gypsum cover an area in the southern part of Kohat Plateau, which is about 130 km long and 15-30 km wide. Its thickness ranges from 35m to 30m. The Jatta Gypsum conformably overlies the Bahadur Khel Salt, Panoba Shale and the Sheikhan Formation in different areas, but conformably underlies the Kuldana Formation throughout (Kazmi and Abassi, 2008). In the Bahadur Khel Salt Tunnel Section the Jatta Gypsum overlies the Bahadur Khel Salt Facies (figure 2.6). The gypsum is light grey to greenish grey and white in colour. In the upper part -

blackish/greenish black shales are present. The Jatta Gypsum is the southernly lateral stratigraphic equivalent of the Sheikhan Formation. Interfingering of the Sheikhan limestone facies and Jatta Gypsum is reported by Meissner et al. (1974) from the Mami Khel Section in the Kohat Basin. No fossils have been reported from the unit. However, its conformable contacts with the Lower Eocene formations, above and below, indicate an Early Eocene age (Kazmi & Abassi, 2008).

### 2.2.6 The Kuldana Formation

The formation was named as "Kuldana Beds" by Wynne (1873), the "Kuldana Series" by Middlemiss (1986), and "Lower Charat Series" by Eames (1952) and "Mami Khel Clay" by Meissner et al. (1973). Latif (1970) renamed it as "Kuldana Formation". The Kuldana Formation can easily be identified in the field as red to brownish red clays with interbedded sandstone layers. It forms conspicuous red coloured gullies because of being soft as compared to the Kohat Formation and other formations exposed in the area.

In the Panoba Nala Section (figure 1.1) the lower part of the Kuldana Formation consists of 30m thick purple to reddish brown clays with occasional sandstone beds while 6m purple grey/greenish grey coloured dolomitic limestone with oysters rich limestone bed at the top marks the Upper Kuldana Formation (figure 2.5).

In the Sheikhan Nala Section (figure 1.1) the Kuldana Formation is comprised of 25m thick purple to reddish brown clays with subordinate sandstone beds (figure 2.6).

In the Bahadur Khel Salt Tunnel Section (figure 1.1), the Kuldana Formation is 38m thick and is represented 12m thick dominant red mudstone facies and minor brownish coloured sandstone in the lower-middle part while in the upper part comprises a 26m thick sequence of greenish grey coloured argillaceous limestone and dolomite is found (figure 2.6) The Kuldana Formation is famous for its vertebrate mammal fossils (Gingerich, 2003). Based on the vertebrate fossils Late Early Eocene to Early Middle Eocene age is assigned to this formation (Shah, 1970).

### 2.2.7 The Kohat Formation

The Kohat Shales of Eames (1950) and the Kohat Limestone of Meissner et al. (1973) were formally renamed as the Kohat Formation by the Stratigraphic Committee of Pakistan (Shah, 1977). The Kohat Formation is predominantly composed of interbedded limestone and subordinate shale. It is confined to the Kohat, northern Potwar and Kalachitta areas (figure 2.1). Its maximum thickness is 170 meters at Chilli Bagh (figure 1.1). The lower contact with the Kuldana Formation is sharp and conformable and is disconformably overlain by the Murree Formation of Miocene age (Shah, 1977).

In the Panoba Nala Section (figure 1.1) the Kohat Formation overlies the Kuldana Formation and comprised of 40m thick bedded to massive fossiliferous limestone unit (figure 2.5). The lower contact with the Kuldana Formation is conformable while the upper contact with the Muree Formation of Miocene age is unconformable.

In the Sheikhan Nala Section (figure 1.1) the Kohat Formation is 67m thick unit which is richly fossiliferous. The lower part which is comprised of 22m thick, thin to medium bedded argillaceous limestone interbedded with Nummulitic shales (figure 2.6) contains larger benthic foraminifera (i.e. *Nummulites, Assilina,* and *Alveolina*), gastropods, bivalves, and echinoids fragments. Oyster beds associated with minor bryozoans appear twice in the unit at 2m and 5m thickness. The *Nummulites* and *Assilina* tests dominate the unit and produce a grainstone fabric. The 10m thick, middle unit has a packstone to grainstone depositional texture and thinning upward facies trend, that grades up-section in to thin to medium bedded grey coloured nodular limestone. The depositional texture is mudstone–wackestone. The upper 45m thick nodular limestone unit has a mudstone–wackestone depositional texture. The limestone is bioturbated and with poorly preserved foraminifera including *Nummulites* and *Operculina*. The uppermost beds of this unit are characterized by the presence of chert nodules.

In the Bahadur Khel Salt Tunnel Section (figure 1.1), the Kohat Formation overlies the Kuldana Formation. It is comprised of a 42m thick sequence of grey coloured highly fossiliferous limestone interbedded with shales (figure 2.6). The lower part consist of a 32m thick sequence of grey coloured argillaceous, thin bedded, nodular limestone, often friable at the weathered surface. The upper part -

consist of 10m thick, grey coloured, massive, hard, highly fossiliferous limestone that has abundant foraminifers and invertebrate fossils (brachiopods, gastropods and bivalves). The Kohat Formation has yielded abundant foraminifers and a Middle Eocene age can be assigned (Shah, 1977).

## 2.3 Paleogene stratigraphy of the Potwar Basin

The well developed marine sequence of the Lockhart, Patala, Nammal, Sakessar and Chorgali Formations of Paleogene age were deposited along most part of the Potwar Basin (Kazmi and Abbassi, 2008). A summary of the field stratigraphic logs of the studied section in the Potwar Basin and TIR is presented in figures 2.7-2.9, while measured stratigraphic sections (Table 2.2) and a detailed description of the stratigraphic units is given below.

### 2.3.1 The Lockhart Formation

Davies (1930) introduced the term "Lockhart Limestone" for a Paleocene limestone unit in the Kohat area and this usage has been extended by the Stratigraphic Committee of Pakistan (Shah, 1977) to similar units in other parts of the Kohat, Potwar and Hazara areas. In the Sikki Village Section (figure 1.2) the Lockhart Formation is 12m thick and consists of grey coloured thick bedded to massive limestone. Lower contact is not exposed while the upper contact with the Patala Formation is conformable (figure 2.7). In the Nammal Gorge Section (figure 1.2) it is 35m thick and consists of fossiliferous, thin to medium bedded, grey coloured nodular limestone (figure 2.8). In the Ziarat Thatti Sharif Section (figure 1.2) it is 129m thick and comprised of thin bedded to massive, grey coloured limestone (figure 2.8). It is exposed in the core of a broad anticline and contains abundant larger benthic foraminifera and small gastropods. In the Kalabagh Hills Section (figure 1.2), it is 122m thick and comprised of grey coloured nodular limestone with subordinate argillaceous limestone. It is full of larger benthic foraminifera, bivalves and other invertebrate fossils (figure 2.9). In the Chichali Nala Section (figure 1.2), it is 35m thick and consists of alternate thin bedded fossiliferous nodular limestone and minor shales (figure 2.9). On the basis of fauna Late Paleocene age is assigned to the Lockhart Formation (Shah, 1977).

| SECTIONS / FORMATIONS | POTWAR BASIN | | | | TRANS INDUS RANGES (TIR) | | Measured stratigraphic thickness |
|---|---|---|---|---|---|---|---|
| | SALT RANGE | | | | | | |
| | EASTERN | | CENTRAL | WESTERN | | | |
| | GHARIBWAL CEMENT FACTORY SECTION | SIKKI VILLAGE SECTION | NAMMAL GORGE SECTION | ZIARAT THATTI SHARIF SECTION | KALABAGH HILLS SECTION | CHICHALI NALA SECTION | |
| LOCKHART FORMATION | Not exposed | 12m | 35m | 129m | 122m | 35m | |
| PATALA FORMATION | Not exposed | 09m | 29m | 50m | 68m | 65m | |
| NAMMAL FORMATION | Not exposed | Not exposed | 163m | Not exposed | Not exposed | 135m | |
| SAKESSAR FORMATION | Not exposed | Not exposed | 143m | Not exposed | Not exposed | 181m | |
| CHORGALI FORMATION | 40m | 39m | Not exposed | Not exposed | Not exposed | Not exposed | |

**Table 2.2.** Measured stratigraphic thicknesses of the Paleogene rocks exposesd in different study sections of the Potwar Basin and Trans Indus Ranges (TIR), northwest Pakistan

### 2.3.1 The Patala Formation (in the Potwar Basin and TIR)

At its type locality and other parts of the Salt Range (figure 1.2) the Patala Formation is comprised of black shale, marl, and subordinate argillaceous and sandy limestone. The shale is calcareous. and dark greenish grey in colour. The limestone is light to dark grey in colour medium bedded and nodular whereas the sandy limestone is yellowish brown and located in upper part of the Formation (Kazmi and Abassi, 2008).

In the Sikki Village Section (figure 1.2) of the Eastern Salt Range the Patala Formation is 9m thick and consists of yellowish brown limestone interbedded with shales (figure 2.7). In the Nammal Gorge Section (figure 1.2) it is 29m thick and consists of dark grey to blackish coloured clays interbedded with skeletal wackestones-packstones (figure 2.8). In the lower part dark-grey shale is dominant and has a thinly bedded packstone at 5m height from the base of the formation. This bed is full of larger benthic foraminifera. In the lower middle part grey coloured shale is interbedded with subordinate medium bedded limestone having mudstone-wackestone depositional texture which at the top of the middle part of the formation has a glauconitic, sandy skeletal packstone-grainstone depositional texture. The upper part is comprised of dark grey shales containing thin to medium bedded mudstones rich in planktonic foraminifers and few alternate beds of argillaceous lime mudstone.

The Patala Formation in the Ziarat Thatti Sharif Section (figure 1.2) of Western Salt Range area consists of 50m thick nodular limestone, which is devoid of any bedding (figure 2.8). In the Chichali Nala Section (figure 1.2) the Patala Formation consists of thick alternating dark grey to blackish coloured clays interbedded with yellowish colored thin to medium bedded, argillaceous and sandy skeletal packstones-grainstones (figure 2.9).

In the Kalabagh Hills Section (figure 1.2) the Patala Formation is composed of 68m thick argillaceous limestone with typical blackish coloured shales with sparse thin beds of limestone in the upper 15m of the formation (figure 2.9). At the contact of the Patala and Nammal Formations a 5m thick greenish coloured grainstone is -

present. Fossils assemblage within this bed includes abundant larger benthic foraminifera (*Nummulities, Assilina* and *Discocyclina*), brachiopods, echinoids and bivalves. Late Paleocene to Early Eocene age is assigned to this formation (Shah, 1977)

### 2.3.3 The Nammal Formation

The basal Eocene limestone and shale, exposed in the Salt Range and Trans Indus Ranges had been described as "Nammal Limestone" by Gee (1935), "Nammal Stage" by Davies & Pinfold (1937) and as "Nammal Marl" by Danilchik and Shah (I967). This unit has been now formalised as the Nammal Formation by the Stratigraphic Committee of Pakistan (Shah, 1977) and derives its name from the Nammal Gorge in the Salt Range.

In the Surghar Range (figure 1.2) the Nammal Formation is composed of light grey to light bluish grey marl containing marine fossils and thin irregular beds and nodules of white limestone (Danilchik and Shah, 1987).

In the Nammal Gorge Section (figure 1.2), the Nammal Formation is 163m thick and conformably overlies the Patala Formation (figure 2.8). In its lower part the bluish grey marl facies dominate and in the upper part ridge forming, flat bedded silty-sandy skeletal mudstones-wackestones are common.

In the Chichali Nala Section (figure 1.2) the Nammal Formation is 135m thick and conformably overlies the Patala Formation (figure 2.9). It consists of 35m thick, thin bedded, bluish grey coloured marls which are full of planktonic foraminifera in its lower part of the formation. A 60m thick sequence of thick bedded to massive, yellowish grey coloured, cliff forming limestone in the middle part and 50m thick thinly bedded thick succession of mudstone in the upper part of the formation is present. The formation is well developed in the Salt and Trans Indus Ranges. On the basis of foraminiferal fauna an Early Eocene age has been assigned to the sediments of this formation (Shah 1977; Kazmi and Abassi, 2008).

### 2.3.4 The Sakessar Formation

Gee (1935) proposed the name Sakessar Limestone for the ridge forming Eocene limestone in the Salt and Trans Indus Ranges (figure 1.2). The Sakessar Formation is well exposed in the Nammal Gorge Section (figure 1.2) and conformably overlies the Nammal Formation (figure 2.8). It is 143m thick, a ridge forming, thick bedded to massive, grey coloured nodular limestone unit with abundant foraminifera and diverse invertebrate fossils. The rock texture is mostly grainstone with some beds in the middle part having a packstone texture.

In the Chichali Nala Section (figure 1.2), the Sakessar Formation conformably overlies the Nammal Formation (figure 2.9). It is exclusively composed of 181m thick, a very thick bedded to massive, grey coloured, ridge forming limestone unit (figure 2.9). Larger benthic foraminifera (*Nummulites* sp*., Assilina* sp., *Lockhartia* sp., and milliolids), algae, gastropods and bivalves are commonly present. On the basis of foraminiferal fauna an Early Eocene age has been assigned to the sediments of this formation (Shah 1977; Kazmi and Abassi, 2008).

### 2.3.5 The Chorgali Formation

The Chorgali Formation was named by the Stratigraphic Committee of Pakistan (Shah, 1977).

In the Eastern Salt Range area the Chorgali Formation is studied in the Gharibwal Cement Factory Section (figure 1.2). It is comprised of a 40m thick, a highly fossiliferous, porcellaneous, hard, massive, yellowish grey coloured limestone with subordinate dolomite and marl (figure 2.7). Large elongate to rounded nodules are common in lower–middle part (from base of the formation to 30m up-section) while in the upper part fossiliferous limestone (8m thick) is overlain by a 2m thick marl bed. The depositional texture of the main limestone unit is grainstone. Larger benthic foraminifera (*Nummulites, Assilina,* and *Alveolina*), brachiopods, molluscs, ostracodes, echinoids and algae are commonly observed.

In the Sikki Village Section of Eastern Salt Range (figure 1.2) the Chorgali Formation consists of 39m thick grey coloured, monotonous nodular limestone (figure 2.7). The limestone is thick bedded to massive, hard and fossiliferous. The fossils are common throughout the exposed unit and include abundant larger benthic foraminifera (*Nummulites* sp., *Assilina* sp., *Discocyclina* sp., *Alveolina* sp., and *Rotalia* sp), brachiopods, molluscs, ostracodes, gastropods, echinoids and algae. On the basis of foraminiferal fauna an Early Eocene age has been assigned to the sediments of this formation (Shah 1977; Kazmi and Abassi, 2008).

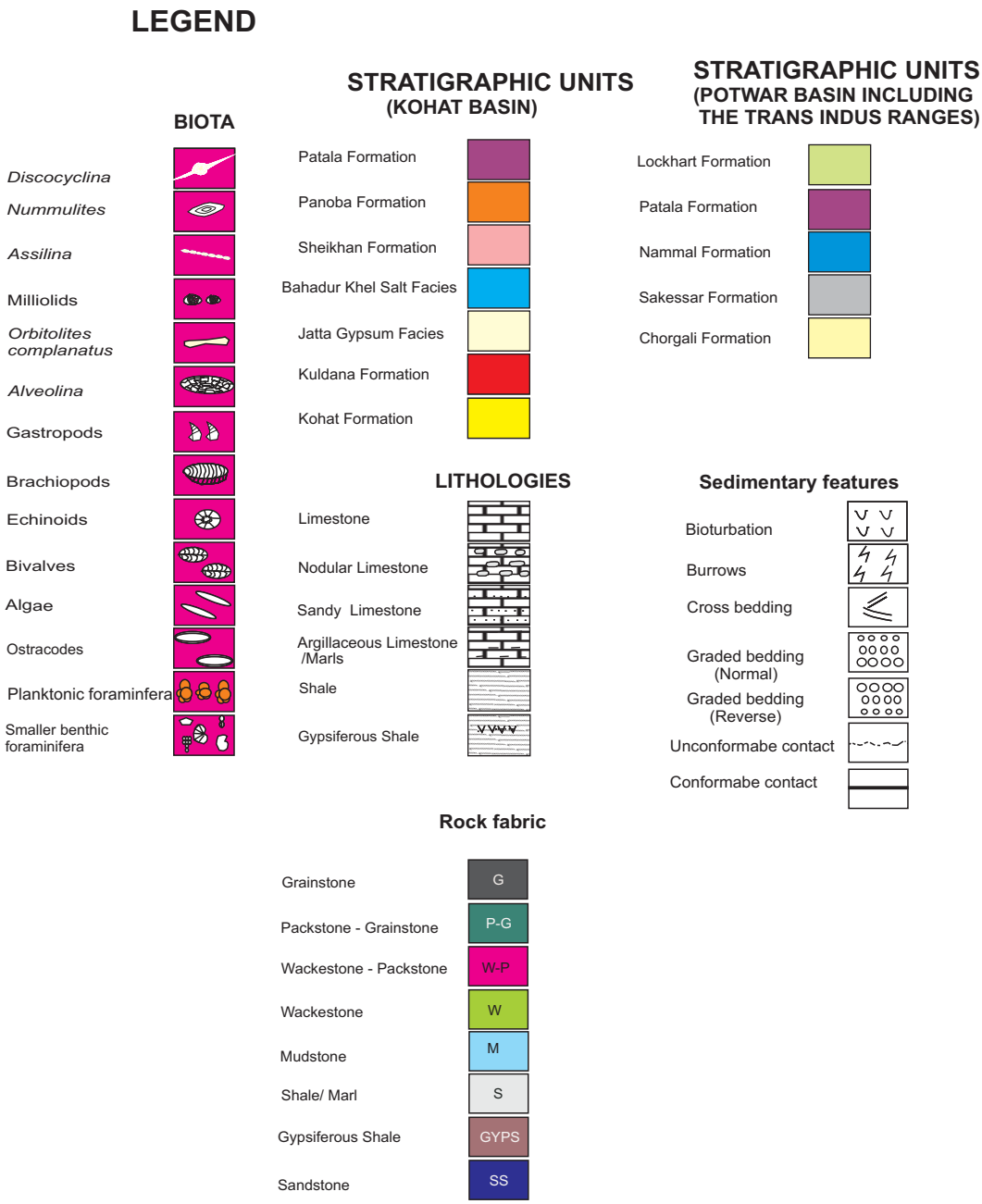


**Figure 2.4.** Key to the different symbols and abbrreviations used in the figures 2.5-2.9.

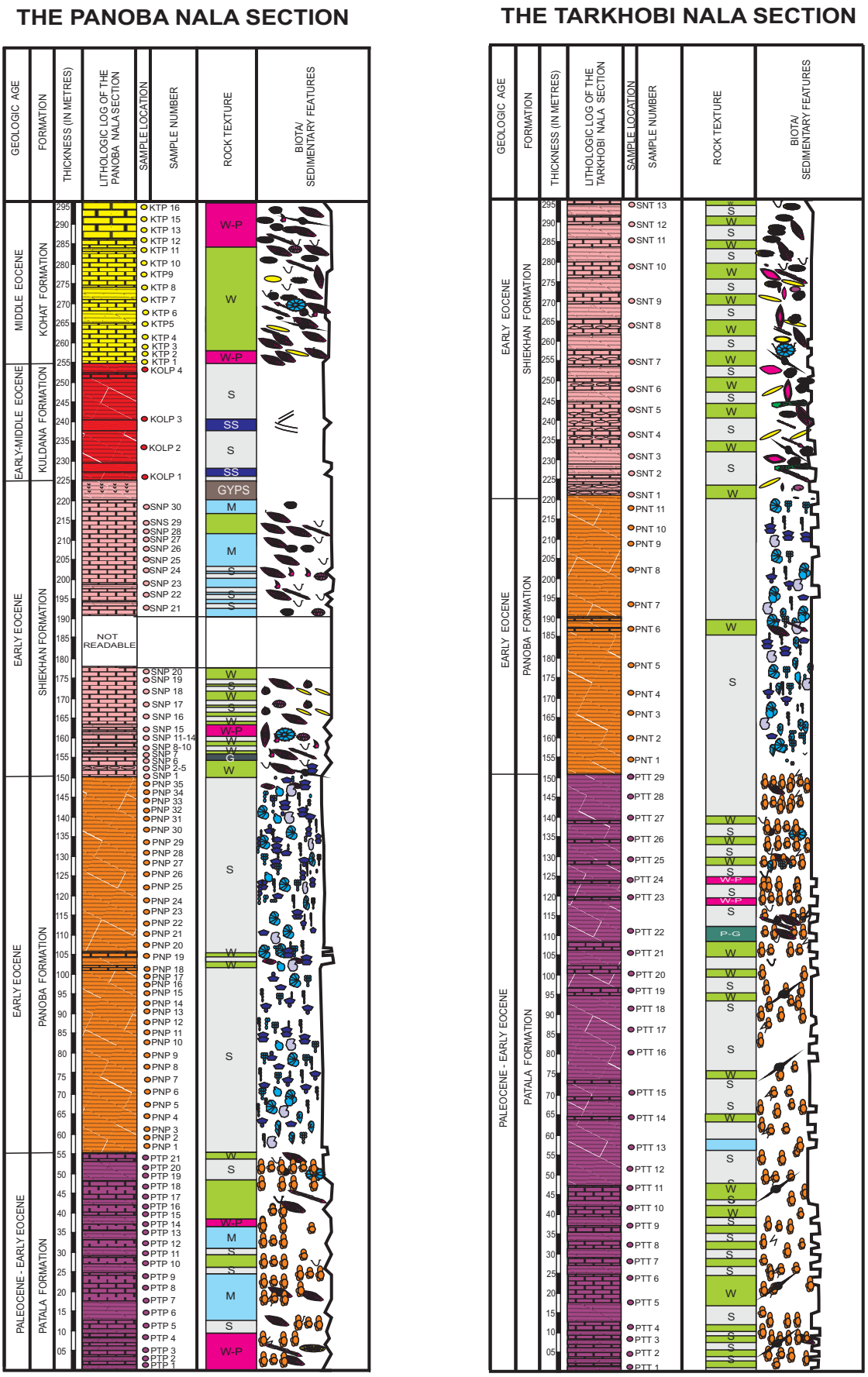


**Figure 2.5.** Composite field stratigraphic log of the Panoba Nala Section and the Tarkhobi Nala Section exposed in the northeastern Kohat Basin (for symbols and abbreviations see figure 2.4).

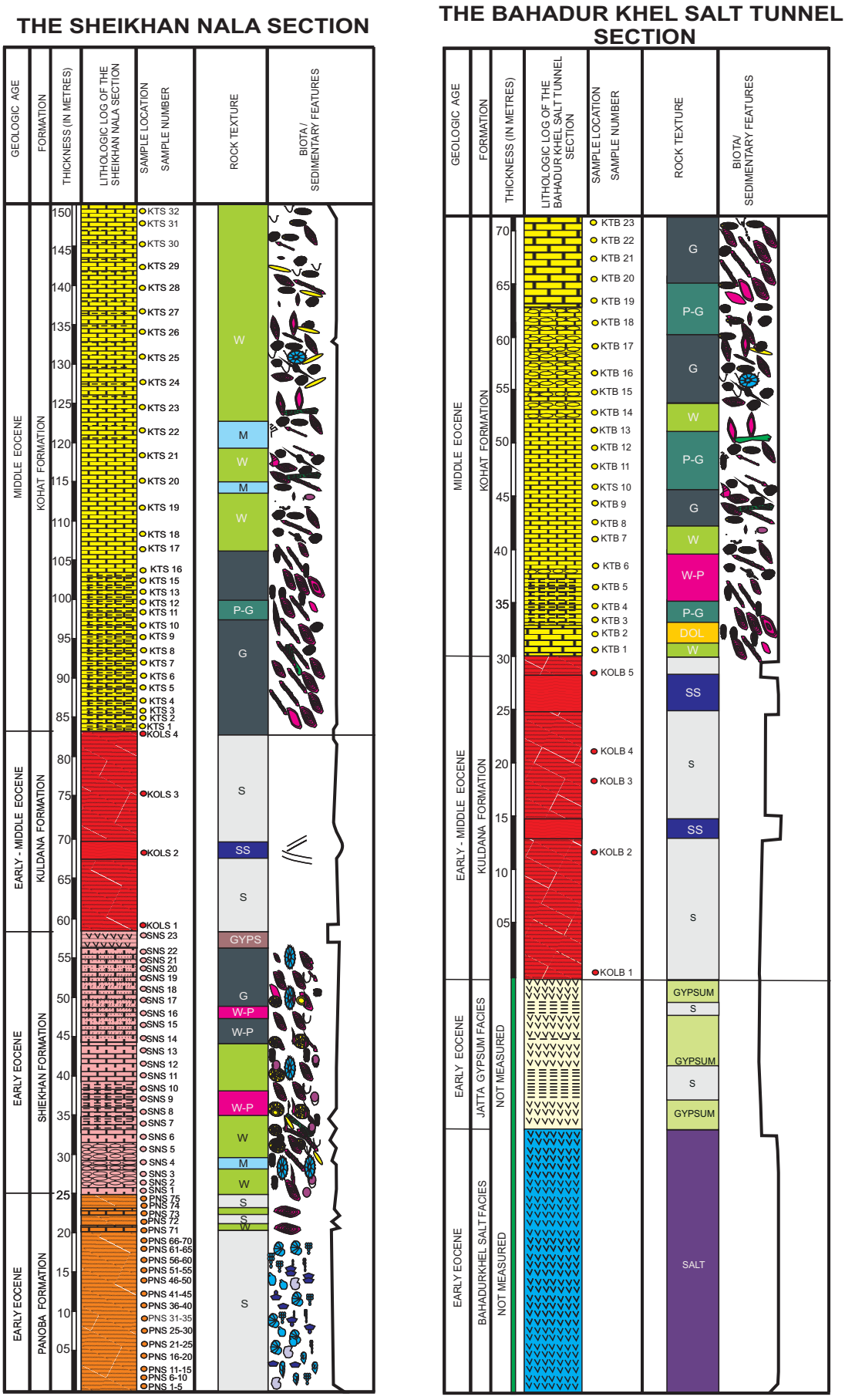


**Figure 2.6.** A Composite stratigraphic log of the Early- Middle Eocene rocks, exposed in the Sheikhan Nala Section and the Bahadur Khel Salt Tunnel Section in the Kohat Basin (for symbols and abbreviations see figure 2.4)

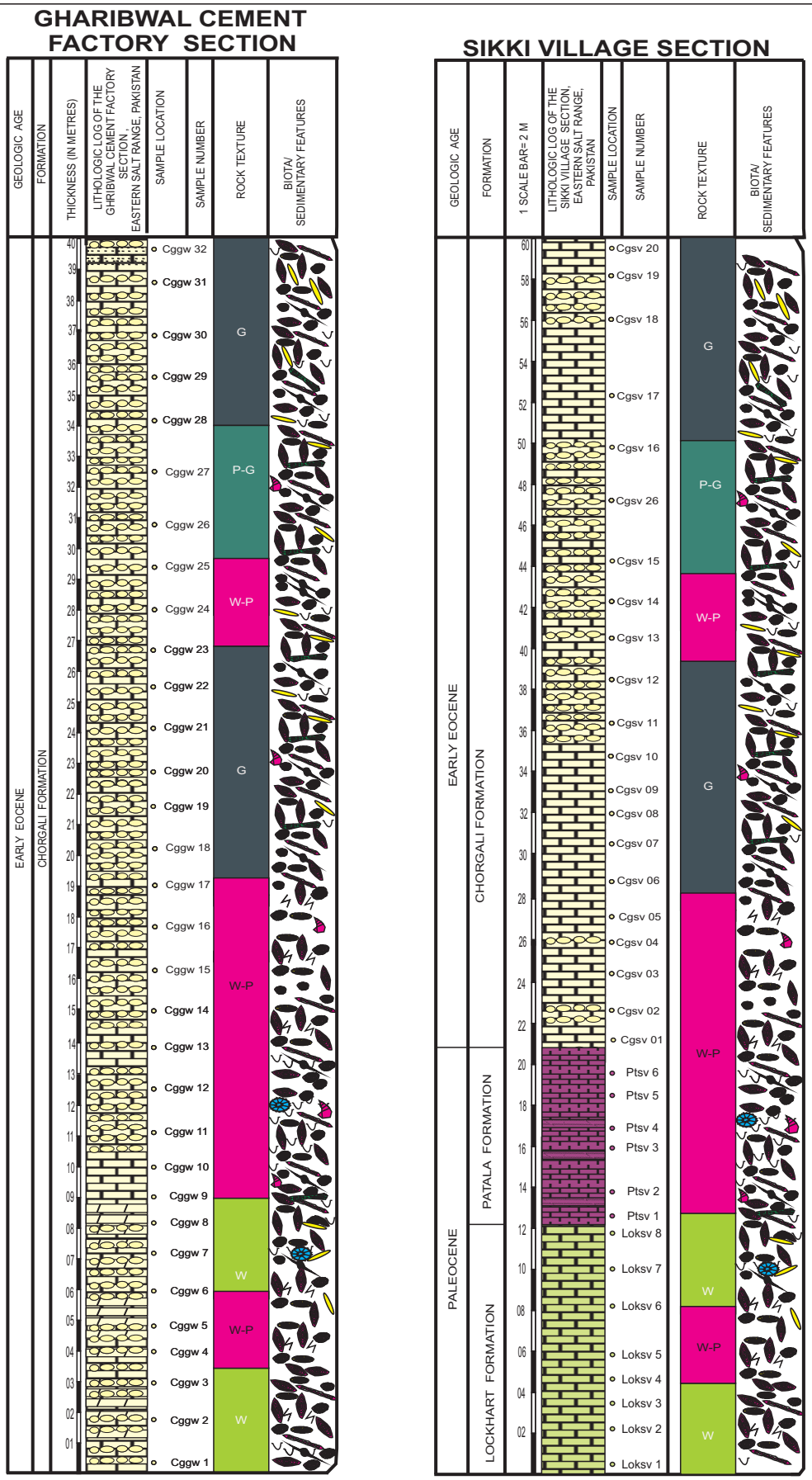


**Figure 2.7.** A Composite stratigraphic log of the Early Eocene Chorgali formation, exposed in the Gharibwal Cement Factory Section and Paleogene rocks exposed in the Sikki Village Section, in the Eastern Salt Range, Potwar Basin (for symbols and abbreviations see figure 2.4).

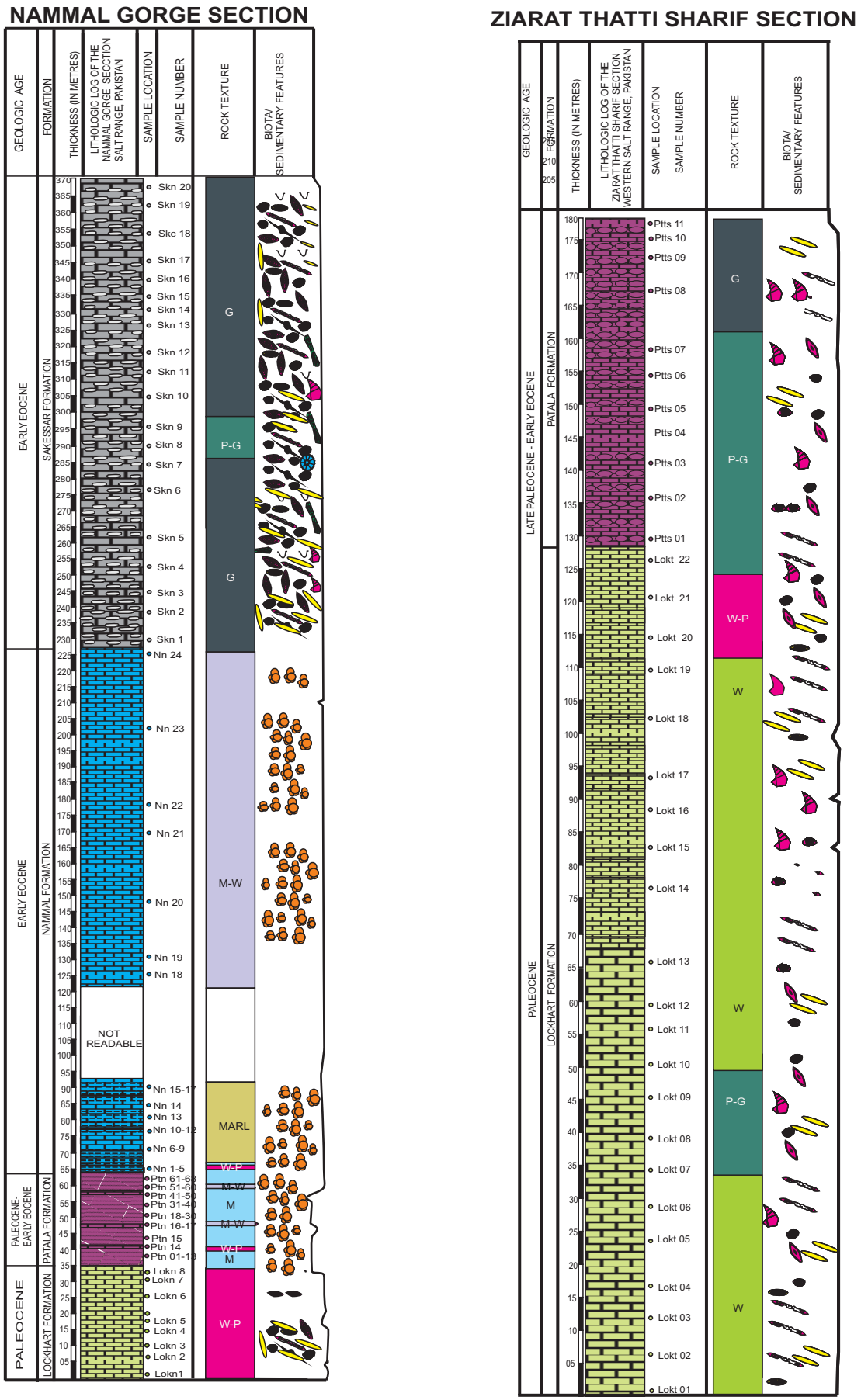


**Figure 2.8.** A Composite stratigraphic log of the Paleogene rocks exposed in the Nammal Gorge Section (Central Salt Range) and the Ziarat Tahtti Sharif Section (Western Slat Range), Potwar Basin (for symbols and abbreviations see figure 2.4)

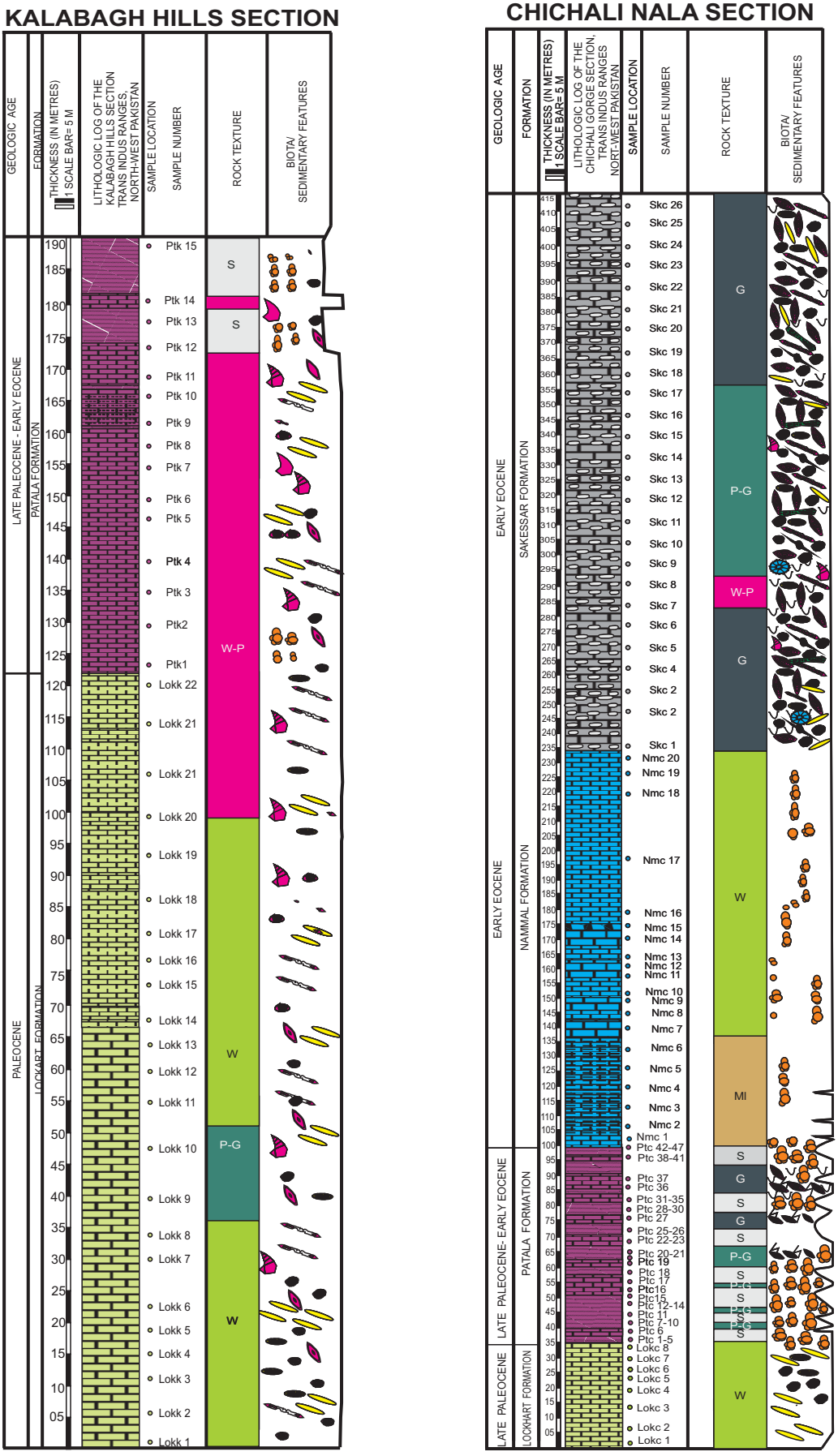


**Figure 2.9.** A Composite stratigraphic log of the Palaeogene rocks exposed in the Kalabagh Hills Section and the Chichali Nala Section ,Trans Indus Ranges (for symbols and abbreviations see figure 2.4)

# Chapter 3

# 3 Foraminiferal paleontology and taxonomy

## 3.1 Larger benthic foraminifera

The Paleogene rocks of the Kohat and Potwar Basins (latter includes the Trans Indus Ranges) of north-west Pakistan have well preserved assemblages of larger benthic foraminifera which are dominated by the genera *Nummulites* and *Assilina*. These genera have a long history of use for stratigraphic analysis (de la Harpe, 1877; Boussac, 1911; Douville, 1919; Eames, 1952; Schaub, 1981; Blondeau, 1966, 1980; Racey, 1995 and Serra Kiel, 1998).

A good and reliable taxonomy of the foraminiferal species is very important in establishing stratigraphy but in case of nummulitid fauna discrepancies exist in the available literature. Therefore this chapter aims to provide a detailed account of the diagnostic paleontology of larger benthic foraminifera that helps in rectifying taxonomy and also provides a quantitative basis for identification of morphologically similar nummulitid fauna. The nomenclature of identified nummulitid species is given in appendix 1 and widely accepted species names are selected in this study.

## 3.2 Morphology of *Nummulites*

The *Nummulites* morphology has been described by Racey (1992) and his terminology is applied herein and briefly summarised below. Figures 3.1-3.3 show the most important features of *Nummulites* and related genera. The terminology outlined below is used for the description of *Nummulites* and associated genera.

***Axial section*:** cut at right angles across the test perpendicular to the plane of symmetry (e.g. figure 3.3, plate 1-1, 2, 3)

***Equatorial section:*** cut through the plane of symmetry in the test showing the median chamber layer (e.g. figure 3.1 C, plate 3-1)

***Lateral section****:* cut immediately below the equatorial section, it shows the structure of septal filaments (plate 3-2)

***Form-A:*** this is the megalospheric generation of the foraminifera which has a large initial chamber and small test size (figure 3.2, plate 2- 8)

***Form-B:*** it is referred to the microspheric generation of the foraminifera which has a small initial chamber and large test size (figure 3.2, plate 2-7)

***Septum/septa:*** a partition between chambers is called a septum / septa (figures 3.1 & 3.2). Spacing and orientation of the septa are important in differentiating species. Septa can be oriented in different ways in equatorial section of the *Nummulites*, for example they can be straight and curved back (figure 3.1 A-B). Although septa and chamber shape are affected by food availability and temperature, they nevertheless constitute reliable characters for the discrimination of species since aberrations from the norm are easily recognised (Racey, 1992; Renema, 2002).

***Septal filaments:*** these are defined as septal extensions situated between successive spiral sheets. Septal filaments change ontogenetically and may show some variation with environmental parameters (Racey, 1992). Quantitative use (number of septal traces, long/short septal traces, secondary septal traces etc) is highly variable and thus unreliable for species discrimination, but in adult specimens presence/absence criteria serve well to discriminate between species groups (Renema, 2002). The following types of septal filaments are known.

***A. Radial:*** straight or slightly curved, extending from the pole to the periphery. All septal filaments are necessarily slightly curved at the peripheral margin (figure 3.1-1)

***B. Sigmoidal:*** curved forwards at the periphery and backwards near the pole. If there is no polar twist, the shape is described as falciform (figure 3.1-2).

***C. Meandrine:*** appearing to wander haphazardly over the lateral surface of the spiral sheet (figure 3.1-3).

***D. Reticulate:*** forming a complex network of filaments in which the individuality of the primary filaments is largely or completely lost (figure 3.1-4).

***E. Subreticulate:*** uniting to form a crude network within the spiral cavity, and showing as septal and filament traces on the outer surface of the spiral wall.

***F. Septal filaments with spiral pillars:*** spiral pillars are seen along the lobe and saddles of the septal filaments (figure 3.1-5).

***Spire Shape:*** the spire may be regularly or irregularly coiled, open or tightly coiled and may show tripartition, doubling and/or reversals (figure 3.1 A).Tripartite spires show a threefold subdivision, each division being characterised by a marked change in tightness, which always follows the sequence tight-loose-tight (Racey, 1995). Intercalatory whorls can form through the bifurcation of the spire by splitting of the marginal cord, so that two whorls are created simultaneously. This character usually involves thinning of the marginal cord (Racey, 1995). In the involute spiral coiling all whorls are visible while in the evolute coiling only the last whorl is seen in external view (figure 3.1 B & C).

***Marginal Cord:*** the marginal cord forms a thickened, imperforate equatorial rim, containing a three-dimensional network of canals that communicate between the chambers (figure 3.2). The thickness of the marginal cord (absolute or relative to the chamber height) can be used as a species character (Schaub, 1981).

***Proloculus size:*** the proloculus size in the macrospheric (Form-A) is an important character for species discrimination. However, proloculus size is shown to vary widely within populations and its size is affected by temperature, water depth and food supply, and that variation was marked, resulting in poor reliability for species discrimination, especially when used on its own (Racey, 1992).

***Pillars:*** Two main types of pillars occur in *Nummulites*: textural and inflational (Racey, 1995; and references therein). Textural pillars are produced by local changes in the texture of the laminae and are visible in axial thin sections but usually do not reach the surface of the test. Inflational pillars are produced by local thickening of the laminae by lamellar superposition. Such pillars may reach the surface to form granules/pustules. Possible pillar arrangements are: 1) arranged so that they form a spire on the outer surface 2) scattered "randomly" all over the test surface either on septal filaments (figure 3.1-5) or between the septal filaments 3) concentrated at the poles to form a large polar pillar (figure 3.3). The pillar location and shape characters (e.g., extending to test surface or not) varies less within populations and may thus constitute valid characters for species discrimination.

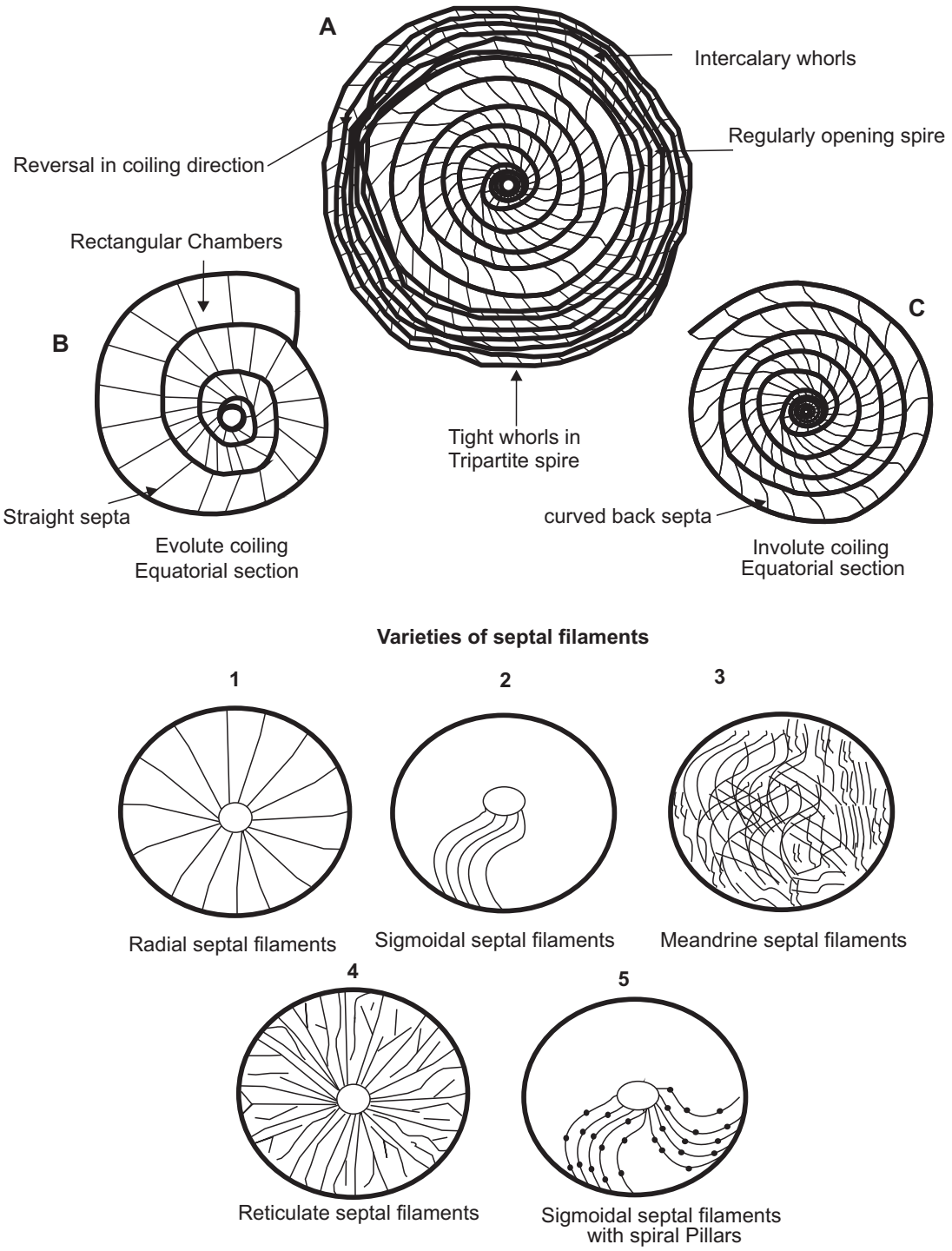


**Figure 3.1.** This figure shows possible variation in the nature of spire (**A.** tripartition and reversal in coiling direction), types of coiling (evolute and involute **B** and **C**) and septal filament varieties **(1-5)** in *Nummulites* and associated genera**.**

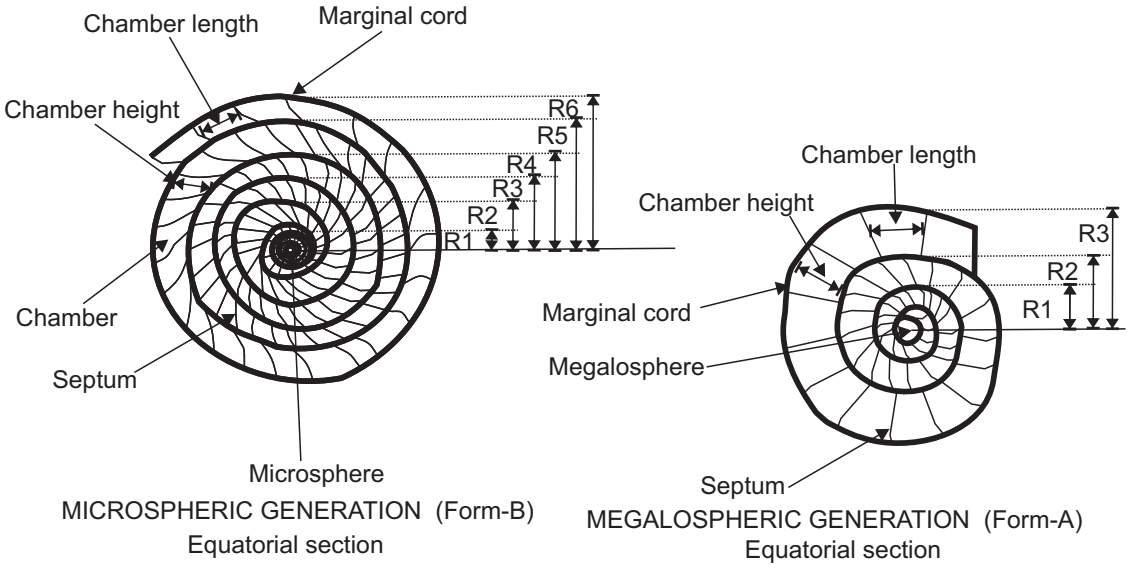


**Figure 3.2.** Figure shows the morphological features (septum, chambers, marginal cord, micro and macrospheres) and procedure of measurement of the radius in microspheric (Form-B) and megalospheric generations (Form-A) in the *Nummulites* and associated genera.

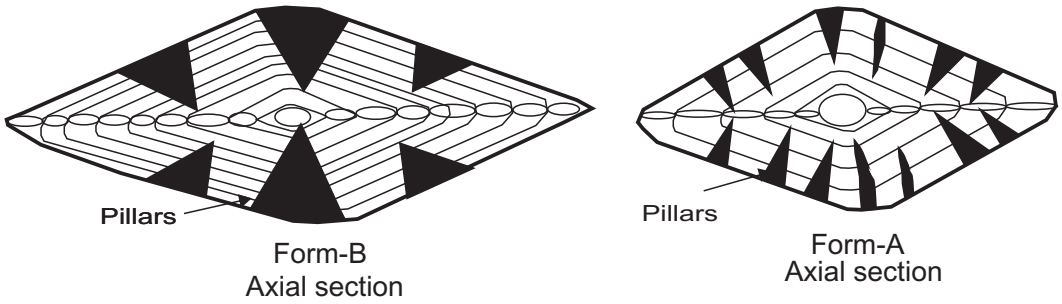


**Figure 3.3.** Axial section of *Nummulites* showing variation in pillar structures of Form A and Form B.

***Test Shape*:** the test shape is defined as a diameter / thickness (D/T) ratio as follows: diameter / thickness shape 1.5- 2.5, inflated lenticular 2.5- 4.5, lenticular 4.5-7 flattened lenticular >7 flat (Racey, 1992). Some species show a highly undulose periphery, whilst others have inflated polar regions and /or variations in the shape of the test margin. Test shape is influenced by environmental parameters and is, as such, of limited taxonomic use (Racey, 1992).

## 3.3 Taxonomy of *Nummulites*

### *General*

It is difficult to define the generic limits in *Nummulites* because of parallel development along several lines (Nagappa, 1959; Blondeau,1972a). Cole (1964) takes the extreme position and lumps together most of the previously recognised genera into *Nummulites* including *Assilina*, *Operculina, Operculinella*, *Operculinoides* and *Ranikothalia*. Hottinger (1977a) bases a generic determination on the stolon and canal system and claims that the traditional description of the *Nummulites* which emphasizes nature of coiling and presence or absence of secondary septa should be abandoned. However, Haynes (1981) suggests that a composite approach combining the traditional criteria and evidence of fine structures can help in discrimination of *Nummulites* genera. The usefulness of species of *Nummulites* in the stratigraphic analysis and correlation of the lower Tertiary of the Indo-Pacific region is widely known but many of these species identifications are difficult to make and intra-specific variations have not been investigated (Sen Gupta., 1965).

In this study, following Gill (1953), Cole (1964), Blondeau (1972a), Hottinger (1977a) and Racey (1995), a range of diagnostic morphological features like alar prolongation, coarseness of the marginal cord, overlap of spiral sheets, type of coiling (evolute/involute), opening of the spire, number of whorls, chambers height, shape and numbers and septal filaments are taken into consideration for identification of *Nummulites* and *Assilina* species.

## 3.4 Format of systematic paleontology

Systematic paleontology of the identified nummulitid and associated fauna is described according to the following format.

***Species name:*** the widely used and accepted name for recorded species is adopted here. Traditionally the microspheric (Form-B) and megalospheric (Form-A) of the nummulitid species were given separate names and these are well entrenched in the literature, therefore to avoid further complications the species naming is based on this traditional style, while description is made with reference to the form A or B of the related species.

***Synonymies:*** the synonymy list for all recorded nummulitid species and associated fauna is based on a review of available literature related to Indian subcontinent (Nuttal, 1924, 1925, 1926; Davies and Pinfold., 1937, 1940; Gill., 1953; Pascoe., 1963; Kureshy., 1975), Indo-Pacific region (Renema, 2002), Mediterranean region (Schaub, 1981) and Tertiary rocks of Oman (Racey, 1995). I have selected the most widely accepted species name in the synonymy list (for details see appendix 1) which will furnish the basis for biostratigraphic zonation.

***Biometric data:*** Description of Form-B is followed by Form-A. Under the heading "Equatorial section" three biometric characters "Whorl", "Radius" and "Chambers" is noted. Whorl refers to the whorl number; radius is the distance (in mm) between the whorl periphery and initial chamber and chambers to the number of chambers per whorl. Details of the biometric data of whorls, Radius and Chambers are given in Tables 3.1-3.2.

***Remarks:*** this section is used to differentiate morphologically similar species and to discuss problems in taxonomic status of the species.

## 3.5 Systematic paleontology of larger benthic foraminifea

**Order** Foraminiferida

**Suborder** Rotaliina Delage & Herouard

**Super family** Nummulitoidea de Blainville

**Family** Nummulitidae de Blainville

**Subfamily** Nummulitinae de Blainville

### 3.5.1 Genus Nummulites Lamarck

**Type species: *Camerina levegata* Bruguirere**

**Diagnosis**

Flattened, discoidal to globular, simple, planispiral spire often tightly coiled, involute, primary septa straight, curved or undulose, septal filaments meandrine, reticulate, radial and traebiculate and fine to moderately thick marginal cord.

**Geological range:** Paleocene to Mid Oligocene in the Tethys area.

***Nummulites pinfoldi* Davies**

Plate 1, figures 1-3, 9; figures 3.4 A-B

**Form-B**

**Diagnosis**

In equatorial section the spire is regularly opening (figure 3.4 A). Chambers are rectangular and higher than long throughout the spire. Septa are straight to slightly twisted in early whorls and curved back in later whorls. Marginal cord has a variable thickness ranging from 1/3$^{rd}$ of the chamber height in the early whorls to 2/3$^{rd}$ of the chamber height in the later whorl. In axial section concentrated polar pillars are present (plate 1, figure 1-2).

**Form-A**

**Diagnosis**

In equatorial section the spire shows regular opening after the second whorl (figure 3.4 B). Chambers are rectangular and higher than long. Septa are straight to slightly curved. The marginal cord is thick throughout the spire (plate 1- figure 4). In axial section alar prolongation is tapering towards the margins and concentrated polar pillars are common (plate 1, figure 5).

***Nummulites pinfoldi* Davies (1940)**

Material: 14 specimens

**Form-B**

**Equatorial section**

| Whorl | 1 | 2 | 3 | 4 | 5 | 6 | 7 |
|---|---|---|---|---|---|---|---|
| Radius (mm) | 0.21 | 0.32 | 0.86 | 1.37 | 2.02 | 2.82 | 3.96 |

**Form-A**

**Equatorial section**

| Whorl | 1 | 2 | 3 | 4 | 5 |
|---|---|---|---|---|---|
| Radius (mm) | 0.34 | 0.73 | 1.32 | 1.83 | 2.48 |

***Nummulites atacicus* Leymerie (1981)** Material: 34 specimens

**Form-B**

| Whorl | 1 | 2 | 3 | 4 | 5 | 6 | 7 | 8 | 9 |
|---|---|---|---|---|---|---|---|---|---|
| Radius (mm) | 0.15 | 0.23 | 0.75 | 0.9 | 1.20 | 1.75 | 2.50 | 3.25 | 4.0 |

***Nummulites subatacicus* Leymerie (1919)** Material: 4 specimens

**Form-A**

**Equatorial Section**

| Whorl | 1 | 2 | 3 | 4 |
|---|---|---|---|---|
| Radius (mm) | 0.55 | 0.82 | 1.34 | 1.90 |
| Chambers | 8 | 16 | 18 | 22 |

***Nummulites globulus* Leymerie (1846)** Material: 24 specimens

**Form-B**

**Equatorial Section**

| Whorl | 1 | 2 | 3 | 4 | 5 | 6 |
|---|---|---|---|---|---|---|
| Radius (mm) | 0.06 | 0.14 | 0.26 | 0.43 | 0.62 | 0.91 |
| Chambers | 15 | 19 | 22 | 24 | 26 | 28 |

| Whorl | 7 | 8 | 9 | 10 | 11 | 12 |
|---|---|---|---|---|---|---|
| Radius (mm) | 1.15 | 1.46 | 1.67 | 2.05 | 2.30 | 2.47 |
| Chambers | 35 | 48 | 53 | 55 | 60 | 66 |

***Nummulites mamilla* Fichtel and Moll (1924)** Material: 14 specimens

**Form-A**

**Equatorial Section**

| Whorl | 1 | 2 | 3 | 4 | 5 |
|---|---|---|---|---|---|
| Radius (mm) | 0.42 | 0.63 | 0.86 | 1.04 | 1.24 |
| Chambers | 10 | 18 | 20 | 29 | 37 |

**Table 3.1** Quantitative biometric data of different *Nummulities* sp (chambers are not recorded in species with only axial sections preserved ).

***Nummulites beaumonti* d' Archiac & Haime (1853)** Material: 60 specimens

**Form-B**

**Equatorial section**

| Whorl | 1 | 2 | 3 | 4 | 5 | 6 | 7 | 8 | 9 | 10 | 11 | 12 |
|---|---|---|---|---|---|---|---|---|---|---|---|---|
| Radius (mm) | 0.12 | 0.24 | 0.40 | 0.69 | 0.80 | 1.85 | 1.20 | 1.79 | 2.18 | 2.54 | 2.88 | 3.18 |
| Chambers | 04 | 20 | 27 | 29 | 33 | 38 | 20 | 48 | 53 | 55 | 60 | 66 |

**Form-A**

**Equatorial section**

| Whorl | 1 | 2 | 3 | 4 | 5 | 6 |
|---|---|---|---|---|---|---|
| Radius (mm) | 0.30 | 0.57 | 0.78 | 1.03 | 1.13 | 1.24 |
| Chambers | 13 | 16 | 21 | 24 | 33 | 40 |

***Nummulites acutus* Sowerby (1840)** Material: 4 specimens

**Form-B**

**Equatorial section**

| Whorl | 1 | 2 | 3 | 4 | 5 | 6 | 7 | 8 | 9 | 10 |
|---|---|---|---|---|---|---|---|---|---|---|
| Radius (mm) | 0.24 | 0.40 | 0.80 | 1.14 | 1.55 | 1.85 | 2.16 | 2.49 | 2.64 | 2.82 |
| Chambers | 17 | 22 | 24 | 26 | 34 | 38 | 44 | 48 | 50 | 56 |

***Nummulites djokdjokartae* Martin (1881)** Material: 19 specimens

**Form-A**

**Equatorial section**

| Whorl | 1 | 2 | 3 | 4 |
|---|---|---|---|---|
| Radius (mm) | 0.47 | 0.68 | 0.86 | 1.01 |
| Chambers | 10 | 20 | 30 | 36 |

***Nummulites pengaroensis* Verbeek (1871)** Material: 8 specimens

**Form-B**

**Equatorial section**

| Whorl | 1 | 2 | 3 | 4 | 5 | 6 | 7 | 8 | 9 | 10 | 11 | 12 |
|---|---|---|---|---|---|---|---|---|---|---|---|---|
| Radius (mm) | 0.12 | 0.24 | 0.40 | 0.69 | 0.80 | 1.20 | 1.85 | 1.79 | 2.18 | 2.54 | 2.88 | 3.66 |
| Chamber | 04 | 20 | 27 | 29 | 33 | 20 | 38 | 48 | 53 | 55 | 60 | 66 |

***Nummulites perforatus De Montfort* (1808)** Material: 19 specimens

**Equatorial section**

| Whorl | 1 | 2 | 3 | 4 | 5 | 6 | 7 |
|---|---|---|---|---|---|---|---|
| Radius | 0.70 | 1.16 | 1.50 | 1.86 | 2.16 | 2.52 | 2.67 |
| Chambers | 12 | 17 | 23 | 32 | 38 | 52 | 58 |

**Table 3.1** (continued)

**Remarks:** this species was identified by Davies (1940) in the Kohat Basin of Pakistan. He describes it as a smaller in size as compared to *N. beaumonti*, having external flattened, excavated postules at each pole. The average thickness to diameter ratio is more or less similar to the ratio of *N. beaumonti* which is 8 -3mm. A trend in gradual decrease in size of the species is seen in the north-eastern corner of the Kohat Basin where in the Sheikhan Nala Section the commonly found specimens are in the Early -Middle Eocene carbonates.

### ***Nummulites atacicus* Leymerie**

Plate 1; figures 7 and 9, plate 2; figure 2, figure 3.4 C

### Form-B

### Diagnosis

The test shape is lenticular. In equatorial section a regularly opening spire is present (figure 3.4 C). The initial five whorls are tightly coiled and later ones are loosely coiled. S-shaped, radiating septal filaments are present in early whorls. Numerous chambers are present which are rectangular and higher than long but in the $7^{th}$ whorl two chambers are longer than high. Septa are straight to gently inclined towards the periphery. A thin marginal cord is present which has a thickness equal $1/4^{th}$ of the chamber height. In axial section a polar pustule is common in young specimens which are sometime buried in adults (plate 1; figure 7, plate 2; figure 2)

**Remarks:** *Nummulites atacicus* Leymerie is the Form-B of *Nummulites subatacicus* Leymerie.

### ***Nummulites subatacicus* Leymerie**

Plate 2, figures 1, figure 3.4 D

### Form-A

### Diagnosis

This species is the megalospheric form of the *Nummulites atacicus* Leymerie. It has a regularly opening spire with straight to inclined septa (figure 3.4 D). The septa are sometimes curved back. Chambers are rectangular and are longer than high.

The marginal cord is thin and uniform with a thickness equal to 1/5$^{th}$ of the chamber height. Proloculus size of the figured specimen is 0.34mm. In axial section a polar pustule is common (plate 2, figure 1).

**Remarks:** *Nummulites subatacicus* Leymerie is the Form-A of *Nummulites atacicus* Leymerie.

### ***Nummulites globulus* Leymerie**

Plate 2, figures 3, 5 and 7; figure 3.4 E

### Form-B

### Diagnosis

The test is small and biconical. Spire is tight and compact in early five whorls then regularly opening in later whorls (figure 3.4 E). Septa are gently curved in early whorls and in later whorls become inclined and sometimes curved back towards the periphery. S-shaped, straight to radiating septal filaments are present. Chambers are rectangular to isometric, higher than long in early whorls but tending to become longer than high in later whorls. The marginal cord is thick but it is non-uniform. In 3$^{rd}$, 5$^{th}$, 7$^{th}$ and 9$^{th}$ whorls the marginal cord has a thickness that equals 2/3$^{rd}$ of the chamber height (plate 2, figures 7). In axial section scattered pillars are seen (plate 2, figure 5).

**Remarks:** *Nummulites globulus* Leymerie is the Form-B of *Nummulites mamilla* Fichtel and Moll.

### ***Nummulites mamilla* Fichtel and Moll**

Plate 2, figures 4, 6 and 8; figure 3.4 F

### Diagnosis

This species is characterized by a rapidly opening spire (figure 3.4 F). Septa are straight to inclined, sometimes curved back. Chambers are rectangular to isometric in shape and longer than high. Septal filaments are S shaped. The marginal

cord is thick and equals 3/4$^{th}$ of the chamber height. The size of proloculus in the figured specimen is 0.36mm. In axial section subrounded alar prolongation, thick polar pillars and a large proloculus are present (plate 2; figure 4 and 6).

**Remarks:** *Nummulites mamilla* Fichtel & Moll is the Form-A of *Nummulites globulus* Leymerie.

### *Nummulites beaumonti* d' Archiac & Haime

Plate 4, figures 1- 6, figure 3.5 A

#### Form-B

#### Diagnosis

In equatorial section the spire is regularly opening (figure 3.5 A). Straight to slightly curved septal filaments are present. Septa are straight, occasionally inclined. Numerous chambers (4 - 66), mostly longer than high and rectangular in shape but subrectangular to isometric chambers are also seen in the last few whorls. The marginal cord is uniform, 1/3-1/4 of the chamber height (plate 4; figure 3). In axial section pillars are commonly scattered. The diameter of figured specimen is 6.36 mm The average thicknesses of 5 studied specimens is 3.8 mm, maximum observed thickness is 4.5 mm and average ratio of the diameter to thickness is 1.8 to 1.

#### Form-A

#### Diagnosis

In the equatorial section the spire displays opening, having six whorls (plate 4, figure 5). Chambers are rectangular to subrectangular in shape and are commonly longer than high, but higher than long chambers are found in the fourth whorl. Septa are mostly straight but inclined in early and last whorls. The marginal cord's thickness equals 1/3$^{rd}$ to 2/3$^{rd}$ of the chamber height. Diameter of the proloculus in the figured specimen is 0.34 mm.

### *Nummulites acutus* Sowerby

Plate 3, figures 1-3 & figure 3.5 C

**Form-B**

**Diagnosis**

In equatorial section the spire is gradually opening (figure 3.5 C). Granules are commonly present along the meandrine septal filaments and generally throughout the spire. Chambers are rectangular occasionally isometric, and are longer than high. Intercalary whorls are present after the 9$^{th}$ whorl (plate 3, figure 2). Septa are gently curved in early whorls and curved back in later whorls. The marginal cord is not uniform; it is thicker in the 1$^{st}$ and 5$^{th}$ whorl and occupies 3/4$^{th}$ of the chamber height (plate 3, figure 1). The average thickness to diameter ratio of the 10 measured specimens varies from 2.5 mm to 1.2 mm.

### *Nummulites djokdjokartae* Martin

Plate 3, figures 4-5; figure 3.5 D

**Form-A**

**Diagnosis**

In equatorial section the spire is gradually opening (figure 3.5 D). Septa are inclined in early whorls becoming straight in later whorls. Chambers are rectangular, longer than high. A thick marginal cord is seen that equals 2/4$^{th}$ -3/4$^{th}$ of the chamber height in thickness (Plate 3, figure 4). In axial section a large proloculus and buried polar pillars are present (plate 3, figure 5)

**Remarks:** the synonymy of this species is discussed by Racey (1995) and Renema (2002). They concluded that *N. djokdjokartae* is the Form-A of N. *acutus* Sowerby whereas *Nummulites vredenburgi* is a juvenile of the N. *djokdjokartae*. This study also supports that N. *djokdjokartae* is the Form-A of *N. acutus* Sowerby.

***Nummulites pengaroensis* Verbeek**

Plate 5, figures 1-2, figure 3.5 E

**Form-B**

**Diagnosis**

In equatorial section the spire is regularly opening, having commonly nine to twelve whorls (figure 3.5 E). Straight septal filaments are common. Septa are straight for most of the spire but inclination of the septa is also seen. Numerous chambers (4 - 66), mostly rectangular, but subrectangular to isometric chambers are seen in the last few whorls. Chambers are longer than high. The marginal cord is uniform and equals the $1/3^{rd}$ -$1/4^{th}$ of the chamber height in thickness (plate 5, figure 1-2). In axial section buried scattered pillars are present (plate 5, figure 4). Diameter of the figured specimen is 7.3 mm.

**Equatorial section**

***Nummulites perforatus* De Montfort**

Plate 5, figures 3, 5-6; figure 3.5 F

**Form-A**

**Diagnosis**

Test is lenticular or inflated lenticular with a rounded periphery. The spire is regular and compact, opening slightly more rapidly in earlier whorls (figure 3.5 F). The marginal cord increasing slowly in thickness usually equals $2/3^{rd}$ of the chamber height (plate 5; figure 3). Chambers are longer than high and septa are strongly inclined to curved back.

## 3.5.2 Genus Assilina dOrbigny

**Type species: *Nummulites spira* Roissy**

The genus *Assilina* embraces all those forms which are morphologically like *Nummulites* but characterized by evolute coiling, whereas in *Nummulites* the coiling is involute. Cole (1960) stated that individual species may grade from involute to-

evolute, and thus he identified *Paleocamerinoides* Cole (genotype *Nummulites exponense* Sowerby) as a junior synonym of *Nummulites*. However Cushman (1948) considered *Assilina* and *Nummulites* as separate genera, the same view is adopted here. In the past megalospheric and microspheric forms of *Assilina* were designated by two different names. As these names are in common use, therefore they are retained here with A and B forms being identified in the diagnosis. The stratigraphic range of *Assilina* is from Paleocene to Eocene.

### *Assilina dandotica* Davies & Pinfold

Plate 6, figures 1-4; figure 3.8 D

#### Form-B

#### Diagnosis

Test is discoidal with a sharp periphery; in equatorial section the spire is tight, regularly opening (figure 3.8 D), granules are common along the septa, septa are straight to slight curved in later whorls, chambers are rectangular, twice higher than long (Plate 6; figure 3). In axial section the spiral sheet completely embraces the succeeding whorls (plate 6; figure 1 and 4).

#### Form-A

#### Diagnosis

In axial section (Form-A) shows a large megalosphere and rapidly opening spiral sheet which is completely enveloping the earlier whorls (plate 6; figure 2).

### *Assilina granulosa* d'Archaic

Plate 6, figures 5-10; figure 3.7 A

#### Form-B

#### Diagnosis

The test is flat, large, smooth and relatively thin in the centre with sharp margins. Granules are concentrated at the pole to form a bunch. Maximum diameter 16mm, thickness to diameter (T/D) ratio of the test ranges between 1: 6- 1:12 with an

average value of 1: 7. Spire is regularly opening (figure 3.7 A, plate 6; figure 6). Septa are curved forward up to 1/3-1/4 than becoming straight along the marginal cord height; Chambers are twice as high as long. In axial section the spiral sheet completely envelops the inner whorls but does not completely envelop the outer whorls (plate 6; figure 5,7)

**Remarks**: this species is the Form-B of *Assilina leymerie* d, Archaic & Haime.

### *Assilina leymerie* d, Archaic & Haime

Plate 6, figures 9, 11 and 12; plate 7, figure 1-3, figure 3.7 B

#### Form-A

#### Diagnosis

Test is lenticular to flat with subrounded periphery and granules are common in the central part of the test. Regularly opening spire, loosely coiled (figure 3.7 B). Septa are straight to inclined but sometimes curved back. Chambers are isometric to rectangular and longer than high. The marginal cord is thick and nonuniform and equals $3/5^{th}$ of the chamber height. In axial section buried polar pillars and a large proloculus are seen (plate 6; figure 12), proloculus size of the figured specimen is 0.83 mm in diameter.

**Remarks**: this is the megalospheric form of *Assilina granulosa* d, Archaic.

### *Assilina pappilata* Nuttal

Plate 8, figures 2 and 4, figure 3.7C

#### Form-B

#### Diagnosis

Test is flat, lenticular with a rounded periphery. Average diameter is about 17mm. The test is characterized by an evolute, lose irregular spire (figure 3.7 C).

***Assilina dandotica* (Davies & Pinfold 1937)** Material: 07specimens

**Form-B**

**Equatorial section**

| Whorl | 1 | 2 | 3 | 4 |
|---|---|---|---|---|
| Radius | 0.27 | 0.56 | 0.94 | 1.39 |
| Chambers | 7 | 14 | 20 | 25 |

***Assilina granulosa* (d'Archaic, 1906)** Material: 28 specimens

**Form-B**

**Equatorial section**

| Whorl | 1 | 2 | 3 | 4 | 5 |
|---|---|---|---|---|---|
| Radius (mm) | 0.21 | 0.63 | 1.10 | 1.63 | 2.04 |
| Chambers | 07 | 11 | 15 | 20 | 26 |

***Assilina leymerie* (d, Archaic & Haime 1853)** Material: 11 specimens

**Form-A**

**Equatorial Section**

| Whorl | 1 | 2 | 3 |
|---|---|---|---|
| Radius (mm) | 0.49 | 1.5 | 2.58 |
| Chambers | 5 | 9 | 20 |

***Assilina pappilata* (Nuttal, 1926a)** Material: 35 specimens

**Form-B**

**Equatorial section**

| Whorl | 1 | 2 | 3 | 4 | 5 | 6 |
|---|---|---|---|---|---|---|
| Radius (mm) | 0.46 | 0.89 | 1.48 | 2.1 | 2.86 | 3.38 |
| Chambers | 8 | 12 | 14 | 20 | 22 | 24 |

***Assilina subpappilata* (Nuttal, 1926a)** Material: 25 specimens

**Form-A**

**Equatorial section**

| Whorl | 1 | 2 | 3 | 4 | 5 |
|---|---|---|---|---|---|
| Radius (mm) | 0.18 | 0.74 | 1.38 | 2.02 | 2.8 |

**Table 3.2** Quantitative biometric data of different *Assilina* sp. (chambers are not recorded in species with only axial sections available).

***Assilina davisie*** **(de Cizancourt, 1938)** Material: 15 specimens

**Equatorial Section**

| Whorl | 1 | 2 | 3 | 4 | 5 |
|---|---|---|---|---|---|
| Radius (mm) | 0.46 | 1.02 | 1.50 | 1.86 | 2.96 |

***Assilina subdavisie*** **(de Cizancourt, 1938)** Material: 12 specimens

**Form A**

**Equatorial Section**

| Whorl | 1 | 2 | 3 | 4 |
|---|---|---|---|---|
| Radius (mm) | 0.35 | 0.60 | 0.90 | 1.12 |

***Assilina spinosa*** **(Davies, 1937)** Material: 25 specimens

**Equatorial section**

| Whorl | 1 | 2 | 3 | 4 | 5 |
|---|---|---|---|---|---|
| Radius (mm) | 0.21 | 0.63 | 1.10 | 1.63 | 2.04 |
| Chambers | 07 | 11 | 15 | 20 | 26 |

***Assilina subspinosa*** **(Davies, 1937)** Material: 15 specimens

**Form-A**

**Equatorial section**

| Whorl | 1 | 2 | 3 | 4 |
|---|---|---|---|---|
| Radius (mm) | 0.6 | 1.2 | 1.8 | 2.5 |
| Chambers | 07 | 14 | 19 | 22 |

***Assilina pustulosa*** **Doncieux (1926)** Material: 10 specimens

**Form-B**

**Equatorial section**

| Whorl | 1 | 2 | 3 | 4 | 5 | 6 |
|---|---|---|---|---|---|---|
| Radius (mm) | 0.46 | 0.89 | 1.48 | 2.1 | 2.86 | 3.38 |
| Chambers | 8 | 12 | 14 | 20 | 22 | 24 |

**Table 3.2** (continued)

***Assilina suteri* Schaub (1981)** Material: 08 specimens

**Form-A**

**Equatorial section**

| Whorl | 1 | 2 | 3 | 4 | 5 | 6 | 7 | 8 |
|---|---|---|---|---|---|---|---|---|
| Radius (mm) | 0.16 | 0.2 | 0.3 | 0.56 | 0.86 | 1.09 | 1.47 | 1.67 |
| Chambers | 5 | 18 | 23 | 34 | 38 | 44 | 46 | 52 |

***Assilina laminosa* Gill (1953)** Material: 15 specimens

**Form-A**

**Equatorial section**

| Whorl | 1 | 2 | 3 | 4 | 5 |
|---|---|---|---|---|---|
| Radius (mm) | 0.12 | 0.96 | 1.88 | 2.91 | 4.04 |
| Chambers | 5 | 9 | 21 | 29 | 34 |

***Assilina sublaminosa* Gill (1953)** Material: 12 specimens

**Form-A**

**Equatorial section**

| Whorl | 1 | 2 | 3 | 4 | 5 |
|---|---|---|---|---|---|
| Radius (mm) | 0.23 | 0.58 | 0.87 | 1.32 | 1.78 |
| Chambers | 5 | 11 | 18 | 25 | 28 |

***Assilina exponense* Sowerby (1840)** Material: 25 specimens

**Form-B**

**Equatorial section**

| Whorl | 1 | 2 | 3 | 4 | 5 | 6 |
|---|---|---|---|---|---|---|
| Radius (mm) | 0.1 | 0.8 | 0.47 | 0.66 | 1.08 | 1.33 |
| Chambers | 4 | 12 | 17 | 20 | 22 | 24 |

| Whorl | 7 | 8 | 9 | 10 | 11 | 12 |
|---|---|---|---|---|---|---|
| Radius (mm) | 1.63 | 1.83 | 2.47 | 3.39 | 4.36 | 5.07 |
| Chambers | 29 | 31 | 36 | 48 | 52 | 62 |

**Table 3.2** (continued)

***Assilina mammilata* d, Archaic & Haime** Material: 15 specimens

**Form-A**

**Equatorial section**

| Whorl | 1 | 2 | 3 | 4 | 5 | 6 |
|---|---|---|---|---|---|---|
| Radius | 0.96 | 1.60 | 2.14 | 2.94 | 3.90 | 4.30 |
| Chambers | 9 | 20 | 26 | 35 | 32 | 43 |

***Assilina cancellata* (Nuttal 1926)** Material: 10 specimens

**Axial section**

| Whorl | 1 | 2 | 3 | 4 | 5 |
|---|---|---|---|---|---|
| Radius (mm) | 0.43 | 0.99 | 1.42 | 1.89 | 2.4 |

***Assilina subcancellata* (Nuttal 1926)** Material: 25 specimens

**Form-A**

**Axial section**

| Whorl | 1 | 2 | 3 | 4 | 5 |
|---|---|---|---|---|---|
| Radius (mm) | 0.24 | 0.51 | 1.05 | 1.52 | 2.1 |

**Table 3.2** (continued)

Initial two whorls are compact, then gradually opening in third and fourth whorl, and again become compact in fifth and sixth whorls. Chambers are isometric to subrectangular, widely spaced, higher than long. Concentrated granules are present throughout the spire. Straight septa are swept back in last few whorls. The marginal cord thickness is variable, 1/3-2/3$^{rd}$ of the chamber height (plate 8; figure 2). In axial section the spiral sheet extended up to 1/3$^{rd}$ of the preceding whorl at the outer margin and does not envelop the inner whorl (plate 8, figure 4).

**Remarks:** this is the microspheric Form-B of *Assilina subpappilata* Nuttal.

### *Assilina subpappilata* Nuttal

Plate 8, figures 1&3, figure 3.7D

#### Form-A

Test is flattened lenticular, with a rounded periphery. Average diameter is 4mm. Regularly opening spire (figure 3.7 D), proloculus size is 0.45-0.75 mm in diameter, septa are widely spaced, mostly straight occasionally curved back in third whorl, chambers are mostly rectangular, higher than long, marginal cord is non uniform and thickness equals 1/4$^{th}$ -2/4$^{th}$ of the chamber height (Plate 8; figure1). In axial section the large proloculus is seen in the centre, while a thick spiral sheet extends up to 2/3$^{rd}$ of the preceding whorl in the middle or near the inner margin and does not completely envelop the inner whorl (Plate 8, figure 3).

**Remarks:** this is the magalospheric Form-A of *Assilina pappilata* Nuttal.

### *Assilina davisie* de Cizancourt

Plate 7, figures 4 and 10, figure 3.7E

#### Form-B

#### Diagnosis

Spire is compact and gradually opening (figure 3.7 E); Septa are straight in the early whorls becoming curved forwards in later whorls. Broad chambers have a rounded margin that are sparsely granulated (plate 7; figure 10). In axial section a clear polar depression is visible due to pinching of the spiral sheet which does not completely envelop the inner whorls and forms a "Bow Tie" structure which is a diagnostic character of this species (plate 7; figure 4).

**Remarks:** this is the microspheric Form B of *Assilina subdavisie* de Cizancourt.

### *Assilina subdavisie* de Cizancourt

Plate 7, figures 6, 7 and 13, figure 3.7F

**Form A**

**Diagnosis**

A much smaller megalospheric form of *Assilina davisie* de Cizancourt has a stout test, heavily granulated with polar depression. Spire is regular and loosely coiled; having 3-4 whorls (figure 3.7 F). Septa are straight in the early part becoming curved forwards in later part; rectangular chambers in early whorls become broad in later whorls (plate 7, figure 13). Average diameter of the test is about 2.3 mm. In the axial section it shows absence of spiral sheets at the poles (plate 7; figure 6).

**Remarks:** this is the megalospheric Form-A of *Assilina davisie* de Cizancourt.

### *Assilina spinosa* Davies

Plate 7, figures 9 & 14, figure 3.8 A

**Form-B**

**Diagnosis**

This is a smaller, stouter, heavily granulated, more tightly coiled form than the typical *Assilina granulosa*. It has a regularly opening spire (figure 3.8 A ), large proloculus, septa curved back throughout the spire, chambers rectangular, higher than long, marginal cord is thick and uniform,1/4$^{th}$ of the chamber height (plate 7; figure 14). In axial section a spiral sheet is totally enveloping the earlier whorls but never completely enveloping the later whorls. Thickness to diameter (T/D) ratio ranges from 1:6 to 1: 10 but averages 1: 5. The adult diameter is usually 5-7 mm.

**Remarks:** this is the microspheric Form B of *Assilina subspinosa* Davies.

### *Assilina subspinosa* Davies

Plate 7, figures 8,11-12, figure 3.8 B

**Form-A**

**Diagnosis**

The test is highly ornamented and heavily granulated in the centre. Granules stand out as spines. Protoconch is double and unequal; chambers are higher than long.

septa are like those in *Assilina spinosa.*

**Remarks:** It is the megalospheric Form-A of *Assilina spinosa* Davies.

### *Assilina pustulosa* Doncieux

Plate 8, figures 5-7, figure 3.8 C

#### Form-B

#### Diagnosis

The microspheric test is stout, flat-lenticular, evolute with a bulging polar region, evenly distributed granules and tight spire (figure 3.8C). Broad rectangular-subrectangular chambers are separated by straight to curved back septa. Chambers are higher than long. In axial section the spiral sheets don't completely envelop the inner whorls and form a central depression in the form of a Bow-Tie shape (plate 8, figure 6 and 7)

**Remarks:** the morphological features are similar in Form B and Form A but the later one is smaller in size.

### *Assilina sutri* Schaub

Plate 9; figure 3-4, figure 3.8 E

#### Form-A

#### Diagnosis

Spire is regularly opening (figure 3.8 E), proloculus size is 0.13mm, septa straight to inclined, occasionally curved back in last few whorls, chambers rectangular to isometric; higher than long. The marginal cord is uniform, $1/4^{th}$ of the chamber height in thickness (plate 9; figure 4). In axial section the spiral sheet of the outermost whorls is very thin at the pole (plate 9; figure 3).

### *Assilina laminosa* Gill

Plate 8, figure 10; Plate 9, figure 1, figure 3.9 A

#### Form-A

#### Diagnosis

Test is inflated, lenticular, involute with sharp periphery. In equatorial section a rapidly opening spire is seen (figure 3.9 A). Chambers are isometric and separated

by closely spaced straight septa. In axial section the spiral sheet of each whorl completely envelops the preceeding whorls. Non-granulated, smooth, numerous pillars structures are common at the poles. A narrow tapering of spiral sheet at the margins, resembling an arrow head shape, is common (plate 8; figure 10).

**Remarks:** this is the microspheric Form–B of *Assilina sublaminosa* Gill.

### *Assilina sublaminosa* Gill

Plate 8, figure 11-12; Plate 9; figure 2, figure 3.9 B

#### Form-A

#### Diagnosis

Test is smooth. In equatorial section a regularly opening spire is seen (figure 3.9 B). A single large proloculus is found in most of the studied specimens (plate 8, figure 12), having an average size of 0.23 mm. Septa are straight in early two whorls becoming inclined in last whorls, sometime curved back, chambers mostly rectangular but some have an isometric shape. Chambers in first two whorls are longer than high, but in later whorls they are higher than long. The marginal cord is thin and uniform, 1/5 of the chamber height in thickness; scattered granules are present throughout the spire (Plate 9, figure 1). In axial section the spiral sheet doesn't envelop the outermost quarter of the preceding whorls. Concentrated polar pillars are also present (plate 8, figure 11-12).

**Remarks:** this is the megalospheric Form-A of *Assilina laminosa* Gill.

### *Assilina exponense* Sowerby

Plate 10; figures 5; text figure 3.9C

#### Form-B

#### Diagnosis

Test flattened lenticular, often with a slight central depression. Spire and septa often visible in relief on the surface of the test. The polar region is markedly pillared. Ornament consists mainly of septal ridges but these are occasionally

replaced by a series of granules (plate 10, figure 5). Granules are also common towards the centre of the chambers. The spire is regular, but compact with some irregularities due to doubling in the middle to outer whorls (figure 3.9 C); chambers are rectangular, higher than long, occasionally isometric,; septa are thin, straight, slightly inclined, gently arcuate towards periphery.

**Remarks:** this is microspheric Form-B of *Assilina mammilata* d, Archaic & Haime.

### *Assilina mamillata* d, Archaic & Haime

Plate 10, figure 6, figure 3.9 D

#### Form-A

#### Diagnosis

The test is evolute, lenticular to flattened lenticular, with a slightly swollen polar region, often with a small polar depression. Ornaments are similar to form-B. The spire is fairly regular (figure 3.9 D). In axial section the granules are distributed throughout the test and scattered buried pillars are commonly present (plate 10; figure 6).

**Remarks:** This is considered as megalospheric Form-A of *Assilina exponense* Sowerby.

### *Assilina cancellata* Nuttal

Plate 10, figures 3-4, figure 3.8 E

#### Form- B

#### Diagnosis

Test is flat, lenticular, with a sharp periphery. It has a large size with an average diameter of 30mm; thickness varies from 3 to 5mm, non ornamented smooth exterior surface. Septa are straight in shape. Chambers are longer than high. In axial section the spiral sheet opens gradually (figure 3.8 E, plate 10, figures 3-4). Proloculus size is 0.19mm. Marginal cord is uniformly thick and granules are present in the centre.

### *Assilina subcancellata* Nuttal

Plate 10, figures 1-2, figure 3.9 F

#### Form-A

#### Diagnosis

The spire is initially tight but later whorls become loosely coiled (figure 3.9 F). Chambers are rectangular, higher than long, separated by straight to gently inclined septa in later whorls (plate 10, figure 1). The axial section shows the same morphological features as that of Form-B but it is smaller in size (plate 10, figure 2).

**Remarks:** this is considered to be the megalospheric Form-A of *Assilina cancellata* Nuttal. Mostly the axial sections were studied and chambers are not recorded.

## 3.6 Quantitative basis of nummulitid taxonomy

In this study we found that different *Nummulites* and *Assilina* species show variability in the opening of the spire and the number and radius of successive whorls For all traditionally (see taxonomy) identified species the number and radius of each whorl, and number of septa are recorded, and graphs (coiling diagrams, figures 3.4-3.11) have been drawn to show the rate of opening of the spire in each species. The procedure for measurement of the radius in each whorl is adopted after Gill (1953), Samanta (1968), Racey (1995) and Renema (2002), see also figure 3.3. The number of specimens of each species described here is given in the explanation of Plates.

These graphs provide an additional basis for species level differentiation, and are particularly helpful in cases where taxa of *Nummulites* and associated genera, are morphologically similar. This is highlighted in the following paragraphs, where various morphologicaly closely taxa can be quantitatively discriminated based on the nature of coiling.

The species of *Nummulites pinfoldi*, *Nummulites globulus* and *Nummulites atacicus* are morphologically very similar, but they show diagnostic difference in the opening of spire and number of septa. *Nummulites pinfoldi* has a regularly opening spire (figure 3.4 A) with straight to slightly twisted septa and has a thin to thick

opening of spire and number of septa. *Nummulites pinfoldi* has a regularly opening spire (figure 3.4 A) with straight to slightly twisted septa and has a thin to thick marginal cord, while in *Nummulites globulus* the spire is tight and compact in the early five whorls and shows regularly opening in later whorls (figure 3.4 E), the septa are gently curved in early whorls and these become inclined in later whorls and are sometime curved back towards the periphery. In *Nummulites atacicus* early whorls are tight in the spire, while later ones are loosely coiled (figure 3.4 C), but the chambers are rectangular and higher than long throughout the spire and septa are straight to gently inclined towards the periphery.

Although species of *Nummulites pengaroensis*, *Nummulites acutus* and *Nummulites beaumonti* are similar to each other, some differences are noted here. In *Nummulites beaumonti* the spire is regularly opening but the eighth whorl shows tightness of the spire and a partial tripartite nature can be seen, because later whorls again show regular opening of the spire (figure 3.5 A). The septa are mostly straight but occasionally inclined. *Nummulites pengaroensis* has a tighter spire than *Nummulites beaumonti*, longer than high chambers in the later spire and has a comparatively thin marginal cord (plate 5; figure 2). *Nummulites acutus* has a regularly opening spire which is a little lose in the $6^{th}$ to $10^{th}$ whorls (figure 3.5C). Septa are gently curved in early whorls and curved back in later whorls.

The Form-A of *Nummulites pinfoldi* closely resembles *Nummulites mamilla.* In axial section *Nummulites pinfoldi* has a small megalosphere as compared to *Nummulites mamilla* and alar prolongation shows lateral tapering (plate 1, figure 5) while it is subrounded in *Nummulites mamilla* (plate 2, figure 6). In the equatorial section both have a loosely coiled spire (figure 3.6 A). The Form-A of the *Nummulites pinfoldi* has rectangular and higher than long chambers which are separated by straight to slightly curved septa and the marginal cord is thick throughout the spire (plate 1, figure 4) and in *Nummulites mamilla* the septa are straight to inclined sometimes curved back, chambers are longer than high and rectangular to isometric in shape. In the Form-A of *Nummulites beaumonti* the spire is regularly opening; septa are mostly straight but inclined in early and last whorls (plate 4, figure 5). Species of *Nummulites subatacicus* has a regularly opening spire which is more loosely coiled than in Form-A of *Nummulites beaumonti* and it is

tighter coiled than in Form-A of *Nummulites pinfoldi* (figure 3.6 A). *Nummulites djokdjokartae* is the Form-A of *Nummulites acutus* having a regularly opening spire and shows doubling in the 3rd whorl (plate 3, figure 4-5). It is more loosely coiled than in Form-A of the *Nummulites beaumonti* (figure 3.6 A).

*Nummulites perforatus* is the form-A of *Nummulites obtusus* (plate 5, figure 5). It is differentiated from the closely resembling *Nummulites subatacicus* and *Nummulites djokdjokartae* by its large megalosphere and lose spire (figure 3.6 A).

The *Assilina* species shows great degree of similarities in their surface features but closely resembling species are discriminated here on the basis of the opening of the spire.

The species *Assilina granulosa* has a more loosely coiled spire than *Assilina davisie,* and it is more tightly coiled than in *Asslina putulosa* and *Assilina pappilata. Assilina putulosa* has a more loosely coiled spire than in *Assilina granulosa, Assilina davisie* and *Assilina pappilata* (figure 3.10). Although *Assilina pappilata* and *Assilina putulosa* show similarities in the opening of the spire in early whorls (1st - 4th), later whorls (5th and 6th) of *Assilina putulosa* are more rapidly opening than in *Assilina pappilata* (figure 3.10). The species *Assilina spinosa* has a more rapidly opening spire than in *Assilina dandotica,* and it is tighter than in *Assilina davisie* (figure 3.10).

Species of *Assilina subdavisie* and *Assilina subpappilata* are similar in their early opening of the spire, but later whorls (3rd-5th) in *Assilina subpappilata* are more loosely coiled. The species *Assilina subspinosa* has a more loosely coiled spire in its early whorls (1st-4th) than in *Assilina subpappilata*, and later whorls are more tightly coiled (figure 3.10). The species *Assilina leymerie* shows very rapid opening of the spire. The species of *Assilina subspinosa*, *Assilina subdavisie* and *Assilina subpappilata* have a more tightly coiled spire than in *Assilina leymerie* (figure 3.10)

The species *Assilina laminosa* is morphologically similar to *Assilina sutri* but the coiling graph shows remarkable difference in coiling of the spire. *Assilina laminosa* has a more rapidly opening spire than in *Assilina sutri* (figure 3.8 E and 3.9 A). The species *Assilina cancellata* and *Assilina laminosa* share a similar pattern in opening of the spire in their earlier whorls (1st and 2nd) but later whorls (3rd-5th) are more loosely coiled in *Assilina laminosa* (figure 3.11).

The species of *Assilina exponense* is more tightly coiled in its earlier whorls ($1^{st}$- $5^{th}$) than in *Assilina laminosa* and *Assilina cancellata,* and later whorls show gradual opening of the spire (figure 3.11).The species of *Assilina subcancellata* and *Assilina sublaminosa* share the same pattern of opening of the spire in their early whorls ($1^{st}$-$3^{rd}$), but later whorls of *Assilina subcancellata* are more tightly coiled. The species of *Assilina mammilata* has a more loosely coiled spire than in *Assilina subcancellata* and *Assilina sublaminosa* (figure 3.11).

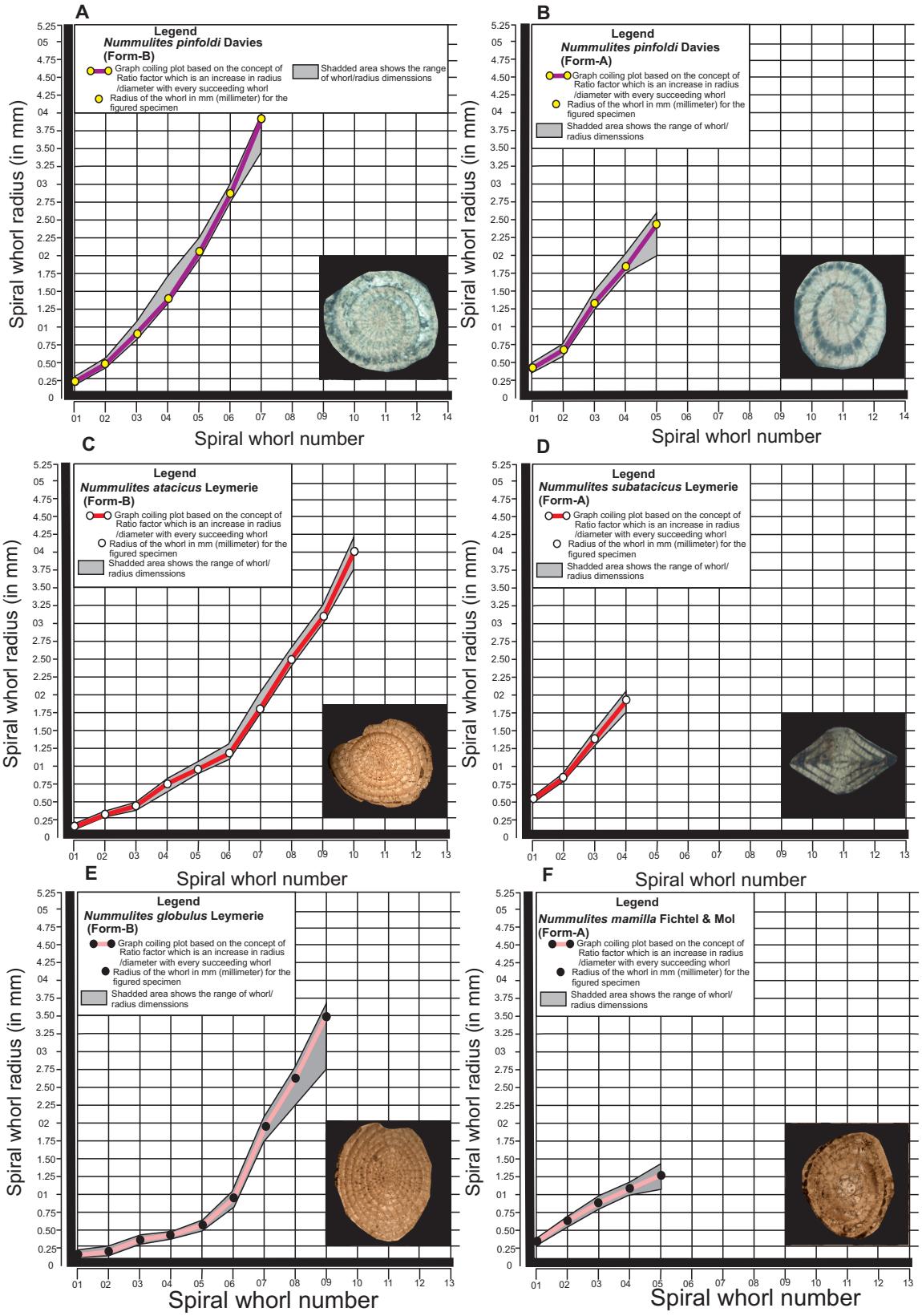


**Figure 3.4.** Graph coiling plot (A-F) shows variation in opening of spire in microspheric (Form B) and megalospheric (Form A) in different species of *Nummulites*. The representatative specimen of each species is figured in these plots.

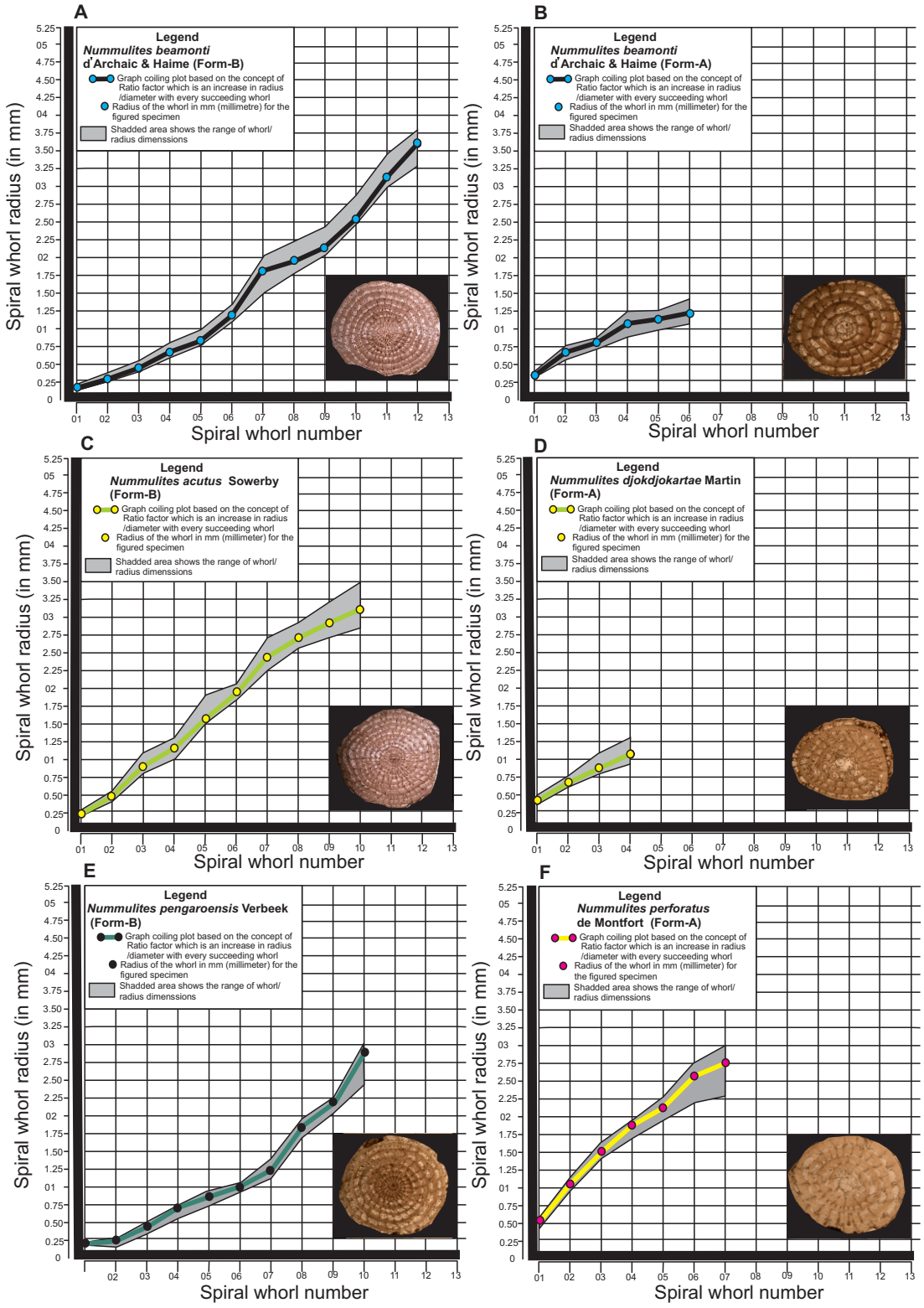


**Figure 3.5.** Graph coiling plot (A-F) shows variation in opening of spire in microspheric (Form B) and megalospheric (Form A) in different species of *Nummulites*.

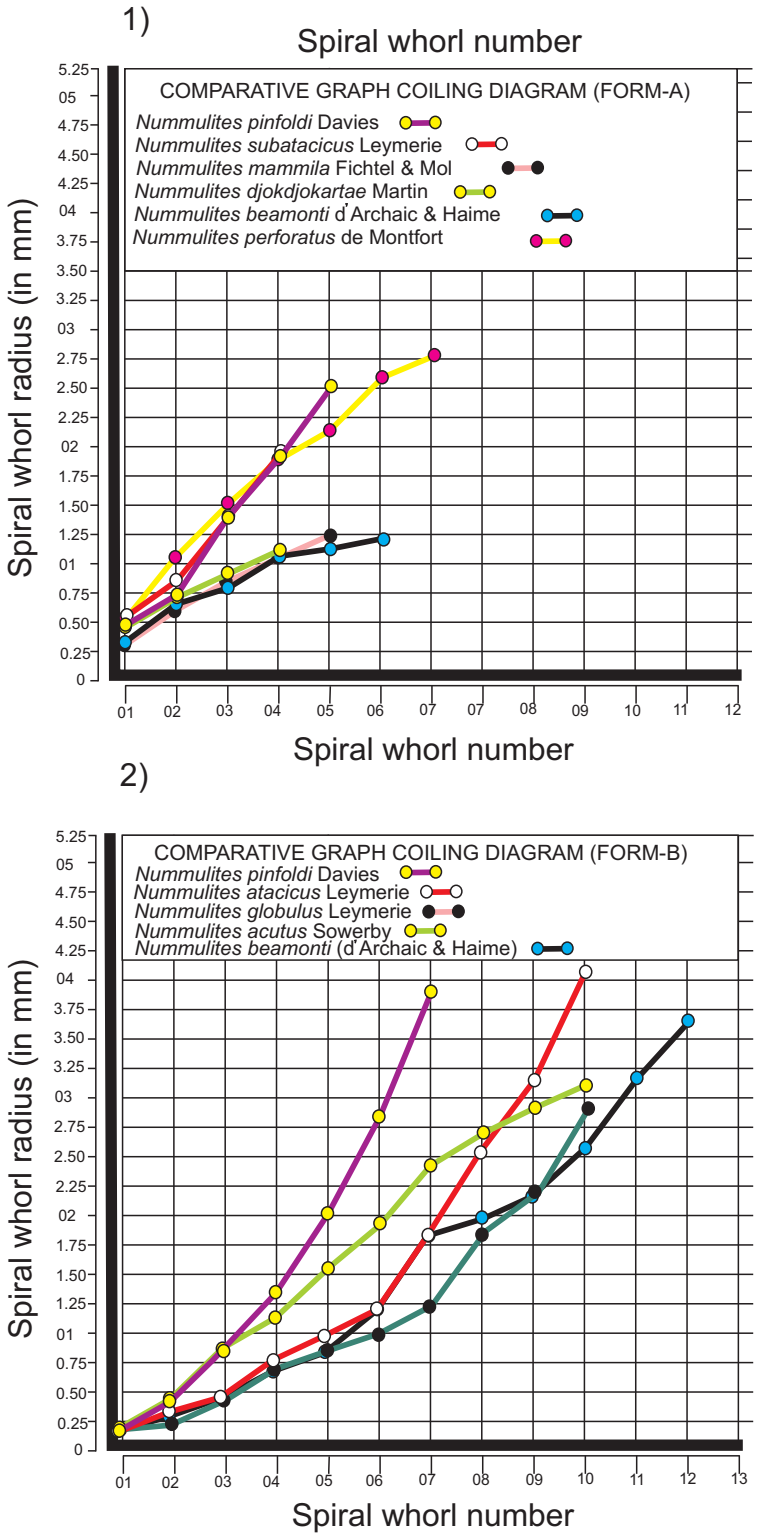


**Figure 3.6.** Comparative graph coiling plot showing variation in rate of opening of the spire 1) i megalospheric (Form A) and 2) Form B of various species of *Nummulites* (see also Table 3.1 f specimens details).

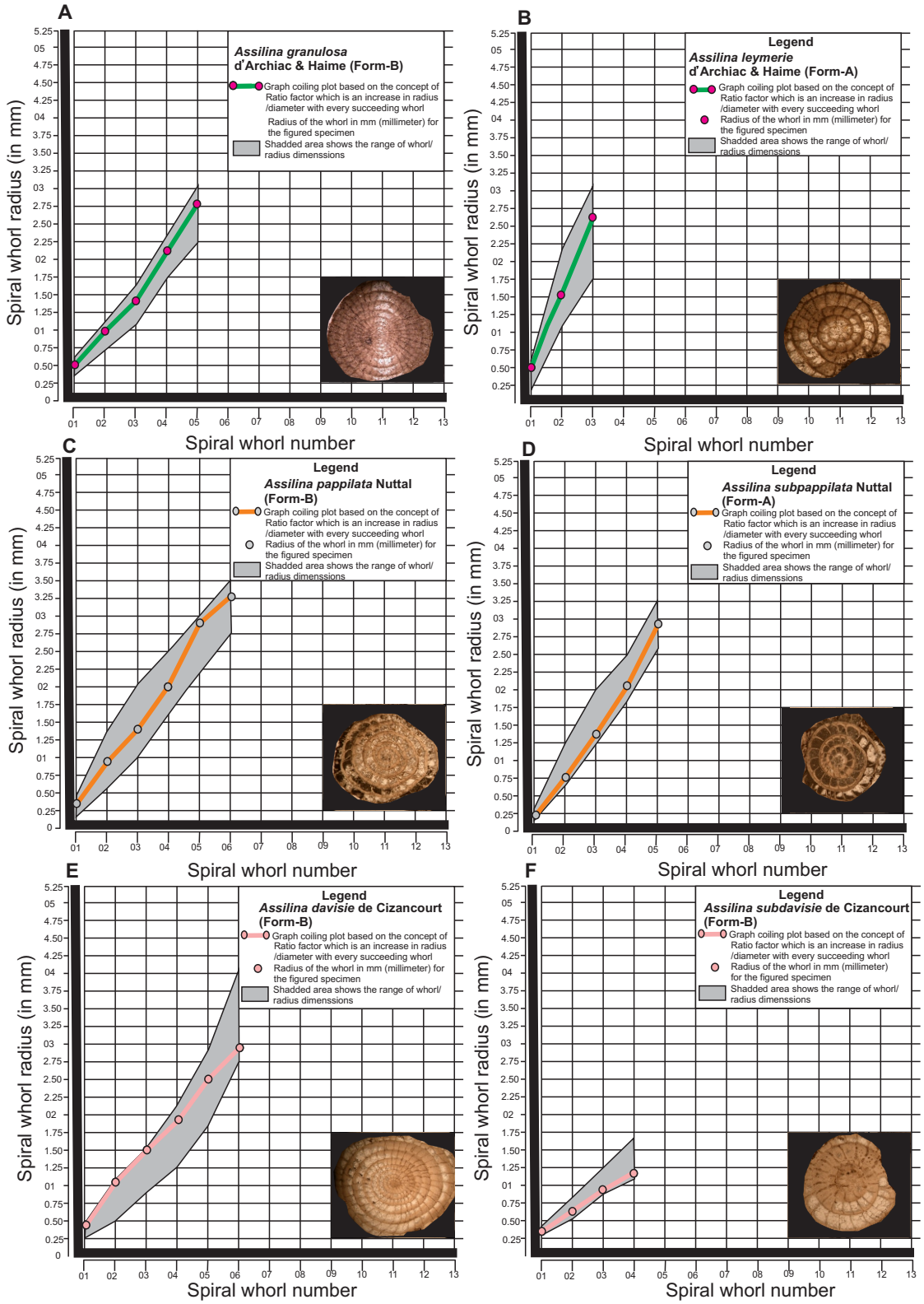


**Figure 3.7.** Graph coiling plot (A-F) shows variation in opening of spire in microspheric (Form B) and megalospheric (Form A) in the figured specimens of *Assilina* species.

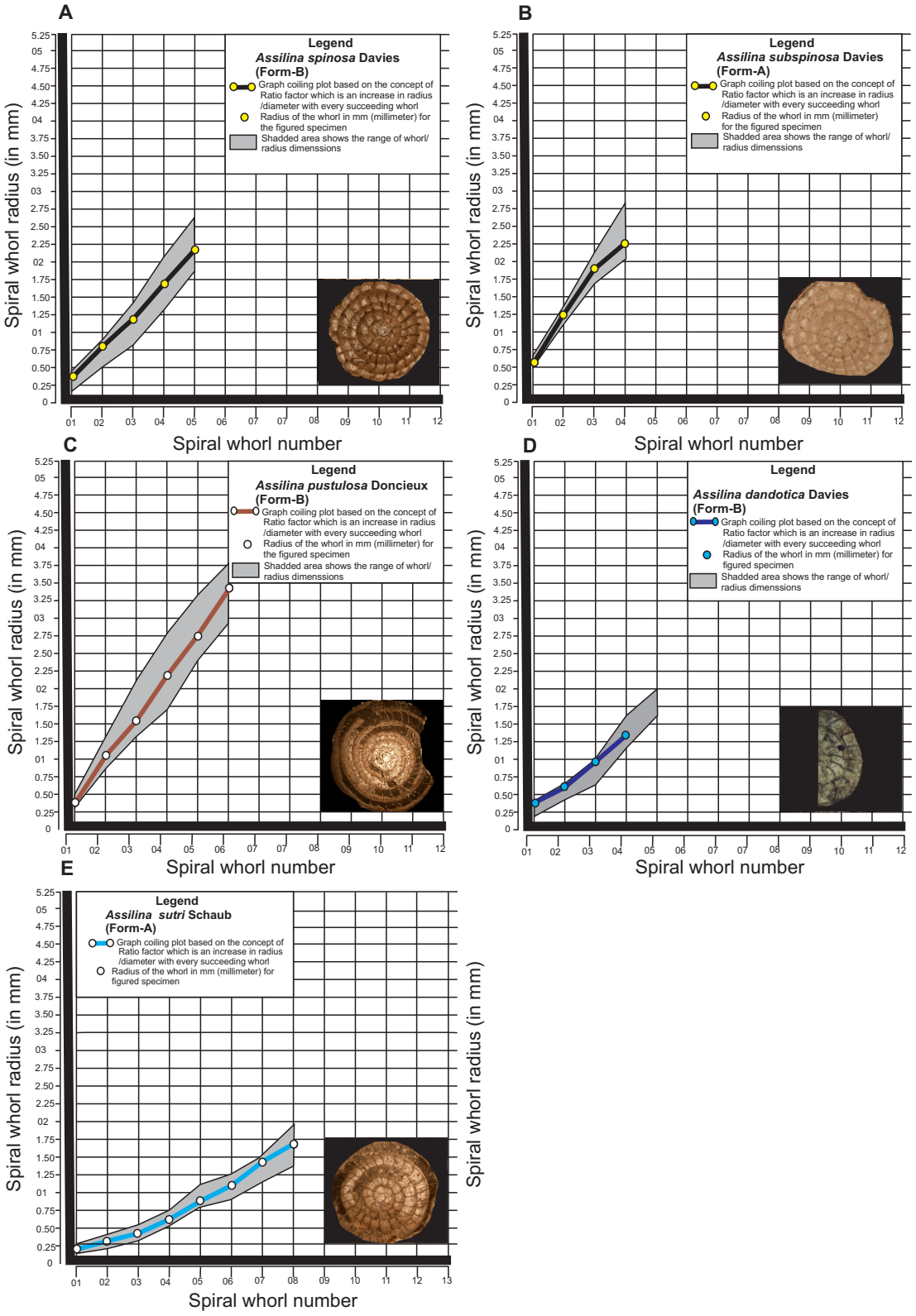


**Figure 3.8.** Graph coiling plot (A-F) shows variation in opening of spire in microspheric (Form B) and megalospheric (Form A) in the figured specimens of *Assilina* species.

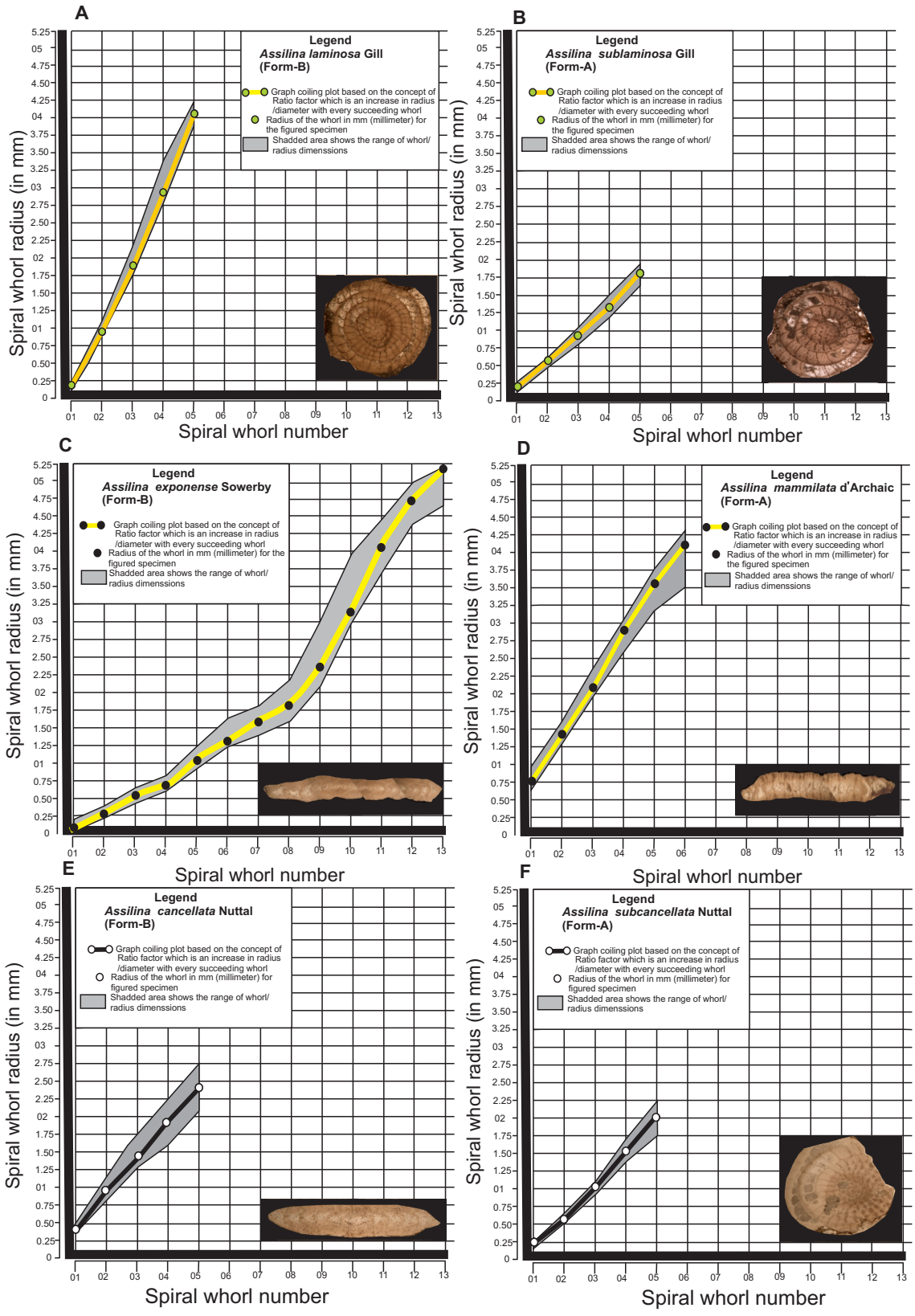


**Figure 3.9.** Graph coiling plot (A-F) shows variation in opening of spire in microspheric (Form-B) and megalospheric (Form-A) in figured specimens of *Assilina* species.

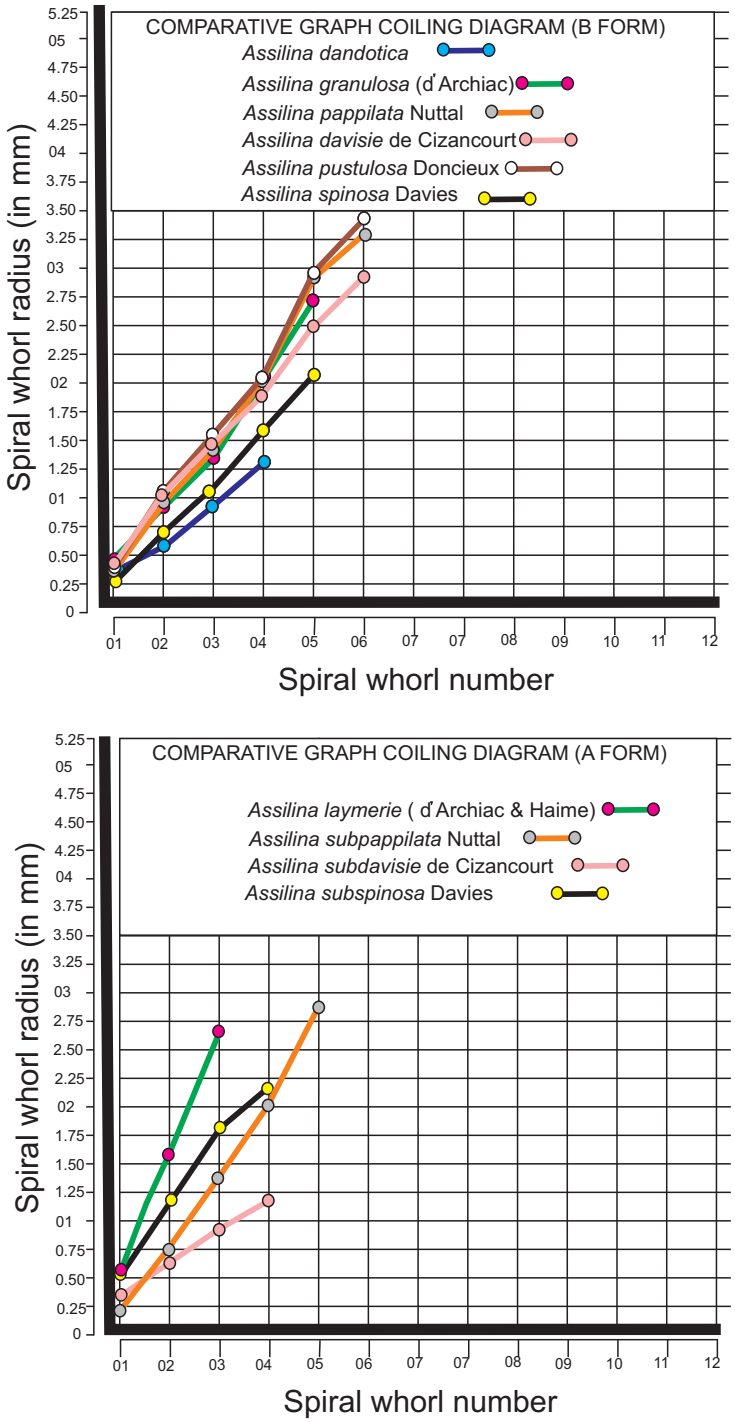


**Figure 3.10.** Comparative graph coiling plot showing variation in rate of opening of the spire in microspheric (Form-B) and megalospheric (Form-A) of different species of *Assilina* (see also Table 3.2 for specimen details).

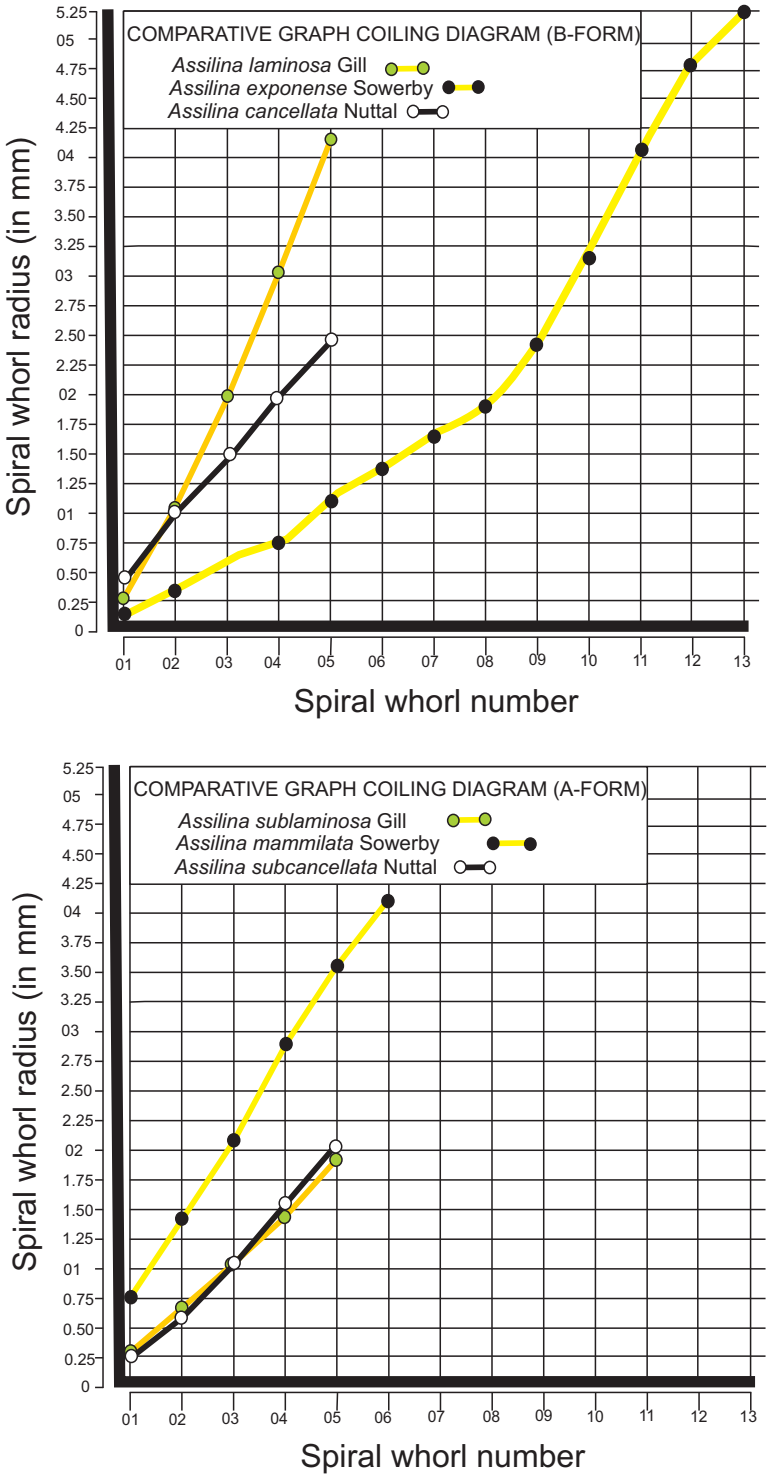


**Figure 3.11.** Comparative graph coiling plot showing variation in rate of opening of the spire in microspheric (Form-B) and megalospheric (Form-A) of different species of *Assilina* (see also Table 3.2 for specimen details).

## 3.7 Smaller benthic foraminifera

In present study for the first time a total of forty four smaller benthic foraminiferal species are recorded from the Early Eocene Panoba and Nammal Formations in the study area. These species belongs to two suborders, 20 super families, 25 families, 13 subfamilies and 27 different genera. Among these foraminifera 27 species are agglutinated and 17 are non agglutinated (Calcareous). Diagnostic morphological features that provide basis for a systematic palaeontology are described first. It is followed by diagnostic morphological features. The description of individual species annotated with the original author name and short references to accessible and quality plates are given in appendix 2. In the remarks brief notes are given on differences between closely resembling species, problematic taxa. The distribution of each species in the study area is also described.

### 3.7.1 Morphology of smaller benthic foraminifera

The smaller benthic foraminiferal species are largely distinguished on the basis of chambers shape and qualitative differences in number and volume while genera are distinguished on the basis of differences in chamber arrangements, aperture position and tooth structure. Wall structure and microstructure were the most important characters for the recognition of suborders. Apertural characters were considered next and chamber arrangement came third (Haynes, 1981).

Classification at supergeneric level is based upon wall structure, form of aperture (figure 3.12) and chamber arrangement taken together with stratigraphic range and evidence of ontogeny (Haynes, 1981).

#### *Wall composition*

Wall compositions are important in recognising species. These include 1) Organic or Chitinous (membranous) i.e. Allogromiina, Lagynacea 2) Agglutinated (test is made up of sand size grains, of sponge spicule, mica flakes or other tests. Grains are commonly cemented by ferruginous cement) 3) Calcareous, which is further subdivided into three groups a) microgranular, calcareous (Fusuliniina, Fusulinacea, and Parathuramminacea) b) porcellaneous calcite (imperforate, high Mg-Calcite i.e. Milliolina, Milliolacea) c) Hyaline perforate (Rotaliina, Rotaliacea). Few exceptions are seen as in the case of the Suborder Spirillinina (single crystal of

calcite), the Suborder Silicoloculinina (test composed of silica) Suborder Involutina and Suborder Carterina (composed of aragonite) 4) Siliceous (truly siliceous tests are only developed in few groups i.e. family Silicinidae from late Jurassic to present oceans (Haynes, 1981)

### *Aperture*

The aperture is the most important part of the test from the standpoint of relationships and descriptive work. It is the main opening of the test from where protoplasm flows out. Various types of the aperture are shown in the figure 3.12.

### *Chambers*

The foraminiferal test has chambers separated by horizontal partitions called as septa and these chambers are connected with each other through small openings called as the "foramina" (the name foraminifera is derived after these openings), Most species of foraminifera build shells with multiple chambers (multilocular) but some species build shells with only a single chamber (unilocular). The most common types of chamber arrangements are explained as following 1) Unilocular; single chamber is present. 2) Uniserial; chambers are arranged in single row. 3) Biserial; chambers are arranged in two rows 4) Triserial; chambers are arranged in three rows. Uni-bi serial, uni-bi-tri serial, bi- tri serial chamber arrangements are also found. 5) Planispiral- biserial; early chambers added in a coil within a single plane while later chambers are arranged in two rows 6) Milioline; chambers arranged in a series where each chamber extends the length of the test, and each successive chamber is placed at an angle of up to 180 degrees from the previous one. 7) Planispiral evolute; planispiral coiling in which chambers in all whorls are visible. 8) Planispiral involute; planispiral coiling in which the last whorl embraces the inner whorl and only the chambers of the last whorl are visible. 9) Streptospiral; where each chamber is half a whorl. 10) Trochospiral; chambers added in a spiral whorl that forms a trochoid shape. The side on which all chambers are visible (evolute) is called the spiral side. On the other side only the final coil is visible (involute) and this is called the umbilical side. 11) Fusuline; a planispiral coil which is elongated along the axis of coiling. Typically each chamber is subdivided by a complex set of internal partitions.

12) Tubular; a simple hollow tube. 13) Arborescent; an erect, branching series of tubes. These forms may live attached to a solid surface or "rooted" in sediment. 14) Irregular; without any definite arrangement of the chambers.

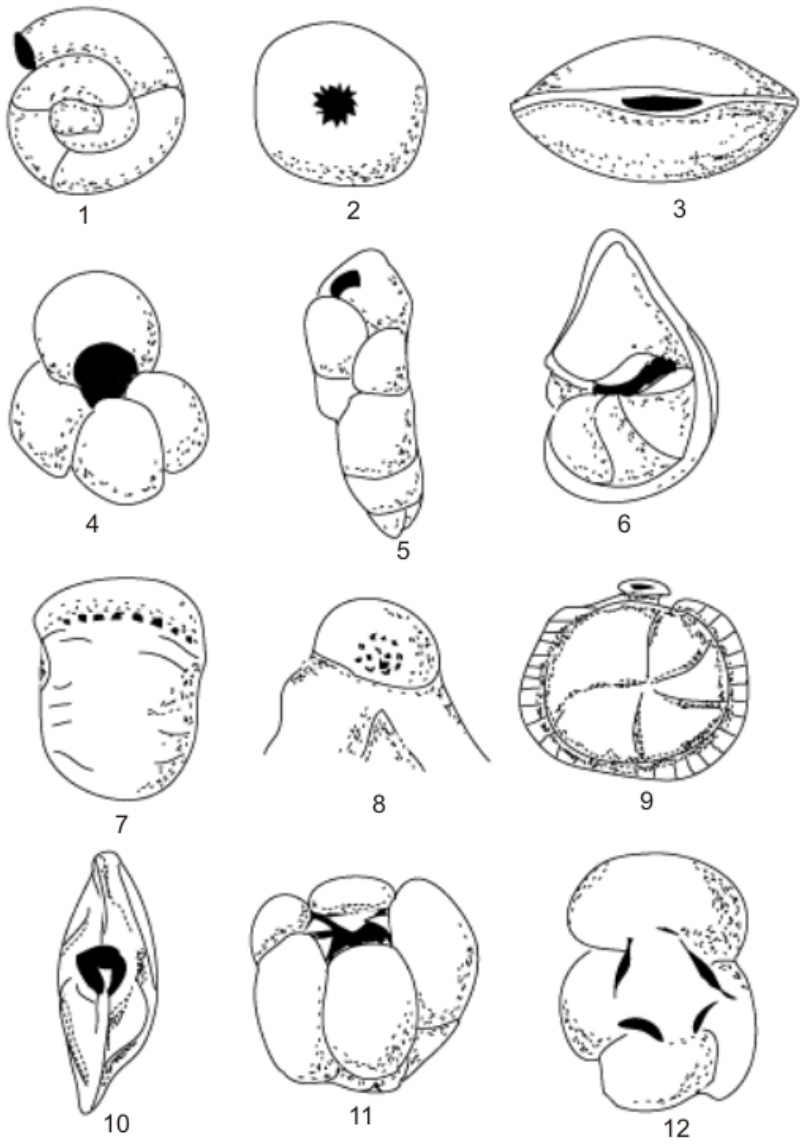


**Figure 3.12.** Various types of Aperture 1) open end of tube 2) terminal radiate 3) terminal slit 4) umbilical 5) loop shaped 6) interiomarginal 7) intereomarginal multiple 8) areal 9) with phialine lip 10) with bifid tooth11) with umbilical teeth 12) with umbilical bulla (Redrawn after Loeblich and Tappan 1964).

## 3.8 Systematic paleontology of smaller benthic foraminifera

The synonymy list of the following species is given in appendix 2.

### *Textularia dibollensis var humblei* Cushman & Applin

**Plate11, figure 1**

**Diagnosis:** The test is small, first few chambers are very narrow forming a pointed end, distinct suture in last three chambers. Chambers increase in height, last chamber is rounded.

**Distribution:** it is recorded from the Early Eocene Panoba Formation exposed in the Sheikhan Nala Section, north-eastern Kohat Basin.

### *Textularia hannai* Davies

**Plate 11, figure 2**

**Diagnosis:** The test is short, rounded periphery, numerous chambers that gradually increase in size, depressed suture, and elongate aperture at the inner margin of the last formed globose chamber.

**Distribution:** it is recorded from the Early Eocene Panoba Formation exposed in the Sheikhan Nala Section, north-eastern Kohat Basin.

### *Textularia cuyleri* Davies

**Plate 11, figure 3**

**Diagnosis:** The test is short, non-smooth, subacute periphery, depressed sutures in last two chambers, broad aperture at the inner margin of last formed subrounded chamber.

**Distribution:** this species is recorded from the Early Eocene Panoba Formation exposed in the Sheikhan Nala Section, north-eastern Kohat Basin

### *Textularia martini* pijpers

**Plate 11, figure 4**

**Diagnosis:** The test is short, furrowed periphery, chambers biserialy arranged; last two chambers are subrounded with distinct depressed sutures arranged at right angles to the periphery of the test, elongate aperture.

**Distribution:** it is recorded from the Early Eocene Panoba Formation exposed in the Sheikhan and Panoba Nala Sections, north-eastern Kohat Basin.

### *Textularia gertrudeana* Davies
### Plate 11, figure 5

**Diagnosis:** The test is elongate, biserially arranged chambers, initial chamber forming pointed apex, last four chambers with distinct depressed sutures forming a zigzag pattern, last two chambers shows abrupt increase in size and change from rectangular to subrounded shape. The aperture is a rounded opening at the margin of the second last chamber.

**Distribution:** This species is recorded from the Early Eocene Panoba Formation exposed in the Sheikhan, Panoab and the Tarkhobi Nala Sections, north-eastern Kohat Basin.

### *Textularia grahamensis* Cushman and Waters
### Plate 11, figure 6

**Diagnosis:** The test is free, agglutinated, typically compressed, zigzag biserial chamber arrangements in the later part, globose periphery, distinct depressed sutures, aperture occurs at the base of the last formed chamber.

**Distribution:** it is recorded from the Early Eocene Panoba Formation exposed in the Sheikhan Nala Section, north-eastern Kohat Basin.

### *Textularia barretti* Jones and Parker
### Plate 11, figure 7

**Diagnosis:** The test is short, agglutinated, triangular at the proximal end and subovoid at the distal end, sharp periphery. Chambers are biserially arranged with gradual increase in size; last chamber shows the greatest width, suture depressed, aperture aerial at the inner margin of last formed chamber.

**Distribution:** it is recorded from the Early Eocene Panoba Formation exposed in the Sheikhan Nala Section, north-eastern Kohat Basin.

### *Textularia losangica* Loeblich & Tappan
### Plate 11, figure 8

**Diagnosis:** The test is small; chambers gradually increase in size, indistinct suture except in last two chambers, subspinose periphery. The aperture occurs at the inner basal margin of last formed chamber**.**

**Distribution:** this species is recorded from the Early Eocene Panoba Formation exposed in the Sheikhan and Panoba Nala Sections, north-eastern Kohat Basin.

### *Bulbobaculites lueckei* Cushman & Renz
### Plate 11; figure 9

**Diagnosis:** The test is small, elongate, agglutinated. Early chambers streptospiraly coiled, later chambers are uncoiled and rectilinear, sutures distinct, depressed and horizontal; wall agglutinated, smoothly finished, interior simple; aperture terminal, a single small rounded opening.

**Distribution:** this species is recorded from the Early Eocene Panoba Formation exposed in the Sheikhan and Panoba Nala Sections, north-eastern Kohat Basin.

### *Conotrochammina cf. dispersa* Finaly
### Plate 11, figure 10

**Diagnosis:** The test is trochoid with raised bosses around umbilicus and last whorl, and the aperture is a small opening at the inner margin of last formed chamber, wall arenaceous with coarse sand grains.

**Distribution:** this species is recorded from the Early Eocene Panoba Formation exposed in the Sheikhan and Panoba Nala Sections, north-eastern Kohat Basin.

### *Bathysiphon eocenicus* Cushman & Hanna
### Plate 11, figure 11

**Diagnosis:** The test is free, straight, wall made up of amorphous sandy material, aperture at the end of the tube.

**Distribution:** this species is recorded from the Early Eocene Panoba Formation exposed in the Sheikhan and Panoba Nala Sections, north-eastern Kohat Basin.

### *Bathysiphon robustus* Grzybowski
### Plate 11, figure 12

**Diagnosis:** The test is a straight unbranched elongate tube, open at both ends, nonseptate but may have slight annular constrictions resulting from periodic growth; wall agglutinated, thick, the aperture occurs at the open end of the tube.

**Distribution:** this species is recorded from the Early Eocene Panoba Formation exposed in the Sheikhan and Panoba Nala Sections, north-eastern Kohat Basin.

### *Arenobulimina truncata* Reuss
### Plate 12, figure 1

**Diagnosis:** Test trochospirally enrolled, agglutinated, four chambers per whorl and sutures are hardly depressed making an acute angle with axis of coiling.

**Distribution:** this species is recorded from the early Eocene Panoba Formation exposed in the Sheikhan, Panoba and Tarkhobi Nala Sections, north-eastern Kohat Basin.

### *Gaudryina tazaensis* Carbonnier
### Plate 12, figure 2

**Diagnosis:** The test is free, elongate, early stage triserial and triangular in section, later becoming biserial and triangular to rounded in section; wall agglutinated, solid, and aperture like ,an arch, occurs at the inner margin of the final chamber.

**Distribution:** this species is recorded from the Early Eocene Panoba Formation exposed in the Sheikhan, Panoba and Tarkhobi Nala Sections, north-eastern Kohat Basin.

### *Lituotuba lituiformis* Brady
### Plate 12, figure 3

**Diagnosis:** The test is free, wall is finely agglutinated, early portion irregular to planispirally coiled, and later portion is uncoiled with the tabular irregularly rectilin-ear chamber arrangement. Surface is smoothly finished, aperture, rounded, occurs at the open end of the tubular chamber.

**Distribution:** this species is recorded from the Early Eocene Panoba Formation exposed in the Sheikhan, Panoba and Tarkhobi Nala Sections, north-eastern Kohat Basin.

### *Ammobaculites lacertae* Beckmann
### Plate 12, figure 4

**Diagnosis:**The test is free, early portion is closely coiled, later tending to become uncoiled and rectilinear, rounded in section; wall coarsely agglutinated, interior simple; aperture is terminal.

**Distribution:** this species is recorded from the Early Eocene Panoba Formation exposed in the Sheikhan, Panoba and Tarkhobi Nala Sections, north-eastern Kohat Basin.

### *Haplophragmoides porrectus* Maslakova
### Plate 12, figure 5

**Diagnosis:** The test wall is agglutinated, planispirally coiled, involute, curved back suture, five chambers which generally increase in size except the third chamber which is comparatively smaller than second chamber. Aperture is single, equatorial in position at the base of the second chamber.

**Remarks:** this species is completely involute and has a basal equatorial aperture along the second chamber. In general it closely resembles *Haplophragmoides mjatliukae* Maslakova which is involute to partially evolute, but has its aperture along the basal equatorial third chamber.

**Distribution:** this species is recorded from the Early Eocene Panoba Formation exposed in the Sheikhan and Tarkhobi Nala Sections, north-eastern Kohat Basin.

### *Haplophragmoides concavus* Chapman
### Plate 12, figure 6

**Diagnosis:** The test wall is agglutinated, planispirally coiled, involute to partially evolute, very scant straight suture, six chambers which gradually increase in size, single equatorial aperture at the base of second last chamber.

**Distribution:** this species is recorded from the Early Eocene Panoba Formation exposed in the Sheikhan, Panoba and Tarkhobi Nala Sections, north-eastern Kohat Basin.

### *Haplophragmoides kirki* Wickenden
### Plate 12, figure 7

**Diagnosis:** The test wall is agglutinated, planispirally coiled, involute, curved back suture, six chambers with rounded to subrounded periphery and gradually increasing in size, single equatorial aperture occurs at the margin of innermost chamber in the last coil is present.

**Distribution:** this species is recorded from the Early Eocene Panoba Formation exposed in the Sheikhan, Panoba and Tarkhobi Nala Sections, north-eastern Kohat Basin.

### *Evolutinella renzi* Beckmann
### Plate 12, figure 8

**Diagnosis:** The test is free, planispiral coiled, almost evolute, wall agglutinated, fine grained, aperture equatorial, at the base of the final chamber.

**Distribution:** this species is recorded from the Early Eocene Panoba Formation exposed in the Sheikhan Nala Section, north-eastern Kohat Basin.

### *Dendrophyra excelsa* Grzybowski
### Plate 12, figure 9

**Diagnosis:** The test is free, large central chamber with branching tubules, wall arenaceous, and aperture at the open end of the tube.

**Distribution:** this species is recorded from the Early Eocene Panoba Formation exposed in the Sheikhan, Panoba and Tarkhobi Nala Sections, north-eastern Kohat Basin.

### *Burmudezina cubensis,* Palmer and Bermudez
### Plate 12, figure 10

**Diagnosis:** Test is similar to *Gaudryina levegata* Frank but with a tooth or tube like projection in the terminal position on the last formed chambers, early part triserial, later biserial with globose chambers gradually increasing in size, depressed sutures, circular aperture at the last formed chamber.

**Distribution:** this species is recorded from the Early Eocene Panoba Formation exposed in the Panoba and Tarkhobi Nala Sections, north-eastern Kohat Basin.

### *Recurvoides cf. walteri* Grzybowiski
### Plate 12, figure 11

**Diagnosis:** The test is free, subglobular, streptospirally enrolled, 6-7 chambers in last whorl, later whorls may tend to be trochospiral to planispiral; wall agglutinated, thin, surface roughly finished; aperture small, areal.

**Distribution:** this species is recorded from the Early Eocene Panoba Formation exposed in the Sheikhan, Panoba and Tarkhobi Nala Sections, north-eastern Kohat Basin.

### *Gaudryina leveagata* Frank
### Plate 12, figure 12

**Diagnosis:** The test has a triangular periphery, longer than broad, early stage is triserial later becoming biserial. Early chambers have inclined sutures, while later chambers have distinct depressed, horizontal sutures. Chambers are inflated in the biserial part, gradually increasing in size, chambers change from elongate to globose shape in the biserial part, 3-5 chambers in later part. Test wall arenaceous, aperture at the margin of last formed chamber.

**Distribution:** this species is recorded from the Early Eocene Panoba Formation exposed in the Sheikhan, Panoba and Tarkhobi Nala Sections, north-eastern Kohat Basin.

### *Hyperammina elongata* Brady
### Plate 13, figure 1

**Diagnosis:** The test is free, elongate, undivided chamber, aperture at the open end of the slightly curved tube.

**Distribution:** this species is recorded from the Early Eocene Panoba Formation exposed in the Sheikhan, Panoba and Tarkhobi Nala Sections, north-eastern Kohat Basin.

### *Guadryinella pussilla* Magneiz-Jannin
### Plate 13, figure 2

**Diagnosis:** The test is thin, arenaceous, compressed; chambers and aperture are obscured due to thick arenaceous walls, however the tri-uniserial chamber arrangement is diagnostic, aperture is terminal.

**Distribution:** this species is recorded from the Early Eocene Panoba Formation exposed in the Sheikhan Nala Section, north-eastern Kohat Basin.

### *Gaudryina pyramidata* Cushman
### Plate 13, figure 3

**Diagnosis:** The test is longer than broad. Triangular periphery with one side flat and other side concave making sharp angles, early part with triserial chambers, last chambers tend to become rounded, rough surface, wall arenaceous, aperture at the base of last formed chamber extending towards the middle.

**Distribution:** this species is recorded from the Early Eocene Panoba Formation exposed in the Tarkhobi Nala Section, north-eastern Kohat Basin.

### *Cibicides cf simplex* Brotzen
### Plate 13, figure 4

**Diagnosis**: The test wall is calcareous, perforate, spiral side concave. Eight chambers separated by deeply incised depressed sutures in the final whorl, involute, strongly convex umbilical side, periphery carinate, spiral side coarsely perforate,

a low interiomarginal equatorial opening that extends a short distance on to the umbilical side.

**Remarks:** the test morphology is similar to *Cibicides simplex* but *C. cf simplex* has a rather thinner and small umbilicus.

**Distribution:** this species is recorded from the Early Eocene Panoba Formation exposed in the Sheikhan, Panoba and Tarkhobi Nala Sections, north-eastern Kohat Basin.

### *Cibicides alleni* Plumer
### Plate 13, figure 5

**Diagnosis:** The test is trochoid, unequal biconvex; wall is calcareous, coarsely perforate. Periphery subrounded with rounded keel, slightly lobate in the later part. On the ventral side the prominent umbo boss of clear shell material is present, 8-9 chambers in the last whorl, uniform shape, gradually increasing in size as added. Sutures are distinct somewhat limbate, slightly curved near the periphery, raised in the early five whorls becoming distinctly depressed in the later chambers. Aperture is present as a small opening at the base of the ninth chamber.

**Remarks:** this species is differentiated from *Cibicides mensilla* Schwager *var. nammalensis* in having more elongate chambers in the last whorl, smaller size, a less rounded periphery, small aperture, more depressed sutures and consistent coarse perforation throughout the later six chambers.

**Distribution:** this species is recorded from the Early Eocene Panoba Formation exposed in the Sheikhan, Panoba and Tarkhobi Nala Sections, north-eastern Kohat Basin.

### *Cibicides mensilla* (Schwager) *var. nammalensis*
### Plate 13, figure 6

**Diagnosis:** The test is trochoid, unequally biconvex, calcareous wall, thickly perforate at the margins, rounded keel along the acute periphery, umbilical area covered with secondary shell material. Eight chambers, broad, sutures are slightly raised in early five chambers and become depressed in later three chambers in the last whorl. These sutures are slightly curved, radiate from the umbo boss and extend to the peripheral margin in the later chambers. The aperture is an interiomarginal opening along the last formed chamber.

**Distribution:** this species is recorded from the Early Eocene Panoba Formation exposed in the Sheikhan, Panoba and Tarkhobi Nala Sections, north-eastern Kohat Basin.

### *Cibicicoides tuxpamensis laxispiralis* Beckmann
### Plate 13, figure 7

**Diagnosis**

The test is a low trochospiral coil, wall calcareous, coarsely perforate, ventral side is convex, multichambered (7-9 in last whorl), slightly curved and depressed sutures in last few chambers; the aperture is an interiomarginal equatorial arch that may extend more onto the umbilical side, with narrow bordering lip.

**Distribution:** this species is recorded from the Early Eocene Panoba Formation exposed in the Sheikhan and Tarkhobi Nala Sections, north-eastern Kohat Basin.

### *Cibicidoides tuxpamensis tuxpamensis* Cole
### Plate 13, figure 8

**Diagnosis:** The test is trochoid, small, wall calcareous, partially perforate along the margins of the test, keel bordering the subacute – rounded periphery, 7-8 chambers gradually increasing in size in the last whorl, slightly raised suture in early chambers and becoming depressed in the last two chambers, Aperture is peripheral which extends inward on to the umbilical side with a bordering lip.

**Distribution:** this species is recorded from the Early Eocene Panoba Formation exposed in the Sheikhan, Panoba and Tarkhobi Nala Sections, north-eastern Kohat Basin.

### *Gavelinella dakotensis* Fox
### Plate 13, figure 9

**Diagnosis:** The test wall is calcareous, perforate, low trochospiral, biconvex, flattened at the margins, 5-6 chambers in the last whorls, involute umbilical side. Umbilicus is partially closed, raised sutures; aperture is peripheral at the base of an early interiomarginal chamber.

**Distribution:** this species is recorded from the Early Eocene Panoba Formation exposed in the Sheikhan and Panoba Nala Sections, north-eastern Kohat Basin.

### *Gavelinella aracajuensis* Petri
### Plate 13, figure 10

**Diagnosis:** The test is planoconvex, calcareous wall, trochospiral coiling, 5-6 inflated subrounded chambers in the last whorls, keeled periphery, umbilical side involute and sutures are slightly curved and depressed, the aperture occurs at the top of last formed chamber.

**Distribution:** this species is recorded from the Early Eocene Panoba Formation exposed in the Sheikhan, Nala Section, north-eastern Kohat Basin.

### *Gavelinella schloenbachi* Reuss
### Plate 13, figure 11

**Diagnosis:** The test is small, trochoid, slightly raised sutures separate the chambers, sparsely perforate, periphery is subrounded, Aperture is interiomarginal, and spiral side is evolute.

**Distribution:** this species is recorded from the Early Eocene Panoba Formation exposed in the Sheikhan, Panoba and Tarkhobi Nala Sections, north-eastern Kohat Basin.

### *Stensioeina excolata*
### Plate 13; figure 12

**Diagnosis:** The test is small, spiral side flat and evolute with chambers enlarging gradually, wall calcareous, coarsely perforate, surface with prominent irregular sutural ridges on the spiral side; the aperture is a low interiomarginal opening between the umbilicus and periphery.

**Distribution:** this species is recorded from the Early Eocene Panoba Formation exposed in the Sheikhan and Tarkhobi Nala Sections, north-eastern Kohat Basin.

### *Loxostomum applinae* Plumer
### Plate 14, figure 1

**Diagnosis:** The test is elongate, compressed, sides flat to concave. Margins are truncate and carinate, wall is calcareous, finely perforate, surface smooth to finely costate, chambers are biserially arranged and increasing in relative breadth as added. Later chambers arched over the midline with a tendency to become nearly uniserial, sutures strongly curved and depressed and slit-like terminal aperture.

**Distribution:** This species is recorded from the Early Eocene Panoba Formation exposed in the Sheikhan, Panoba and Tarkhobi Nala Sections, north-eastern Kohat Basin.

### *Valvulineria patalensis*
### Plate 14, figure 2

**Diagnosis:** The test is rounded in outline, trochospirally coiled, wall calcareous, optically radial, finely perforate, umbilical side with depressed umbilicus, 5-6 chambers, enlarging gradually as added, sutures straight to gently curved, thickened, radial and depressed surface smooth; aperture an interiomarginal- umbilical arch.

**Distribution:** this species is recorded from the Early Eocene Panoba Formation exposed in the Sheikhan Nala Section, north-eastern Kohat Basin.

### *Nonionella Jacksonenesis* Cushman var minuta
### Plate 14, figure 3

Diagnosis: The test is longer than broad (about 120 μm length and 70 μm width of the figured specimen), calcareous wall, smooth, perforate, aperture extending from the periphery along the lower edge of the last formed chamber towards the umbilical region. Periphery subrounded to elongate, earlier whorls are visible on dorsal side, 8-9 distinct chambers, increasing in size with growth. The last chamber shows greatest width and covers the umbilical region on the ventral side, sutures distinct, slightly curved back towards the periphery.

**Remarks:** this species is differentiated from the *Nonionella jacksonensis* Cushman in having much smaller size and more rounded periphery.

**Distribution:** this species is recorded from the Early Eocene Panoba Formation exposed in the Sheikhan, Panoba and Tarkhobi Nala Sections, north-eastern Kohat Basin.

### *Praebulimina cf seabeensis* Tappan
### Plate 14, figure 4

**Diagnosis:** The test is trochospirally enrolled. Ovoid chambers are triserially arranged, two chambers in last whorl are large, subrounded, separated by distinct depressed sutures, wall is calcareous, finely perforate, surface smooth, looped aperture occurs at the base of last formed chamber.

**Distribution:** This species is recorded from the Early Eocene Panoba Formation exposed in the Sheikhan and Panoba Nala Sections, north-eastern Kohat Basin.

### *Bulimina stokesi* Cushman and Renz

**Plate 14, figure 5**

**Diagnosis:** The test is elongate, chambers are triserially arranged, thick ornamentation, sutures are distinct, raised; wall is calcareous, perforate, surface rough, marginal aperture.

**Remarks:** This species is distinguished from the somewhat similar *Bulimina midwayensis* by coarser ornamentation and larger size.

**Distribution:** this species is recorded from the Early Eocene Panoba Formation exposed in the Sheikhan, Panoba and Tarkhobi Nala Sections, north-eastern Kohat Basin.

### *Uvigerina gallowayi basicordata* Cushman and Renz

**Plate 14, figure 6**

**Diagnosis:** The test is elongate, wall is calcareous, perforate, triserial, early chambers are narrow, later ones are wide and inflated, sutures distinct and depressed, low angle oblique, longitudinal plan costae on the surface are prominent ornamentations, terminal aperture.

**Distribution:** this species is recorded from the Early Eocene Panoba Formation exposed in the Sheikhan and Tarkhobi Nala Sections, north-eastern Kohat Basin.

### *Uvigerina spinicostata* Cushman & Jarvis

**Plate 14, figure 7**

**Diagnosis:** The test is elongate, triserial, chambers are inflated, and sutures are distinct. depressed, slightly oblique, wall calcareous, perforate. Surface with longitudinal plan costae or striae, aperture terminal.

**Remarks:** it is distinguished from *Uvigerina gallowayi basicordata* by its more elongated test, less inflated chambers, absence of phialine lip around the aperture and relatively fine ornamentation.

**Distribution:** this species is recorded from the Early Eocene Panoba Formation exposed in the Sheikhan, Panoba and Tarkhobi Nala Sections, north-eastern Kohat Basin.

### *Bolivinoides decoratus decoratus* Jones
### Plate 14, figure 8

**Diagnosis:** The test is large, robust, laterally compressed to lenticular in section Chambers are low, increasing rapidly in breadth as added, bi-tri serial witl longitudinal costae. Sutures high angle oblique, obscured by the surface ornamen tation, wall calcareous, finely perforate. Surface with strong tubercles, aperture ai elongate narrow opening with smooth border and short internal tooth-plate at the bas of last formed chamber.

**Distribution:** this species is recorded from the Early Eocene Panoba Formatio exposed in the Sheikhan, Panoba and Tarkhobi Nala Sections, north-eastern Koha Basin.

# EXPLANATION OF PLATES

## LARGER BENTHIC FORAMINIFERA

### Plate 1

#### *Nummulites pinfoldi* Davies

1 & 8: Axial sections 2: Equatorial section of Form-B; 3 & 5: Axial section 4: Equatorial section of Form-A of *Nummulites pinfoldi* Davies recorded from the Chorgali Formation in the Gharibwal Cement Factory Section in the Eastern Salt Range, Potwar Basin.

#### *Nummulites atacicus* Leymerie

7: Axial section of *Nummulites atacicus* Leymerie (Form-B) recorded from the Chorgali Formation in Gharibwal Cement Factory Section in the Eastern Salt Range, Potwar Basin, Pakistan. 6: Axial section 9: Equatorial section of the *Nummulites atacicus* Leymerie (Form-B) recorded from the Sheikhan Formation in the Sheikhan Nala Section, north-eastern Kohat Basin.

### Plate 2

#### *Nummulites atacicus* Leymerie

2: Axial section of *Nummulites atacicus* Leymerie (Form-B) recorded from the Sakessar Formation in the Chichali Nala Section, Trans Indus Ranges.

#### *Nummulites subatacicus* Leymerie

1: Axial section of *Nummulites subatacicus* Leymerie recorded from the Patala Formation in the Ziarrat Thatti Sharif Section, Western Salt Range, Potwar Basin.

#### *Nummulites globulus* Leymerie

3: Axial section of *Nummulites globulus* Leymerie (Form-B) recorded from the Sakessar Formation in the Chichali Nala Section, Trans Indus Ranges, Pakistan. 5: Axial section 7: Equatorial section of *Nummulites globulus* Leymerie (Form-B) recorded from the Kohat Formation in the Sheikhan Nala Section, north-eastern Kohat Basin.

#### *Nummulites mammila* Fichtel and Moll

4: Axial section of *Nummulites mammila* Fichtel and Moll recorded from the Chorgali Formation in the Gharibwal Cement Factory Section, Eastern Salt Range, Potwar Basin, Pakistan. 6: Axial section 8: Equatorial section of *Nummulites mamilla* Fichtel and Moll from the Kohat Formation in the Sheikhan Nala Section, north-eastern Kohat Basin.

**Plate 3**

***Nummulites acutus* Sowerby**

1: Equatorial section 2: Lateral section 3: Axial section (Form-B) of *Nummulites acutus* Sowerby recorded from the Kohat Formation in the Sheikhan Nala Section, north-eastern Kohat Basin.

***Nummulites djokdjokartae* Martin**

4: Equatorial section 5: Axial section of *Nummulites djokdjokartae* Martin recorded from the Kohat Formation in the Sheikhan Nala Section, north-eastern Kohat Basin.

**Plate 4**

***Nummulites beaumonti* d' Archiac & Haime**

1-2 and 4: Axial sections 3: Equatorial section (Form-B) and 5: equatorial section 6: Axial section (Form-A) of *Nummulites beaumonti* d' Archiac & Haime recorded from the Kohat Formation in the Sheikhan Nala Section, north-eastern Kohat Basin.

**Plate 5**

***Nummulites pengaroensis* Verbeek**

1: Axial section 2: Equatorial section (Form-B) of *Nummulites pengaroensis* Verbeek recorded from the Kohat Formation in the Sheikhan Nala Section, north-eastern Kohat Basin.

***Nummulites perforatus* de Montforte**

3: Lateral section 5: Axial section 6: Equatorial section of *Nummulites Perforatus* de Montforte recorded from the Kohat Formation in the Sheikhan Nala Section, north-eastern Kohat Basin.

**Plate 6**

***Assilina dandotica* Davies**

1 and 4: Axial section 3: Equatorial section (Form-B) 2: Axial section (Form-B) of *Assilina dandotica* Davies recorded from the Patala Formation in the Chichali Nala Section, Trans Indus Ranges.

***Assilina granulosa* d' Archiac & Haime**

1, 7 and 8: Axial section 6: Equatorial section (Form-B) of *Assilina granulosa* d' Archiac & Haime recorded from the Sheikhan Formation and Kohat Formation in the Panoba Nala Section, north-eastern Kohat Basin.

***Assilina* Leymerie**

10-12: Axial section 9: Equatorial section of *Assilina* Leymerie recorded from the Nammal Formation in the Chichali Nala Section, Trans Indus Ranges, Pakistan.

## Plate 7

### *Assilina leymerie*

1 and 3: Axial section 2: Equatorial section of the *Assilina leymerie* recorded from the Sakessar Formation in the Nammal Gorge Section, Central Salt Range, Potwar Basin.

### *Assilina davisie* de Cizancourt

4: Axial section 10: Equatorial section (Form-B) of *Assilina davisie* Cizancourt recorded from the Sakessar Formation in the Nammal Gorge Section, Central Salt Range, Potwar Basin.

### *Assilina sub davisie* de Cizancourt

6: Axial section 13: Equatorial section of *Assilina subdavisie* Cizancourt recorded from the Sheikhan Formation in the Panoba Nala Section north-eastern Kohat Basin.

### *Assilina spinosa* Davies

9: Axial section 14: Equatorial section of the *Assilina spinosa* Davies recorded from the Chorgali Formation in the Gharibwal Cement Factory Section in the Eastern Salt Range, Potwar Basin.

### *Assilina subspinosa* Davies

8 and 11: Axial section 12: Equatorial section of the *Assilina subspinosa* Davies recorded the Nammal Formation in the Chichali Nala Section, Trans Indus Ranges.

## Plate 8

### *Assilina pappilata* Nuttal

4: Axial section 2: Equatorial section of the *Assilina Pappilata* Nuttal recorded from the Kohat Formation in the Sheikhan Nala Section, north-eastern Kohat Basin.

### *Assilina subpappilata* Nuttal

3: Axial section 1: Equatorial section of the *Assilina subpappilata* Nuttal recorded from the Kohat Formation in the Sheikhan Nala Section, north-eastern Kohat Basin.

### *Assilina pustulosa* Doncieux

5: Equatorial section 6-7: Axial section (Form-B) 9: Axial section 8: Equatorial section (Form-A) of *Assilina pustulosa* Doncieux recorded from the Chorgali Formation in the Gharibwal Cement Factory Section in the Eastern Salt Range, Potwar Basin.

### *Assilina laminosa* Gill

10: Axial section (Form-B) of *Assilina laminosa* Gill recorded from the Kohat Formation in the Sheikhan Nala Section, north-eastern Kohat Basin.

### *Assilina sublaminosa* Gill

11-12: Axial section of *Assilina laminosa* Gill recorded from the Kohat Formation in the Sheikhan Nala Section, north-eastern Kohat Basin.

## Plate 9

### *Assilina laminosa* Gill

1: Equatorial section (Form-B) of *Assilina laminosa* Gill recorded from the Chorgali Formation in the Gharibwal Cement Factory Section in the Eastern Salt Range, Potwar Basin.

### *Assilina sublaminosa* Gill

2: Equatorial section of *Assilina sublaminosa* Gill recorded from the Chorgali Formation in the Gharibwal Cement Factory Section in the Eastern Salt Range, Potwar Basin.

### *Assilina sutri* Schaub

3: Axial section 4: Equatorial section (Form-A) of *Assilina sutri* Schaub recorded from the Kohat Formation in the Sheikhan Nala Section, north-eastern Kohat Basin.

## Plate 10

### *Assilina cancellata* Nuttal

3-4: Axial section (Form-B) of *Assilina cancellata* Nuttal recorded from the Kohat Formation in the Sheikhan Nala Section, north-eastern Kohat Basin.

### *Assilina subcancellata* Nuttal

1: Equatorial section 2: Axial section (Form-A) of *Assilina subcancellata* Nuttal recorded from the Kohat Formation in the Sheikhan Nala Section, north-eastern Kohat Basin.

### *Assilina exponense* Sowerby

5: Axial section (Form-B) of *Assilina exponense* Sowerby recorded from the Kohat Formation in the Sheikhan Nala Section, north-eastern Kohat Basin.

### *Assilina mammilata* Sowerby

1: Equatorial section 2: Axial section (Form-A) of *Assilina mammilata* Sowerby (5 specimens) recorded from the Kohat Formation in the Sheikhan Nala Section, north-eastern Kohat Basin.

# SMALLER BENTHIC FORAMINIFERA

## Plate 11

### 1: *Textularia dibollensis var humblei* Cushman & Applin

It is recorded from the Panoba Formation in the Sheikhan Nala Section, north-eastern Kohat Basin (Side view).

**2*: Textularia hannai* Davies**

It is recorded from the Panoba Formation in the Sheikhan Nala Section, north-eastern Kohat Basin (Side view).

**3: *Textularia cuyleri* Davies**

It is recorded from the Panoba Formation in the Sheikhan Nala Section, north-eastern Kohat Basin (Side view).

**4: *Textularia martini* Pijpers**

It is recorded from the Panoba Formation in the Sheikhan Nala Section, north-eastern Kohat Basin, Pakistan (Side view).

.

**5: *Textularia gertrudeana* Davies**

It is recorded from the Nammal Formation in the Chichali Nala Section, Trans Indus Ranges, Pakistan (Side view).

**6: *Textularia grahamensis* Cushman and Waters**

It is recorded from the Panoba Formation in the Sheikhan Nala Section, north-eastern Kohat Basin, Pakistan (Side view).

**7: *Textularia barrettii* Jones and Parker**

It is recorded from the Panoba Formation in the Sheikhan Nala Section, north-eastern Kohat Basin, Pakistan (Side view).

**8: *Textularia losangica* Loblich &Tappan**

It is recorded from the Panoba Formation in the Sheikhan Nala Section, north-eastern Kohat Basin, Pakistan (Side view).

**9: *Bulbobaculites lueckei* Cushman & Renz**

It is recorded from the Panoba Formation in the Sheikhan Nala Section, north-eastern Kohat Basin, Pakistan.

**10: *Conotrochammina cf dispersa* Finlay**

It is recorded from the Panoba Formation in the Panoba Nala Section, north-eastern Kohat Basin, Pakistan..

**11: *Bathysiphon eocenicus* Cushman & Hanna**

It is recorded from the Nammal Formation in the Chichali Nala Section, Trans Indus Ranges, Pakistan.

**12: *Bathysiphon robustus* Grzybowski**

It is recorded from the Panoba Formation in the Panoba Nala Section, north-eastern Kohat Basin, Pakistan.

**Plate 12**

**1: *Arenobulimina truncate* Reuss**

It is recorded from the Panoba Formation in the Sheikhan Nala Section, north-eastern Kohat Basin, Pakistan.

**2: *Gaudryina tazaensis* Carbonnier**

It is recorded from the Panoba Formation in the Sheikhan Nala Section, north-eastern Kohat Basin, Pakistan.

**3: *Lituotuba lituiformis* Brady**

It is recorded from the Panoba Formation in the Panoba Nala Section, north-eastern Kohat Basin, Pakistan.

**4: *Ammobaculites lacerate* Beckmann**

It is recorded from the Nammal Formation in the Chichali Nala Section, Trans Indus Ranges, Pakistan

**5: *Haplophragmoides porrectus* Maslakova**

It is recorded from the Nammal Formation in the Chichali Nala Section, Trans Indus Ranges, Pakistan

**6: *Haplophragmoides concavus* Chapman**

It is recorded from the Panoba Formation in the Sheikhan Nala Section, north-eastern Kohat Basin, Pakistan

**7: *Haplophragmoides kirki* Wickenden**

It is recorded from the Panoba Formation in the Panoba Nala Section, north-eastern Kohat Basin, Pakistan.

**8: *Evolutinella renzi* Beckmann**

It is recorded from the Panoba Formation in the Sheikhan Nala Section, north-eastern Kohat Basin, Pakistan

**9: *Dendrophyra excelsa* Grzybowski**

It is recorded from the Panoba Formation in the Sheikhan Nala Section, north-eastern Kohat Basin, Pakistan.

**10: *Burmudezina cubensis* Palmer and Bermudez**

It is recorded from the Panoba Formation in the Panoba Nala Section, north-eastern Kohat Basin, Pakistan.

**11: *Recurvoides cf walteri* Grzybowiski**

It is recorded from the Panoba Formation in the Panoba Nala Section, north-eastern Kohat Basin, Pakistan.

**12: *Gaudryina leveagata* Frank**

recorded from the Panoba Formation in the Panoba Nala Section, north-eastern Kohat Basin.

## Plate 13

**1: *Hyperammina elongata* Brady**

It is recorded from the Panoba Formation in the Panoba Nala Section, north-eastern Kohat Basin, Pakistan.

### 2: *Guadryinella pussilla* Magneiz-Jannin

It is recorded from the Panoba Formation in the Panoba Nala Section, north-eastern Kohat Basin, Pakistan

### 3: *Gaudryina pyramidata* Cushman

It is recorded from the Panoba Formation in the Sheikhan Nala Section, north-eastern Kohat Basin, Pakistan.

### 4: *Cibicides cf simplex* Brotzen

It is recorded from the Panoba Formation in the Sheikhan Nala Section, north-eastern Kohat Basin, Pakistan.

### 5: *Cibicides alleni* Plumer

It is recorded from the Panoba Formation in the Sheikhan Nala Section, north-eastern Kohat Basin, Pakistan.

### 6: *Cibicides mensilla* (Schwager) var. nammalensis

It is recorded from the Panoba Formation in the Sheikhan Nala Section, north-eastern Kohat Basin, Pakistan.

.

### 7: *Cibicicoides tuxpamensis laxispiralis* Beckmann

It is recorded from the Panoba Formation in the Sheikhan Nala Section, north-eastern Kohat Basin, Pakistan.

### 8: *Cibicidoides tuxpamensis tuxpamensis* Cole

It is recorded from the Panoba Formation in the Sheikhan Nala Section, north-eastern Kohat Basin, Pakistan.

### 9: *Gavelinella dakotensis* Fox

It is recorded from the Panoba Formation in the Panoba Nala Section, north-eastern Kohat Basin, Pakistan.

### 10: *Gavelinella aracajuensis* Petri

It is recorded from the Panoba Formation in the Tarkhobi Nala Section, north-eastern Kohat Basin.

### 11: *Gavelinella schloenbachi* Reuss

It is recorded from the Panoba Formation in the Panoba Nala Section, north-eastern Kohat Basin, Pakistan.

### 12: *Stensioeina excolata*

It is recorded from the Panoba Formation in the Panoba Nala Section, north-eastern Kohat Basin, Pakistan.

## Plate 14

**1: *Loxostomum applinae* Plumer**

It is recorded from the Panoba Formation in the Panoba Nala Section, north-eastern Kohat Basin, Pakistan

**2: *Valvulineria patalensis***

It is recorded from the Panoba Formation in the Panoba Nala Section, north-eastern Kohat Basin, Pakistan

**3: *Nonionella Jacksonenesis* Cushman var minuta**

It is recorded from the Panoba Formation in Sheikhan Nala Section, north-eastern Kohat Basin.

**4: *Praebulimina cf seabensis* Tappan**

It is recorded from the Patala Formation in the Panoba Nala Section, north-eastern Kohat Basin

**5: *Bulimina stokesi* Cushman and Renz**

It is recorded from the Patala Formation in the Panoba Nala Section, north-eastern Kohat Basin.

**6: *Uvigerina gallowayi basicordata* Cushman and Renz**

It is recorded from the Panoba Formation in the Panoba Nala Section, north-eastern Kohat Basin.

**7: *Uvigerina spinicostata* Cushman and Jarvis**

It is recorded from the Panoba Formation in the Panoba Nala Section, north-eastern Kohat Basin.

**8: *Bolivinoides decoratus decoratus* Jones**

It is recorded from the Panoba Formation in the Panoba Nala Section, north-eastern Kohat Basin.

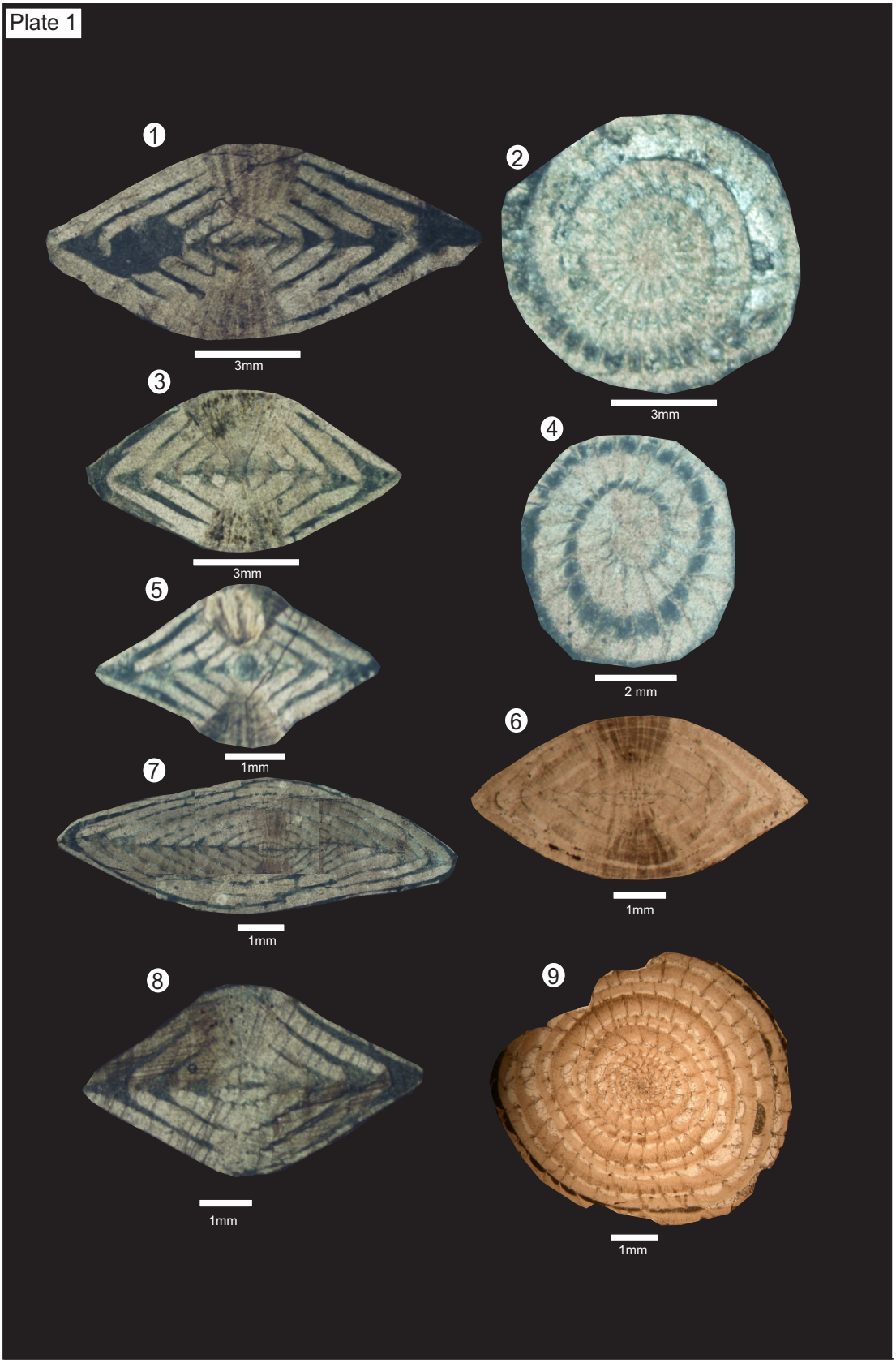
Plate 1
1
3mm
2
3mm
3
3mm
4
2 mm
5
1mm
6
1mm
7
1mm
8
1mm
9
1mm

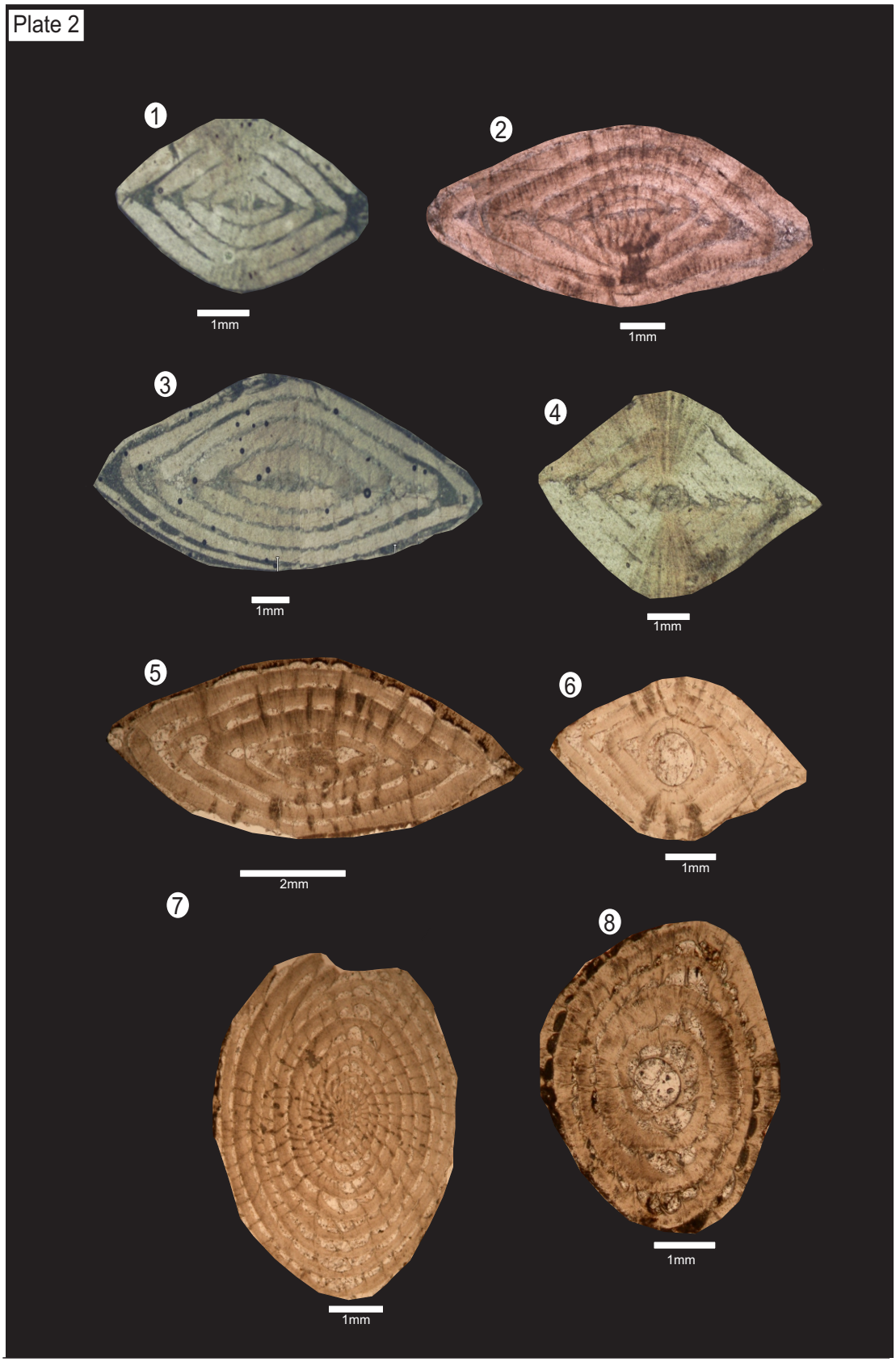
Plate 2
1
1mm
2
1mm
3
1mm
4
1mm
5
2mm
6
1mm
7
1mm
8
1mm

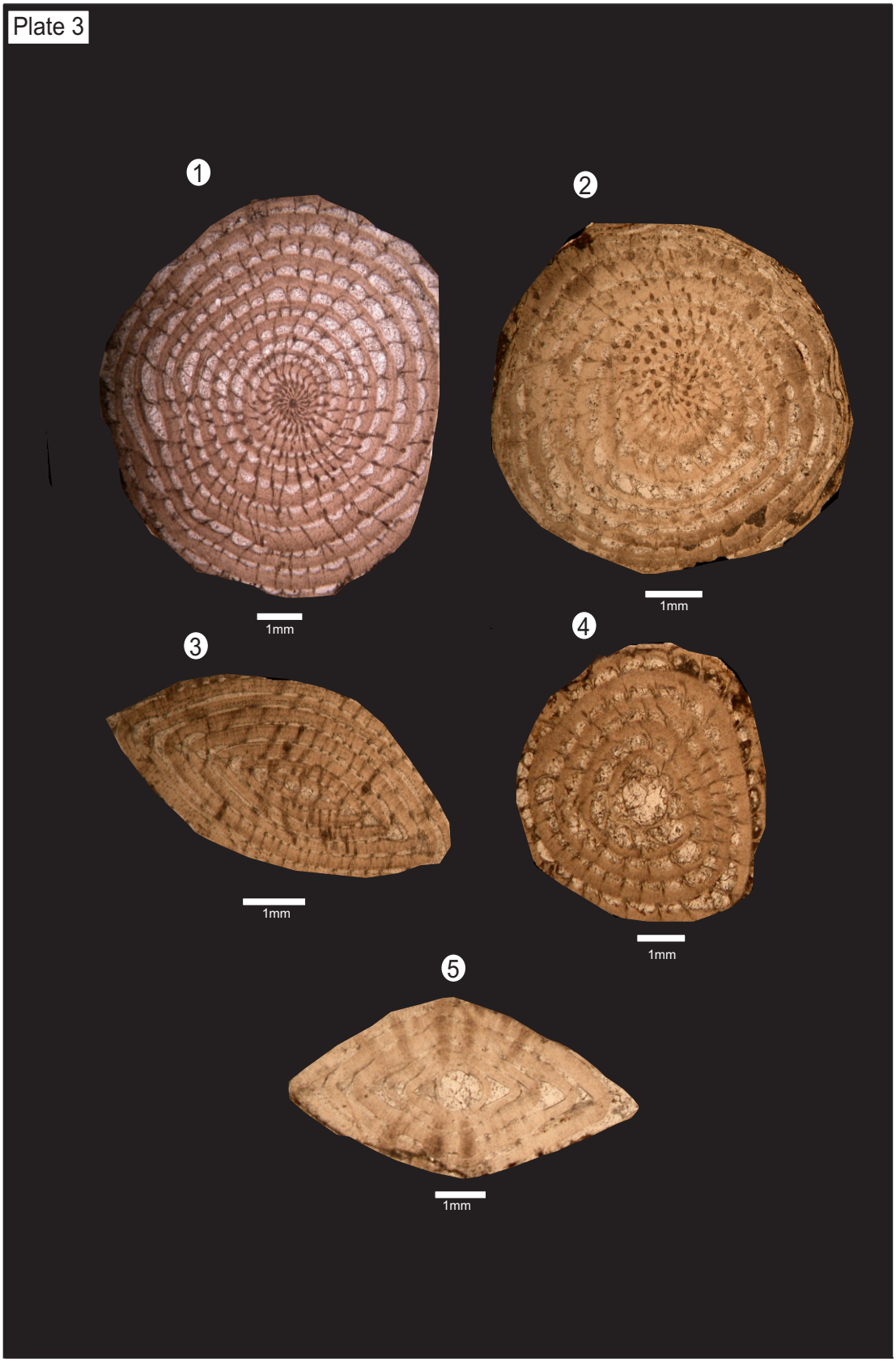
Plate 3
1
1mm
2
1mm
3
1mm
4
1mm
5
1mm

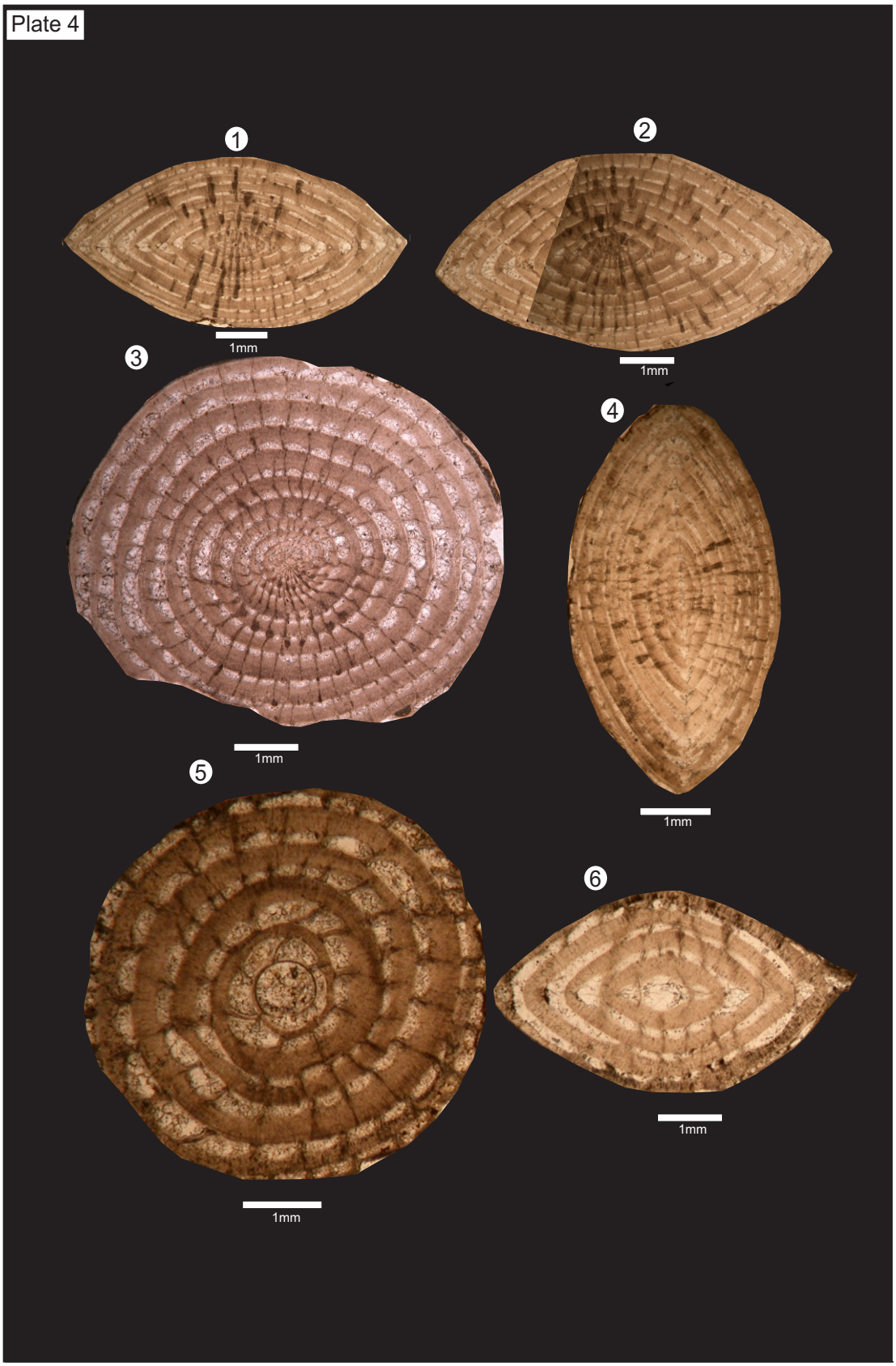
Plate 4
1
1mm
2
1mm
3
1mm
4
1mm
5
1mm
6
1mm

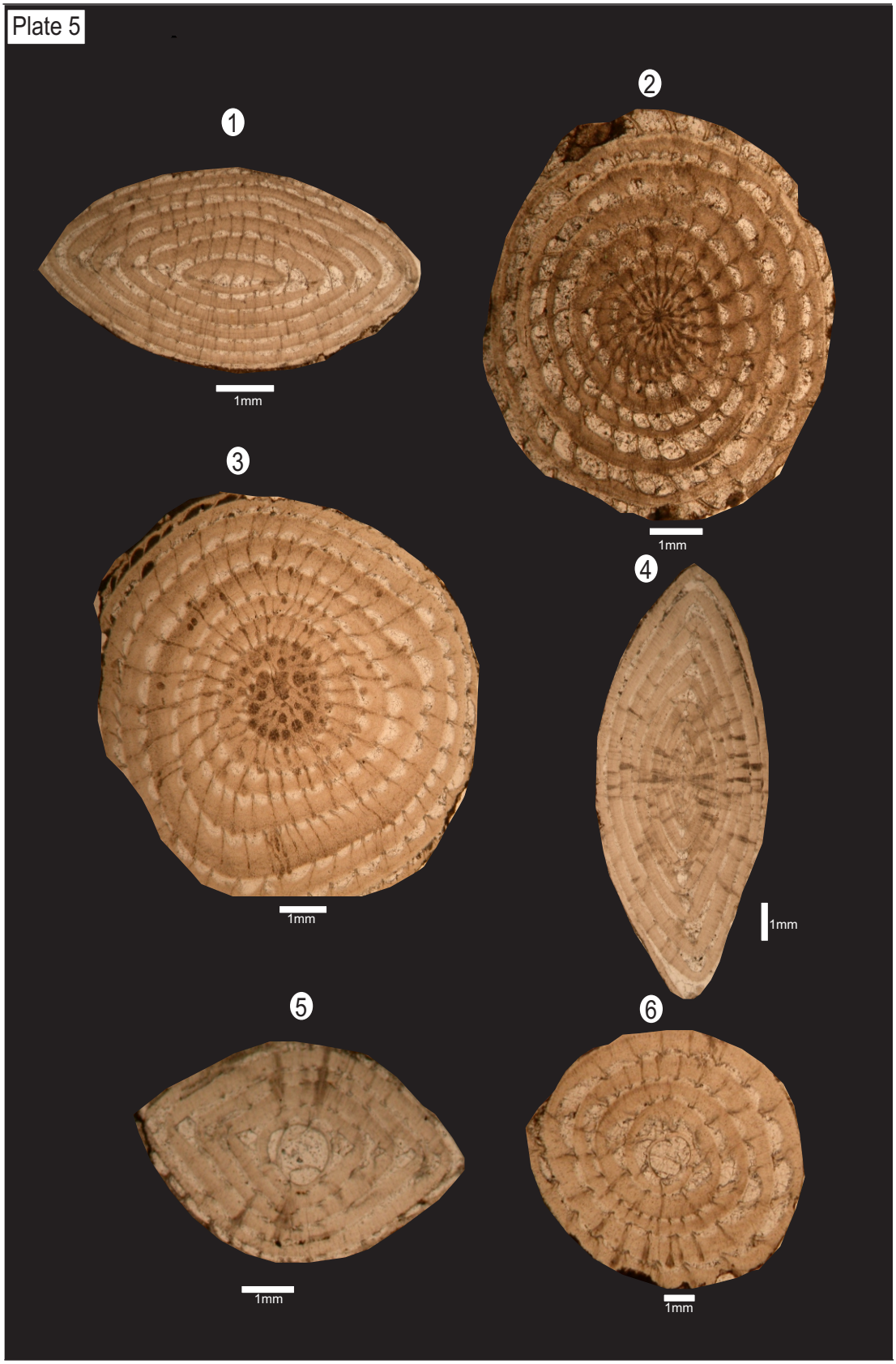
Plate 5
1
1mm
2
1mm
3
1mm
4
1mm
5
1mm
6
1mm

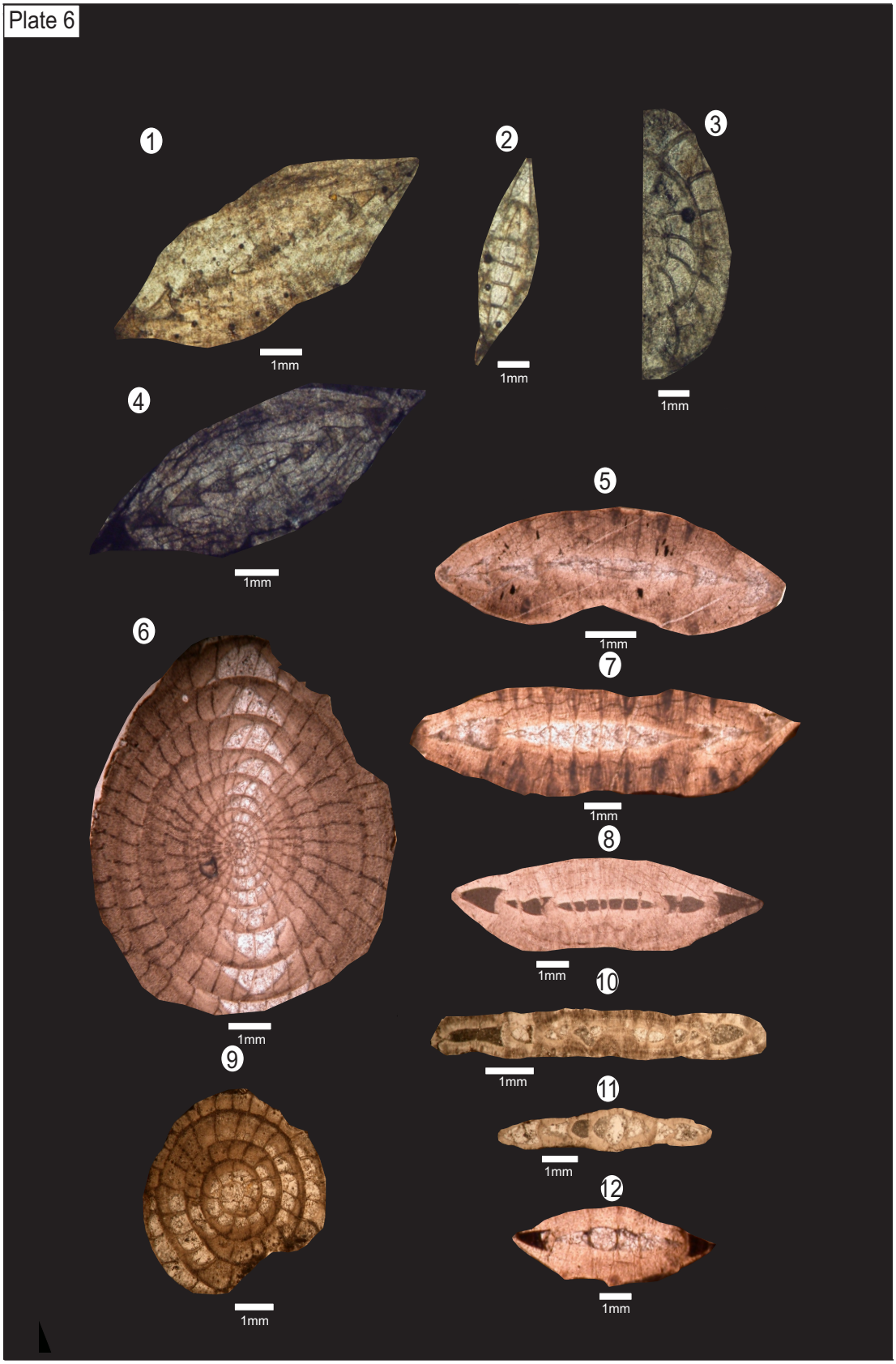
Plate 6
1
1mm
2
1mm
3
1mm
4
1mm
5
1mm
6
1mm
7
1mm
8
1mm
9
1mm
10
1mm
11
1mm
12
1mm

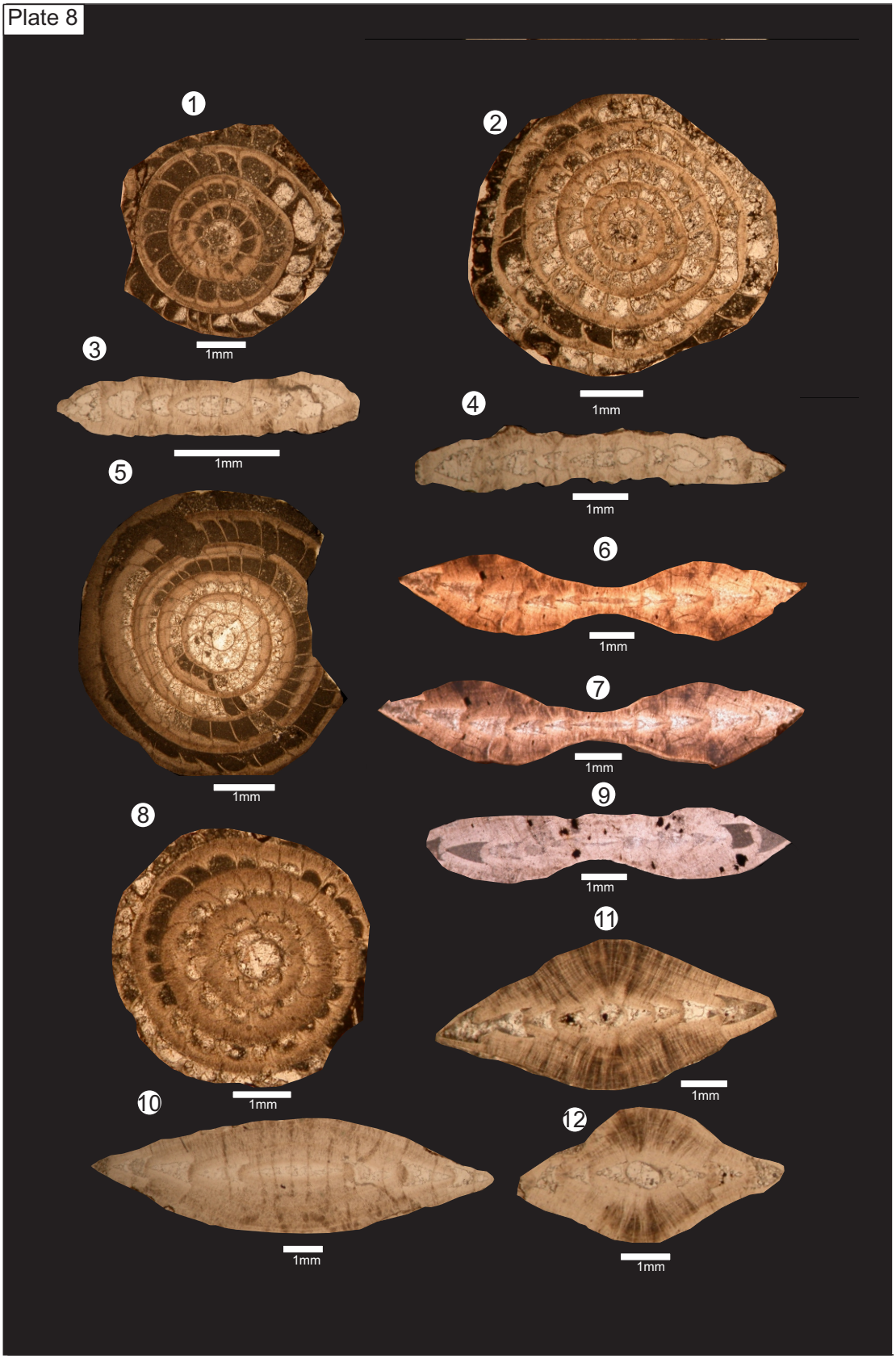
Plate 8
1
1mm
2
1mm
3
1mm
4
1mm
5
1mm
6
1mm
7
1mm
8
1mm
9
1mm
10
1mm
11
1mm
12
1mm

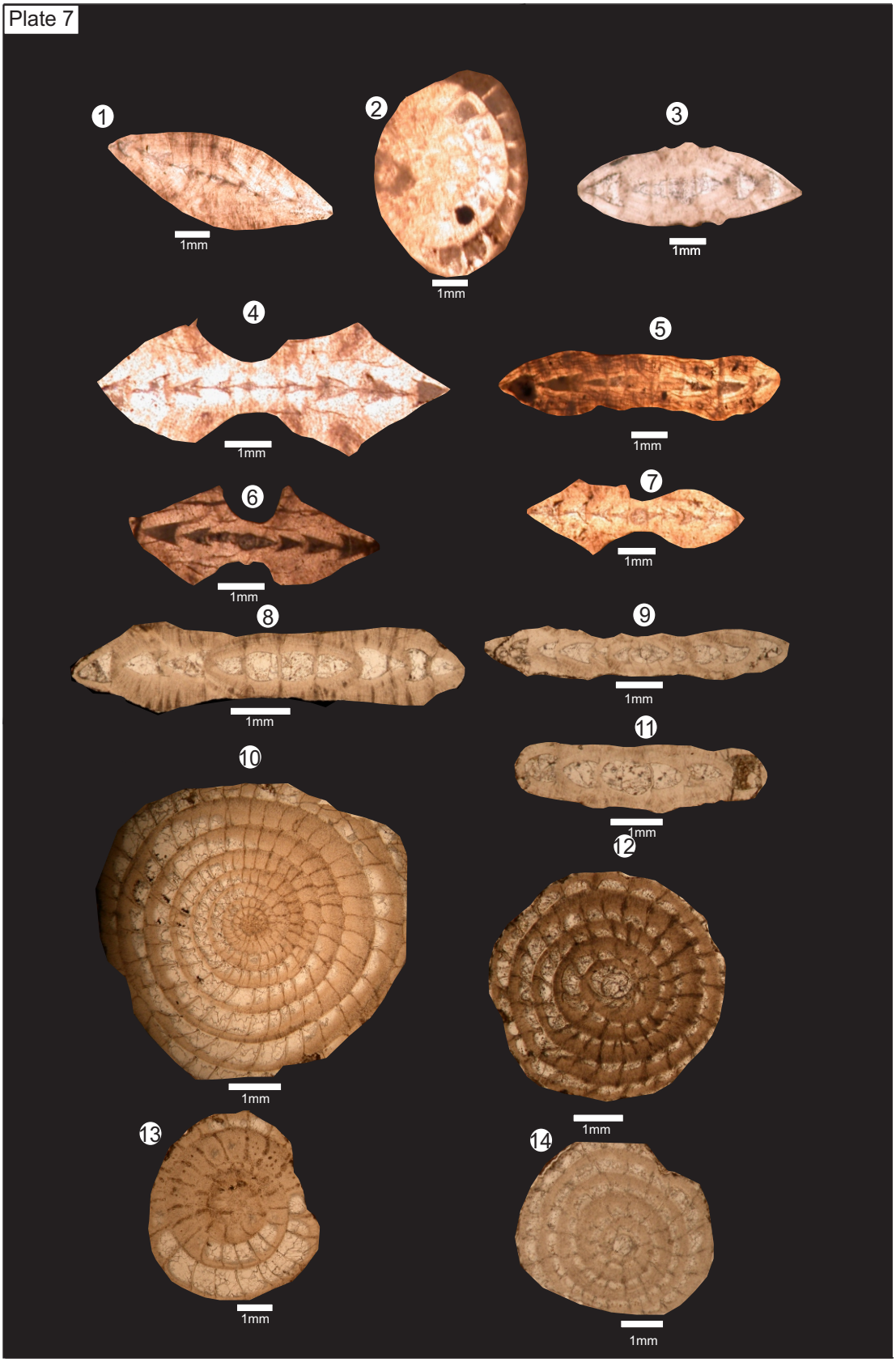
Plate 7
1
1mm
2
1mm
3
1mm
4
1mm
5
1mm
6
1mm
7
1mm
8
1mm
9
1mm
10
1mm
11
1mm
12
1mm
13
1mm
14
1mm


Plate 9
1
1mm
2
1mm
3
1mm
4
1mm


Plate 10
1
1mm
2
1mm
3
1mm
4
1mm
5
1mm
6
1mm

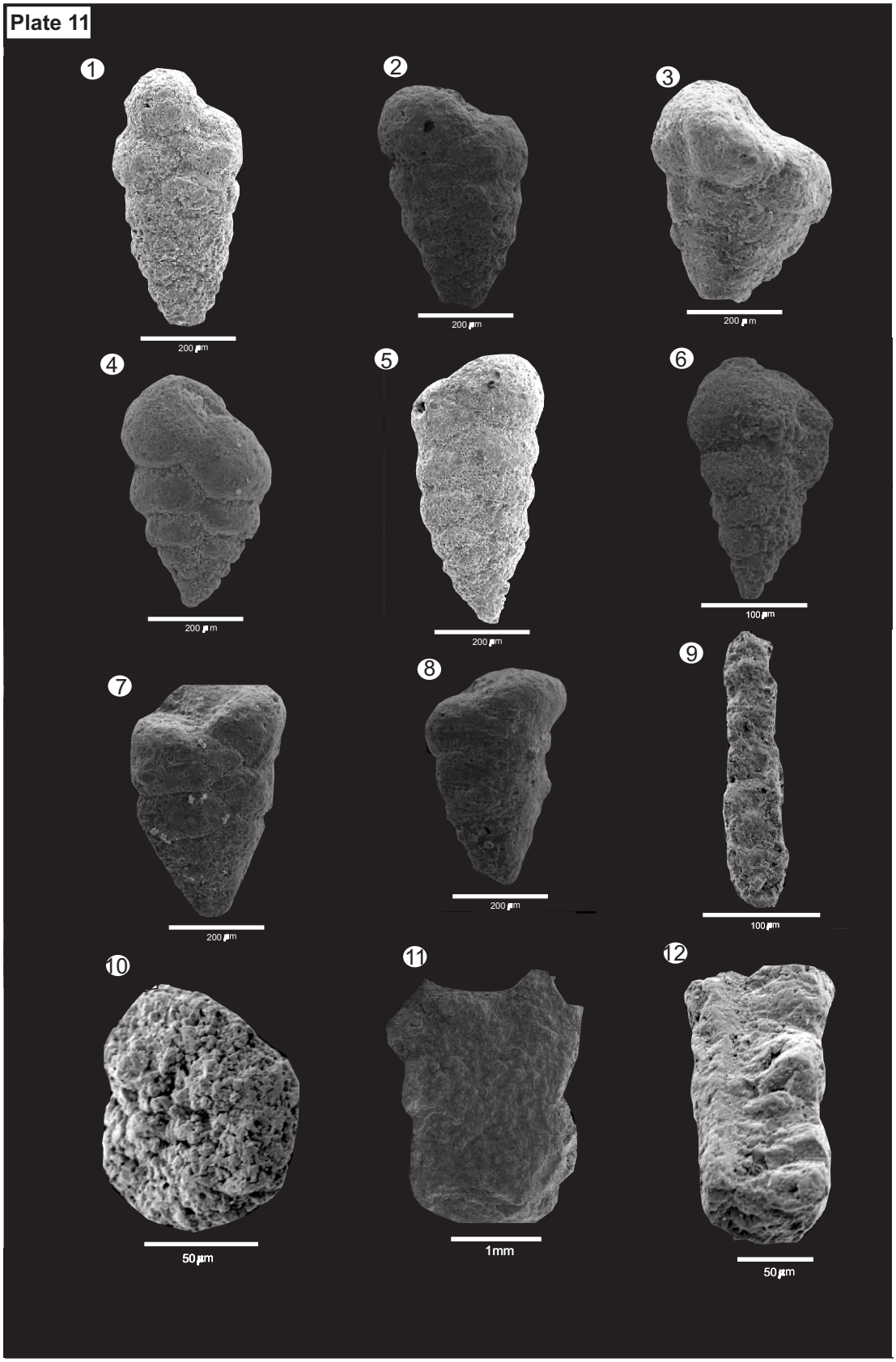
Plate 11
1
200 µm
2
200 µm
3
200 µm
4
200 µm
5
200 µm
6
100 µm
7
200 µm
8
200 µm
9
100 µm
10
50 µm
11
1mm
12
50 µm

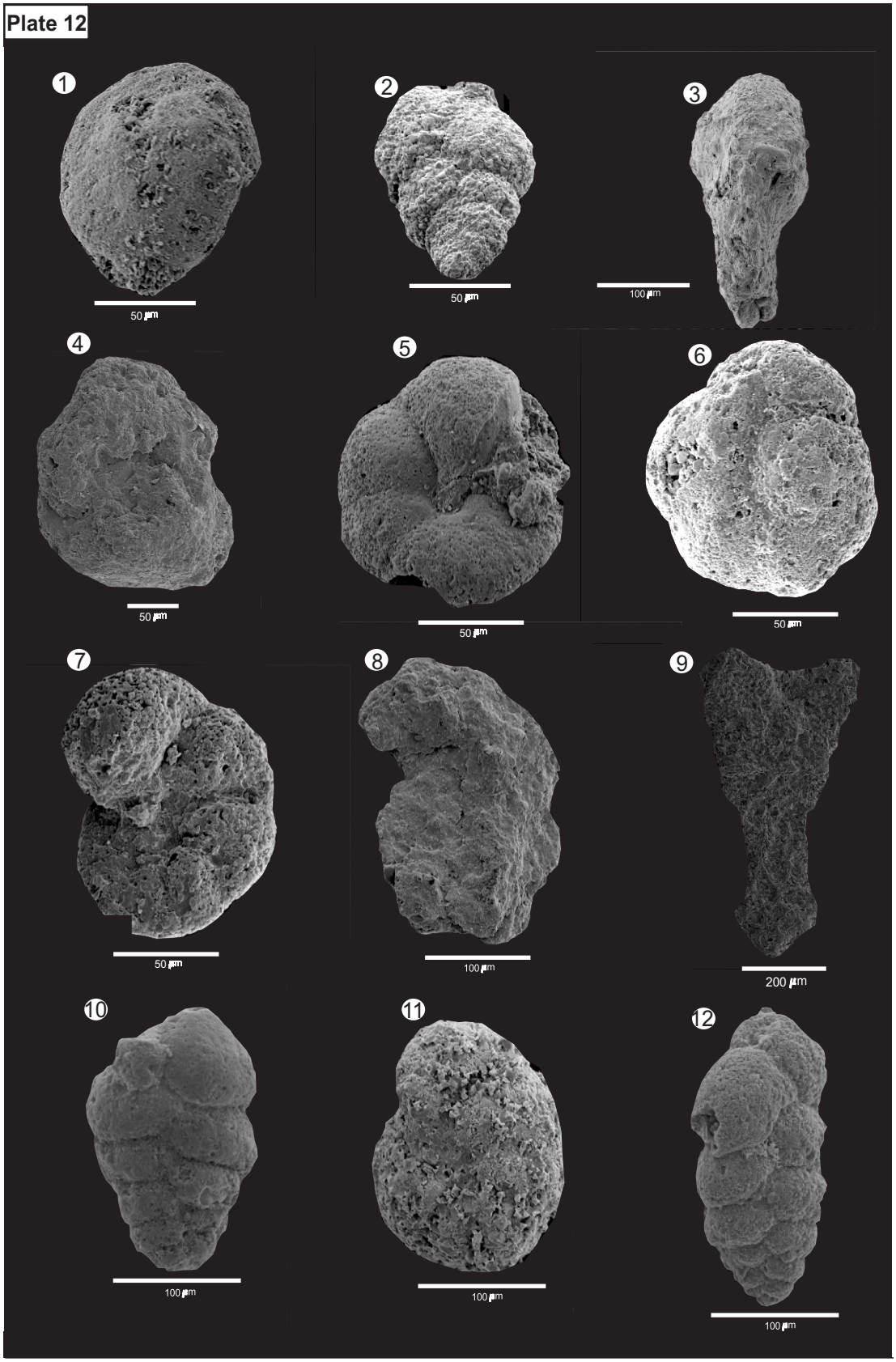
Plate 12
1
50 µm
2
50 µm
3
100 µm
4
50 µm
5
50 µm
6
50 µm
7
50 µm
8
100 µm
9
200 µm
10
100 µm
11
100 µm
12
100 µm

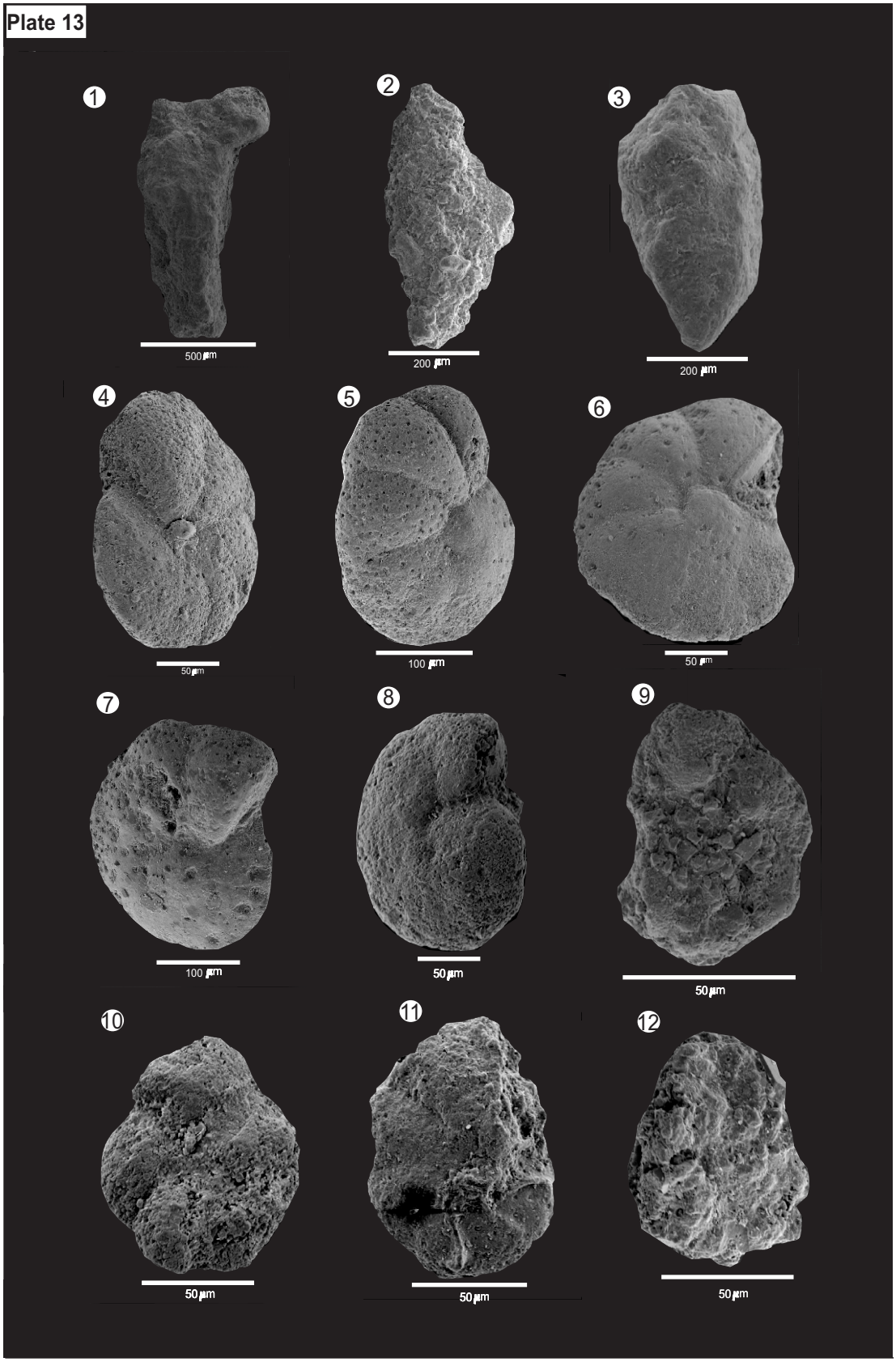
Plate 13
1
500 µm
2
200 µm
3
200 µm
4
50 µm
5
100 µm
6
50 µm
7
100 µm
8
50 µm
9
50 µm
10
50 µm
11
50 µm
12
50 µm

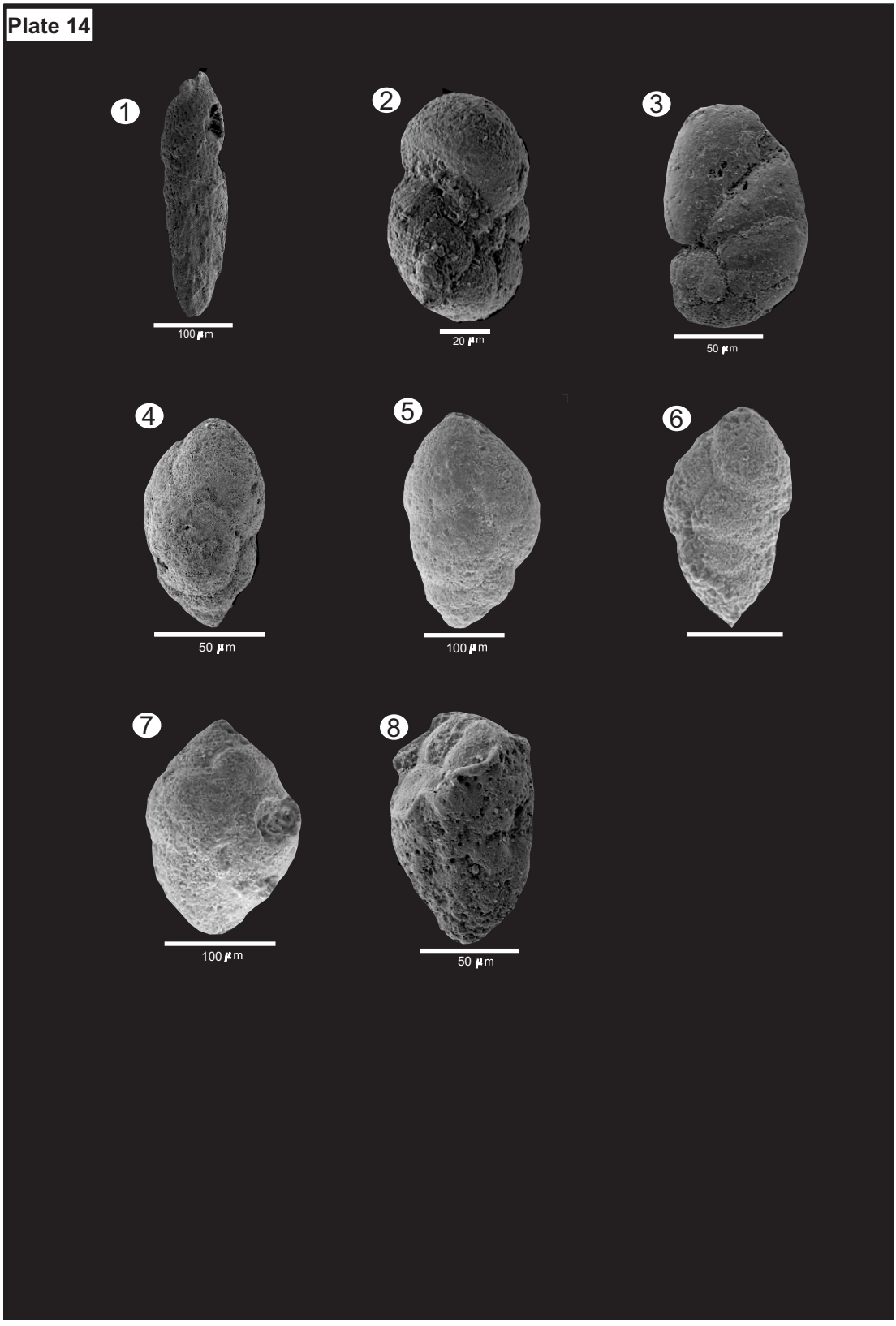
Plate 14
1
100 µm
2
20 µm
3
50 µm
4
50 µm
5
100 µm
6
7
100 µm
8
50 µm

# Chapter 4

# 4 Larger benthic foraminiferal biostratigraphy of the Kohat Basin

## 4.1 Introduction

The biostratigraphic zonal schemes which were developed on the basis of phylogeny of larger benthic foraminifera (alveolinids, nummulitids, and assilinids) by Höttinger (1960), Blondaeau (1972) and Schaub (1981) have been integrated into the Shallow Benthic Zones (SBZ) for the Paleogene strata as proposed by Serra Kiel et al. (1998). These biozonation schemes have been successfully used for constraining the ages of the Tertiary rocks in Oman (Racey, 1995). The applicability of these biozonations is tested here for the Paleogene rocks of the Kohat Basin which contains well preserved larger benthic foraminifera.

## 4.2 Previous Work

The pioneering work of the following authors contributed significantly to the understanding of the stratigraphy and regional distribution of Paleogene rocks across the Indus Basin including those of the Kohat-Potwar Plateax. Blanford (1876) used the term Ranikot series for the Paleocene and Kirthar Series for the Middle Eocene rocks of the Indus Basin. These terms were commonly used by later workers in the Kohat Basin. Noetling (1903) used the term Laki Series for Early Eocene rocks of the Lower Indus Basin and later authors used the same term for the Early Eocene rocks exposed in the Kohat Basin. Vredenburg (1906) established local biozones and described *Nummulites millecaput* Boubee at the base of the upper Kirthar beds and *Nummulites beaumonti* d, Archaic and Haime near the top of the upper Kirthar (Upper Middle Eocene) beds in the Kohat Basin. According to Vredenburgh (1906) the lowest zone of upper Kirthar contains *Assilina spira*, and *Nummulites perforatus* which continues into the overlying zone, while third zone contains *Nummulites complanatus*. Nuttal (1926) recorded age diagnostic foraminifera from the Laki Series of the Kohat Basin and classified them according to their septal filament types.

Davies (1940) synonymises the species in Vredenburg (1906) Zone 1 *Assilina spira* with *Assilina pappilata* and its larger derivative *Assilina irregularis*, *Nummulites perforatus* with *Nummulites obtusus/Nummulites uroniensis* in Zone 2, and *Nummulites complanatus* with *Nummulites millecaput* Boubee in Zone 3. Davies (1940) claimed that there is no paleontological evidence to define an upper / middle Kirthar boundary in the Kohat area. Eames (1950) presented the local palaeontological subdivisions and correlated the Eocene rocks of the Kohat Plateau with the Rakhi Nala and Zinda Pir area in the Lower Indus Basin. He concluded that more work is needed to be done on collections from different facies of the Laki and Kirthar Series before any regional subdivision on paleontological grounds could be attempted. Gill (1953) described various Laki age *Assilina* species from the Kohat Basin. Naggapa (1959) and Pascoe (1963) reported Early Eocene *Alveolina oblonga, Assilina daviesi, Assilina laminosa, Nummulites atacicus and Orbitolites complanatus* from the Kohat area. Kureshy (1968) provides an overview of the taxonomy and a range distribution of the larger benthic foraminiferal species recorded from different parts of Pakistan including few representatives of the Laki and the Kirthar age from the Kohat Basin. Meissner et al. (1967) also confirmed larger benthic foraminifera of the Eocene age from the Kohat Basin. Roohi and Baqri (2004) found Middle-Upper Eocene foraminiferal species of *Nummulites mamillatus, N. atacicus, N. globosa, N. subirregularis, Operculina patalensis, Operculina sp., Assilina exponens, A. granulosa, A. spinosa, A. subspinosa, A. laminosa, A. dandotica, Discocyclina despansa, Dictyoconoides sp., Alveolina elliptica* and *Alveolina stercumeris* from the Kohat Formation in the Kohat Basin.

## 4.3 Present study

It is clear from the literature review above that there are two different views about the existence of Upper Kirthar (Upper Middle Eocene) beds in the Kohat Basin. Vredenburg (1906), Davies (1940) , Eames (1950), and Rohi & Baqri (2004) support the existence of the Upper Kirthar (Upper-Middle Eocene) strata, while Gill (1953), Meissner (1974) did not report beds younger than the Middle Kirthar (Middle Eocene) in the Kohat Basin. The aim of present study is to distinguish between the above claims and to propose a more detailed biostratigraphic framework in the study area.

In this study biostratigraphic zonation is based on the identification of diagnostic larger benthic foraminifera which mainly include *Nummulites* and *Assilina* species. These are systematically described, illustrated and commented upon with reference to taxonomic status of morphologically close species (see chapter 3).

In this chapter the concept of stages and biozones is discussed (figure 4.1-4.2) and a larger benthic foraminiferal biostratigraphic zonation scheme for the Paleogene (Ranikot, Laki and Kirthar) rocks is presented (figures 4.3–4.6). These biozones are correlated within the Panoba Nala, the Tarkhobi Nala, the Sheikhan Nala and the Bahdur Khel Salt Tunnel Sections and a biostratigraphic correlation chart is constructed across these sections (figure 4.7). A comparson of local biozones with the standard biozonation (Hottinger, 1960; Schaub, 1981; Serra Kiel, 1998) is presented (figure 4.8). Stratigraphic ranges of the recorded species are shown in figure 4.9 which are compared with the nummulitid Lineage Charts (figure 4.10 A-C) of Schaub (1981).

## 4.4 Stage and biozone concept

The stage can be defined as a group of strata containing the same major fossil assemblages while the biozone is defined as body of strata characterized by a specific kind of fossil contained in it. It is the fundamental biostratigraphic unit. Biozones are divided in to following principal kinds (figures 4.1 and 4.2).

***A) Taxon range biozone:*** known as a teilzone, local zone, local-range zone, or topozone characterized by the known stratigraphic and geographic range of occurrence of a single taxon.

***B) Concurrent range biozone:*** this is also referred to as an overlap zone or range-overlap zone and includes the concurrent, coincident, overlapping part of the range of two specified taxa. The concurrent range zone concept is distinguished from the taxon range zone concept by being based on more than a single taxon, and from the assemblage zone concept by not including all elements of a naturally occurring assemblage of fossil organisms.

***C) Abundance biozone (ACME):*** those strata in which the abundance of a particular taxon or group of taxa is significantly greater than in the adjacent part of the section is known as abundance biozone.

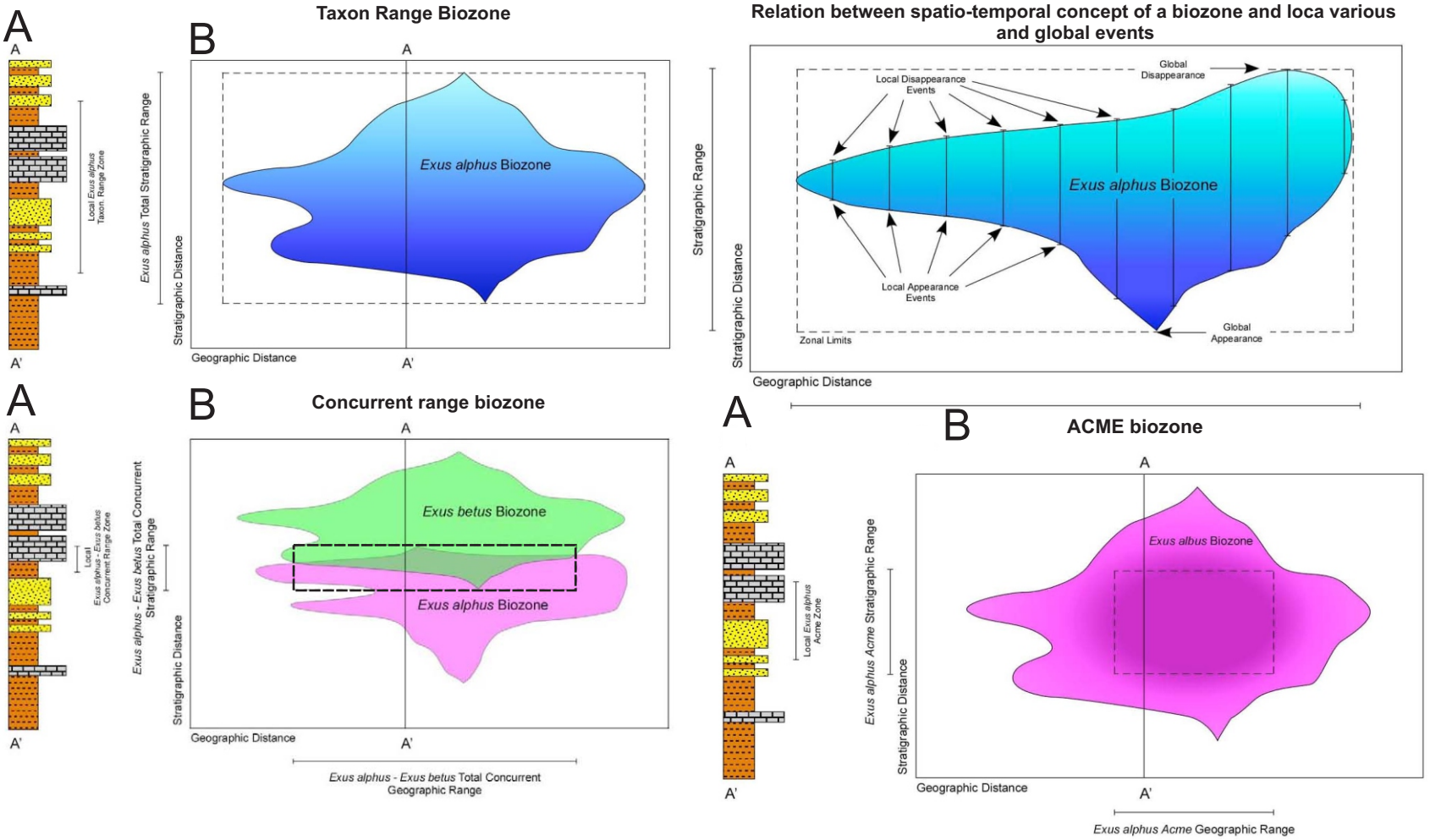


**Figure 4.1.** One dimensional (A) and two dimensional (B) representation of various types of biozones where speciation and extinction events define a spatio temporal region within which inferred Total Stratigraphic Range (vertical distribution) and Total Geographic Range (Horizontal) of the taxon are defined (dashed lines), however in local sections the biozones will be represented by a one dimensional interval whose boundaries are included in the within taxon,s global biozones ( Note: species names are hypothetical which serves the purpose of illustration). (Reference: Macleod, N. in Press. Biozones. *in* R.C. Selly, L.R.M. Cooks and I.R. Plimer (eds), *Encyclopedia of Geology*, Academic Press, London )

***D) Oppel biozone*:** defined by the ranges and range-limits of a group of fossil taxa selected in such a way as to minimize zonal boundary diachrony and maximize the geographic scope of the interval so defined.

***E) Lineage biozone*:** also referred to as a phylozone, evolutionary zone, lineage zone, morphogenic zone, phylogenetic zone, or morphoseries zone, defined by strata containing species representing a specific segment of an evolutionary lineage or the combined biostratigraphic range of the series of ancestral descendant species in a lineage.

***F) Interval biozone***: also referred to as an inter biohorizon zone, gap zone, or a partial-range zone is the strata between two specific biostratigraphic surfaces. It can be based on lowest or highest occurrences.

***G) Assemblage biozones****:* also referred to as a cenozone, ecozone, ecological zone, faunizone, biofacies zone and association zone is the strata that contain a unique association of three or more taxa.

## 4.5 Biostratigraphy

The present study is based on the high resolution foraminiferal analysis of the Paleogene rocks of the Kohat Basin. Systematic rock sampling has been carried out by collecting a total of 305 rock samples from the Patala, the Panoba, the Sheikhan, and the Kohat Formations in a younging up sequence exposed in the Panoba Nala, the Tarkhobi Nala, the Sheikhan Nala and the Bahadurkhel Salt Tunnel Sections. About 500 thin sections were made including oriented sections of the individual foraminiferal tests derived from the marl units. A total of fifty one larger benthic foraminifera species (sixteen *Nummulites,* twelve *Assilina*, five *Alveolina*, seven *Discocyclina*, three *Operculina*, two *Ranikothalia,* three *Lockhartia*, one *Orbitolites,* one *Misccellanea* and *one Rotalia* species are recorded. These species are identified after Nuttal (1926), Davies (1940), Gill (1953), Naggapa (1959), Höttinger (1960), Kureshy (1968), Schaub (1981) and Racey (1995). For the first time forty four smaller benthic foraminiferal species are recorded from the Palaogene rocks of the Kohat Basin. These species are identified after Davies (1940), Haque (1956) and Bolli et al. (1994). Their distribution provide further support for demarcation of zonal boundaries.

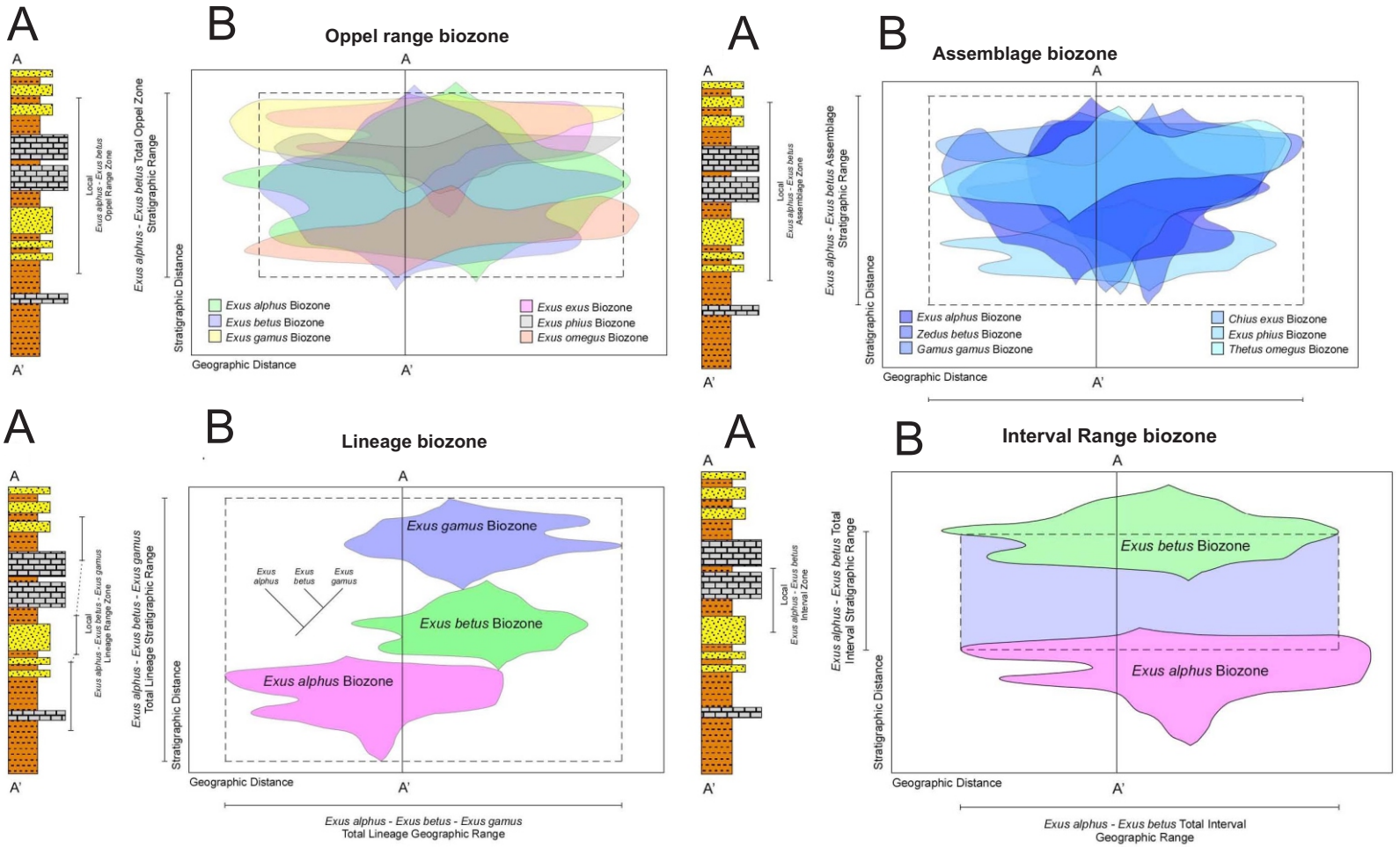


**Figure 4.2.** One dimensional (A) and two dimensional (B) representation of various types of biozones where speciation and extinction events define a spatio temporal region within which inferred Total Stratigraphic Range (vertical distribution) and Total Geographic Range (Horizontal) of the taxon are defined (dashed lines) however in local sections the biozones will be represented by a one dimensional interval whose boundaries are included in the within taxon global biozones (Note: species names are hypothetical which serves the purpose of illustration). (Reference: Macleod, N. in Press. Biozones. *in* R.C. Selly, L.R.M. Cooks and I.R. Plimer (eds), *Encyclopedia of Geology*, Academic Press, London )

In this study a biozonation scheme is developed which is based on the biostratigraphic range of identified foraminiferal species. The first and last occurrence of the age diagnostic species of nummulitids and associated foraminifera provide the basis for establishing biozone boundaries. These zonal boundaries divide Paleogene rocks of the Kohat Basin into six local larger benthic forminiferal biozones which are taxa, lineage and assemblage types and abbreviated as BFZK (Benthic Foraminiferal Zones of the Kohat Basin). For constraining relative ages of the strata, stratigraphic ranges of the nummulitid species (figure 4.10 A-C) as developed by Schaub (1981), alveolinid species for Biozones of Höttinger (1960) and Shallow Benthic Foraminiferal Zones (SBZ) as proposed by Serra Kiel et al. (1998) are used. A comparative biozonation chart (figure 4.8) and stratigraphic range chart of the identified larger benthic foraminifera (figure 4.9) are also presented. The chronologic calibration of the biozones is based on magnetostratigraphy as presented in Geological Time Scale developed by Bergeren et al. (1995). In this study BFZK1-BFZK 6 Biozones are defined and described as following.

### 4.5.1 BFZK 1 (A) Biozone

**Definition:** the stratigraphic range of *Miscellanea miscella* and *Ranikothalia sindensis* defines base and top of this biozone.

***Associated assemblages:*** the associated larger benthic foraminifera include *Miscellanea stampi*, *Operculina salsa, Asterocyclina alticosta, Lockhartia haime* and *Ranikothalia nuttali.*

***Age:*** this biozone is Thanitian

### 4.5.2 BFZK 1 (B) Biozone

***Definition:*** the base of this biozone is taken at the first occurrence of *Assilina granulosa* and the top is taken at the first occurrence of *Assilina aff. pustulosa*.

***Associated assemblages:*** the associated larger benthic foraminifera include *Nummulites irregularis, Nummulites pinfoldi, Nummulites thalicus, Assilina daviesie, Assilina subdavisie, Operculina salsa, Alveolina ludwingi, Alveolina vredenburgi,*

*Asterocyclina alticosta, Discocyclina sella, Discocyclina undulata, Discocyclina despensa, Discocyclina fortisie, Discocyclina roberti, Discocyclina scalaris* and *Lepidocyclina fortisi.* Several age diagnostic smaller benthic foraminifera range through this zone and include *Textularia dibollensis var humblei, Textularia hannai, Textularia cuyleri, Textularia martini, Textularia gertrudeana, Textularia grahamensis, Textularia barrettii, Textularia losangica, Bulbobaculites lueckei, Conotrochammina cf dispersa, Bathysiphon eocenicus, Bathysiphon robustus, Arenobulimina truncate, Gaudryina tazaensis, Lituotuba lituiformis, Ammobaculites lacerate, Haplophragmoides porrectus, Haplophragmoides concavus, Haplophragmoides kirki, Evolutinella renzi, Dendrophyra excelsa , Burmudezina cubensis, Recurvoides cf walteri, Gaudryina leveagata, Hyperammina elongata, Guadryinella pussilla,* and *Gaudryina pyramidata*. Non-agglutinated associated species are *Cibicides cf simplex, Cibicides alleni, Cibicides mensilla (var. nammalensis, Cibicicoides tuxpamensis laxispiralis, Cibicidoides tuxpamensis tuxpamensis, Gavelinella dakotensis, Gavelinella aracajuensis, Gavelinella schloenbachi, Stensioeina excolata, Loxostomum applinae, Valvulineria patalensis, Nonionella Jacksonenesis Cushman var minuta, Praebulimina cf seabeensi, Bulimina stokesi, Uvigerina gallowayi basicordata, Uvigerina spinicostata, Bolivinoides decoratus decoratus* and *Bolivinoides delicatulus curtus.*

***Age:*** this biozone is Lower Lllerdian 1.

### 4.5.3 BFZK 2 Biozone

***Definition:*** the Base of this biozone is taken at the first occurrence of *Assilina aff pustulosa, Assilina pustulosa* and the top is marked by the first occurrences of *Nummulites atacicus* and *Nummulites globulus.*

***Associated assemblages:*** the associated benthic foraminifera include *Assilina spinosa, Assilina subspinosa, Assilina granulosa, Assilina leymerie, Assilina pustulosa, Discocyclina sella, Discocyclina undulata, Discocyclina despensa, Discocyclina fortisie, Discocyclina roberti, Discocyclina scalaris, Alveolina vredenburgi, Alveolina ludwingi, Lockhartia pustulosa, Rotalia trochidoformis. humblei, Textularia hannai*, *Textularia cuyleri*, *Textularia martini*, *Textularia gertrudeana*, *Textularia grahamensis*, *Textularia barrettii*, *Textularia losangica*,

*Cibicides cf simplex, Cibicides alleni*, *Bulimina tuxpamensis* and *Praeglobobulimina ovata*, *Stensioeina excolata, Loxostomum applinae, Valvulineria patalensis, Nonionella Jacksonenesis Cushman var minuta, Praebulimina cf seabeensi, Bulimina stokesi, Uvigerina gallowayi basicordata, Uvigerina spinicostata, Bolivinoides decoratus decoratus* and *Bolivinoides delicatulus curtus*

***Age:*** this biozone is Lower LlIerdian 2 - Middle Lllerdian 1.

### 4.5.4 BFZK 3 (A) Biozone

***Definition:*** the base of this zone is taken at the first occurrence of *Nummulites globulus* and *Nummulites atacicus* while the top is defined by the first occurrence of *Alveolina rotundata.*

***Associated assemblages:*** the larger benthic foraminifera *Nummulites thalicus, Nummulites pinfoldi, Assilina granulosa, Assilina leymerie, Assilina spinosa, Assilina subspinosa, Assilina putulosa, Discocyclina sella, millioids, Lockhartia tipperi, Lockhartia putulosa, Lockhartia conditi, Dictyoconus indicus, Dictyoconus daviesie, Rotalia trochidoformis, Asterocyclina alticosta, Alveolina ludwingi, Alveolina paraloculinoides* and *Alveolina elliptica* range through this biozone.

**Age:** this biozone is Middle Lllerdian 2.

### 4.5.5 BFZK 3 (B) Biozone

***Definition:*** the base of this zone is taken at the first occurrence of *Alveolina rotundata* and the top is defined by the synchronous occurrences of *Assilina laxispira, Nummulites palnulatus,* and *Orbitolites complanatus.*

***Associated assemblages:*** *Rotalia trochidoformis, Asterocyclina alticosta, Alveolina ludwingi, Alveolina paraloculinoides*, *Sakessaria*, *Alveolina elliptica, Nummulites pinfoldi, Nummulites globulus, Assilina granulosa, Assilina leymerie, Assilina spinosa, Assilina subspinosa, Discocyclina sella, Discocyclina fortisie. Lockhartia tipperi, Lockhartia putulosa, Lockhartia conditi, Dictyoconus indicus* and *Dictyoconus daviesie* species range through this biozone.

***Age:*** this biozone is Upper Lllerdian-Middle Cuisian.

### 4.5.6 BFZK 4 Biozone

***Definition:*** the base of this zone is taken at the first synchronous occurrences of *Nummulites beaumonti, Nummulites acutus and Assilina pappilata* and the top is taken at the first occurrence of *Assilina exponense.*

***Associated assemblages:*** the larger benthic foraminifera, *Nummulites beaumonti, Nummulites globulus, Nummulities perforatus, Nummulites pinfoldi, Nummulites acutus, Nummulites mammila, Nummulites pengaroensis*, *Rotalia trochidoformis*, *Assilina subpappilata, Assilina laminosa, Assilina sublaminosa, Assilina spinosa, Assilina subspinosa*, *Assilina granulosa*, *Assilina leymerie* and *Assilina sutri* range through this zone.

***Age:*** this biozone is Middle Lutetian 1.

### 4.5.7 BFZK 5 Biozone

***Definition:*** the base of this zone is taken at the first occurrence of *Assilina exponense* and the top is taken at the first occurrence of *Assilina cancellata*.

***Associated assemblages:*** the larger benthic foraminifera *Nummulites beaumonti, Nummulites globulus, Nummulites pinfoldi, Nummulites mamilla, Nummulites thalicus, Assilina pappilata, Assilina subpappilata, Assilina mammilata, Assilina laminosa, Assilina sublaminosa, Assilina spinosa, Assilina subspinosa*, *Assilina granulosa*, *Assilina leymerie* and *Assilina sutri* range through this zone.

***Age:*** this biozone is Middle Lutetian 2.

### 4.5.8 BFZK 6 Biozone

***Definition:*** the stratigraphic range of the *Assilina cancellata* defines the base and top of this biozone.

***Associated assemblages:*** the larger benthic foraminifera *Nummulites perforatus, Nummulites mamilla, Assilina subspinosa, Assilina pappilata,, Assilina subpappilata, Operculina petalensis, Operculina bermudezi, Alveolinia elliptica* and *Alveolina periloculinoids* range through this zone.

## 4.6 Biostratigraphic correlation of the studied sections

The biostratigraphic ranges of the larger benthic foraminiferal species, recorded from the Paleogene rocks of the Kohat Basin, are plotted in figures 4.3-4.6. In this study the stratigraphic ranges of *Miscellanea miscella, Ranikothalia sindensis, Assilina granulosa, Assilina aff. putulosa, Assilina putulosa, Assilina laxispira, Assilina pappilata, Assilina exponense, Assilina cancellata, Nummulites globulus, Nummulites atacicus, Nummulites planulatus, Nummulites beaumonti*, *Nummulites acutus, Alveolina rotundata* and *Orbitolites complanatus* are useful in establishing the biozonal boundaries. The biostratigraphic correlation across the studied sections is summarized in figure 4.7 and described as following.

The first synchronous occurrence of *Miscellanea miscella, Ranikothanlia sindensis* species in the BFZK 1 (A) Biozone (representing Thanitian age) is recorded at the base of the Patala Formation in the Panoba Nala and the Tarkhobi Nala Sections while the top is recorded at 24m above the base of the Patala Formation in the Panoba Nala Section and 78m above the base of the Patala Formation in the Tarkhobi Nala Section. This Biozone is restricted to the Panoba Nala and the Tarkhobi Nala Sections.

The first occurrence of *Assilina granulosa* species in the BFZK 1 (B) Biozone (representing lower Lllerdian 1 age) is recorded at a stratigraphic level 16 m above the base of the Panoba Formation in the Sheikhan Nala Section, 24m above the base of the Patala Formation in the Panoba Nala Section and 78 m above the base of the Patala Formation in the Tarkhobi Nala Section respectively. The first synchronous occurrences of *Assilina aff. putulosa*/*Assilina putulosa,* which mark the upper boundary of the BFZK 1 (B) Biozone and by definition the lower boundary of the BFZK 2 Biozone (representing lower Lllerdian 2-Middle Lllerdian 1 age) are recorded at a stratigraphic level 2m below the base of the Sheikhan Formation in the Sheikhan Nala Section and 4m above the base of the Sheikhan Formation in the Panoba Nala Section, and at 8m below the base of the Sheikhan Formation in the Tarkhobi Nala Section respectively (figure 4.7). The synchronous first occurrences of *Nummulites globulus* and *Nummulites atacicus*, which mark the upper boundary of the BFZK 2 Biozone and by definiition the lower boundary of the BFZK 3 (A) Biozone (representing Middle Lllerdian 2) are recorded at the stratigraphic level 13m

above the base of the Sheikhan Formation in the Sheikhan Nala Section, 24m above the base of the Sheikhan Formation in the Panoba Nala Section and 22m above the base of the Sheikhan Formation in the Tarkhobi Nala Section respectively. The upper boundary of the BFZK 3 (A) Biozone is recorded at 22m, 23m, and 24m below the top of the Sheikhan Formation in the Sheikhan Nala Section, the Panoba Nala Section and the Tarkhobi Nala Section repesctively. The lower boundary of the BFZK 3 (B) biozone by definition is same as the upper boundary of the BFZK 3 (A) Biozone. The upper boundary of the BFZK 3 (B) Biozone and the lower boundary of the BFZK 4 Biozone are not defined due to the deposition of evaporitic and fluvial facies above the platform carbonates of the Sheikhan Formation. Lack of larger benthic foraminifera in the evaporitic facies (Bahadur Khel Salt, Jatta Gypsum) in the south-western part (Bahadur Khel Salt Tunnel Section) and fluvial facies (Kuldana Formation red beds in the Sheikhan Nala, the Panoba Nala and Bahadurkhel Salt Tunnel Sections) in the Kohat Basin hinders biostratigraphic correlation of the BFZK1- BFZK3 (B) Biozones between platform and marginal marine sections (figure 4.7).

The first synchronous occurrences of *Nummulites beaumonti*, *Nummulites acutus* and *Assilina pappilata* which mark the lower boundary of the BFZK 4 Biozone (representing Middle Lutetian 1 age), are recorded at the base of the Kohat Formation in the Sheikhan Nala Section. The first occurrence of *Assilina exponense* marks the upper boundary of the BFZK 4 Biozone and by definition the lower boundary of the BFZK 5 Biozone (representing Middle Lutetian 2 age). It is recorded at a stratigraphic level 31m above the base of the Kohat Formation in the Sheikhan Nala Section, while it is not identified in the Panoba, the Tarkhobi and the Bahadur Khel Salt Tunnel Sections. The first occurrence of *Assilina cancellata*, that marks the upper boundary of the BFZK 5 Biozone and by definition the lower boundary of the BFZK 6 Biozone (representing Upper Lutetian age) is recorded at a stratigraphic level 25m below the top of the Kohat Formation in the Sheikhan Nala Section, at the base of the Kohat Formation in the Panoba Nala and the Bahdur Khel Salt Tunnel Sections and the top is taken at the top of the Kohat Formation in the Sheikhan, the Panoba and the Bahadur Khel Salt Tunnel Sections (figure 4.7).

## 4.7 Comparison and discussion

The BFZK 1 Biozone is equivalent to the Eames Biozone 2 (1950), *Assilina prisca* Zone of Schaub (1981), *Alveolinia cucumiformis* Zone of Höttinger (1960) and the SBZ 5 Zone of Serra Kiel et al. (1998). The Eames (1950) local biozones for the Eocene rocks in the Kohat basin don't provide realistic ranges of benthic foraminiferal species and are rectified here. For instance, the top of the local Biozone 2 is not clear, because (i.e. in the north-eastern part of the Kohat Basin in the Sheikhan Nala Section) it included beds where no diagnostic fossils are present. In the present study *Nummulites thalicus*, *Assilina putulosa* and several other Early Eocene age diagnostic smaller benthic foraminifers characterize this biozone.

Racey (1995), while comparing the Tertiary foraminifera of Oman with the nummulitid zonal scheme of Schaub (1981) regarded *Assilina granulosa* as a synonym of *Assilina laxispira* of middle – upper Cuisian age. When his illustration of *Assilina laxispira* ( plate 9, figure 11-16 in Racey, 1995) is compared with the *Assilina granulosa* in the Kohat Basin (in Chapter 3, Plate 6, figure 5-10) it is clear that *Assilina granulosa* is different from *Assilina laxispira* species. In this study *Assilina granulosa* is considered as a distinct species and is regarded as the microspheric generation (Form-B) of *Assilina leymerie* (Davies, 1940; Gill, 1953). In the study area the stratigraphic range of *Assilina granulosa* (Form-B of *Assilina leymerie*) is Lower Lllerdian 1 to the Middle Lutetian 2 (figure 4.9).

According to the stratigraphic ranges of *Assilina aff putulosa* and *Assilina putulosa* (figure 4.10 c) (Schaub, 1981) the BFZK 2 Biozone is equivalent to the *Assilina arenensis* and *Assilina aff. arenensis* Zone of Schaub (1981), *Alveolina ellipsoidalis* Zone of Höttinger (1960), the SBZ 6 and 7 Zones of Serra Kiel et al. (1998), and the Eames Biozone 3a (1950) (figure 4.8). In this study *Assilina aff. pustulosa* is considered a synonym of *Assilina davisie* de Cizancourt and *Assilina putulosa* a synonym of *Assilina davisie* de Cizancourt var. *nammalensis* described by Gill (1953) from the Upper Indus Basin of Pakistan. Both species represent a lineage zone in which *Assilina aff. putulosa* appeared in Lower Lllerdian 2 as ancestor followed by *Assilina putulosa* that ranges through Middle Lllerdian 1-Middle Lllerdian 2 in the Kohat Basin (figure 4.9).

The BFZK 3 (A) Biozone is equivalent to the *Nummulites globulus* Zone of Schaub (1981), *Alveolina carbarica* Zone of Höttinger (1960), the SBZ 8 Zone of Serra Kiel et al. (1998) and Eames Biozone 3a and 3b (1950) (figure 4.8). The usefulness of this biozone can be tested not only in the Kohat Basin but can also be satisfactorily tested in adjacent areas. Schaub (1981) considered that *Nummulites globulus* ranges from Middle Lllerdian 2 to Early-Late Lllerdian and is a zonal marker for the Middle Lllerdian 2. However in the Kohat Basin, it has an extended range because it was found also in the Middle Lutetian 2 age rocks together with its megalospheric generation (Form-A) which is known as *Nummulites mamilla*. Similarly Blondeau (1972) extended its range to Late Cuisian; Racey (1995) extended its range to Lower Cuisian in Tertiary rocks of Oman. However the stratigraphic range of associated *Nummulites atacicus* in Schaub (1981) (figure 4.10 A-B) confirms a Middle Lllerdian 2 age (figures 4.8-4.9) for this biozone while the upper boundary of this biozone is diachronous worldwide.

The species of *Alveolina rotundata* appears in the BFZK 3 (B) Biozone along with *Assilina laxispira* and *Orbitolites complanatus* in a condensed section found in the upper part of the Sheikhan Formation. The *Alveolina rotundata* represents SBZ 9, *Assilina laxispira* represents SBZ 10 and *Orbitolites complantas* is found in SBZ 11-12 (Serra Kiel et al., 1998). The BFZK 3 (B) is interpreted as a condensed horizon where telescoping of sediments caused mixing of the diachronous species. The minimum and maximum age constraints of these species indicate that BFZK (B) Biozone represents Upper Lllerdian–Middle Cuisian age.

According to the stratigraphic ranges of *Nummulites beaumonti* and *Assilina pappilata* in Schaub (1981) (figure 4.10 B) the BFZK 4 Biozone is equivalent to the upper part of the *Assilina spira spira* Zone of Schaub (1981), *Alveolina munierie* Zone of Höttinger (1960), the SBZ 14 Zone of Serra Kiel et al.(1998) and the Eames Biozone 4a (1950) (figure 4.8).

According to the stratigraphic range of *Assilina exponense* in Schaub (1981) (figure 4.10 C), the BFZK 5 Biozone is equivalent to the *Assilina planospira* Zone of Schaub (1981), *Alveolina proerecta* Zone of Höttinger (1960), the SBZ 15 Zone of Serra Kiel et al. (1998) and the Eames Biozone 4a and 4b (1950).

According to the stratigraphic range of *Assilina cancellata* in Schaub (1981) (figure 4.10 C), the BFZK 6 Biozone is equivalent to the *Assilina giagantea* Zone of Schaub (1981), the SBZ 16 Zone of Serra Kiel et al. (1998) and the Eames Biozone 4a and 4b (1950*)* (figure 4.8). Eames (1950) defined a boundary between his local subzone 4a and 4b on the basis of simultaneous presence of *Assilina cancellata* and *Assilina subcancellata,* while in the present study it is found that *Assilina subcancellata* is the Form-A of *Assilina cancellata*; they were present together throughout this zone.

## 4.8 Summary and conclusions

In this study four stratigraphic sections are selected for detailed foraminiferal biostratigraphic analysis of the Paleogene rocks of the Kohat Basin, north-west Pakistan. These sections lie in the north-east (the Panoba, the Tarkhobi and the Sheikhan Nala Sections) to south-west (the Bahurkhel Salt Tunnel Section). These sections provide a complete picture of the different facies from margin to the deepest part of the basin. Fifty one larger and forty four smaller benthic foraminiferal species are identified (details are in Chapter 3) that provide a biostratigraphic framework through which the Paleogene rocks of the Kohat Basin can be correlated.

The following conclusions are drawn from this study.

- The Early Eocene (Laki age) sediments of the Upper Patala, the Panoba and the Sheikhan Formations and Upper Middle Eocene (Upper-Middle Kirthar age) sediments of the Kohat Formation are marine in nature. The larger benthic foraminifera allow development of a local biozonation scheme.
- The stratigraphic range distributions of *Miscellanea miscella, Ranikothalila sindenis, Alveolina rotundata, Orbitolites complanatus, Assilina aff pustula, Assilina putulosa, Assilina laxispira, Nummulites atacicus, Nummulites globulus, Nummulites planulatus, Nummulites beoumonti, Assilina pappilata, Assilina exponense,* and *Assilina cancellata* species provide sound basis for establishing biozonal boundaries. The local larger benthic foraminiferal biozones of the Kohat Basin are named as BFZK 1- BFZK 6 and compared

with the nummulitid Biozones of Schaub (1981), alveolinid biozones of Höttinger (1960), SBZ Biozones of Serra Kiel et al. (1998) and Eames local Biozones (1950).

- The BFZK 1 (A) Biozone (representing Thanitian age) is recorded in the lower-middle part of the Patala Formation. It is equivalent to the SBZ 3 Zone of Serra Kiel et al. (1998)
- The BFZK 1 Biozone (representing Lower Lllerdian 1 age) is recorded from the upper part of the Patala Formation and extends up section to the top of the Panoba Formation. It is equivalent to the *Assilina prisca* Zone of Schaub (1981), *Alveolinia cucumiformis* Zone of Höttinger (1960) and the SBZ 4- 5 Zone of Serra Kiel et al. (1998) and the Eames Biozone 2.
- The BFZK 2 Biozone (representing Lower Lllerdian 2-Middle Lllerdian 1 age) is recorded from the top most part of the Panoba Formation. According to the stratigraphic ranges of *Assilina aff pustulosa* and *Assilina pustulosa* (Schaub, 1981) this zone is equivalent to the *Alveolina ellipsoidalis* Zone of Höttinger (1960), *Assilina arenensis* and *Assilina aff. arenensis* Zone of Schaub (1981), the SBZ 6 and 7 Zones of Serra Kiel et al. (1998) and the Eames Biozone 3a (1950).
- The BFZK 3 (A) Biozone (representing Middle Illerdian 2 age) was recorded in the middle part of the Sheikhan Formation.This biozone is equivalent to the *Nummulites globulus* Zone of Schaub (1981), the *Alveolina carbarica* Zone of Höttinger (1960), the SBZ 8 Zone of Serra Kiel et al. (1998) and the Eames Biozone 3a and 3b (1950).
- The BFZK 3 (B) Biozone (representing Upper Lllerdian-Middle Cuisian age) was recoded in the condensed section found in the upper part of the Sheikhan Formation. This biozone is equivalent to the SBZ 9-11 Zones of Serra Kiel et al (1998) and the Eames Biozone 3 b (1950).
- The BFZK 4 Biozone (representing Middle Lutetian 1 age) is recorded from the lower-middle part of the Kohat Formation. According to the stratigraphic ranges of *Nummulites beaumonti* and *Assilina pappilata* in Schaub (1981) (figure 4.10 A-B) this biozone is equivalent to the upper part of the *Assilina*

*spira spira* Zone of Schaub (1981), the *Alveolina munierie* Zone of Höttinger (1960), the SBZ Zone 14 of Serra Kiel et al. (1998) and the Eames Biozone 4a (1950).

- The BFZK 5 Biozone (representing Middle Lutetian 2 age) is recorded from the upper middle part of the Kohat Formation. According to the stratigraphic range of *Assilina exponense* in Schaub (1981) (figure 4.10 C), this biozone is equivalent to the *Assilina planospira* Zone of Schaub (1981), the *Alveolina proerecta* Zone of Höttinger (1960), the SBZ 15 Zone of Serra Kiel et al., (1988) and the Eames Biozone 4a and 4b (1950).
- The BFZK 6 Biozone (representing Upper Lutetian age) is recorded from the upper part of the Kohat Formation, and it is equivalent to the *Assilina giagantea* Zone of Schaub (1981), the SBZ 16 Biozone of Serra Kiel et al. (1998) and the Eames Biozone 4a and 4b (1950)
- In the north-eastern part of the Kohat Basin in the Sheikan Nala Section all biozones (BFK1-BFK6) are identified while in the Panoba Nala Section the BFKZ 4 and 5 Biozones are missing, representing a break in sedimentation from Upper Lllerdian-Middle Lutetian 2. In the Tarkhobi Nala Section only three biozones BFZK 1-BFZK 3 (B) are identified.
- The upper boundary of the Biozone BFZK 3 (B) and lower boundary of the Biozone BFZK 4 are not defined due to the period of regression and deposition of evaporitic and continental red beds facies (representing Upper Illerdian- Lower Lutetian 2 age) in all parts of the Kohat Basin.
- The Upper Kirthar (Upper Middle Eocene) age fauna is seen in the studied sections.
- The proposed zonal scheme provides a framework for regional correlation of Paleogene rocks and is open for further contribution and refinements.

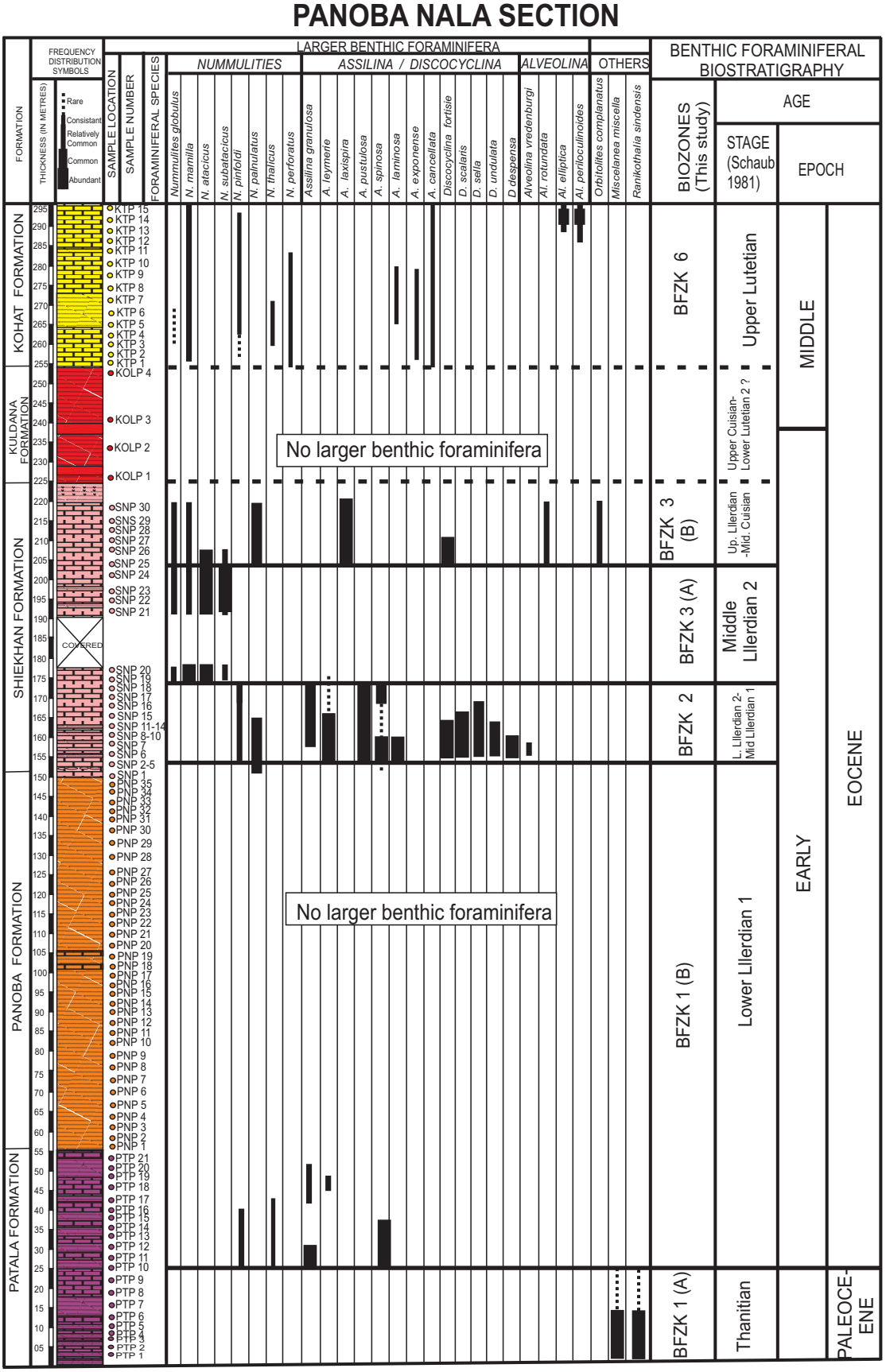


**Figure 4.3.** Range distribution and biostratigraphic chart of the larger benthic foraminifera in Paleogene rocks of the Panoba Nala Section, Kohat Basin, northwest Pakistan.

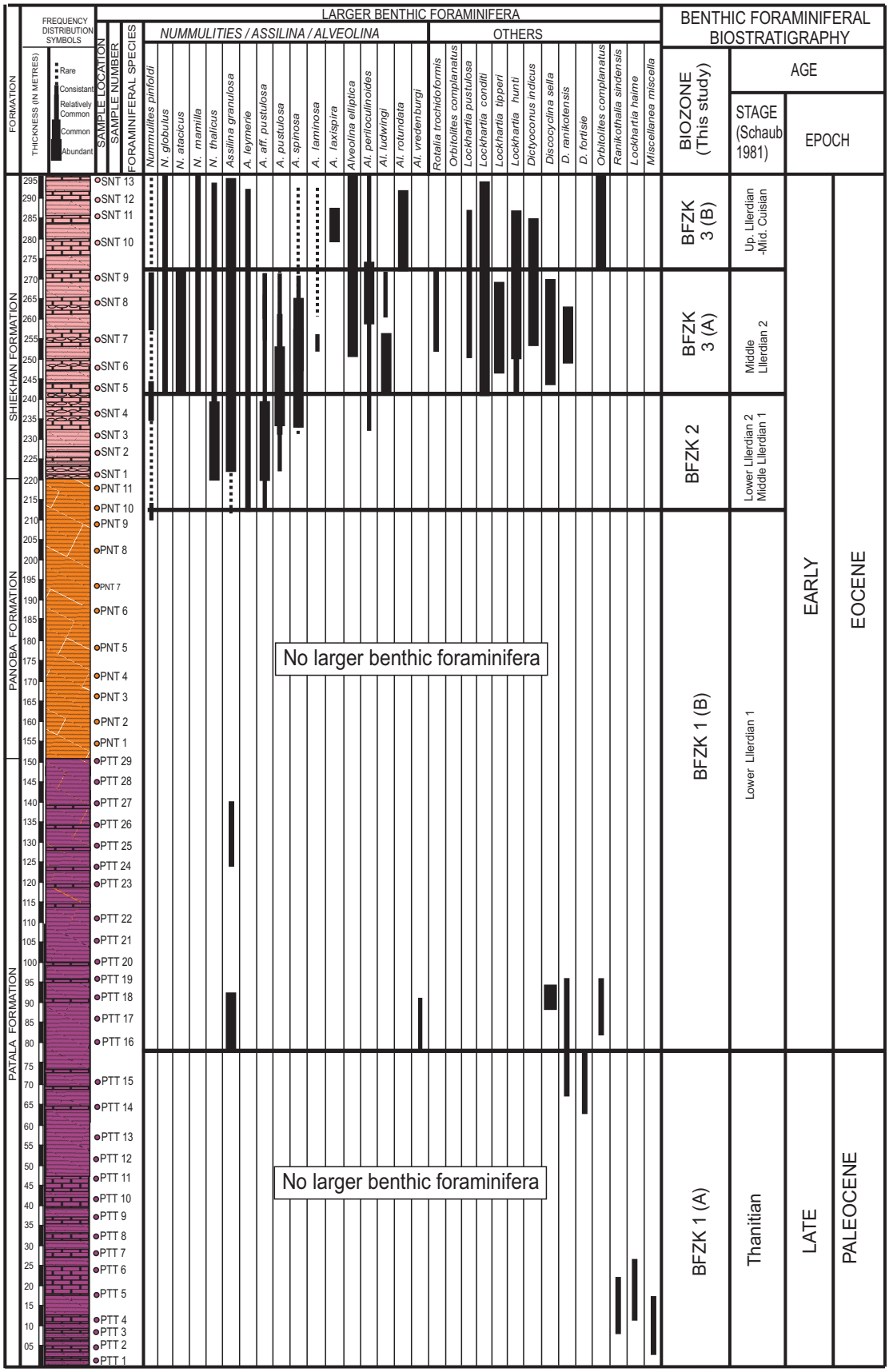


**Figure 4.4.** Range distribution and biostratigraphic chart of the larger benthic foraminifera in Paleogene rocks of the Tarkhobi Nala Section, Kohat Basin, northwest Pakistan.

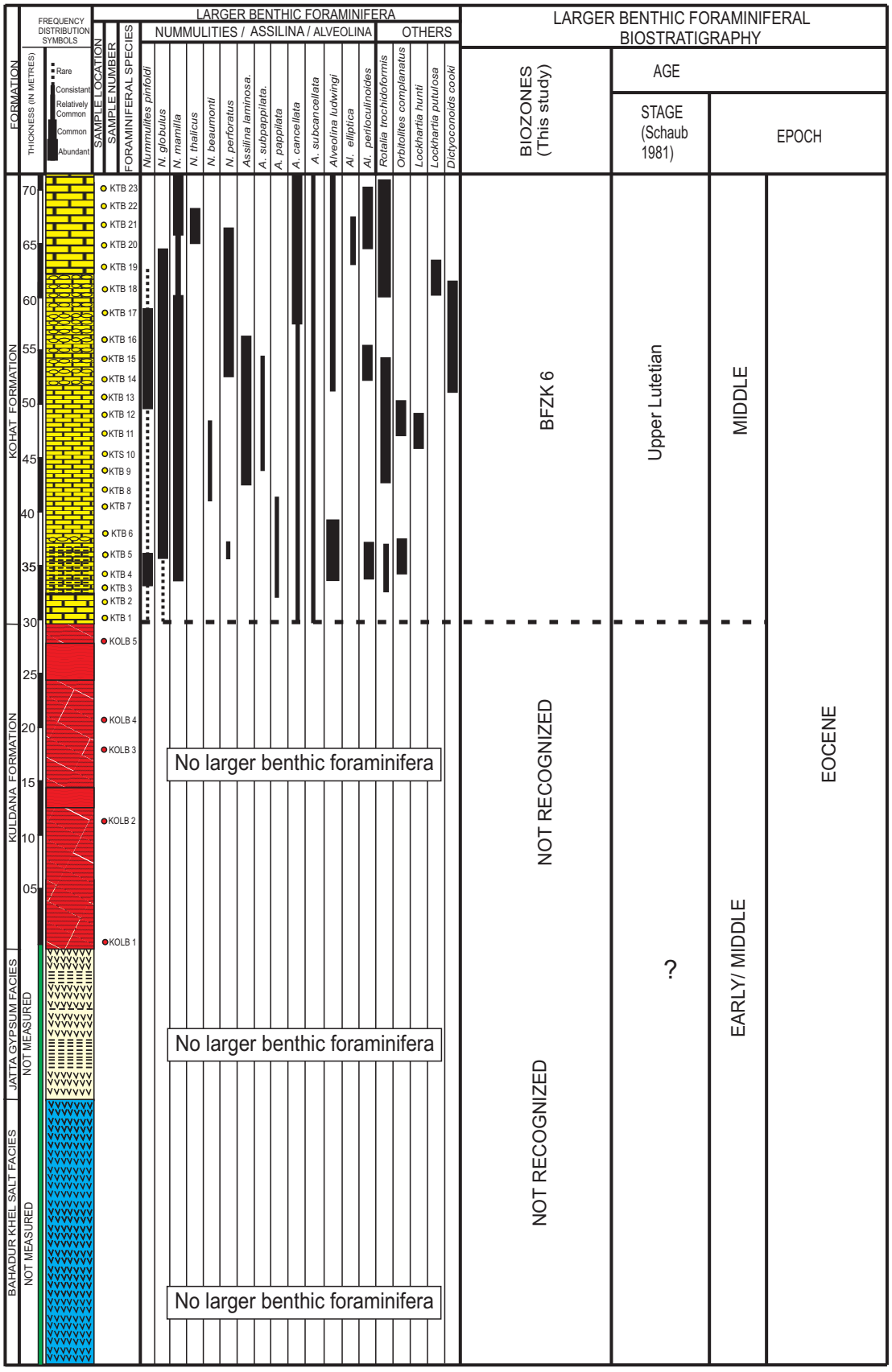


**Figure 4.6.** Range distribution and biostratigraphic chart of the larger benthic foraminifera in Eocene rocks of the Bahadur Khel Salt Tunnel Section, Kohat Basin, northwest Pakistan.

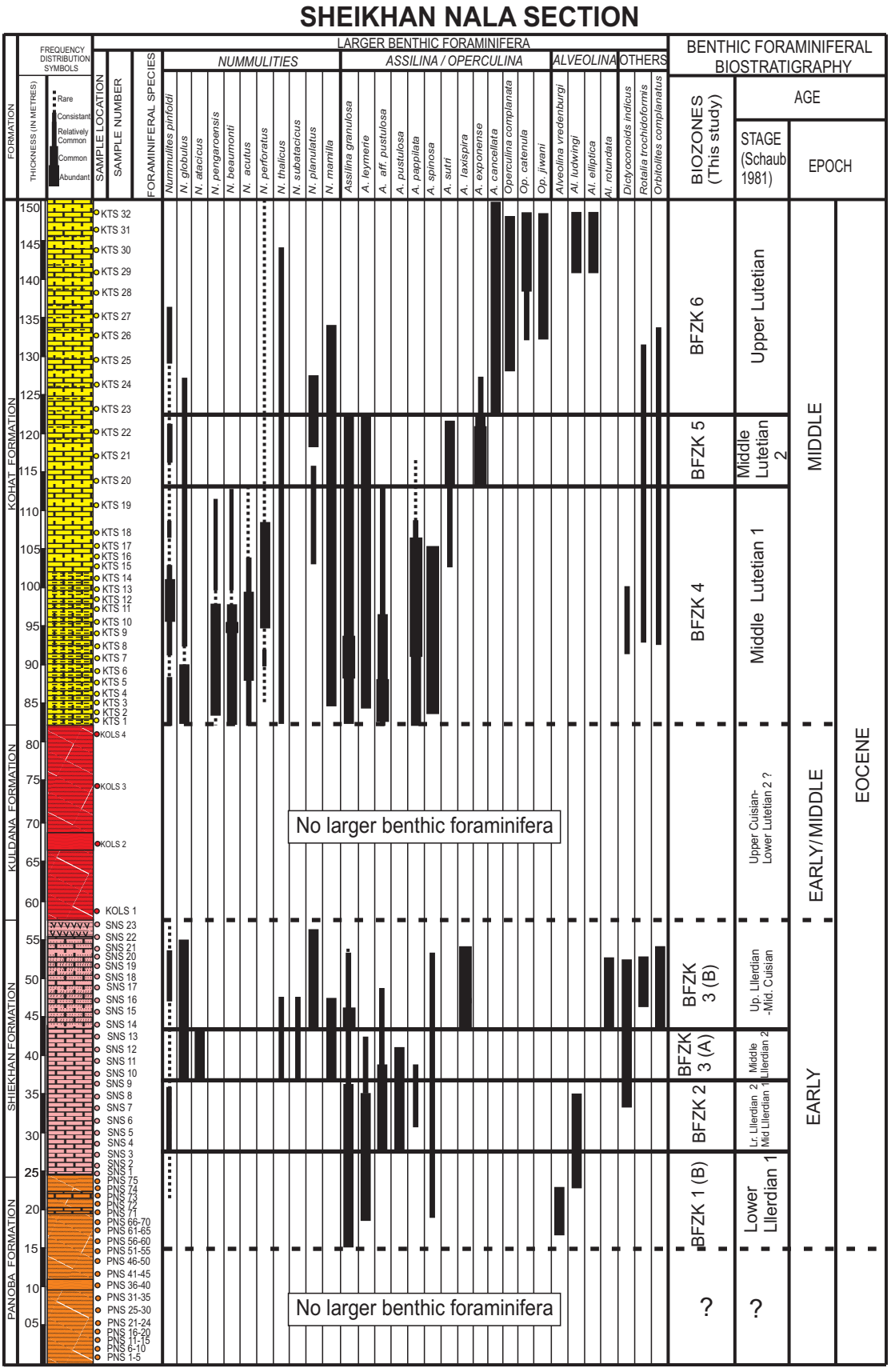


**Figure 4.5.** Range distribution and biostratigraphic chart of the larger benthic foraminifera in Eocene rocks of the Sheikhan Nala Section, Kohat Basin, northwest Pakistan.

# Biostratigraphic correlation chart of the Kohat Basin

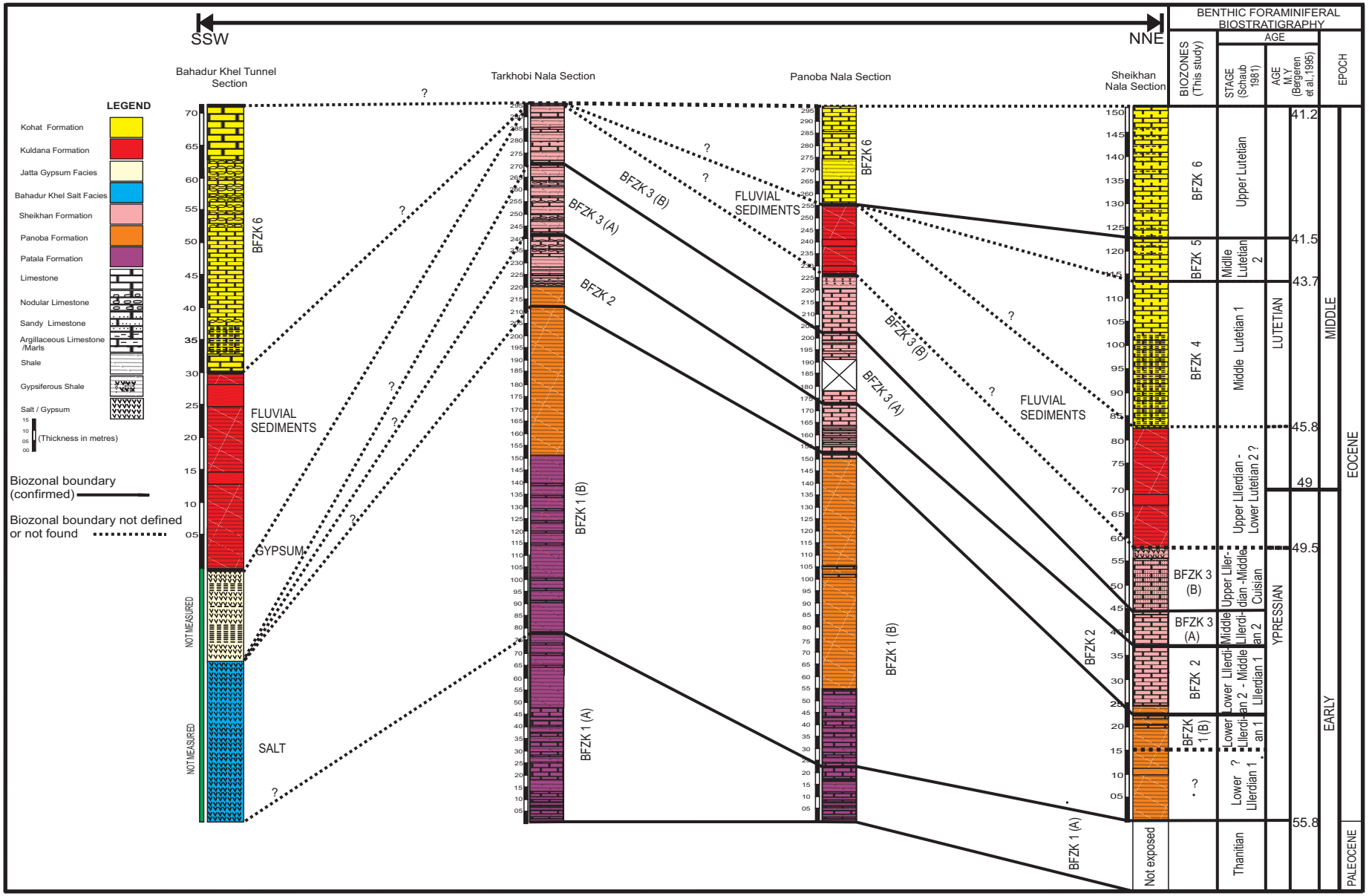


**Figure 4.7.** Biostratigraphic correlation of the Paleogene rocks in studied sections of the Kohat Basin, northwest Pakistan.

## Biostratigraphic comparison chart of the Kohat Basin

| EPOCH | | STAGE (Holland et al., 1978) | STAGE (Schaub, 1981) | | Nummulitid Biozone (Schaub, 1981): Nummulities brogniatri group | Nummulitid Biozone (Schaub, 1981): Nummulities perforatus group | Nummulitid Biozone (Schaub, 1981): Nummulities others group | Nummulitid Biozone (Schaub, 1981): Assilina | Alveolinid Biozone (after Hottinger, 1960) | SBZ (after Serra Kiel et al., 1998) | (Eames Biozones, 1950) | Biozone (This study) | Plankton and Nannoplankton Zones (Cavalier & Pomerol, 1985) | | (Harland et al., 1989) |
|---|---|---|---|---|---|---|---|---|---|---|---|---|---|---|---|
| OLIGO-CENE | Lower | Repelian | Stampian | | | | *fichteli* | | | | | Not Recognized (Regressive facies) | P 18 | | P17 |
| EOCENE | Upper | Priabonian | Priabonian | | | | *fabianii* | | *Neoalveolina* | SBZ 19 | | | P 17<br>P 14 | | |
| | Middle | Bartonian | Biarritzian | | *brogniatri* | *perforatus* | *ptukhiani* | | *elongata* | SBZ 18<br>SBZ 17 | | | P 15 | | P13<br>P12 |
| | | Lutetian | Lutetian | U | *herbi* | *atauricus* | *bullatus* | *giagantea* | | SBZ 16 | 4a and 4b | BFZK 6 | | | |
| | | | | M 2 | *sordensis* | *crasus* | | *planospira* | *proerecta* | SBZ 15 | | BFZK 5 | | | |
| | | | | M 1 | *gratus* | *beneharnensis* | | *spira spira* | *munierie* | SBZ 14 | | BFZK 4 | | | |
| | | | | L 2 | *laevigatus* | *obesus* | | *spira abradi* | *stipes* | SBZ 13 | | Not Recognized (Regressive facies) | P 10 | NP15 | P10 |
| | | | | L 1 | | *gallensis* | | | | | | | | | |
| | Lower | Ypresian | Cuisian | U | *manfredi* | *campesinus* | *formosus* | *major* | *violae* | SBZ 12 | | | P 9 | NP14 | P9 |
| | | | | M | *praelaevigatus* | *burd. cantabricus* | *nitidus* | *laxispira* | *dainelli* | SBZ 11 | | | | | |
| | | | | L 2 | *planulatus* | *burdigalensis burdigalensis* | *aff. laxus* | *plana* | *oblonga* | SBZ 10 | | BFZK 3 (B) | | | |
| | | | | L 1 | | | | | | | | | | | |
| | | | Llerdian | U | *involutus* | *pernotus* | *laxus* | *adrianensis* | *trempina* | SBZ 9 | | | | | |
| | | | | M 2 | *exilis* | | *globulus* | *leymeriei* | *carbarica* | SBZ 8 | 3 a and 3b | BFZK 3 (A) | | | |
| | | | | M 1 | *robustiformis* | | *minervensis* | *Assilina aff arenensis* | *moussoulensis* | SBZ 7 | | BFZK 2 | | | P6 |
| | | | | L 2 | *frassi* | | | *Assilina arenensis* | *ellipsoidalis* | SBZ 6 | | | | | |
| | | | | L 1 | | | *deserti* | *Assilna prisca* | *cucumiformis* | SBZ 5 | | BFZK 1 (B) | P5 | NP9 | |
| PALAEOCENE | Upper | Thanetian | Thanetian | | | | | | | | | BFZK 1 (A) | P4 | NP8 | P3 |
| | | | | | | | | | | | | | P3b | | |
| | Low | Danian | Danian | | | | | | | | | | P3a | | P2 |

**Figure 4.8.** Comparison of larger benthic foraminiferal biostratigraphic zonation of the Eocene rocks of the Kohat Basin with Nummulitids Biozones of Schaub 1981, Alveolinid Biozones of Hottinger (1960), SBZ Biozone of Sierra Kiel et al. (1998) and Eames Biozones (1950).

# Foraminiferal stratigraphic range distribution chart of the Kohat Basin

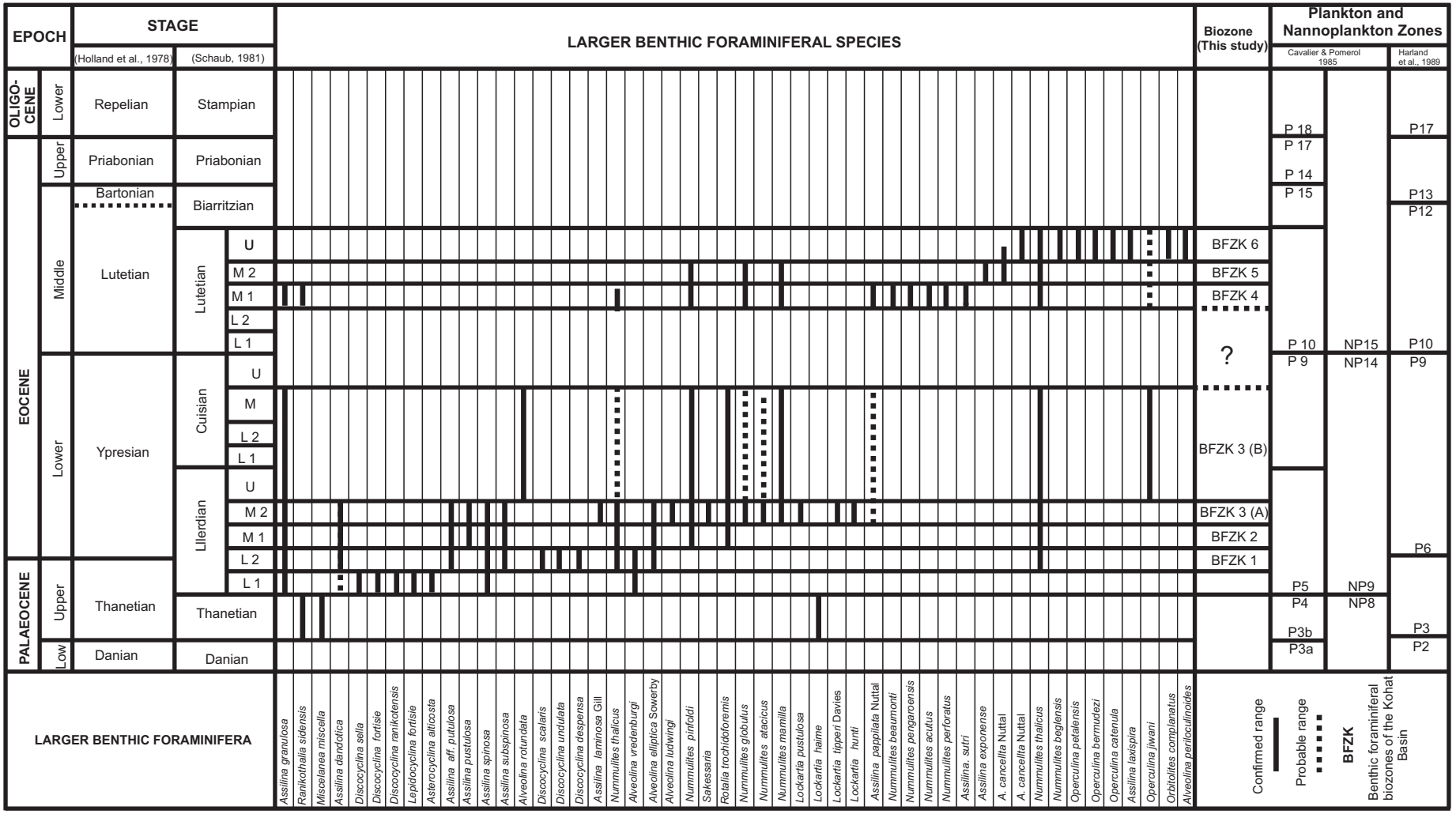


**Figure 4.9** Stratigraphic range of the important larger benthic foraminifera in Paleogene rocks of the Kohat Basin.

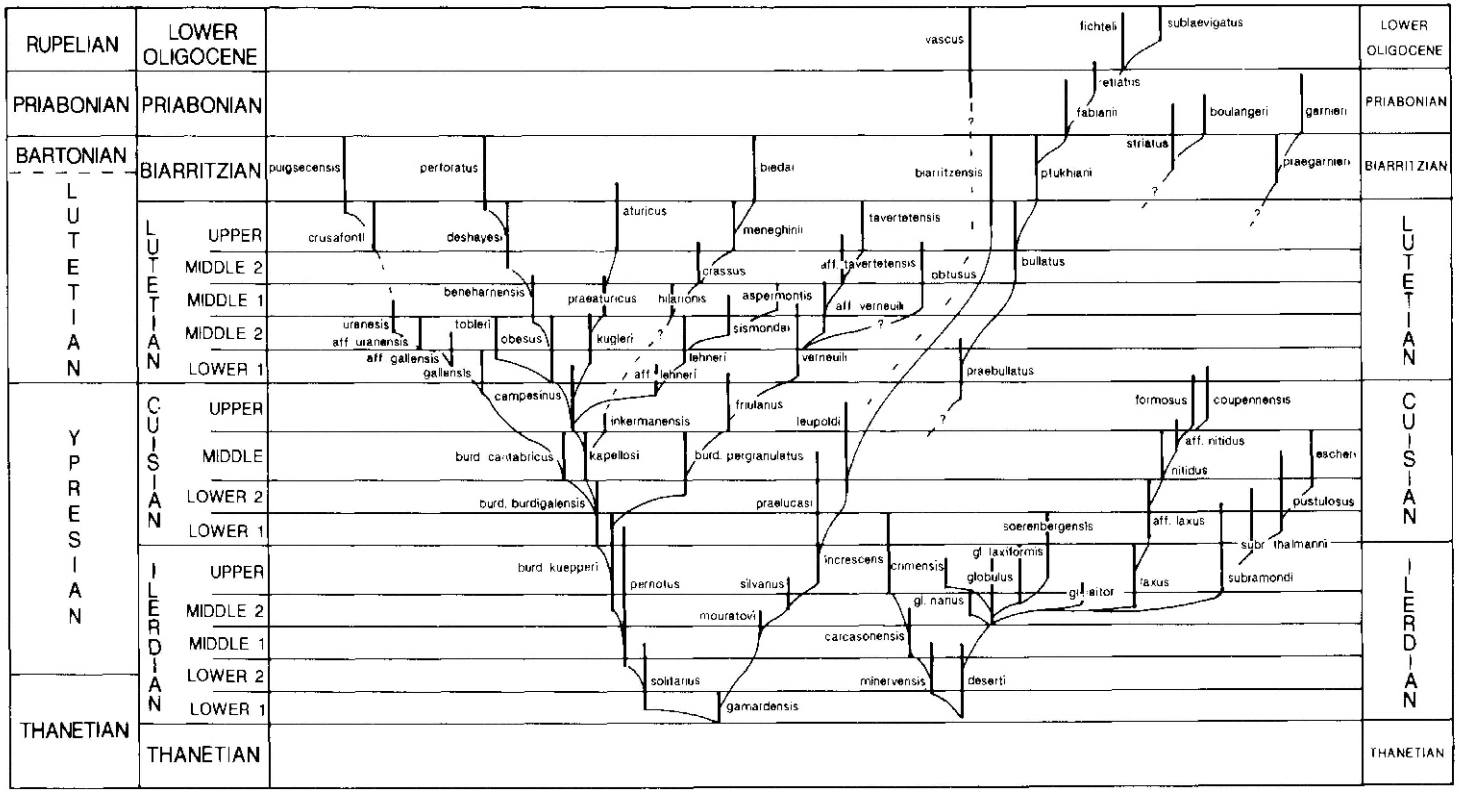


**Figure 4.10 (A).** Stratigraphic ranges of different *Nummulites* species lineages (after Schaub, 1981)

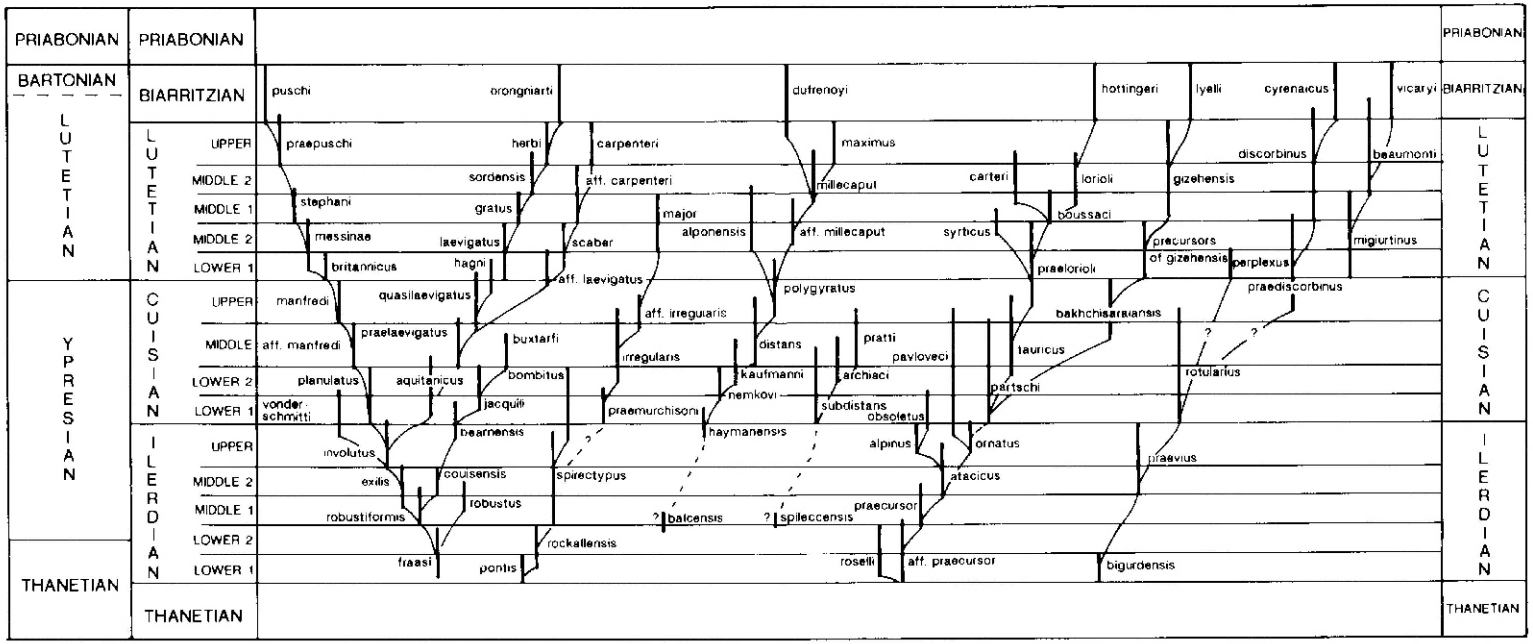


**Figure 4.10 (B).** Stratigraphic ranges of different *Nummulites* species lineages (after Schaub, 1981)

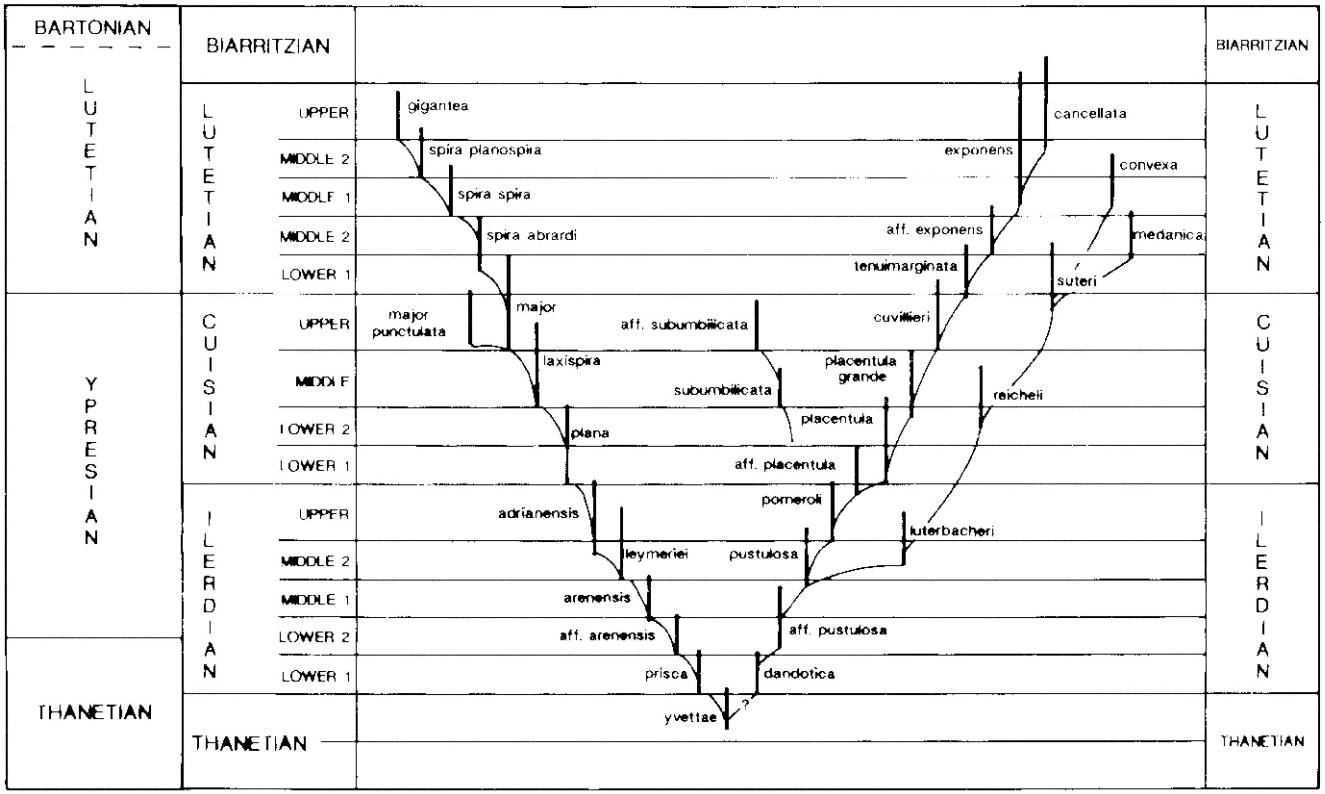


**Figure 4.10 (C).** Stratigraphic ranges of different *Assilina* species lineages (after Schaub, 1981)

# Chapter 5

# 5. Larger benthic foraminiferal biostratigraphy of the Potwar Basin and Trans Indus Ranges (TIR)

## 5.1 Previous work

The work of Afzal (1998, and references therein) represents the most comprehensive investigation of larger benthic foraminiferal biostratigraphy of the Patala and Nammal Formations in the Potwar Basin, specifically in the Salt Range area. The Lower Eocene Sakessar and Chorgali Formations have not been investigated yet in most parts of the Potwar Basin and the Trans Indus Ranges (TIR).

The aim of the present investigation is to refine the existing biozonation for the Patala and Nammal Formations in the two new stratigraphic sections, i.e. in the Ziarat Thati Sharif and Kalabagh Hill Sections, and to develop a biozonation for the Sakessar and Chorgali Formations in the Potwar Basin and the TIR.

## 5.2 Present work

In the present study the Paleogene rocks of the Potwar Basin and the TIR are revisited for comprehensive documentation of the larger benthic foraminiferal distribution in the Gharibwal Cement Factory Section, the Sikki Village Section (in the Eastern Salt Range), the Ziarat Thatti Sharif Section (in the Western Salt Range), the Nammal Gorge Section (in the Central Salt Range), the Kalabagh Hills Section and the Chichali Nala Section (in the Trans Indus Ranges).

A total of 336 outcrop samples (see table 1.1) were analysed. Four Paleogene larger benthic foraminiferal biozones are established for the Potwar Basin and the TIR. These biozones are abbreviated as BFZP (Larger Benthic Foraminiferal Zones of the Potwar Basin and TIR). In this chapter larger benthic foraminiferal range distribution, abundance and biozonation (figure 5.1-5.6), and a biostratigraphic correlation chart of the studied sections (figure 5.7) are presented. A biostratigraphic comparison with earlier biozonal schemes is discussed and a biostratigraphic correlation between sections of the Kohat and Potwar Basins is proposed (figure 5.8).

## 5.3 Biostratigraphy

In this study three assemblage range biozones BFZP 1 - BFZP 3 (A) and one taxa range biozone BFZP 3 (B) is identified and described as following.

### 5.3.1 BFZP 1 Biozone

***Definition**:* the base of this biozone is taken at the first occurrence of *Ranikothalia sindensis* and the top is taken at the synchronous first occurrences of *Assilina dandotica* and *Discocyclina despensa.*

***Associated assemblages*:** the larger benthic foraminifera that range through this zone include *Miscellanea miscella, Lockhartia haime, Lockhartia hunti, Lockhartia newboldi, Miscellanea stampi, Operculina salsa, Operculina subsalsa, Operculina petalensis, Discocyclina ranikotensis, Discocyclina seunesi, Operculina petalensis, Assilina spinosa, Nummulites thalicus* and *Nummulites pinfoldi*.

**Age**: this biozone is Upper Thanitian

### 5.3.2 BFZP 2 Biozone

***Definition**:* the base of this biozone is defined by the synchronous first occurrences of *Assilina dandotica*, *Alveolina vredenburgi, Alveolina globula, Alveolina pasticilata* and *Discocyclina despena,* while the top is defined by the simultaneous first occurrences of *Assilina aff. pustulosa*, *Assilina putulosa*, *Ranikothalia sahini*, *Nummulites planulatus, Nummulites atacicus* and *Nummulites globulus.*

***Associated assemblages:*** the larger benthic foraminifera that range through this zone are *Nummulites thalicus, Alveolina pasticilata, Alveolina conradi, Alveolina elliptica, Lockhartia conica, Lockhartia conditi, Lockhartia hunti, Assilina spinosa, Assilina laminosa, Operculian salsa, Operculina subsalsa, Discocyclina ranikotensis, Operculina petalensis* and *Ranikothalia nuttali.*

**Age:** this biozone is Lower Lllerdian 1 - Middle Lllerdian 1

### 5.3.3 BFZP 3 (A) Biozone

***Definition:*** the base of this biozone is taken at the synchronous first occurrences of *Nummulites atacicus, Nummulites globulus, Assilina pustulosa, Assilina leymerie*, *Assilina granulosa, Discocyclina scalaris, Discocyclina sella* and *Discocyclina*

*undulata* while the top of this biozone is defined by the last occurrences of *Alveolina globula and Alveolina pasticilata.*

***Associated assemblages:*** the larger benthic foraminifera that range through this zone include *Ranikothalia sahini, Ranikothalia nuttali*, *Nummulites thalicus, Nummulites lahiri, Nummulites pinfoldi, Assilina spinosa, Assilina laminosa*, *Sakessaria cottorie, Rotalia trochidoformis, Discocyclina fortisie, Discocyclina scalaris, Lockhatia conditi, Lockhartia hunti, Lockhartia conica,* and *Operculina petalensis*.

***Age:*** this biozone is Middle Lllerdian 2.

### 5.3.4 Biozone BFZP 3 (B)

***Definition:*** the base of this biozone is taken at the first occurrence of *Alveolina rotundata* and the top is taken at the last occurrences of the *Assilina laxispira* and *Orbitolites complanatus.*

***Associated assemblages:*** the larger benthic foraminifera that range through this zone include*, Lockhartia hunti, Lockhartia tipperi, Lockhartia conditi, Discocyclina undulata, Assilina spinosa, Assilina laminosa* and *Rotalia trochidoformis*.

***Age:*** this biozone is Upper Lllerdian to Middle Cuisian.

## 5.4 Biostratigraphic correlation of the studied sections

In the present study the stratigraphic ranges of *Ranikothalia sindensis*, *Assilina dandotica, Assilina granulosa, Assilina leymerie, Assilina aff. putulosa, Assilina putulosa, Assilina laxispira, Nummulites globulus, Nummulites atacicus, Discocyclina despensa, Discocyclina sella, Discocyclina scalaris, Alveolina vredenburgi, Alveolina globula, Alveolina pasticilata* and *Alveolina rotundata* were found useful in establishing the biozonal boundaries. A biostratigraphic correlation across the studied sections in the Potwar Basin and the TIR is summarized in figure 5.7 and described as below.

The first occurrence of *Ranikothalia sindensis* in association with *Miscellanea miscell*a and *Lockhartia haime* in the BFZP 1 Biozone (representing

Upper Thanitian) is recorded at the base of the Lockhart Formation in the Chichali Nala, Nammal Gorge, Ziarat Thatti Sharif, Kalabagh Hills and the Sikki Village Sections. The first synchronous occurrences of *Assilina dandotica*, *Alveolina vredenburgi, Alveolina globula, Alveolina pasticilata* and *Discocyclina despensa* mark the upper boundary of the BFZP 1 Biozone and by definition lower boundary of the BFZP 2 Biozone (representing Lower Lllerdian 1- Middle Lllerdian 1). These species are recorded at a stratigraphic level 35m above the base of the Patala Formation in the Chichali Nala Section, at 25m above the base of the Patala Formation in the Nammal Gorge Section, at 32m below the base of the Patala Formation in the Ziarat Thatti Sharif Section and at 13m above the base of the Patala Formation in the Kalabagh Hills Section respectively, but were not found in the Sikki Village Section (figure 5.7). The first synchronous occurrences of *Nummulites atacicus, Nummulites globulus, Assilina pustulosa, Assilina leymerie, Assilina granulosa, Discocyclina scalaris, Discocyclina sella* and *Discocyclina undulata* mark the upper boundary of the BFZP 2 Biozone and by definition lower boundary of the BFZP 3 (A) Biozone (representing Middle Lllerdian 2). These species are recorded at the base of the Nammal Formation in the Chichali Nala Section, at 2m above the base of the Nammal Formation in the Nammal Gorge Section, at the base of the Chorgali Formation in the Gharibwal Cement Factory Section respectively, but were not found in the Sikki Village Section due to the unconformable contact of the Patala and the Chorgali Formations (figure 5.7). The last occurrences of *Alveolina globula* and *Alveolina pasticilata* mark the upper boundary of the BFZP 3 (A) Biozone. These species are recorded at a stratigraphic level that marks the top of the Sakessar Formation in the Chichali Nala and Nammal Gorge Sections and at the top of the Chorgali Formation in the Gharibwal Cement Factory Section and 6.5m above the base of the Chorgali Formation in the Sikki Village Section respectively. The first occurrence of *Alveolina rotundata* mark the lower boundary of the BFZP 3 (B) Biozone (representing Upper Lllerdian). It represents a condensed section in which mixing of diachronous species is seen due to telescoping of sediments. The presence of *Assilina laxispira* and *Orbitolites complanatus* indicates Upper Llerdian to Middle Cuisian deposition. This first occurrence of these species is recorded at a stratigraphic level that starts at 6.5m above the base of the Chorgali Formation and

extends up to the top of the Chorgali Formation in the Sikki Village Section. The BFZP 3 (B) Biozone is restricted to the Eastern Salt Range area (Sikki Village Section) and it is not found in the other studied sections.

## 5.5 Biostratigraphic correlation of the Potwar and the Kohat Basins

In the present study the Paleogene foraminiferal biostratigraphic zonation of the Potwar Basin and the TIR reveals that Late Paleocene (Upper Thanitian) to Early Eocene (Middle Lllerdian) rocks can be biostratigraphically correlated with the Paleogene (Lower Lllerdian 1 to Middle Lllerdian 2) rocks of the Kohat Basin (figure 5.8).

The larger benthic foraminifera which are of great value for this correlation across both basins include species of *Ranikothalia sindensis*, *Discocyclina ranikotensis* for the Upper Thanitian strata, *Discocyclina despensa*, *Alveolina vredenburgi*, *Assilina dandotica* and *Assilina aff. pustulosa* species for the Lower Lllerdian 1- Middle Lllerdian 1 strata. In addition *Nummulites atacicus, Nummulites globulus, Assilina granulosa*, *Assilina leymerie* and *Alveolina pasticilata* are useful for biostratigraphic correlation of the Middle Lllerdian 2 strata in both areas.

The BFZP 1 Biozone (representing Upper Thanitian) in the Potwar Basin and the TIR is correlated with the BFZK 1 (A) Biozone (representing Upper Thanitian) in the Kohat Basin (figures 5.8-5.9). The foraminiferal species which are common in BFZP 1 (A) and BFZK 1 (A) Biozones include *Miscellanea miscella, Ranikothalai sindensis, Lockhartia haime, Discocyclina ranikotensis* and *Operculina petalensis*.

The BFZP 2 Biozone (representing Lower Illedian 1–Middle Lllerdian 1) in the Potwar Basin and the TIR is correlated with the BFZK 1 (B)-BFZK 2 Biozones in the Kohat Basin (figures 5.8-5.9). The species of *Assilina aff. putulosa, Discocyclina despensa*, *Discocyclina undulata*, *Discocyclina sella* and *Discocyclina scalaris* are common in these biozones in both areas.

The BFZP 3 (A) Biozone (representing Middle Lllerdian 2) in the Potwar Basin and the TIR is correlated with the BFZK 3 (A) Biozone in the Kohat Basin (figures 5.8-5.9).

The species of *Nummulites atacicus, Nummulites globulus, Assilina leymerie, Assilina granulosa* and *Assilina pustulosa* are common in the BFZK 3 (A) and the BFZP (A) biozones.

The species of *Alveolina rotundata, Assilina laxispira* and *Orbitolites complanatus* characterizes the BFZP 3 (B) Biozone (representing Upper Lllerdian to Middle Cuisian) in the Potwar Basin and the TIR is correlated with the BFZK 3 (B) Biozone of the Kohat Basin. In both Basins these biozones represents a condensed section (figures 5.8-5.9).

## 5.1 Biostratigraphic comparison with other biozonal schemes

A comparison of the Paleogene Larger Benthic Foraminiferal Biozones (abbreviated as BFZP 1-BFZP 3 (B) of the Potwar Basin and the TIR with the nummulitid Biozones of Schaub (1981), alveolinid Biozones of Höttinger (1960), the Weiss Biozones (1988, 1993), the SBZ Biozones of Serra Kiel et al. (1998), and the Local Biozones of Afzal (1997) is summarized in figure 5.8. and as described below.

The BFZP 1 Biozone is correlated with the SBZ 5 Zone of Serra Kiel et al. (1998), the *Assilina Prisca*/*Nummulites deserti* Zone of Schaub (1981), the *Alveolina cucumiformis* Zone of Höttinger (1960), the SRX 2 and SRX 3 Zones of Afzal (1997) and the upper part of the *Lockhartia haime-Dictyokathina simplex* Zone of Weiss (1988, 1993).

The BFZP 2 Biozone is correlated with the SBZ 6-7 Zones of Sierra Kiel et al. (1998), the *Assilina arenensis*/*Nummulites frassi* Zone of Schaub (1981), the *Alveolina pasticilata* Zone of Höttinger (1960), the SRX 4 Zone of Afzal (1997), and the lower part of *Assilina dandotica-Discocyclina ranikotensis* Zone of Weiss (1988, 1993).

The BFZP 3 (A) Biozone is correlated with the SBZ 8 Zone of Serra Kiel et al. (1998), the *Assilina leymerie*/*Nummulites globulus* Zone of Schaub (1981), the *Alveolina carbarica* Zone of Höttinger (1960), the SRX 5 Zone of Afzal (1997), and the lower part of the *Assilina leymerie-Nummulites fossulata-Discocyclina ranikotensis* Zone of Weiss (1988, 1993).

The BFZP 3 (B) Biozone is correlated with the SBZ 9-11 Zones of the Serra Kiel et al. (1998), the SRX 7 Zone of Afzal (1997) and the *Assilina spinosa-Flosculina glubosa-Dictyokathina cooki* Zone of Weiss (1988, 1993).

## 5.7 Discussion

During the course of this study comparison of the recorded larger benthic foraminiferal species of *Alveolina vredenburgi, Alveolina globula, Alveolina pasticilata, Nummulites planulatus, Nummulites globulus, Nummulites atacicus, Assilina putulosa, Assilina granulosa* and *Assilina leymerie* with the nummulitid biozonal scheme of Schaub (1981), alveolinid Biozones of Hottinger (1960), SRX biozones of Afzal (1997), SBZ Biozone of Serra Kiel et al. (1998) shows a distinct variation in their biostratigraphic ranges, which are discussed here.

*Alveolina vredenburgi* (considered as a synonym of *Alveolina curcumiformis* in Höttinger, 1960) is recorded from the BFZP 2 Biozone (representing Lower Lllerdian 1 - Middle Lllerdian 1) in the Potwar Basin and the TIR and in the BFZK 1 (B)-BFZK 2 Biozones (representing lower Lllerdian 1- Middle Lllerdian 1) in the Kohat Basin. The biostratigraphic range of *Alveolina vredenburgi* in the SBZ Zones of Serra Kiel et al. (1998) and alveolinid Zones of Höttinger (1960) is Lower Lllerdian 1, but it is found also upwards in the Middle Lllerdian 1 in the study area.

*Alveolina globula* in association with *Alveolina pasticilata* is recorded in the BFZP 2-BFZP 3 (A) Biozones (representing Lower Lllerdian 1- Middle Lllerdian 2) in the Potwar Basin and BFZK 1 (B)-BFZK 3 (A) Biozones (representing Lower Lllerdian 1-Middle Lllerdian 2) in the Kohat Basin. The stratigraphic range of *Alveolina globula* in SBZ Zones of Serra Kiel et al. (1998) shows that it ranges from Lower Lllerdian 1-Lower Lllerdian 2 but its range extends to Middle Lllerdian 2 in the study area.

*Nummulites planulatus* is recorded in the BFZP 2 to BFZP 3 (B) Biozones (representing the Lower Lllerdian 1-Middle Cuisian) in the Potwar Basin and the TIR and the BFZK 2 to BFZK 3 (B) Biozones (representing the Lower Lllerdian 2-Middle Llledian 2) in the Kohat Basin. It is recorded in the SBZ Zones of Serra Kiel et al. (1998) with a stratigraphic range from the Upper Lllerdian to the Lower Cuisian.

Its biostratigraphic range in the study area shows its first occurrence in the Lower Lllerdian 1 and last occurrence in the Middle Lllerdian 2.

*Nummulites globulus* is recorded in the BFZP 2–BFZP 3 (B) Biozones (representing the Lower Lllerdian 2- Middle Cuisian) in the Potwar Basin and the TIR and in the BFZK 2 to BFZK 5 Biozones (representing the Lower Lllerdian 2–Middle Lutetian 1) in the Kohat Basin. It is recorded in the nummulitid Zones of Schaub (1981) and the SBZ Zones of Serra Kiel et al. (1998) having a stratigraphic range from the Upper Lllerdian to Lower Cuisian. Thus its stratigraphic range is found substantially extended upwards in this study.

*Nummulites atacicus* is recorded in the BFZP 3 (A) to BFZP 3 (B) Biozones (representing the Middle Lllerdian 2–Middle Cuisian) in the Potwar Basin and the TIR and in the BFZK 3 (A) to BFZK 3 (B) Biozones (representing the Middle Lllerdian 2 to Middle Cuisian) in the Kohat Basin. It is recorded as in the nummulitid Biozones of Schaub (1981) and SBZ Biozones of Serra Kiel et al. (1998) with a stratigraphic range in the Middle Lllerdian 2. Thus its stratigraphic range is substantially extended upwards in this study.

*Assilina putulosa* (synonym of *Assilina daviesie* of Gill (1953) is recorded in the BFZP 2–BFZP 3 (B) Biozones (representing the Lower Lllerdian 1-Middle Cuisian) in the Potwar Basin and the TIR and in the BFZK 2-BFZK 3 Biozones (representing the Lower Lllerdian 1-Middle Lllerdian 2) in the Kohat Basin. The biostratigraphic range of *Assilina pustulosa* according to Schaub (1981) and Serra Kiel et al. (1998) is Middle Lllerdian 2. Therefore its biostratigraphic range is substantially extended upwards in the study area.

*Assilina granulosa* and *Assilina leymerie* are recorded in the BFZP 3 (A)–BFZP 3 (B) Biozones (representing Lower Lllerdian 1–Middle Cuisian) in the Potwar Basin and the TIR and in the BFZK 1 (B)-BFZK 4 Biozones (representing Lower Lllerdian-Middle Lutetian 1) in the Kohat Basin. *Assilina leymerie* is Form-A of *Assilina granulosa* and represents Middle Lllerdian 2 in the nummulitid Zones of Schaub (1981) and in the SBZ Zones of Serra Kiel et al. (1998). Therefore its range is found substantially extended upwards in the study area.

*Alveolina pasticilata* is recorded in the BFZP 1 Biozone (Thanetian-Lower Lllerdian 1) to the BFZP 3 (A) Biozone (representing Middle Lllerdian 2) in the Potwar Basin and the BFZK 1 (B) Biozone (Lower Lllerdian 1) to the BFZK 3 (B) Biozone (Middle Cuisian) in the Kohat Basin. The stratigraphic range of *Alveolina pasticilata* in SBZ Zones of Serra Kiel (1998) is Lower Lllerdian 2. Thus its stratigraphic range in the study area is extended upward.

## 5.8 Summary and conclusions

In this study six Paleogene stratigraphic sections of the Potwar Basin and the TIR are investigated for a detailed biostratigraphy. Larger benthic foraminiferal species of nummulitids, alveolinids and discocyclinids provide a sound basis for biozonal boundaries. A total of four biozones are identified, among these three are assemblage range biozones and one is a taxa range biozone. A Paleogene biostratigraphic correlation among the studied sections across the Potwar and Kohat Basin is presented. The following conclusions are drawn from this study.

- The first and last occurrences of *Ranikothalia sindensis*, *Assilina dandotica, Assilina granulosa, Assilina leymerie, Assilina aff. putulosa, Assilina putulosa, Nummulites globulus, Nummulites atacicus, Discocyclina despensa, Discocyclina sella, Discocyclina scalaris, Alveolina vredenburgi, Alveolina globula, Alveolina pasticilata* and *Alveolina rotundata* are useful in establishing boundaries for the Paleogene biozones in the study area.
- The Late Paleocene (Upper Thanitian) to Early Eocene (Upper Lllerdian) biozones are abbreviated as BFZP 1-BFZP 3.
- The BFZP 1 Biozone represents the Upper Thanitian and it is recorded in the Lockhart Formation in all studied sections, but extends upwards into the overlying Patala Formation in the Sikki Village, the Chachali Nala, the Kalabagh Hills and the Nammal Gorge Sections. It correlates with the BFZK 1 (A) Biozone of the Kohat Basin.
- The BFZP 2 Biozone represents the Lower Lllerdian 1 – Middle Lllerdian 1 in the upper part of the Lockhart Formation and extends upwards into the overlying Patala Formation in the Ziarat Thatti Sharif Section and it is

Nammal Formation in the Nammal Gorge Section. This biozone correlates with the BFZK 1 (B) - BFZK 2 Biozones of the Kohat Basin.

- The BFZP 3 (A) Biozone represents the Middle Lllerdian 2. It is only recorded in the Nammal and the Sakessar Formations in the Chichali Nala and the Nammal Gorge Sections and in Chorgali Formation in the Gharibwal Cement Factory Section. It correlates with the BFZK 3 Biozone of the Kohat Basin.
- The BFZP 3 (B) Biozone represents Upper Lllerdian to Middle Cuisian and it is only recorded in the Sikki Village Section of the Eastern Salt Range area in the Potwar Basin. This biozone is correlated with the BFZK 3 (B) Biozone of the Kohat Basin.
- The biostratigraphic age of the Lockhart Formation in the Potwar Basin ranges from the Late Paleocene (Upper Thanitian) to Early Eocene (Lower Lllerdian 1) while in the Kohat Basin it is Late Paleocene (Upper Thanitian).
- The biostratigraphic age of the Patala Formation in the Potwar and Kohat Basins ranges from Late Paleocene (Upper Thanitian) to Early Eocene (Middle Lllerdian 1).
- The biostratigraphic age of the Nammal Formation in the studied sections is Early Eocene (Lower Lllerdian 1 to Middle Lllerdian 2). It correlates with the upper part of the Patala Formation, the Panoba Formation and lower middle to upper part of the Sheikhan Formation in the Kohat Basin.
- The biostratigraphic age of the Sakessar Formation in all studied sections is Early Eocene (Middle Lllerdian 2). It correlates with the middle to middle-upper part of the Sheikhan Formation in the Kohat Basin.
- The biostratigraphic age of the Chorgali Formation in the study area is Early Eocene (Middle Lllerdian 2–Middle Cuisian). It correlates with the middle-uppermost part of the Sheikhan Formation.

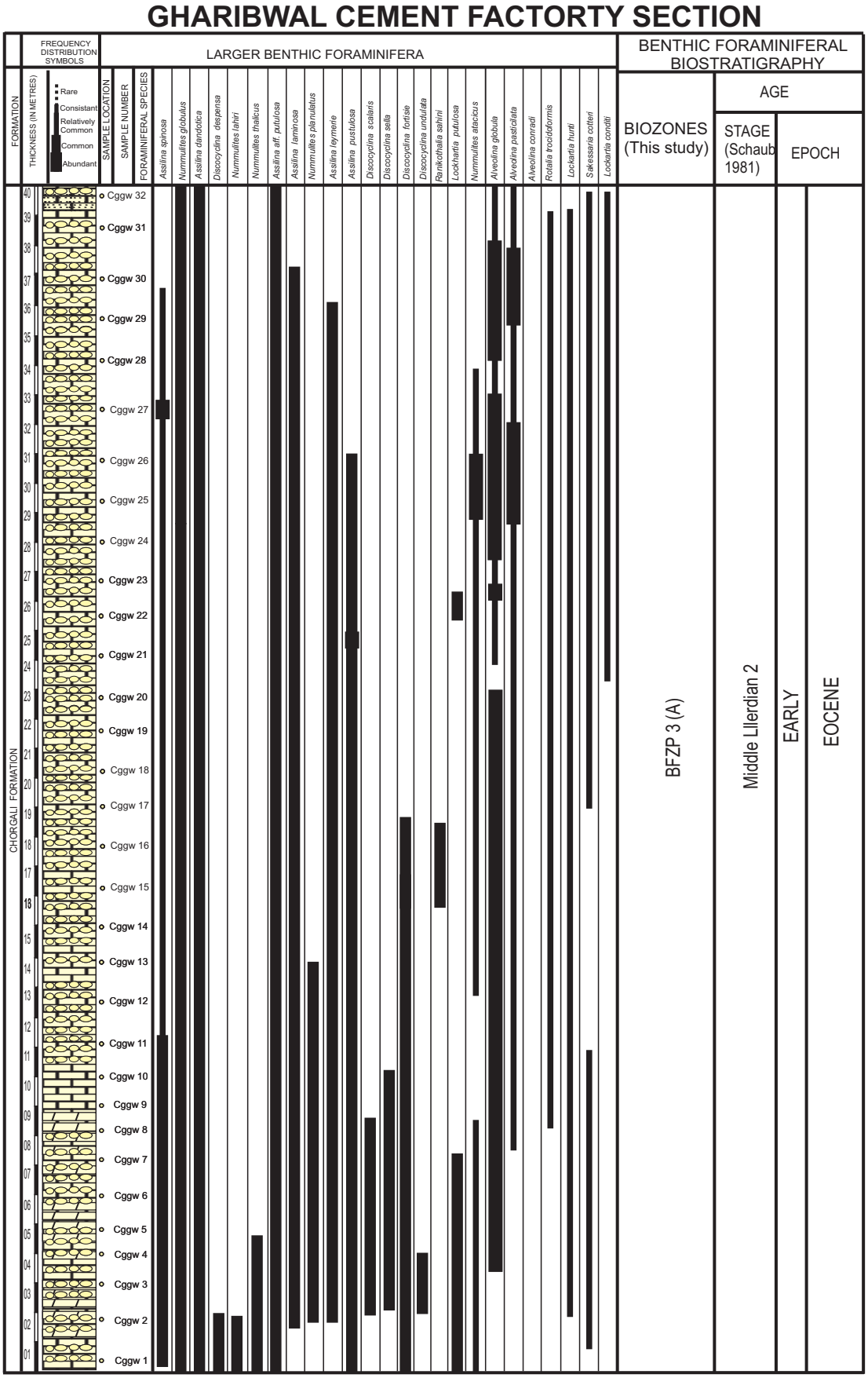


**Figure 5.1.** Range distribution, abundance and biozonation chart of larger benthic foraminifera in Early Eocene rocks of the Gharibwal Cement Factory Section, Eastern Salt Range, Potwar Basin, north-west Pakistan.

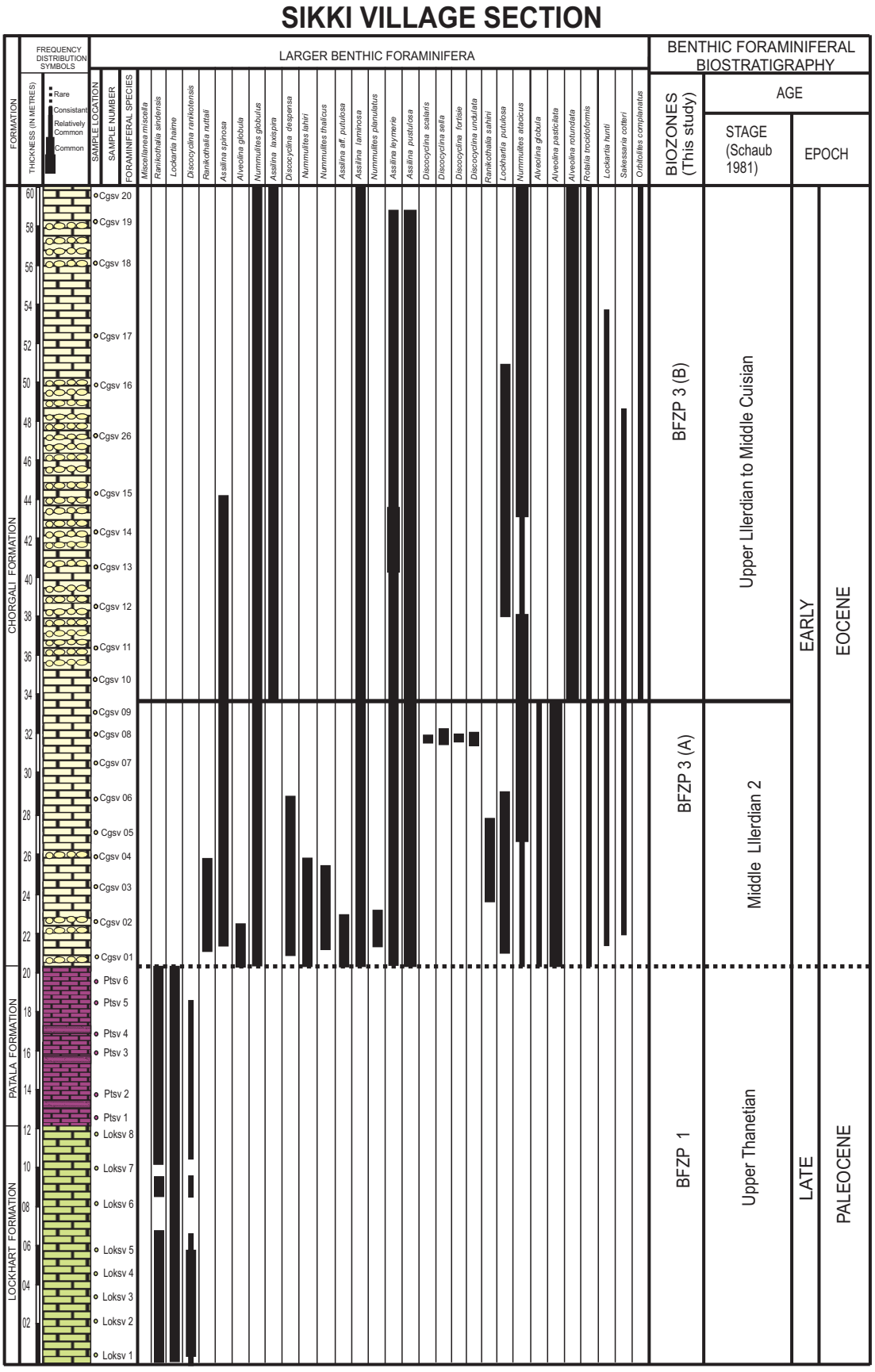


**Figure 5.2.** Range distribution, abundance and biozonation chart of larger benthic foraminifera in the Paleogene rocks of the Sikki Village Section, Eastern Salt Range, Potwar Basin, north-west Pakistan.

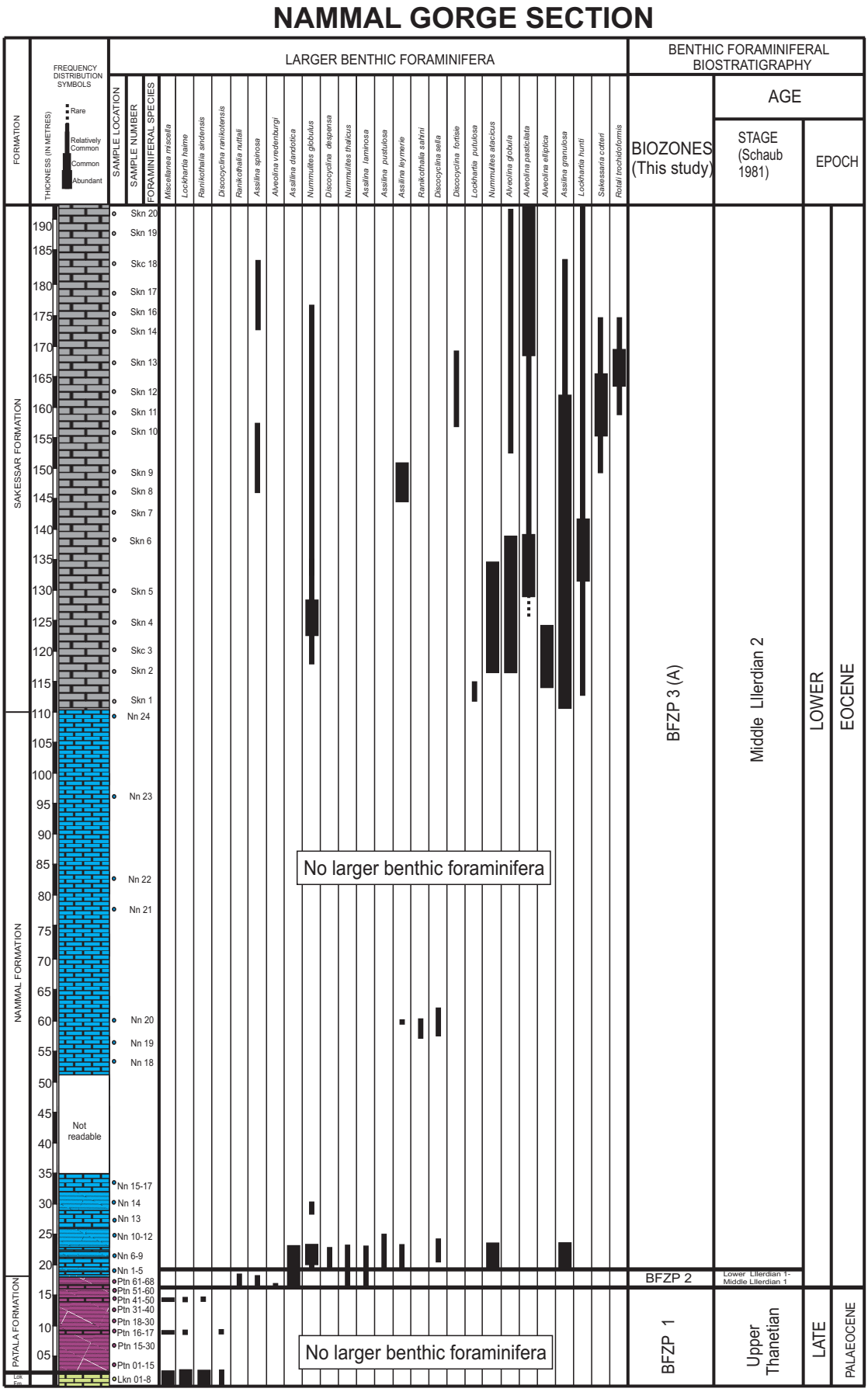


**Figure 5.3.** Range distribution, abundance and biozonation chart of larger benthic foraminifera in Paleogene rocks of the Nammal Gorge Section, the Central Salt Range, Potwar Basin, north-west Pakistan.

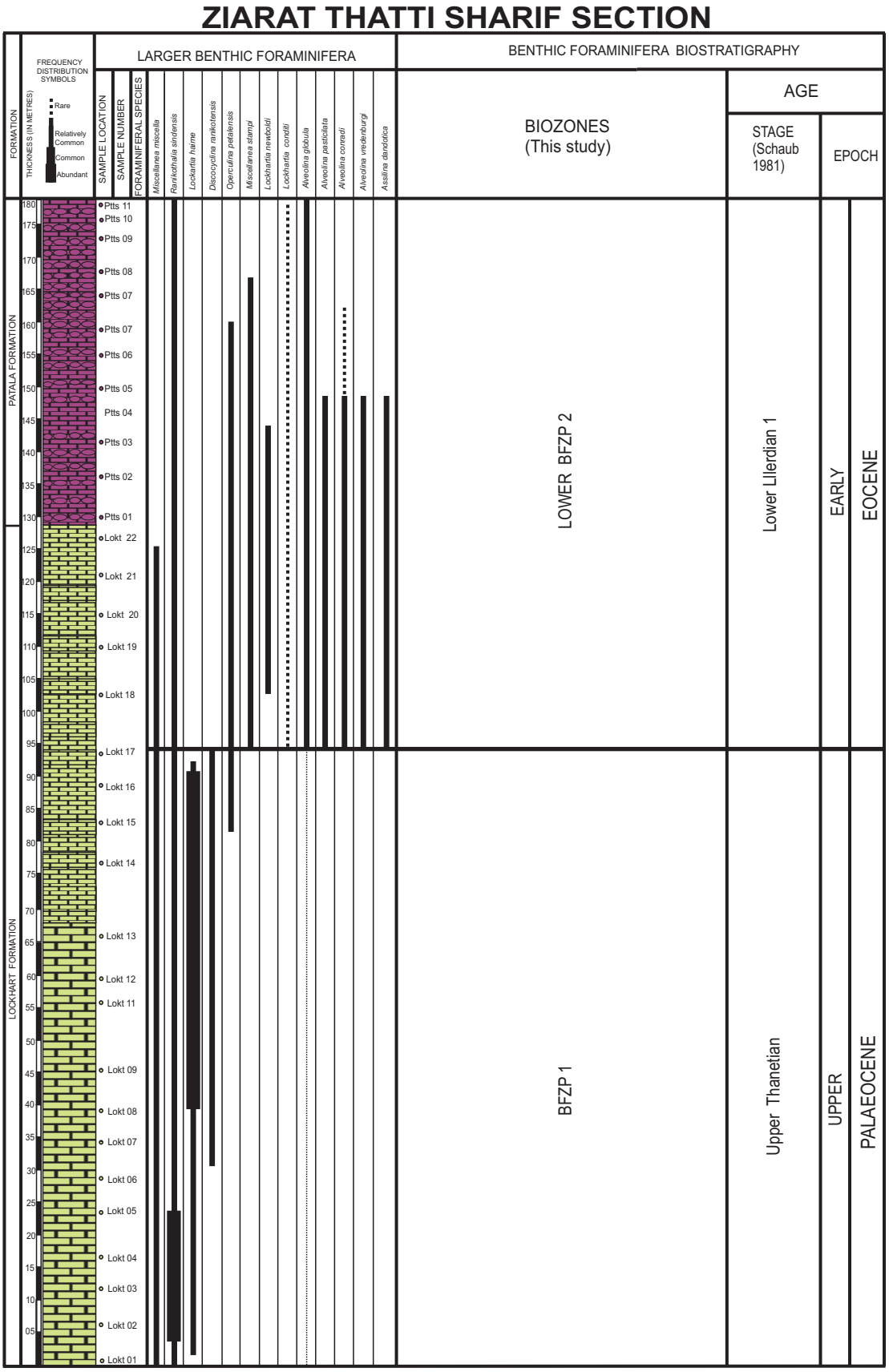


**Figure 5.4.** Range distribution, abundance and biozonation chart of larger benthic foraminifera in Paleogene rocks of the Ziarat Thatti Sharif Section, the Western Salt Range, Potwar Basin, north-west Pakistan.

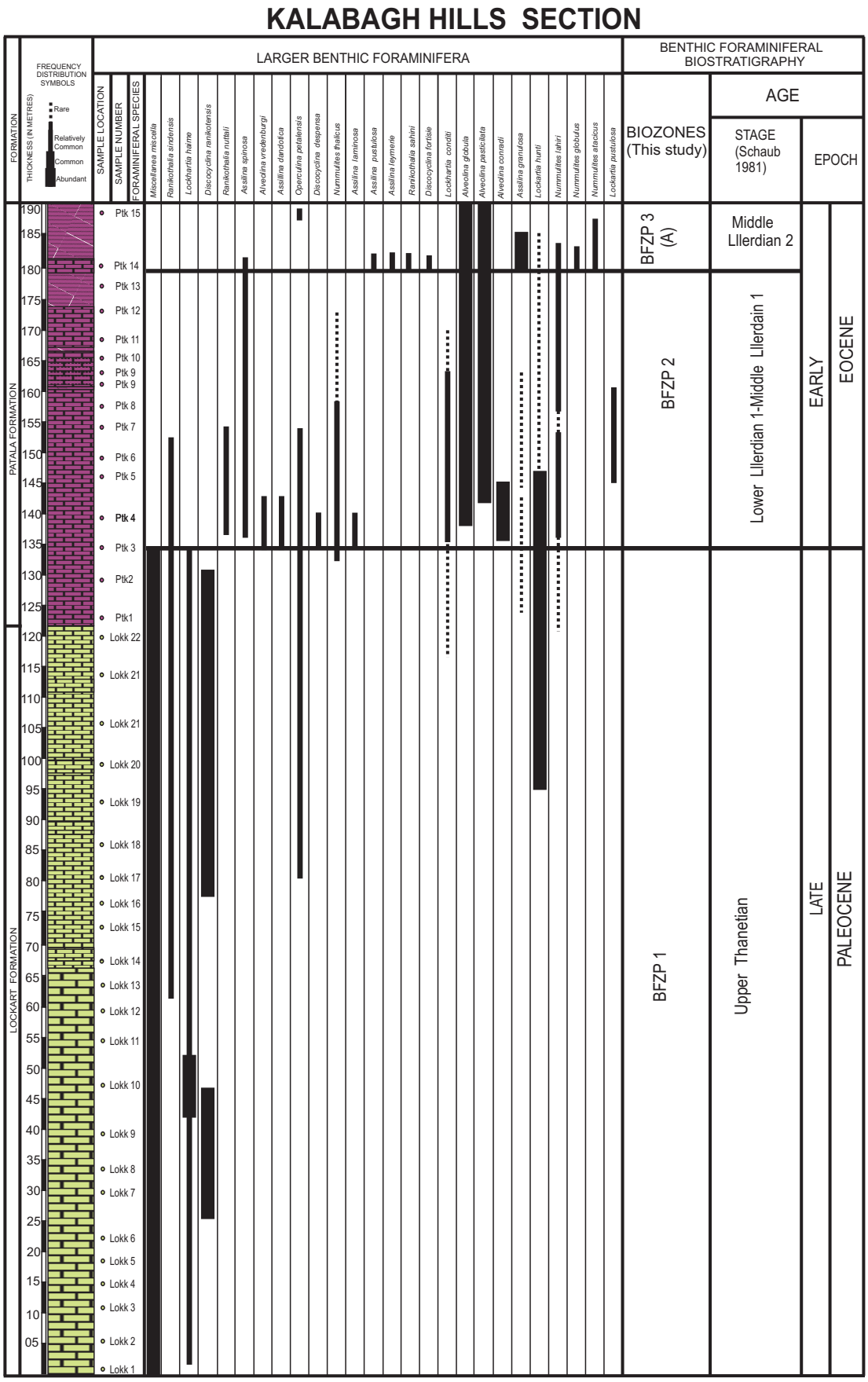


**Figure 5.5.** Range distribution, abundance and biozonation chart of larger benthic foraminifera in Paleogene rocks of the Kalabagh Hills Section, Trans Indus Ranges, north-west Pakistan.

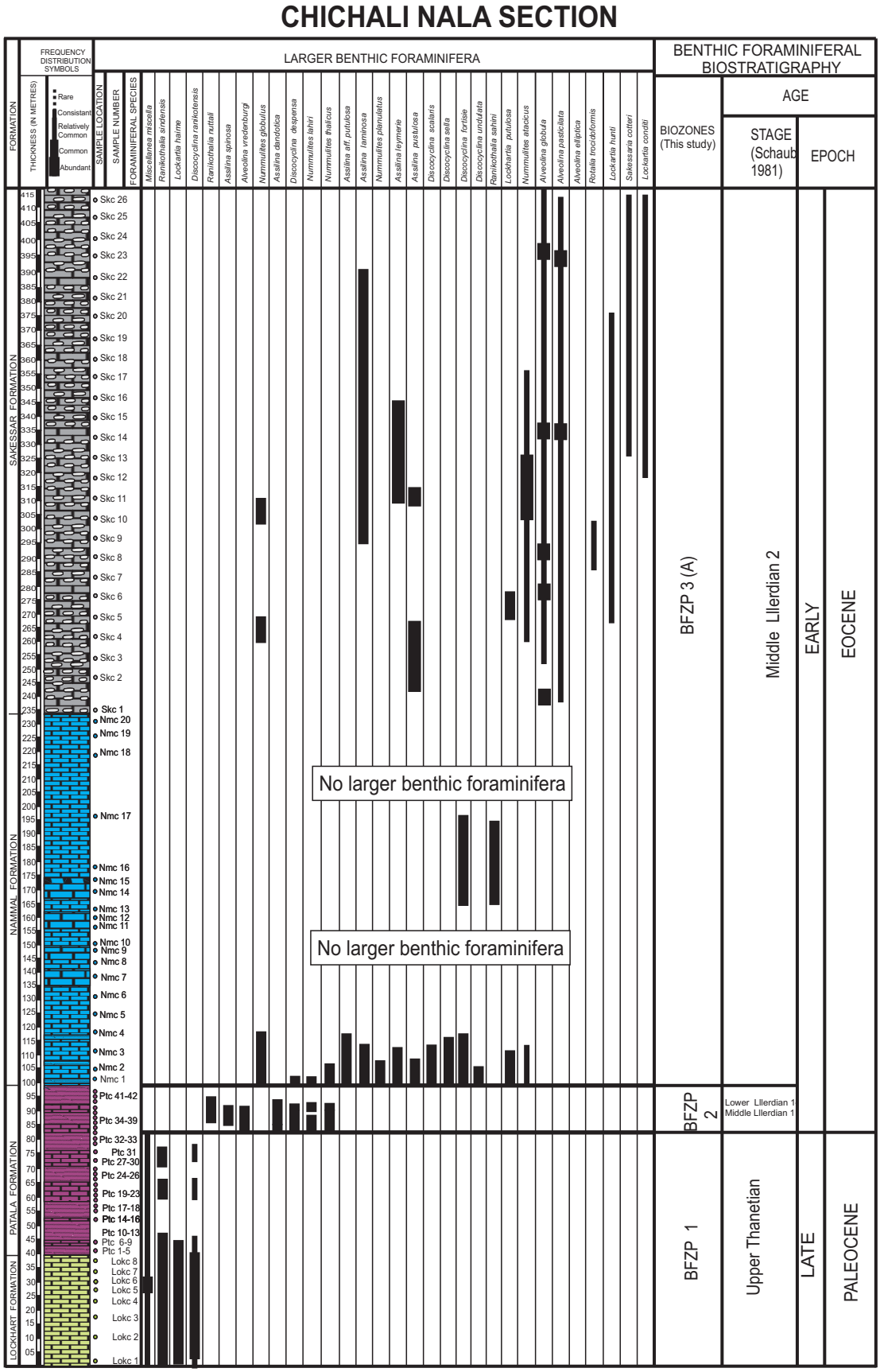


**Figure 5.6.** Range distribution, abundance and biozonation chart of larger benthic foraminifera in Paleogene rocks of the Chichali Nala Section, Trans Indus Ranges, north-west Pakistan.

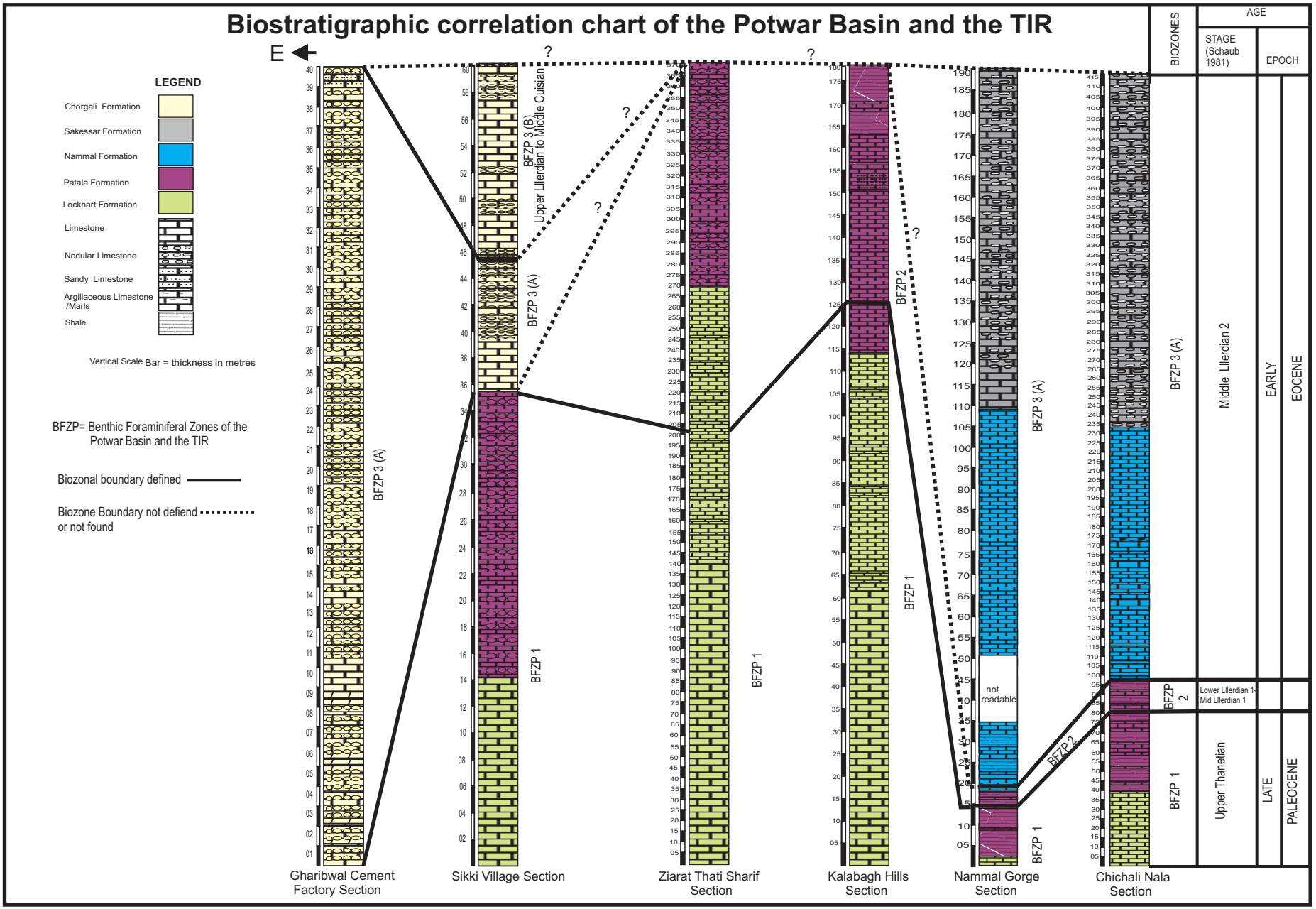


**Figure 5.7.** Paleogene foraminferal biostratigraphic correlation of the studied sections in the Potwar Basin and the TIR.

## Biostratigraphic comparison chart of the Potwar and Kohat Basins

| EPOCH | | STAGE (Holland et al., 1978) | STAGE (Schaub 1981) | | Nummulitid Biozone (Schaub., 1981): *Nummulites* brogniatri group | *Nummulites perforatus* group | *Nummulites* others group | *Assilina* | Alveolinid Biozone (after Hottinger., 1960) | SBZ (after Serra Kiel et al., 1998) | Local Bizones (Afzal. J 1997) | Biozones (Kohat Basin) (see Chapter 4) | Biozones (Potwar Basin) including the Trans Indus Ranges (This study) |
|---|---|---|---|---|---|---|---|---|---|---|---|---|---|
| OLIGO-CENE | Lower | Repelian | Stampian | | | | *fichteli* | | | | | Not recognized (Regressive facies) | (No deposition uplifting phase) |
| EOCENE | Late | Priabonian | Priabonian | | | | *fabianii* | | *Neoalveolina* | SBZ 19 | | | |
| | Middle | Bartonian | Biarritzian | | *brogniatri* | *perforatus* | *ptukhiani* | | *elongata* | SBZ 18<br>SBZ 17 | | | |
| | | Lutetian | Lutetian | U | *herbi* | *atauricus* | *bullatus* | *giagantea* | | SBZ 16 | | BFZK 6 | |
| | | | | M 2 | *sordensis* | *crasus* | | *planospira* | *proerecta* | SBZ 15 | | BFZK 5 | |
| | | | | M 1 | *gratus* | *beneharnensis* | | *spira spira* | *munierie* | SBZ 14 | | BFZK 4 | |
| | | | | L 2 | *laevigatus* | *obesus* | | *spira abradi* | *stipes* | SBZ 13 | | | |
| | | | | L 1 | | *gallensis* | | | | | | | |
| | Early | Ypresian | Cuisian | U | *manfredi* | *campesinus* | *formosus* | *major* | *violae* | SBZ 12 | | | |
| | | | | M | *praelaevigatus* | *burd. cantabricus* | *nitidus* | *laxispira* | *dainelli* | SBZ 11 | | | |
| | | | | L 2 | *planulatus* | *burdigalensis burdigalensis* | *aff. laxus* | *plana* | *oblonga* | SBZ 10 | | BFZK 3 (B) | BFZP 3 (B) |
| | | | Lllerdian | U | *involutus* | *pernotus* | *laxus* | *adrianensis* | *trempina* | SBZ 9 | SRX 7 | | |
| | | | | M 2 | *exilis* | | *globulus* | *leymeriei* | *carbarica* | SBZ 8 | SRX 5 | BFZK 3 | BFZP 3 (A) |
| | | | | M 1 | *robustiformis* | | *minervensis* | *Assilina aff arenensis* | *moussoulensis* | SBZ 7 | | BFZK 2 | BFZP 2 |
| | | | | L 2 | *frassi* | | | *Assilina arenensis* | *ellipsoidalis* | SBZ 6 | | | |
| PALAEOCENE | Upper | Thanetian | | L 1 | | | *deserti* | *Assilna prisca* | ***cucumiformis*** | SBZ 5 | SRX 4 | BFZK 1 (B) | |
| | | | Thanetian | | | | | | | | SRX 3 | BFZK 1 (A) | BFZP 1 |
| | Low | Danian | Danian | | | | | | | | | | |

**Figure 5.8.** Comparison of larger benthic foraminiferal biostratigraphic zonation of the Paleogene rocks of the Potwar Basin (including the Trans Indus Ranges) and the Kohat Basin and also with the Nummulitids Biozones of Schaub (1981), the Alveolinid Biozones of Hottinger (1960), the SBZ Biozone of Serra Kiel et al. (1998) and Local Biozones of Afzal .J (1997).

# Chapter 6

# 6 Paleogene facies analysis of the Kohat Basin with implications for paleoenvironments

## 6.1 General

The most practical definition of the term facies was given by Middleton (1978). He defines the term facies as "lithological, structural and organic aspects of a rock which can be detectable in the field. The term microfacies in carbonate rocks refers to the total of all the paleontological and sedimentological criteria which can be classified in thin sections, peel and polished slabs (Flügel, 2004). Different microfacies types can be identified using the limestone composition, depositional texture and fossil distribution of specific samples (Tucker & Wright, 1990; Flügel, 2004). The lateral subdivision of a stratigraphic unit on the basis of fauna, trace fossils and lithology are described as biofacies, ichnofacies, and lithofacies. The facies which are genetically related and have some environmental significance are grouped as facies associations, while a vertical succession of facies characterized by a change in one or more parameters, e.g. abundance of sand, grain size, or sedimentary structures, is termed a facies succession. A general summary of a particular depositional system involving many examples from recent sediments and ancient rocks is known as a facies model. A facies model is said to be static when interpreted under a fixed pattern of processes while a dynamic facies model is used for interpreting lateral and vertical facies distribution formed under different conditions.

## 6.2 Present study

The Paleogene biostratigraphic framework of the Kohat Basin (for details see Chapter 4), is very useful in establishing paleoenvironments of the synchronous depositional systems in the studied sections. In this chapter the paleoecology of larger benthic foraminifera (LBF), facies and paleoenvironments of the Paleogene rocks are described. These rocks include the Patala Formation, the Panoba Formation, the Kuldana Formation and the Kohat Formation in a younging up sequence.

## 6.3 Paleoecology

The larger benthic foraminifera (LBF) and algae are common constituents of the Paleogene rocks of the Kohat Basin. An overview of the literature on the paleoecology of LBF (table 6.1) and algae is presented here. This information can be used to critically appraise the observed distributions of foraminifera and algae for the interpretation of paleoenvironments in the study area.

### 6.3.1 Larger benthic foraminifera (LBF)

LBF live in symbiotic relationship with unicellular algae. In tropical carbonate reef and shoal environments LBF house various algae including dinophyceans, diatoms, chlorophyceans and rhodophyceans. These symbioses provide nutrients from photosynthesis that facilitate life in different water depth and favour maximum carbonate production by carbon dioxide intake (Flügel, 2004). Stable, oligotrophic, nutrient deficient conditions are highly advantageous but they cannot respond competitively when nutrient resources become plentiful (Hallock, 1985). LBF may obtain all or part of their nutritional requirements from their endosymbionts (McEnery and Lee, 1981). Nutrient availability is often linked to temperature and salinity; upwelling adds nutrients whilst reducing temperature, runoff adds nutrients whilst reducing salinity, and evaporation concentrates nutrients whilst raising salinity (Hallock and Schlager, 1986).

Höttinger (1983) noted that at extreme values, temperature and salinity are limiting factors for all LBF, whilst at intermediate values they have a negligible selective effect and short lived extreme values, as observed in tidal pools, often produce contorted tests. The quantity of available nutrients depends on the substrate (Gerlach, 1972). Substrate comprises inorganic particles (including shell debris) and organic particles (e.g. plant material, faecal pellets and detritus) plus interstitial water and air. Silty and muddy substrates are often rich in organic debris and the small pore spaces may contain bacterial blooms, which can support large populations of foraminifera. Many of these foraminiferal species are delicate, often elongate forms.

Foraminifera from the coarser substrates may be thick shelled, heavily ornamented and of biconvex or fusiform shape (Brasier, 1980). Different wall structures reflects differences in light attenuation through the water column and of water energy (Haynes, 1965). These include small spaces within the test walls that harbour algae (Hansen and Dalberg, 1979), pits on the interior of the chamber walls in which the algal cells reside (Hansen and Reiss, 1972; McEnery and Lee, 1981).

An investigation into the ecology and distribution of LBF (larger rotallids) has been made in the Red Sea (Gulf of Elat) by Reiss et al. (1977) and by Hallock in the Pacific (1979). Around the Caroline Island and Hawaii Hallock (1979) has studied the distribution of fifteen species including *Amphistigina* (a descendent of the Lepidocyclines), *Calcarina*, *Operculina*, *Baculogypsina* and *Heterostegina.* She concludes that light and water motion influence test morphology. Many studies have documented systematic morphology changes with variation in habitat depth in living, symbiont bearing species (e.g., Haynes, 1965; Höttinger and Dreher, 1974; Larsen, 1976; Hansen and Buchardt, 1977; Höttinger, 1977a; Larsen and Drooger, 1977). Although living distribution patterns of the symbiont-bearing LBF are confined to tropical and subtropical shallow marine environments, their distribution is determined by a complex set of inter-related parameters such as temperature, nutrient levels and light (Renema, 2002).

Since Carboniferous, LBF have thrived in the shallow warm marine environments. Their remarkable abundance and diversity is due to their ability to grow to a variety of sizes, to their ability to exploit a range of ecological niches and to their ability to transform their shells into greenhouses for symbionts (Fadel, 2008). However, attaining large size made some forms very specialised and vulnerable to rapid ecological changes. For this reason larger foraminifera show a tendency to suffer periodic major extinctions at different geological times. This makes them valuable biostratigraphic zone fossils (Fadel, 2008).

The paleoecological analysis of the recent LBF can be utilized to deduce the paleoenviromental reconstruction of their habitat. In the study area abundant LBF are

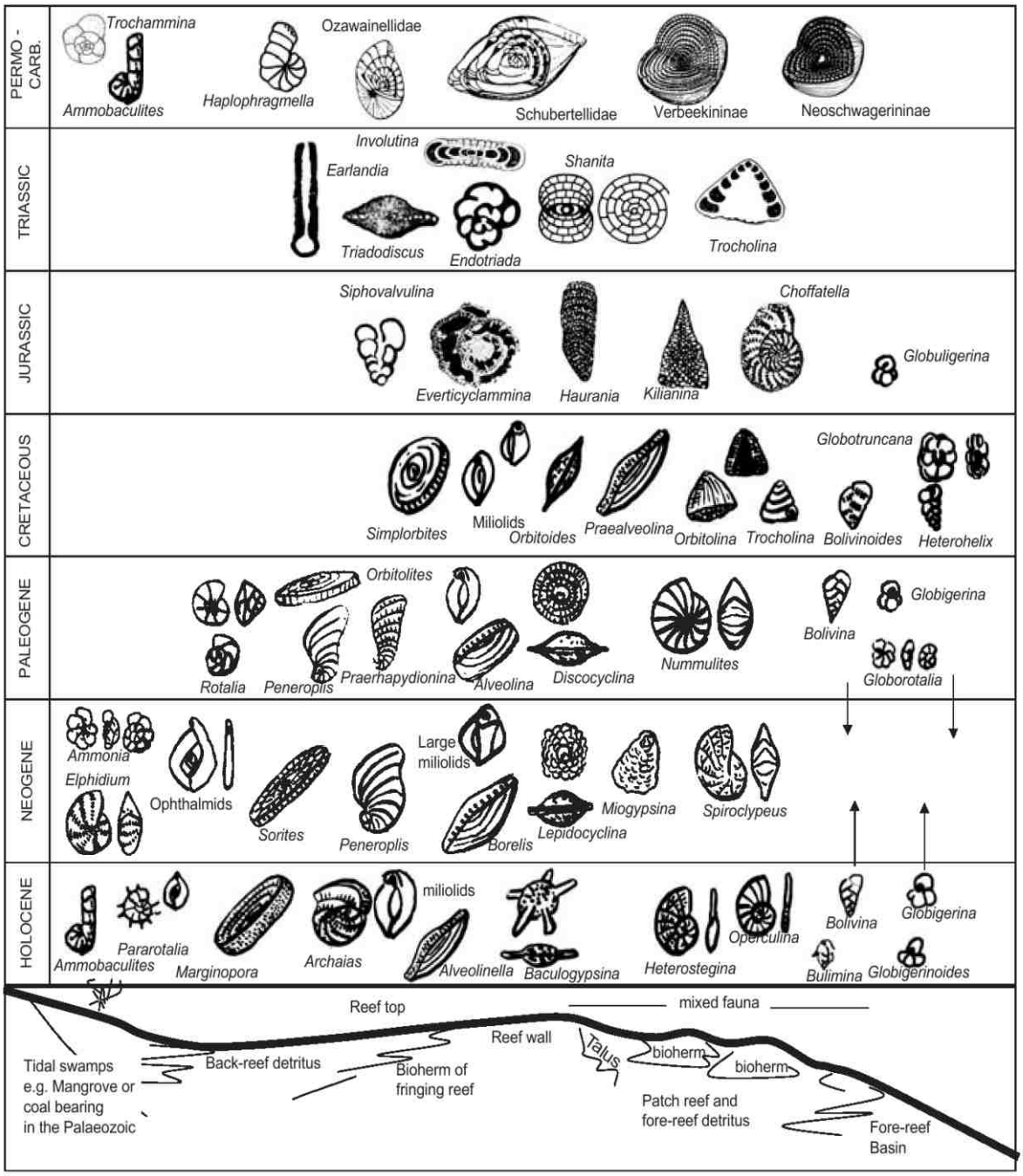


**Table 6.1**. The ecological distribution of larger and key smaller benthic and planktonic foraminifera through time and space (modified from Fadel, 2008).

*Assilina sp., Alveolina sp., Operculina sp.,* milliolids and *Discocyclina sp*. Their paleoecology and depth distribution are briefly described as follows.

#### 6.3.1.1 *Nummulites*

*Paleonummulites venosus* species is found in the depth range of 15-85 m, in quiet back- and forereef areas on a sandy substrate below fair weather wave base (FWWB) in Okinawa, Sessoko, Jima and Mina Island of Japan (Hohenegger, 2000), and on coarser sand in the west Pacific (Langer and Hottinger, 2000). In SW Sulawesi, Indonesia it is found at the reef base (Renema and Troelstra, 2001).

Fossil *Nummulites* is reported from the El Garia Formation in Tunisia (Racey, 2001), the Jdeir Formation offshore Libya (Anketell and Mriheel, 2000), the Seeb Formation in Oman (Racey, 1994), representing a mid ramp environment. These are also reported from Eocene inner shoal ramps of the French Alps (Sinclair et al., 1998). Sandy near shore deposits of southern Tethys have *Nummulites perforatus* (Herbs, 1988). They are also reported from the inner shoal to mid ramp grainstones to bioturbated mudstone facies in the Pyrenean Basin (Gilham and Bistrow, 1998). They are associated with *Assilina* and *Spiroclypeus* representing middle to upper ramp settings in northern Italy (Bassi, 1998). *Nummulites* is found associated with red algae and *Discocyclina* representing allochthonous shelf edge banks in northern Italy (Arni and Lanterno, 1972) and in accumulations from the Middle Eocene Mukhatam Formation in Egypt (Aigner, 1983).

#### 6.3.1.2 *Assilina*

*Assilina* is reported from the Pyrenean Basin in association with *Discocyclina* representing the outer ramp environment (Luterbacher, 1998), Helvic Nappes Switzerland (Herb, 1988) and Oman (Racey, 1994). Ghose (1977) reported *Assilina* from turbid water fore- and backreef facies from the Paleogene of northern India.

#### 6.3.1.3 *Operculina*

*Operculina complata* is reported from the deepest photic zone, in 80 m deep clear water on a sandy substrate in Okinawa, Japan (Hohenegger, 2000).

Fossils of *Operculina* are recorded from the Eocene French Alps, representing lower mid ramp environment below fair weather wave base (FWWB) (Sinclair et al., 1998). It is also reported from the Early Eocene Sierra del Cadi platform in south - eastern Pyrenean Basin, representing the back barrier to outer ramp environment and representing the distal fore bank deposit in the Sirite Basin, Libya (Arni, 1965).

#### 6.3.1.4 *Alveolina*

Species of *Alveolinella quoyi* represents 3-5 m very shallow protected waters where it is located on algal covered rubbles as an epibiont, and it lives also in the range of 20-30 m water depth, on stable substrates with inorganic detritus in Papua New Guinea (Serverin and Lipps, 1989). It is also reported from the shallow shelf between 5-75 m water depth range in the Sesoko Island, Japan (Hohenegger et al., 1999) and within the 3-50 m depth range from the reef base on hard substrate in the SW Sulawesi, Indonesia (Renema and Troelstra, 2001). *Alveolinella* sp. is another example which is recorded from the 10-80 m water depth range in fore- and backreef of tropical seas (Reichel, 1964; Hottinger, 1973). It is reported from the Great Barrier Reef on a sandy substrate laterally adjacent to seagrass (Maxwell et al., 1961), from a < 30m deep lagoon (Newell, 1956), from the back reef shoals where no clastic input occurs (Henson, 1950) in Raroia Atoll.

In the fossil record, *Alveolina* is found in association with *Orbitolites* from the Eocene Jdeir Formation in the offshore Libya, representing a back ramp environment (Anketell and Mirheel, 2000). It is also reported associated with milliolids and *Orbitolites* from the shallow protected lagoon in inner ramp settings of the Pyrenean Basin (Gilham and Bristow, 1998; Luterbacher 1998). In the Southern Tethys the Early Eocene–Middle Eocene record indicates inner shallow platform margin settings (Sartorio and Venturini, 1988). *Alveolina* was found leeward of the backbank facies in the Sirite Basin Libya (Arni, 1965).

#### 6.3.1.5 Orbitolites

Species of *Orbitolites* in association with *Alveolina* represent the restricted shallow clear water environment between the *Nummulites* bank and shoreline in the Catalan Basin (Serra Kiel and Reguant, 1984).

#### 6.3.1.6 Milliolids

Species of milliolids prefer low turbulence waters and a soft substrate and their high abundance indicates hypersaline, nutrient rich backreefs and a restricted lagoonal setting (Geel, 2000).

#### 6.3.1.7 Discocyclina

*Discocyclina* sp. represent normal marine conditions below FWWB, found slightly deeper than *Assilina* sp. but shallower than *Operculina* sp. When it is found associated with *Alveolina* sp. and milliolids, *Discocyclina* sp. represent the backreef environment (Geel, 2000). Broken *Discocyclina* sp. tests associated with *Nummulites* sp. and *Assilina* sp. are recorded from the Eocene Jdeir Formation in offshore Libya, representing a forebank environment (Anketell and Mirheel, 2000). The ovate forms found in the inner ramp above FWWB and flattened forms occur in the mid to outer ramp settings in the El Garia Formation, Tunisia (Loucks et al., 1998). Robust forms are recorded from fore shoals above FWWB, flattened form from back shoal lagoons (5-20m) below FWWB in the French Alps (Sinclair et al., 1998). Largest forms have been recorded from the Late Eocene, inner-mid ramp deposits in the northern Italy (Bassi, 1998). *Discocyclina* is recorded from the outer ramp deposits of Oman (Racey, 1994) and from the Pyrenean Basin (Gilham and Bristow, 1998). It represents middle to outer bank, reef core and forereef areas (large and stout form) in the Paleogene rocks of India (Ghose, 1977). Other rotalliids are symbiotic, robust, and highly ornamented. They represent shallow turbulent water (0-40m) in the shore zone of carbonate sands, reef and inner reef areas (Geel, 2000).

### 6.3.2 Dasycladacean green algae

Dasycladacean green algae informally referred to as dasyclads are a group of benthic calcified unicellular green algae. These are important fossil calcareous algae which appeared in the Cambrian and were important rock builders in the Late Paleozoic, Mesozoic and Cenozoic eras. Calcification in the dasyclads can preserve branching pattern and position of reproductive structures. These details have been utilized extensively in taxonomic treatments of the group and to assess phylogenetic development (Berger and Kaever, 1992). The dasyclad algae are valued as significant paleoecological proxies and for stratigraphic zonation (Flügel, 2004). The living dasyclads are mm to cm sized upright growing plants which are attached to firm or soft substrate by rhizoids. As a result of this calcification, dasyclads have a better fossil record than any other marine green algae, and the long-term development of the group is known in considerable detail (e.g., Pia, 1920; Flügel, 1985 and 1991; Barattolo, 1991; Berger and Kaever, 1992; De Castro, 1997).

Present-day dasyclads are typical of warm, shallow bays and backreef lagoons (Berger and Kaever, 1992). Paleoecologic studies indicate that this environmental predisposition has not changed substantially during the long history of the group (Flügel, 1985 and 1991).

## 6.4 Facies analysis

A complete transect from (NE-SW) represents Paleogene deep basinal, slope, shallow platform, marginal marine and non-marine facies of the Kohat Basin. North-eastern key Paleogene studied sections include the Panoba Nala, the Tarkhobi Nala and the Sheikhan Nala Sections and the Bahadur Khel Salt Tunnel Section lies in the southwest. The Paleogene rocks of the Kohat Basin are represented by seven stratigraphic units. These are named as the Patala Formation, the Panoba Formation, the Bahadur Khel Salt, the Jatta Gypsum, the Sheikhan Formation, the Chashmai Formation, the Kuldana Formation and the Kohat Formation respectively. A detailed description of the facies distribution, depositional facies models (figures 6.26-6.27) and a summary of the paleoenvironments in the key stratigraphic sections (figure 6.28-6.31) of the Kohat Basin is presented.

### 6.4.1 Materials and methods

A total of 317 rock samples were collected for detailed facies analysis at macro- and microscale. The lithofacies description is based on the outcrop investigations, biofacies is based on the foraminifera collected after sieving and microfacies analysis is based on microscopic investigation of thin sections. The microfacies analysis details the allochems, matrix, textural features, fossils content, diagenetic fabric and reservoir rock characteristics. Abundance, type and size of the foraminiferal tests along with invertebrate fauna (brachiopods, bivalves, gastropods, echinoids, and ostracodes), flora (algae) and non-skeletal components (peloids and intraclasts) provide valuable information for the interpretation of depositional environments. The petrographic classification of rocks follows the Dunham (1962) classification of carbonate rocks. The identification and semi-quantitative data on the component distribution of thin sections (see appendix 3) was collected using Comparison Charts (see appendix 5) produced by Baccelle and Bosselini (1965).

### 6.4.2 Facies of the Patala Formation

The microfacies of the Patala Formation are abbreviated as PTK 1-PTK 4 where PT stands for the Patala Formation, K stands for the Kohat Basin and 1-4 are various types of recorded microfacies.

#### *6.4.2.1 Planktonic foraminiferal wackestone microfacies (PTK 1)*

The PTK 1 microfacies is represented by thin bedded, grey coloured, limestone interbedded with black shales in the lower part of the Patala Formation in the Panoba Nala Section.

In thin sections the PTK 1 microfacies is characterized by a wackestone depositional texture. The allochems are dominated by a rich assemblage of planktonic foraminifera (figure 6.1). Micritic matrix dominates and its abundance ranges from 60 to 90 % with an average of 75 %. Black shales are enriched in planktonic foraminifers and are interbedded with the wackestones.

**Depositional environment:** the rich assemblage of the planktonic foraminifers within the micritic matrix indicates that PTK 1 microfacies was deposited in a deep basinal setting (Flügel, 2004).

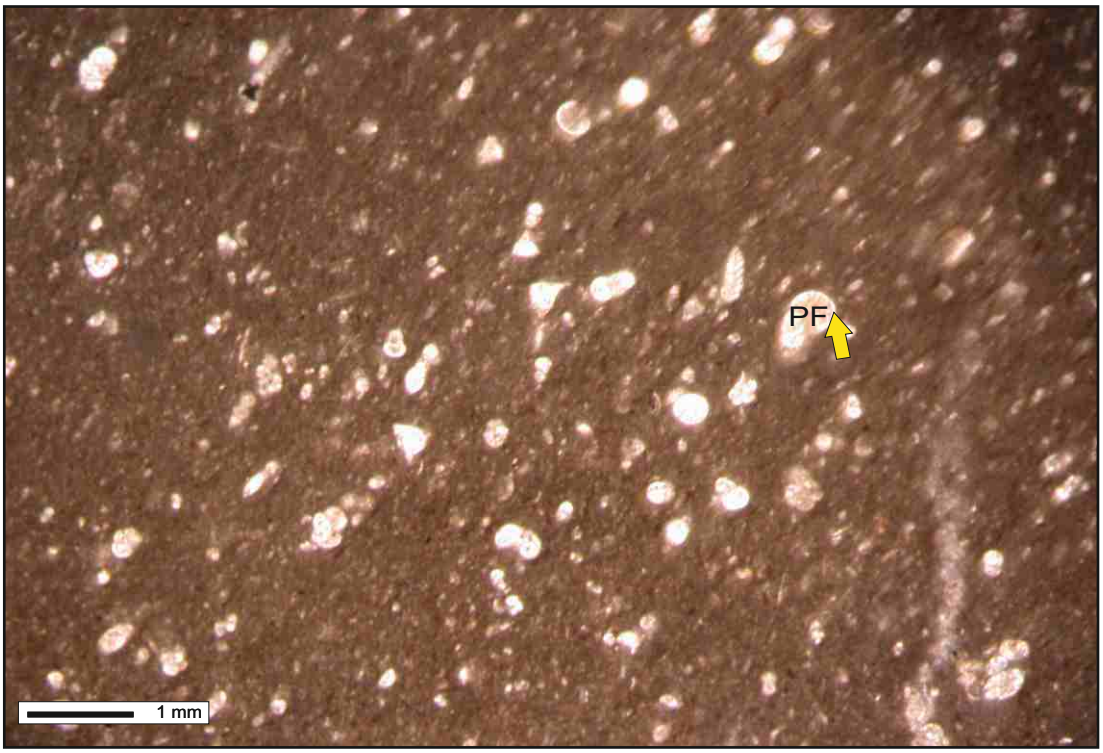


**Figure 6.1. Planktonic wackestone microfacies (PTK 1):** allochems in the PTK 1 microfacies dominantly comprise planktonic foraminifera (PF).

### *6.4.2.2 Nummulitic wackestone microfacies (PTK 2)*

The PTK 2 microfacies is represented by thin bedded, grey coloured, nodular limestone in the lower middle part of the Patala Formation in the Panoba Nala and the Tarkhobi Nala sections.

In thin section the PTK 2 microfacies is characterized by a wackestone depositional fabric. Allochems are dominated by LBF including *Nummulites* sp. and algae (figure 6.2). The micritic matrix dominates and its abundance ranges from 50 to 90 % with an average of 70%.

**Depositional environment:** the presence of *Nummulites* sp. and *Assilina* sp.. along with the micritic matrix suggests that the PTK 2 microfacies was deposited in a middle ramp setting, below FWWB (Racey, 1994; Luterbacher, 1998; Anketell and Mriheel, 2000).

### *6.4.2.3 Mixed faunal wackestone to packstone microfacies (PTK 3)*

The PTK 3 microfacies is represented by a limestone conglomerate in the middle part of the Patala Formation in the Panoba Nala Section.


**Figure 6.2. Nummulitic wackestone microfacies (PTK 2):** *Nummulites globulus* test (NM) shows full preservation in the dominantly micritic matrix.

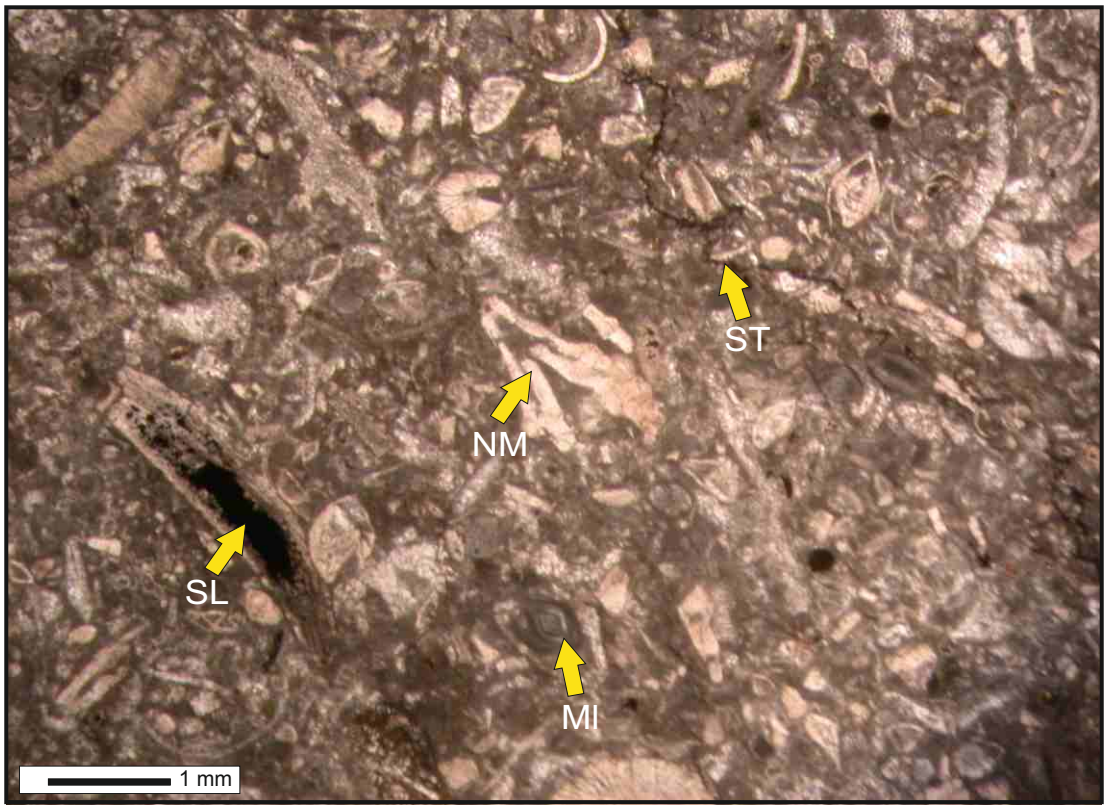


**Figure 6.3. Mixed faunal wackestone to packstone microfacies (PTK 3):** bioclasts of *Nummulites* (NM), milliolids (Ml), and echinoid clasts with evidence of silicification (SL) are present. Stylolites (ST) show chemical compaction of the rock.

In thin sections the PTK 3 microfacies is characterized by a packstone depositional fabrics. Allochems are dominated by LBF including *Nummulites* sp., *Assilina* sp., *Alveolina* sp., *Orbitolites* sp. and also mixed shallow water fauna that include milliolids, ostracodes and bivalves. The allochems abundance ranges from 60 to 80 % with an average of 65 %.

**Depositional environment:** The mixture of shallow and deep water fauna indicates deposition along the ramp slope settings (Racey, 1995; Anketell and Mriheel, 2000).

#### *6.4.2.4 Diverse foraminiferal packstone microfacies (PTK 4)*

The PTK 4 microfacies is represented by thin bedded limestone interbedded with black shales in the upper part of the Patala Formation in the Panoba and the Tarkhobi Nala sections. In thin sections the PTK 4 microfacies is characterized by a wackestone depositional fabric. Allochem abundance ranges from 70 to 90 %, with an average of 80 %, and comprised of *Nummulites* sp., *Assilina* sp., and *Discocyclina* sp. (figure 6.4). The matrix abundance ranges from 20 to 30 % with an average of 22 %.

**Depositional environment:** The moderate faunal biodiversity and micritic matrix indicate that the PTK 4 microfacies was deposited in the distal middle ramp settings (Luterbacher, 1998; Anketell and Mriheel, 2000).

### 6.4.3 Facies of the Panoba Formation

The Panoba Formation consists of greenish coloured calcareous clays/marls in the Panoba Nala, the Sheikhan Nala and the Tarkhobi Nala sections. The clay samples were chemically treated for separation of benthic foraminifera (for details see smaller benthic foraminifera in Chapter 3). Useful bathymetric indicator species among the agglutinated and non-agglutinated benthic foraminifera are identified (details are in Chapter 3) and are used here to define the following biofacies (BF 1-BF 3, here BF stands for biofacies) in the Panoba Formation.

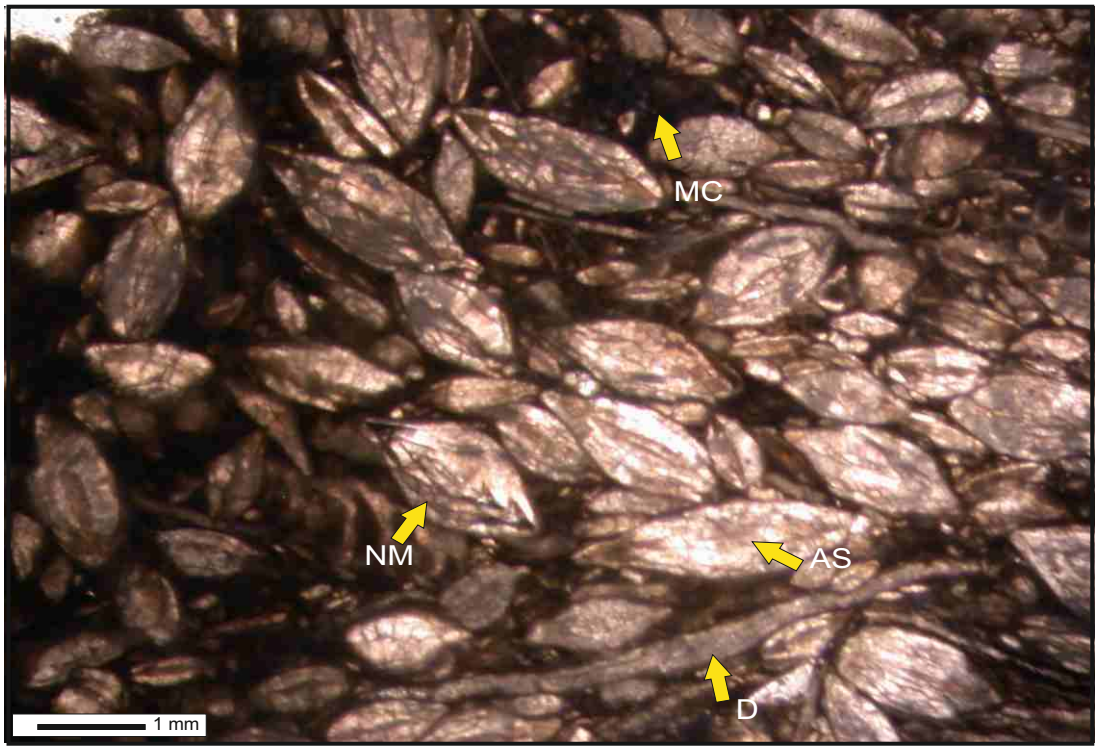


**Figure 6.4. Diverse foraminiferal packstone microfacies (PTK 4):** the allochems of *Discocyclina* (D), *Nummulites* (NM), *Assilina* (AS) are present and micritic matrix filling the intergranular spaces (MC).

### *6.4.3.1 Bulimina biofacies (BF 1)*

The BF 1 biofacies is represented by the green colour clays/marl unit, 9m thick in the lower-middle and 2m thick in the upper part of the Panoba Formation in the Sheikhan Nala Section, and it is represented by typical green coloured clays, 18m thick in the lower part, 19m thick in the middle part and 5m thick in the upper most part in the Panoba Nala Section, northeastern Kohat Basin.

The BF 1 biofacies is characterized by a low to high foraminiferal biodiversity represented by species of *Bulimina gracilis, Bulimina tuxpamensis*, *Praeglobobulimina ovata, Textularia barrettii*, *Textularia martini, Textularia dibollensis*, *Textularia cuyleri*, *Textularia hannai* and *Textularia getrudeana*.

**Depositional environment:** the foraminiferal assemblage of the BF 1 biofacies is compared and found consistent with the *Bulimina gracilis* biofacies defined by Miller et al. (1997) and it represents the middle neritic environment (50-80 m paleodepth of water) in middle ramp settings.

### *6.4.3.2 Uvigerina biofacies (BF 2)*

The BF 2 biofacies is characterized by 2 m thick green coloured clays in the middle part of the Panoba Formation in the Sheikhan Nala Section and represented by 19 m thick, green coloured clays/marls in the lower middle part of the Panoba Formation in the Panoba Nala Section.

The BF 2 biofacies has a high foraminiferal biodiversity and it is characterized by species of *Uvigerina rustica, Uvigerina gallowayi basicordata*, *Uvigerina spinicostata*, *Cibicides cf. simplex*, *Cibicides alleni*, *Cibicidoides tuxpamensis laxispiralis*, *Cibicidoides tuxpamensis tuxpamensis, Gavelinella dakotensis, Gavelinella aracajuensis, Gavelinella schloenbachi, Stensioeina excolata, Loxostomum applinae, Valvulineria patalensis, Nonionella Jacksonenesis*, *Praebulimina cf. seabeensis*, *Bulimina strokesi* and *Bolivinoides decoratus decoratus.*

**Depositional environment:** the species of *Uvigerina rustica, Uvigerina gallowayi basicordata*, *Uvigerina spinicostata* in the BF 2 biofacies are consistent with those in the *Uvigerina* biofacies defined by Miller et al. (1997). This assemblage indicates deposition in the middle to outer neritic environment (> 75m paleodepth of water) in the distal middle-outer ramp depositional setting. This interpretation is supported by the high diversity of foraminifera present.

### *6.4.3.3 Bathysiphon/Gaudryina biofacies (BF 3)*

The BF 3 biofacies is represented by the 8m thick, green coloured clays/marl unit in the middle upper part of the Panoba Formation in the Sheikhan Nala Section and represented by 37m thick, green coloured clays in the middle upper part of the Panoba Formation in the Panoba Nala Section.

The BF 3 biofacies has a moderate to high foraminiferal diversity and is characterized by the species *Bathysiphon eocenicus*, *Bathysiphon robustus, Gaudryina tazaensis*, *Gaudryina leveagata, Guadryinella pussilla*, *Gaudryina pyramidata, Haplophragmoides porrectus*, and *Haplophragmoides concavus*,

Non-agglutinated calcareous species found in the BF 3 biofacies include *Cibicides cf. simplex, Cibicides alleni, Cibicides mensilla* (Schwager) *var. nammalensis, Cibicicoides tuxpamensis laxispiralis*, *Cibicidoides tuxpamensis,*

*Gavelinella dakotensis, Gavelinella aracajuensis*, *Gavelinella schloenbachi*, *Stensioeina excolata, Loxostomum applinae*, *Valvulineria patalensis, Nonionella Jacksonenesis*, *Praebulimina cf seabeensis*, and *Bulimina stokesi.*

**Depositional environment:** the faunal assemblage within the BF 3 biofacies indicates deposition along the ramp slope setting. Similar fauna is recorded from the Eocene of the Carpathian Flysch, Poland (Malecki,1973).

### 6.4.4 Facies of the Sheikhan Formation

The microfacies of the Sheikhan Formation are abbreviated as SHF 1-SHF 9, where SH stands for the Sheikhan Formation, F denotes the microfacies and 1-9 are various types of recorded microfacies.

#### *6.4.4.1 Diverse bioturbated/burrowed wackestone - packstone microfacies (SHF 1)*

The SHF 1 micofacies is represented by alternate yellowish grey clays interbedded with thin nodular yellowish grey limestone in the Panoba Nala Section and is observed in the lower part of the Sheikhan Formation in the Sheikhan Nala Section.

In thin sections, the SHF 1 microfacies is characterized by a rich allochemic constituent of gastropods, echinoids, small brachiopods, *Nummulites* sp., and sparse ostracode shells (figure 6.5 B-H). Many of the ostracode shells are concentrated in small nests. Some intraclasts of less than 1mm size are found. Gastropods constitute the dominant allochem ranging from less than 1 mm size to 3mm size. Mostly gastropods show replacement of aragonite by sparry calcite (figure 6.5 E).

Large scattered echinoid clasts and well preserved echinoid spines are seen (less than 2mm size). Foraminifers are commonly present, including *Assilina* sp. and *Nummulites* sp. which are mostly preserved but ocassionaly replaced by microspar.

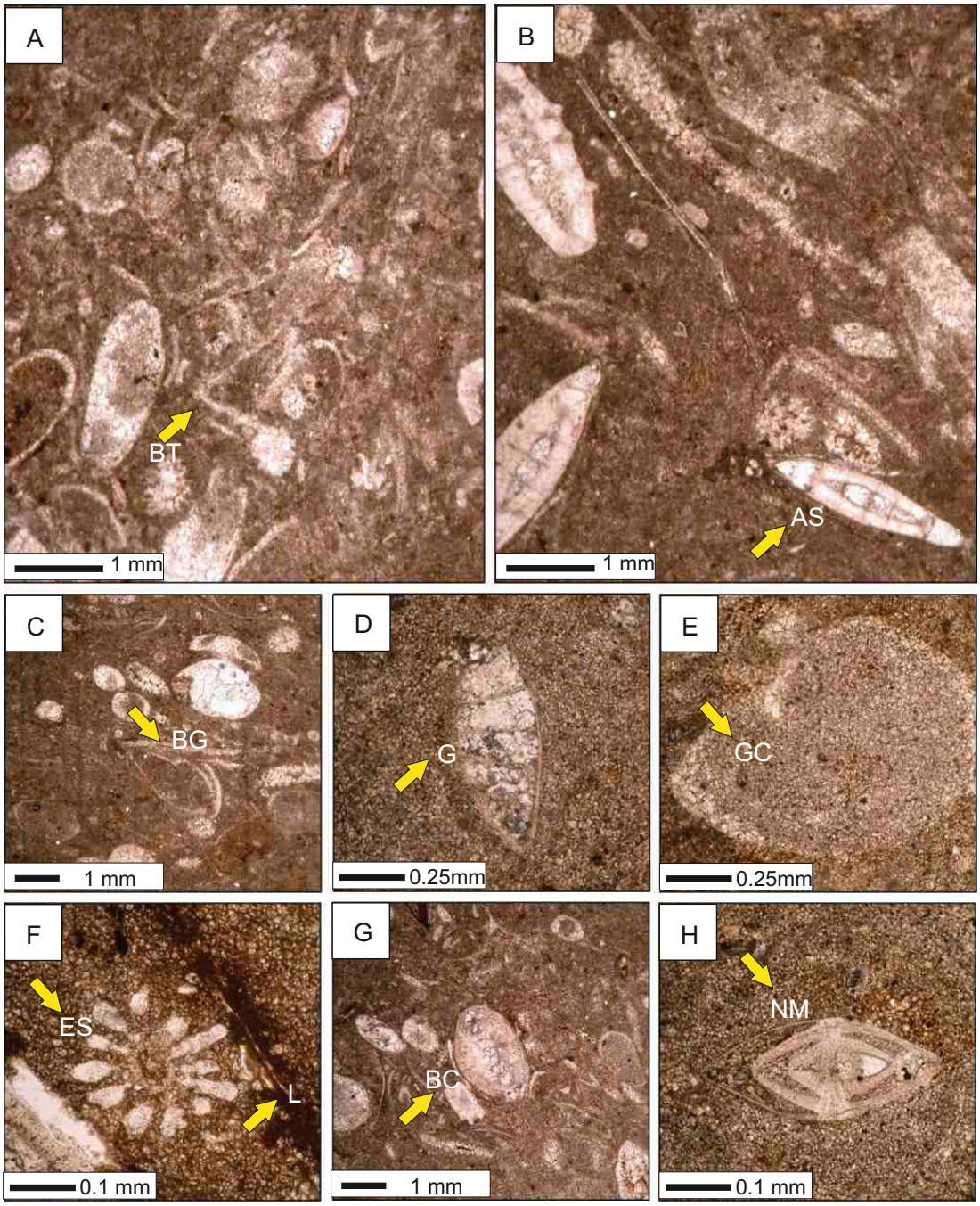


**Figure 6.5. Diverse bioturbated / burrowed wackestone - packstone microfacies (SHF 1):** intense bioturbation contributing sparry matrix (BT in **A,** BG **in C**), diversity of fauna is indicated by presence of *Assilina leymerie* (AS in **B**), gastropod carotid (GC in **E**), echinoid spine (ES in **F**), unidentified bioclasts (BC in **G**) and *Nummulites* (NM in **H**). Diagenetic fabric shows neomorphic alterations forming coarse sparry cement, internal micritization of the bioclasts (GC in **E**) and patchy limonite replacement (L in **F**). Moldic porosity is common (GC in **E** and BG in **C**).

*Nummulites* sp. have preserved internal pillars but along the marginal cord (alar prolongaton) test is mostly micritized (figure 6.5 H). Small ostracode cartoids with internal replacement and biogenic encrustation are present. The matrix is grey coloured allomicrite, thoroughly bioturbated, ranges in abundance from 40-60 %, with an average of 50% (figure 6.5 A). Microspar forms the intergranular cement. Nonskeletal constituents are peloids of varied composition (algal and echinoidal). No preferential orientation of the grains is found.

Detrital quartz of silt size with angular to subrounded shaped grains are found. These grains have abundance range of 1-5 % with an average of 2 %. Fracture filling and neomorphic sparry calcite ranges from 5-15% with an average of 8%. Limonite is common and found in patches. Porosity type includes moldic, intragranular, intergranular and shelter type.

The diagenetic fabric is marked by compaction, neomorphisn and microbial micritization.

**Depositional environment:** The presence of a diverse assemblage of open marine fauna i.e. bivalves, gastropods, foraminifers, echinoids suggests an open marine middle ramp setting (Tucker & Wright, 1990; Flügel, 2004). The presence of micritic matrix, well preserved burrows and bioturbation indicate deposition below FWWB under normal conditions.

#### *6.4.4.2 Bioclastic wackestone microfacies (SHF 2)*

The SHF 2 microfacies is represented by thin-bedded, grey coloured highly bioturbated nodular limestone in the lower part of the Sheikhan Formation in the Sheikhan Nala Section.

The allochemic abundance in the SHF 2 microfacies ranges from 60–80 %, with an average of 65 %. Small gastropods, brachiopods, milliolids, *Nummulites* sp., distorted echinoid spines and algal peloids constitute the main allochemic constituents (figure 6.6 A-H). Scattered gastropod shells range in size from <1mm - 1 mm. Neomorphic alteration (replacement of aragonite by calcite) is seen in many allochems especially in milliolids, *Nummulites* sp. and gastropods.

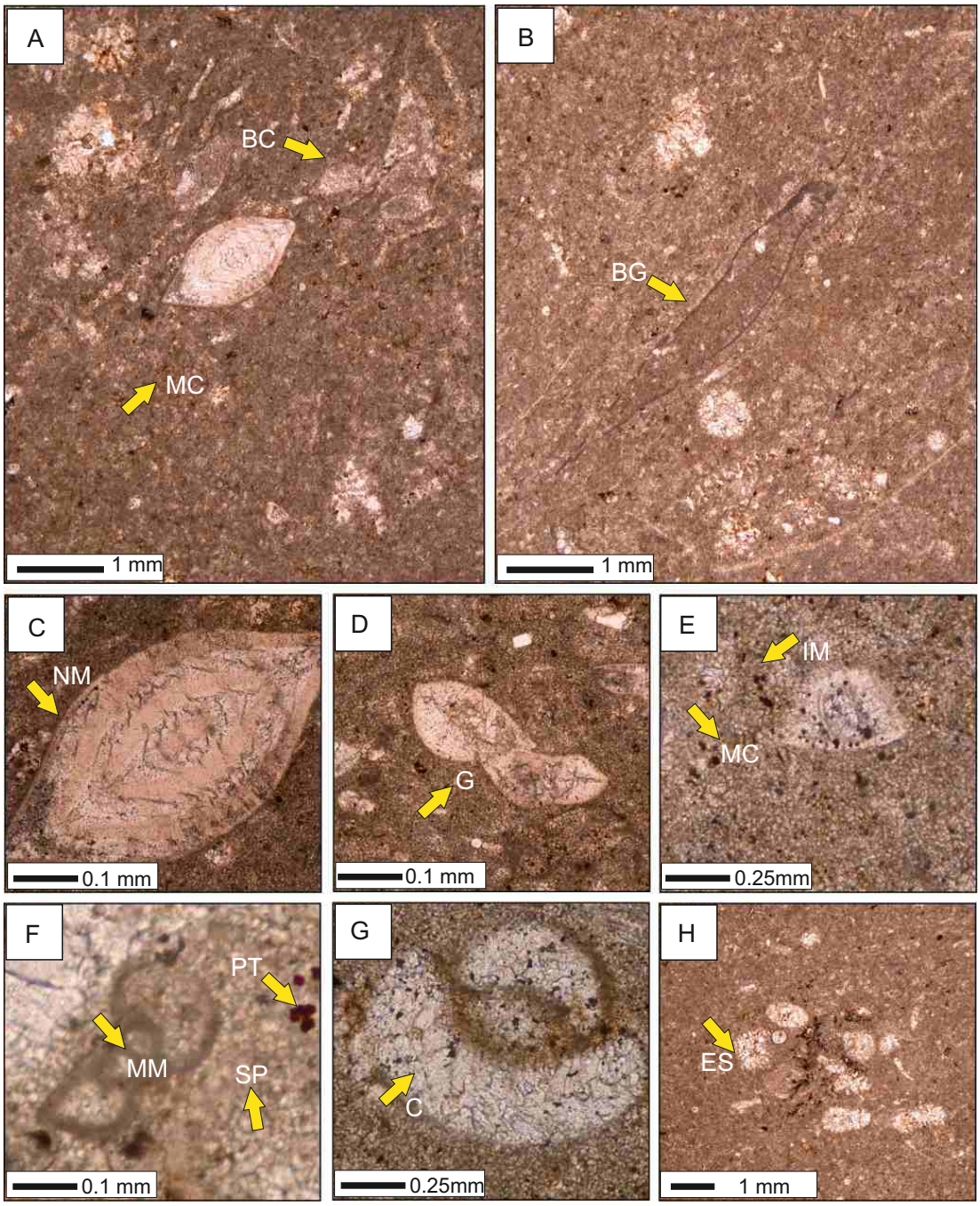


**Figure 6.6. Bioclastic wackestone microfacies (SHF 2):** the allochems of the SHF 2 microfacies include *Nummulites lahiri* (NM in **C**), brachiopods (BG in **B**), gastropods (G in **D**) and scattered bioclasts (BC in **A** and ES in **H**). The diagenetic fabric is characterized by internal micritization of bioclasts (BG in **B**, IM in **E)** microbial micritization (MM in **F**), replacement by coarse sparry cement (C in **G,** SP in **F**) and pyrite (PT in **F**). Intergranular and moldic porosity (BG in **B**) are common.

The micritic matrix ranges in abundance from 40 to 60 %, with an average of 45 %. The diagenetic fabric is characterized by biogenic encrustation around the spar filled small gastropod clasts (figure 6.6 F), internal micritization of the bioclasts forming ghost structures (figure 6.6 B), neomorphic alteration of bioclasts (figure 6.6 G) and spar filled micro fractures. Chemical compaction resulted in development of a variety of stylolites including irregular, anastomizing and columnar types. Limonite patches and less than 2 % detrital quartz are seen scattered in the micritic matrix. Porosity types identified are moldic, intragranular and intergranular porosity.

**Depositional environment:** the intense bioturbation, reworking, micritization of bioclasts and impoverished faunal assemblages of dominantly small gastropods, milliolids and bivalves (Tucker & Wright, 1990) suggest deposition of the SHF 3 microfacies in the distal inner ramp to proximal middle ramp setting.

#### *6.4.4.3 The peloidal – Alveolina rich bioclastic wackestone - packstone microfacies (SHF 3)*

In the Sheikhan Nala Section the SHF 3 microfacies is represented by yellowish to yellowish grey coloured thin-bedded, nodular limestone in the lower-middle part of the Sheikhan Formation.

In thin sections the SHF 3 microfacies is characterized by a wackestone to packstone depositional textures. The dominant allochems are *Alveolina* sp., milliolids, echinoids, brachiopods, gastropods, green algae and few scattered ostracodes (figure 6.7 A-H). *Alveolina* sp. clasts are >3mm size and specimens show partial replacement of the test by spar and micrite (figure 6.7 A). Milliolid and uni-bi-tri serial foraminifers are identified showing internal micritization and biogenic encrustation of the test (figure 6.7 H). Echinoid biodebris and spines are commonly scattered in the matrix (figure 6.7 C). Small micritized brachiopod shells form the relic ghost structures. Geopetal fabric is also seen in small brachiopods shells. Small boring gastropods of < 1mm size with biogenic encrustation around the chambers are seen (figure 6.7 E). The bioturbation has resulted in the breakdown and alteration of the bioclasts but still these bioclasts have a preferred orientation.

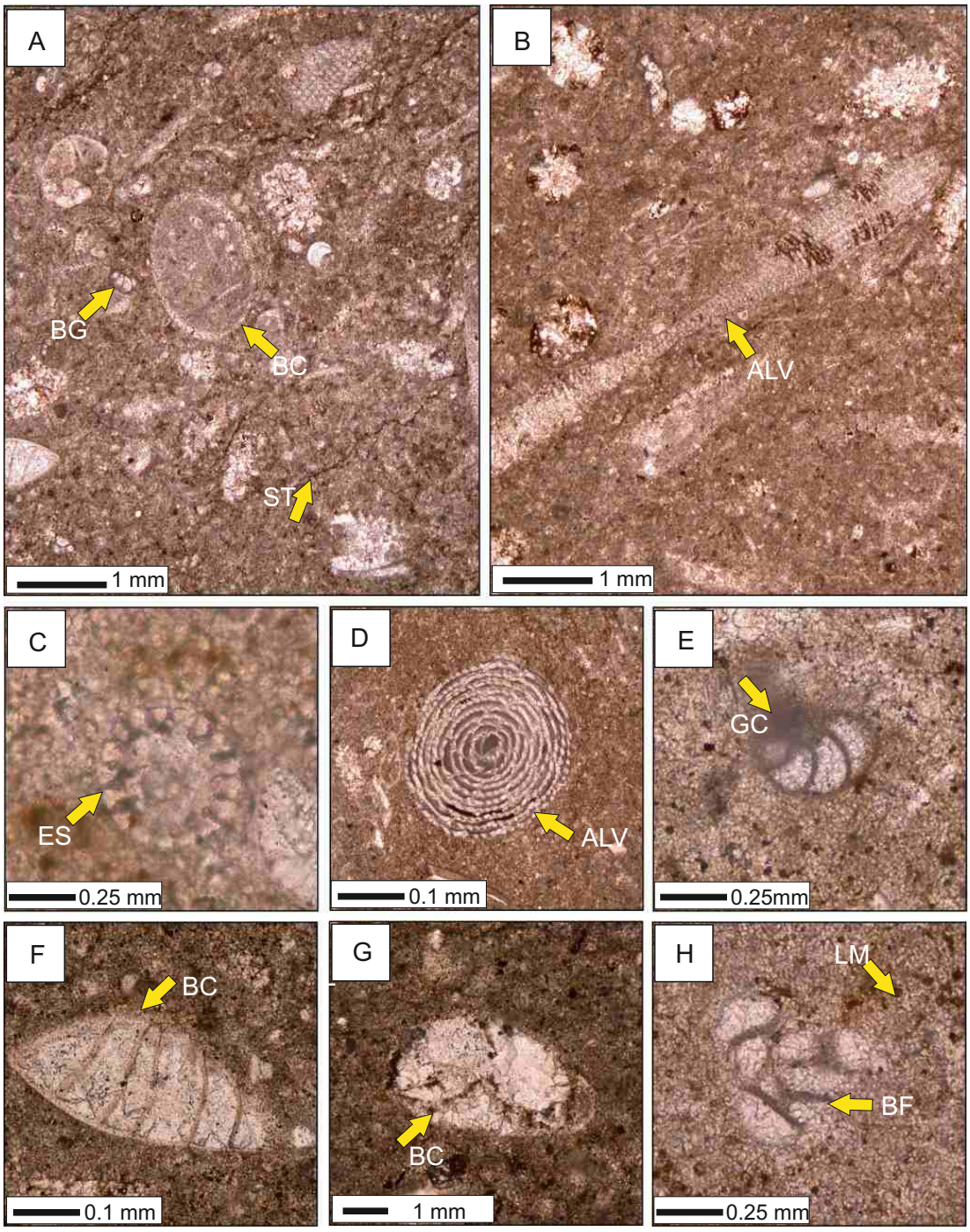


**Figure 6.7. Peloidal - *Alveolina* rich bioclastic wackestone - packstone microfacies (SHF 3):** allochems of the SHF 3 microfacies include common micritized brachiopod (BC in **A, F** and **G**), boring gastropods (BG in **A** and GC in **E**), *Alveolina* bioclasts (ALV in **B, and D**) and echinoid spine (ES in **C**). The diagenetic fabric is characterized by internal micritization of bioclasts (BC in **A**, GC in **E**), coarse sparry cement (BC in **F** and **G**) and limonite (LM in H) replacement and chemical compaction forming stylonodular fabric (ST in **A**). Moldic porosity (BC in **A**) is seen.

The nonskeletal constituents include about 20-25 % peloids of varying sizes and shapes. Peloids are found in irregular, rounded, and random shapes, associated with bioturbation of algae and echinoids. The allomicrite matrix abundance ranges from 40-60 %, with an average of 40 %. The distribution of micrite is associated with the packing and distribution of the peloids. When the packing of peloids is low and bioturbation is common, then the sparitic matrix dominates and where the packing of the peloids is high and poses difficulty in identification, then micritic matrix dominates.

The diagenetic fabric is characterized by chemical compaction resulting in stylonodular fabric, microbial and internal micritization. Neomorphic alteration and pyrite replacement is common. Porosity types include moldic and intragranular porosity.

**Depositional environment:** Peloids are particularly common in recent shallow subtidal to intertidal environments (Flügel, 1982). The dominance of peloids and only a small percentage of bioclastic material suggest deposition in shallow, yet restricted environments. Wilson (1975), Tucker and Wright (1992) suggested peloids usually typify environments with moderate or restricted circulation. The association of peloids, *Alveolina* sp., milliolids, green algae suggests that SHF 3 microfacies was deposited in a proximal inner ramp settings.

#### *6.4.4.4 Diverse bioclastic/burrowed mudstone - wackestone microfacies (SHF 4)*

The SHF 4 microfacies is represented by yellowish grey coloured, thin bedded nodular limestone, alternating with yellowish marls and calcareous shale in the middle part of the Sheikhan Formation in the Sheikhan Nala Section.

In thin section the SHF 4 microfacies is characterized by diverse allochems that include *Alveolina* sp., *Nummulites* sp., *Assilina* sp., milliolids, echinoids, brachiopods, gastropods, ostracodes, bivalves and minor green algae (figure 6.8 A-H). The allomicrite matrix dominates and its abundance ranges from 30-70 %, with an average of 55 %. *Alveolina* sp. bioclasts are > 3mm size and these show partial replacement of the test by spar (figure 6.8 C). Milliolids are scattered and show

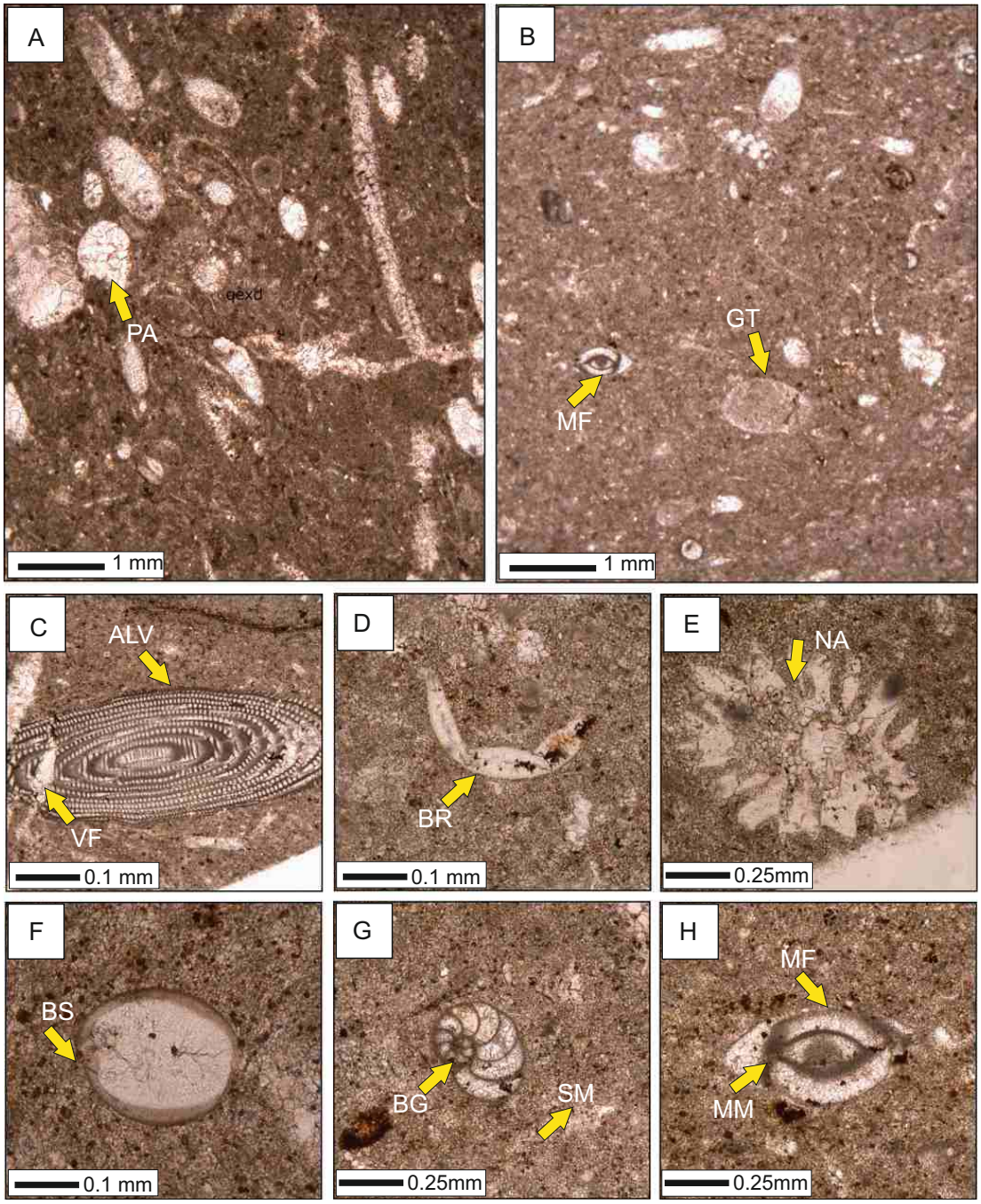


**Figure 6.8. Diverse bioclastic/burrowed mudstone - wackestone microfacies (SHF 4):** the allochems of the SHF 4 Microfacies are scattered in allomicritic matrix and include bioclasts of brachiopod (BR in **D**) and brachiopod spine (BS in **F**), *Alveolina* (ALV in **C**), milliolid forams (MF in **B** and **H**), boring gastropods (BG in **G**). Diagenetic fabric is characterized by internal micritization of bioclasts (GT is **B**), post depositional calcite filled veins that has disturbed the chamber arrangements of *Alveolina* (VF in **C**), neomorphic alteration (NA in **E** & BG in **G**) and replacement by pyrite (BR in **D**). Moldic porosity is common (GT in **B**).

evidence of biogenic encrustation (figure 6.8 F). *Nummulites* sp.and *Assilina* sp. tests are broken up into scattered clasts of less than 1mm size and are partially preserved. Pyrite has replaced the *Nummulites* sp. tests along the test margins. Small brachiopods of < 2mm size with neomorphic alteration are commonly present. Echinoid clasts are scattered but spines are occasionally preserved after escaping micritization. Small boring gastropods of < 1mm size are seen (figure 6.8 E). Occasionally small ostracodes < 2mm size are identified. Green algae are preserved with preferred orientation. Most of the algal bioclasts are micritized or replaced by blocky spar cement (figure 6.8 A). Limonite is less than 3 % and found around the bioclasts. Stylonodular fabric is common. Irregular and low amplitude stylolites are identified. Scattered silt size quartz grains less than 3 %, of variable shapes (i.e. subrounded, angular and elongate) are seen. Sorting of the bioclasts is poor. Spar filled micro-fractures are present. Porosity types identified are moldic, intragranular and fracture porosity.

**Depositional environment:** The high faunal biodiversity and presence of lime mud as matrix suggest that the SHF 4 micofacies was deposited below FWWB under normal marine conditions of middle ramp settings (Flügel, 2004)

#### *6.4.4.5 Siliciclastic mixed bioturbated wackestone - packstone microfacies (SHF 5)*

The SHF 5 microfacies is represented by thin to medium bedded, yellowish brown coloured, arenaceous limestone in the middle upper part of the Sheikhan Formation, exposed in the Sheikhan Nala Section.

In thin sections, the SHF 6 microfacies is characterized by a rich diversity allochemic constituents of brachiopods, *Nummulites* sp., echinoids, green algae and gastropods (figure 6.9 A–H). Brachiopods constitute the dominant allochem type with a size range from < 1 mm to > 3mm. The internal structure of large brachiopod shells is completely micritized or sometimes altered by aggrading neomorphism. *Nummulites* sp. are also identified with completely preserved axial sections (figure 6.9 A). *Lockhartia*, a larger benthic foraminifer genus, is commonly found (figure

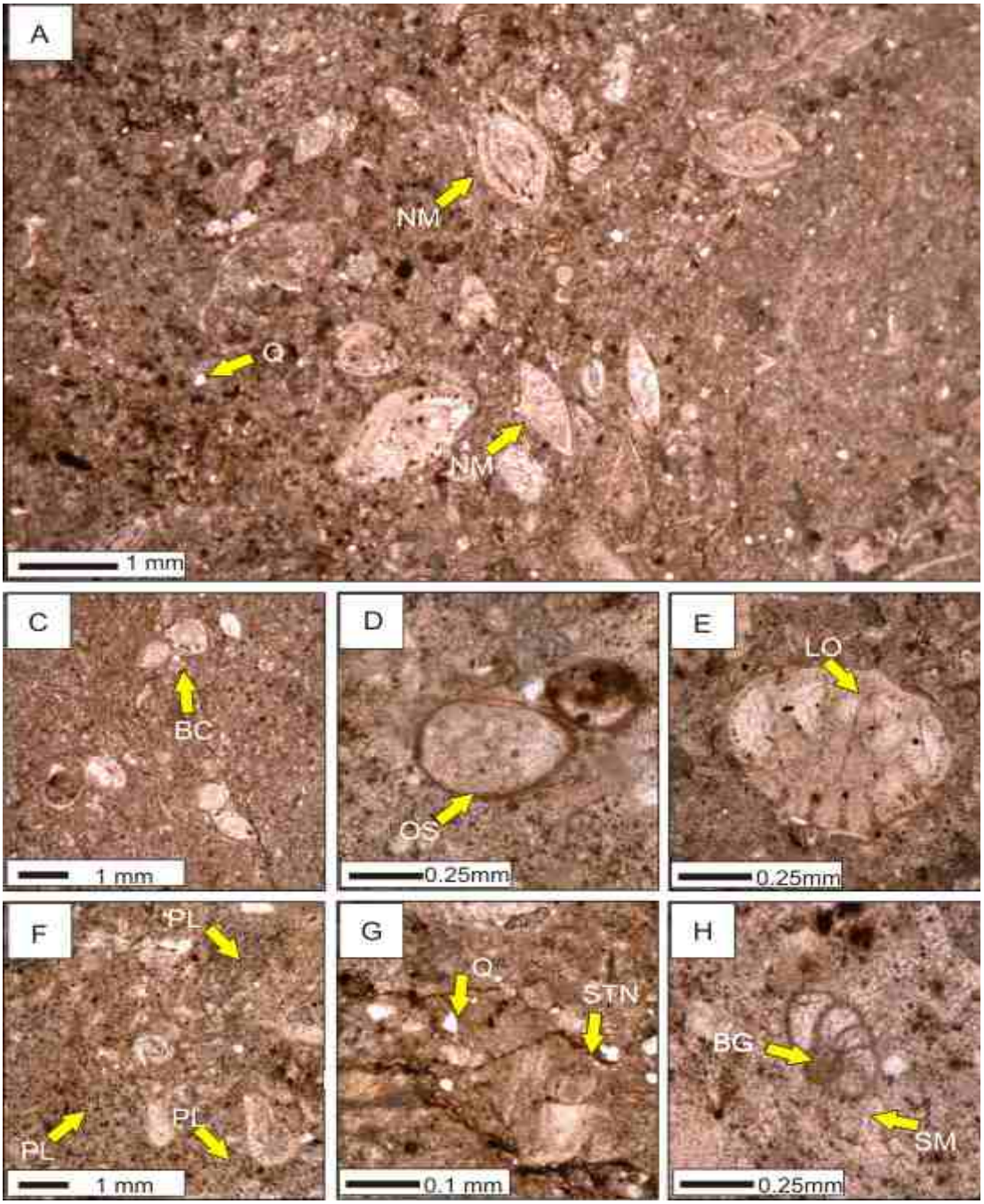


**Figure 6.9. Siliciclastic mixed bioturbated wackestone-packstone microfacies (SHF 5):** the allochems of the SHF 5 Microfacies include *Nummulites* (NM in **A**), *Lockhartia* (LO in **E**), ostracodes (OS in **D**) and boring gastropods (BG in **H**). The diagenetic fabric is characterized by chemical compaction forming stylonodules (STN in **G**), microbial micritization of bioclasts (BG in **H**), and limonite replacement (patchy distribution in **A**). Scattered quartz grains indicate terrestrial influx during storms (Q in **A** and **G**).

biogenic encrustation are identified (figure 6.9 D and H). The bioclasts does not have any preferred orientation and sorting is poor. Echinoid and brachiopod geopetals are recognized. Sparry matrix constitutes 30-55 %, with an average of 40 %. Limonite is scattered in the sparry matrix and constitutes less than 5 % of the total volume. Quartz grains of angular, subrounded and elongate shapes are scattered in the matrix (6.9 A). Stylonodular fabric is characterized by irregular and smooth stylolites (figure 6.9 G). Bioturbation has resulted in a dismicrite fabric, with blocky calcite spar filling the fractures and voids in the mud matrix. Microfratures filled with blocky spar cement are identified.

The diagenetic fabric is characterized by compaction, neomorphism, microbial micritization and post depositional fracture filling. A variety of porosity types are recognized which includes moldic, fracture, interparticle and shelter porosity.

**Depositional environment:** the presence of diverse benthic fauna (i.e. echinoids, foraminifers, brachiopods, gastropods) and flora (algae) indicate normal salinity while sparry matrix indicates high energy conditions of distal inner ramp setting (Flügel, 2004).

#### *6.4.4.6 Milliolid rich packstone-grainstone microfacies (SHF 6)*

The SHF 6 microfacies is represented by thin to medium bedded, yellowish brown coloured, arenaceous limestone in the upper part of the Sheikhan Formation in the Sheikhan Nala Section.

In thin section the SHF 6 microfacies shows the milliolid rich packstone to wackestone depositional textures. Allochems range in abundance from 40-80 %, with an average of 60 %. The allochems show dominance of foraminifera i.e. milliolids, *Alveolina* sp., *Nummulites* sp., *Operculina* sp. and *Lockhartia* sp. (figure 6.10 A - H). Some ostracodes are also seen. Sparry cement has filled the intergranular space. Less than 10 % micritic matrix is seen. Biogenic encrustation of the bioclasts have either partially distorted the internal structure or completely micritized the test and only relic ghosts are seen (figure 6.10 E). Limonite is very commonly found around and inside the foraminiferal test chambers (figure 6.10 A, B, E, G and H).

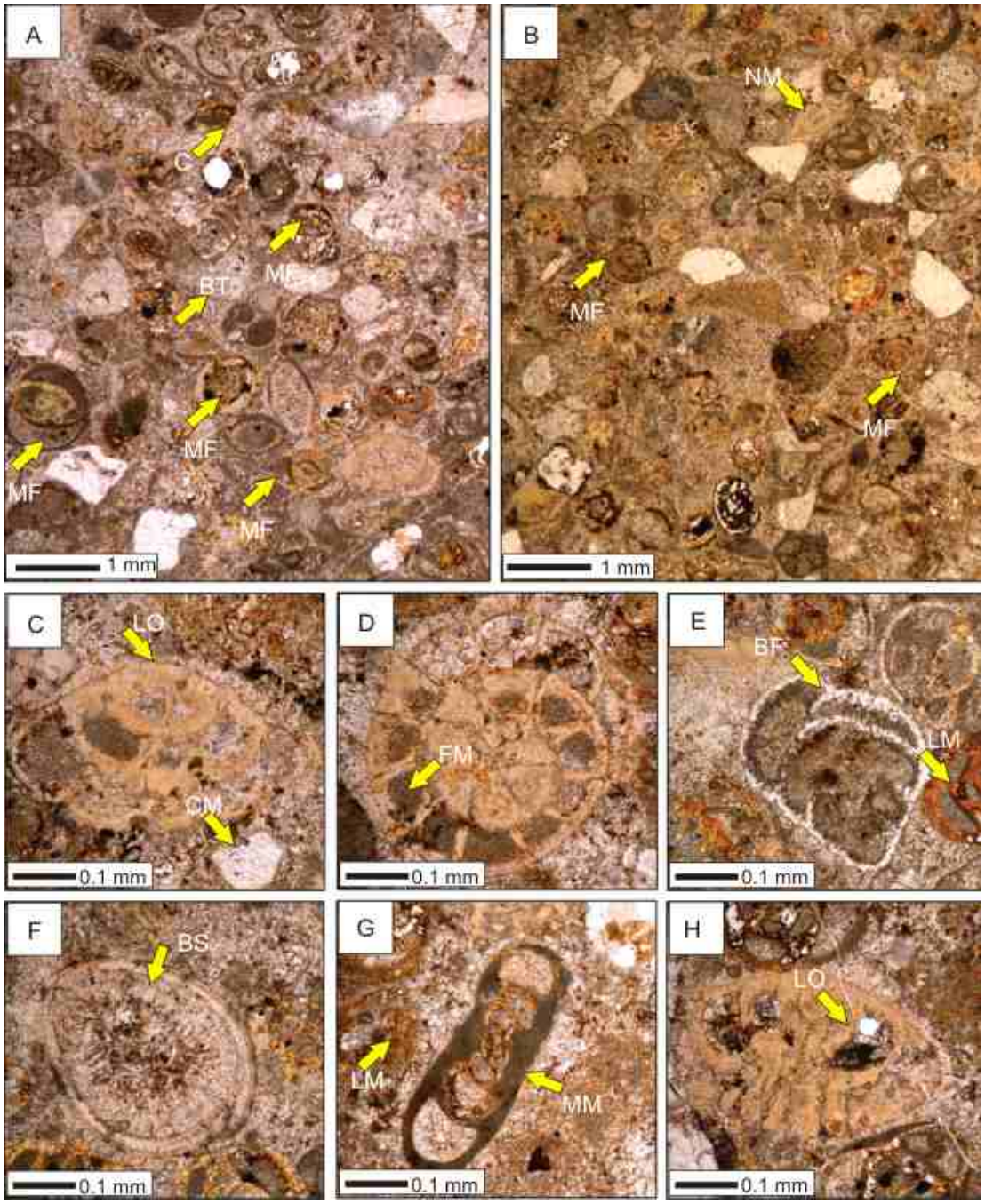


**Figure 6.10. Milliolid rich packstone-grainstone microfacies (SHF 6)**: the allochems of the SHF 6 microfacies include milliolid forams (MF in **A** and **B**), *Nummulites* (NM in **B**), *Lockhartia* (LO in **C**), biserial foram (BF in **E**), brachiopod spine (BS in **F**). The diagenetic fabric is characterized by microbial (MM in G) and internal micritization (FM in **D**) of the bioclasts, limonite and spar replacement (LM in **E** and CM in **C**).

The diagenetic fabric is characterized by neomorphic alteration, micritization, pyritization and chemical compaction that form irregular and columnar stylolites. Intragranular, moldic, intergranular and stylolitic porosity types are identified.

**Depositional environment:** Abundance of milliolid foraminifera indicates shallow water, low turbulence, and saline to hyper saline restricted lagoon conditions (Geel, 2000; Chassefiere et al., 1969). Terrigenous quartz indicates input from the continent under occasional stormy conditions. The SHF 6 microfacies is interpreted as deposited under restricted marine conditions of the inner ramp lagoonal setting.

#### *6.4.4.7 Discocyclina rich wackestone microfacies (SHF 7)*

The SHF 7 microfacies is represented by thin to medium bedded, grey coloured nodular limestone in the lower part of the Sheikhan Formation in the Panoba Nala Section.

In thin sections the SHF 7 microfacies shows the wackestone depositional texture which is dominated by a rich LBF including *Discocyclina* sp. associated with *Nummulites* sp. and *Assilina* sp. (figure 6.11 A - D). The *Discocylina* sp. tests are completely preserved (figure 6.11 A and C) and scattered bioclasts are also common (figure 6.11 B and D). Bioclasts have angular, subangular and subrounded morphologies with poor sorting. Bioretexturing is also common. Occasionally stylonodular fabric is seen. Small (< 1 mm) size boring gastropods are also present. Echinoid spines are also seen mixed in fine grained allomicritic matrix, showing single grain complete extinction under cross light. Brachiopod, gastropod and foraminiferal cartoids are also common. Matrix is inhomogeneous allomicrite that ranges in abundance from 60 to 80 %, with an average of 70 % (figure 6.11 B). Biogenic content is mostly benthic fauna with good preservation. The bioclasts are randomly arranged. The intergranular micrite cement and replacement spar cement is seen. Limonite patches are found around the chambers of *Nummulites* sp. A variety of smooth, columnar and irregular stylolites shows chemical compaction. Diagenetic fabric is characterized by micritization and neomorphic alteration of bioclasts. Porosity types include moldic, intergranular and intragranular.

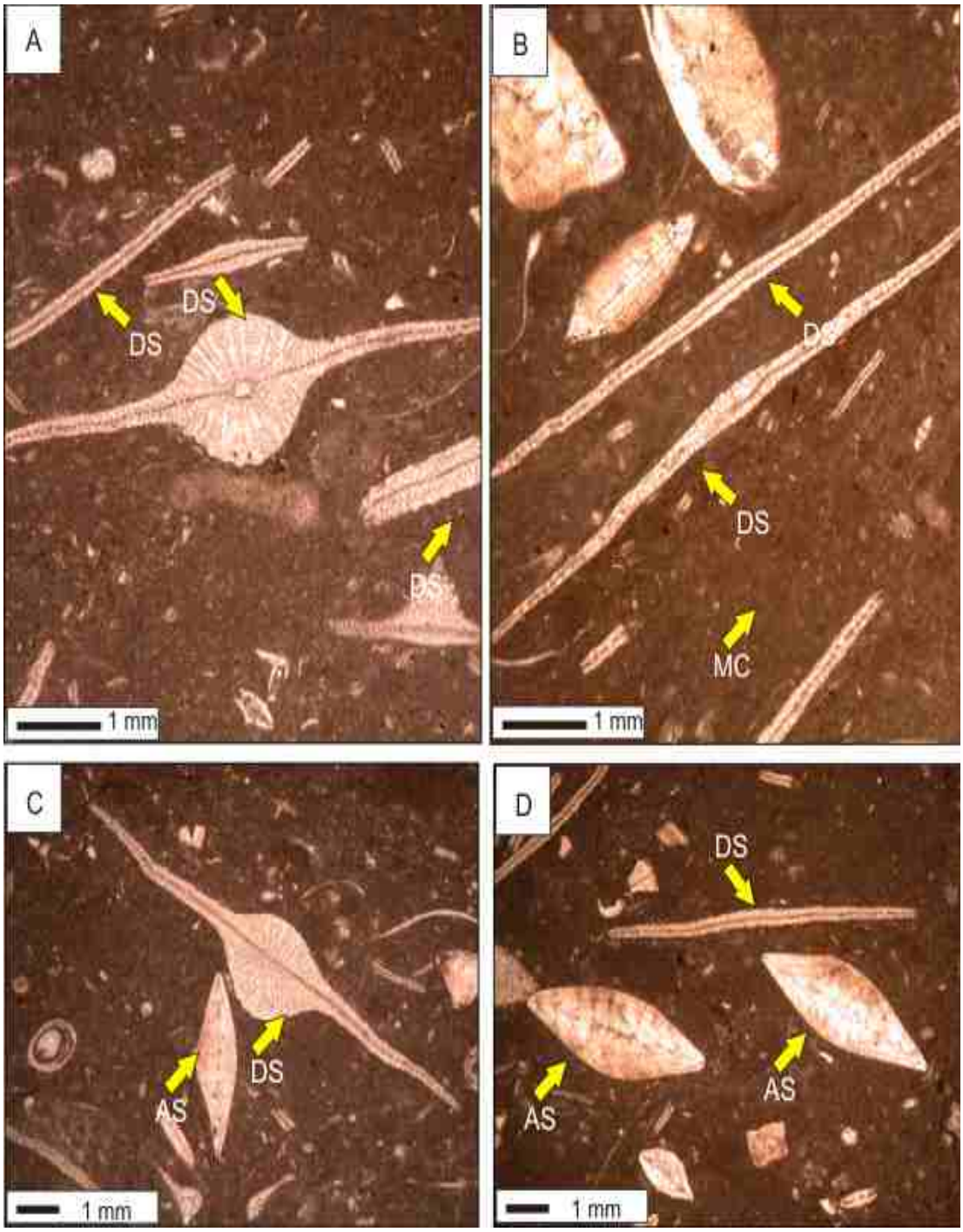


**Figure 6.11. *Discocyclina* rich wackestone microfacies (SHF 7):** the allochems of the SHF 7 microfacies are dominated by *Discocyclina* (DS in **A** -**D**), *Assilina* (AS in **C** and **D**), which are scattered in a micritic matrix (MC in **B**).

**Depositional environment:** the abundance of *Discocylina* sp. indicates normal marine conditions, in slightly deeper water than *Assilina* sp. but in shallower water than *Operculina* sp. representing an outer ramp environment (Racey, 1994). Abundance of *Discocylina* sp. along with *Nummulites* sp. *Assilina* sp., echinoid clasts, and micritic matrix indicate that the SHF 7 microfacies was deposited in open marine conditions of the distal middle ramp setting.

#### *6.4.4.8 Assilina rich bioclastic wackestone - packstone microfacies (SHF 8)*

The SHF 8 microfacies is represented by thin to medium bedded, grey coloured nodular limestone in the lower part of the Sheikhan Formation in the Panoba Nala Section.

In thin sections the SHF 8 microfacies is characterized by the wackestone to packstone depositional textures. The preservation of the biogenic content is good. The dominant allochems are bioclasts of *Assilina* sp. (figure 6.12 A), and subordinate *Lockhartia* sp., echinoid clasts, small brachiopods are found. The allochemic abundance ranges from 40 to 80 %, with an average of 65 %. *Assilina* sp. bioclasts dominate and have a size range from 1 mm to 4 mm (figure 6.12 A). The echinoid clasts are scattered in inhomogeneous allomicritic matrix which ranges in abundance from 40 to 50 %, with an average of 35 % (figure 6.12 A).

Bioretexturing is seen in small brachiopod shells. The internal structure of small brachiopod is either filled with neomorphic spar or due to biogenic encrustation a micrite envelope is found around the shell margin. Intergranular and neomorphic microspar cement is present.

The diagenetic fabric is characterized by microbial micritization, chemical compaction forming stylondular fabric (figure 6.12 C), post depositional spar filled fractures and neomorphic alteration of the bioclasts. Porosity types include intraparticle, fracture and moldic porosity.

**Depositional environment:** *Assilina* sp. have been reported to occupy a mid ramp environment (Ghose, 1977). The dominance of *Assilina* sp., echinoid bioclasts,

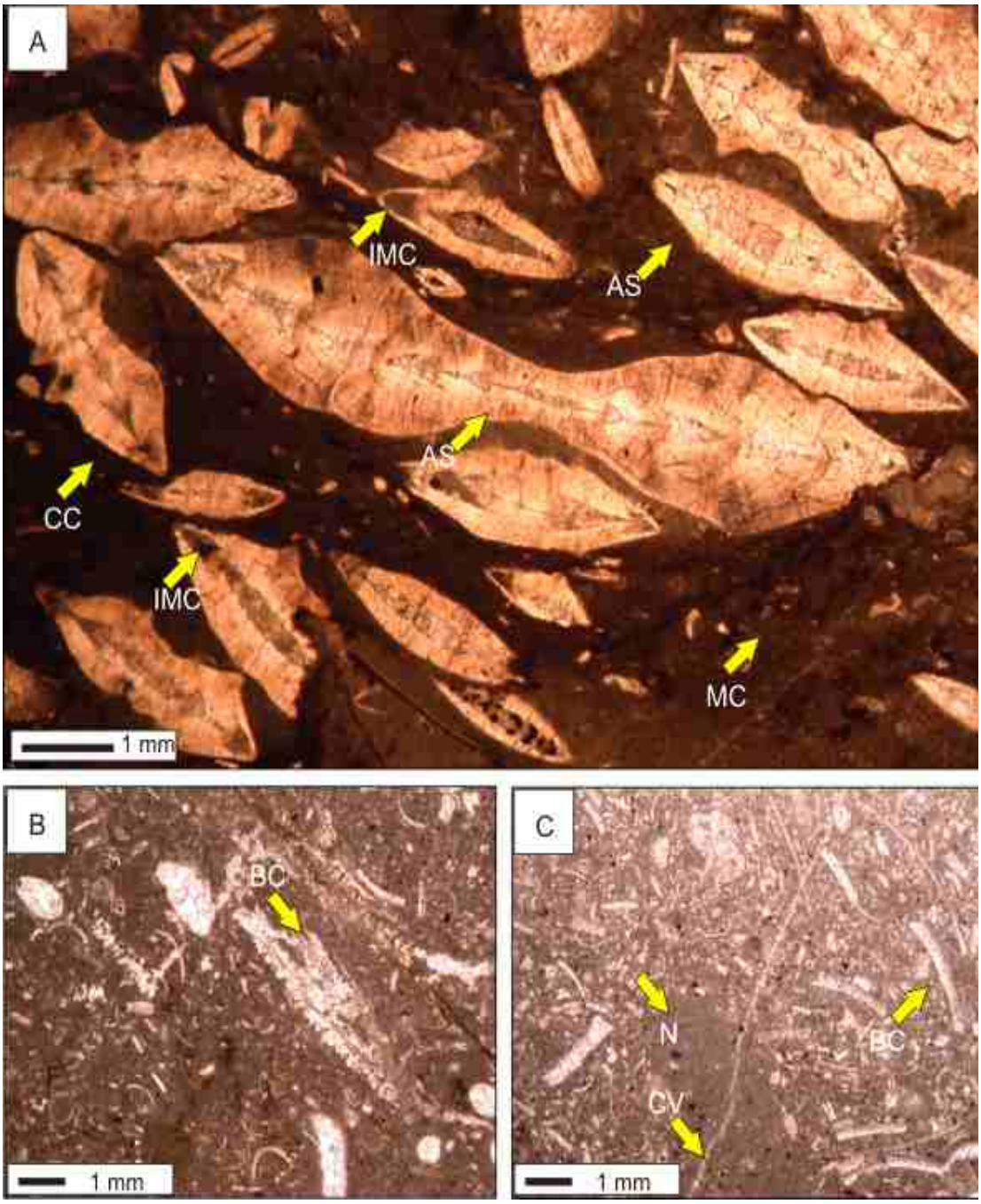


**Figure 6.12. *Assilina* rich bioclastic wackestone - packstone Microfacies (SHF 8):** the allochems of the SHF 8 Microfacies includes *Assilina* (AS in **A**) and echinoid bioclasts (BC in **B**). Matrix is allomicrite (MC in **A**).The diagenetic fabric is characterized by internal micritization of bioclasts (IMC in **A**), post depositional calcite filled fractures (CV in **C**) and nodules (N in **C**).

allomicritic matrix and absence of terrigenous influx indicates that SHF 8 microfacies was deposited FWWB in middle ramp settings (Tucker & Wright, 1990; Flügel, 2004).

#### *6.4.4.9 Poorly fossiliferous lime mudstone/dolomicrite microfacies (SHF 9)*

The SHF 9 microfacies is represented by medium to thick bedded dolomitic limestone capped by gypsiferous shales in the upper part of the Sheikhan Formation in the Panoba Nala Section.

In thin sections the SHF 9 microfacies shows poorly preserved biogenic content dominated by foraminifera and algal peloids (figure 6.13 E). Micritic matrix ranges from 70-90 %, with an average of 85 % (figure 6.13 A). The allochems are mostly benthic foraminifers which include *Nummulites* sp. (figure 6.13 D) and rare biserial foraminiferal tests (figure 6.13 C). Biogenic encrustations are common around the chambers of the biserial foraminifera. Detrital quartz (less than 2 %) of angular, subrounded and irregular shapes is scattered in the matrix (figure 6.13 B). Stylolitic fabric is very prominent and different varieties of stylolites are recognized including irregular, smooth and columnar types. Stylonodular fabric is also identified (figure 6.13 B). In the sparry matrix < 1mm size boring gastropods are sometimes found. Few neomorphic ghosts are also identified. The diagenetic fabric is characterized by dolomitization (figure 6.13 C) and chemical compaction.

**Depositional environment:** a relatively low diversity fauna and flora in the SHF 9 microfacies indicate that environmental conditions were not suitable for the establishment of diverse normal marine fauna that characterises open marine conditions. Presence of dolomite indicates shallow supratidal inner ramp platform conditions (Tucker & Wright, 1990; Flügel, 2004).

### 6.4.5 Facies of the Chashmai Formation

In the north-western corner of the Kohat Basin in the Haji Khel area near Hangu City the Chashmai Formation is identified. Meissner (1975) correlated the -

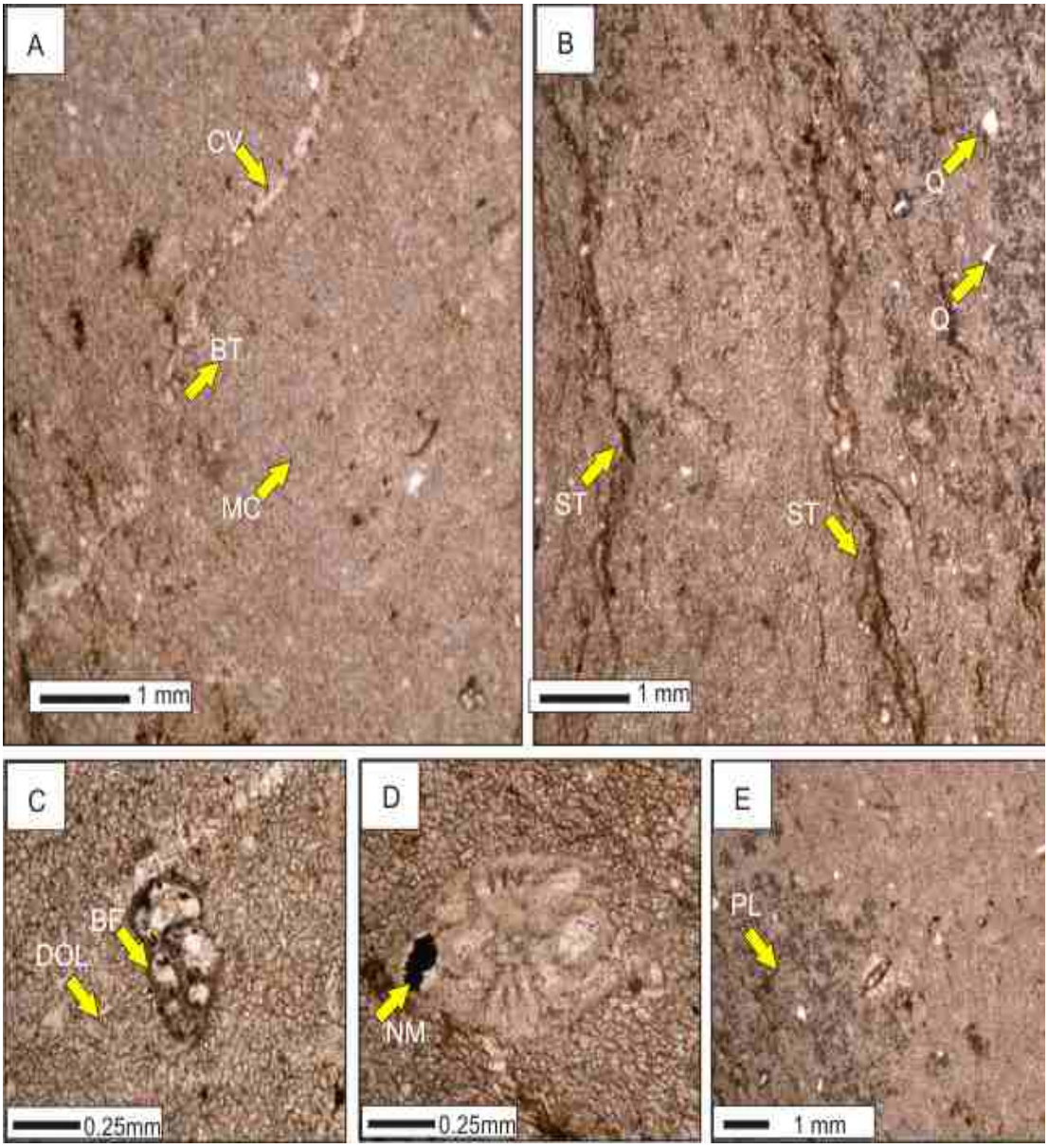


**Figure 6.13. Poorly fossilferous lime mudstone/dolomicrite microfacies (SHF 9):** the allochems of the SHF 8 microfacies comprised of poorly preserved biserial forams (BF in **C**) and *Nummulites* (NM in **D**) found in micritic matrix (MC in **A**). Non bioclastic grains are dominated by peloids that are concentrated in bunches (PL in **E**). Scattered quartz is found (Q in **B**). The diagenetic fabric is characterized by chemical compaction forming stylolites (ST in **B**), aggrading neomorphic alteration forming coarse sparry cement. Dolomite crystals are also seen (DOL in **C**). Pyritization of the bioclasts is seen (**NM** in D).

Chashmai Formation with the upper part of the Panoba Formation while Wells (1984) correlated it with the lower part of the Kuldana Formation. However, along the western margin of the Kohat Basin, Kazmi and Abassi (2008) placed it between the Panoba and the Kuldana Formation as a stratigraphic equivalent of the Sheikhan Formation in the north-eastern part and Bahadur Khel Salt/Jatta Gypsum in the central part of the Kohat Basin. The Chashmai Formation is comprised of olive green clay and grey sandstone with subordinate conglomerate (Kazmi and Abassi, 2008). The conglomerate contains pebbles of limestone, chert and quartzite. The facies shows a coarsening upward sequence. The lower contact is not clear while it has an unconformable upper contact with the Kohat Formation.

**Depositional environment:** the clastics of the Chashmai Formation are deposits of deltas and stream fed beaches. Larger benthic foraminifera are a very common constituent of the conglomerate beds, and thus these beds contain transported bioclasts of *Nummulites* sp., *Alveolina* sp., *Operculina* sp., *Lockhartia* sp. and milliolids from the upper part of the Sheikhan Formation. Limonite crust is often seen in the conglomerate indicating oxidizing conditions. Here, the Chashmai Formation is interpreted to represent a lateral facies of the Kuldana Formation.

### 6.4.6 Facies of the Bahadur Khel Salt

In the study area (Bahadur Khel Salt Tunnel Section), the Bahadur Khel Salt is exposed in the core of a regional anticline and it is conformably capped by the Jatta Gypsum. The salt is bedded to massive crystalline and grey/blackish coloured (figure 6.14), thickness of the Salt is difficult to measure due to its diapiric nature and its estimated thickness is over 100m.

**Depositional environment:** according to Tanoli et al. (1993) the Salt was deposited in shallow marine restricted small basin, which were local shoals of Early Eocene regression. The basins were recharged with saline sea water either through inlets or by overtopping the barrier during storms. However, this study supports Wells (1984), who proposed that more than 300m thick Bahadur Khel Salt must have been deposited in the centre of a deep barred basin.

This study suggests that uplift of the northeastern Kohat Basin and subsequent sea regression caused restriction of marine conditions in the southwest and deposition of thick salt is attributed to hot arid climatic conditions of deep but restricted basinal settings.


**Figure 6.14:** a northeast looking view of the massive salt facies of the Bahadur Khel Salt, exposed in the Bahadur Khel Salt Tunnel Section, southern Kohat Basin.

### 6.4.7 Facies of the Jatta Gypsum

The "Upper Kohat Saline Series" of Gee (1945) has been renamed as Jatta Gypsum by Meissner et al. (1974) from exposures in the Jatta Salt Quarry in the Kohat Basin.

In the study area (Bahadur Khel Salt Tunnel Section) the Jatta Gypsum overlies the Bahadur Khel Salt. The gypsum is light grey to greenish grey, laminated, massive to well bedded (figure 6.15) and contains greenish coloured clays in the upper part (figure 6.16). The Jatta Gypsum is mostly pure and homogeneous and has

organic rich bituminous clays having a strong hydrocarbon odour. Oil shales are reported from Pathan Algad near the intersection of the Jatta Salt Quarry with the Shakardara- Kohat road. The Jatta Gypsum is exposed along a 15-20 Km wide and about 60m long E-W trending belt in the central Kohat Basin (Kazmi and Abassi, 2008). Meissner (1974) reported maximum thickness of 70m from the Bahadur Khel Salt Tunnel Section (study area). Interfingering of the Sheikhan Formation and Jatta Gypsum is reported by Meissner (1974) from the Mamikhel Section where 40m thick gypsum is underlain by 25m thick limestone. Further southward of the basin the Sheikhan Formation is completely replaced by the Jatta Gypsum and it has a conformable contact with the overlying Bahadur Khel Salt. Based on the stratigraphic position the Jatta Gypsum has been assigned an Early Eocene age (Kazmi and Abassi, 2008).

**Depositional environment:** Gypsum is deposited in variety of settings in the marine realm, ranging from deep basinal to shallow marine or supratidal sabkhas. The association of the Jatta Gypsum with the shallow marine and fluvial facies rule out deep basin origin and shallow marine intertidal to supratidal environment is considered likely for the Jatta Gypsum (Kazmi and Abassi, 2008).

The upper part of the Jatta Gypsum where it passes to the Kuldana Formation flood plain clastics represent extremely shallow water to an emergent environment (figure 6.17). The bulk of gypsum, laminated, variegated clays and interbedded green shales suggest deposition under low energy conditions in a shallow water photic zone (10m-20m to less than 1m depth range). The green shale that locally succeeds the gypsum formed in gypsum floored bays and lagoons with fine clastics which halted the gypsum deposition. The gypsiferous shales (14m thick in the Panoba Nala Section) represent a sabkha environment (Wells, 1984).

### 6.4.8 Facies of the Kuldana Formation

The Kuldana Formation can easily be identified in the field as red to brownish red clay with interbedded sandstone layers. It forms conspicuous red coloured gullies because of being soft as compared to the Kohat Formation and other formations exposed in the area. The formation is approximately 50-60 meters thick,

**Figure 6.15:** massive gypsum facies in lower part of the Jatta Gypsum exposed in the Bahadur Khel Salt Tunnel Section, southwestern Kohat Basin (see hammer for scale).


**Figure 6.16:** green coloured clays in the upper part of the Jatta Gypsum exposed in the Bahadur Khel Salt Tunnel Section, southwestern Kohat Basin.

and usually composed of clay, sandstone, limestone and bleached dolomite. The clay is red to brownish red, soft, calcareous and gypsiferous. The sandstone is reddish brown, thick bedded, hard medium to coarse grained and cross-bedded. The Kuldana Formation overlies the Sheikhan Formation.

Wells (1983) divided the Kuldana Formation into two, the Lower Kuldana (red to purple colour mudstone with some sandstone and minor grey limestone) and the Upper Kuldana (green and brown calcareous mudstone and few limestone beds). The Kuldana Formation is famous for its vertebrate mammal fossils (Gingerich, 2003).

In the Panoba Nala Section, the Lower Kuldana Formation consists of 24m thick purple to reddish brown continental clays with occasional sandstone beds. The Upper Kuldana Formation is represented by purple grey/greenish grey coloured dolomitic limestone that grades upward into an oysters rich limestone bed which marks the boundary between the Upper Kuldana Formation and the overlying Kohat Formation.

In the Sheikhan Nala Section, Lower Kuldana Formation is identified and it is composed of 25m thick purple to reddish brown continental clays with subordinate sandstone beds.

In the Bahadur Khel Salt Tunnel Section, the Kuldana Formation is represented by dominant red mudstone facies with subordinate brownish coloured sandstone in the lower- middle part while in the upper part (referred to as Upper Kuldana by Wells, 1984) a 26m thick sequence of greenish grey coloured argillaceous limestone and dolomite (with a persistent oysters rich bed) is present (figure 6.18).

**Depositional environment:** the Kuldana Formation has a fluvial origin and was deposited by rapidly flowing streams in a semi-arid basin at the end of a marine regression (Wells, 1983). The uniform brick red shale beds in the Lower Kuldana contains enriched mammal bones and represents deposition in an over bank flood plain. The Upper Kuldana Formation contains ostracodes, bivalves and represents a marginal marine environment of deposition.

**Figure 6.17:** emergent gypsum facies having upper contact with the flood plain red beds of the Kuldana Formation exposed in the Bahadur Khel Salt Tunnel Section, southwestern Kohat Basin.

**Figure 6.18.** A northeast looking view of the Kuldana Formation, which is exposed in the Bahadur Khel Salt Tunnel Section, southern Kohat Basin. Thick reddish / purple colour sandstone and shale interbeds characterize the Lower Kuldana and the Upper Kuldana is characterized by sandstone, dolomite and few limestone beds (see person standing in figure for scale).

### 6.4.9 Facies of the Kohat Formation

The microfacies of the Kohat Formation are abbreviated as KTF 1-KTF 7 (KT stands for the Kohat Formation, F stands for microfacies and 1-7 are various types of recorded microfacies).

#### *6.4.9.1 Foraminiferal packstone microfacies (KTF 1)*

The KTF 1 microfacies is represented by highly fossiliferous shales and thin to medium bedded argillaceous limestone in the lower part of the Kohat Formation in the Sheikhan Nala Section.

In thin sections the KTF 1 microfacies is characterized by the packstone depositional texture. Predominance of *Assilina* sp. bioclasts is noted with good biogenic preservation. The size of *Assilina* sp. bioclasts is ranging from 2 mm to 6 mm (figure 6.19 A). *Nummulites* sp. tests are also seen having spar filled chambers (figure 6.19 A and B). Packing of the bioclasts is lose to moderate and they have poor sorting. The micritic matrix and scattered biodebris of *Assilina* sp. and *Nummulites* sp. filled the intergranular space. The diagenetic fabric is characterized by micritization and aggrading neomorphic alteration is also common in the bioclasts. A variety of intergranular, intragranular and fracture porosity is identified.

**Depositional environment:** *Assilina* sp. lived in the outer ramp environment (Herb, 1988). Thinner tests of *Assilina* sp. with elongate form indicate increasing water depth (Racey, 2004). In the KTF 1 microfacies the dominance of asexually produced elongated *Assilina* sp. Form-A bioclasts with minor proportion of *Nummulites* sp. tests indicates deposition in the deeper part of the depth range. This microfacies is interpreted to have been deposited in a moderate energy forebank environment.

#### *6.4.9.2 Nummulitic packstone -grainstone microfacies (KTF 2)*

The KTF 2 micofacies is represented by highly fossiliferous medium bedded argillaceous limestone in the lower part of the Kohat Formation in the Sheikhan Nala Section.

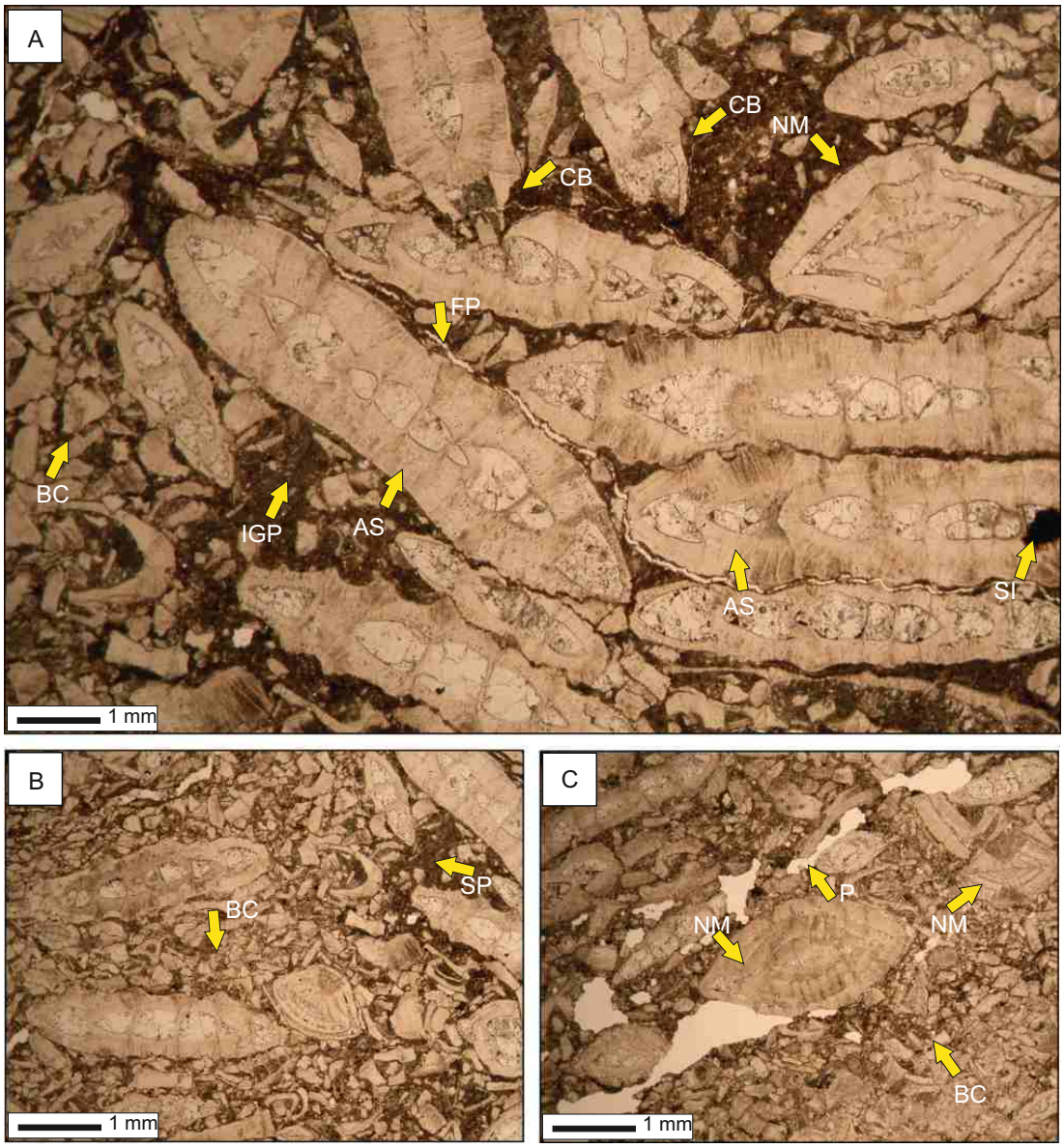


**6.19. Foraminiferal packstone microfacies (KTF 1):** The allochems of the KTF 1 microfacies include dominance of *Assilina* bioclasts (AS in **A**), *Nummulites* (NM in **A** and **C**) and broken foraminiferal bioclasts (BC in **A - C**). Cross bedding fabric (CB in **A**) is shown by *Assilina* bioclasts. Micritic matrix filled the intergranular space. Diagenetic fabric is characterized by silicification of bioclasts (Sl in **A**). Porosity types identified are Intergranular (IGP in **A**), fracture porosity (FP in **A**)

In thin sections the KTF 2 microfacies is characterized by the packstone to grainstone depositional fabrics with dominant allochemic component of *Nummulites* sp. and subordinate *Assilina* sp. (figure 6.20 A). The *Nummulites* sp. and *Assilina* sp. bioclasts range in size from 1 mm to 6 mm. These bioclasts have good sorting and well packed (figure 6.20 A). The *Assilina* bioclasts show an imbricated fabric. Brachiopod spines are also found having the characteristic feature of a foliated lamellar structure, fused and amalgamated and made up of calcite layers having wavy banded appearance (figure 6.20 B). The biogenic content is mostly benthic and shows good preservation. Interparticle space is filled by spar cement (figure 6.20 C). The diagenetic fabric is characterized by pyrite replacement, neomorphism, and compaction of the bioclasts. The KTF 2 microfacies shows intergranular, intragranular and fracture porosity.

**Depositional environment:** The dense packing, poor to moderate sorting of *Nummulites* sp. bioclasts and presence of spar indicate post-mortem allochthonous deposition by high energy currents (Flügel, 2004).

The processes leading to the formation of Tertiary grainstone, packstone or wackestone with nummulitid foraminifera can be derived from the abundance and proportion of the large and small tests, their orientation and amount of carbonate mud occurring together with the foraminifera (Flügel, 2004). The KTF 2 microfacies shows poor to moderate sorting, dense packing, very rare to absent micrite which has been winnowed by high energy currents. The bioclasts are not worn which indicates limited transport. The proportional dominance of small *Nummulites* sp. tests (form-A) over the large (Form-B) tests also suggests deposition in the shallower part of the fore bank environment.

#### *6.4.9.3 Operculina rich mudstone-wackestone microfacies (KTF 3)*

The KTF 3 micofacies is represented by medium bedded argillaceous limestone in the middle upper part of the Kohat Formation in the Sheikhan Nala Section. In thin sections the KTF 3 microfacies is characterized by the mudstone to wackestone depositional fabric. The biogenic content is well preserved and includes bioclastic assemblages of *Operculina* sp., rare small *Nummulites* sp., *Assilina* sp. and

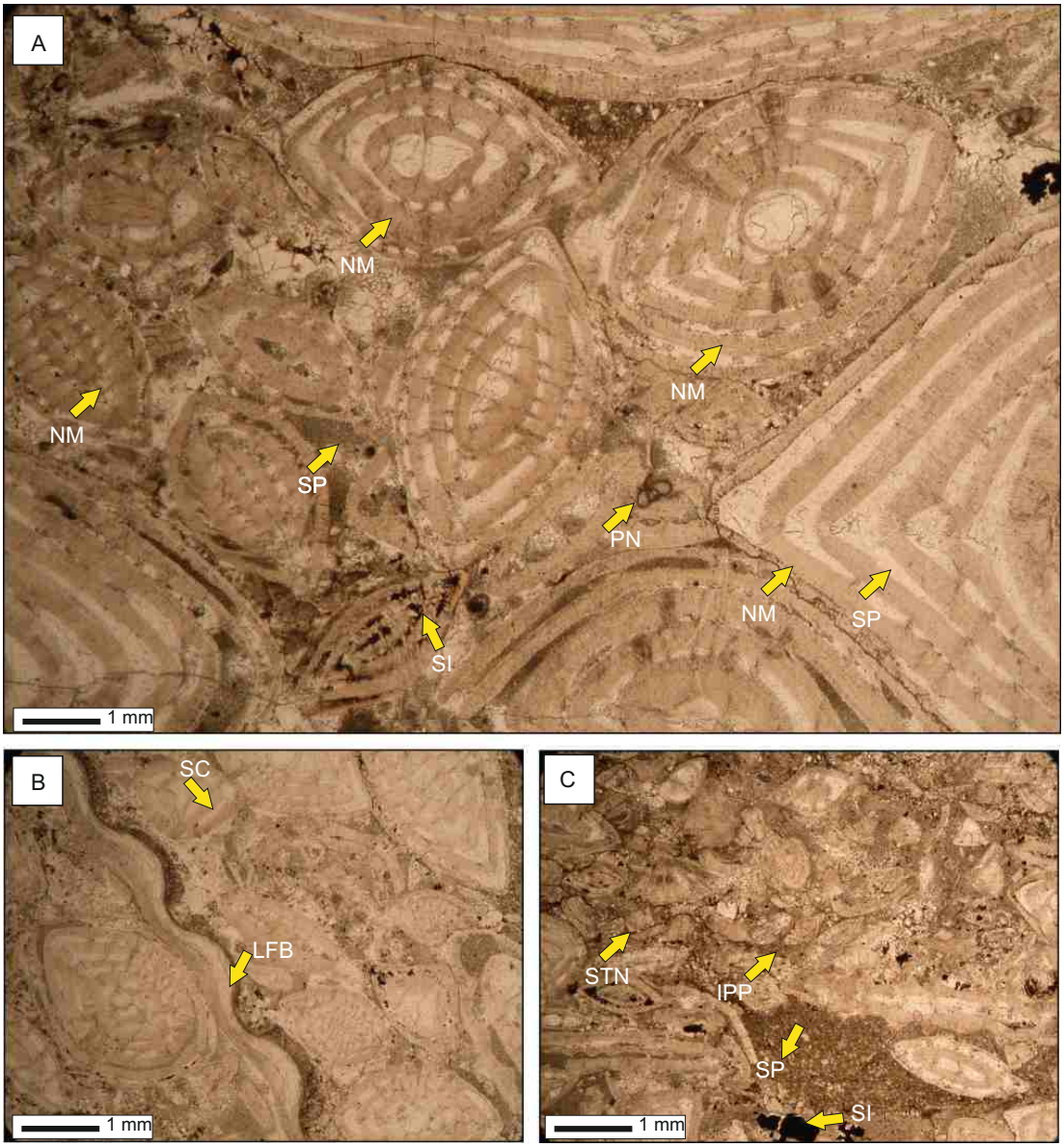


**6.20. Nummulitic packstone-grainstone microfacies (KTF 2):** the allochems of the KTF 2 microfacies include dominance of Form-A *Nummulites* (NM in **A**). A rare planktonic foram is also seen (PN in **A**). Brachiopod spines show characteristic foliated and lamellar feature (LFB in **B**). Diagenetic fabric is characterized by silicification of bioclasts (Sl in **C**), neomorphic alteration of the bioclasts (SP in **A**) and stylonodular fabric (STN in **C**). Porosity types identified are intergranular (IPP in **C**), fracture porosity (FP in **A**).

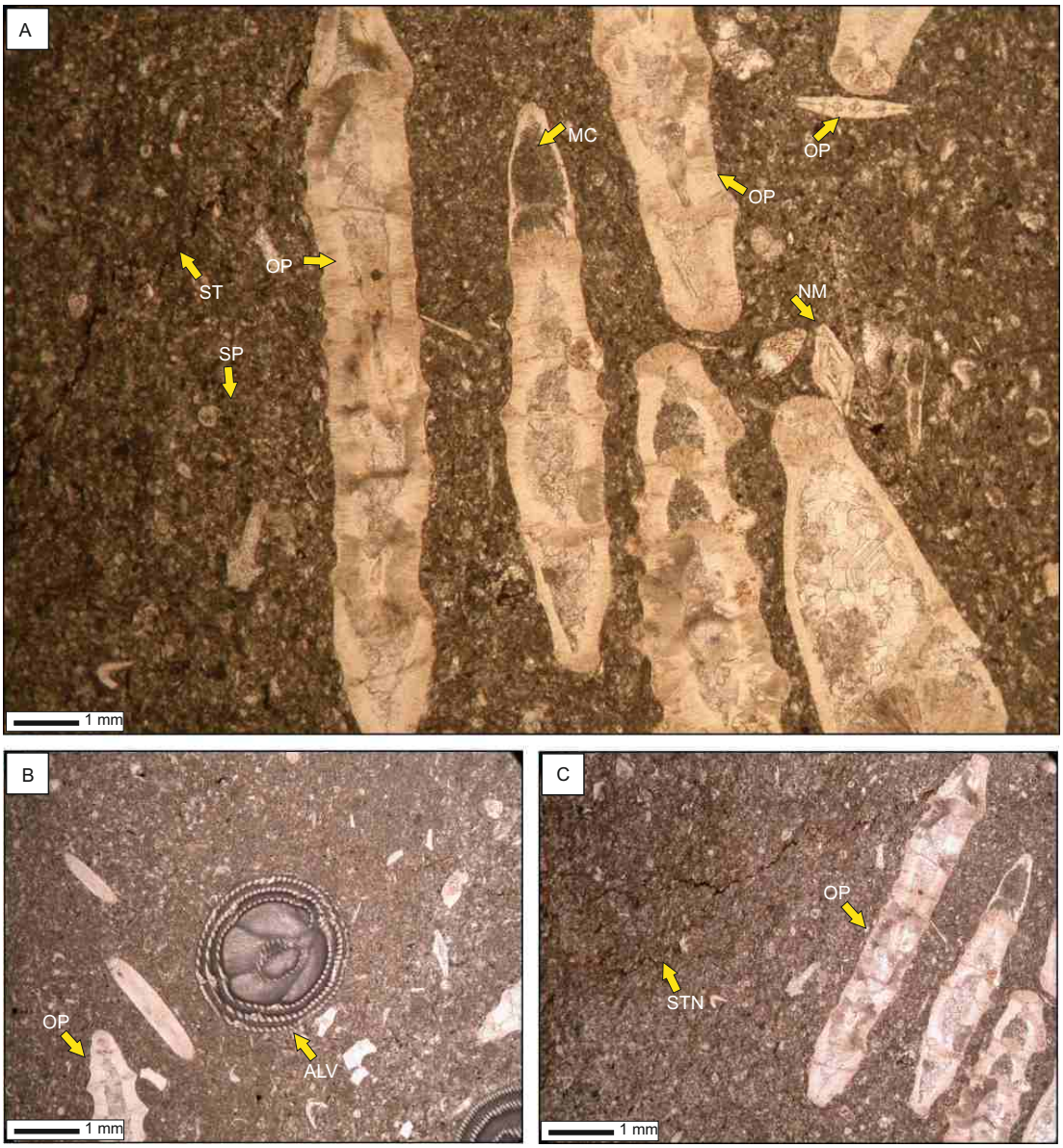


**Figure 6.21. *Operculina* rich mudstone - wackestone microfacies (KTF 3):** the allochems of the KTF 3 microfacies include *Operculina* bioclasts (OP in **A-C**), *Alveolina* (ALV in **B**) and *Nummulites* (NM in **A**). Diagenetic fabric is characterized by stylolites (ST in **A**), stylonodular fabric (STN in **C**) and internal micritization of the bioclasts (MC in **A**).

**Depositional environment:** *Operculina* sp. occupies the mid ramp environments below fair weather wave base (Sinclair et al., 1998). The KTF 3 microfacies hosts a rich variety of elongated *Operculina* sp. tests preferentially aligned in micritic matrix. Presence of *Alveolina* sp. along with *Operculina* sp. and small *Nummulites* sp. indicates a barrier backbank, low energy environment of deposition.

#### *6.4.9.4 Alveolina rich wackestone microfacies (KTF 4)*

The KTF 4 microfacies is represented by thin bedded argillaceous limestone in the middle-upper part of the Kohat Formation in the Sheikhan Nala Section.

In thin sections the KTF 4 microfacies is characterized by dominance of monospecific assemblage of *Alveolina* sp. scattered in a micritic matrix which ranges from 25-55 %, with an average of 35 %. Sparse biodebris of *Nummulites* sp., *Assilina* sp., echinoids and small gastropods are also found (figure 6.22 A, C and E). The diagenetic fabric is characterized by neomorphic alteration, compaction and post depositional spar filled fractures (figure 6.22 A). Limonite patches are found scattered in matrix and also around the smooth type stylolites. Stylonodular fabric is common (figure 6.22 D). Porosity type includes fracture, stylolitic and intragranular porosity.

**Depositional environment:** *Alveolina* sp. lived in 0-75m water depth (Geel. 2000). When alveolinids are associated with milliolids and *Orbitolites,* this indicates the leeward ramp setting (Sartorio and Venturini, 1988). The dominance of *Alveolina* sp. along with some *Nummulites* sp. indicates that KTF 4 microfacies was deposited in the distal inner ramp setting.

#### *6.4.9.5 Nummulitic wackestone microfacies (KTF 5)*

The KTF 5 microfacies is represented by thick bedded limestone in the upper part of the Kohat Formation in the Panoba Nala and the Bahadur Khel Salt Tunnel Sections.In thin section the KTF 5 microfacies is characterized by the mudstone to wackestone depositional fabrics. The bioclasts include *Nummulites* sp., *Assilina* sp. (figure 6.23 A) and rare small boring gastropods. The bioclasts abundance ranges from 30 to 50 %, with an average of 35 %. The allomicrite matrix is dominant and it

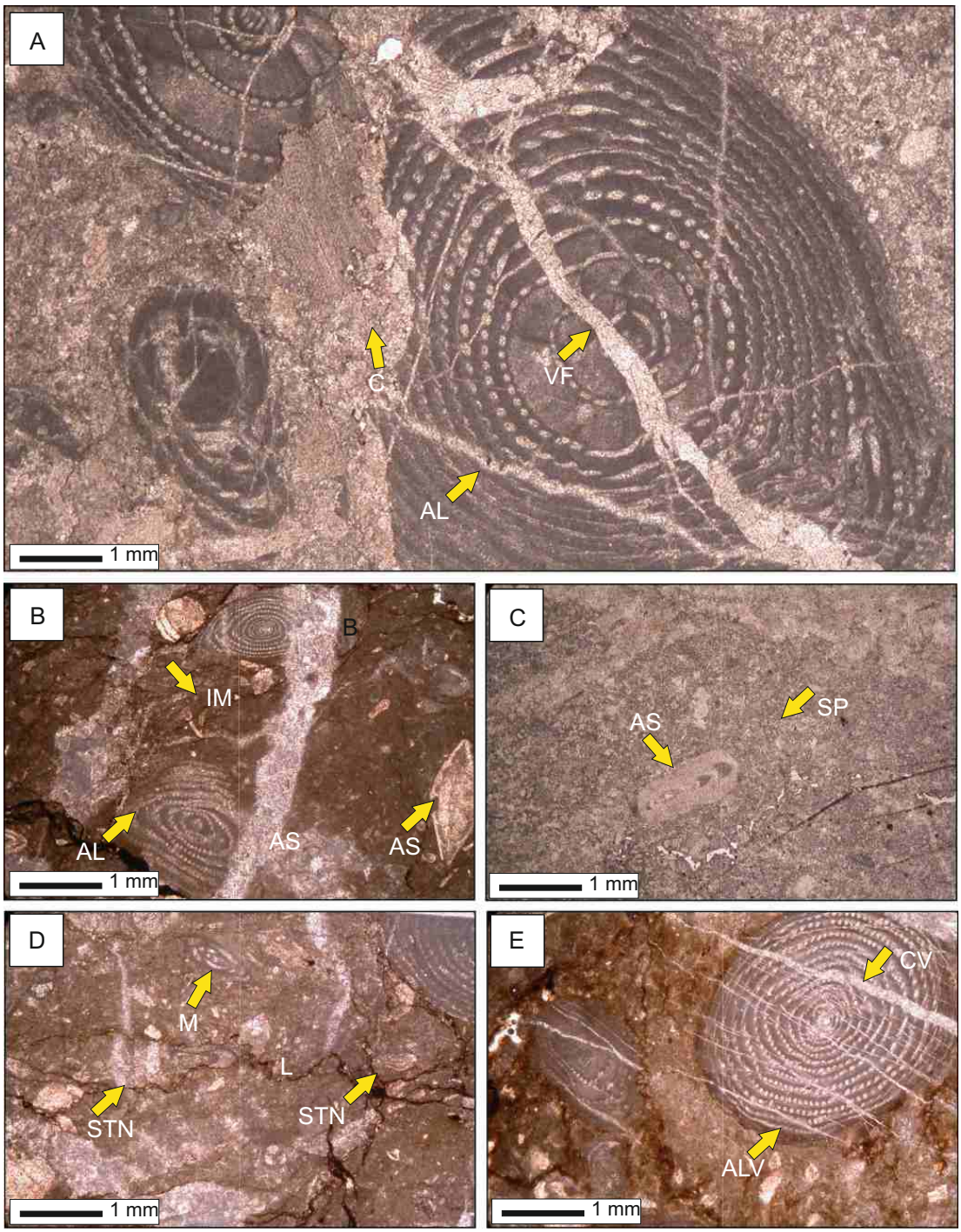


**Figure 6.22. *Alveolina* rich wackestone microfacies (KTF 4):** the allochems of the KTF 4 microfacies includes dominance of *Alveolina* (ALV in **A**, **B** and **E**), subordinate *Assilina* (AS in **B** and **C**), and milliolids (M in **D**). The diagenetic fabric is characterized by chemical compaction forming stylonodular fabric (STN in **D**), post depositional spar filled veins (VF in **A**). Fracture and stylolitic porosity is very prominent.

is enriched with scattered bioclasts of foraminifera. The matrix is ranging from 40 - 80 %, with an average of 45 %. Microspar is 10-30%, with an average of 22 %, found as cement filling the intergranular space and a replacement product due to aggrading neomorphism. The bioclasts do not show preferred orientation although some grains show a cross bedding relationship (figure 6.23 A). The biogenic content has fair to good preservation. The bioclasts show effects of diagenetic alteration in the form of micritization, neomorphic alterarion and chemical compaction. Irregular and anatomizing stylolites are common. Along the sutured stylolites residual iron oxide is common. Post depositional spar filled microfractures show the equispaced parallel set pattern (figure 6.23 B - C). The KTF 5 microfacies shows intergranular and stylolitic porosity.

**Depositional environment:** The presence of the micritic matrix and abundance of *Nummulites* sp. (Sinclair et al., 1998) suggests that the KTF 5 microfacies was deposited in the low energy back bank environment, seaward of the KTF 4 microfacies.

#### *6.4.9.6 Gastropodal mudstone- wackestone microfacies (KTF 6)*

The KTF 6 micofacies is represented by thick bedded to massive limestone in the upper part of the Kohat Formation in the Panoba Nala and the Bahadur Khel Salt Tunnel Sections.

In thin sections the KTF 6 microfacies is characterized by mudstone to wackestone depositional textures. Bioclastic constituents include dominance of small gastropods and rare *Nummulites* sp. The small gastropods are mostly < 1 mm size, internally micritized, or replaced by neomorphic microspar, but in most cases only the outline of the gastropod shell is preserved (figure 6.24 A). Few bioclasts of *Nummulites* sp. having <1 mm size and shows partial to complete micritization (figure 6.24 B). Scattered small articulated brachiopods having <2 mm size and few >5mm size brachiopod spines are also observed. Echinoid spines are scattered in allomicrite (figure 6.24 C). The biogenic content is mostly benthic fauna and it is poor to moderately preserved, with no preferred orientation. Allomicritic matrix is

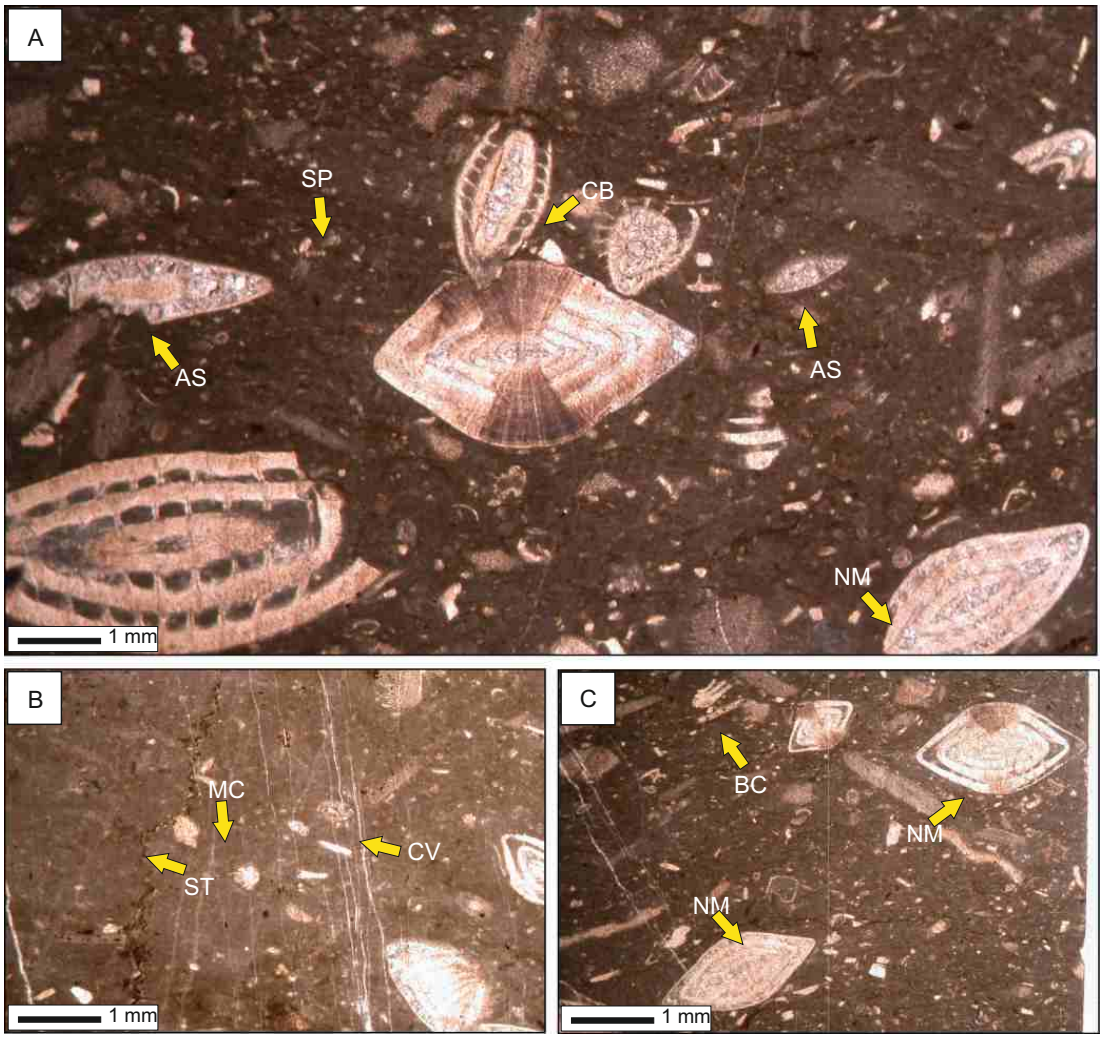


**Figure 6.23. *Nummulitic* wackestone microfacies (KTF 5):** the allochems of KTF 5 microfacies includes *Nummulites* (NM in **A** and **C**), and *Assilina* (AS in **A**) scattered in micritic matrix (MC in **C**). *Nummulites* also shows cross bedding fabric (CB in **A**). The diagenetic fabric is characterized by internal micritization of the bioclasts (IMC in **A**), chemical compaction forming stylolites (ST in **B**) and post depositional spar filled veins (CV in **C**).

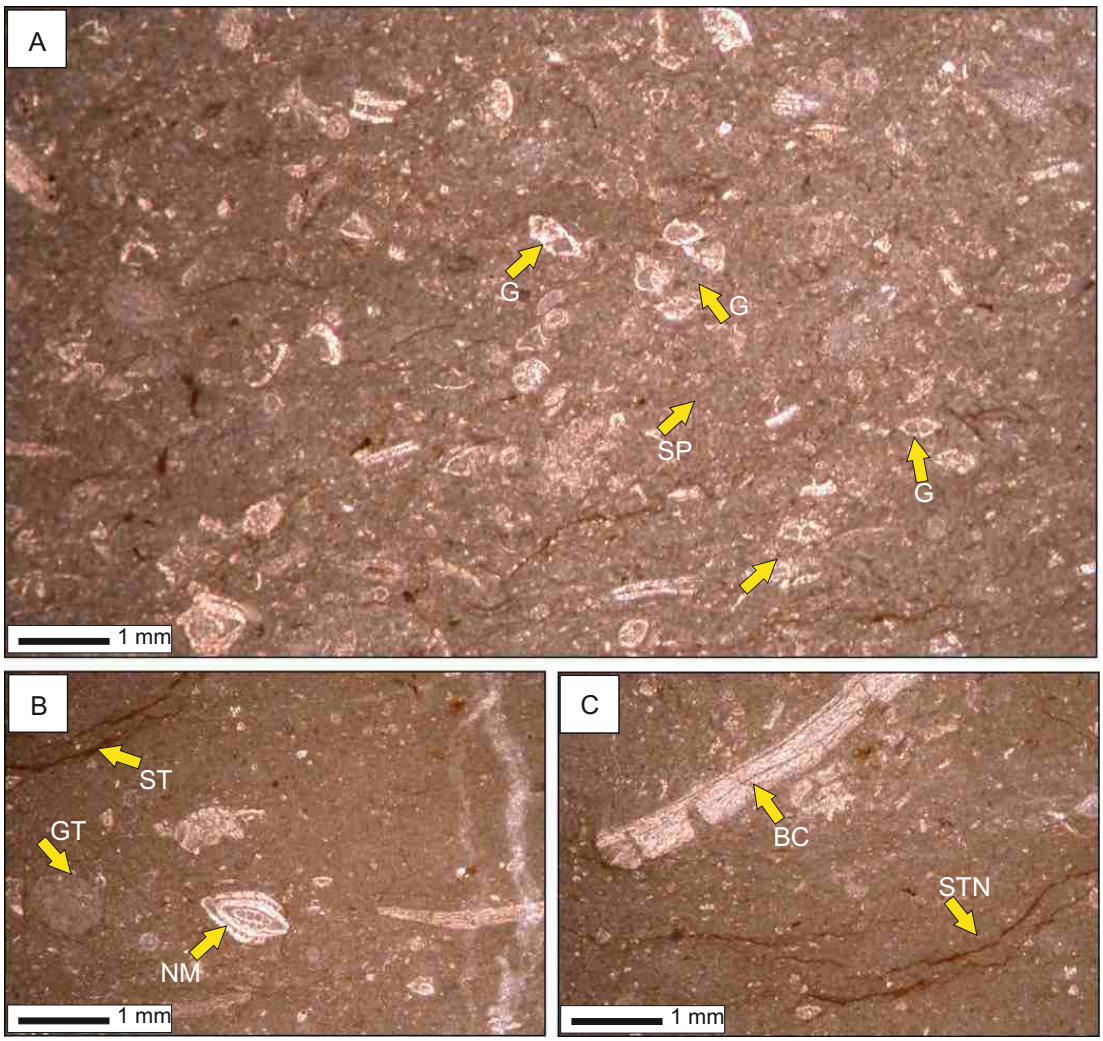


**Figure 6.24. Gastropodal mudstone-wackestone microfacies (KTF 6):** the allochems of the KTF 6 microfacies includes dominance of small gastropods (G in **A**), *Nummulites* (NM in **B**) and echinoidal bioclastic debris (BC in **C**). The diagenetic fabric is characterized by chemical compaction forming smooth stylotites (ST in **B**), stylonodular fabric (STN in **C**). Intergranular and stylolitic porosity is common.

common and its abundance is ranging from 40-60 %, with an average of 45 %. Spar constitutes 20-40 %, either as a product of aggrading neomorphism or interparticleand fracture filling cement. Bioclasts abundance is ranging from less than 5 to 30 % with an average of 18 %. Poor to moderate sorting of mostly elongated grains is seen. The diagenetic fabric is characterized by chemical compaction forming stylolites that include columnar, irregular, anastomizing, and smooth types (figure 6.24 B-C). Stylonodular fabric is characterized by the patchy iron oxide seams around the nodules (figure 6.24 C). Inter and intraparticle porosity is very common while moldic and fracture porosity is also found in gastropods and brachiopod bioclasts.

**Depositional environment:** the low diversity of fauna and micritic matrix suggests deposition of the KTF 6 microfacies in the inner ramp, backbank, low energy environment.

### *6.4.9.7 Intraclastic-bivalve rich wackestone microfacies (KTF 7)*

The KTF 7 microfacies is represented by massive limestone in the upper part of the Kohat Formation in the Panoba Nala Section.

In thin sections the KTF 7 microfacies is characterized by the wackestone depositional texture. Biogenic content is mostly benthic in origin and it is moderately preserved. The bioclasts abundance ranges between 10 - 20 %, with an average of 14 %. Intraclasts abundance is ranging from 30-50 %, with an average of 40 %. The intraclasts are ranging in size from < 1mm to 2 mm, found in small nests, patches and are randomly oriented. Inter and intra particle spar cement is commonly seen. The dominant bioclasts include bivalves, which are completely micritized (figure 6.25 A). The size of bivalve bioclasts is variable ranging from 1 mm to 3 mm. The *Nummulites* sp. are rare and their internal structure is destroyed by partial to complete micritization, only outline is preserved (figure 6.25 B). Small gastropods are seen scattered in an allomicritic matrix. Very rare detrital quartz grains are found.

The diagenetic imprints include hummocky, columnar, parallel and anastomizing varieties of stylolites (figure 6.25 C) . Residual limonite seams are found around the bioclasts. Moldic porosity is very common.

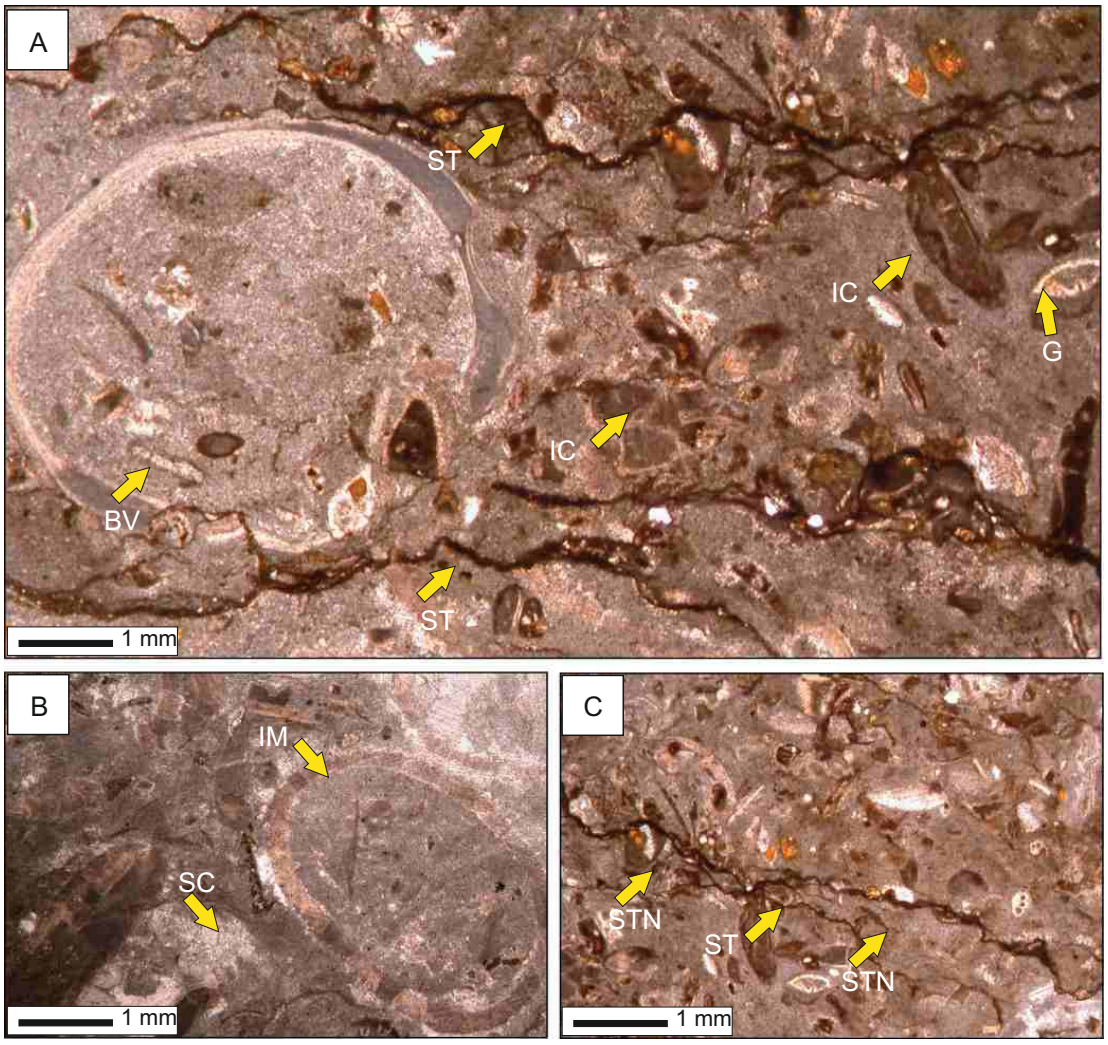


**Figure 6.25. Intraclastic–bivalve rich wackestone microfacies (KTF 7):** the allochems of KTF 7 microfacies include dominance of bivalves (BV in **A**), small gastropods (G in **A**) and intraclasts (IC in **A**). The diagenetic fabric is characterized by chemical compaction forming stylolites (ST in **A**) and stylonodular fabric (STN in **C**), internal micritization of the bioclasts (IM in **B**) and aggrading neomorphic alteration (SC in **B**).

**Depositional environment:** the low diversity fauna (with the dominance of monospecific bivalve assemblage) and lime mud matrix indicate that the KTF 7 microfacies was deposited in a low energy shallow proximal inner ramp setting.

## 6.5 Facies depositional model

The facies analysis suggests that Paleogene rocks of the Kohat Basin were deposited in the carbonate ramp platform setting. Ramps are a type of carbonate platforms which are characterized by less than 1° slope gradient and have no slope break. In the classification of ramps (Markello and Read, 1981; Aigner, 1984; Calvet and Tucker, 1988; Buxton and Pedley, 1989; Somerville and Strogen, 1992 and Burchette and Wright, 1992), the fair weather wave base (FWWB) and storm wave base (SWB) are used as interfaces between the inner ramp (above the FWWB), the mid ramp (between the FWWB and the SWB), and the outer-ramp (belown the SWB up to the basin). Ramps can be divided into homoclinal and distally steepened ramps. In a homoclinal ramp no platform-slope break is present while a distally steepened carbonate ramp platform has a slope break between the outer ramp and the basin and can be recognized by slumpings and slope apron deposits (Burchette and Wright, 1992; Flügel, 2004). Facies analysis of the Paleogene rocks in the Kohat Basin allows construction of the depositional profile and three dimensional facies architecture. The depositional profile is consistent with a distally steepened ramp (*sensu* Read, 1982, 1985). Facies of the Patala, Panoba, Sheikhan and Kohat Formations represents deposition in a distally steepened carbonate ramp platform (figure 6.26-27). This model is based on following differentiating criteria from a shelf platform 1) Absence of reef building organisms, 2) presence of storm related features with fragmented fauna, 3) wedge shape geometry of the deposits indicated by a thickening upward trend, 4) the proximal platform setting is charecterized by packstone-grainstone textures while the distal parts show wackstones-packstones textures.

The inner ramp facies consists of delta and stream fed beach sandstone, clays and conglomerates. These lithofacies passes down dip into siliciclastic mixed-milliolid rich packstones. Abundance of milliolids indicates hypersaline, nutrient rich and low turbulent water conditions (Geel, 2000). Siliciclastic input (mostly quartz) indicates occasional stormy episodes. Basinward of the siliciclastic mixed milliolid packstones, the algal - foraminiferal wackestone to packstone textures dominate-

## FACIES

Planktonic wackestone microfacies (PTK 1)

Nummulitic wackestone microfacies (PTK 2)

Mixed faunal wackestone to packstone microfacies (PTK 3)

Diverse foraminiferal packstone microfacies (PTK 4)

*Bulimina* biofacies (BF 1)

*Uvigerina* biofacies (BF 2)

*Bathysiphon/Gaudryina* biofacies (BF3)

Diverse bioturbated/burrowed wackestone to packstone microfacies (SHF 1)

Bioclastic wackestone microfacies (SHF 2)

Peloidal–*Alveolina* rich bioclastic wackestone to packstone microfacies (SHF 3)

Diverse bioclastic / burrowed mudstone to wackestone microfacies (SHF 4)

Siliciclastic mixed bioturbated wackestone to packstone microfacies (SHF 5)

Milliolid rich packstone to grainstone microfacies (SHF 6)

*Discocyclina* rich wackestone microfacies (SHF 7)

*Assilina* rich bioclastic wackestone to packstone microfacies (SHF 8)

Poorly fossiliferous lime mudstone / dolomicrite microfacies (SHF 9)

Foraminiferal packstone microfacies (KTF 1)

*Nummulitic* packstone to grainstone microfacies (KTF 2)

*Operculina* rich mudstone to wackestone microfacies (KTF 3)

*Alveolina* rich wackestone microfacies (KTF 4)

*Nummulitic* wackestone microfacies (KTF 5)

Gastropodal mudstone to wackestone microfacies (KTF 6)

Intraclastic–bivalve rich wackestone microfacies (KTF 7)

## LEGEND

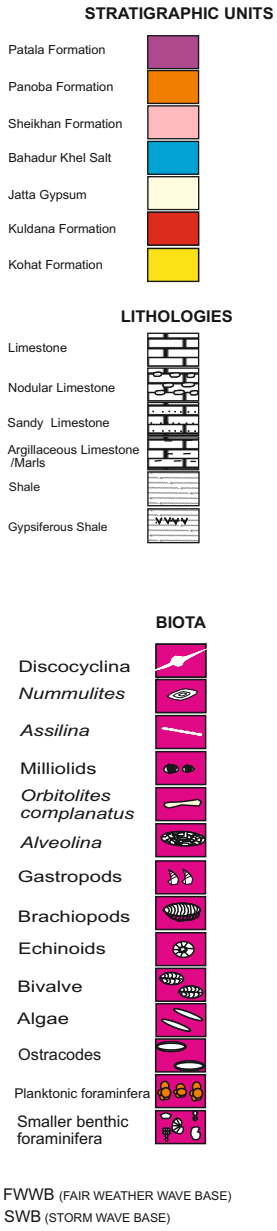


**Figure 6.26** Key to Paleogene facies types, symbols for biota, stratigraphic units, various lithologies shown in the figure 6.27.

# Facies Model

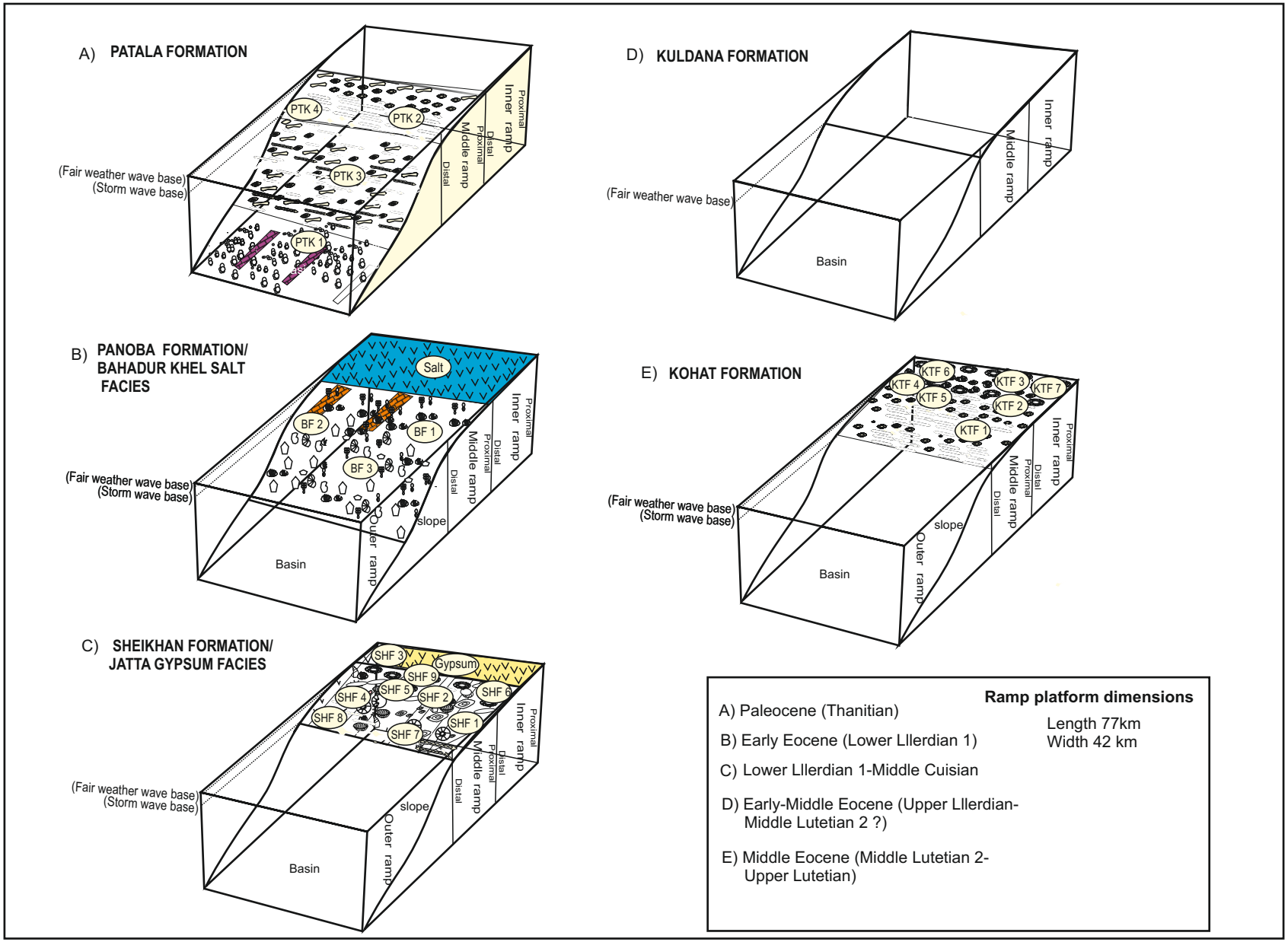


**Figure 6.27.** A distally steepened ramp platform facies depositional model showing distribution of the Paleogene siliciclastic-carbonate mixed facies of the Kohat Basin (A-D indicates various depositional units in chronological order, for details of symbols and abbreviations see figure 6.26).

carbonates in the distal inner ramp setting. These are interpreted as shallow water sediments in which larger benthic foraminifera live in symbiotic relationship with the dasycladacean green algae. The carbonates of the proximal middle ramp setting are characterized by algal-bioclastic mudstone and wackestone textures, having high diversity macrofauna that indicates normal marine conditions.

A high bioclast ratio and intense bioturbation and biodebris show deposition below FWWB in the photic zone. A distal middle ramp setting is inhabited by the larger benthic foraminifera (i.e. *Nummulites* sp*., Assilina* sp. and *Discocyclina* sp.) that characterize foraminiferal wackestones in the mesophotic zone. Basinward of the middle ramp setting slope facies of pelagic clays, enriched in highly diverse assemblage of flysch type agglutinated foraminifera i.e. *Bathysiphon eocenicus*, *Bathysiphon robustus, Gaudryina tazaensis*, *Gaudryina leveagata,* and *Haplophragmoides* and a mix of shallow water depth indicators like milliolids*,* textularids*,* bolivinids*,* uvigerinids and *Cibicides* sp. shows deposition in an upper slope setting. Slope apron carbonate facies include mixed faunal wackestone to packstone textures dominated by larger benthic foraminifera including *Nummulites* sp*., Assilina* sp*., Alveolina* sp*.,* and *Orbitolites* sp. with a mixed shallow water fauna that include milliolid, ostracodes and bivalves. The bioclasts are broken and abraded. Well bedded and intact upper and lower facies contact rule out tectonic orgin of the ramp slope facies. While allochthonous orgin is supported by intraclastic nature of the limestone which was originally deposited under middle ramp settings, but later on transported by gravity flow and deposited in a ramp slope settings. Outer ramp to basinal setting is characterized by planktonic foraminiferal rich wackestone. Planktonic foraminifera (e.g. *globigerinids*) live in pelagic environment and represents deposition into deep water associated with the slope and deep basinal settings (Flügel, 2004).

## 6.6 Paleoenvironments

The following paleoenviromental interpretation of the Paleogene stratigraphic units is based on the detailed facies analysis in the studied sections of the Kohat Basin (figure 6.28-6.31).

### 6.6.1 Paleoenvironments of the Patala Formation

In the Kohat Basin, the Patala Formation represents deposition in deep basin, slope and middle to outer ramp settings (figure 6.27).

In the Panoba Nala Section (figure 6.28),outer ramp-deep basinal setting is represented by the 17m thick PTK 1 microfacies. Gradual shallowing of the facies is represented by the 18m thick, PTK 2 microfacies that was deposited in distal middle ramp setting. In the middle upper part, the 8m thick PTK 3 microfacies, representing slope settings, grades upward into the PTK 4 microfacies, which is 12m thick and indicates deposition in distal middle ramp settings.

In the Tarkhobi Nala Section (figure 6.29), the Patala Formation represents deposition in deep marine, slope and middle to outer ramp settings. The lower 20m thick PTK 1 microfacies represents outer ramp-deep basinal settings. The overlying 8m thick PTK 2 microfacies, representing middle to outer ramp settings, grades into 24m thick PTK 3 microfacies, deposited in ramp slope setting. The PTK3 microfacies is overlain by 98m thick the PTK4 microfacies which represent distal middle ramp settings.

The composite relative sea level curve (figure 6.32) and facies fence diagram (figure 6.33) indicate ramp backstepping (retrogradation) followed by a shallowing upward (progradational) facies trend during the deposition of the Patala Formation.

### 6.6.2 Paleoenvironments of the Panoba Formation

In the Kohat Basin, the Panoba Formation represents deposition in middle ramp-outer ramp and slope settings (figure 6.27). In the Panoba Nala Section (figure 6.28), the lower part of the Panoba Formation is represented by the 18m thick BF1 biofacies, representing deposition in middle neritic environment (50-80 m paleodepth of water) in proximal middle ramp settings. In the middle part the 18m thick BF2 biofacies represents distal middle ramp settings, pointing towards the deepening of the paleoenvironments. In the middle upper part sea level fluctuations are indicated by the 18m thick, middle ramp BF1 bioacies overlain by the 36m thick BF 3 biofacies that shows deposition along the ramp slope setting. In the upper most part of the Panoba Formation, shallower biofacies BF1 graded upward into proximal middle ramp facies of the Sheikhan Formation.

In the Tarkhobi Nala Section (figure 6.29), the Panoba Formation represents deposition along middle ramp to slope settings. The BF 1 biofacies characterizes the lower 21m thickness and uppermost 7m thickness of the Panoba Formation, representing proximl middle ramp settings. In the lower middle part 31m thickness is represented by the distal middle ramp BF 2 biofacies. Ramp slope setting is represented by 11m thick, BF 3 biofacies in the middle upper part of the Panoba Formation.

In the Sheikhan Nala Section (figure 6.30), the Panoba Formation represents deposition in middle ramp to ramp slope settings. The lower part is represented by the 9m thick BF I biofacies representing proximal middle ramp setting. Deepening of the environment from proximal middle to distal middle ramp settings is shown by the 2m thick BF 2 biofacies in the middle part of the Panoba Formation. In the upper part the 12m thick BF 3 biofacies is found which represents ramp slope settings. The uppermost 2m thick BF 1 biofacies transitionally changes to the overlying middle ramp facies of the Sheikhan Formation.

The composite relative sea level curve (figure 6.32) and facies fence diagram (figure 6.33) indicate a dominant shallowing upward facies trend intrupted by deepening during the deposition of the Panoba Formation. The Panoba Formation is well exposed in the northeastern corner of the Kohat Basin and towards southwest it laterally changes to the stratigraphically equivalent evaporite facies of the Bahadur Khel Salt which shows deposition in semiarid enclosed basinal settings.

### 6.6.3 Paleoenvironments of the Sheikhan Formation

The microfacies analysis of the Sheikhan Formation suggests that its lower part was deposited in a flat carbonate middle ramp environment and upper part in restricted lagoon conditions (figure 6.27).

In the Panoba Nala Section (figure 6.28), in the lower part of the Sheikhan Formation, 17m thick SHF 8 microfacies was deposited in distal middle ramp settings. The 2m thcik distal middle ramp SHF 7 microfacies grades upward into

42m thick shallow inner ramp SHF 9 microfacies. At the top 14m thick gypsiferous shales represents restricted lagoonal settings.

In the Tarkhobi Nala Section (figure 6.29) 34m thick proximal inner ramp microfacies (SHF 3) is overlain by 19m thick middle ramp-lagoonal microfacies (SHF 9). The distal middle ramp microfacies (SHF 7) is 7m thick and is found between the SHF 9 microfacies above and below. The 5m thick gypsiferous shales mark the top of the unit.

In the Sheikhan Nala Section (figure 6.30), in the lower part of the Sheikhan Formation, 3m thick, the SHF 1 microfacies was deposited in a middle ramp settings. It is follwed by 9m thick SHF 2 microfacies representing distal middle ramp settings and in the middle part the 2m thick SHF 3 proximal inner ramp facies and 4m thick middle ramp facies occurs. The restriction of the environmental conditions is indicated by abundance of milliolids and ostracodes in the 12m thick, SHF 5 microfacies found in the upper part of the Sheikhan Formation. The SHF 5 microfacies grades upward into 4m thick, gypsiferous shales that indicates evaporitic enclosed basin conditions.

The SHF 5 microfacies in the Sheikhan Nala Section is equivalent of the SHF 9 microfacies in the Panoba Nala Section. In the Panoba Nala Section (figure 6.28) the upper Sheikhan Formation has a 14m thick gypsiferous shale unit above the dolomicrites. This gypsiferous shale facies laterally change into thick bedded gypsum facies in the southwestern Kohat Basin and is referred to as Jatta Gypsum. In the Bahadur Khel Salt Tunnel Section (figure 6.31), the bulk of gypsum is laminated with variegated clays and contains interbedded green shales. All of which suggests deposition under low energy conditions in shallow lagoons.

The composite relative sea level curve (figure 6.32) and facies fence diagram (figure 6.33) indicate a common shallowing upward facies trend during the deposition of the Sheikhan Formation in ramp progradation (shedding). Minor deepening in an overall shallowing is also seen in the Panoba Nala Section. The restriction of the platform is indicated by gypsiferous clays and thick gypsum in the southwestern part of the basin.

### 6.6.4 Paleoenvironments of the Kuldana Formation

In the Kohat Basin, the Kuldana Formation represents deposition in a fluvial to marginal marine depositional setting. In the Panoba Nala Section (figure 6.28), the Kuldana Formation was deposited in fluvial channels, flood plains and marginal marine settings. The Lower Kuldana Formation consists of 24m thick purple to reddish brown clays, which indicates deposition in a fluvial flood plain environment. Marginal marine environment is represented by 6m purple grey/greenish grey coloured dolomitic limestone in the upper part of the Kuldana Formation.

In the Sheikhan Nala Section (figure 6.30), the Kuldana Formation is comprised of 25m thick purple to reddish brown continental clays with subordinate sandstone beds representing deposition in the fluvial flood plains and fluvial channels.

In the Bahadur Khel Salt Tunnel Section (figure 6.31), the Lower Kuldana Formation was deposited in a fluvial flood plain, fluvial channels, whilst the Upper Kuldana indicates marginal marine settings. In the western Kohat Basin, the Kuldana Formation laterally changes into clastics facies known as the Chashmai Formation, which shows its deposition in the stream and delta fed beach settings.

The composite relative sea level curve (figure 6.32) and facies fence diagram (figure 6.33) indicate that deposition of the Kuldana Formation is associated with a major sea level fall that has exposed the whole basin. Continued progradation of the more proximal fluvial facies onto the restricted marine evaporitic facies has occurred. However a renewed phase of marine sedimentation is seen in the Upper Kuldana Formation facies indicatig the start of a relative sea level rise and and backstepping of the ramp facies (figure 6.32).

### 6.6.5 Paleoenvironments of the Kohat Formation

In the Kohat Basin, the Kohat Formation shows deposition in the barrier back- bank to distal middle ramp settings (figure 6.27).

In the Panoba Nala Section (figure 6.28), the lower part of the Kohat Formation has 6m thick the KTF 5 microfacies that represent deposition in a back -

## 6.7 Summary and conclusions

In this Chapter Paleogene facies, depositional models and paleoenvironments of the Kohat Basin are presented in detail. Four key stratigraphic sections are selected and studied in detail. Sections to the northeast (the Panoba Nala, the the Tarkhobi Nala and the Sheikahn Nala sections) represent deep basinal, slope, shallow platform, marginal marine and non-marine facies while in the southwest part of the Kohat Basin (the Bahadur Khel Salt Tunnel Section) the evaporitic facies are well developed. These rocks are represented by seven different stratigraphic units. These units are named as the Patala Formation, the Panoba Formation, the Bahadur Khel Salt, the Jatta Gypsum, the Sheikhan Formation, the Chashmai Formation, the Kuldana Formation and the Kohat Formation.

The following conclusions are drawn from the present investigations.

- The Paleogene siliciclastic mixed carbonate rocks are deposited in distally steepened carbonate ramp platform setting.
- Facies of the Patala, the Panoba, the Sheikhan and the Chashmai Formations, representing deposition in such a distally steepened carbonate platform.
- The Patala Formation is well exposed in the northesastern Kohat Basin (Panoba and the Tarkhobi Nala Sections) and represents deposition in the deep basin, slope and middle to outer ramp settings. The composite relative sea level and facies fence diagram indicate backstepping of the ramp during the deposition of the Patala Formation.
- The Panoba Formation is well exposed in the Panoba Nala, the Sheikhan Nala and Tarkhobi Nala Sections in the northeastern Kohat Basin. Biofacies analysis shows that the Panoba Formation was deposited in middle ramp to ramp slope settings. It is the stratigraphic equivalent of the Bahadur Khel Salt Facies, and is well exposed in the Bahadur Khel Salt Tunnel Section, south-western Kohat Basin, representing restricted marginal basin conditions. The composite relative sea level curve and -

.

bank lagoon environment. In the middle upper part 12m thick, the KTF 6 microfacies and 19m thick, the KTF 7 microfacies represent backbank lagoonal setting.

In the Sheikhan Nala Section (figure 6.30), the lower part of the Kohat Formation is represented by 14m thick, the KTF 1 microfacies and 9m thick, the KTF 2 microfacies, which represents proximal-distal barrier forebank settings respectively. The KTF 3 microfacies (14m thick) and KTF 4 microfacies (38m thick) representing backbank lagoonal settings, shows that the upper part of the Kohat Formation was deposited in a deeper environment but having restricted circulation and the fauna is dominated by *Operculina* sp. and *Alveolina* sp.

In the Bahadur Khel Salt Tunnel Section (figure 6.31), the Kohat Formation shows deposition in the backbank lagoon settings, where the 9m thick KTF 5 microfacies, 25m thick KTF 6 microfacies in the lower middle part and 6m thick, the KTF 7 microfacies in the upper part were deposited.

The composite relative sea level curve (figure 6.32) and facies fence diagram (figure 6.33) indicate that in the northeastern part of the Kohat Basin (the Panoba, and Sheikhan Nala Sections) deeper environment of proximal middle ramp to distal middle ramp prevailed. The deepest facies are found in the Sheikhan Nala Section (figures 6.30 and 6.33). The deposition of backbank lagoonal facies is associated with the restriction of the environment due to development of the Nummulitic barrier banks in the northeast of the basin.

facies fence diagram show progradation of the Panoba Formation.

- The Sheikhan Formation is well exposed in the Sheikhan Nala and the Panoba Nala sections in the northeastern Kohat Basin. The microfacies analysis suggests that the lower part of the formation was deposited in a flat carbonate middle ramp setting and upper part in restricted lagoonal setting. The gypsiferous shale facies in the upper part of the Sheikhan Formation is a stratigraphic equivalent of the thick bedded gypsum facies exposed in the southwestern Kohat Basin and is known as Jatta Gypsum. The composite relative sea level curve and facies fence diagram shows progradation of the ramp during the deposition of the Sheikhan Formation.
- In the Kohat Basin, the Kuldana Formation is well exposed in the north-east (the Panoba and the Sheikhan Nala sections) and to the southwest (Bahadur Khel Salt Tunnel Section). The lower part of the Kuldana Formation represents deposition in a fluvial environment and the upper part indicates deposition in marginal marine settings. In the western part of the Kohat Basin, the Kuldana Formation laterally changes into the clastics facies of the Chashmai Formation in southwest, which shows its deposition in the stream and delta fed beach settings. The composite relative sea level and facies fence diagram show major sea level fall and a continued progradation of the ramp during the deposition of the lower Kuldana Formation and backstepping of the ramp during the deposition of the Upper Kuldana Formation.
- The Kohat Formation is well exposed in the Sheikhan Nala, the Panoba Nala and the Bahadur Khel Salt Tunnel sections. Facies analysis suggests its deposition in the backbank to distal middle ramp settings. The mean relative sea level curve and facies fence diagram show continued sea level rise and a continued backstepping of the ramp during the deposition of the Kohat Formation.

# THE PANOBA NALA SECTION

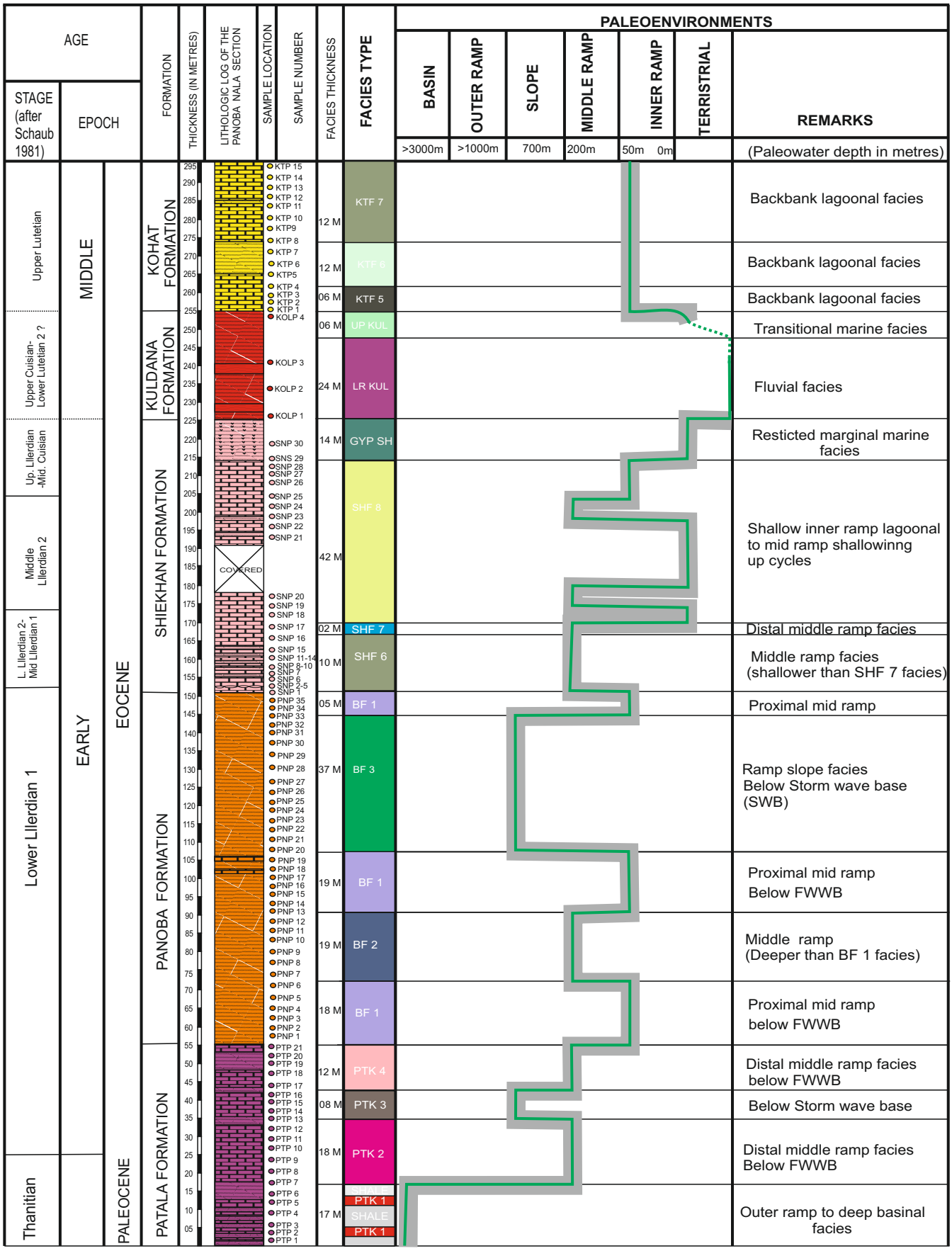


**Figure 6.28.** Composite chart showing facies distribution, paleoenvironments and a mean relative sea level curve infered from the faunal paleoecology (Racey. 1995) and facies critaria (Flugel. 2004) of the Paleogene rocks exposed in the Panoba Nala Section, northeastern Kohat Basin (the shaded area shows the range of variation in the environment of deposition).

# THE TARKHOBI NALA SECTION

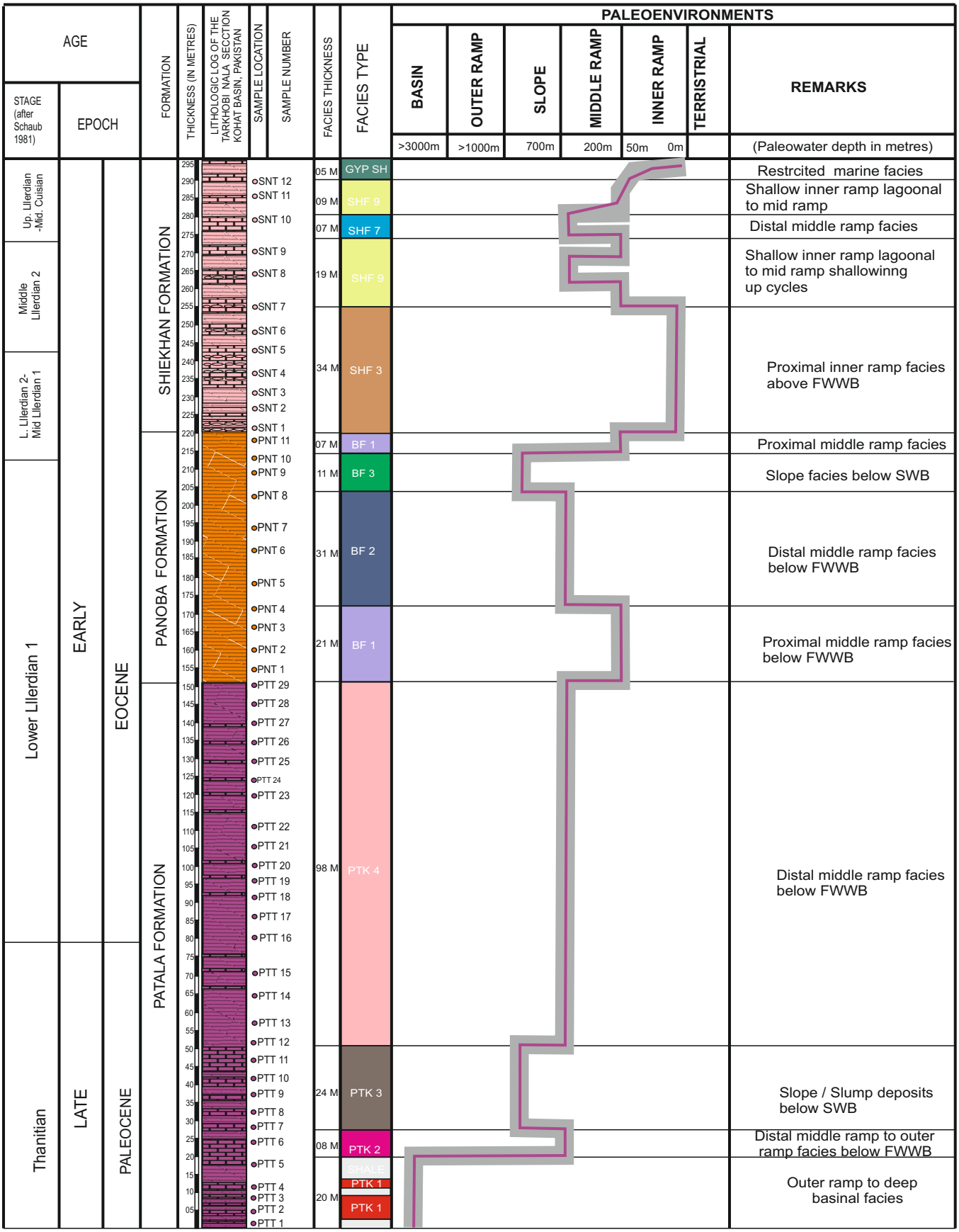


**Figure 6.29.** Composite chart showing facies distribution, paleoenvironments and a mean relative sea level curve infered from the faunal paleoecology (Racey. 1995) and facies critaria (Flugel. 2004) of the Paleogene rocks exposed in the Tarkhobi Nala Section, northeastern Kohat Basin (the shaded area shows the range of variation in the environment of deposition).

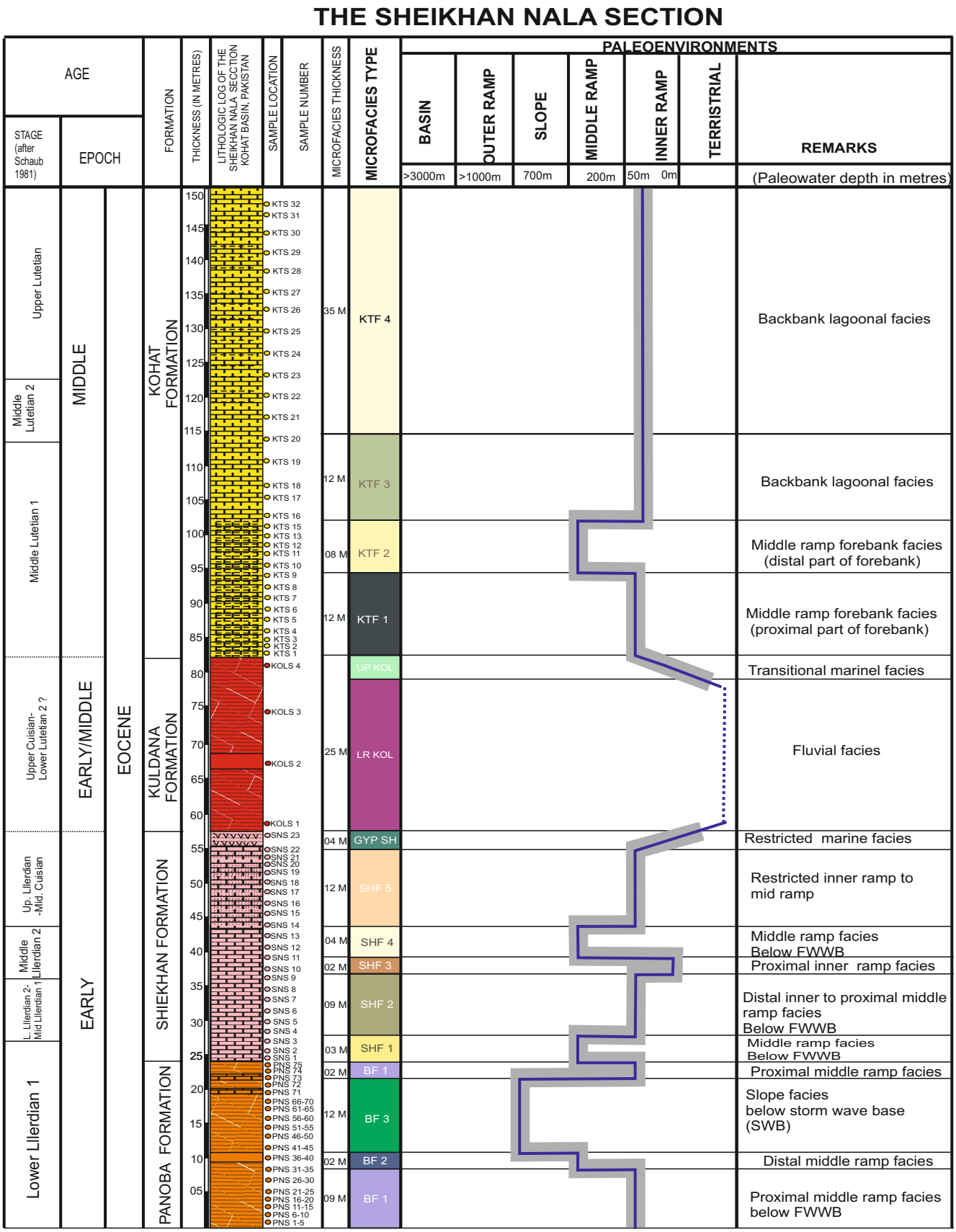


**Figure 6.30.** Composite chart showing facies distribution, paleoenvironments and a mean relative sea level curve infered from the faunal paleoecology (Racey. 1995) and facies critaria (Flugel. 2004) of the Paleogene rocks exposed in the Sheikhan Nala Section, northeastern Kohat Basin (the shaded area shows the range of variation in the environment of deposition).

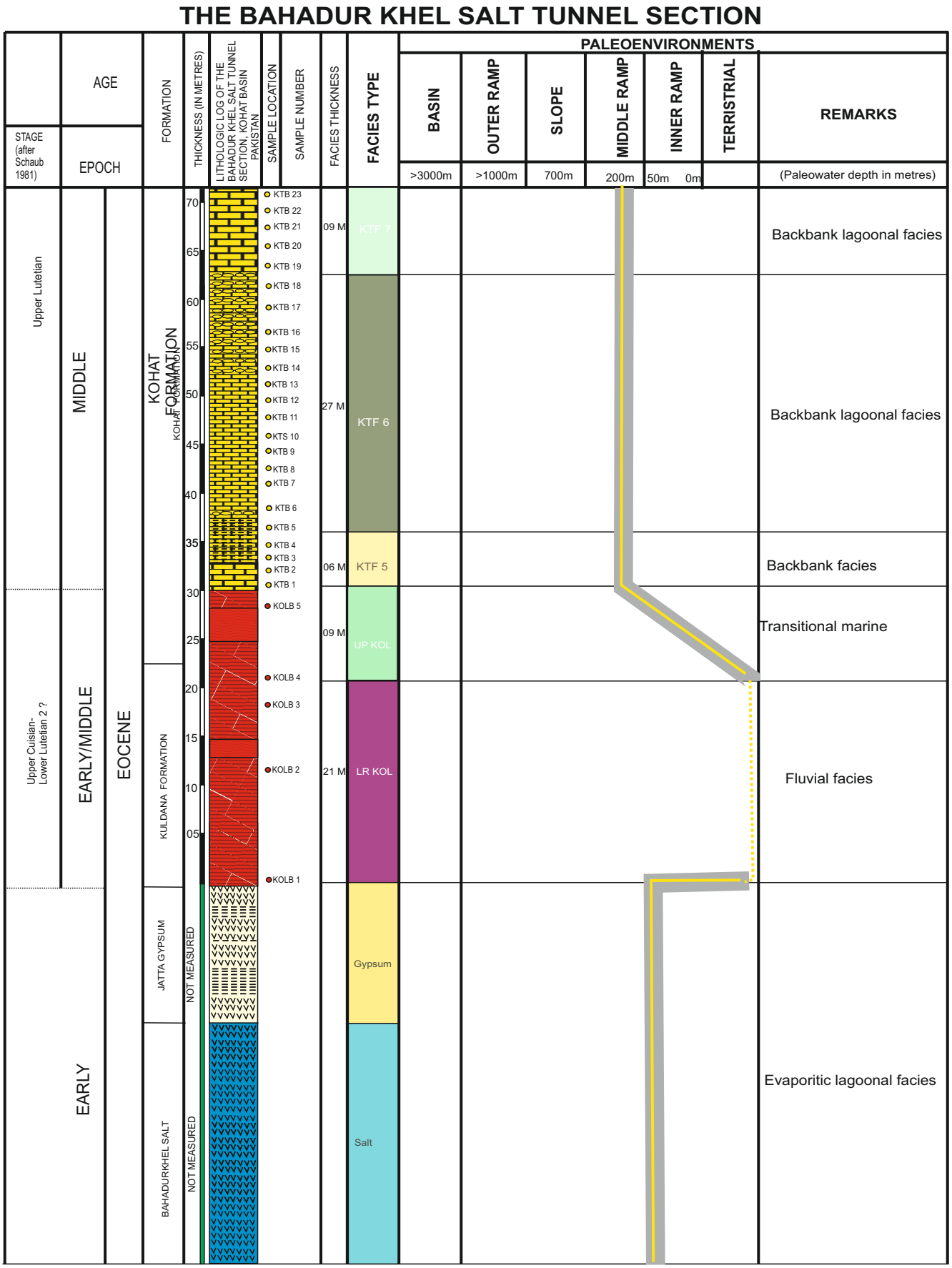


**Figure 6.31.** Composite chart showing facies distribution, paleoenvironments and a mean relative sea level curve infered from the faunal paleoecology (Racey. 1995) and facies critaria (Flugel. 2004) of the Paleogene rocks exposed in the Bahadur Kkhel Salt Tunnel Section, northeastern Kohat Basin (the shaded area shows the range of variation in the environment of deposition).

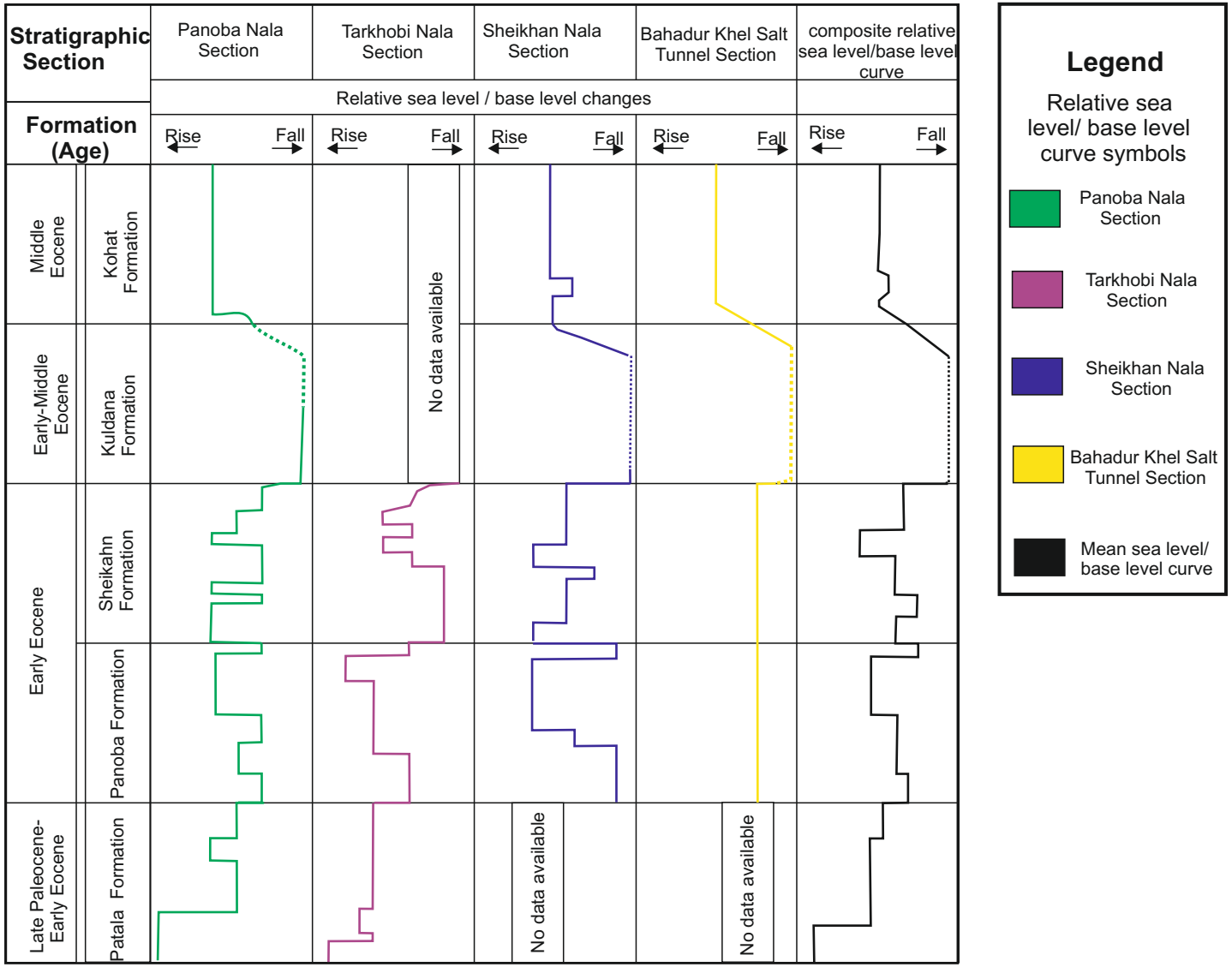


**Figure 6.32** Relative sea level curves of the Paleogene rocks exposed in the different study sections and a composite relative sea level curve derived from the average relative sea level shift and facies variation in the Kohat Basin, northwest Pakistan.

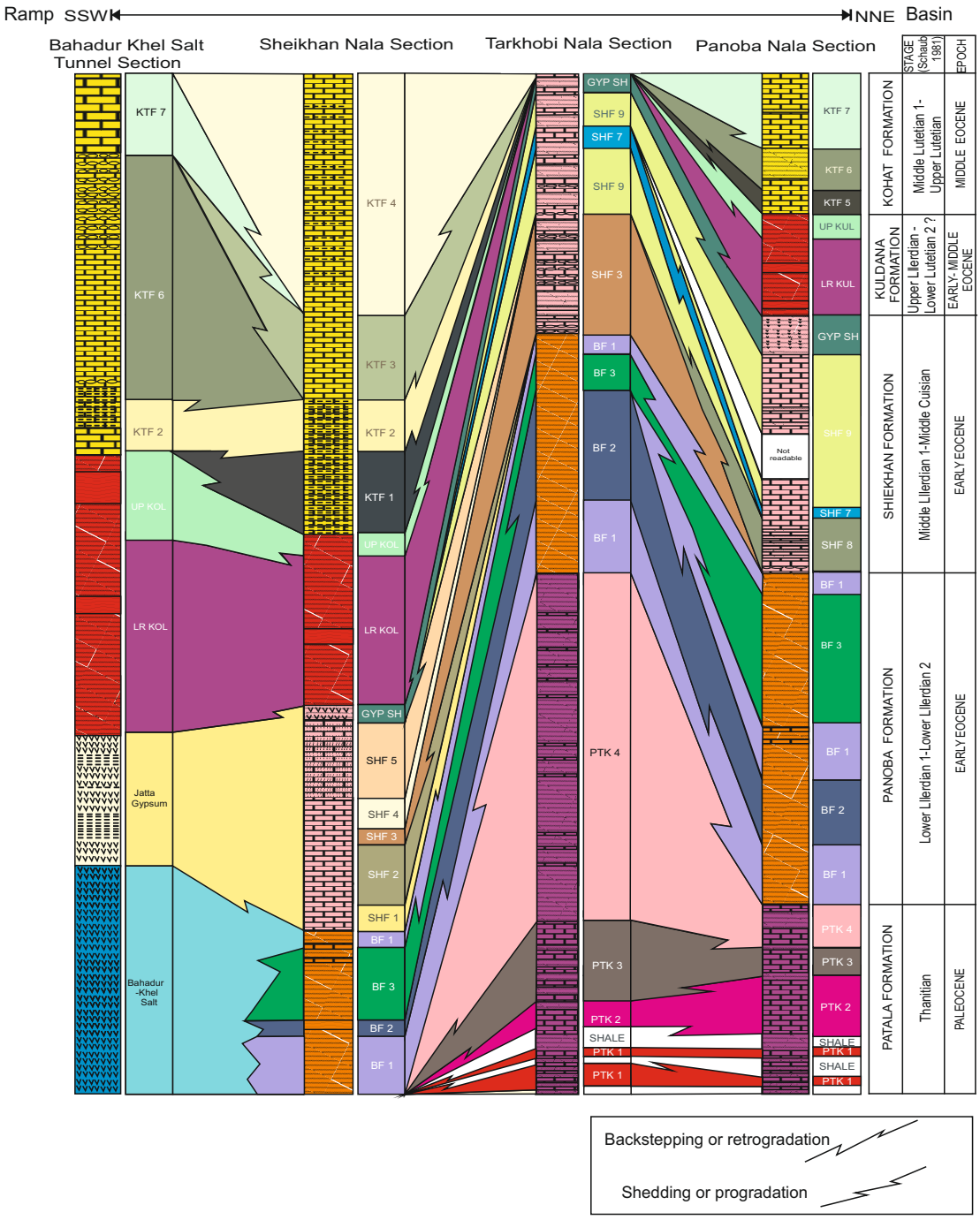


**Figure 6.33.** Paleogene facies fence diagram showing correlation of different facies, backstepping and progradation of the distally steepened ramp in the Kohat Basin (for details of symbols see figure 6.26 on pg 207).

# Chapter 7

# 7 Paleogene facies analysis of the Potwar Basin and the Trans Indus Ranges (TIR) with implications for paleoenvironments

## 7.1 Introduction

In this chapter the detailed microfacies of the Paleocene Lockhart and the Patala Formations and the Early Eocene Nammal, Sakessar and Chorgali Formations are presented. A total of six key Paleogene stratigraphic sections in the Potwar Basin (including the Trans Indus Ranges) were logged and sampled. The microfacies information is based on study of 336 petrographic thin sections (see Chapter 1 for techniques). A detailed microfacies scheme is presented here which provides the basis for paleoenviromental analysis and also encompasses information regarding reservoir rock quality (porosity) and diagenetic fabric of the rocks.

In this chapter a facies model is proposed that represents evolution of the paleoenvironments in this area during a critical time in the tectonic evolution of the region. The detailed description of the Paleogene microfacies in the study area is given below.

## 7.2 Facies of the Lockhart Formation

Microfacies of the Lockhart Formation are abbreviated as LKF 1-LKF 4 (here LK stands for the Lockhart Formation, F stands for microfacies and 1-4 are various types of recorded microfacies).

### *7.2.1 Algal foraminiferal wackestone-packstone microfacies (LKF 1)*

In the study area the LKF 1 microfacies is represented by grey coloured limestone in the lower part of the Lockhart Formation. In thin section, the LKF 1 microfacies is characterized by a wackestone-packstone depositional texture. The biogenic content is well preserved. The allochemic constituent ranges from 40-80 %, with an average of 60%. The microfloral components are dominated by calcareous green algae with an abundance that ranges from 40-60 % of the total allochems. The micritic matrix dominates and its abundance ranges from 25-45 % with an average of 30 %. The identified algal flora includes *Ovulites arabica* (Pfender, 1938), *Ovulites*

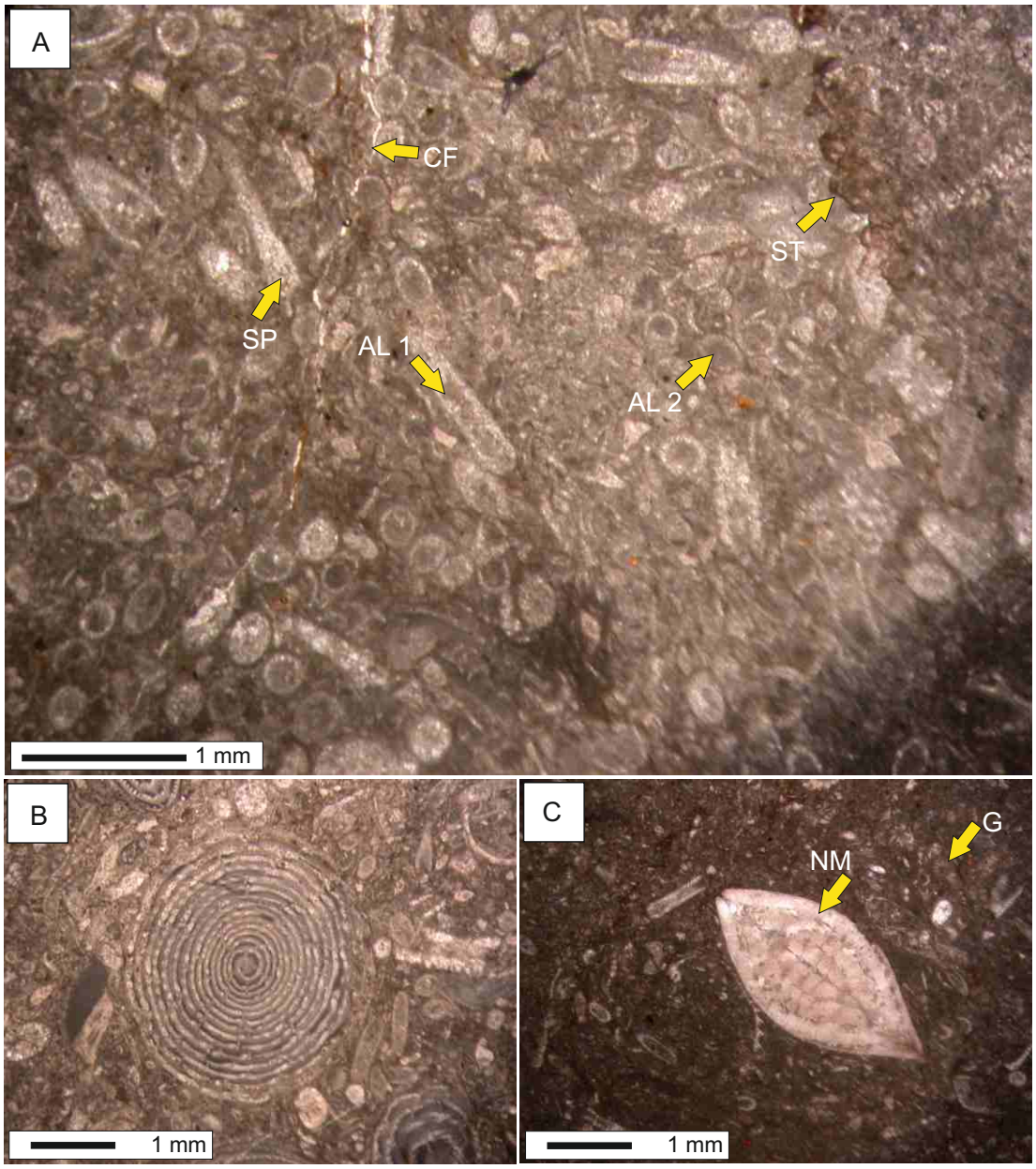


**Figure 7.1. Algal foraminiferal wackestone-packstone microfacies (LKF 1):** the allochems are represented by **A)** algae include *Ovulites Arabica (AL 1*), internal micritization in the thali of the *Ovulites margaritula (AL 2)* the diagenetic fabric is shown by stylolites (ST), and coarse spar formed by aggrading neomorphism within calcite filled fracture (CF) **B)** Well preserved *Alveolina vredenburgi* test surrounded by various size bioclasts of algae **C)** Note the micritic matrix and well preserved test of *Nummulites deserti* (NM) and small boring gastropods (G).

*arabica* (Pfender, 1938), *Ovulites margaritula* and *Ovulites elongata*. Mass accumulations of the algal thali segments show partial to complete internal micritization (figure 7.1A). Larger benthic foraminifera are commonly scattered through the allomicritic matrix. Well preserved foraminiferal species of *Miscellanea miscella, Alveolina vredenburgi* (figure 7.1B), *Nummulites deserti* (figure 7.1 C), *Assilina spinosa, Alveolina globula,* and *Lockharti haime* are identified. Subordinate occurrence of bioclastic invertebrate fauna includes brachiopods (1mm - 3mm size range), ostracodes (2mm – 3mm size range), and small boring gastropods (less than 2 mm size). Most of the grains have poor to moderate sorting and do not show any preferred orientation.

The diagenetic fabric is characterized by microbial micritization, neomorphic alteration and presence of microfractures, filled with spary calcite (figure 7.1 A). The LKF 1 microfacies is characterized by intergranular, moldic and fracture type porosities.

**Depositional environment:** the LKF 1 microfacies shows moderate floral and faunal diversity. The presence of algae along with shallow benthic foraminifera (e.g. *Alveolina*), ostracodes and gastropods indicate deposition in a shallow marine, restricted but normal salninity, warm water proximal inner ramp setting.

### 7.2.2 *Alveolina rich bioclastic wackestone-packstone microfacies (LKF 2)*

The LKF 2 microfacies is represented by grey to yellowish grey coloured fossiliferous limestone of the Lockhart Formation. In thin section, the LKF 2 microfacies is characterized by a wackestone-packstone depositional texture having abundant allochems ranging from 40-70 %, with an average of 55%. Among the allochems alveolinid foraminifera dominate with good biogenic preservation (figure 7.2 A). Other foraminiferal species include milliolids (figure 7.2 B) and *Lockhartia pustulosa* (figure 7.2 D). The foraminiferal tests show partial to complete micritization (figure 7.2 E) and silicification of the internal chambers. Gastropods are the second most abundant allochems ranging in size from 0.5 mm to 2 mm with burrowing and boring modes (figure 7.2 A-B). The grains are poorly sorted and show

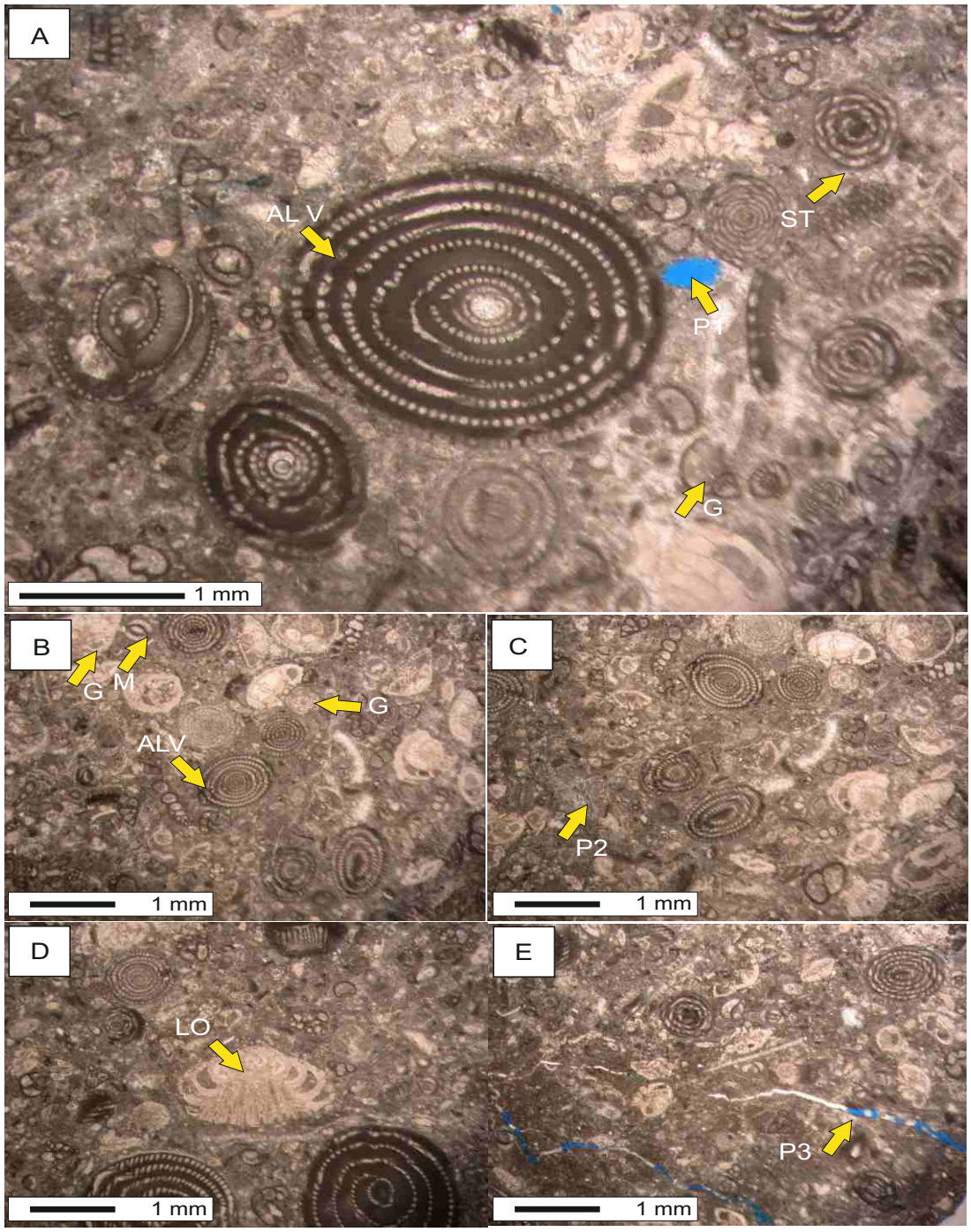


**Figure 7.2. *Alveolina* rich bioclastic wackestone-packstone Microfacies (LKF 2): A)** The allochems of LKF 2 include *Alveolina globula* (ALV) and small micritized boring gastropods (G), the diagenetic fabric shows low amplitude stylolites (ST), and coarse spary cement. Reservoir rock characters include vuggy porosity (P1) Intergranular porosity (P2 in **C**) fracture porosity (P3 in **E**) **B)** Shallow benthic fauna includes *milliolid* foraminifera (M**),** gastropods (G) and (ALV) *Alveolina* bioclasts in micritic matrix. **D)** Test of *Lockhartia pustulosa* showing partial micritization of the chambers.

no preferred orientation. The micritic matrix ranges in abundance from 20–50 %, with an average of 30 %. Sparry cement fills the intergranular spaces (figure 7.2 A). The diagenetic fabric is characterized by neomorphism, chemical compaction, calcite filled fractures and stylonodular fabric. The LKF 2 microfacies shows intergranular, vuggy, moldic and fracture porosity (figure 7.1 A, C and E).

**Depositional environment:** the co-occurrence of abundant *Alveolina*, milliolid and gastropods in the LKF 2 microfacies reflects shallow water, low energy conditions in distal inner ramp settings.

### *7.2.3 Diverse benthic foraminiferal wackestone-packstone microfacies (LKF 3)*

In the study area, the LKF 3 microfacies is represented by grey coloured nodular limestone of the Lockhart Formation. In thin sections, the LKF 3 microfacies is characterized by a wackestone-packstone depositional texture.

The biogenic content is well preserved having a rich allochemic constituent of larger benthic foraminifera ranging in abundance from 50-70%, with an average of 55%. The identified foraminiferal species are *Discocyclina ranikotensis*, *Miscellanea miscella, Operculina salsa, Lockhartia haime, Nummulites pinfoldi, Ranikothalia sindensis, Assilina spinosa* and *Alveolina globula* (see figure 7.3 A-E). The size of these foraminiferal bioclasts ranges from 2mm to 5mm. The micritic matrix abundance ranges from 30–60 %, with an average of 45%. The matrix has shown evidence of bioturbation and burrowing of small gastropods, ostracodes, algal thali and bivalves. The brachiopod bioclasts (up to 5mm in size) show partial to complete internal micritization and only the outline is preserved forming ghost structures (figure 7.3 E). Some terrestrial influx is seen in the form of scattered quartz grains ranging in abundance from 3-6 %, with an average of 2%. The diagenetic fabric is characterized by chemical compaction that resulted in the stylonodular fabric (figure 7.3 C), neomorphic alteration and spar filled fractures (figure 7.3 D). The LKF 3 microfacies is characterized by moldic, intergranular, fracture and intragranular porosities (figure 7.3 A-E).

**Depositional environment:** the moderate to high diversity of foraminifera, absence of restricted marine fauna and matrix supported rock fabric suggest that the

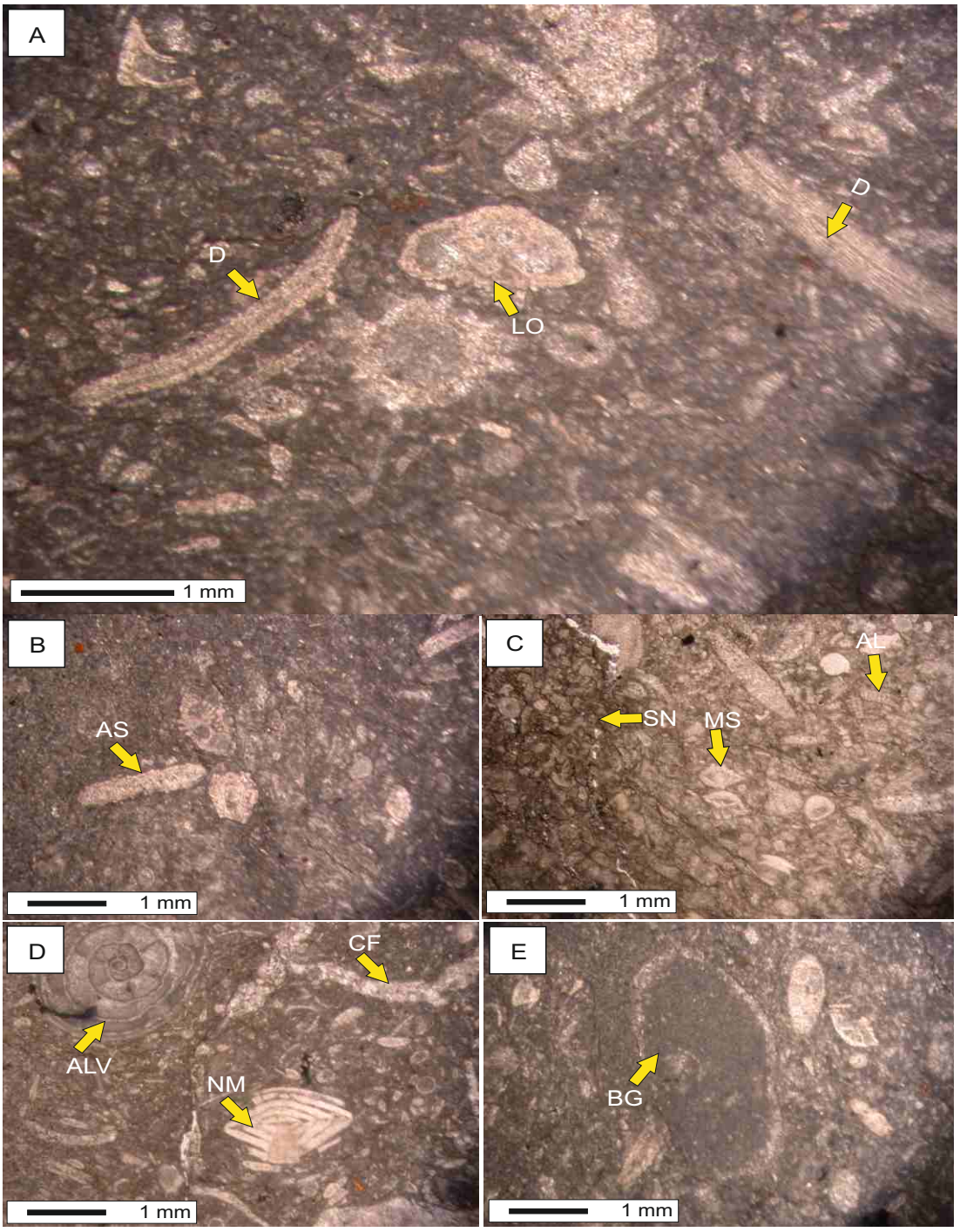


**Figure 7.3. Diverse benthic foraminiferal wackestone-packstone microfacies (LKF 3):** the allochems of the LKF 3 microfacies include *Discocyclina ranikotensis* (D) *Lockhartia* (LO), *Assilina spinosa* (AS in **B**), *Miscellanea stampi* (MS in **C**), *Nummulites pinfoldi* (NM in **D**), *Alveolina globula* (ALV in **D**) and Algae (AL in **C**). The diagenetic fabric is characterized by the stylonodular fabric (SN in **C**), complete internal micritization of brachiopod shell forming ghost structure (BG in **E**), post depositional spar filled fractures (CF in **D**) and neomorphic spar replacement of bioclasts (LO in **A** and AS in **B**).

LKF 3 microfacies was deposited in distal middle ramp settings.

### *7.2.4 Planktonic-benthic mixed foraminiferal lime mudstone - wackestone microfacies (LKF 4)*

In the study area, the LKF 4 microfacies is represented by medium bedded grey coloured nodular limestone of the Lockhart Formation. In thin section, the LKF 4 Microfacies is characterized by a lime mudstone-wackestone depositional textures. A well preserved biogenic content is seen, containing both planktonic and benthic foraminifera. The abundance of the allochems ranges from 10 –30 %, with an average of 18 %. Species of the larger benthic foraminifera include *Ranikothalia sahini* (figure 7.4 B)*, Operculina salsa*, *Miscellanea miscella* and *Discocyclina ranikotensis* having an abundance range of 30-45% of the total allochems. The planktonic foraminifera include genera of *Globorotalia, Globigerina* and *Planorotalites* and their abundance ranges from 10 to 20 % of the total allochems. Some planktonic foraminiferal tests show silicification and internal micritization of the chambers (figure 7.4 A). The micritic matrix dominates and ranges in abundance from 60-90 %, with an average of 75 %. Less than 5 % scattered quartz is also present in the allomicritic matrix.

The diagenetic fabric is characterized by neomorphic alteration, planer to wavy grain contacts, stylolites with iron oxide residue and calcite filled fractures showing post depositional deformation (figure 7.4 C). The LKF 4 microfacies has intragranular and fracture type porosities.

**Depositional environment:** the presence of the micritic matrix, mixed planktonic and larger benthic foraminifera and absence of shallow marine flora and fauna suggest that the LKF 4 microfacies was deposited in low energy outer ramp settings. Storm surges have contributed some quartz within the microfacies.

## 7.3 Facies of the Patala Formation

The microfacies of the Patala Formation are abbreviated as PTF 1-PTF 6 (here PT stands for the Patala Formation and F stands for the microfacies in the Potwar Basin and the TIR and 1-6 are various types of recorded microfacies).

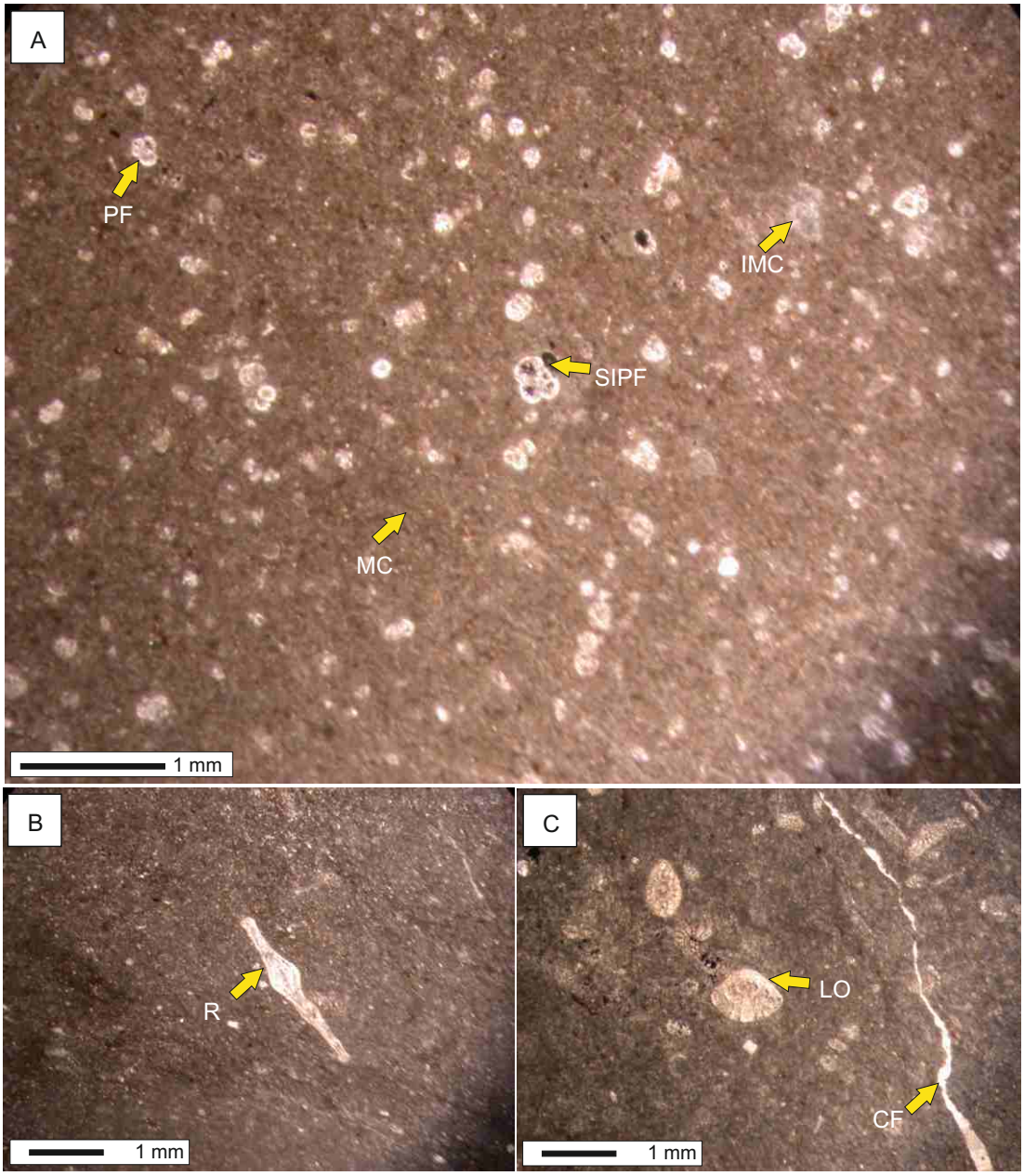


**Figure 7.4. Planktonic-benthic mixed foraminiferal lime mudstone-wackestone microfacies (LKF 4):** the allochems of the LKF 4 microfacies include planktonic foraminifera (PF in **A**), benthic foraminifera i.e. *Ranikothalia sahini* (R in **B**) and *Lockhartia conditi* (LO in **C**)**.** The diagenetic fabric is characterized by complete internal micritization (IMC in **A**) and silicification (SIPF in **A**) of the planktonic foraminiferal test and post depositional spar filled fractures (CF in **C**).

### 7.3.1 Algal-milliolid rich bioclastic wackestone-packstone microfacies (PTF 1)

In the study area the PTF 1 microfacies is represented by thin bedded yellowish brown coloured fossiliferous limestone in the lower part of the Patala Formation. In thin section, the PTF 1 microfacies is characterized by a wackestone-packstone depositional texture. The biogenic content is moderately preserved. The allochems are dominated by algae and milliolid foraminifera (figure 7.5 A) that range in abundance from 40-60 %, with an average of 50 %. Ostracodes, bivalves and small gastropods are also present with an abundance range from 5-20 %, with an average of 12 %. The micrite matrix ranges in abundance from 50-70%, with an average of 45 %.

The diagenetic fabric is characterized by neomorphic alteration and internal micritization of bioclasts (figure 7.5 C) and post depositional spar filled fractures. The PTF 1 microfacies shows fracture, moldic (figure 7.5 A) and intragranular porosities.

**Depositional environment:** the abundance of algae and milliolid foraminifera indicates that the PTF 1 microfacies was deposited in shallow water restricted conditions of proximal inner ramp settings.

### 7.3.2 Fenestral bioclastic mudstone-wackestone microfacies (PTF 2)

In the study area, the PTF 2 microfacies is represented by medium–bedded, yellowish coloured fossiliferous limestone of the Patala Formation. In thin section, the PTF 2 microfacies is characterized by a mudstone to wackestone depositional texture. The allochems are dominated by algae and benthic foraminifera (figure 7.6 B and C).The abundance of bioclasts ranges from 5 to 40 % with an average of 25 %. These bioclasts are poorly preserved, have poor sorting and lack any preferred orientation. The sparry matrix dominates and ranges in abundance from 50 – 75 %, with an average of 60 %. The fenestral fabric is a prominent feature of the PTF 2 microfacies. The fenestral openings are synsedimentary in origin, filled with calcite and are ranging in size from 0.2mm to 2mm. The geopetal fabric is also seen in the fenestrae (figure 7.6 A). These fenestrae are classified as laminoid, irregular and tabular types, have complex interconnecting network (figure 7.6 A and C).

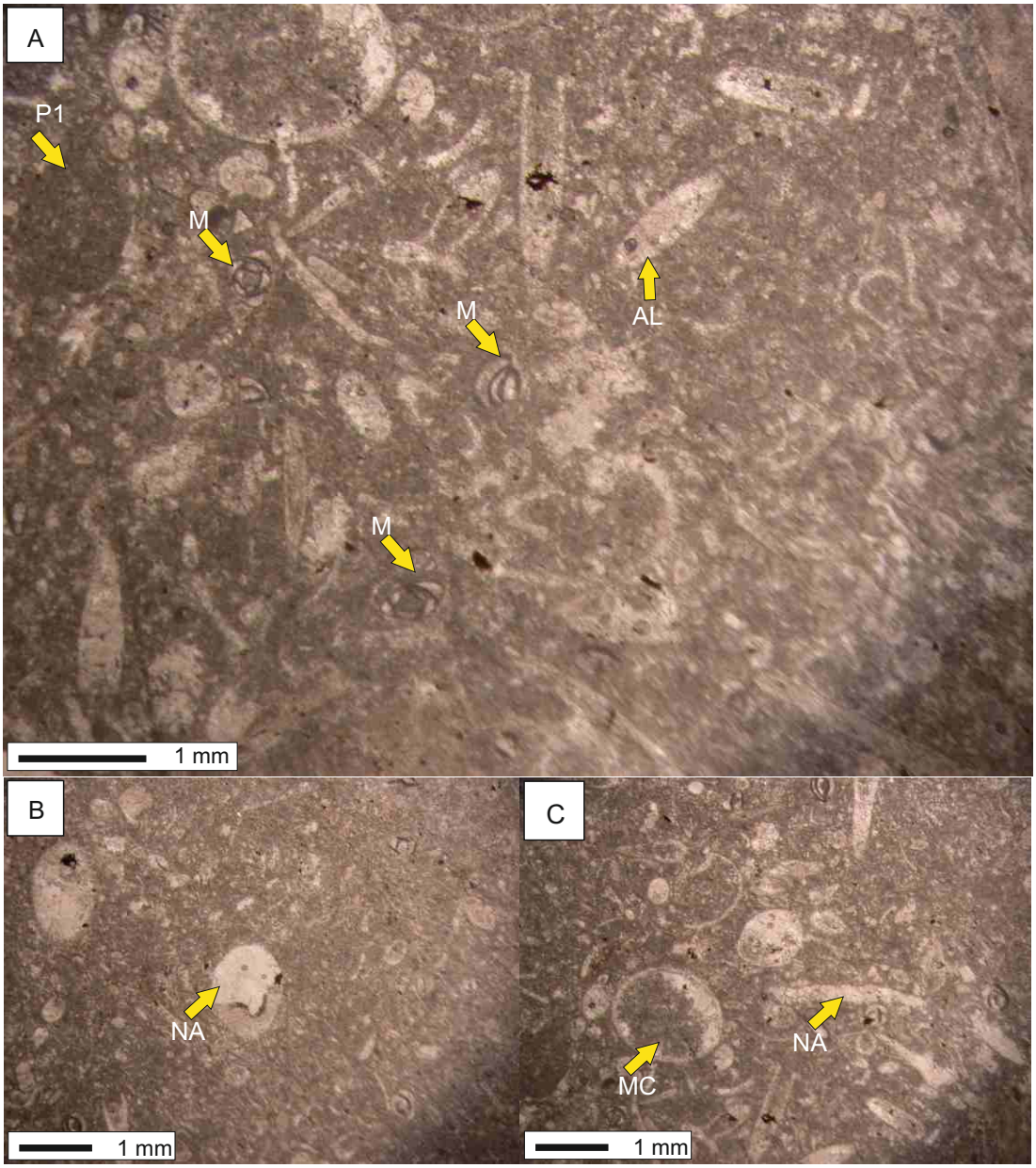


**Figure 7.5. Algal-milliolid rich bioclastic wackestone-packstone microfacies (PTF 1):** the allochems of the PTF 1 microfacies include algae (AL in **A**), benthic foraminifera i.e. milliolids (M in **A**) and *brachiopod* ghosts (MC in **C**)**.** The diagenetic fabric is characterized by internal micritization (MC in **C**), Aggrading neomorphic alteration (NA in **B** and **C**) of the bioclasts. Moldic porosity is common (P1 in **A**).

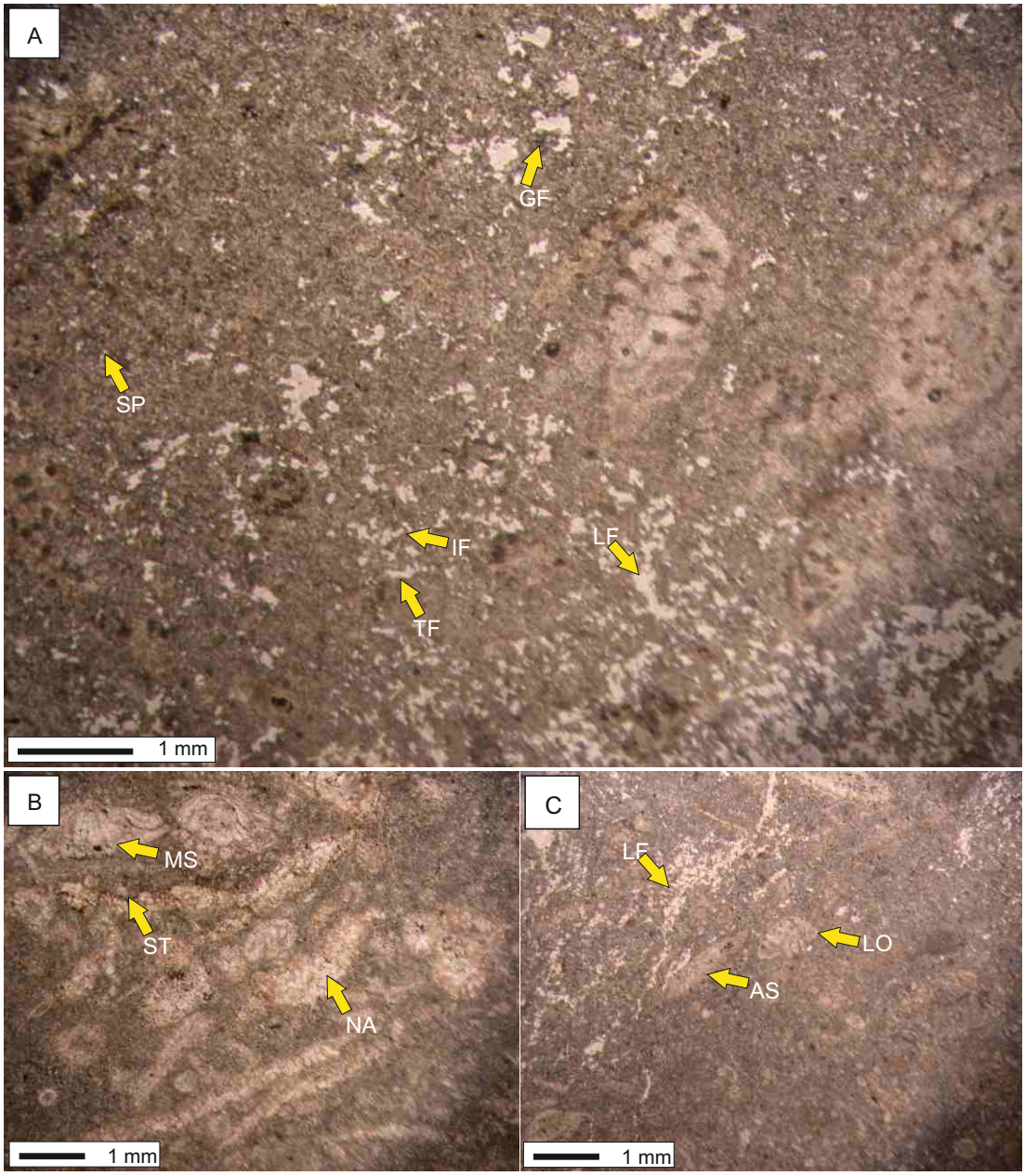


**Figure 7.6. Fenestral bioclastic mudstone-wackestone microfacies (PTF 2):** allochems of the PTF 2 microfacies include benthic foraminifera i.e. *Miscellanea miscella* (MS in **B**) *Assilina spinosa* (AS in **C**) and *Lockhartia conditi* (LO in **C**)**.** Fenestral fabric is characterized by interconnecting network of laminoid fenestrae (LF in **A** and **C**), Irregular fenestrae (IF in **A**), Tabular fenestrae (TF in **A**) and a geopetal fabric is also seen (GF in **A**). Spary matrix is dominant (SP in **A**). The diagenetic fabric is characterized by partial internal micritization, chemical compaction forming low amplitude stylolites (ST in **B**) and aggrading neomorphic alteration of the bioclasts (NA in **B**).

The diagenetic fabric of the PTF 2 microfacies is characterized by smooth stylolites with iron residue along the sutured seams and neomorphic alteration (figure 7.6 B and C) of the bioclasts. Pyrite alteration is commonly found in the matrix and also within the bioclasts (figure 7.6 B).

**Depositional environment:** the fenestra structure has different origins. Laminoid fenestrae are common in the intertidal to supratidal zone and are believed to form through desiccation processes. The irregular fenestrae are formed in intertidal to supratidal environments (Flügel, 2004). The presence of distinctive fenestral morphologies, poorly preserved foraminifera and spary matrix indicate that the PTF 2 microfacies is deposited in high energy intertidal to supratidal conditions in a proximal inner ramp setting.

### *7.3.3 Foraminiferal packstone microfacies (PTF 3)*

In the study area the PTF 3 microfacies is represented by medium bedded yellowish brown coloured, highly fossiliferous sandy limestone in the upper part of the Patala Formation. In thin section, the PTF 3 microfacies is characterized by a packstone depositional texture. The biogenic content is well preserved, with good sorting, preferred orientation and graded bedding fabric of the bioclasts (figure 7.7 C). The allochems are dominated by foraminiferal bioclasts that range in abundance from 70–90 %, with an average of 80 %. The foraminiferal bioclasts include *Assilina dandotica, Assilina laminosa, Assilina leymerie, Nummulites lahiri, Nummulites deserti, Discocyclina ranikotensis* and *Discocyclina despensa* (figure 7.7 A-C).

The diagenetic fabric of the PTF 3 microfacies is characterized by silicification of the bioclasts, smooth stylolites and neomorphic alteration of the bioclasts (figure 7.7 C). The PTF 3 microfacies show intergranular, intragranular and fracture porosities (figure 7.7 A-C).

**Depositional environment:** the high diversity foraminiferal fauna of middle ramp affinity and micritic matrix indicate deposition in low energy conditions of middle ramp settings.

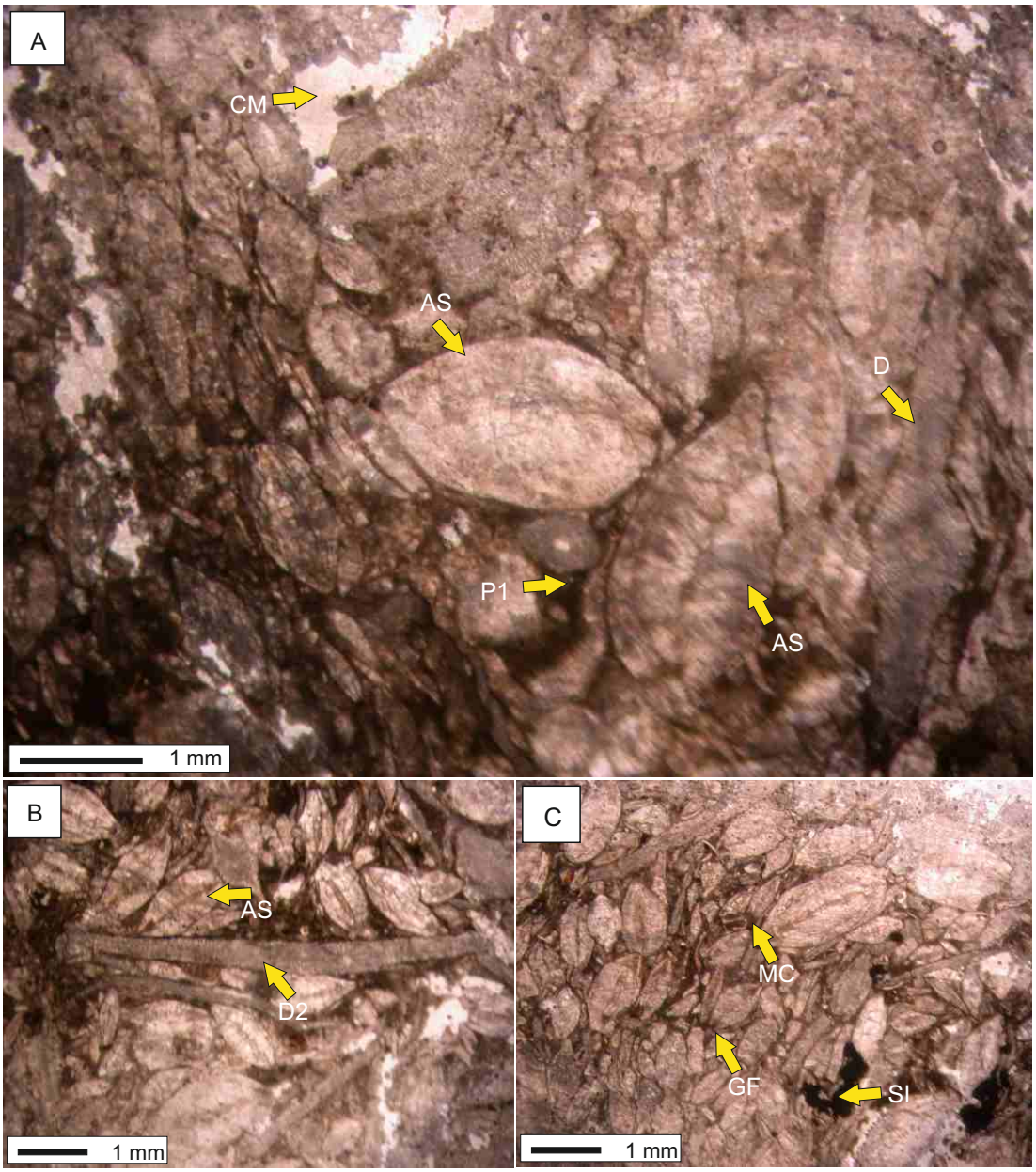


**Figure 7.7**. **Foraminiferal packstone microfacies (PTF 3):** the allochems of the PTF 3 microfacies include larger benthic foraminifera i.e. *Assilina dandotica, Assilina laminosa* (AS in **A** and **B**), *Discocyclina ranikotensis* (D2 in **B**). Preferred grain orientation and graded bedding fabric (GF in **C**) is seen. The diagenetic fabric is characterized by partial internal micritization, neomorphism and silicification of the bioclasts (SI in **C**). Micritic matrix (MC in **C**). and calcite cement (CM in **A**) filled the intergranular space. Intergranular porosity is common (P1 in **A** and **B**)

### 7.3.4 Peloidal mudstone microfacies (PTF 4)

In the study area the PTF 4 microfacies is represented by thin to medium bedded grey coloured limestone in the lower part of the Patala Formation. In thin section, the PTF 4 microfacies is characterized by a mudstone to wackestone depositional textures. The biogenic content is poorly preserved and rare planktonic and larger benthic foraminiferal bioclasts are found scattered in the micritic matrix (figure 7.8 A and B). The micritic matrix ranges in abundance from 70 to 90 %, with an average of 85 % (figure 7.8 B). Peloids are very common ranging in size from 0.1 to 0.3mm, and found in nests, scattered and isolated forms (figure 7.8 B). The diagenetic fabric is characterized by chemical compaction forming stylolites, internal micritization and pyritization of the bioclasts. The PTF 4 microfacies show intragranular and stylolitic porosities (figure 7.8 A and B).

**Depositional environment:** Peloids are commonly found in shallow subtidal to intertidal environments (Flügel, 2004). The presence of the micritic matrix, rare planktonic and larger foraminifera indicate that the PTF 4 microfacies was deposited in low energy conditions in the inner ramp setting.

### 7.3.5 Diverse foraminiferal wackestone-packstone microfacies (PTF 5)

In the study area, the PTF 5 microfacies is represented by medium bedded yellowish coloured, highly fossiliferous nodular limestone of the Patala Formation. In thin section, the PTF 5 microfacies is characterized by a wackestone-packstone depositional texture (figure 7.9). The biogenic content is well preserved. The allochems are diverse and ranging in abundance from 40–60 %, with an average of 50 %. These allochems mainly include larger benthic foraminifera (i.e. *Ranikothalia sindensis, Ranikothalia sahini, Miscellanea miscella, Dictyoconiodes cooki, Nummulites lahiri, Operculina salsa, Lockhartia pustulosa* and *Lockhartia haime*), Bivalves, brachiopods, ostracodes and scattered echinoid clasts are also present (figure 7.9 A-C). The micritic matrix dominates and its abundance ranges from 30 – 60 %, with an average of 40 %. Sparry calcite is also found as cement, filling the large fractures and intergranular spaces. The matrix is allomicritic in nature and related to the breakdown of the skeletal material.


**Figure 7.8. Peloidal mudstone microfacies (PTF 4):** the allochems of the PTF 4 microfacies include rare planktonic foraminifera (PL in **A**) and abraded bioclasts of benthic foraminifera. Peloids are rounded in shape (PL in **B**). The diagenetic fabric is characterized by smooth low amplitude stylolites (ST in **A**), pyrite replacement (PY in **A**) and laminated fabric (L1 and L2 in **A**). The micritic matrix is abundant (MC in **B**).

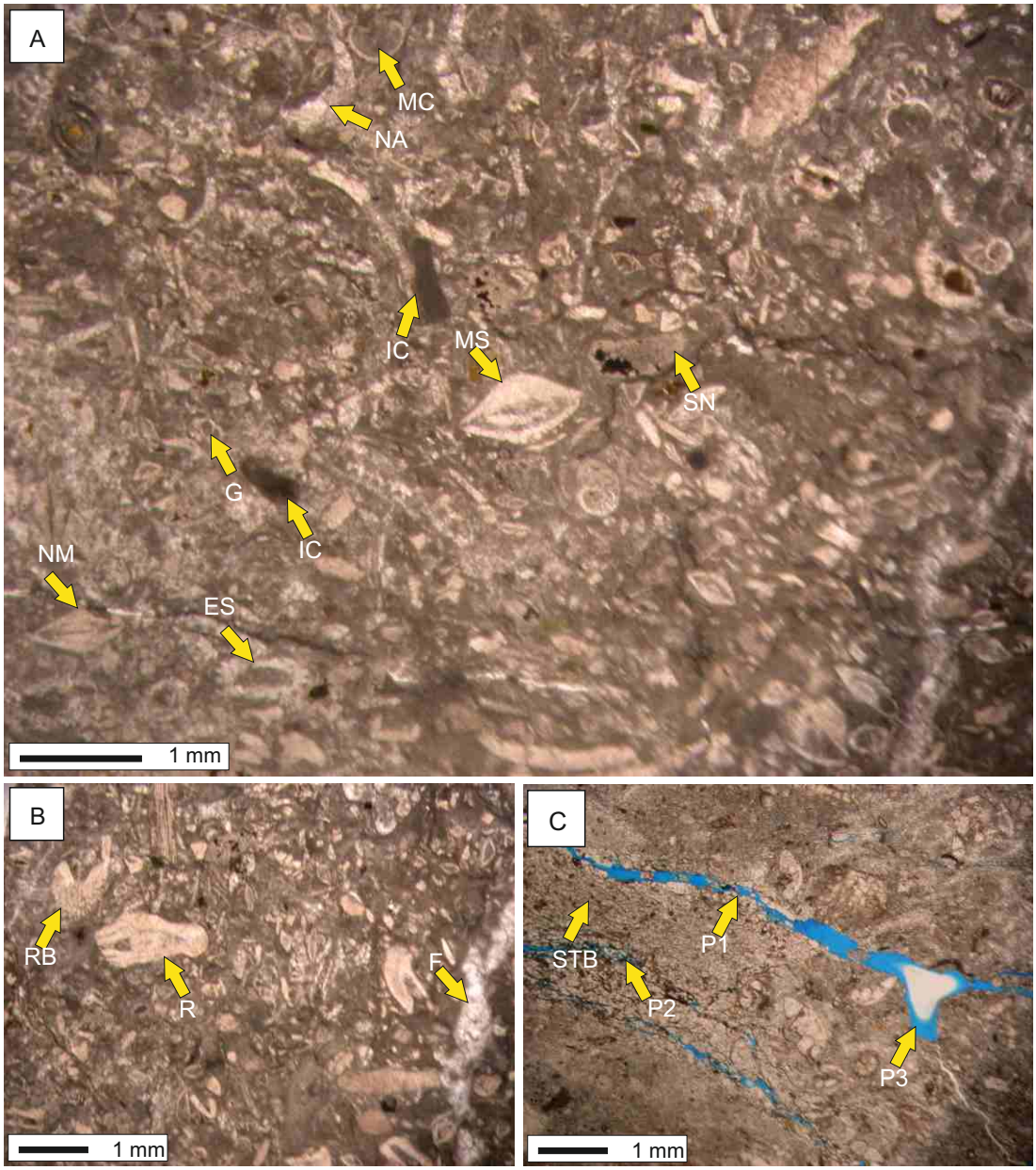


**Figure 7.9**. **Diverse foraminiferal wackestone-packstone microfacies (PTF 5):** allochems of the PTF 5 microfacies include diverse larger benthic foraminifera i.e. *Miscellanea miscella* (MS in **A**), *Nummulites lahiri* (NM in **A**), *Ranikothalia sidensis* bioclasts (R and RB in **B)** and echinoderm spines (ES in **A**) and small gastropods (G in **A**). Intraclast are also found (IC in **A**). The diagenetic fabric is characterized by partial internal micritization (MC in **A**), neomorphism (NA in **A**) and post depositional spar filled fracures (F in **B**). Chemical compaction is evidenced by stylonodular (SN in **A**) and stylobrecciated (STB in **C**) fabrics. Fracture (P1 in **C**), intergranular (P2 in **C**) and vuggy (P3 in **C**) porosities are identified.

The diagenetic fabric of the PTF 5 microfacies is characterized by stylolaminated, stylobrecciated and stylonodular fabrics. Post depositional calcite filled fractures, silicification, micritization and low to medium amplitude stylolites are common diagenetic imprints (figure 7.9 A-C). The PTF 5 microfacies shows intergranular, intragranular, moldic, and fracture type porosities (figure 7.9 C). **Depositional environment:** high faunal diversity, micritic matrix and absence of shallow water fauna (Flügel, 2004) indicate that PTF 5 microfacies was deposited below FWWB, in normal salinity conditions of the proximal middle ramp setting.

### *7.3.6 Coralline red algal-stromatolite mudstone- wackestone microfacies (PTF 6)*

In the study area the PTF 6 microfacies is represented by thin bedded yellowish coloured, nodular limestone with interbeds of calcareous clays in the lower part of the Patala Formation. In thin section, the PTF 6 microfacies is characterized by a mudstone to wackestone depositional textures. The PTF 6 microfacies show presence of red coralline algae forming stromatolites. The stromatolites are having spaced hemispheroids which are laterally linked (LLH) with each other and stacked hemispheroids (domes) which are not linked (SH) with each other (figure 7.10 A and C). Occasional planktonic foraminifera are also present. The micritic matrix dominates and its abundance ranges from 70 to 90 %, with an average of 85 %. The diagenetic fabric is characterized by microbial micritization of bioclasts forming ghost structures and replacement of bioclasts by spar. The PTF 6 microfacies shows intragranular and moldic porosities.

**Depositional environment:** the morphology of coralline red algal crusts reflects different water energy (Bosence, 1983). The modern coralline algae range from tropical to polar oceans and extend from intertidal areas to depths of 250m. They reflect normal salinities and grow on hard substrates. The stromatolites are formed by several mechanisms but most commonly a peritidal environment is envisaged for their deposition (Demicco and Hardie, 1994). The presence of coralline red algae, LLH and SH type stromatolites, occasional planktonic foraminifera and the micritic

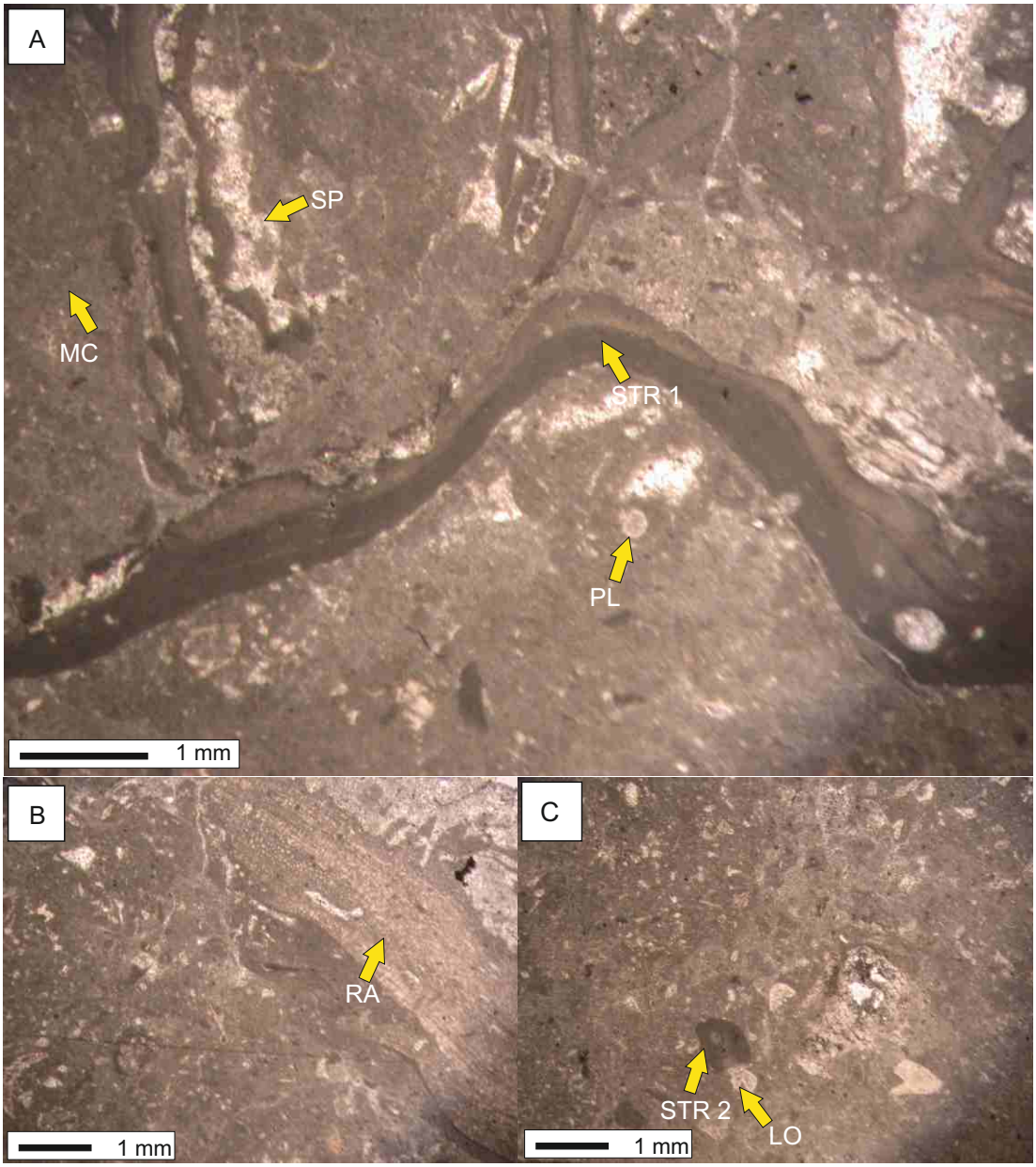


**Figure 7.10. Coralline red algal–stromatolite mudstone - wackestone microfacies (PTF 6)**: the allochems of the PTF 6 microfacies include coralline red algae (RA in **B**), rare planktonic foraminifera (PL in **A**), *Lockhartia conica* (LO in **C**) and few abraded bioclasts of larger benthic foraminifera. Algal stromatolites are very prominent including (LLH type) stromatolites with laterally linked hemispheroids (STR 1 in **A**), and (SS type) stromatolite with vertical stacking and lacking any lateral link (STR 2 in **C**). The diagenetic fabric is characterized by partial internal micritization (PL in **A**) and neomorphism (SP in **A**).

matrix suggest that the PTF 6 microfacies was deposited below FWWB in normal marine conditions of the distal middle ramp settings.

## 7.4 Facies of the Nammal Formation

The microfacies of the Nammal Formation are abbreviated as NMF 1- NMF 6 (NM stands for the Nammal Formation, F stands for the Potwar Basin and the TIR and 1-6 are various types of recorded microfacies) and are described below.

### *7.4.1 Nummulites- Discocyclina rich packstone microfacies (NMF 1)*

In the Chichali Nala and Nammal Gorge Sections the NMF 1 microfacies is represented by a bluish grey to brownish yellow coloured, 1.5 m thick fossiliferous limestone in the lowermost part of the Nammal Formation. In thin section, the NMF 1 microfacies is characterized by a packstone-grainstone depositional textures having a rich allochemical constituent of larger benthic foraminifera (dominated by > 50 % - <80 % , with an average of 70%, allochems of *the Assilina, Nummulites, Discocyclina, Ranikothalia* and *Operculina*) (figure 7.11). Size of the *Nummulites* test ranges from 2mm to 4mm, *Discocyclina* size ranges from 2mm to 5mm, *Ranikothalia* size ranges from 3mm to 7mm, *Operculina* size ranges from 1mm to 4mm, and *Assilina* size ranges from 1mm to 4mm. In spite of the presence of broken bioclasts of *Discocylina* the overall biogenic preservation is good. The grains show a cross bedded fabric (figure 7.11 C), sorting of the grains is moderate. The micritc matrix is ranging from 10% - 30 %, with an average of 15%.

The diagenetic fabric is characterized by partial micritization and silicification of the foraminiferal test chambers. In the NMF 1 microfacies intergranular, intragranular and fracture porosities are identified (figure 7.11 D - E).

**Depositional environment:** The foraminiferal diversity in the NMF 1 microfacies and presence of micritic matrix indicate deposition in low energy normal marine distal middle ramp setting.

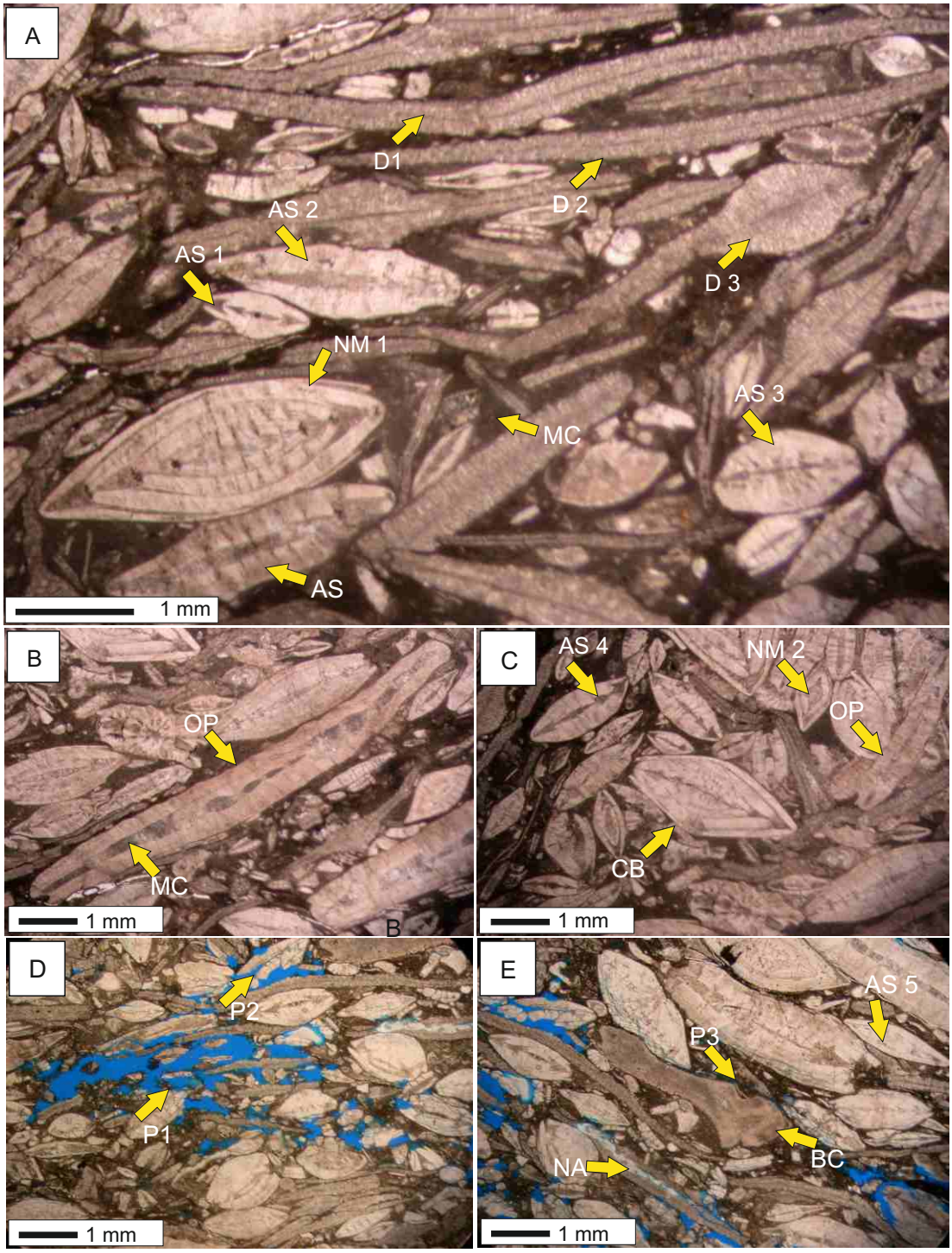


**Figure 7.11**. ***Assilina- Discocyclina* rich packstone microfacies (NMF 1):** the allochems of the NMF 1 microfacies include diverse larger benthic foraminifera i.e. *Nummulites palnulatus* (NM 1 in **A**), *Nummulites lahiri* (NM 2 in **C**), *Ranikothalia sindensis* bioclasts (BC in **E),** *Operculina salsa* (OP in **A** and **C**), *Assilina granulosa* (AS and AS 2 in **A**), *Assilina spinosa* (AS 1 in **A** and AS 4 in **C**), *Assilina dandotica* (AS 3 in **A**), *Assilina leymerie* (AS 5 in **E**) and *Discocyclina* (D1 – D4 in **A**). Intergranular micrite is commonly seen (MC in **A**). The diagenetic fabric is characterized by partial internal micritization (MC in **B**) and neomorphism (NA in **E**). Various porosity types including intergranular (P1 in **D**), intragranular (P 2 in **D**) and fractures (P3 in **E**) are identified.

### 7.4.2 Foraminiferal bioclastic wackestone microfacies (NMF 2)

In the Chichali Nala and the Nammal Gorge sections the NMF 2 microfacies is represented by bluish grey coloured marls in the lower most part of the Nammal Formation. In thin sections, the NMF 2 microfacies is characterized by wackestone-packstone depositional texture. The allochems are mainly larger benthic foraminifera (i.e. *Assilina spinosa*, *Ranikothalia sahini* and *Discocyclina*) ranging in abundance from 10-40%, with an average of 25 %. The brachiopod bioclasts of up to 3mm size show internal micritization (figure 7.12 B) and rare *Assilina spinosa* and ostracode bioclasts are partially silicified (figure 7.12 A and D). The sparry matrix ranges from 30-50 %, with an average of 40 %. Some planktonic foraminifera are also found within the sparry matrix. The bioclasts show graded bedding fabrics (normal and reverse) and increased sorting upward which is typical of the main zone of an allodopic turbidite limestone of the Meischner sequence (1964) (figure 7.12 A and E). Allodopic limestone in the Meischner sequence refers to a limestone bed consisting of graded carbonate debris, deposited in high energy carbonate platform slope settings (Meischner, 1964).

The diagenetic fabric is characterized by partial internal micritization and silicification of the bioclasts (figure 7.12 A and D). The NMF 2 microfacies shows fracture, intergranular, intragranular and moldic porosities (figure 7.12 A and E).

**Depositional environment:** presence of the sparry matrix and mixing of the ecologically different fauna that includes some of the larger benthic foraminiferal species (*Assilina spinosa*, *Discocyclina*), micritized brachiopods, silicified ostracodes, coral debris, and graded bedding (normal and reverse) indicate that the NMF 2 microfacies was deposited as an allodopic limestone turbidite. The NMF 2 microfacies can be compared with the main phase (part 1) of the Meischner sequence (1964) of an allodopic limestone turbidite and was deposited in a distally steepened ramp slope setting.

### 7.4.3 Planktonic-Discocyclina rich wackestone-packstone microfacies (NMF 3)

In the Chichali Nala and Nammal Gorge section the NMF 3 microfacies is represented by thin to medium bedded blueish grey coloured limestone in the middle

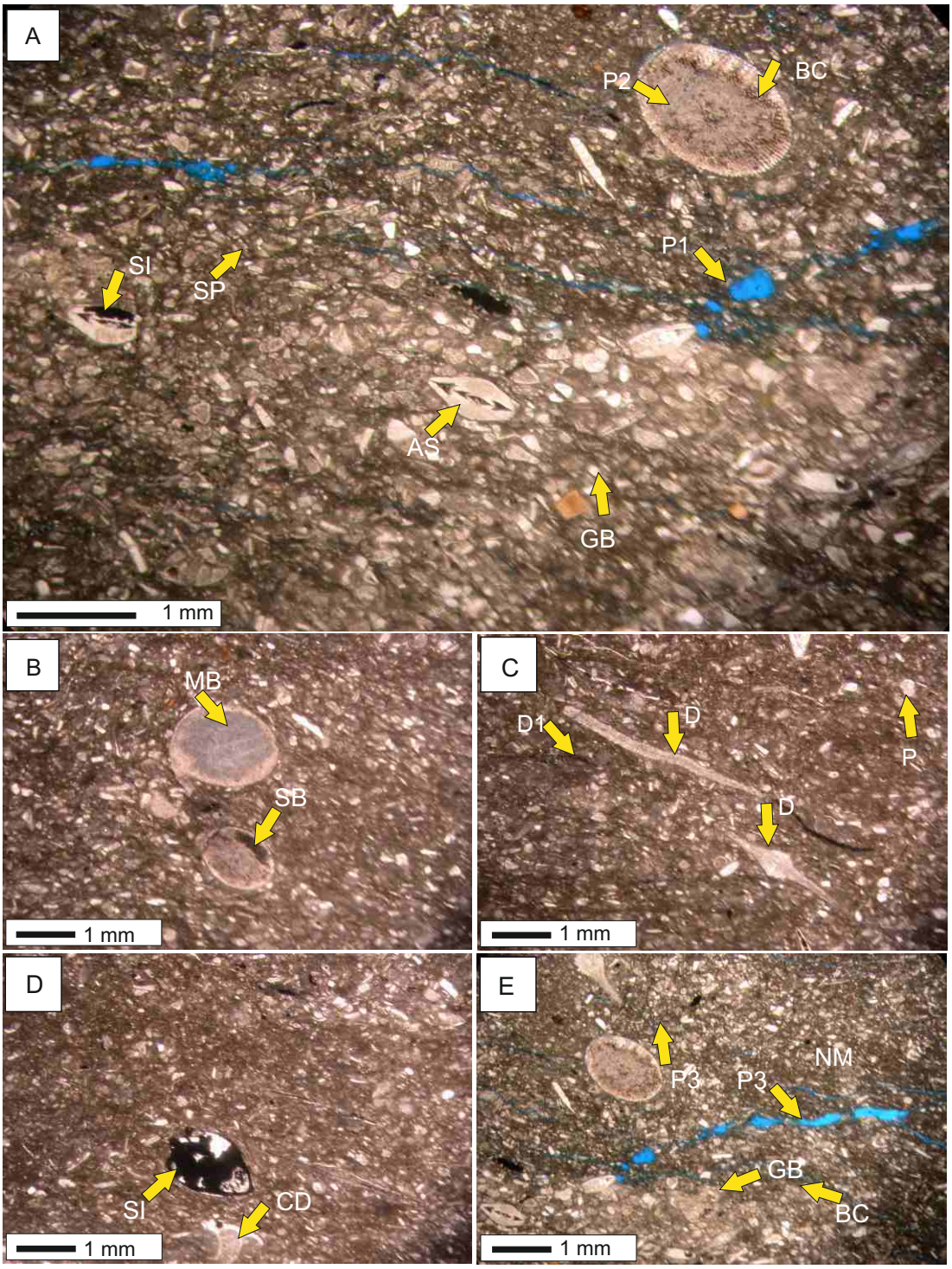


**Figure 7.12. Foraminiferal bioclastic wackestone microfacies (NMF 2)**: the allochems of the NMF 2 microfacies include larger benthic foraminifera i.e. *Assilina spinosa* (AS in **A**) and *Discocyclina* (D1 and D in **A** and **C**), brachiopods (BC in **A** and SB in **B**), silicified ostracodes (Sl in **D**), coral debris (CD in **D**) and broken bioclasts (BC in **E**). The diagenetic fabric is characterized by internal micritization shown by brachiopod bioclast (MB in **B**) and silicification of the ostracode and *Assilina spinosa* bioclasts (Sl in **A** and **D**). Note mixing of the ecologically different fauna (ostracode, brachiopods, coral debris and *Assilina*) in a typical allodopic limestone turbidite showing graded and reverse graded bedding (GB in **A** and **E**) (Zone 1 A of Meischner sequence, 1964). Various porosity types including intergranular (P1 in **A**), intragranular (P 2 in **A**) and fracture (P 3 in **E**) are identified.

part of the Nammal Formation. In thin section, the NMF 3 microfacies is characterized by a wackestone-packstone depositional texture (figure 7.13 A and D). The biogenic content is well preserved. The allochems are dominated by a mixture of planktonic and benthic forams, abundance of allochems ranges from 40-60 %, with an average of 50 %. The planktonic foraminifera include globorotaliids while larger benthic foraminifera are dominated by species *Discocyclina sella* and *Discocyclina scalaris*. *Discocyclina* bioclasts range in size from 3mm to 6mm and are mostly found in small nests and sometime scattered in the micritic matrix (figure 7.13 A). The abundance of the micritic matrix ranges from 40 – 60 %, with an average of 45 %. The diagenetic fabric shows silicification of *Discocyclina* tests and micritization of internal chambers in the planktonic foraminiferal tests. The spar filled fracture and veins are commonly present and show aggrading neomorphism (7.13 B). These fractures also show diagenetic faults which have displaced the *Discocyclina* tests (figure 7.13 C). Grains have poor to moderate sorting. The porosity types identified are fracture (figure 7.13 E) and intergranular.

**Depositional environment:** *Discocyclina* is found in mid–outer ramp settings (Racey 1994; Anketell and Miriheel, 2000). The planktonic foraminifera indicate a pelagic environment. The mixing of shallow and deep water fauna (ostracodes, bivalves, benthic foraminifera and planktonic foraminifera) and presence of the micritic matrix in the NMF 3 microfacies indicate that *Discocyclina* tests are eroded from the distal middle ramp platform and redeposited in the open marine ramp slope setting. Presence of diagenetic faults, micritic matrix and pelagic foraminifers compares NMF 3 microfacies with the zones 2 and 3 of the Meischner (1964) allodopic limestone turbidite sequence and shows deposition in a distally steepened upper ramp slope setting.

### *7.4.4 Pelagic mudstone -wackestone microfacies (NMF 4)*

In the Chichali Nala and Nammal Gorge Sections the NMF 4 microfacies is represented by medium to thick bedded bluish grey coloured limestone in the middle-upper part of the Nammal Formation. In thin sections, the NMF 4 microfacies is characterized by a mudstone-wackestone depositional textures. Abundant planktonic foraminifera are found within the micritic matrix (figure 7.14).

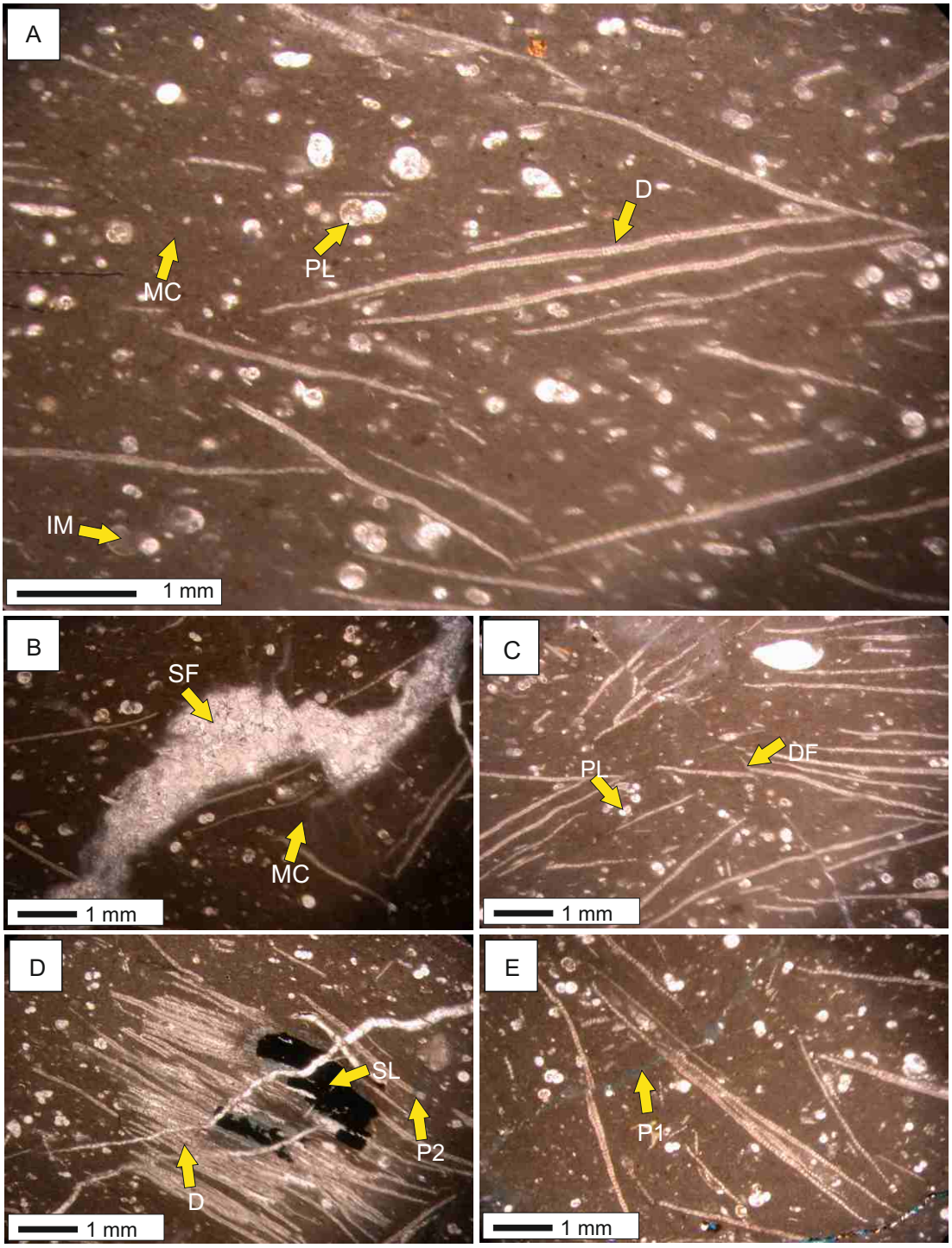


**Figure 7.13. Planktonic-*Discocyclina* rich foraminiferal wackestone–packstone microfacies (NMF 3)**: note mixing of the fauna, larger benthic foraminifera i.e. *Discocyclina* (D in **A**) and planktonic foraminifera (PL in **A** and **C**) scattered in a micritic matrix (MC in **A**). The diagenetic fabric is characterized by internal micritization shown by planktonic foraminiferal bioclasts (IM in **A**), silicification (SL in **D**), diagenetic faults exhibited by displacement of *Discocylina* test (DF in **C**), and spar filled post depositional fractures showing aggrading neomporphism (SF in **B**). Various porosity types including fracture (P 1 in **E**) and intragranular (P 2 in **D**) are identified.

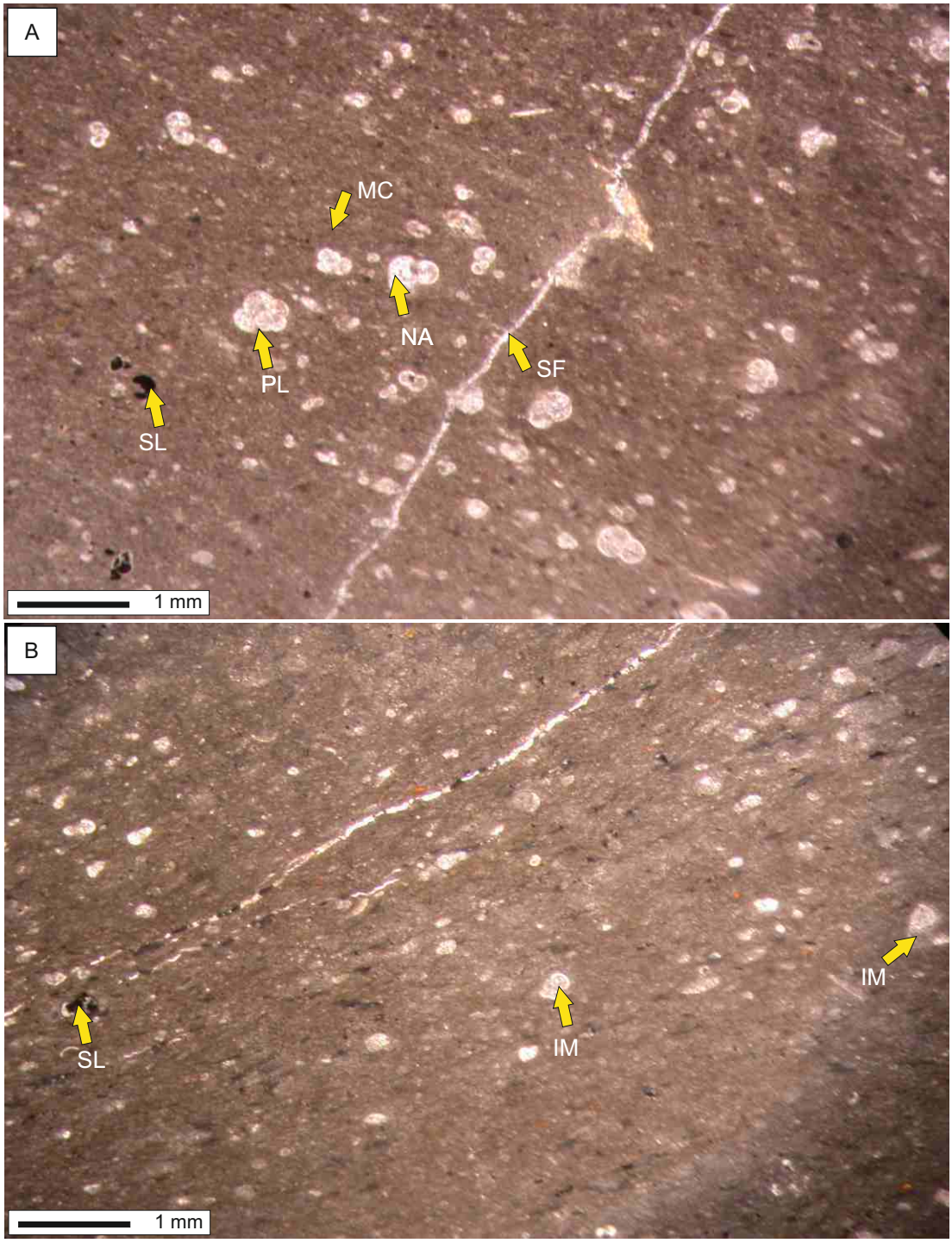


**Figure 7.14. Pelagic mudstone-wackestone microfacies (NMF 4):** the allochems of the NMF 4 microfacies include planktonic foraminifera (PL in **A**) which are scattered in micritic matrix (MC in **A**). The diagenetic fabric is characterized by internal micritization shown by planktonic foraminiferal test (IM in **B**), silicification (SL in **A** and **B**), spar filled post depositional fractures (SF in **A**) and bioclasts showing aggrading neomorphism and NA in **A**).

The planktonic foraminiferal abundance ranges from 10 to 20 %, with an average of 15 %. The micritic matrix ranges from 50 to 80 %, with an average of 70 %. The diagenetic fabric is characterized by internal micritization and silicification of the bioclasts and spar filled fractures showing aggrading neomorphism (figure 7.14 A and B). Intergranular, intragranular and fracture porosities are common in the NMF 4 microfacies.

**Depositional environment:** presence of the micrite matrix with abundance of the planktonic foraminifera indicates that NMF 4 microfacies was deposited in open marine conditions in outer ramp to deep basinal settings.

### *7.4.5 Planktonic foraminiferal wackestone-packstone microfacies (NMF 5)*

In the Chichali Nala and Nammal Gorge sections the NMF 5 microfacies is represented by thin bedded bluish grey coloured marls in the middle - upper part of the Nammal Formation. In thin section, the NMF 5 microfacies is characterized by a dolomitic lime mudstone to wackestone depositional textures. In thin section, the NMF5 microfacies is characterized by abundance of planktonic foraminifera and dolomicritic matrix (figure 7.15). The diagenetic fabric is characterized by neomorphism, post depositional spar filled fractures and pyritization (figure 7.15). Intergranular and fracture porosities are common.

**Depositional environment:** the presence of planktonic foraminifera and abundance of the micritic matrix suggest that the NMF 5 microfacies was deposited in low energy conditions in an open marine pelagic environment of the outer ramp setting.

### *7.4.6 Peloidal lime mudstone microfacies (NMF 6)*

In the Chichali Nala and Nammal Gorge Sections the NMF 6 microfacies is represented by thin bedded blueish grey coloured marls in the upper part of the Nammal Formation. In thin section, the NMF 6 microfacies is characterized by a lime mudstone depositional texture. In thin section studies the NMF 6 is characterized by an abundance of peloids and sparse larger benthic foraminifera i.e. *Ranikothalia sahini* (figure 7.16 C), rare gastropods and ostracodes. The micritic matrix is abundant and ranges from 50 to 70 %, with an average of 55 %.

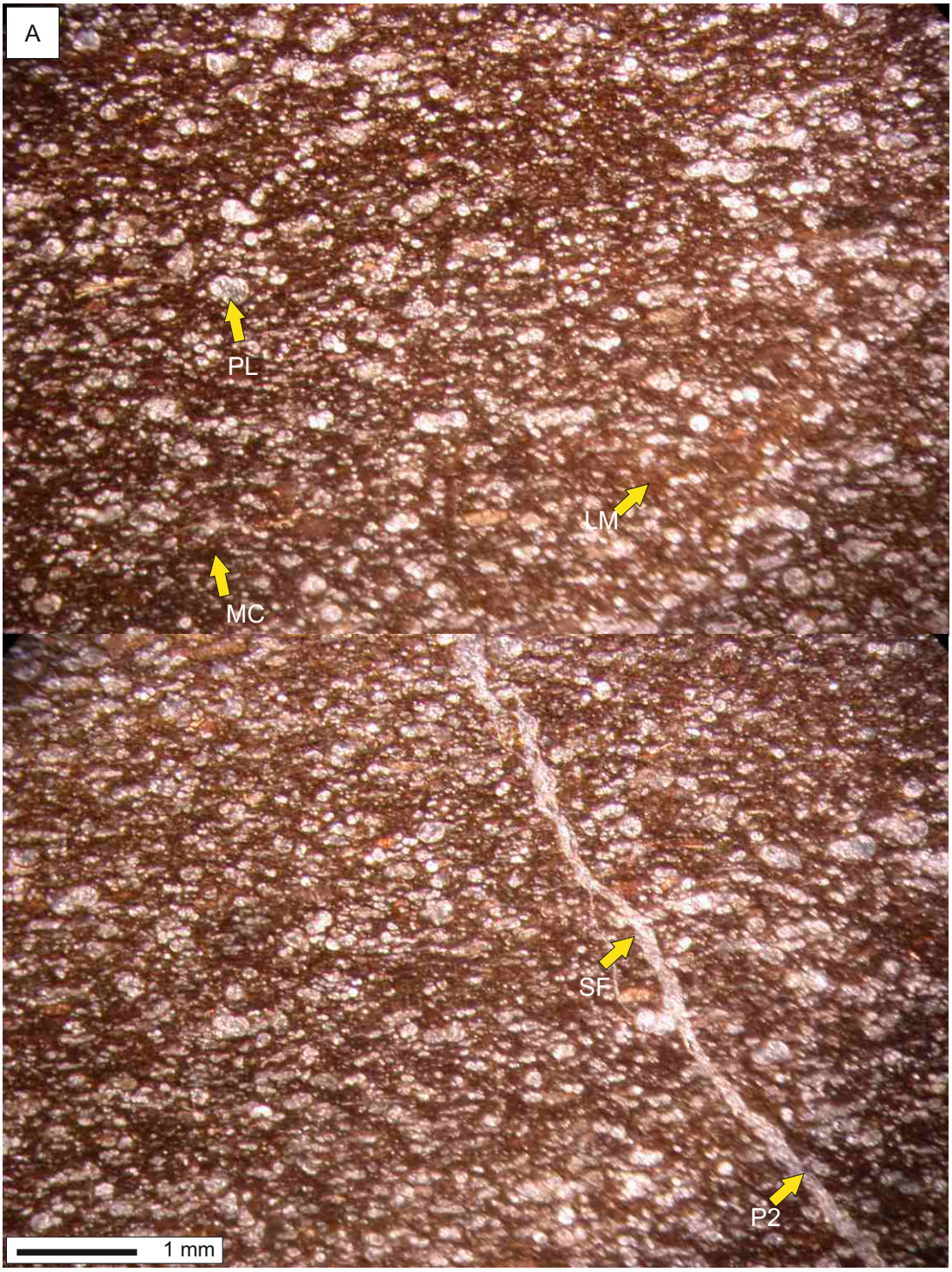


**Figure 7.15. Planktonic foraminiferal wackestone-packstone microfacies (NMF 5):** the allochems of the NMF 5 microfacies include planktonic foraminifera (PL) which are scattered in a micritic matrix. The diagenetic fabric is characterized by internal micritization shown by planktonic foraminiferal tests (PL in **A**), spar filled post depositional fractures showing aggrading neomorphism (SF in **A**) and limonite (LM in **A**) is scattered in the matrix. Intragranular (PL) and fracture porosities (P2 in **A**) are common.

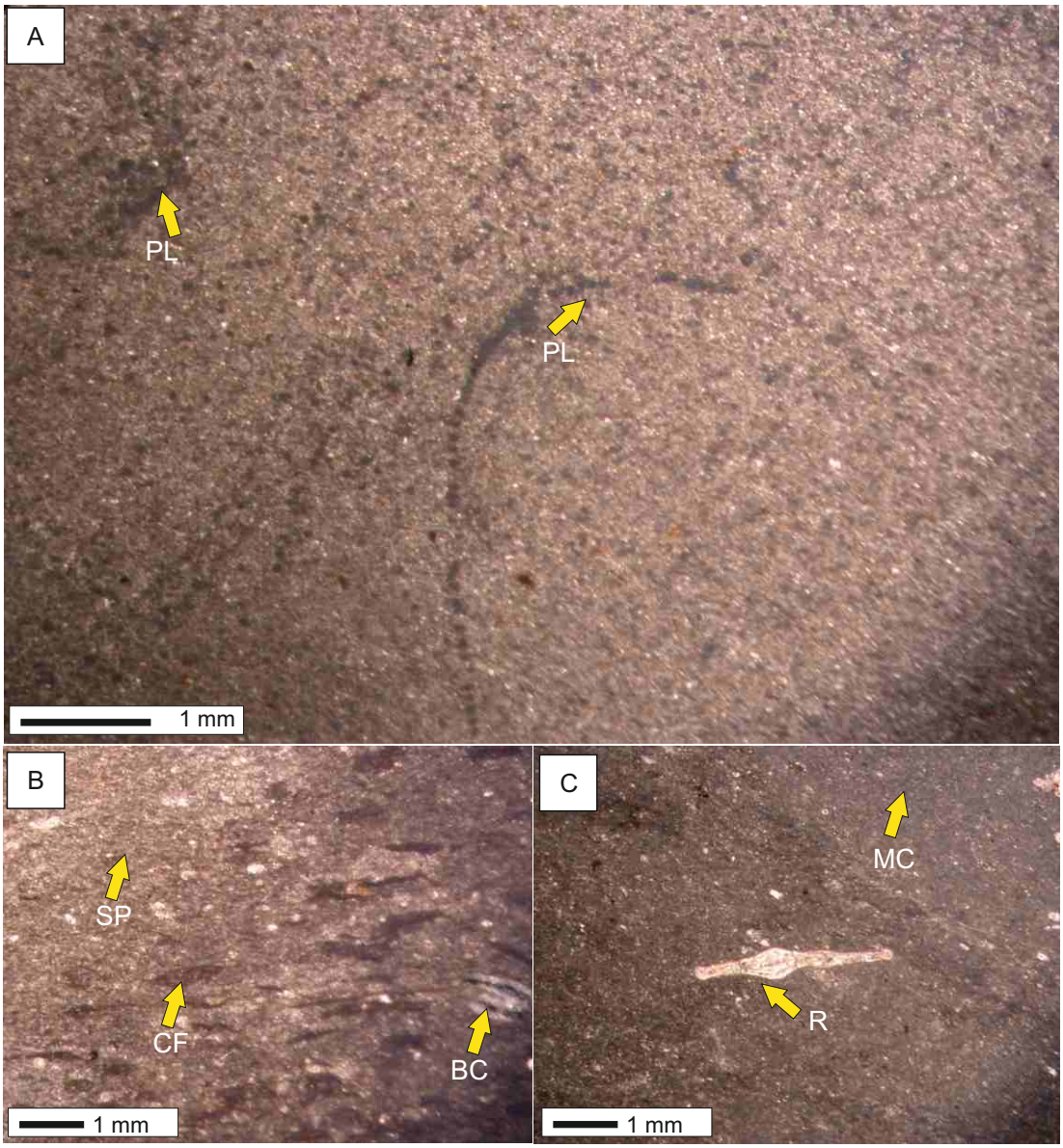


**Figure 7.16. Peloidal lime mudstone microfacies (NMF 6):** note abundance of the peloids forming nests (PL in **A**) and amalgamated clotted fabric (CF in **B**). Benthic foraminiferal bioclasts are i.e. *Ranikothalia* (R in **C**) and abraded *Nummulites* bioclasts (BC in **B**) scattered in the micritic matrix (MC in **C**). The diagenetic fabric is characterized by transformation of micrite into spar (SP in **B**).

Peloids are very common ranging in abundance from 20 to 40 % with an average of 25 %, and are found in small patches as well as scattered in the matrix (figure 7.16 A). Peloids are rounded as well as showing amalgamated clotted fabric formed by recrystallization of limemud to microspar (figure 7.16 B). Intergranular and fracture porosities are common.

**Depositional environment:** rare presence of macrofossils and abundance of peloids suggest that the NMF 6 microfacies was deposited in a restricted environment such as a pond or bay in the inner ramp setting. Occasional presence of the planktonic foraminifera may suggest a maintained inlet to the restricted ponds from the main ocean.

## 7.5 Facies of the Sakessar Formation

The microfacies of the Sakessar Formation are abbreviated as SKF 1-SKF 3 (SK stands for the Sakessar Formation, F stands for the microfacies in the Potwar Basin and the TIR and 1-3 are various types of recorded microfacies) and are described below

### *7.5.1 Algal-peloidal lime mudstone to wackestone microfacies (SKF 1)*

In the Chichali Nala and the Nammal Gorge sections the SKF 1 microfacies is represented by the massive grey coloured nodular limestone of the Sakessar Formation. In thin section, the SKF 1 microfacies is characterized by a lime mudstone-wackestone depositional textures. The biogenic content is poorly preserved and grains are mostly micritized. Phylloid algal bioclasts are the dominant allochems (figure 7.17 A) while few brachiopods (figure 7.17 A) and gastropods (figure 7.17 B) are also seen. The bioclasts abundance ranges from 30-60 %, with an average of 45 %. The micritic matrix ranges from 30 to 60 % with an average of 45 %. The subordinate spar presence is related to the breakdown of the algal biodebris (figure 7.17 A and C). Abundant peloids are found in the sparry matrix. Mud peloids are very common, having rounded shape and less than 0.2 mm size (figure 7.17 C). Some peloids with larger grain size characterize a clotted microfabric (figure 7.17 B). Grains have poor to moderate sorting.

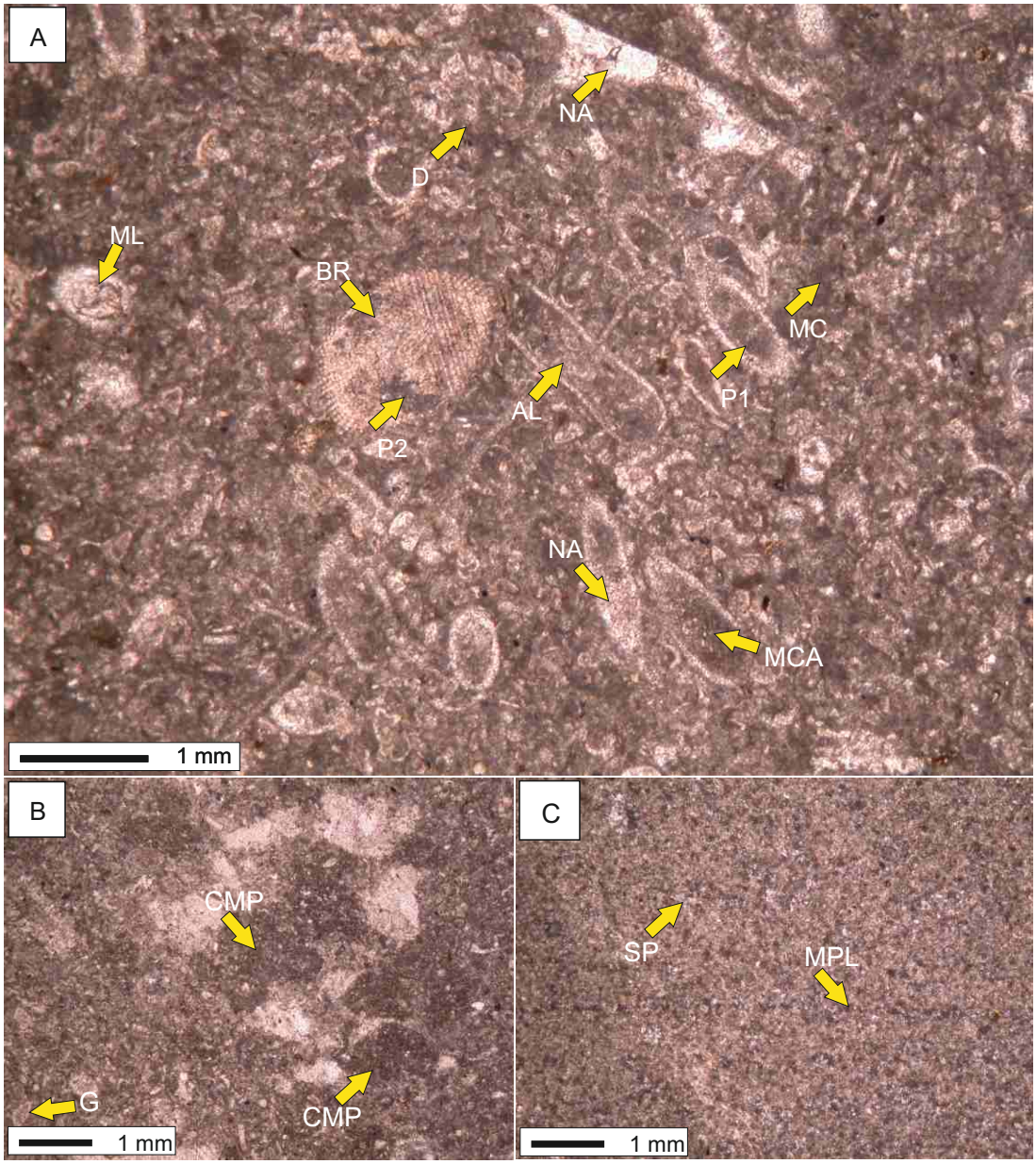


**Figure 7.17. Algal–peloidal lime mudstone-wackestone microfacies (SKF 1):** the allochems of the SKF 1 microfacies include phylloid algae (AL in **A**), milliolid foraminifera (ML in **A**), brachiopods (BR in **A**) and small gastropods (G in **B**) scattered in a micritic matrix (MC in **A**). The diagenetic fabric is characterized by internal micritization shown by algal bioclasts forming ghost structures (MCA in **A**), aggrading neomorphism (NA in **A**). Note the clotted peloidal fabric (CMP in **B**) and various mud peloids (MPL in **C**) in a micritic matrix and minor microspar (SP in **C**). Various porosity types such as moldic (P 1 in **A**) and intragranular (P 2 in **A**) are identified.

The diagenetic fabric is characterized by micritization and neomorphic alteration of the bioclasts (figure 7.17 A). The porosity types identified are moldic, intragranular and intergranular.

**Depositional environment:** Phyloid algae live around barrier mounds in back reef settings where constant baffling of waves by algae contributes to the formation of the spary matrix (Flügel, 2004). The peloids with a clotted microfabric are formed by transformation of micrite into spar and the break down of the algal debris. The flora and fauna show that the SKF 1 microfacies was deposited in the semi-restricted proximal inner ramp setting.

### *7.5.2 Algal–gastropod rich bioclastic wackestone-packstone microfacies (SKF 2)*

In the Chichali Nala and Nammal Gorge Section the SKF 2 microfacies is represented by massive grey coloured nodular limestone. In thin section, the SKF 2 microfacies is characterized by a wackestone-packstone depositional texture. The biogenic content is moderately preserved. The allochems are dominated by dasycladacean algae and small micritized boring gastropods while subordinate milliolid forams and brachiopods are also found (figure 7.18 A-C). The algae abundance ranges from 30-50%, with an average of 45 % while gastropod abundance ranges from 5-10%, with an average of 4 %. The micritic matrix ranges in abundance from 40 – 60 %, with an average of 45 %. The allomicritic matrix is associated with the break down of bioclasts.

Some large ghost bivalve structures are seen with well preserved outlines of the shell and showing neomorphic alteration (figure 7.18 B). Boring and burrowing is a common feature within the SKF 2 microfacies (figure 7.18 A). Most of the grains have poor to moderate sorting (figure 7.18 C). The porosity types identified are moldic, intragranular and intergranular (figure 7.18 A).

**Depositional environment:** a low floral and faunal diversity, presence of brachiopods, small gastropods and milliolid foraminifera suggest that the SKF 2 microfacies was deposited in semi-restricted conditions of the inner ramp setting.

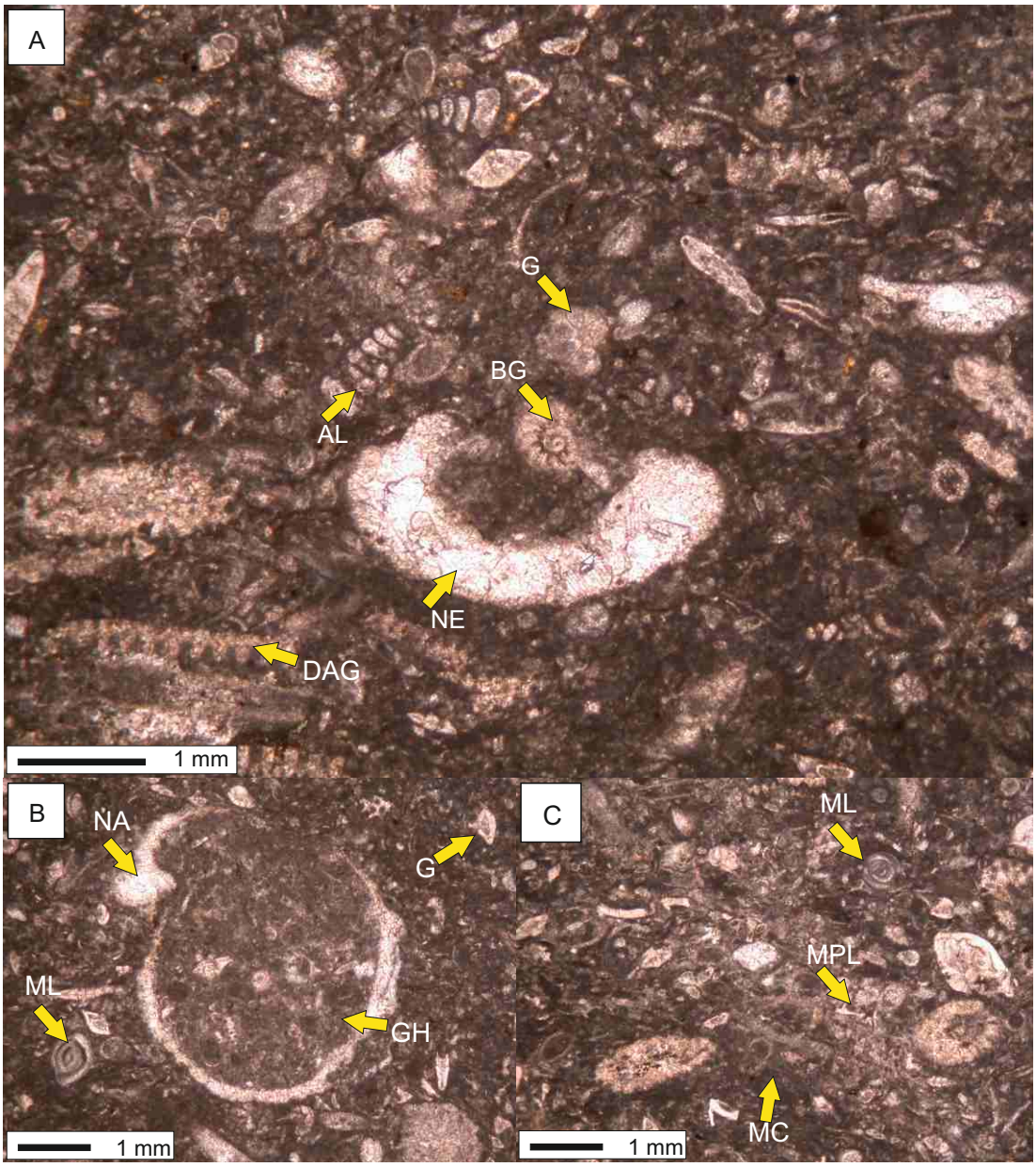


**Figure 7.18. Algal–gastropod rich bioclastic wackestone - packstone microfacies (SKF 2):** the allochems of the SKF 1 microfacies include algae (AL and DAG in **A**), boring gastropods (BG in **A**), milliolid foraminifera (ML in **B** and **C**) and brachiopods (GH in **B**) which are scattered in a micritic matrix (MC in **C**). The diagenetic fabric is characterized by internal micritization shown by the brachiopod bioclasts forming ghost structures (GH in **B**). Aggrading neomorphic alteration (NA in **B**) is also common. Sorting of the bioclasts is poor (**A** and **C**). Various porosity types such as moldic (P 1 in **A**) and intragranular (P 2 in **A**) are identified.

### *7.5.3 Foraminiferal bioclastic wackestone-packstone microfacies (SKF 3)*

In the Chichali Nala and the Nammal Gorge Sections the SKF 3 microfacies is represented by massive grey-coloured nodular limestone. In thin section, the SKF 3 microfacies is characterized by a wackestone-packstone depositional texture. The biogenic content is well preserved. The allochems are dominated by the larger benthic foraminifera i.e. *Alveolina globula*, *Nummulites globulus* and subordinate algae (figure 7.19 A-C). The abundance of foraminifera ranges from 40-50%, with an average of 45 %, while algae abundance ranges from 5-10%, with an average of 3 %. The sparry matrix ranges from 40–60 %, with an average of 45 % and is associated with the bioturbation and break down of the bioclasts while minor proportion of micrite is associated with the micritization of the bioclasts. Most of the grains have poor to moderate sorting.

The diagenetic fabric is characterized by neomorphic alteration; partial micritization and stylobrecciated fabric (figure 7.19 A-C). The porosity types identified are moldic, intragranular and intergranular.

**Depositional environment:** high faunal diversity, sparry matrix and absence of shallow water fauna indicate that the SKF 3 microfacies was deposited above the fair weather wave base , in normal salinity water conditions in the middle ramp setting.

## 7.6 Microfacies of the Chorgali Formation

The microfacies of the Chorgali Formation are abbreviated as CGF 1-CGF 5 (Here CG stands for the Chorgali Formation, F stands for the microfacies in the Potwar Basin and the TIR while 1-5 are various types of recorded microfacies) and are described below.

### *7.6.1 Diverse foraminiferal wackestone-packstone microfacies (CGF 1)*

In the Gharibwal Cement Factory and the Sikki Village sections, the CGF 1 microfacies is represented by cream coloured thick bedded to massive nodular limestone. In thin section, the CGF 1 microfacies is characterized by a wackestone-

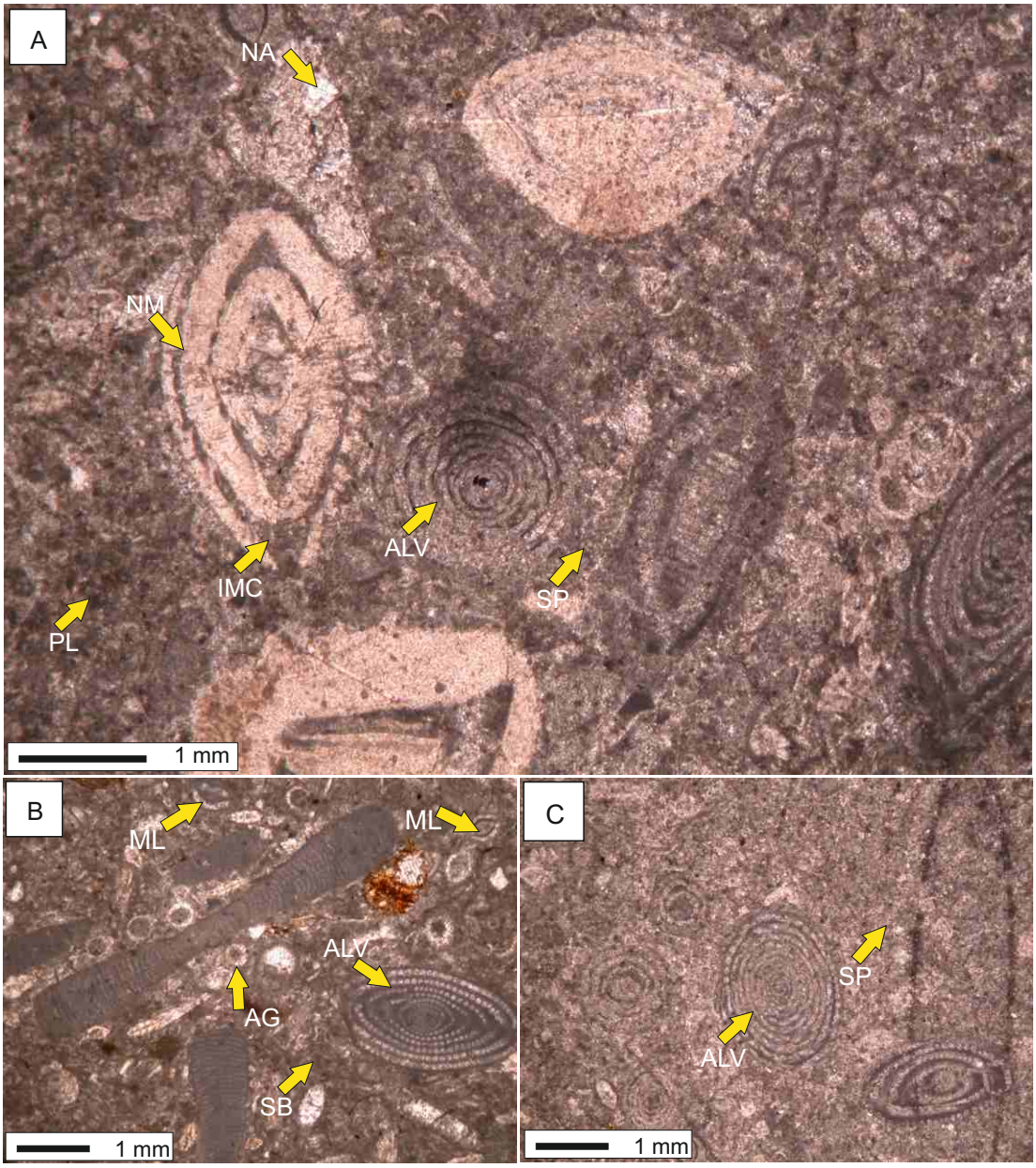


**Figure 7.19. Foraminiferal bioclastic wackestone-packstone microfacies (SKF 3):** the allochems of the SKF 3 microfacies include larger benthic foraminifera i.e. *Nummulites globulus* (NM in **A**), *Alveolina* (ALV in **A**, **B** and **C**, milliolid forams (ML in **B**), algal thali segments (**AG** in B) and peloids (PL in **A**) which are scattered in a spary matrix (SP in **A**). The diagenetic fabric is characterized by partial internal micritization as shown by *Nummulites globulus* (IMC in **A**), transformation of micrite into microspar (SP in **C**), aggrading neomorphic alteration (NA in **A**) and stylobrecciated fabric (SB in **B**) is common.

packstone depositional textures. The biogenic content is well preserved and allochems abundance ranges from 30-60%, with an average of 45 %.

The dominant allochems are larger benthic foraminifera i.e. *Nummulites atacicuc, Nummulites globulus, Nummulites mammilatus, Assilina granulosa, Assilina leymerie, Assilina pustulosa, Alveolina globula, Alveolina rotundata, Lockhartia pustulosa* and *Discocyclina fortisie* (figure 7.20 A-C). These foraminiferal bioclasts have a size range from 2mm to 5mm. Some small gastropods are internally micritized, scattered in micritic matrix and are having less than 2mm size. Overall the micritic matrix dominates and ranges in abundance from 40 to 70 %, with an average of 40 %. 5-10 % dolomite crystals are also found. 1-2 % pyrite is seen filling the stylolitic seams and internal chambers of the foraminiferal tests (figure 7.20 A-B).

The diagenetic fabric is characterized by the stylonodular fabric having anastomizing, irregular and columnar stylolite varieties. Internal micritization, post depositional spar filled fractures showing aggrading neomorphism and pyrite replacement of the bioclasts indicate prominent diagenetic imprints (figure 7.20 A-C). The porosity types identified are fracture, vuggy, stylolitic, intergranular and intragranular.

**Depositional environment:** the presence of diverse larger benthic foraminifera (*Nummulites, Assilina, Alveolina* and *Discocyclina*) and the micritic matrix show deposition of the CGF 1 microfacies in low energy, below fair weather wave base in the distal middle ramp setting.

### 7.6.2 Algal-foraminiferal wackestone-packstone microfacies (CGF 2)

In the Gharibwal Cement Factory and the Sikki Village sections the CGF 2 microfacies is represented by cream coloured thick bedded nodular limestone. In thin section, the CGF 2 microfacies is characterized by a wackestone-packstone depositional texture. The biogenic content is moderately preserved and bioclasts abundance ranges from 40-70%, with an average of 50 %. The dominant allochems are green algae and larger benthic foraminifera i.e. *Alveolina globula, Rotalia trochidoformis,* milliolids*, Lockhartia pustulosa, Nummulites mamilla* and *Assilina*

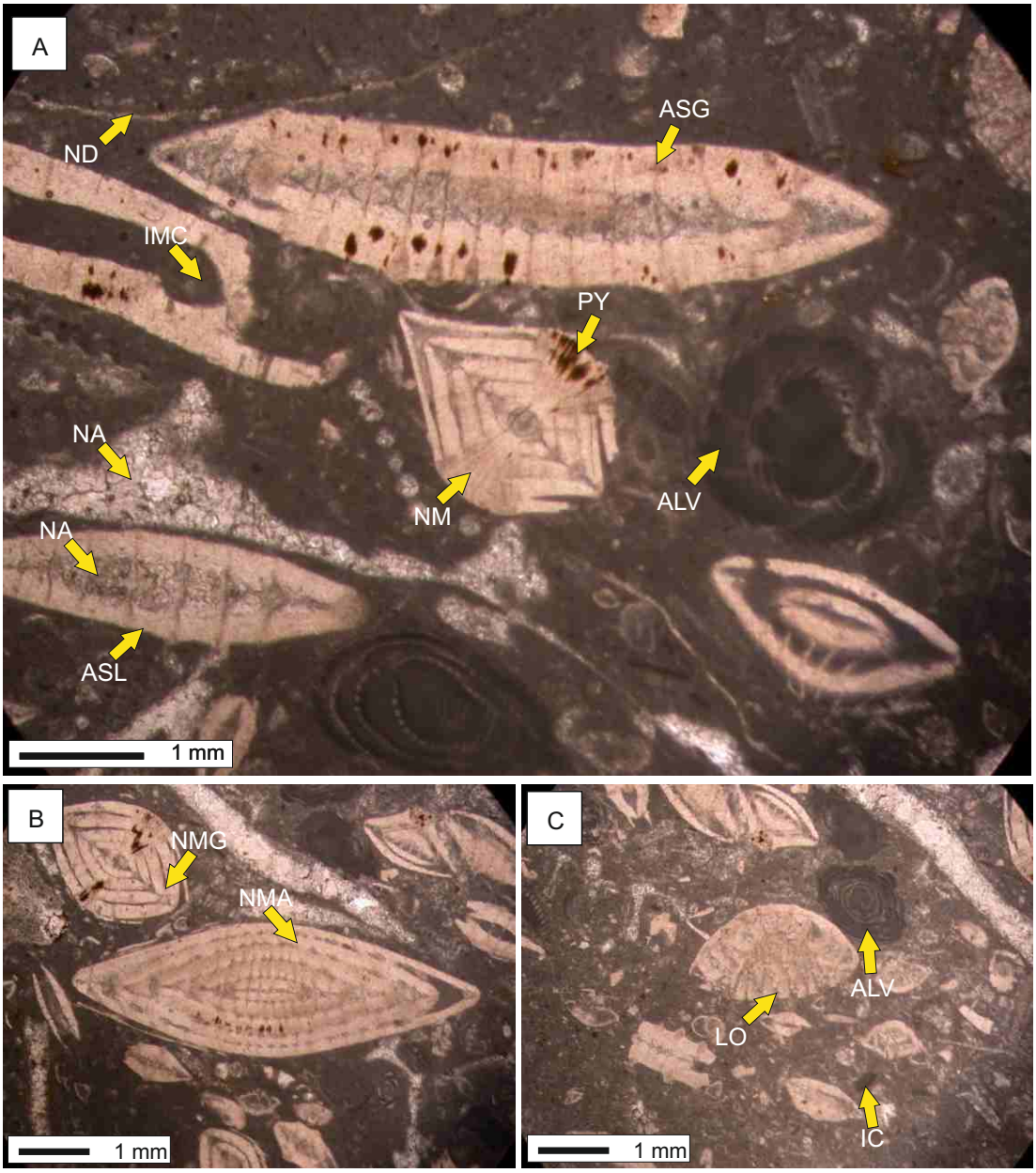


**Figure 7.20. Diverse foraminiferal wackestone-packstone micofacies (CGF 1):** the allochems of the CGF 1 microfacies include larger benthic foraminifera i.e. *Nummulites mammila* (NM in **A**), *Nummulites globulus* (NMG in **B**), *Nummulites atacicus* (NMA in **B**), *Assilina granulosa* (ASG in **A**), *Assilina leymerie* (ASL in **A**), *Alveolina* (ALV in **A** and **C**) and *Lockhartia* (LO in **C**). The diagenetic fabric is characterized by partial internal micritization (IMC in **A**), spar filled fractures showing aggrading neomorphic alteration (NA in **A**) and pyrite replacement of bioclasts (PY in **A**). Note the presence of nodules (ND in **A**).

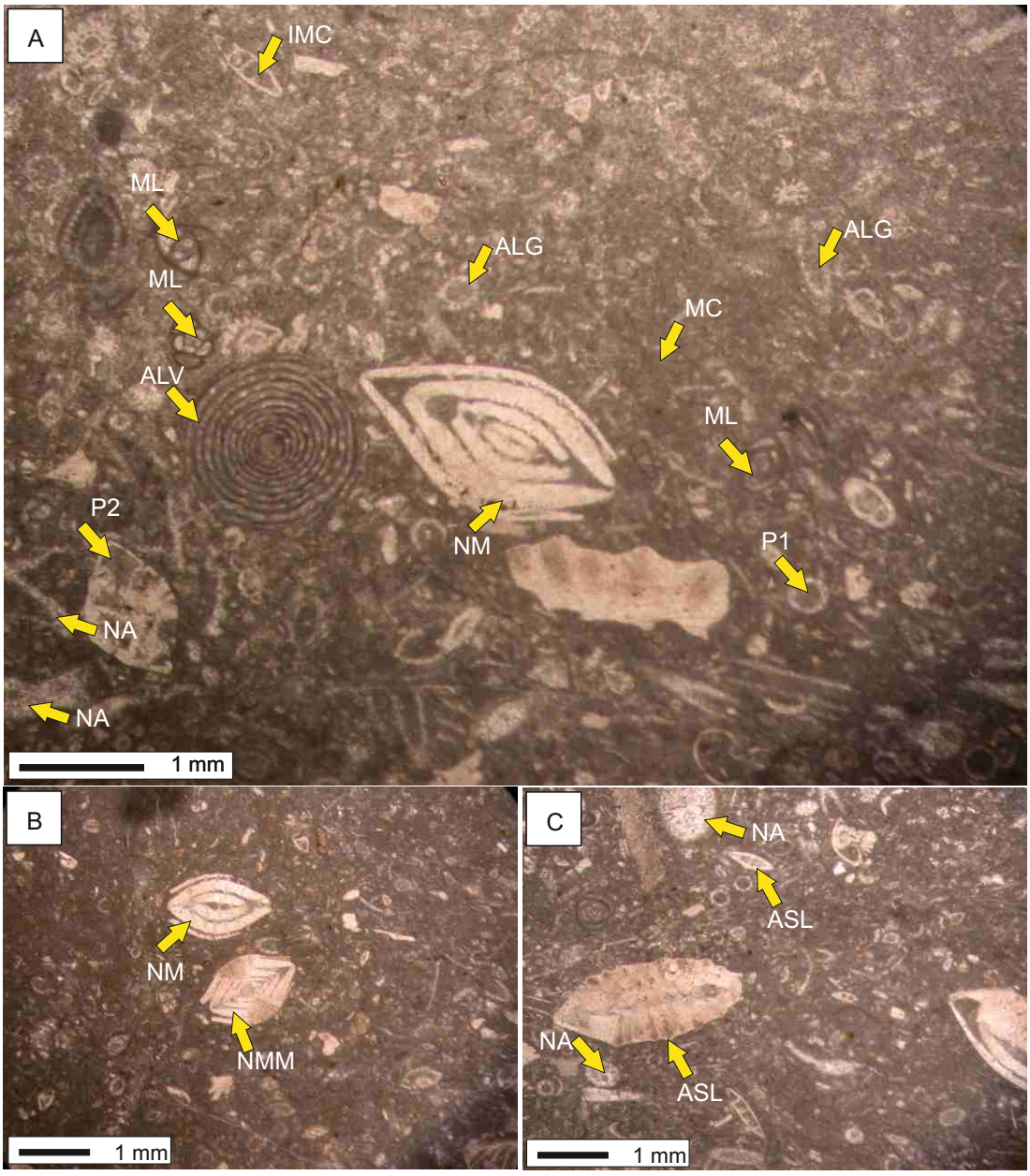


**Figure 7.21. Algal-foraminiferal wackestone-packstone microfacies (CGF 2):** the allochems of the CGF 2 microfacies include algal thali segments (ALG in **A**), larger benthic foraminifera i.e. *Nummulites mamilla* (NMM in **B**), *Nummulites globulus* (NMG in **B**), *Nummulites atacicus* (NM in **A**), *Assilina laminosa* (ASL in **C**), *Alveolina* (ALV in **A** and **C**) and *milliolids* (ML in **A**) scattered in micritic matrix (MC in **A**). The diagenetic fabric is characterized by partial internal micritization of the bioclasts i.e. *Assilina leymerie* (IMC in **A** and ASL in **C**), spar filled fractures and bioclasts showing aggrading neomorphic alteration (NA in **A** and **C**). Moldic and intragranular porosities are common (P1 and P2 in **A**).

*Assilina spinosa* (figure 7.21 A-C). Algal thalli segments and ostracodes are also seen. The matrix is dominated by micrite associated with the biodebris of the foraminiferal and algal bioclasts and ranging in abundance from 20-40 %, with an average of 25 %. Algal peloids are common and their abundance ranges from 5-10 %. Sorting of the bioclasts is poor and no preferred grain orientation is seen. The diagenetic fabric is characterized by the stylonodular fabric, internal micritization, neomorphic alteration and spar filled post depositional fractures (7.21 A-C). The identified porosity types are fracture, moldic, stylolitic, intergranular and intragranular.

**Depositional environment:** the CGF 2 microfacies is characterized by moderate diversity of faunal and floral constituents with dominant benthic foraminifera and dasycladacean algae. Dasycladacean algae are reported to occur in warm water, not more than few metres deep and are more common between depths of 12-15 metres with restricted circulation (Heckel, 1972; Wilson 1975; Flügel 2004). The association of small gastropods and ostracodes, milliolid forams and minor dolomite indicates increasing salinity and a shallowing upward depositional trend. The micritic matrix suggests low energy conditions. Based on the paleoecology of the flora and fauna and micritic matrix the CGF 2 microfacies is interpreted as deposited in the low energy shallow proximal inner-ramp setting.

### *7.6.3 Dolomitized fenestral lime mudstone microfacies (CGF 3)*

In the Gharibwal Cement Factory and the Sikki Village sections, the CGF 3 microfacies is represented by cream coloured thick bedded to massive nodular dolomitic limestone. In thin section, the CGF 3 microfacies is characterized by a dolomitized mudstone depositional texture. The biogenic content is poorly preserved and bioclasts abundance ranges from 5-8 %, with an average of 4 %. The dominant allochems are larger benthic foraminifera including *Nummulites* (figure 7.22 B). The dolomite is fabric retentive, medium grained and crystalline. Crystals are euhedral to subhedral (figure 7.22 A). Peloids are also seen, their abundance ranges from 5-10%, with an average of 2%. Spar abundance ranges from 10-20%, with an average of 12 %. Chert is also found and its abundance ranges from 1-3 %. Laminoid and irregular fenestral fabrics are found (figure 7.22 A and C) and are forming an interconnecting

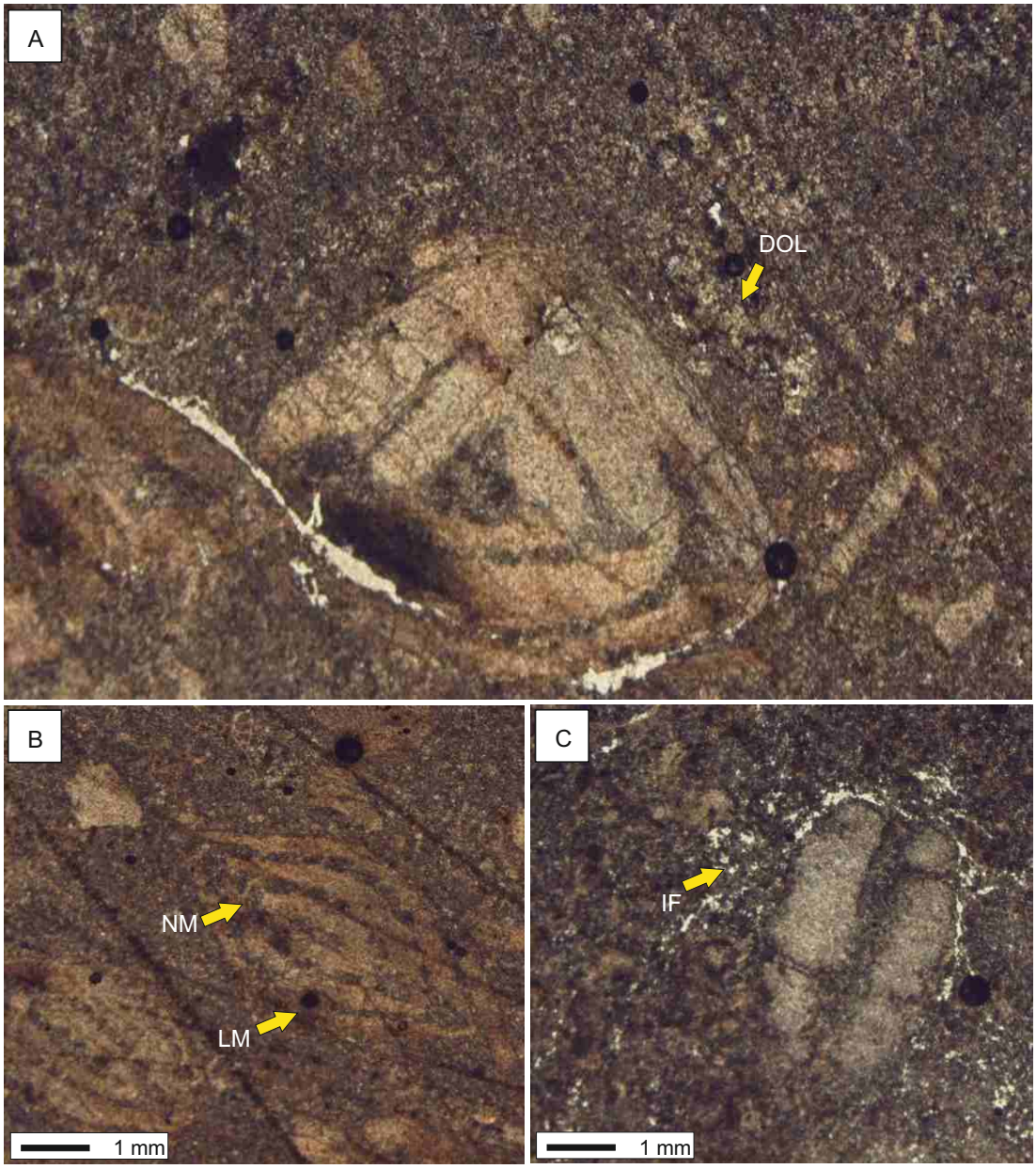


**Figure 7.22. Dolomitize fenestral lime mudstone microfacies (CGF 3):** the allochems of the CGF 3 microfacies include rare larger benthic foraminifera i.e. *Nummulites mammila* (NM in **B**). Note the dolomite crystals (DOL in **A**), limonite replacement of the bioclasts (LM in **B**) and fenestral fabric shown irregular fenestrae (IF in **C**) forming an interconnecting network.

network. The diagenetic fabric is characterized by dolomitization and pyritization. The porosity types identified are fracture, vuggy, stylolitic, intergranular and intragranular.

**Depositional environment:** the dominance of dolomitized micrite and rare fauna suggest hypersaline conditions. The presence of fine to very fine crystalline dolomites (fabric retentive) is exclusively confined to supratidal to intertidal setting. Their texture (small crystal size and planar intercrystal boundaries) are typical of dolomite formed in near surface low temperature conditions (Sibley and Gregs, 1987). The CGF 3 microfacies is interpreted as deposited in a hypersaline intertidal pond of the proximal inner ramp setting.

### *7.6.4 Algal stromatolite lime mudstone microfacies (CGF 4)*

In the Gharibwal Cement Factory Section the CGF 4 microfacies is represented by cream coloured thick bedded to massive nodular limestone. In thin section, the CGF 4 microfacies is characterized by a mudstone depositional texture. The biogenic content is poorly preserved and rare foraminiferal bioclasts and algae are present and their abundance ranges from 0-8 %, with an average of 3 % (figure 7.23). The sparry matrix dominates while algal peloids (0-5 %) contributed towards the subordinate micrite in the CGF1 microfacies (figure 7.23). Dolomite is also found having an abundance of 5-15 %, with an average of 8 %. Detrital quartz is sparsely distributed in the spary matrix.

The diagenetic fabric is characterized by stylobrecciated fabric and low amplitude stylolitic seams (figure 7.23). The porosity types identified are fracture, intergranular and intragranular.

**Depositional environment:** Presence of the low diversity fauna, sparry matrix and algal mats indicate that the CGF 4 microfacies was deposited in the restricted proximal inner ramp setting.

### *7.6.5 Assilina-Discocyclina rich bioclastic wackestone-packstone microfacies (CGF 5)*

In the Sikki Village Section, the CGF 5 microfacies is represented by the grey coloured thin to medium bedded nodular limestone. In thin section, the CGF 5 microfacies is characterized by a wackestone-packstone depositional texture.

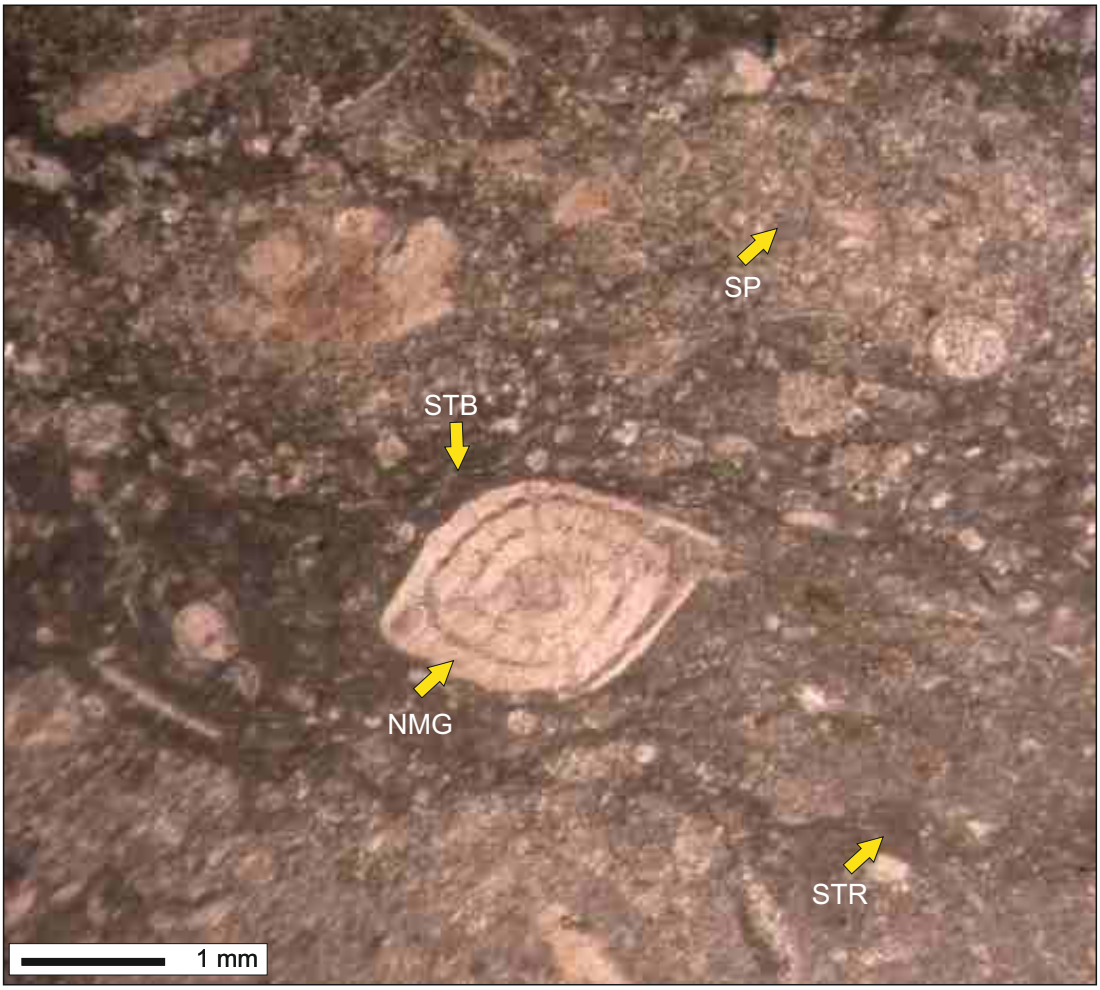


**Figure 7.23. Algal stromatolite lime mudstone microfacies (CGF 4):** the allochems of the CGF 3 microfacies include larger benthic foraminifera i.e. *Nummulites globulus* (NMG in **A**). Note the algal stromatolites (STR), stylo- brecciated fabric (STB) and coarse spary bioclastic matrix (SP).

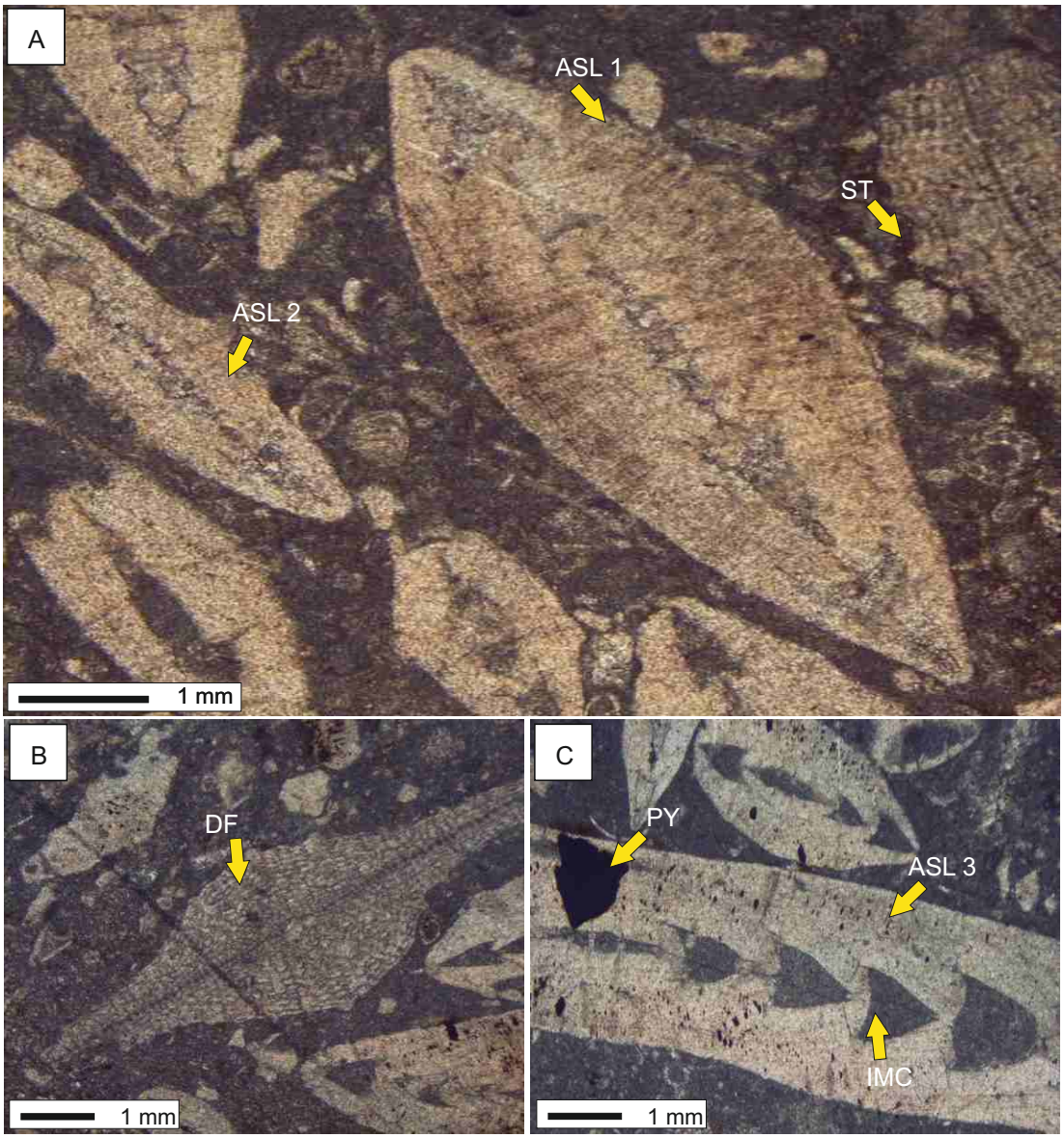


**Figure 7.24. *Assilina-Discocyclina* rich bioclastic wackestone-packstone microfacies (CGF 5)**: the allochems of the CGF 5 microfacies include larger benthic foraminifera i.e. *Assilina laminosa* (ASL 1 in **A**), *Assilina leymerie* (ASL 2 in **A**), *Assilina laxispira* (ASL 3 in **C**) and *Discocyclina fortisie* (DF in **B**) Note the internal micritization and pyrite replacement of the *Assilina granulosa* chambers (IMC and PY in **C**). Low amplitude stylolites (ST in **A**) found around the *Discocyclina* bioclasts.

biogenic content is well preserved having dominance of foraminiferal bioclasts with abundance ranges from 30-70%, with an average of 45 %. The foraminiferal assemblage is dominated by *Assilina laminosa, Assilina pustulosa, Assilina granulosa, Assilina laxispira, Assilina spinosa, Nummulites globulus, Nummulites mamillatus, Alveolina rotundata, Alveolina globula, Operculina salsa* and *Discocyclina fortisie* (figure 7.24). Most of the foraminiferal bioclasts have a size range between 2mm to 5mm. The micritic matrix dominates and its abundance ranges from 40 to 70 %, with an average of 55 %. Some spar is related to the foraminiferal biodebris. The diagenetic fabric is characterized by pyrite replacement, stylolitic fabric, neomorphic alteration and internal micritization of the bioclasts (figure 7.24 A-C). The porosity types identified are fracture, vuggy, stylolitic, intergranular intragranular and moldic.

**Depositional environment:** *Assilina* represents the mid-outer ramp setting slightly deeper than that of *Nummulites* and shallower than *Discocyclina*. The presence of the high diversity *Assilinia* fauna and association with *Discocyclina* indicates that the CGF 5 microfacies was deposited in the distal middle ramp setting in low energy conditions below FWWB.

## 7.7 Facies Model

Architecture of the Paleogene facies of the Potwar Basin and the TIR indicates that deposition took place along a distally steepened carbonate ramp. The absence of continuous reefal build ups, scarcity of reef forming organisms and presence of slope facies supports this model. A distally steepened carbonate ramp has a slope break between the outer ramp and the basin and can be recognized by slumping and slope apron deposits (Burchette and Wright, 1992; Flugel, 2004). Facies of the Lockhart, Patala, Nammal, Sakessar and Chorgali Formations were deposited in such a distally steepened ramp setting (figure 7.25-7.26).

The proximal inner ramp settings were dominated by algal meadows, milliolid foraminifera and small gastropods, resulting in algal-foraminiferal mixed bioclastic wackestones and packstones. Peloids and fenestrae fabric in facies indicate the presence of nearby intertidal ponds.

## List of Microfacies

**Microfacies of the Lockhar Formation:**

LKF 1: Algal foraminiferal wackestone - packstone microfacies

LFK 2: *Alveolina* rich bioclastic wackestone - packstone microfacies

LFK 3: Diverse benthic foraminiferal wackestone - packstone microfacies:

LKF 4: Planktonic - benthic mixed foraminiferal lime mudstone - wackestone microfacies:

**Microfacies of the Patala Formation:**

PTF 1: Algal-miliolid rich bioclastic wackestone - packstone microfacies

PTF 2: Fenestral bioclastic mudstone - wackestone microfacies

PTF 3: Foraminiferal grainstone microfacies

PTF 4: Peloidal mudstone microfacies

PTF 5: Diverse foraminiferal wackestone - packstone microfacies

PFT 6: Coralline red algal - stromatolite mudstone - wackestone microfacies

**Microfacies of the Nammal Formation**

NMF 1: Nummulitic - Discocyclinid rich packstone-grainstone microfacies

NMF2: Foraminiferal bioclastic wackestone microfacies

NMF 3: Planktonic – Discocyclina rich foraminiferal wackestone – packstone microfacies

NMF4: Pelagic mudstone - wackestone microfacies

NMF 5: Planktonic foraminiferal wackestone - packstone microfacies

NMF 6: Peloidal lime mudstone Microfacies

**Microfacies of the Sakessar Formation**

SKF 1: Algal – peloidal lime mudstone - wackestone micofacies

SKF 2: Algal – gastropod rich bioclastic wackestone - packstone microfacies

SKF 3: Foraminiferal bioclastic wackestone- packstone microfacies

**Microfacies of the Chorgali Formation**

CGF1: Diverse foraminiferal wackestone - packstone micofacies

CGF 2: Algal-foraminiferal wackestone - packstone microfacies

CGF3: Dolomitized fenestral lime mudstone microfacies

CGF 4: Algal stromatolite lime mudstone microfacies

CGF5: *Assilina - Discocyclina* rich bioclastic wackestone - packstone microfacies

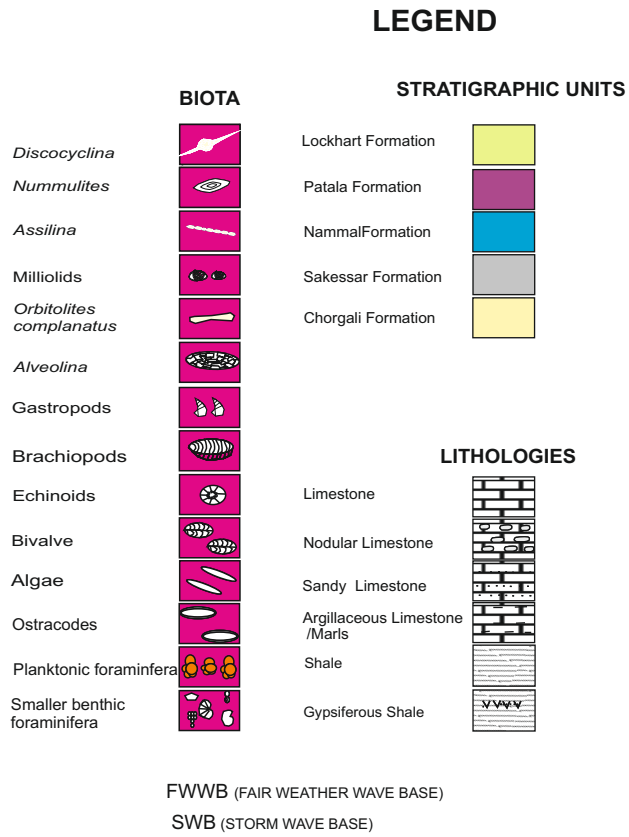


**Figure 7.25** Key to Paleogene facies types, symbols for biota, stratigraphic units, various lithologies shown in the figure 7.26.

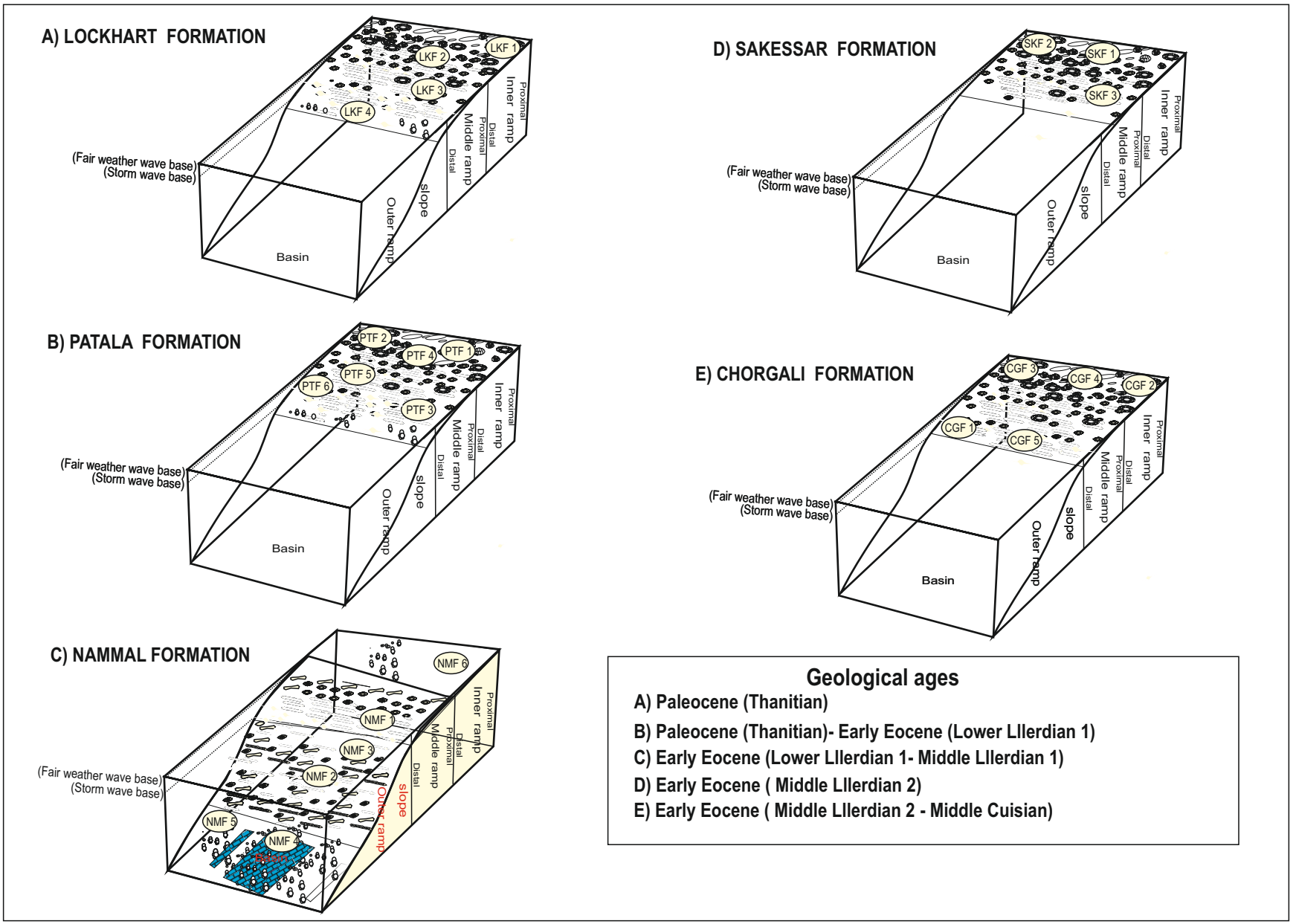


**Figure 7.26.** Facies depositional model of a distally steepened carbonate ramp representing chronological distribution of the Paleogene facies in the Potwar Basin and the TIR, northwest Pakistan (for symbols and abbreviations used here see figure 7.25).

The conditions were hypersaline in these ponds but favourable for the milliolid populations. Bioclastic wackestone-packstones facies change downdip to *Alveolina* rich algal-foraminiferal wackestone-packstones in the distal inner ramp settings. The proximal middle ramp was essentially covered by diverse assemblages of larger benthic foraminifera (*Nummulites*, *Alveolina* and *Assilina*) and invertebrate macrofauna (brachiopods, echinoids, gastropods and echinoids). These faunal clasts form wackestone-packstone depositional texture. Further downdip towards the basin diversity of the foraminifera is further increased in the distal middle ramp setting, where *Discocyclina*, *Operculina* and *Ranikothalia* species dominate the packstone-grainstone facies. Oligotrophic conditions were prevailent on the middle ramp. The coralline red algae also inhibited the distal middle ramp setting and were only found in Eastern Salt Range area of the Potwar Basin. Storm surges on the middle ramp may have contributed terrestrial quartz within the wackestone-packstone facies. The upper slope facies consists of planktonic-benthic mixed foraminiferal wackestones - packstones with evidence of slumping and turbidity movements. Resedimented *Discocyclina* tests are found in the planktonic foraminiferal mustones - wackstones. An ecologically distinct fauna is encountered in the middle slope setting and includes ostracodes, bivalves and those foraminifera having middle ramp affinity. These form graded and reverse graded bedding structures typical of redeposited limestones, e.g. turbidites. Outer ramp to deep basin settings are characterized by planktonic foraminiferal mudstones and wackstones. Pelagic shales with abundant planktonic forams represent deposition in the deeper part of the basin.

## 7.8 Paleoenvironments

Following paleoenviromental interpretation of the Paleogene stratigraphic units of the Potwar Basin and the TIR is based on the detailed microfacies analysis in the key studied sections (figures 7.27-7.32).

### 7.8.1 Paleoenvironments of the Lockhart Formation

In the study area the Lockhart Formation represents deposition in an inner ramp to outer carbonate ramp setting with the following subenvironments.

**Inner ramp:** The algal foraminiferal wackestone-packstone microfacies LFK 1 and *Alveolina* rich bioclastic wackestone-packstone microfacies LKF 2 represent the shallow water, subtidal inner ramp environment of deposition. The LKF 1 microfacies is 23m thick in the Chichali Nala Section, 5m thick in the Nammal Gorge section, 62m thick in the Kalabagh Hills Section, 82m thick in the Ziarat Thatti Sharif Section and 08m thick in the Sikki Village Section. Similarly the LKF 2 microfacies is 13m thick in the Nammal Gorge Section and 48m thick in the Kalabagh Hills Section and was not found in other sections.

**Middle ramp**: The diverse benthic foraminiferal wackestone-packstone microfacies LKF 3 represents deposition in low energy middle ramp, below FWWB, subtidal conditions. The presence of quartz suggests episodic storm surges on the middle ramp. The LKF 3 microfacies is 12m thick in the Chichali Nala Section, 17m thick in Nammal Gorge section, 12m thick in Kalabagh Hills Section, 18m thick in Ziarat Thatti Sharif Section and 2m thick in the Sikki Village Section.

**Outer ramp:** The planktonic-benthic mixed foraminiferal lime mudstone - wackestone microfacies LKF 4 shows the presence of a micritic matrix, mixed planktonic and larger benthic foraminifera and absence of shallow marine flora and fauna. This suggests that the LKF 4 microfacies was deposited in low energy, subtidal carbonate ramp conditions, where occasional storm surges have contributed some quartz within the microfacies. The LKF 4 microfacies is 2m thick and it is only identified in the Sikki Village Section in the Eastern Salt Range.

The composite sea level curve (figure 7.33) and facies fence diagram (figure 7.34) indicate that during the deposition of the Lockhart Formation sea level was high in the beginning which gradually decreased and resulted in shedding (progradation) of the carbonate ramp. An exceptional high sea level has been seen in the Chichali Nala section indicating backstepping (retrogradation) of the carbonate ramp.

### 7.8.2 Paleoenvironments of the Patala Formation

In the study area the Patala Formation represents deposition in inner ramp to deep basinal settings with the following subenvironments.

**Inner ramp**: The algal-milliolid-rich bioclastic wackestone-packstone microfacies (PTF 1) was deposited in the inner ramp, in shallow water restricted lagoonal conditions. The PTF 1 microfacies is 4m thick in the Chichali Nala Section, 3m

thick in the Nammal Gorge section, 2.2m thick in the Sikki Village Section and it is not identified in other sections. The fenestral bioclastic mudstone to wackstone microfacies (PTF 2) is deposited in high energy intertidal to supratidal conditions in the inner ramp environment. The PTF 2 microfacies is 11m thick, and repeated three times in the Chichali Nala Section and it is not found in other sections. The peloidal mudstone microfacies PTF 4 was deposited in the shallow subtidal inner ramp environment. The PTF 4 microfacies is 3m thick and it is only found in the Kalabagh Hills Section.

**Middle ramp:** The benthic foraminiferal grainstone microfacies PTF 3 shows high diversity foraminiferal faunas of middle ramp affinity and this combined with the micritic matrix indicates subtidal FWWB, distal middle ramp conditions of deposition. The PTF 3 microfacies is only found in the Chichali Nala Section, having 3m thickness. The diverse foraminiferal wackestone-packstone microfacies PTF 5 was deposited below FWWB, in normal salinity middle ramp subtidal conditions. The PTF 5 microfacies is 3m thick in the Chichali Nala Section, 6m thick in the Nammal Gorge Section, 34m thick in the Kalabagh Hills Section, 50m thick in the Ziarat Thatti Sharif Section and 6.4m thick in the Sikki Village Section. The coralline red algal–stromatolite mudstone-wackstone microfacies PTF 6 shows deposition in the middle ramp, below FWWB conditions. The PTF 6 microfacies is only found in the Chichali Nala Section, having 1.8m thickness.

**Outer ramp-deep basin:** The pelagic shales with abundant planktonic foraminifera are interbeded with the PTK 5 and PTK 6 microfacies and represents outer ramp to deep basinal conditions.

The composite relative sea level curve (figure 7.33) and facies fence diagram (7.34) show alternate cycles of backstepping (retrogradation) and shedding (progradation) of the carbonate ramp during the deposition of the facies of the Patala Formation. The deepening upward trend is prominant in the lower and middle part while shallowing upward facies trend is found in the upper parts of the Patala Formation.

### 7.8.3 Paleoenvironments of the Nammal Formation

In the study area the Nammal Formation represents deposition in the inner ramp, middle ramp, slope and deep basinal settings with the following subenvironments.

**Inner ramp:** The peloidal lime mudstone microfacies NMF 6 shows rare presence of macro fossils and high abundance of peloids which suggest that the NMF 6 microfacies was deposited in a restricted pond or bay in the inner ramp environment. Occasional presence of the planktonic foraminifera is related to the storm water inlet to the restricted ponds from the main ocean. It is 57m thick in the Chichali Nala Section and 37m thick in the Nammal Gorge Section.

**Middle ramp:** The *Nummulites–Discocyclina* rich packstone microfacies NMF 1 shows deposition in a distal middle ramp setting. It is 4m thick in the Chichali Nala Section and 11m thick in the Nammal Gorge Section.

**Ramp slope:** The foraminiferal bioclastic wackstone–packstone microfacies NMF 2, was deposited as a turbidite in high energy ramp slope settings. It is 28m thick in the Chichali Nala Section and 18m thick in the Nammal Gorge Section. The planktonic–*Discocyclina* rich foraminiferal wackestone NMF 3 shows mixing of shallow and deep water fauna. This combined with the presence of micritic matrix in the NMF 3 microfacies indicate that *Discocyclina* tests were eroded from the mid-outer ramp and redeposited in the ramp slope environment. The NMF 3 microfacies is 10m thick in the Chichali Nala Section and it is not found in the Nammal Gorge Section.

**Outer ramp-open marine basin:** The pelagic mudstone-wackestone microfacies NMF 4 and planktonic foraminiferal wackestone-packstone microfacies NMF 5 show abundance of planktonic foraminifera which suggests deposition in low energy conditions in an open marine pelagic environment. The NMF 4 microfacies is 27m thick in the Chichali Nala Section and 45m thick in the Nammal Gorge Section. The NMF 5 microfacies is restricted to the Chichali Nala Section and having 5m thickness.

The composite sea level curve (figure 7.33) and facies fence diagram (figure 7.34) indicate backstepping (retrogradation) of the carbonate ramp which is followed by the shedding (progradation) of the platform during the deposition of the Nammal Formation. The deepening upward facies trend is seen in the lower and middle part which are separated by shallowing upward facies in the middle-upper part of the Nammal Formation.

### 7.8.4 Paleoenvironments of the Sakessar Formation

In the study area the Sakessar Formation was deposited in inner ramp to middle ramp setting with the following subenvironments.

**Inner ramp:** The algal–peloidal lime mudstone to wackestone microfacies SKF 1 and algal–gastropod-rich bioclastic wackestone-packstone microfacies SKF 2 represent deposition in the inner ramp, in subtidal semi- restricted lagoonal settings. The SKF 1 microfacies is 68m thick in the Chichali Nala Section and 63m thick in the Nammal Gorge Section while the SKF 2 microfacies is 97m thick in the Chichali Nala Section and 50m thick in the Nammal Gorge Section.

**Middle ramp**: The foraminiferal bioclastic wackstone-packstone microfacies SKF 3 has a high faunal diversity. This combined with the absence of shallow water fauna indicates that the SKF 3 microfacies was deposited in normal salinity, mid ramp settings below FWWB. The SKF 3 microfacies is 16m thick in the Chichali Nala Section and 30m thick in the Nammal Gorge Section.

The composite relative sea level curve (figure 7.33) and facies fence diagram (figure 7.34) indicate an overall lowering of the relative sea level, causing shedding (progradation) of the facies. A deepening facies trend in the middle part of the Sakessar Formation indicate that local subsidence induced deepening of the environment.

### 7.8.5 Paleoenvironments of the Chorgali Formation

In the study area the Chorgali Formation shows deposition in inner ramp to outer ramp conditions which are summarised as follows.

**Inner ramp:** The algal-foraminiferal wackestone-packstone microfacies CGF 2 was deposited in the low energy shallow subtidal inner ramp lagoonal environment.

The CGF 2 microfacies is 29m thick in the Gharibwal Cement Factory Section and 28.4m thick in the Sikki Village Section. The dolomitized fenestral lime mudstone microfacies CGF 3 is interpreted as deposited in the hypersaline intertidal ponds. It is 4.3m thick in the Gharibwal Cement Factory Section and 2.8m thick in the Sikki Village Section. The algal stromatolite lime mudstone microfacies CGF 4 shows low diversity fauna, spary matrix and algal mats which indicate that the CGF 4 microfacies was deposited in the inner ramp in restricted sabkha environmental setting. It is only identified in the Sikki Village Section, having 1.8m thickness.

**Middle ramp:** The diverse foraminiferal wackstone-packstone microfacies CGF 1, has diverse larger benthic foraminifera (*Nummulites, Assilina, Alveolina and Discocyclina*). This together with the micritic matrix show that deposition of the CGF 1 microfacies occurred in low energy, below FWWB, in the distal middle ramp settings. It is 7.6m thick in the Gharibwal Cement Factory Section and 6.5m thick in the Sikki Village Section. The *Assilina-Discocyclina* rich bioclastic wackestone-packstone microfacies CGF 5 was deposited in the distal middle ramp setting in low energy conditions. It is only identified in the Sikki Village Section, having 3.5m thickness.

The composite relative sea level curve (figure 7.33) and facies fence diagram (figure 7.34) shows alternate shallowing-deepening upward facies trends in an overall shedding (progradation) of the carbonate ramp.

## MICROFACIES OF THE GHARIBWAL CEMENT FACTORY SECTION

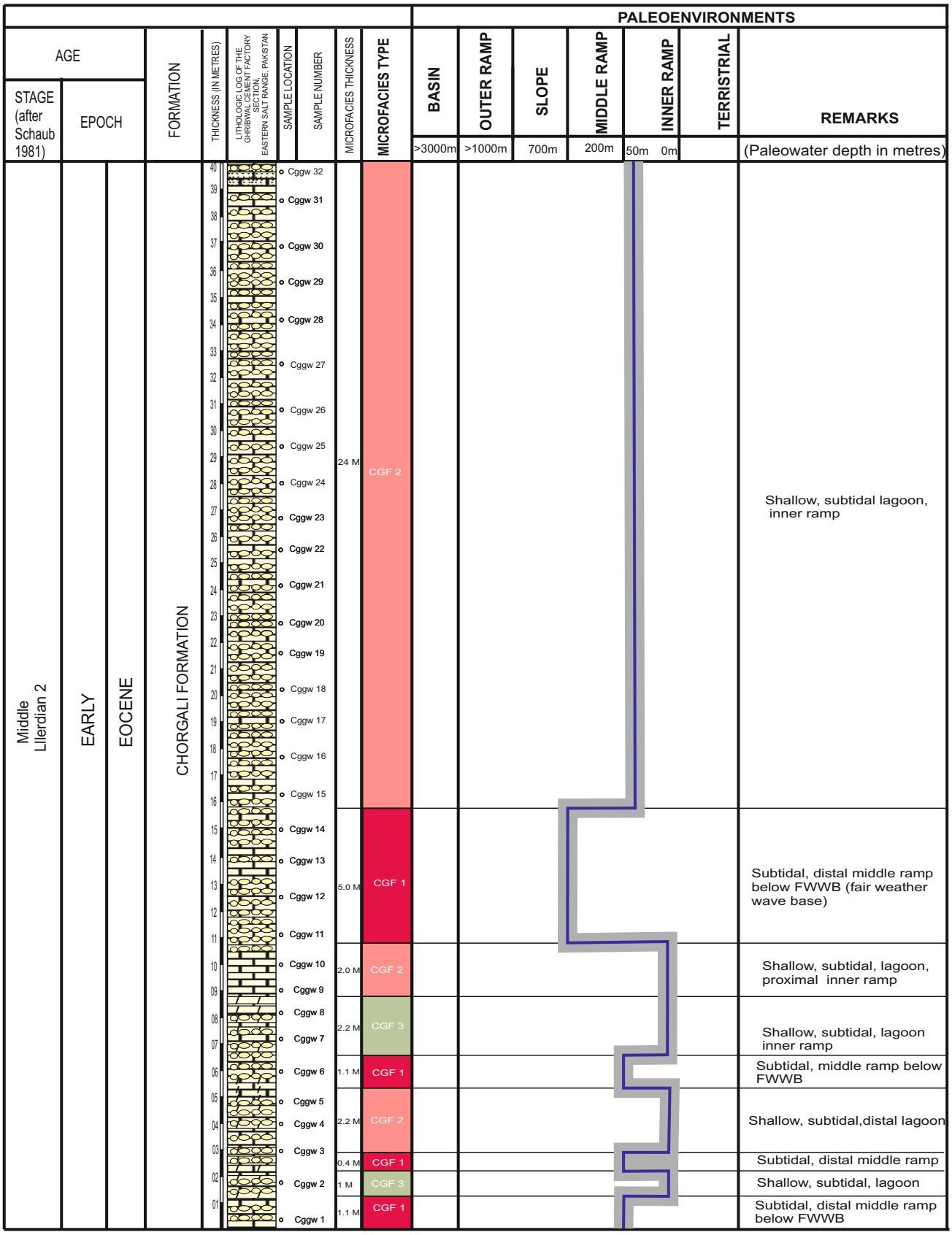


**Figure 7.27.** Composite chart showing facies distribution, paleoenvironments and a mean relative sea level curve infered from the faunal paleoecology (Racey. 1995) and facies criteria (Flugel. 2004) of the Eocene rocks exposed in the Gharibwal Cement Factory Section, Eastern Salt Range, Potwar Basin, northwest Pakistan (the shaded area shows the range of variation in the environment of deposition).

## MICROFACIES OF THE SIKKI VILLAGE SECTION

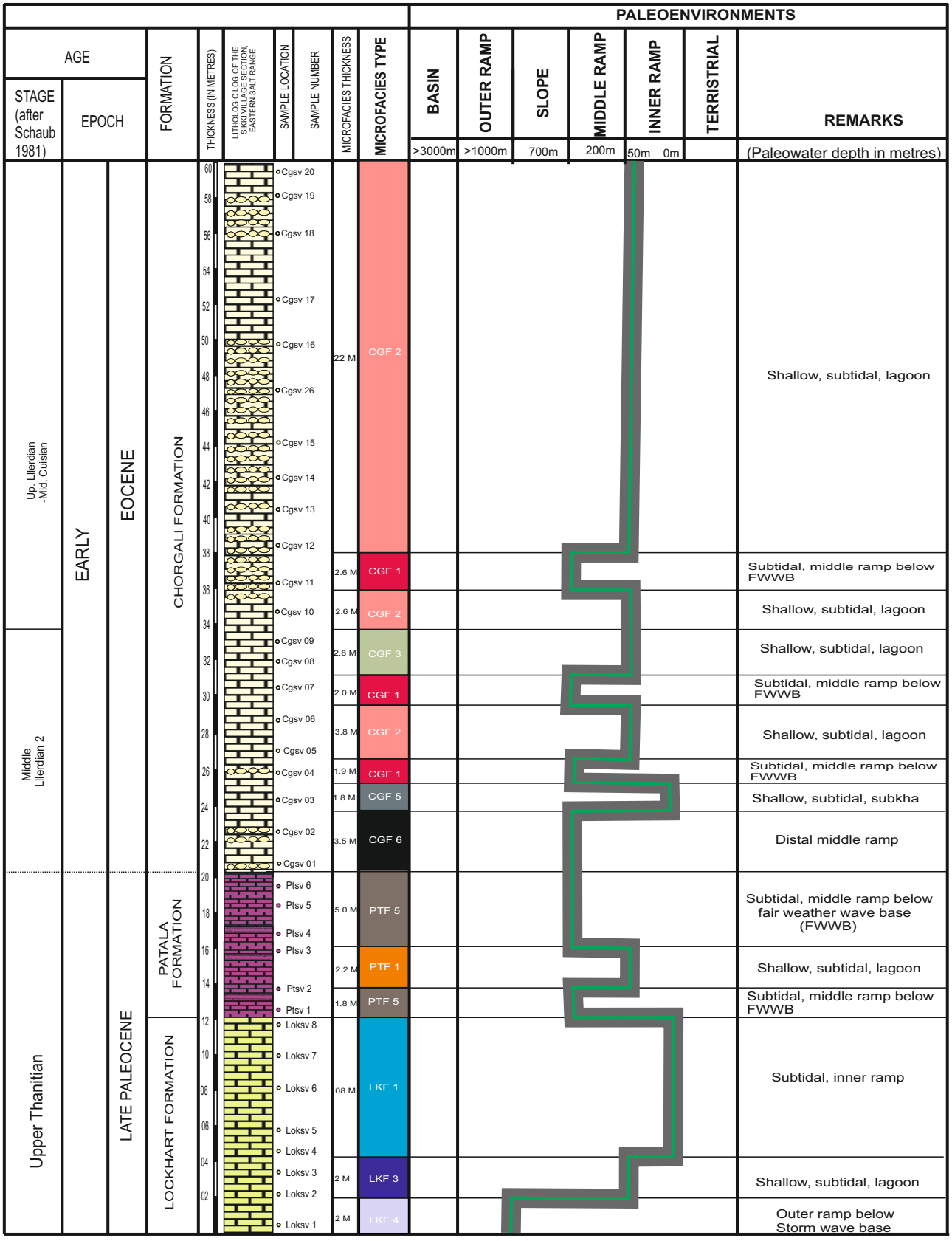


**Figure 7.28.** Composite chart showing facies distribution, paleoenvironments and a mean relative sea level curve infered from the faunal paleoecology (Racey. 1995) and facies criteria (Flugel. 2004) of the Paleogene rocks exposed in the Sikki Village Section, Eastern Salt Range,Potwar Basin, norhwest Pakistan (the shaded area shows the range of variation in the environment of deposition).

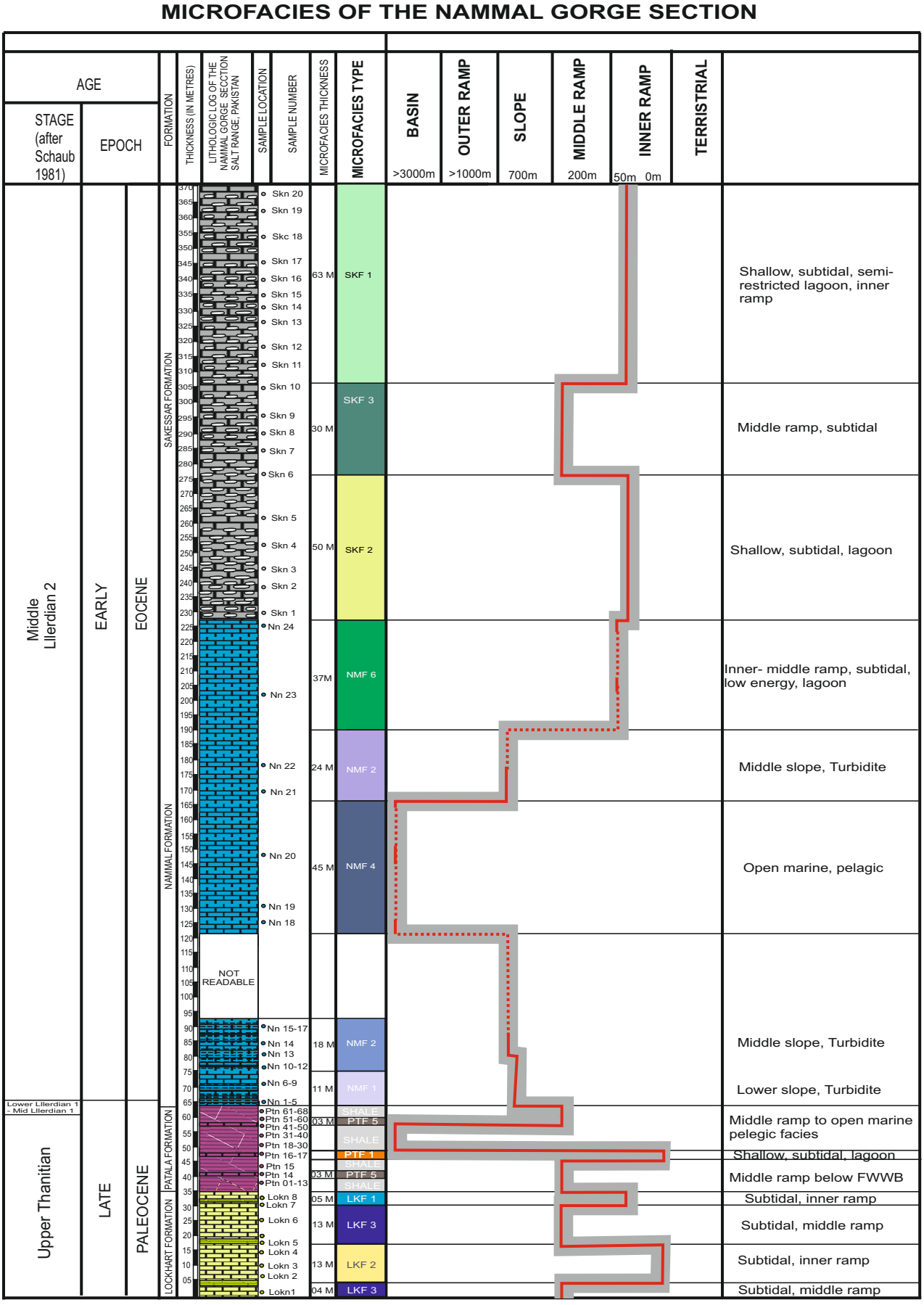


**Figure 7.29.** Composite chart showing facies distribution, paleoenvironments and a mean relative sea level curve infered from the faunal paleoecology (Racey. 1995) and facies criteria (Flugel. 2004) of the Paleogene rocks exposed in the Nammal Gorge Section, Central Salt Range, Potwar Basin, northwest Pakistan (the shaded area shows the range of variation in the environment of deposition).

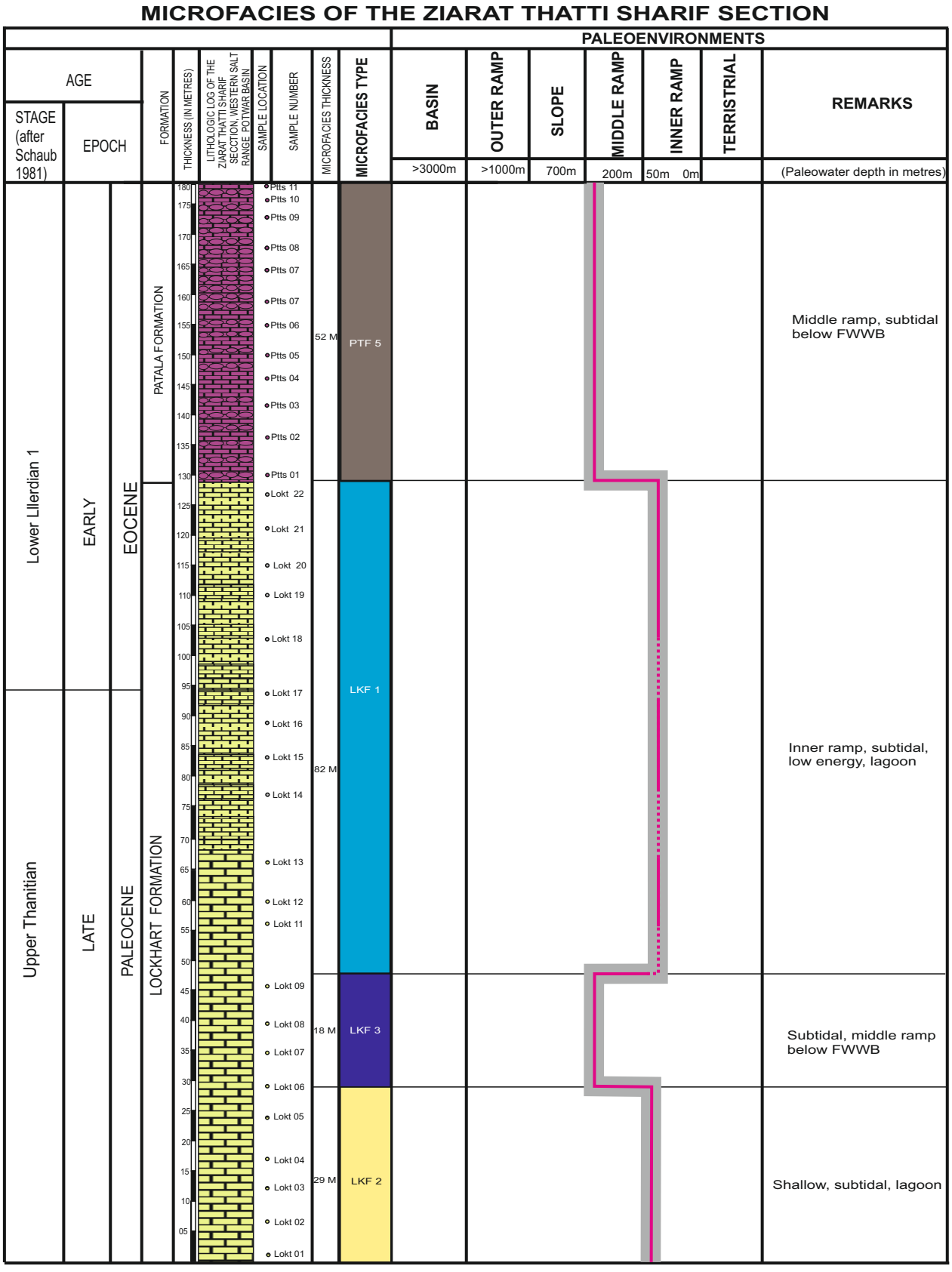


**Figure 7.30.** Composite chart showing facies distribution, paleoenvironments and a mean relative sea level curve infered from the faunal paleoecology (Racey. 1995) and facies criteria (Flugel. 2004) of the Paleogene rocks exposed in the Ziarat Thatti Sharif Section, Western Salt Range, Potwar Basin, northwest Pakistan (the shaded area shows the range of variation in the environment of deposition).

## MICROFACIES OF THE KALABAGH HILLS SECTION

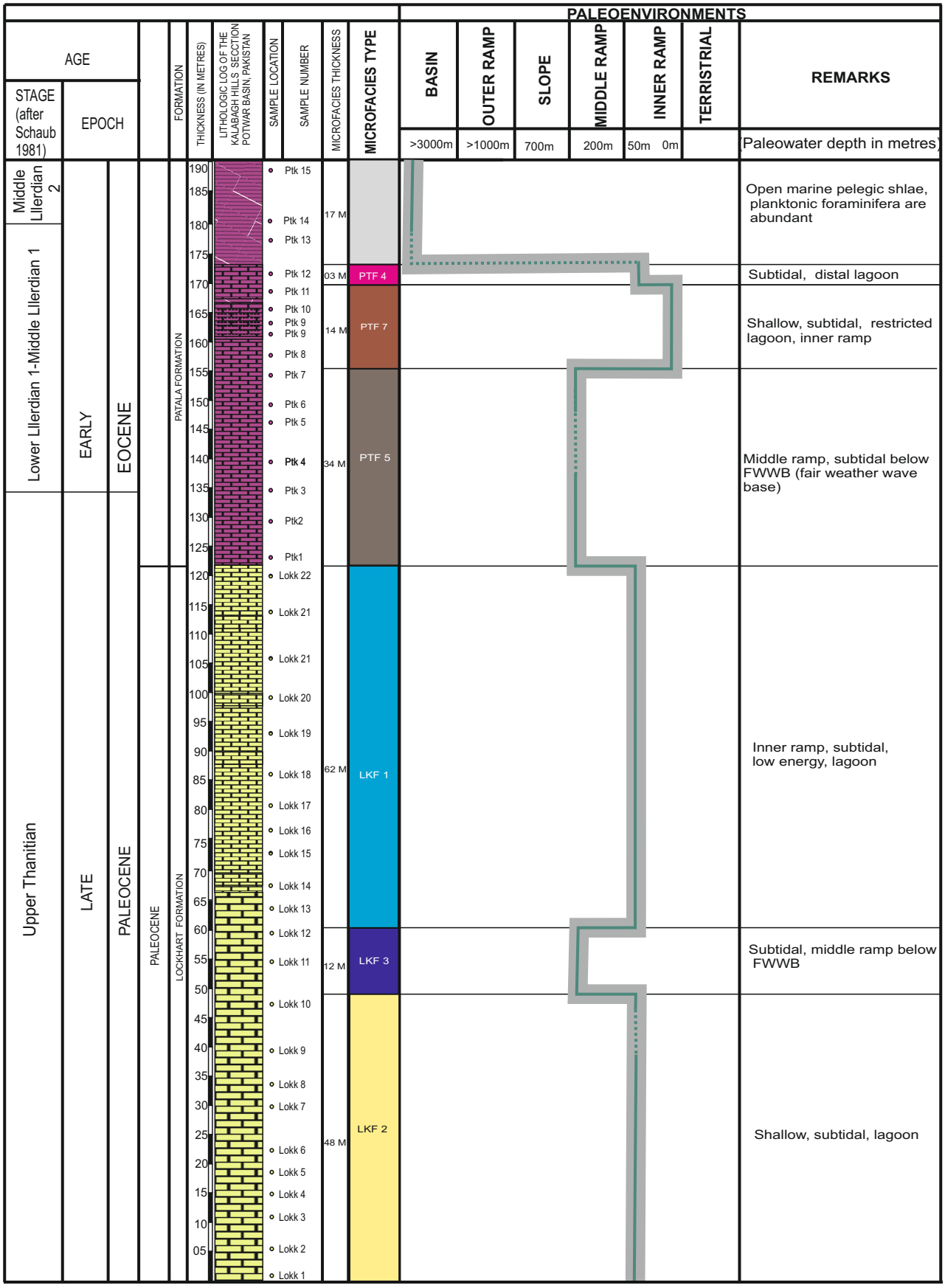


**Figure 7.31.** Composite chart showing facies distribution, paleoenvironments and a mean relative sea level curve inferred from the faunal paleoecology (Racey. 1995) and facies criteria (Flugel. 2004) of the Paleogene rocks exposed in the Kalabagh Hills Section, the Trans Indus Ranges (TIR), northwest Pakistan (the shaded area shows the range of variation in the environment of deposition).

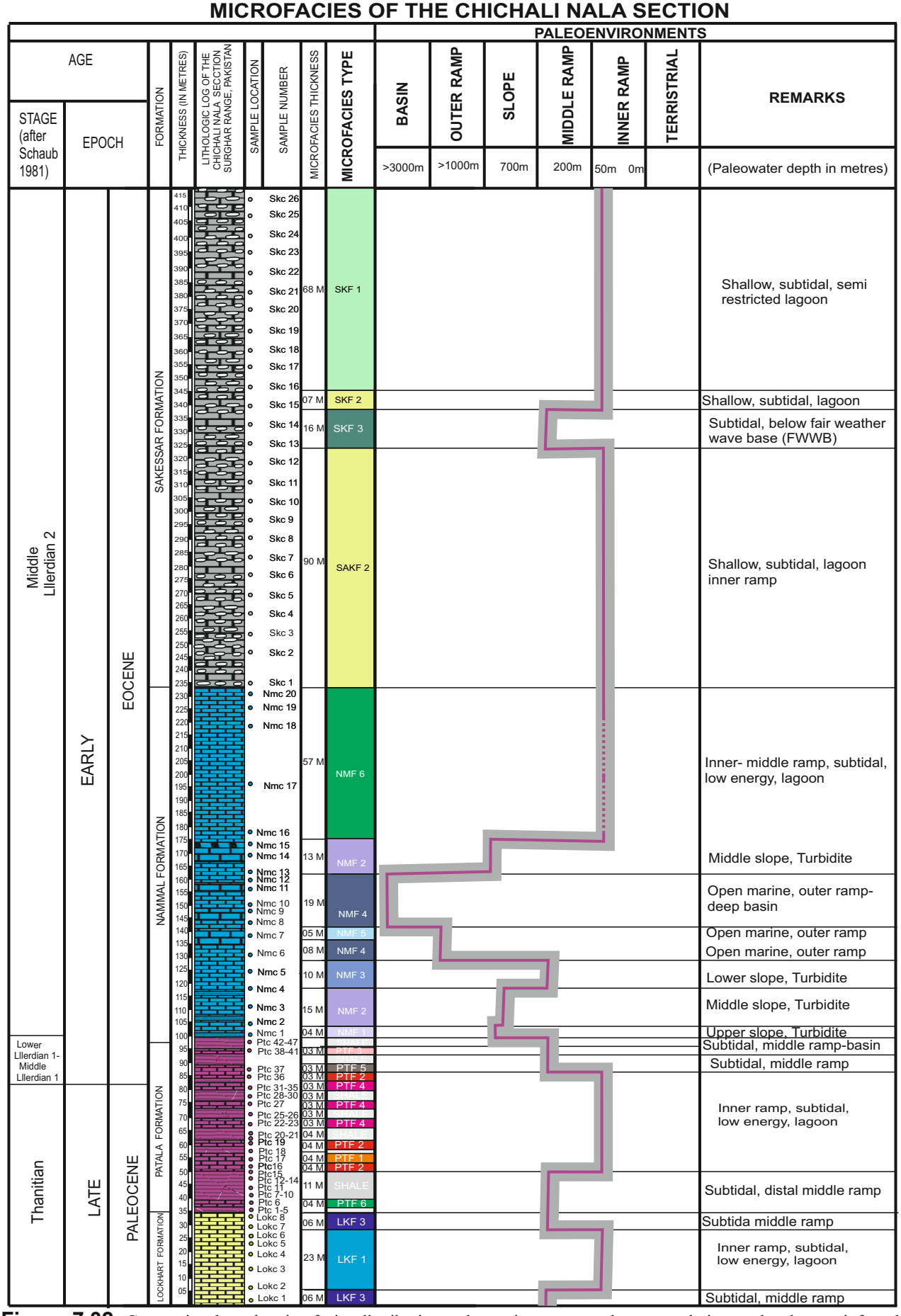


**Figure 7.32.** Composite chart showing facies distribution, paleoenvironments and a mean relative sea level curve inferred from the faunal paleoecology (Racey. 1995) and facies criteria (Flugel. 2004) of the Paleogene rocks exposed in the Chichali Nala Section, the Trans Indus Ranges, northwest Pakistan (the shaded area shows the range of variation in the environment of deposition).

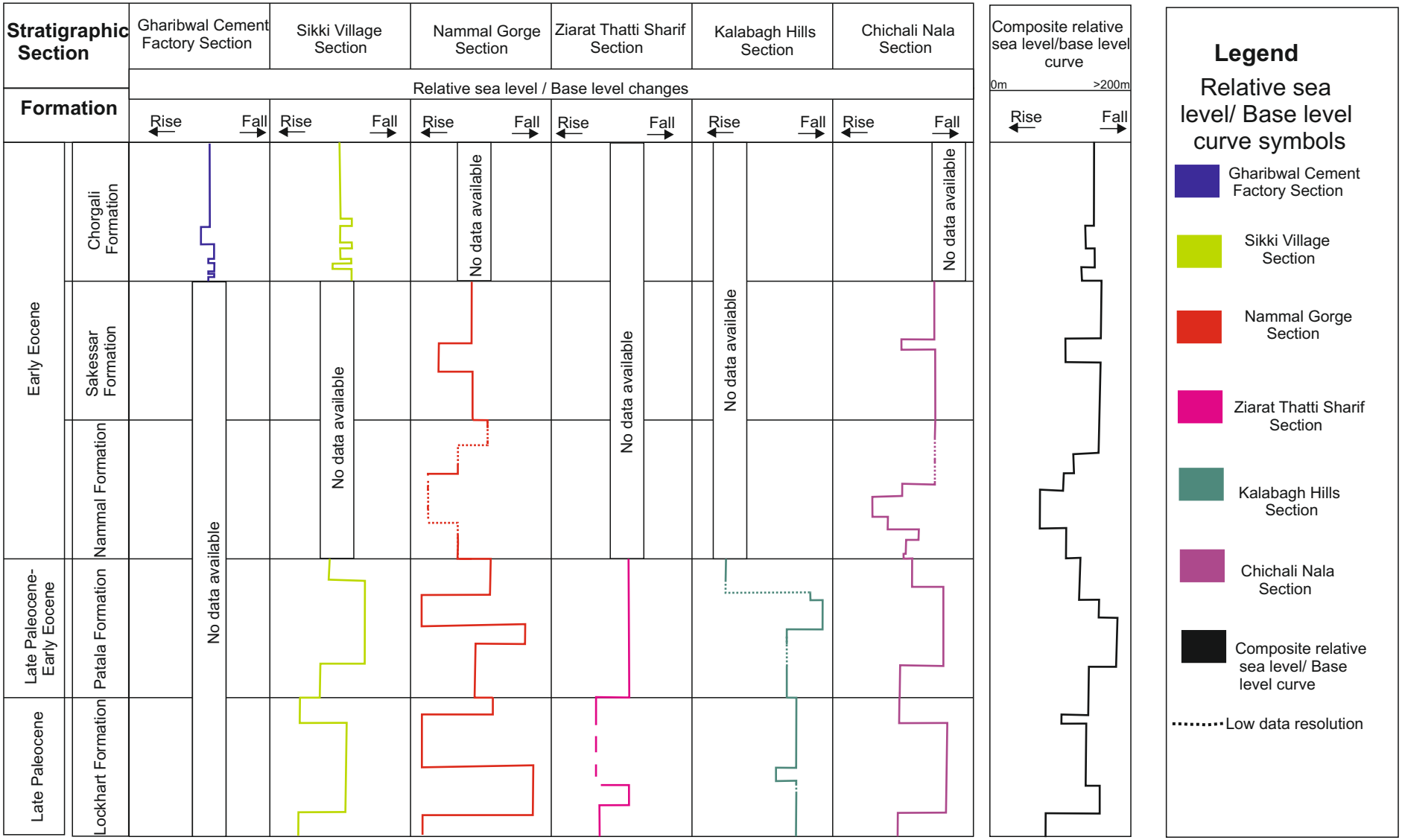


**Figure 7.33.** Relative sea level curves in different study sections and a composite sea level curve drawn from the variation in the dominant facies trend and relative sea level) of the Paleogene rocks of the Potwar Basin and the TIR.

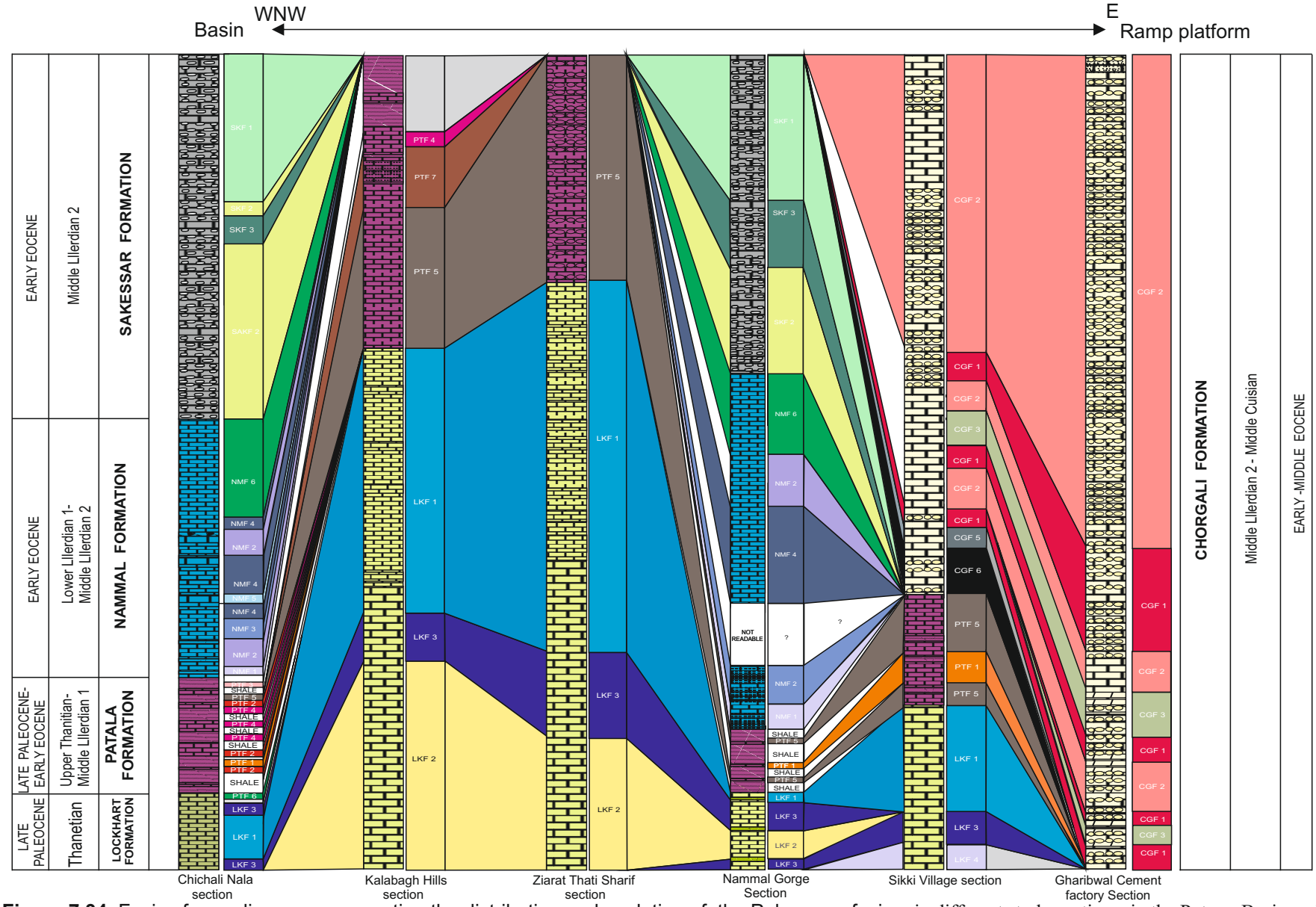


**Figure 7.34.** Facies fence diagram representing the distribution and evolution of the Paleogene facies in different study sections in the Potwar Basin and TIR (for location map of study sections see figure 1.1 and for symbols and abbreviations used here see figure 7.25 on page 266).

# Chapter 8

# 8 Tectono-stratigraphic evolution of the Kohat Basin Potwar Basin and the TIR

## 8.1 Introduction

The Kohat and Potwar Basins form the western deformed terrains of the Himalayan mountain belt that was formed by north-south shortening and crustal thickening during convergence between the Indian and Asian Plates after their collision at about 45 Ma (Gansser, 1964; LeFort, 1975). The Early Cenozoic collision of the Indian plate with the south eastern Afghanistan plate margin resulted in deep seas on the continental margin in the west and deltas in the east of Kohat Basin. The development of the basin from a Paleocene shelf sea with free circulation in north Central Pakistan into an enclosed and salty Eocene inland sea resulted from the closure of north-western Indo-Pakistan against Eurasia's former southern shore (Wells, 1984). Paleocene and Early Eocene sediments found in and adjacent to the Potwar Basin represent deposition in a "basinal" setting within the center of a trough developed between the Afghanistan and Pakistan-India plates (figure 8.1) and in a "shelfal" setting along the margin of the Pakistan-India plate (Warlaw et al., 1992 ).

In this chapter Paleogene foraminiferal stratigraphy and facies information are combined to augment understanding of the tectonic and eustatic control on the stratigraphic evolution of depositional sequences during a crucial time in the tectonic history of the Kohat Basin, Potwar Basin and the the Trans Indus Ranges (TIR) of northwestern Pakistan. In this study the larger benthic foraminiferal stratigraphy of the Paleogene rocks (detailed in chapter 4) constrains the geological ages of the stratigraphic units to a much higer resolution than has previously been achieved. The facies data provide information on the environment of deposition of sedimentary units. In this chapter I describe the depositional sequences in a bio-chronostratigraphic context and discuss their tectono-stratigraphic evolution in the study area.

## 8.2 Depositional sequences

The term "Sequence" was defined by Mitchum (1977) as "genetically related conformable succession of strata bounded at its base and top by unconformities".

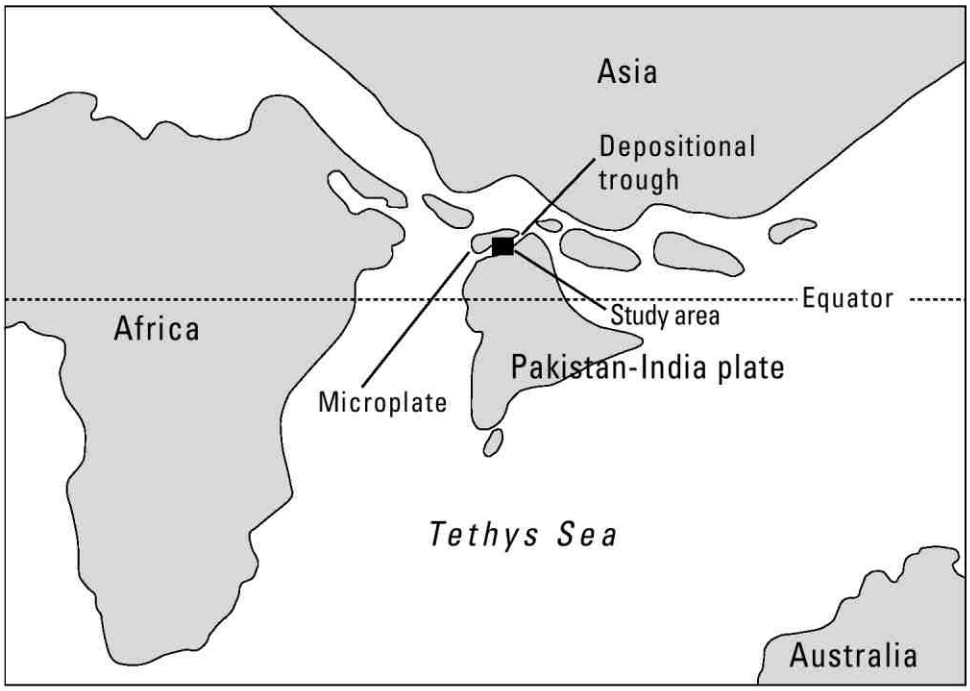


**Figure.8.1.** Paleogene continental configuration of the Pakistan-India Plate and a microplate showing a Paleocene-Eocene depositional trough (modified from Warwick et al., 1992). The microplate is part of the Afghanistan plate.

These sequences represent different episodes of deposition occurring in periods of falling and rising sea level. The depositional architectures of these sequences are affected by the rate of sediment supply and the relative sea level change. The major facies architectures recognized are progradational, aggradational, and retrogradational geometries (Emery and Myer, 1996, Catuneanu, 2006). When the rate of sediment supply is greater than the space available for sedimentation than a progradational geometry develops and the facies belts migrate basinward. The aggradational geometry occurs when the sediment deposition and the sea level change are in balance, and vertical stacking of the facies occurs. In the retrogradational geometry the rate of sediment supply is less than the space available for sedimentation and the facies belts migrate landward.

The deposits associated with these sequences occur in depositional packages known as systems tracts (Posametier and Vail 1988; Emery and Myers, 1996; Catuneanu, 2006). System tracts records deposition in third order cycles and its main types are: lowstand systems tract (LST), transgressive systems tract (TST) and highstand systems tract (HST). The LST consists of submarine fans deposited during a fall in the sea level that passes the offlap break margin and progradational facies architecture develops. The TST develops during a period of relative sea level rise and maximum transgression is represented by a maximum flooding surface (MFS). The facies architecture in TST follows a retrogradational pattern that depends on sediment input and rate of relative sea level rise. A decelerating sea level rise during transgression results in deposition of HST which is characterized by aggradational and progradational facies architecture (Posametier and Vail 1988; Emery & Myers, 1996). The sequence stratigraphy model was modified and applied to carbonates rocks by Sarg (1988). He described the depositional sequences of platforms and carbonate shelf margins. Subsequently carbonates sequence stratigraphy models were also developed by Calvet et al. (1990), Tucker and Wright (1990), Hunt and Tucker (1993) and Tucker et al. (1993). Schlager (2005) provided a modern view on sequence sratigraphy in carbonates and identifies drowning unconformities. In these models the general concepts remained the same, their fundamental difference is in their consideration of the influence of the sediment supply. Carbonate sedimentation is strongly influenced by environmental factors and is governed by the biogenic

production, water depth, temperature, and water chemistry while siliciclastic sedimentation depends on the sediment influx from continental margin sources.

The paleontological and sedimentological data help constraining the sequence stratigraphic models (Gregory and Hart, 1992). There are no fossils that are unique to certain system tracts/sequences that help in identifying position in system tract (Van Gorsel, 1988), but foraminiferal diversity and abundance in condensed sections can be used to constrain sequence boundaries and system tracts (Rosen and Hill 1990; Vail and Wornardt, 1988). The arenaceous benthic forams (flysch fauna) reflect rapid mud deposition in deep marine facies which are most likely representing a lowstand fan or distal lowstand wedge portion of a lowstand system tract (Van Gorsel, 1988). Transgressive systems tract are dominated by marine processes (waves, tides), low water turbidity favoring the presence of larger forams, glauconitic/calcareous beds and reefal buildups (Van Gorsel, 1988). In turbid waters of highstand system tracts, fluvially dominated (HST) foraminifera like *Ammonia* and *Pseudorotalia* dominate in shallow parts of the water colomn while *Bolivina* dominates in deeper parts (Van Gorsel, 1988). Sequence boundaries calibrated with biostratigraphy can be correlated across the carbonate platform from proximal to distal positions, in comparison with the global sequence stratigraphic framework most exposure surfaces correlate with sequence boundaries (Hardenbol et al., 1997). Biostratigraphy allows us to utilize the full suite of paleontological data for more detailed stratigraphic applications. Quantitative techniques result in more precise geochronology, recognition of depositional environments, paleobathymetry, and key stratal surfaces (condensed intervals, maximum flooding surfaces and unconformities), rates of sediment accumulation, and climatic changes (Wescott, 1998). Microfacies analysis aided with outcrop and fossils interpretation yields sufficient information about paleoenvironments, sea level changes and is important for the construction of a sequence stratigraphic framework for carbonate/clastic mixed systems (Serra Kiel et al., 2003)

In this chapter I use foraminiferal biostratigraphy and paleoecology along with facies and outcrop data to delineate depositional sequences, their bio-chronostratigraphic framework and to elucidate tectono-stratigraphic evolution of the Paleogene rocks in the Kohat Basin, Potwar Basin and the TIR.

## 8.3 Depositional sequences and bio-chronostratigraphic framework of the Kohat Basin

In the Kohat Basin two Paleogene Transgressive-Regressive Cycles TRK 1 and TRK 2 are identified (here TR is the abbreviation for Transgression-Regression and K stands for the Kohat Basin). Two depositional sequences SK 1 and SK 2 characterize these cycles (here S is the abbreviation for the depositional sequence and K stands for the Kohat Basin).

### 8.3.1 First Transgressive–Regressive Cycle (TRK 1)

The large benthic foraminiferal Biozones BFZ K 1-BFZK 3 are identified in the TRK 1 Cycle in the Kohat Basin. Deposition during this cycle is spanning from Thanitian to Middle Cuisian (figure 8.19A & C).

#### *8.3.1.1 Transgressive phase 1*

During the transgressive phase 1 the first Sequence SK 1 was deposited in the Kohat Basin. It is comprised of sediments of the Patala Formation (deep basinal to outer ramp facies), overlain by the sediments of the Panoba Formation (middle ramp to ramp slope deposits) which are in turn overlain by the sediments of the Sheikhan Formation (ramp platform carbonates and lagoonal facies) and the Jatta Gypsum sediments (Sabkha/lagoonal evaporites) (figure 8.19 A & C). Within the Sequence SK 1 a transgressive system tract (denoted as TSTK 1) and a subsequent highstand systems tract (denoted as HSTK 1) are identified. In the north-eastern part of the Kohat Basin, black shales and bluish grey limestone of the Patala Formation are characterizing the upper Thanitian BFZK 1 (A) Biozone and they are exposed in the Panoba Nala and the Tarkhobi Nala Sections (figure 1.1 ). Depth and age diagnostic foraminifera are recorded in the TSTK 1. In the lower part of the Patala Formation the pelagic shales and interbedded limestone (figure 8.2) planktonic foraminiferal wackestone microfacies (PTK 1) deposited in deep basinal settings, mark the maximum flooding surface (MFSK 1) in the TSTK 1 (figure 8.19 A & C). This surface is defined on the basis of abundant planktonic foraminifera. A decelerating sea level rise during Lllerdian 1 initiated the deposition of HSTK 1 in the study area (figure 8.3). In the Panoba Nala and the Tarkhobi Nala Sections (figure 1.1) HSTK 1

is characterized by the Nummulitic wackestone microfacies (PTK 2) in the lower middle part of the Patala Formation representing distal middle ramp settings. During highstand progradation a mixed faunal packstone to grainstone microfacies (PTK 3) was deposited in a ramp slope setting; and occurs in the middle part of the Patala Formation in the Tarkhobi Nala and the Panoba Nala sections. The bioclastic mudstone-wackestone microfacies (PTK 4) that occurs in the upper part of the Patala Formation grades upward into green coloured clays, the Panoba Formation (figure 8.3), which are well exposed in the Panoba Nala, the Tarkhobi Nala and the Sheikhan Nala sections. The green clays of the Panoba Formation represent the continued progradation (figure 8.19 A) of the more proximal middle ramp *Bulimina* biofacies (BF 1) and distal middle ramp *Uvigerina* biofacies (BF 2) onto the ramp slope *Bathysiphon*/*Gaudryina* biofacies (BF3). The shallowing upward depositional trend continues and shallow ramp carbonates/marls of the Sheikhan Formation (figure 8.4) were deposited within the HSTK 1 (figure 8.19 A). In the Sheikhan Nala Section the lower part of the Sheikhan Formation is characterized by inner ramp deposits succeeded by open marine middle ramp to restricted inner ramp deposits. In the Panoba Nala Section the distal middle ramp facies occurs in the lower part of the sequence. In the middle part interbedded clays and limestone grade upward into thick bedded dolomicrites deposited in a sabkha environment during late stage of HSTK 1 (figures 8.4 & 8.19 A). The characteristic foraminiferal fauna of the proximal topsets representing middle ramp settings during HSTK 1 deposition includes *Alveolina globula, Alveolina rotundata, Alveolina pasticilata, Lockhartia* sp*, Nummulites pinfoldi,* and *Nummulites thalicus.* The distal middle ramp foraminiferal fauna of the HSTK 1 includes *Assilina granulosa*, *Assilina daviesi, Assilina dandotica, Assilina laxispira Discocyclina sella, Discocyclina despansa, Discocyclina fortisie, Discocyclina roberti, Discocyclina scalaris* and *Lepidocyclina* sp.

#### *8.3.1.2 Regressive phase 1*

During regressive phase 1, before the complete exposure of the Kohat Basin, gypsiferous shales were deposited in a coastal sabkhas forming along the margin of the Sheikhan carbonate platform (figure 8.5 & 8.19 A) in the northeast and thick Jatta Gypsum and Bahadur Khel Salt (figures 8.6 & 8.19 A) were deposited in the southwest in the restricted hypersaline lagoons. The evaporites demarcate the first -

sequence boundary SBK 1 (figures 8.19 A & C) in the Kohat Basin (here SB abbreviates sequence boundary and K stands for the Kohat Basin). Subsequently the Kuldana Formation fluvial channel sandstone, flood plain red clays, pebbly conglomerates and common enriched in mammal bones indicate deposition in lowstand systems tract (LST) under terrestrial conditions (figures 8.7, 8.8 & 8.19 A ).

### 8.3.2 Transgressive-Regressive Cycle (TRK 2)

The large benthic foraminiferal Biozones BFZK 4-BFZK 6 are identified in the TRK 2 cycle in the Kohat Basin. Deposition during the TRK 2 cycle occurs during the Middle Lutetian 1 to Upper Lutetian (figure 8.19 A & C).

#### *8.3.2.1 Transgressive Phase 2*

Sequence SK 2 comprises the transitional marine incised valley fill deposits of the Kuldana Formation (figure 8.8) and the ramp platform carbonates of the Kohat Formation (figures 8.9 & 8.10). A purple grey/greenish grey coloured dolomitic limestone including the oysters-rich bed in the upper part of the Kuldana Formation marks the transgressive surface (TS) of the TSTK 2. In the Sheikhan Nala Section the maximum flooding surface (MFSK 2) within TSTK 2 is represented by the highly fossiliferous thin bedded argillaceous limestone of the Kohat Formation. Latter consists of foraminiferal bioclastic packstone microfacies (KTF 1 deposited during maximum transgression in the foraminiferal forebank barrier (Racey, 1995) setting. Foraminiferal fauna that characterize the MFSK 2 include *Assilina granulosa, Assilina spinosa, Assilina subspinosa, Assilina pappilata, Assilina subpappilata, Nummulites beaumonti* and *Nummulites globulus.* Subsequent highstand systems tract (HSTK 2) is represented by the thick sequence of thinly bedded grey coloured nodular limestone (representing BFZK 4-BFZK 6 Biozones, of the Lower Lutetian 2-Upper Lutetian age) in the Sheikhan Nala Section. Due to local tectonics, e.g. uplift, of the Kohat Basin a brief period of non-deposition (from Lower Lutetian 2 to Middle Lutetian 1) in the Panoba Nala Section and the Bahadur Khel Salt Tunnel Section is recorded by the absence of the BFZK 4 and BFZK 5 Biozones (figure 8.19 A & C).

In the Bahadur Khel Tunnel Section only thick bedded to massive -Limestone (representing BFZK 6 Biozone) is present. During the HSTK 2 facies deposition of the bioclastic mudstone- wackestone microfacies KTF 3 and the *Operculina* rich bioclastic mudstone- -wackestone microfacies KTF 4, representing deep barrier backbank lagoonal settings, are well developed in the Sheikhan Nala Section, while the proximal barrier backbank gastropod-rich mudstone-wackestone microfacies (KTF 5), proximal barrier forebank *Nummulitic* mudstone-wackestone microfacies (KTF 6) and distal barrier backbank *Alveolina*-rich bioclastic wackestone microfacies (KTF 7) dominates in the Panoba Nala (figure 8.10) and the Bahadur Khel Salt Tunnel sections.

#### *8.3.2.2 Regressive Phase 2*

In the Kohat Basin marine conditions vanished in Upper Lutetian times due to the collision of Indian and Eurasian plates and Himalayan orogeny and subsequent molasses sedimentation started in Miocene to Pliocene. The Kohat Basin became a foreland basin and a thick accumulation of the fluviatile sediments occured in most part of the basin (figure 8.11). The molasses represents deposition after second sequence boundary SBK 2 in the region and (8.19 A & C) comprised of mudstones, sandstones, and coarsely bedded conglomerates laid down when the region was a vast basin during Middle Miocene, to Upper Pleistocene times.

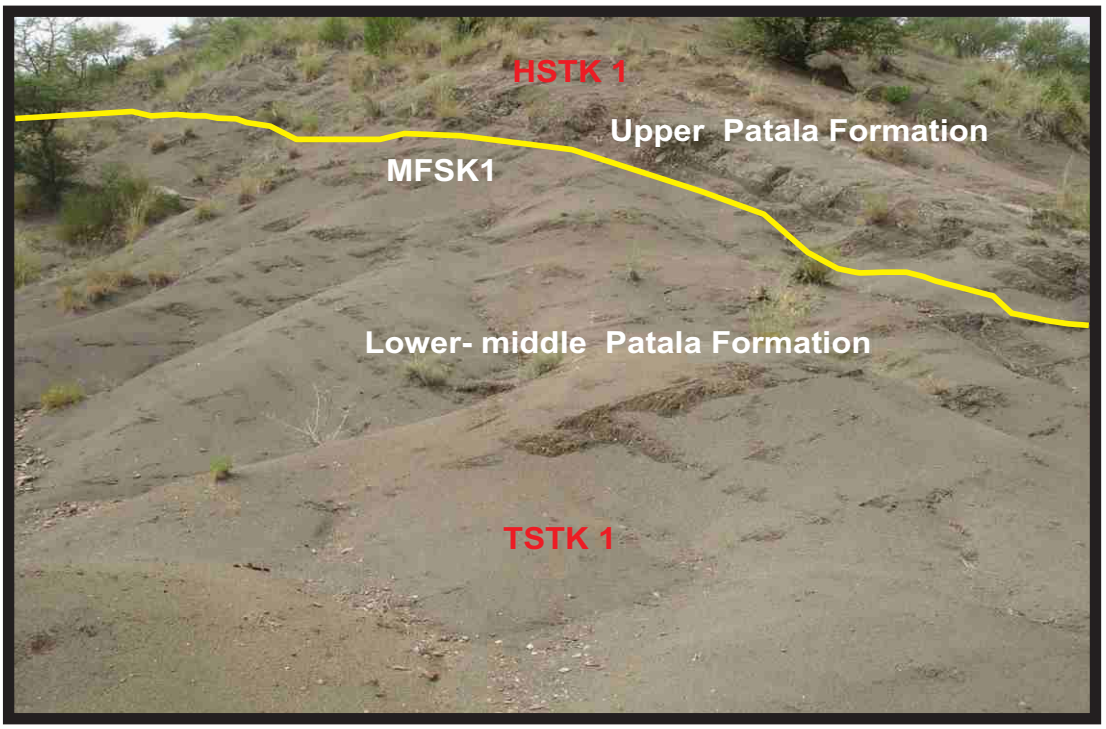


**Figure 8.2.** A north-east looking view of the Patala Formation showing the transgressive system tract (TSTK 1) and highstand systems tract (HSTK 1) within Sequence SK 1 and are separated by the maximum flooding surface (MFSK 1) in the Tarkhobi Nala Section, Kohat Basin.

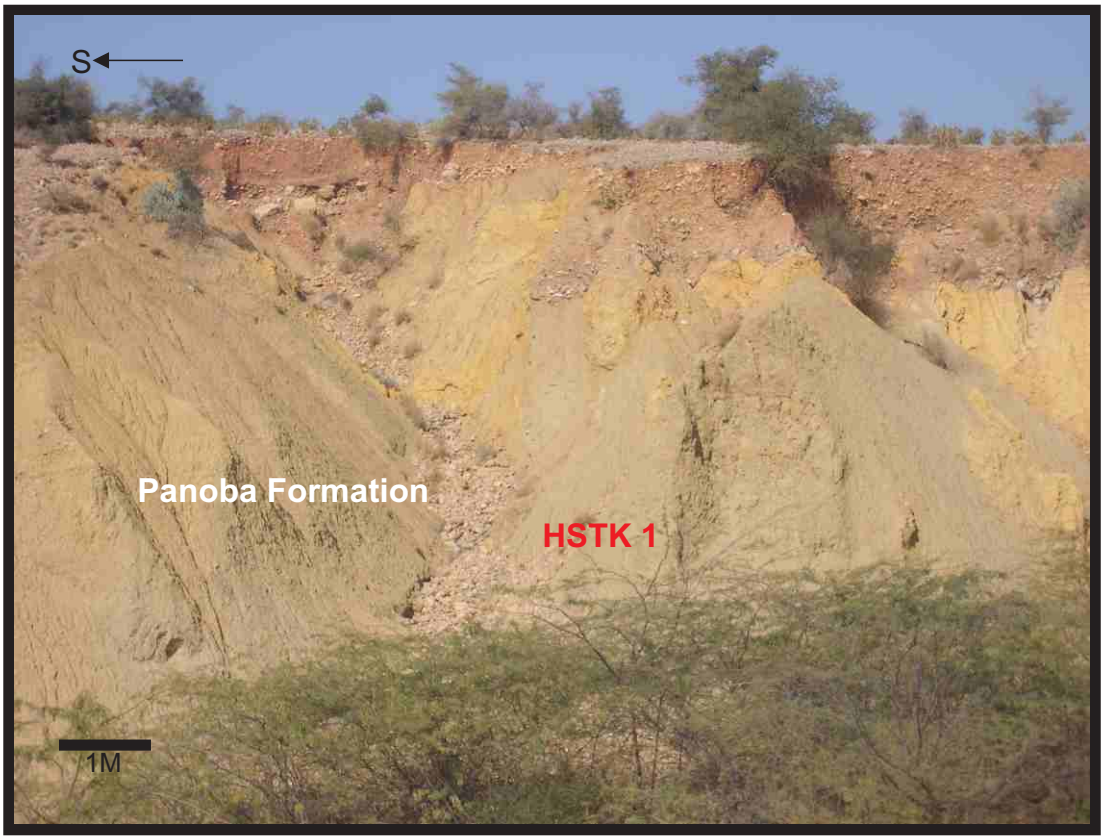


**Figure 8.3.** Green clays of the Panoba Formation showing deposition during the first highstand systems tract (HSTK 1) deposition within Sequence SK 1, exposed in the Sheikhan Nala Section, Kohat Basin.


**Figure 8.4.** Thinly bedded nodular limestone representing lower-middle part of the Sheikhan Formation showing deposition in the carbonate ramp depositional setting during the first highstand systems tract (HSTK 1) within the Sequence SK 1, exposed in the Sheikhan Nala Section, Kohat Basin.


**Figure 8.5.** Thinly bedded arenaceous limestone interbedded with gypsiferous shales representing the start of regressive phase 1 within the upper part of the Sheikhan Formation during late highstand systems tract (HSTK 1) deposition within the Sequence SK 1, exposed in the Sheikhan Nala Section, Kohat Basin.

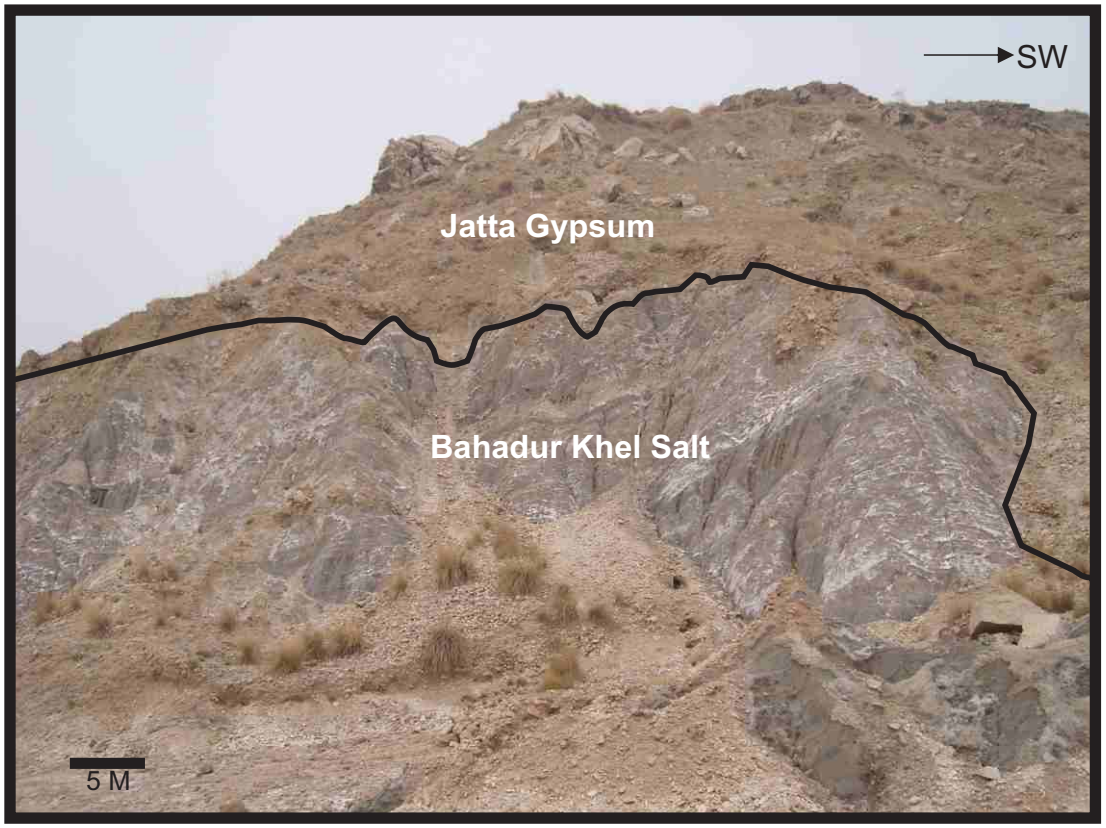


**Figure 8.6.** The massive Bahadur Khel Salt Facies and overlying Jatta Gypsum Facies representing deposition in the regressive phase 1 of the TRK cycle 1, and represented by the first sequence boundary SBK 1, in the Bahadur Khel Salt Tunnel Section, southwestern Kohat Basin.


**Figure 8.7.** At the end of regressive phase 1 in TRK 1 cycle the facies progradation is represented by the fluvial sandstones and flood plain clays of the Lower Kuldana Formation, representing deposition in a lowstand systems tract (LST) in the Bahadur Khel Salt Tunnel Section, southwestern Kohat Basin.

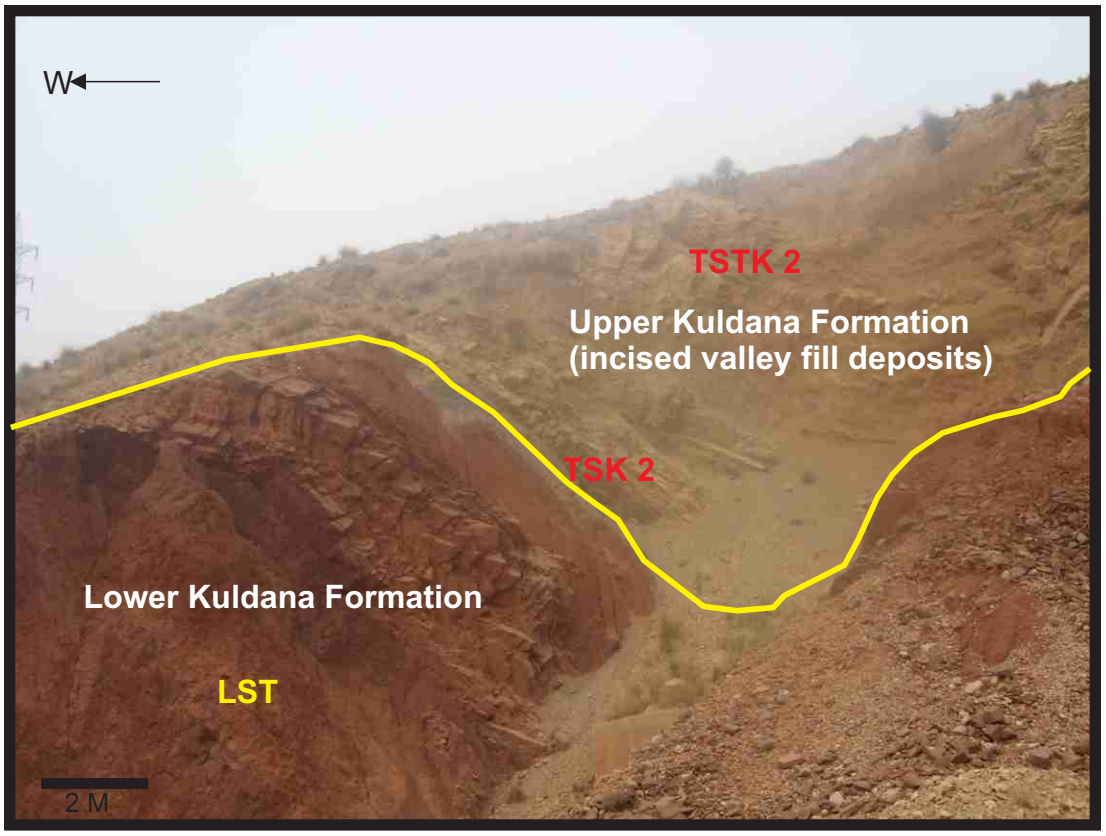


**Figure 8.8.** The marginal marine facies of the upper Kuldana Formation marks the transgressive surface (TSK 2) in TRK 2 cycle. The incised valley fill deposits (marginal marine) are formed during the deposition TSTK 2 in the Bahadur Khel Salt Tunnel Section, southwestern Kohat Basin.

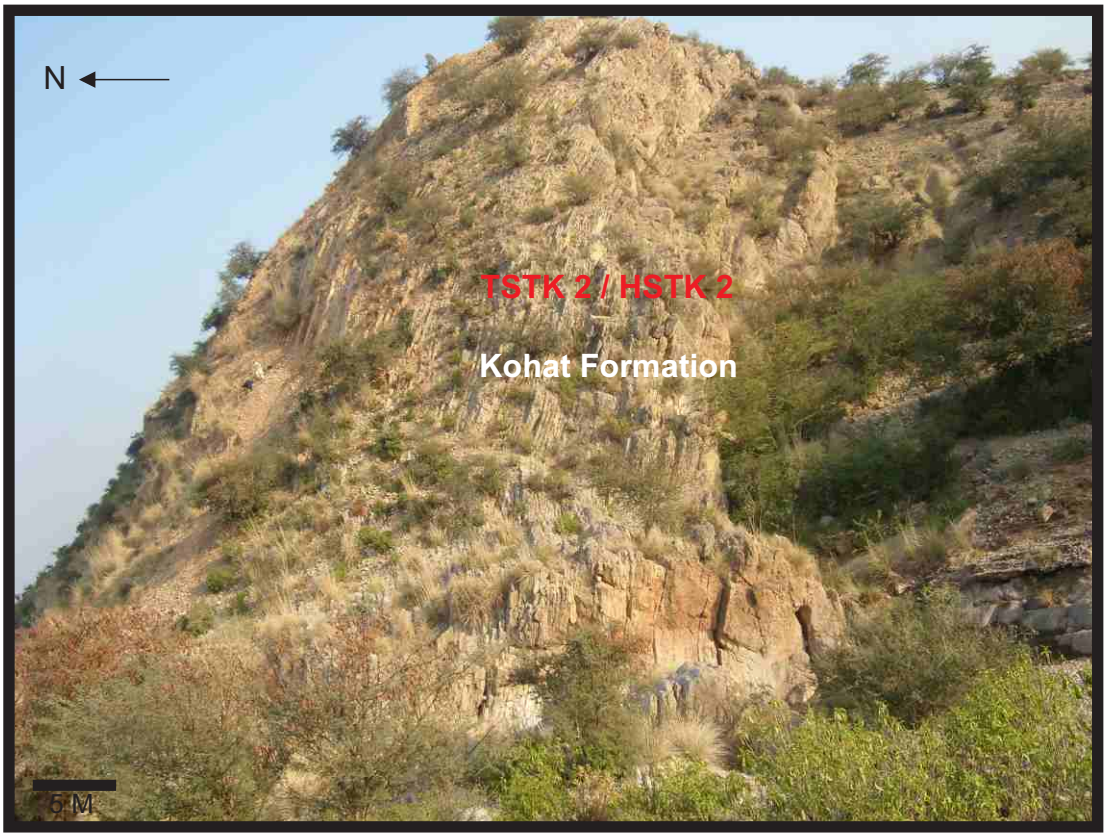


**Figure 8.9.** The ramp carbonates of the Kohat Formation were deposited in the second Sequence SK 2 in TSTK 2 and HSTK 2, exposed in the Sheikhan Nala Section, northeastern Kohat Basin.


**Figure 8.10.** The HSTK 2 in the TRK 2 cycle is dominated by the deposition of barrier backbank lagoonal facies characterized by the benthic foraminifera in the thick bedded to massive limestones of the Kohat Formation exposed in the Panoba Nala Section, northeastern Kohat Basin.


**Figure 8.11.** The Miocene mollasses deposits representing the SBK 2 sequence boundary, and were deposited in a foreland basin in the regressive phase of TRK 2 cycle in the Kohat Basin

## 8.4 Depositional sequences and bio-chronostratigraphic framework of the Potwar Basin and the TIR

In the Potwar Basin and the TIR Upper Paleocene (Thanitian) to Lower Eocene (Middle Cuisian) rocks show deposition in three Transgressive-Regressive cycles. TRP 1, TRP 2 and TRP 3 (here TR represents Transgression-Regression and P stands for Potwar Basin and the TIR). These cycles are described as following.

### 8.4.1 Transgressive-Regressive cycle TRP 1

The large benthic foraminiferal Biozones BFZ P 1 is identified in the TRP 1 cycle. Deposition during the TRP 2 cycle is spanning Late Paleocene (Thanitian) in the Potwar Basin and the TIR (figures 8.19 B-C).

#### *8.4.1.1 Transgressive Phase 1 (TSTP 1)*

The first marine transgression during the Late Paleocene (Thanitian) deposited the first Sequence SP 1 in the Potwar Basin and the TIR (here S represents Sequence and P stands for the Potwar Basin and TIR). Sequence SP 1 consists of the carbonate ramp deposits of the Lockhart Formation and lower part of the Patala Formation (figure 8.12) TSTP 1 is represented by thick carbonates of Lockhart Formation, and interbedded pelagic shales and carbonates in lower part of the Patala Formation (figure 8.12 & 8.19 B). A diverse assemblage of age and depth diagnostic foraminiferal fauna, that characterizes the topsets of TSTP 1 and include *Ranikothalia sindensis, Ranikothalia nuttali, Miscellanea miscella, Lockhartia* sp., *Miscellanea stampi, Operculina salsa, Operculina subsalsa, Discocyclina ranikotensis, Discocyclina seunesi, Operculina petalensis*, *Assilina spinosa, Nummulites lahiri, Nummulites thalicus, Nummulites pinfoldi, Alveolina vredenburgi, Alveolina pasticilata, Alveolina conradi* and *Alveolina globula.* Shallow marine ramp invertebrate fauna (gastropods, pelecypods, brachiopods) and flora (green algae) accompany the foraminiferal fauna. The microfacies which characterize the proximal topsets of the TSTP 1 includes the algal foraminiferal wackestone-packstone microfacies (LFK 1) and the *Alveolina*-rich bioclastic wackestone to packstone microfacies (LKF 2) suggesting deposition in shallow water, subtidal inner ramp setting. The distal middle ramp topsets of TSTP 1 include

diverse benthic foraminiferal wackestone- packstone microfacies (LKF 3) that represents deposition in distal part of middle ramp settings. The ramp slope (clinoform) transect of TSTP 1 is characterized by the planktonic- benthic mixed foraminiferal lime mudstone-wackestone microfacies (LKF 4). It has a micritic matrix with mixed planktonic and larger benthic foraminifera and contains no of shallow marine flora and fauna. This suggests that LKF 4 microfacies was deposited in the distal part of the middle ramp to outer ramp setting. The first maximum flooding surface (MFSP 1) within TSTP 1 is marked by pelagic shale enriched in the planktonic firaminifera interbedded with the distal middle ramp microfacies (i.e. PTF 5). The shales have a high diversity of planktonic foraminiferal fauna representing deposition in an open marine, pelagic environment, outer ramp to basinal settings. The peloidal mudstone microfacies (PTF 4) prograded over the deep marine pelagic shale (PTF 5) during HSTP 1 deposition.

#### *8.4.1.2 Regressive phase 1*

Before the onset of the second transgressive cycle a subaerial exposure mark the sequence boundary SBP 1 (here SB abbreviates sequence boundary). The SBP 1 (figure 8.19 B-C) is indicated by the absence of age diagnostic benthic foraminifera, i.e. *Assilina aff pustulosa* in the lower part of the BFZP 2 Biozone (representing lower Lllerdian 2) (figure 8.19 C) in the Chichali Nala Section (figure 1.1). Sequence boundary SBP 1 is controlled by local tectonics. The barrier beach sands with thick iron crusts (figure 8.13) and the fenestral bioclastic mudstone- wackestone microfacies (PTF 2) of an intertidal to supratidal origin indicates subaerial exposure.

### 8.4.2 Transgressive-Regressive cycle TRP 2

The large benthic foraminiferal Biozone BFZP 2 is identified in the TRP 2 cycle in the Potwar Basin and the TIR. Deposition during the TRP 2 cycle is spanning Lower Lllerdian 2-Middle Lllerdian 1 (figure 8.19 B-C).

#### *8.4.2.1 Transgressive phase 2 (TSTP 2)*

The transgressive phase 2 in the TRP 2 cycle the second Sequence SP 2, was deposited and it consists of the upper part of the Patala Formation and lower part of the Nammal Formation (figures 8.19 B-C) (here in SP 2, S represents Sequence and P stands for Potwar Basin and the TIR).

The TSTP 2 is characterized by the deposition of limestone and shale interbeds in the upper part of the Patala Formation and grey coloured marls in the lower middle part of the Nammal Formation (figure 8.14), marking the transgressive surface. The retrogradational topsets (figure 8.19 B) of the TSTP 2 contains a diverse foraminiferal fauna that includes *Nummulites thalicus, Nummulites lahiri, Alveolina globula, Alveolina pasticilata, Alveolina conradi, Discocyclina despensa, Discocyclina fortisie, Discocyclina scalaris, Lockhartia conica, Assilina leymerie, Operculina salsa, Operculina subsalsa, Discocyclina ranikotensis, Operculina petalensis*, *Ranikothalia nuttali* and *Assilina sp*. The retrogradational topsets of the TSTP 2 are also characterized by the benthic foraminiferal packstone microfacies (PTF 3), the diverse foraminiferal wackestone-packstone microfacies (PTF 5) and the coralline red algal–stromatolite mudstone-wackestone microfacies (PTF 6). All shows deposition in distal middle ramp settings (*sensu* Read, 1985). The PTF 6 microfacies is restricted to the Chichali Nala Section. The maximum flooding surface (MFSP 2) within the TSTP 2 is characterized (figure 8.14) by deep basinal pelagic shale bed overlying the distal middle ramp platform microfacies (PTF 5). The HSTP 2 progradation (figure 8.19 B) of the shallow ramp platform microfacies (beach barrier sand) on the deeper facies is seen in the lower part of the Nammal Formation that indicates deceleration of sea level rise.

The progradational clinoforms (figure 8.19 B) of the HSTP 2 are characterized by foraminiferal bioclastic wackestone–packstone microfacies (NMF 2) and the planktonic–*Discocyclina*-rich foraminiferal wackestone microfacies (NMF 3) that shows deposition on a distally steepened carbonate ramp slope settings. Mixing of shallow (milliolids/*Nummulites*/*Assilina*/*Discocyclina*) and deep-water

fauna (planktonic foraminifera) indicate redeposition during HSTP 2 facies progradation. Allodopic turbidites were common in the deep basinal settings during HSTP 2 deposition.

#### *8.4.2.2 Regressive Phase 2*

During the regressive phase 2 exposure of the platform is evidenced by thick bedded to massive limestone in the middle part of the Nammal Formation having eroded rubbles in fine matrix (figure 8.15). It indicates sequence boundary SBP 2 in the Potwar Basin and the TIR (figures 8.19 B-C).

### 8.4.3 Transgressive-Regressive cycle TRP 3

The large benthic foraminiferal Biozones BFZP 3 (A) and BFZP 3 (B) are identified in TRP 3 cycle. Deposition during the TRP 3 cycle is spanning Middle Lllerdian 1-Middle Cuisian (figures 8.19 B-C)..

#### *8.4.3.1 Transgressive Phase 3 (TSTP 3)*

During TSTP 3 of TRP 3 cycle, sequence SP 3 was deposited. It consists of middle-upper part of the Nammal Formation, the Sakessar Formation and the Chorgali Formation (figures 8.14, 8.16 and 8.17) (here in SP 3, S represents sequence and P stands for the Potwar Basin and the TIR) (figures 8.19 B-C).

TSTP 3 was recorded in the bluish coloured marls/limestone in the upper part of the Nammal Formation (figure 8.16). The planktonic foraminiferal wackestone-packstone microfacies (NMF 5) marks the transgressive surface of the TSTP 3 and is characterized by an abundance of planktonic foraminifera which suggests deposition under low energy conditions in an open marine pelagic environment. The NMF 5 microfacies is restricted to the Chichali Nala Section and has 5m thickness. The gradual decrease in the sea level rise is seen in the subsequent highstand system tract (HSTP 3), when a thick shallow marine sequence of thinly bedded carbonates was deposited. These carbonates are characterized by the inner ramp peloidal lime mudstone microfacies (NMF 6) in upper part of the Nammal Formation. The shallowing upward trend continues (figure 8.19 B), although occasional deepening of the environment is seen in the thick ramp carbonates of the Sakessar (SKF 1 and

SKF 2) (figure 8.17) and the Chorgali Formations (CGF 2 and CGF 3) (figure 8.18). The progradational topsets of the HSTP 3 (figure 8.19 B) hosts a diverse and rich assemblage of the foraminifera. These foraminifera are *Nummulites atacicus, Nummulites globulus, Nummulites thalicus, Nummulites lahiri, Nummulites pinfoldi, Assilina pustulosa, Assilina leymerie*, *Assilina granulosa, Assilina spinosa, Assilina laminosa, Discocyclina scalaris, Discocyclina sella, Discocyclina undulata, Lockhartia hunti, Lockhartia tipperi, Lockhartia conditi, Assilina spinosa, Assilina laminosa*, *Rotalia trochidoformis, Orbitolites complanatus, Ranikothalia sahini* and *Ranikothalia nuttali*. The progradational proximal topsets are dominated by the foraminifera (milliolid and alveolinid), dasycladacean algae and ostracodes. The progradational distal topsets are differentiated by the presence of *Alveolina* sp./*Nummulites* sp./*Assilina* sp. dominated fauna in the proximal part and *Nummulites* sp./*Assilina* sp/*Discocyclina* sp./*Operculina* sp. dominated fauna in the distal part of the middle ramp setting.

#### *8.4.3.2 Regressive Phase 3*

The regressive phase 3 is evidenced by the presence of Miocene fluvial molasses deposits overlying the Early Eocene Chorgali Formation and marks the third sequence boundary (SBP 3) (figures 8.19 B-C) as seen in the Gharibwal Cement Factory Section (figure 8.18).

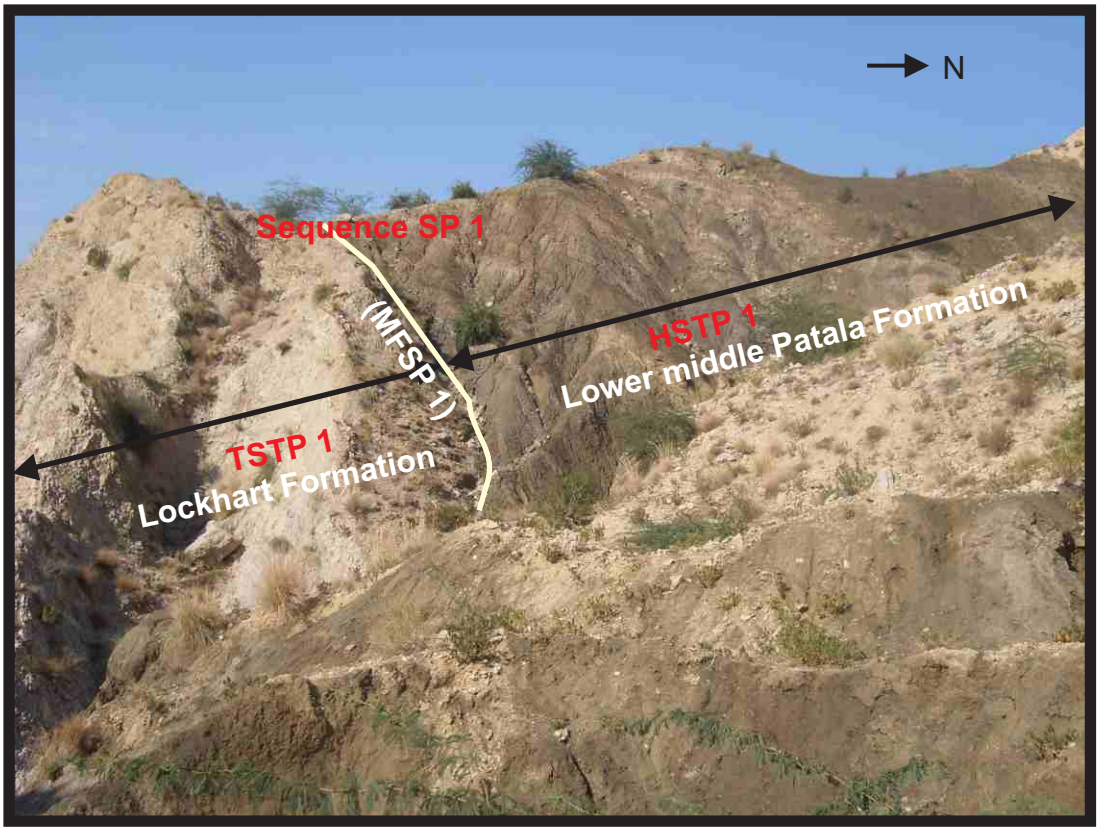


**Figure 8.12.** The sequence SP 1 comprises of the Lockhart Formation and lower middle part of the Patala Formation. A maximum flooding surface (MFSP 1) separates the transgressive systems tract (TSTP 1) deposits from the highstand systems tract (HSTP 1) deposits exposed in the Ziarat Tahtti Sharif Section, Potwar Basin.


**Figure 8.13.** The regressive phase in the TRP 1 cycle created the sequence boundary (SBP 1) which is shown by presence of iron crust (non deposition surface) on the sandstone of the Patala Formation exposed in the Kalabagh Hills Section, Trans Indus Ranges, north-west Pakistan.

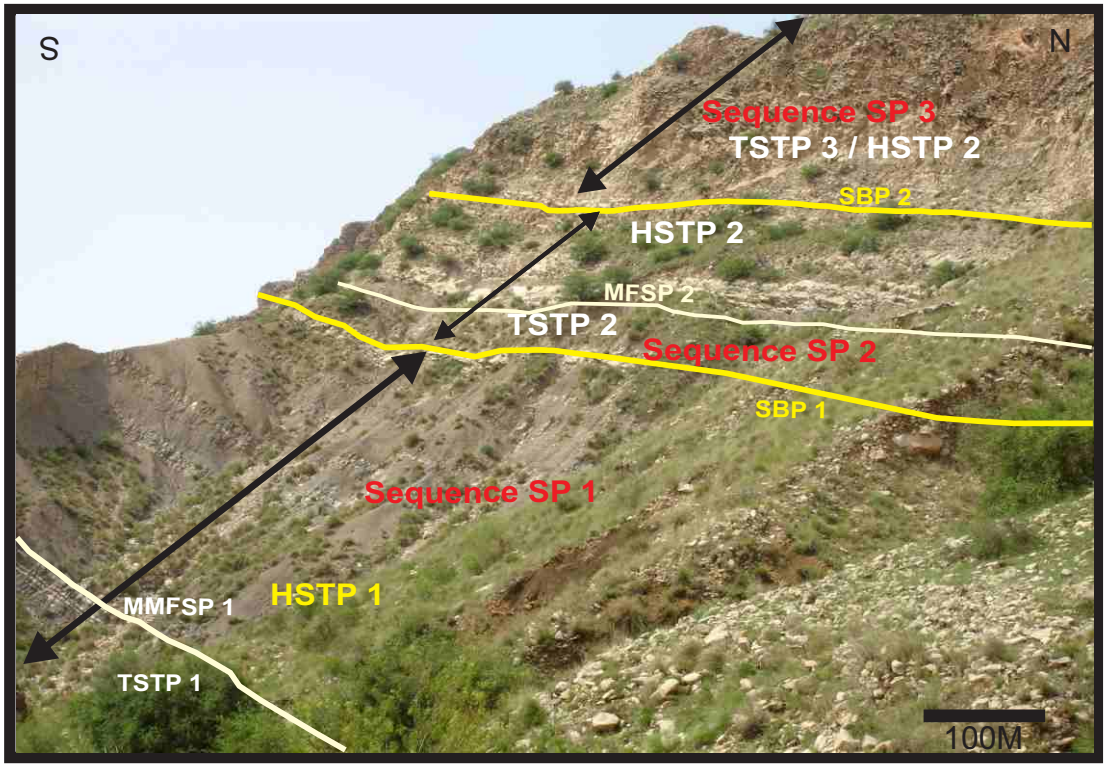


**Figure 8.14.** The sequence SP1 and sequence SP 2 are separated by the sequence boundary (SBP 1). SP 2 sequence consists of the lower middle part of the Nammal Formation which was deposited in the TSTP 2 and the HSTP 2 is separated by a maximum flooding surface (MFSP 2). It is separated from the overlying sequence SP 3 by the sequence boundary (SBP 2) in the Nammal Gorge Section, Central Salt Range, Potwar Basin.

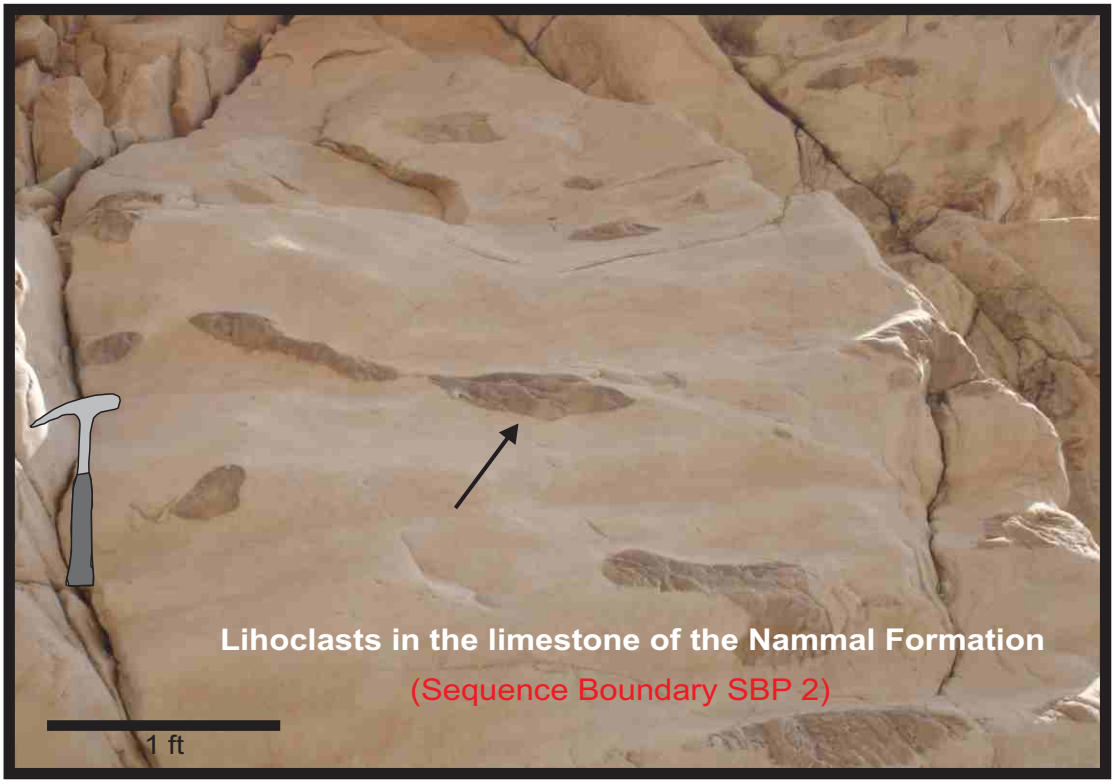


**Figure 8.15.** The embedded lithoclasts of limestones within the massive limestone of Nammal Formation indicates exposure of the carbonate platform in the Nammal Gorge Section, Central Salt Range, Potwar Basin.


**Figure 8.16.** The upper part of the Nammal Formation shows deposition in the HSTP 3 in the Nammal Gorge Section, Central Salt Range, Potwar Basin.

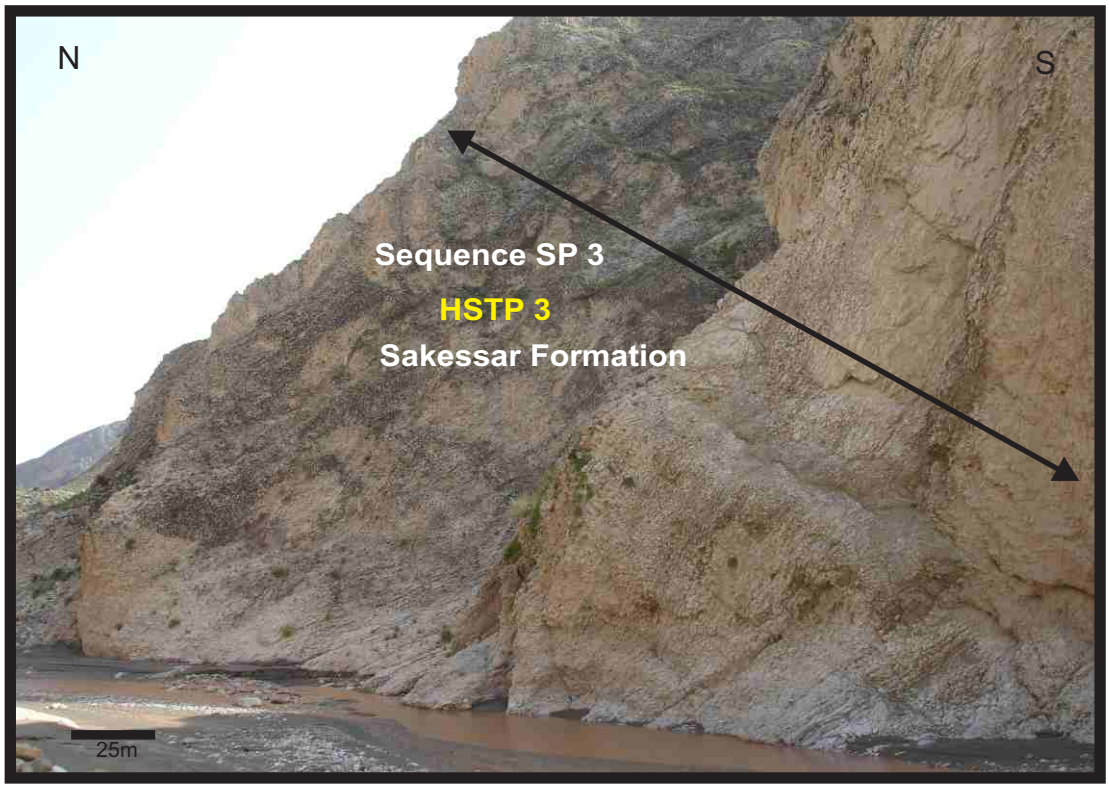


**Figure 8.17.** Thick bedded to massive ramp platform carbonates of the Sakessar Formation show a shallowing upward trend in the HSTP 3 in the Chichali Nala Section, the Trans Indus Ranges, north-west Pakistan.

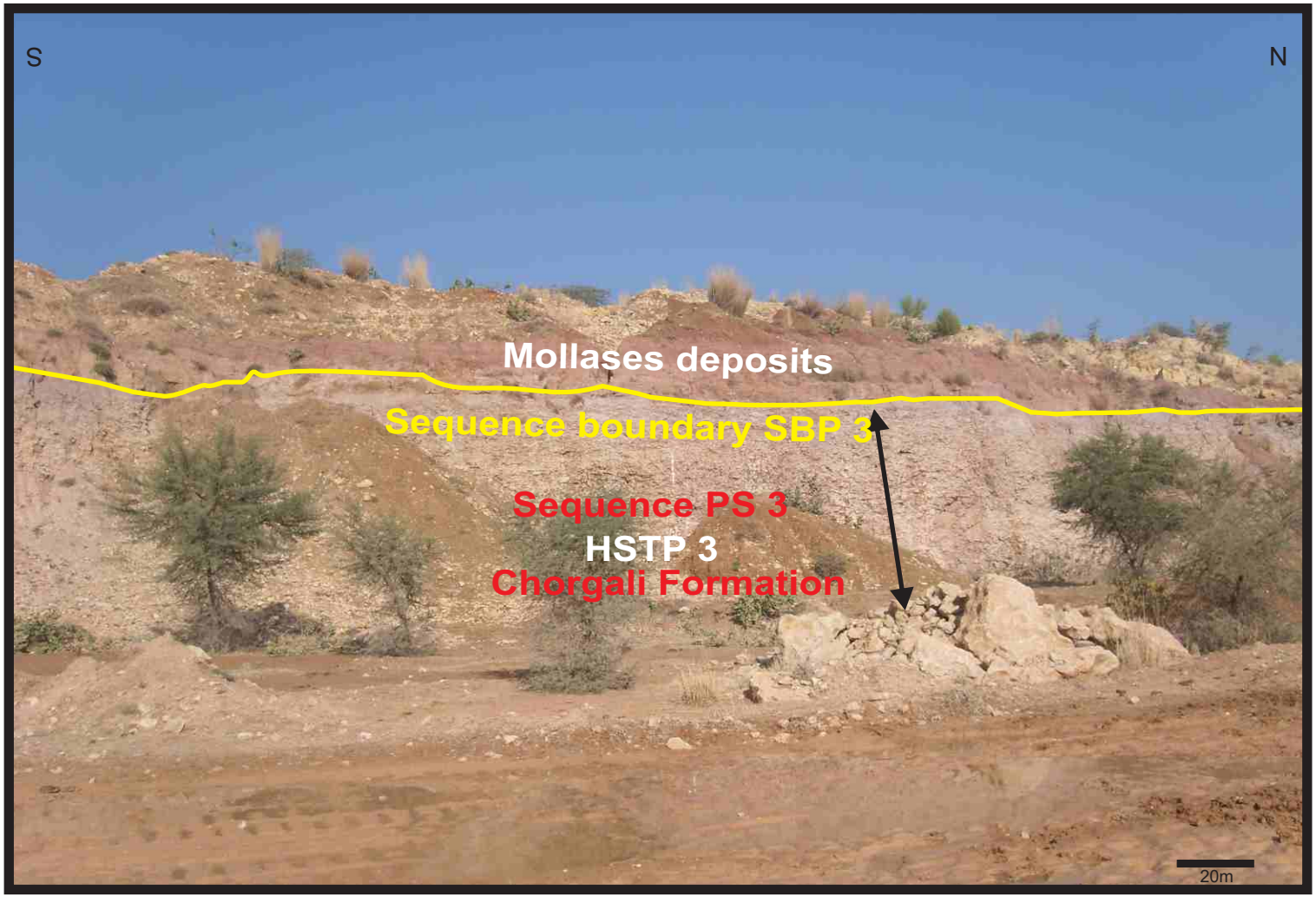


**Figure 8.18.** Thick bedded to massive ramp platform carbonates of the Chorgali Formation shows deposition during HSTP 3. The SP 3 is separated from the overlying Miocene mollasses deposits by the the sequence boundary SBP 3, exposed in the Gharibwal Cement Factory Section, Eastern Salt Range, Potwar Basin.

## 8.5 Tectono-stratigraphic evolution of depositional sequences

### 8.5.1 Thanitian-Lower LIlerdian 1

During the Thanitian the deposition of inner ramp to distal middle ramp carbonates of the Lockhart Formation was interrupted by the introduction of a deep marine to outer ramp clastic carbonate mixed facies of the Patala Formation in the Kohat and Potwar Basins and the Trans Indus Ranges (TIR) (figures 8.20 & 8.24). The deepening of the basin is most likely related to lithospheric flexural subsidence (figure 8.22) caused by initial loading of Asian plate rocks onto the Indian margin (e.g., Beaumont, 1981; Walcott, 1970; and others), and argues for Early Paleocene collision with Asia (Pivnik and Wells, 1996). Evidence of similar collapse and drowning of Tethyan carbonate shelves as a result of tectonism has been noted from Early Cenozoic rocks in the Mediterranean region (e.g., Bosellini, 1989). The Patala Formation (Shah, 1977), is the equivalent of the Paleocene to Middle Eocene Subathu Formation (Mathur, 1978) in India that is comprised of limestones and mudstones with some fine grained sandstones (Mathur, 1978; Blondeau, 1986). The petrographic indicators of the Patala Formation show orogenic input similar to Subathu clastics in India (Najman et al., 2004). The Subathu Formation composition reflects provenance influence from the Indus suture zone during latest Paleocene–Middle Eocene time, indicating initiation of continent-continent collision and development of a foreland basin by this time (Najman et al., 2004). Onset of the continental collision and initial subsidence of the Himalayan foreland basin is documented by a drastic compositional change in sediments close to the Paleocene-Eocene boundary (Garzanti et al., 1996). Sediments of the Kohat Basin, the Potwar Basin and the TIR record eustatic sea-level changes (figure 8.23) during this period of initial collision between the Indian and Asian Plates (Pivinick & Wells, 1996). The presence of a diverse planktonic foraminiferal fauna in lower-middle part of the Patala Formation during the TSTK 1 deposition in the Kohat Basin and during TSTP 1 deposition in the Potwar Basin and the TIR represents drowning of the carbonate

ramp around 56.6 Ma (figures 8.22 and 8.24). A close match up exists between this episode of platform flooding and the transgressive systems tract in the Paleocene (Tahitian) stratigraphic cycle TEJAS A (TA 2.1) in global sea level charts of Haq et al. (1987) (figure 8.22). The Lllerdian 1, exposure (56.2 Ma) of the platform is seen in the upper part of the Patala Formation in the Potwar Basin and the TIR and marks the sequence boundary SBP 1 (figure 8.19 C).

The sediments of second sequence SP 2 include uppermost part of the Patala Formation to lower part of the Nammal Formation, which were deposited during the TSTP 2 and subsequent HSTP 2 in the Potwar Basin and the TIR (figure 8.19 B). In the Kohat Basin the lithostratigraphic signature of the platform exposure is not clear, but a very distinct faunal turnover from the *Miscellanea* sp/*Discocyclina* sp/*Lockhartia* sp dominated assemblage to the *Assilina* sp/*Nummulites* sp/*Alveolina* sp dominated assemblage in the upper part of the Patala Formation is seen. The Lower Lllerdian 1 progradational sedimentation in the HSTK 1 continues and follows deposition of the lower-middle part of the Panoba Formation in the Kohat Basin (figures 8.19 A & 8.20) and deposition of the chronostratigraphically equivalent lower part of the Nammal Formation (Lower Lllerdain 1) in the Potwar Basin and the TIR. The lower-middle part of the Panoba and the lower part of the Nammal Formations show deposition in a ramp slope setting with a shallow (*Bulimina, Uvigerina*, milliolids, ostracodes) and deep (*Discocyclina* sp*, Assilina* sp*, Bathysiphon/Guadryina*) mixed assemblages found together. The source of Panoba clastics is attributed to erosion of an uplifted nort-western margin of the Kohat Basin (Pivinick & Wells, 1996). Shallowing and deepening up signatures of the facies are common in the Patala, the Panoba and the Nammal Formations (figures 8.19 A-B).

### 8.5.2 Lower Lllerdian 2- Middle Lllerdian 2

The Lower Lllerdian 2-Middle Lllerdian 2 strata in the Kohat Basin are represented by the upper part of the Panoba Formation, lower to middle upper part of the Sheikhan Formation and the deposition of the chronostratigraphically equivalent middle upper part of the Nammal, Sakessar and Chorgali Formations in the Potwar-

Basin and the TIR (figures 8.20 & 8.24). During this period the HSTK 1 sedimentation in the Kohat Basin was continuous, while in the Potwar Basin and the TIR, HSTK 1 deposition during Lower Lllerdian 2 was interrupted twice by the exposure-flooding event on the carbonate ramp during the deposition of the lower-middle part of the Nammal Formation. These exposure-flooding events in the Potwar Basin and the TIR are dated as 56.2 Ma and 55 Ma. Although these exposure-flooding events show good correlation with the global sea level charts of Haq et al. (1987) (figure 8.23), it is not found in all studied sections and is also not seen in the Kohat Basin, which implies that local tectonics were also controlling the sedimentation and exposure of the basin. The progradation of the shallow proximal inner ramp facies on the middle ramp facies of the Nammal and the Sakessar Formations with seldom deepening up signatures are also found (figures 8.20, 8.21). The Sheikhan carbonates in the Kohat Basin represent inner to middle ramp conditions with inherited undulations in the depositional basin profile that is fabricating the shallow ramp and restricted lagoonal facies (figures 8.19 B, 8.20-8.21). In the Potwar Basin and the TIR, Nammal marls were deposited in the inner ramp to deep basinal settings, overlain by shallow inner ramp to proximal middle ramp carbonates of the Sakessar and Chorgali Formations (figures 8.19 B, 8.20-8.21). The foraminifera, gastropods, algae, bivalves and brachiopods were dominant in a carbonate ramp setting while reef building organisms were rare or totally absent in both areas.

### 8.5.3 Upper Lllerdian-Middle Cuisian

The Upper Lllerdian-Middle Cusian is represented by the middle to upper part of the Sheikhan Formation in the north-east and Jatta gypsum facies in the south-west of the Kohat Basin (figures 8.19 A & 8.21). The onset of the first regression (figure 8.24) in the Kohat Basin started around 52.8 Ma when a condensed sequence of the sandy arenaceous limestone with interbeds of the gypsiferous shales started deposition in a restricted marine enclosed basinal setting (figure 8.19 C). The biostratigraphic age marker species of *Alveolina rotundata, Assilina laxispira* and *Orbitolites complanatus*, representing Biozones BFZP 3 (B) appear in a condensed section, which indicates mixing of the species due to telescoping of sediments in the regression phase (figure 8.19 C). The condensed section represents deposition during

Middle Lllerdian 2-Middle Cuisian. This condensed section is also seen in the chronostratigraphically equivalent BFZP 3 (B) Biozone in the middle upper part of the Chorgali Formation exposed in the Eastern Salt Range. The species of *Nummulites, Assilina, Operculina* and *Discocyclina* characterize the condensed section in the Potwar Basin. Similar foraminiferal fauna is recorded in the condensed section of a ramp carbonate platform setting in the south-eastern Pyrenean foreland basin (NE Spain), western Tethys (Serra Kiel et al., 2003). Although regression in the Kohat and Potwar Basin started earlier as evidenced in the condensed section, The biostratigraphic data presented here suggest that a complete exposure of the basin took place around 49.5 Ma (figures 8.19 A & C). This is the time of an eustatic sea level fall in the Global Sea Level Charts of Haq et al. (1987) ( figure 8.23). Thus, the collisional tectonics clearly played an important role in the restriction of the sea, caused complete cessation of the marine sedimentation in the area. These data suggest that this regression was accelerated by the global sea-level fall around 49.5 Ma. This fall defines the sequence boundary SBK 1 in the Kohat Basin and sequence boundary SBP 3 in the Potwar Basin and the TIR (figures 8.19 A-C, & 8.24).

### 8.5.4 Upper Cuisian-Lower Lutetian 2

After the Middle Cuisian eustatic sea level regression (ca. 49.5 Ma) (figure 8.23), fluvial continental deposits of the Kuldana Formation were deposited in the Kohat Basin during a lowstand systems tract progradation (figure 8.19 A) in the Upper Cuisian to Lower Lutetian 2 (figure 8.21). The Kuldana Formation comprises flood plain red clays and fluvial channel sandstones and marginal marine clastic facies. In this study, Late Cuisian to Early Lutetian 2 age of the Kuldana Formation is corroborated by the foraminiferal biostratigraphic evidence from the underlying Middle Cuisian Sheikhan Formation and the overlying Middle Lutetian 1, Kohat Formation in the Kohat Basin (figures 8.19 A & C). Our biostratigraphic age data reinforce the Early-Middle Eocene age of the Kuldana Formation assigned to it on the basis of mammal and other vertebrate remains (Gingerich, 2003). The lowstand systems tract deposits of the Kuldana Formation in the Kohat Basin are chronostratigraphicaly equivalent to the intervening lowstand system tract in the -

stratigraphic cycle TEJAS A TA 3.1, shown in the global sea level charts of Haq et al (1987) (figure 8.23). In the southeastern Pyrenean foreland basin (NE Spain), western Tethys (Serra Kiel et al., 2003), facies similar to the Kuldana Formation are recorded in the Pontils Formation (Ferrer, 1971), upgraded to the Pontils Group by Anadón (1978a) which is composed of red mudstone, siltstone, sandstone and conglomerate, and limestone of lacustrine facies. It is up to 900 m thick and is attributed to the Late Ypresian-Early Bartonian age (Anadón and Feist, 1981). In the Paris Basin there is a known unconformity (Hottinger & Schaub 1960, Aubry 1985), due to a major sea-level drop, between the Sables de Cuise (*Nummulites planulatus* beds, Cuisian, upper Zone NP12) and the Calcaire grossier (*Nummulites laevigatus* beds, Lutetian, upper Zone NP14) (Molina, 2006). This comparison allows us to reinforce the notion that the lowstand sedimentation of the Kuldana Formation was a possible consequence of the global sea-level fall at 49.5 Ma (figure 8.23). When the Lower-Middle Eocene mammal-bearing sections of northern Pakistan are considered in geographic context there is a trend toward greater sediment accumulation and, by inference, more rapid subsidence toward the southwest, with less accumulation and less rapid subsidence in the northeast. However, paleocurrent directions in fluvial parts of the Kuldana Formation indicate sediments derivation from an upland source or sources in the northwest (figure 8.22), with rivers flowing toward the southeast across the outcrop belt (Wells, 1983; Pivnik and Wells, 1996), making northwest-southeast the likely orientation of any onshore-offshore trend in paleogeography (Gingerich, 2003).

Petrographic studies of foreland basin sedimentary rocks in India and Pakistan document orogenic-derived detritus in Eocene strata (Critelli and Garzanti, 1994; Najman and Garzanti, 2000; Pivnik and Wells, 1996). By contrast, coeval sedimentary rocks of the Eocene Bhainskati Formation (Sakai, 1989; Sakai et al., 1992) along strike to the east in the foreland basin in Nepal show scant petrographic evidence of orogenic input (DeCelles et al., 1998a). In Nepal and farther east in the Bengal Basin, Bangladesh (Uddin and Lundberg, 1998), the earliest clear evidence of erosion from the Himalaya is found in Miocene rocks. Such data open the potential for substantial along-strike diachroneity of the collision zone (e.g., Najman and Garzanti, 2000; Uddin and Lundberg, 1998). The facies analysis and biostratigraphic

age constraints of the Kuldana Formation in Kohat Basin indicate that clastic input was synorogenic and the likely souce of clastics was situated northwest of the study area.

### 8.5.5 Middle Lutetian 1-Upper Lutetian

The deposition of Kohat Formation on Middle Lutetian 1-Upper Lutetian carbonate ramp was restricted to the Kohat Basin and there is no chronostratigraphic equivalent in the Potwar Basin and the TIR (figures 8.19 A & C). The Kohat Formation shows deposition in a wave washed foraminiferal barrier forebank-backbank lagoonal conditions within carbonate ramp settings (figure 8.21). The foraminiferal fauna thrived on the ramp and indicates productive oligotrophic conditions. Reef building organisms were absent and early development of the foraminiferal banks created a barrier in the Middle Lutetian 1-Middle Luteteian 2, and restricted but deep lagoonal backbank muddy ramp settings in the Upper Lutetian time. The backbank muddy ramp setting was deep enough to favour deposition of the micritic mudstones and wackestones. Forebank foraminiferal barrier (figure 8.21) setting favoured deposition of the high energy foraminiferal bank facies with an increasing depth gradient. *Alveolina* sp./*Nummulites* sp. dominated assemblage occurred in the proximal part and *Nummulites* sp./*Assilina* sp. dominated assemblage occurred in the distal part of the forebank settings. The Middle Lutetian 1 reestablishment of marine conditions in the Kohat Basin is possibly related to a renewed phase of uplift and crustal loading at the Himalayan suture (Pivinick and Wells, 1996). Additional loading would have caused flexural subsidence in the foreland, creating a relative sea-level rise that allowed open-marine water into the formerly restricted basin (fgures 8.22 & 8.24). The eastward transition from carbonate to muddy coastal deposits reflects a clastic source to the east of the Kohat Basin, possibly the clastic wedge described by Bossart and Ottiger (1989) in the Kashmir syntaxis (Pivinick and Wells, 1996). Our data show that Middle Lutetian eustatic sea level rise has affected dynamics of the depositional processes in the Kohat Basin and can be correlated with the transgressive system tract deposited during eustatic sea level rise in the TEJAS A TA 3 stratigraphic cycle in the global sea level charts of Haq et al. (1987) (figure 8.23). The early transgression has deposited the Upper-

transitional marine facies of the Upper Kuldana Formation were deposited overlying the fluvial deposits of the Lower Kuldana Formation and a full fledged transgression of the platform is seen in the carbonates of the Kohat Formation in the TSTK 2/HSTK 2 in the Kohat Basin (figures 8.19 A & 8.22). Naggapa (1959) described the distribution of foraminiferal fauna and facies in Pakistan/India/Burma and concluded that the Kirthar Transgression (Kirthar was used as an equivalent to Middle Lutetian stage by him) was a major transgression covering India (Weastern Narbada Valley, South of Combay, Cutch, Aasam), Pakistan (Sind, Baluchistan, Kohat and Potwar), Burma (Anarkan, Andamans) and whole of Indonesia. The Lutetian transgression, where a dozen of identical species of *Nummulites* have been found in the Alps and in the Himalaya during the Lutetian, indicates that the transgression was not only continuous but synochronous intercontinentaly (Sarkar, 1967). In the stratotype section of the Lutetian in the Paris Basin the sedimentation took place on a marine continental shelf, a transgression allowed the development of *Nummulites laevigatus* in the Lower and Middle Lutetian, but the presence of *Alveolina boscii* and *Orbitolites complanatus* indicates that the environment gradually became restricted since the Middle Lutetian (Blondeau, 1981). In the Kohat Basin the species of *Nummulites beaumonti, Nummulites globulus, Nummulites acutus, Assilina pappilata, Assilina granulosa, Assilina laminosa, Assilina exponense* and *Assilina cancellata* are dominating the carbonate platform forming forebank and deep backbank lagoonal facies. These species are showing a high degree of diversity, increase in size, and high degree of flosculization as seen in *Alveolina* sp (Naggapa, 1959) that indicates favourable conditions for living. The geographic and age distribution of these species lend support to the theory of aneustatic sea level rise during Middle Lutetian 1.

The foraminiferal biostratigraphy implies that Middle Lutetian 1 transgression persisted up to the Upper Lutetian and final closure of the Tethys Ocean took place around 41.2 Ma in the Kohat Basin (figures 8.19 A, 8.19 C & 8.22). The most often quoted age of India-Asia collision is 55–50 Ma (de Sigoyer et al., 2000; Klootwijk et al., 1992; Searle et al., 1997), but the degree of diachroneity is disputed (Rowley, 1996, 1998; Searle et al., 1997). Metamorphism of the subducting Indian crust took place after the collision, possibly diachronous from west to east. Eclogite facies-

metamorphism occurred by 49 Ma (Pognante and Spencer, 1991; Tonarini et al., 1993). Another phase of later metamorphism have also been recognized: phase 1 metamorphism (M1) at ca. 40 Ma was the result of the crustal thickening due to thrust stacking of the India Plate (Staubli, 1989; Searle and Rex, 1989; Metcalfe, 1993). The timing of the later phase of the metamorphism (M 1) at ca. 40 Ma supports the comparable timing of the complete closure of the Tethys Ocean due to collision of the India and Asia in the Kohat Basin. Our data also allow the biostratigraphic and facies record to be brought into better alignment with the marine $^{87}Sr/^{86}Sr$ isotopic record where a marked rise in the $^{87}Sr/^{86}Sr$ values around ~40 Ma is attributed to the Himalayan erosion (Richter et al., 1992).

### 8.5.6 Foreland basin deposits

The Miocene–Pliocene foreland basin sediments of the study area include the Muree, the Kamilial, the Chiji, the Nagri and the Dhok Pathan Formations respectively. The Muree Formation is composed of dark greyish brown, greenish grey and occasionally purple, medium to coarse-grained sandstone, purple or reddish brown siltstone and shale and subordinate intra-formational conglomerate. The formation is mainly unfossiliferous and only a few plant remains and vertebrate fossils have been reported. It is overlain by the Kamlial Formation, dated as 18–14 Ma (Johnson et al., 1985). The Kamlial Formation consist of purple-grey and dark brick-red sandstone which is medium to coarse grained and contains interbeds of hard purple shale and yellow and purple intra-formational conglomerate. A number of fossil mammals have been recorded from the formation, which indicate middle to late Miocene age to the formation. The formation is conformably overlain by the Chinji Formation of the Siwalik Group of middle Miocene to Pleistocene (Johnson et al., 1985). The Chinji formation mainly consists of red shale with frequent intervals of grey to green, soft sandstone. The Chinji Formation conformably underlies the Nagri Formation (Danilchik and Shah, 1967). The age assigned to the formation is late Miocene. The Nagri Formation is mainly composed of grey to greenish-grey sandstone with 30% of red shale and minor conglomerate in the Kohat Plateau. Early Pliocene age is assigned to the Nagri Formation the Kohat-Potwar Basins (Shah, 1977). The Dhok Pathan Formation is the youngest unit and consists of conglomerate and sandstones and it conformably overlies the Nagri Formation.

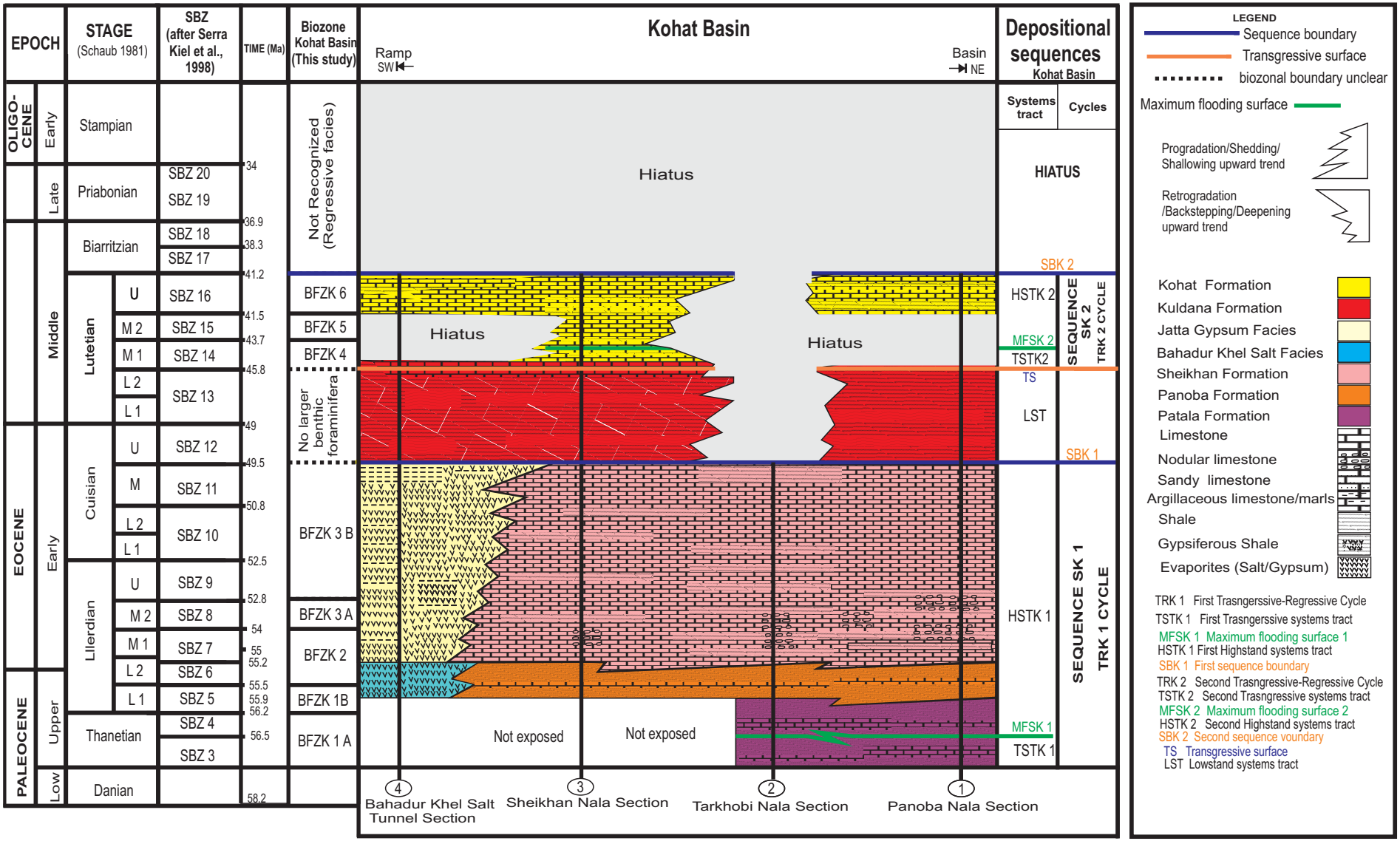


**Figure 8.19 A**. The archectecture of the Paleogene depositional sequences showing retrogradation (backstepping) and progradation (shedding) of the carbonate ramp in different study sections (for location map of study sections see also figure 1.1) in the Kohat Basin, northwest Pakistan.

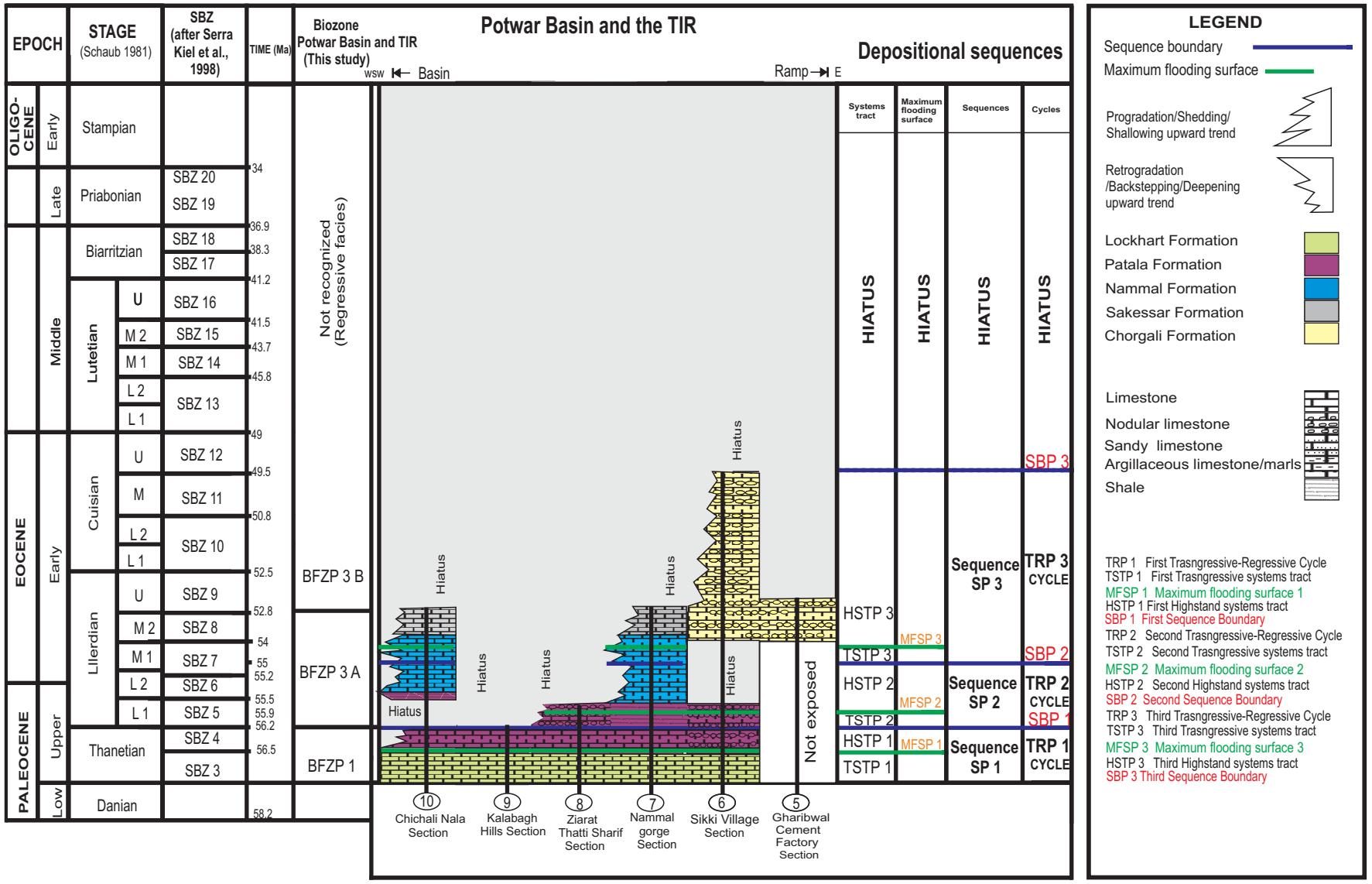


**Figure 8.19 B**. The architecture of Paleogene depositional sequences showing retrogradation (backstepping) and progradation (shedding) of the carbonate ramp in different study sections (for location map of study sections see also figure 1.2) in the Potwar Basin and the TIR, northwest Pakistan.

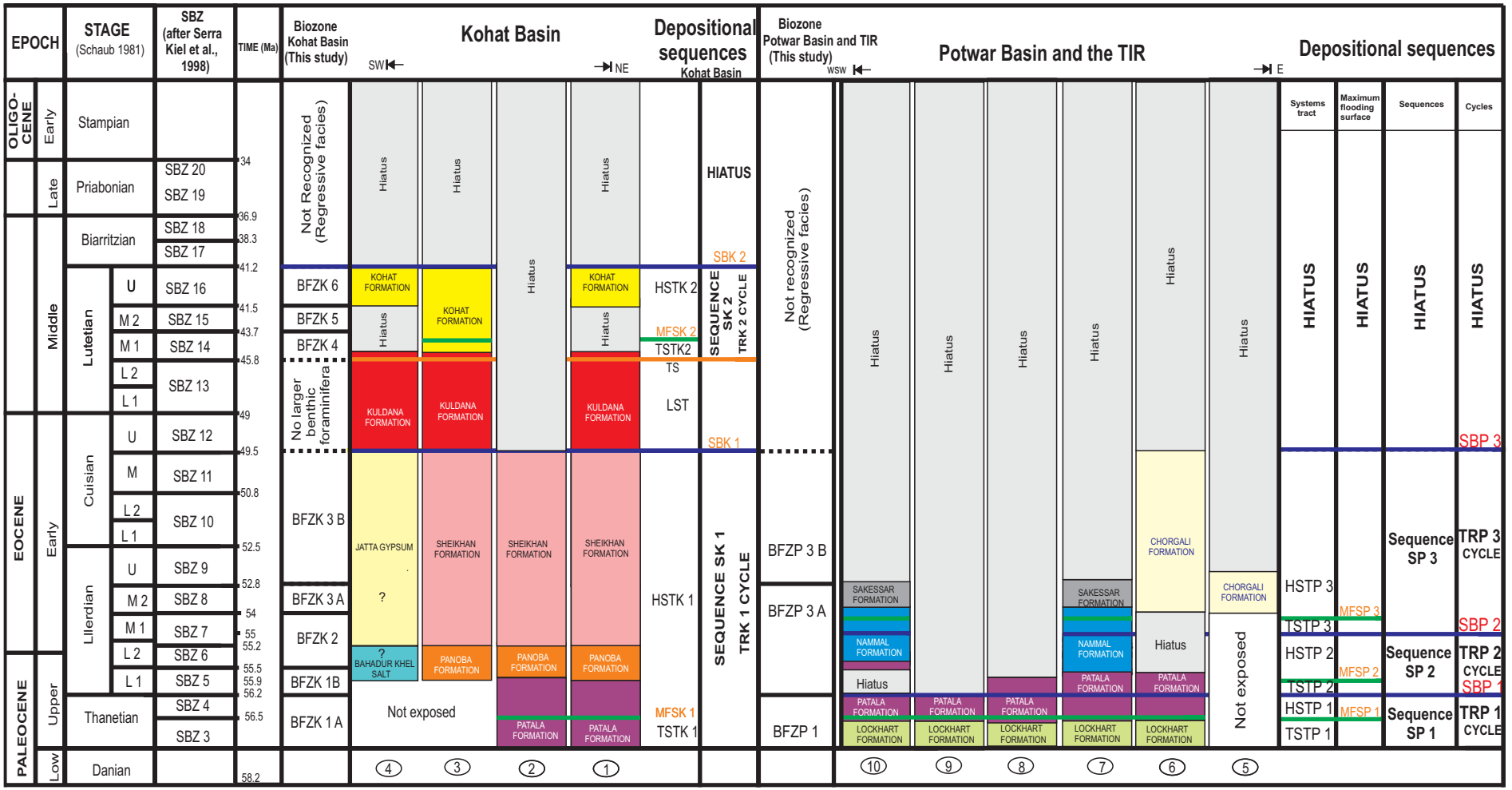


**Figure 8.19C** Bio-chronostratigraphic framework of the Paleogene rocks of the Kohat Basin, Potwar Basin and the TIR, northwest Pakistan. (see page number 314 for full description)

**Symbols**

- Sequence boundary
- Transgressive surface
- biozonal boundary unclear
- Maximum flooding surface
- ? Age not confirmed

**(Figure 8.19 C).** Depositional sequences and bio-chronostratigraphic framework of the Paleogene rocks of the Kohat Basin, Potwar Basin and the TIR, northwest Pakistan is presented. Paleogene larger benthic foraminiferal biozones of the Kohat Basin (BFZK 1-BFZK 6 Biozones) and Potwar Basin and the TIR (BFZP 1-BFZP 3) are compared with shallow benthic foraminiferal Biozones of Serra Kiel et al. (1998) and calibrated with the standard chronostartigraphy that follows Berggeren et al. (1995) to constrain geological ages of the stratigraphic units. The Paleogene depositional sequences of the Kohat Basin were depsoited in two Transgressive-Regressive cycles (TRK 1 and TRK 2). The TRK 1 cycle is represented by the BFZK 1-BFZK 3 Biozones and shows deposition of the Sequence SK 1 during Thanitian to middle Cuisian time in a transgressive phase which has deposited a transgressive system tract (TSTK 1) and a highstand system tract (HSTK 1). The regressive phase of the TRK1 cycle is marked by the sequence boundary SBK 1 at 49.5 Ma . It follows the the deposition of fluvial deposits in a lowstand systems tract (LST) during Upper Cuisian to Lower Lutetain 2, time. The second Transgressive- Regressive cycle (TRK 2) is represented by the BFZK 4-BFZK 6 Biozones shows deposition in Lower to Middle Lutetian 1 time in a transgressive phase, depositing a transgressive system tract (TSTK 2) and a higstand system tract (HSTK 2). The final closure of the Kohat Basin is recorded at 41.2 Ma in Upper Lutetian time as shown by the BFZK 6 Biozone. The Late Eocene to Oligocene time represents a hiatus in the region. In the Potwar Basin and the TIR three depositional sequences (SP 1, SP 2 and SP3) were deposited in three Transgressive-Regressive cycles (TRP 1 cycle, TRP 2 cycle and TRP 3 cycle). The TRK 1 cycle is represented by the BFZP 1 and BFZP 2 Biozones) deposited Sequence SP 1 during Thanitian to Lower Lllerdian 1 time and comprises a transgressive systems tract (TSTP 1) and a highstand systems tract (HSTP 2) which are separated by a maximum flooding surface (MFSP 1). The regressive phase of the TRP 1 cycle is represented by the SBP 1 sequence boundary. The TRP 2 cycle (represented by the Upper part of BFZP 2 Biozone) deposited Sequence SP 2 in Lower Lllerdian 1 to Middle Lllerdian 2 time in a transgressive systems tract (TSTP 2) separated by maximum flooding surface (MFSP 2) from the subsequent highstand systems tract (HSTP 2). The regressive phase of the TRP 2 cycle is represented by the SBP 2 sequence boundary. The TRP 3 cycle (represented by the BFZP 3 A and BFZP 3 B Biozones) deposited Sequence SP 3 during middle LIlerdian 2 to middle Cuisian time in a transgressive syatems tract (TSTP 3) which is separated by a maximum flooding surface (MFSP 3) from the subsequent highstand systems tract (HSTP 3). The regressive phase is represented by a sequenc boundary SBP 3 around 49.5 Ma which is equivalent to the timing of the SBK 1 sequence boundary in the Kohat Basin. The Tethyan marine sedimentation came to an end with the closure of the Potwar Basin and the TIR in Middle Cuisian (49-49.5 Ma) time. The Middle Eocene to Oligocene time represents a Hiatus in the Potwar Basin and the TIR. From Miocene-Pliocene time the Kohat Basin, Potwar Basin and the TIR became a foreland basin and received thick molasses sediments from the Himalayan erosion in a fluvial system. Different studied sections in the Kohat Basin, Potwar Basin and the TIR are numbered from 1-10 where 1) the Panoba Nala Section (northeastern Kohat Basin) 2) the Sheikhan Nala Section (northeastern Kohat Basin) 3) the Tarkhobi Nala Section (northeastern Kohat Basin) 4) the Bahadur Khel Salt Tunnel Section (southwestern Kohat Basin) 5) the Gharibwal Cement Factory Section (Eastern Salt Range, Potwar Basin) 6) the Sikki Village Section (Eastern Salt Range, Potwar Basin) 7) the Nammal Gorge Section (Central Salt Range, Potwar Basin) 8) the Ziarat Tahtti Sharif Section (Western Salt Range, Potwar Basin), 9) the Kalabagh Hills Section (the Trans Indus Ranges) and 10) the Chichali Nala Scetion (the Trans Indus Ranges)

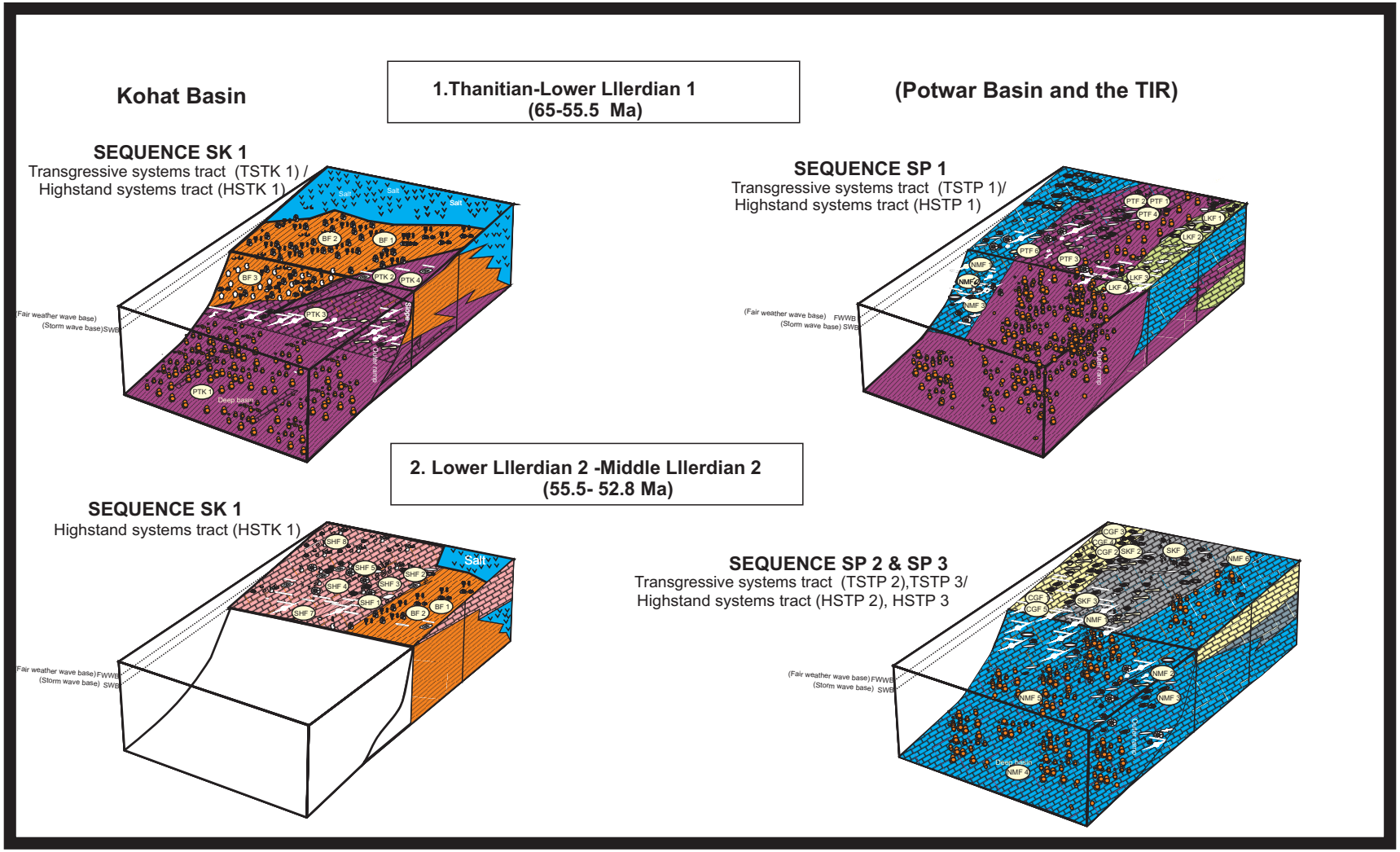


**Figure 8.20.** The figure shows stratigraphic evolution of the Kohat Basin, Potwar Basin and the TIR during the deposition of Sequence SK 1 and Sequences SP 1-3 **1) From Thanitian to Lower Lllerdian 1 (65-55.5 Ma)** deposition of the Patala Formation, the Panoba Formation and the Bahadur Khel Salt represents the transgressive systems tact (TSTK 1) and the subsequent highstand systems tract (HSTK 1) in the Kohat Basin. In the Potwar Basin and the TIR Thanitian to Lower Lllerdian 1 time is characterized by the deposition of Patala Formation and Nammal Formation in the transgressive system tract (TSTP 1) and the higshtand systems tract (HSTP 1) **2) During the Lower Lllerdain 2- Middle Lllerdian 2 (55.5-52.8 Ma)** the Sheikhan Formation carbonates prograded during the HSTK 2 in the Kohat Basin, Potwar Basin and the TIR, deposition of the Nammal Formation, Sakessar Formation and the Chorgali Formation represents shallowing upward sequence of the TSTP 2, HSTP 2, TSTP 3 and HSTP 3 (for details of symbols e.g see figures 6.26 & 7.25).

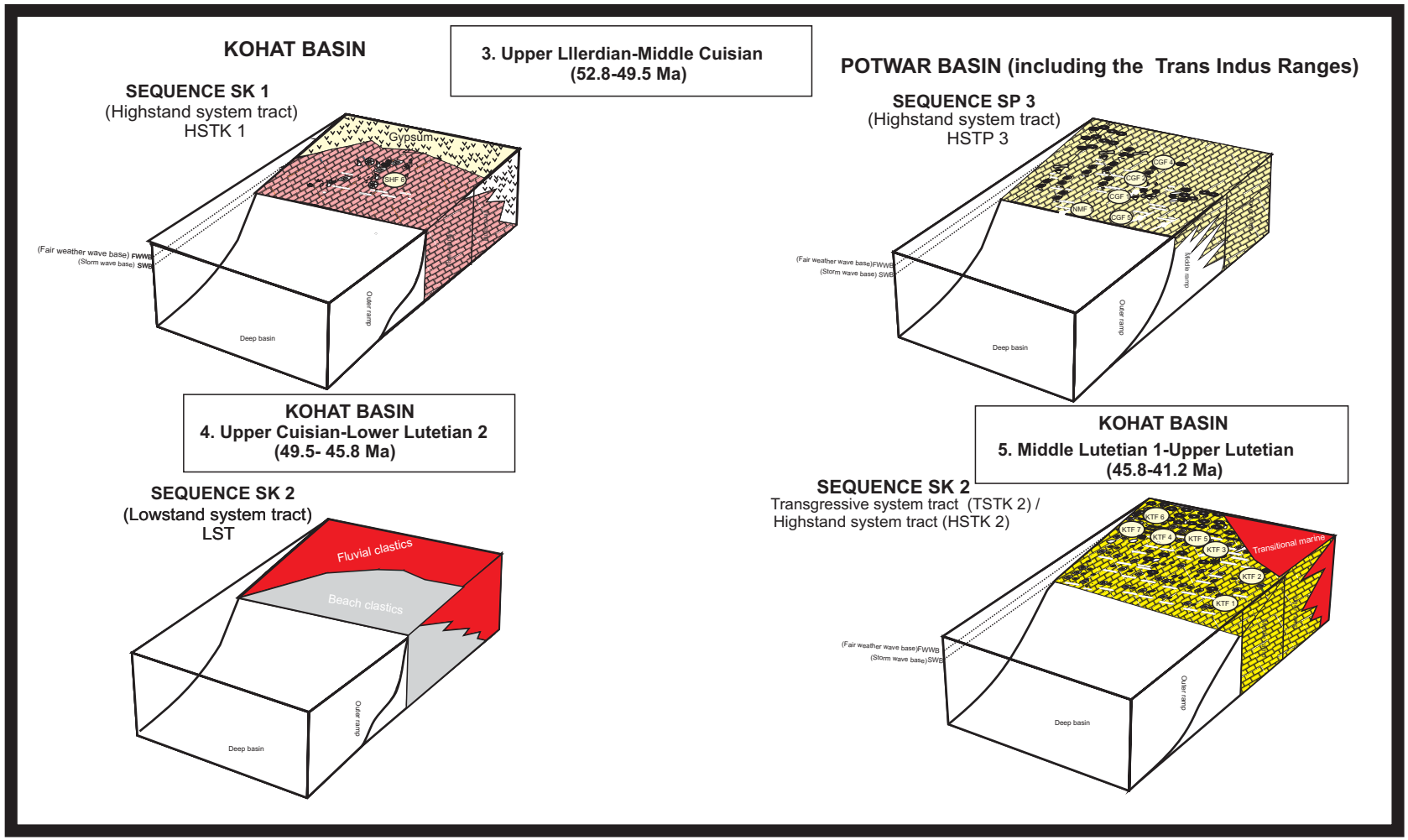


**Figure 8.21.** The figure shows stratigraphic evolution of the Kohat Basin, Potwar Basin and the TIR during the deposition of Sequences SK 1, SK 2 and SP3 **3) From Upper Llerdian to Middle Cuisian (52.8-49.5 Ma)** the upper part of the Sheikhan Formation and the Jatta Gpsum Facies were deposited in a shallowing upward sequence of HSTK 1 in the Kohat Basin while in the Potwar Basin and the TIR the Chorgali Formation shows deposition in the HSTP 3. **4) From Upper Cuisian to Lower Lutetian (49.5-45.8 Ma)** the progradational Kuldana Formation was deposited in the Kohat Basin during the LST while during the same time in the Potwar Basin and the TIR no sedimentation is recorded **5) From Middle Lutetian 1-Upper Lutetian** the transitional marine facies of the Upper Kuldana Formation and thick carbonates of the Kohat Formation were deposited in the Kohat Basin (for details of symbols e.g see figures 6.26 & 7.27).

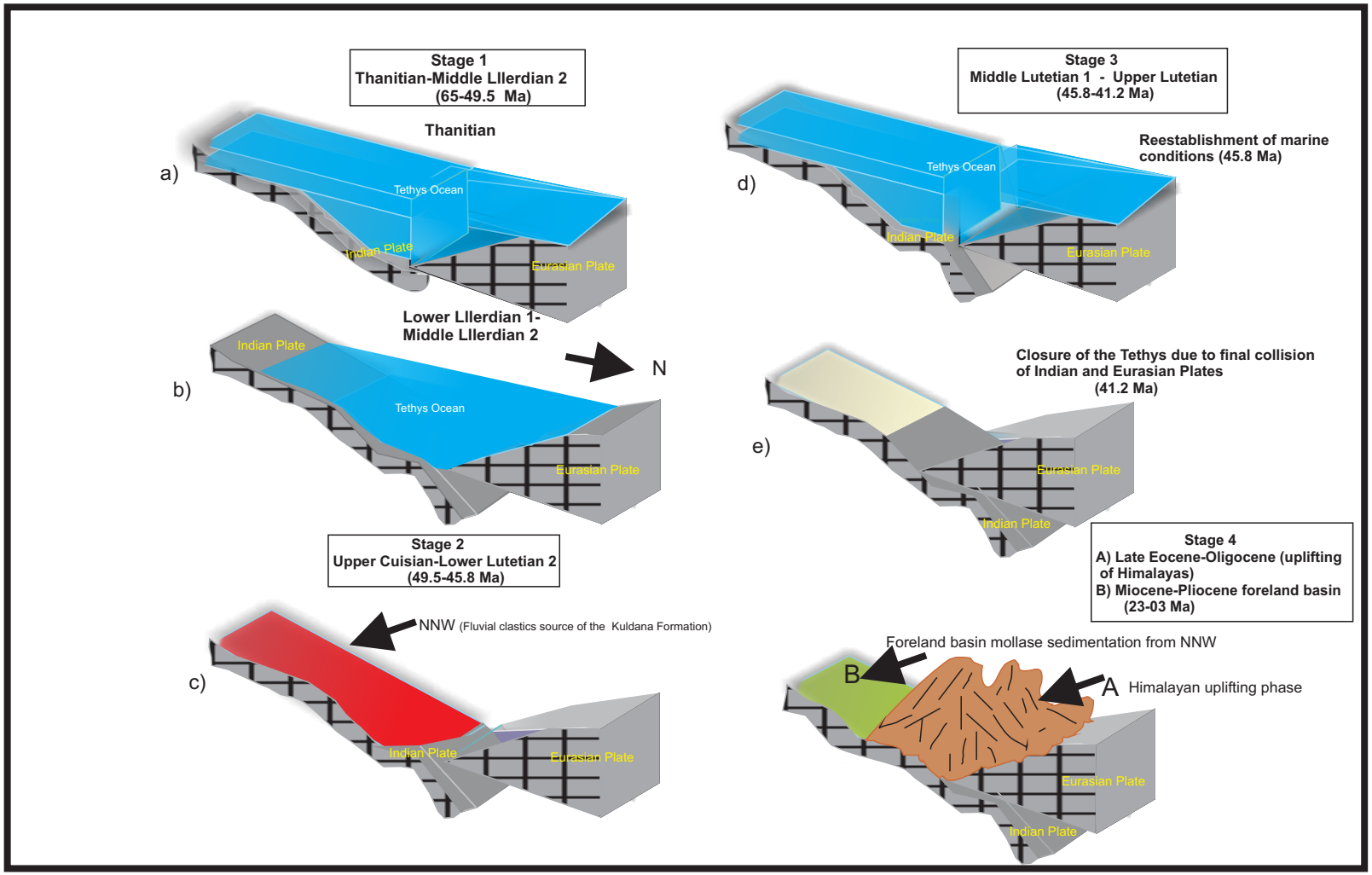


**Figure 8.22.** Paleogene tectonic evolution of the study area in the context of India - Asia collision. **Stage 1** a) initial collision of the India- Asia **b)** restriction of the Tethys Ocean due to uplift in the NNW of the study area (Pivinick & Wells, 1996) **Stage 2:** proto-closure of the Tethys Ocean is followed by synorogenic lowstand clastic progradational sedimentation from the NNW of the study area **Stage 3:** reestablishment of the marine conditions due to continued subsidence related to flexural loading of the Indian Plate (Pivink & Wells 1996) and final closure of the Tethys at 41.2 Ma. **Stage 4 A)** after the collision of the Indian and Eurasian Plates uplifting phase of Himalayas began during Late Eocene-Oligocene time **B)** post-collisional development of a foreland basin and mollasse sedimentation in the study area started during Miocene-Pleistocene)

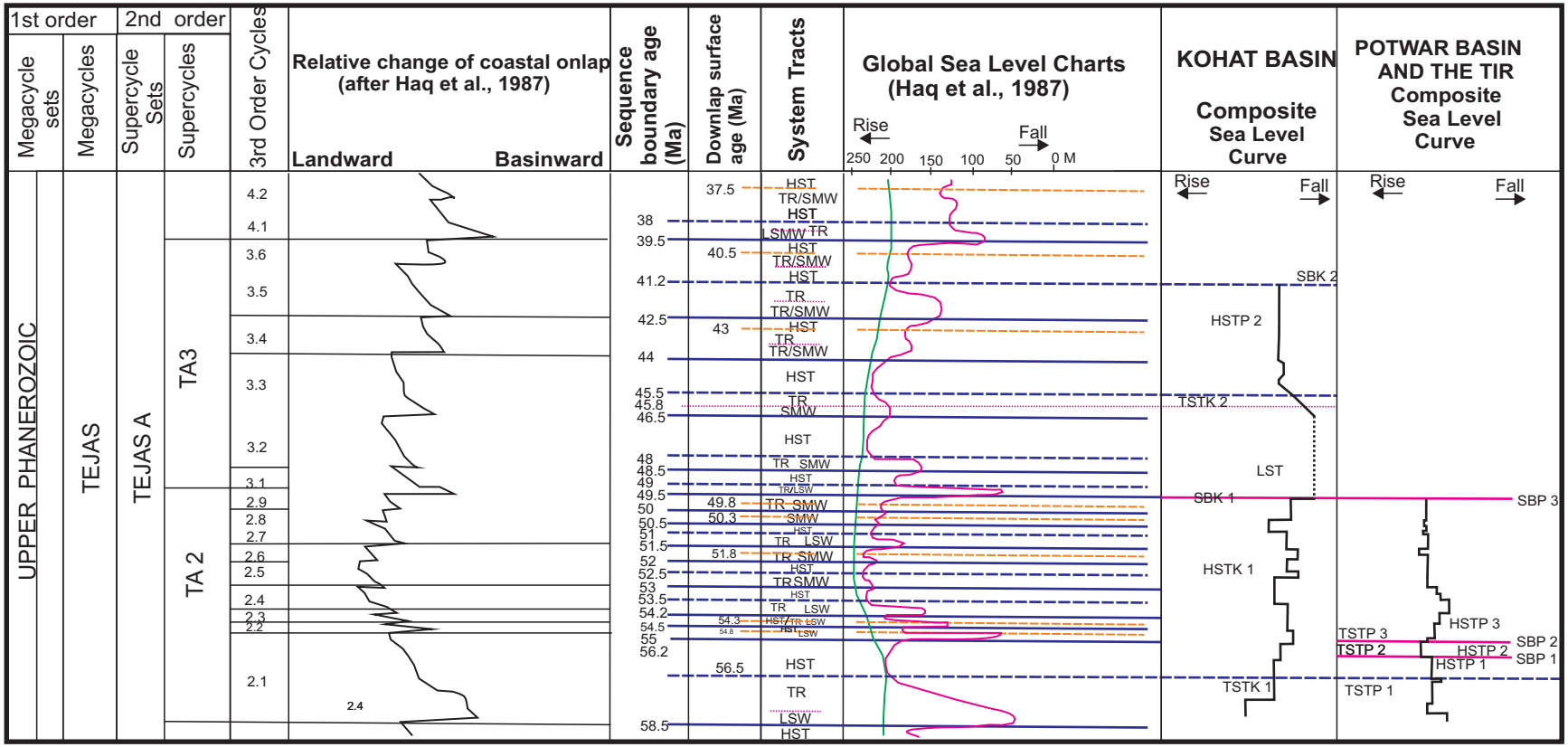


**Figure 8.23:** Comparison of the Paleogene global sea level charts of Haq et al. (1987) with the composite sea level charts inferred from the Paleogene rocks in the Kohat Basin, Potwar Basin and the TIR, nothwest Pakistan. The first marine flooding is compared in the transgressive system tract TSTK 1 in the Kohat Basin and TSTP 1 in the Potwar Basin at 56.5 Ma. The sea level variations in the Potwar Basin between 56.5 and 55 can possibly be compared with 55 Ma eustatic sea level fall in the Haq charts. A major regression at 49.5 Ma is compared with the sea level fall in the Kohat Basin and the Potwar Basin. Eustatic sea level rise at 45.8 Ma can be compared with the TSTK 2/HSTK 2 sedimentation in the Kohat Basin. At 41.2 Ma marine sedimentation in the Kohat Basin was ceased due to the final Indian and Asia collision.(Thick solid lines indicate the major sequence boundaries while dotted lines represents the minor sequence boundaries).

## 8.6. Geohistory of the Kohat Basin, the Potwar Basin and the TIR

Geohistory diagrams were constructed (figure 8.24 A-E, figure 8.25 A-|G) by using biostratigraphic age and paleobathymetric conclusions obtained from the biostratigraphic zonation and relative sea level plots and combining these data with sediment thickness obtained from the outcrop studies.

The foraminiferal biostratigraphy is used to correlate the studied sections within the basin. The paleobathymetric estimates were made by studying the larger benthic foraminifera and other associated macro fauna from all samples. Certain depth zones are demarcated and relative sea level plots are constructed while mean ranges of established depth zones were selected for the construction of geohistory diagrams.

The sediment thickness plots are constructed by calculating sediment thickness for discrete time slices. Based on the biozonal boundaries the ages of the individual rock samples within these stratigraphic units were approximated by extrapolation.

The Geohistory analysis shows that sediments of the Kohat Basin records both periods of subsidence and uplift. During the Late Paleocene (Thanetian) thick exposure of the marine sediments (the Patala Formation) shows gradual increase in subsidence in the northeast due to tectonic pulses and a masked eustatic effect (Haq et al., 1987). In the Lower-Middle Lllerdian continued gradual subsidence due to tectonic pulsation contributed thick sediments of the Panoba Formation and carbonate–clastic mixed sediments of the sheikhan Formation in the northeast (figure 8.24 A-C). Interruption of the gradual subsidence is evidenced in the southwest when restriction of the basin by an emergent barrier (Sheikhan dolomite) is seen that caused deposition of the evaporates (figure 8.24 D) in the isolated hypersaline deep lagoons.

The mean Geohistory diagram (figure 8.24 E) shows that phases of the removal of the portion of sediments which contains the information about the initiation of the uplift and subsequent erosion occurred during Upper Cusian- Middle Lutetian 1. During this period fluvio-marine deposit of the Mamikhel Formation shows an increase in sediment thickness from south to north and a greater subsidence is inferred towards the south. The cessation of marine sedimentation and onset of the fluvio-marine sedimentation is regarded as a consequence of the combined effect of the eustatic sea level fall (Haq et al., 1987) and India-Asia collision. The Middle Lutetian 1 indicates a renewed phase of the marine sedimentation in the Kohat Basin. The north-eastern part of the basin (figure 8.24 A) received thinly bedded, thick succession of carbonates as compared to the southwest (figure 8.24 D), where sediment thickness

decreases substantially, which implies that a grater rate of subsidence was prevailing in the northeast due to tectonic pulsation of the Indian plate. Complete closure of the basin due to India-Asia collision occurred in upper Lutetian.

In the Potwar basin and the Trans Indus Ranges (TIR), the rapid spatial vertical movements complicated the lateral facies distribution but longer periods of quite subsidence may record high frequency eustatic cycles in their stratal patterns and facies sequences. During the Late Paleocene (Thanetian) a greater rate of subsidence related to the flexural loading of the India plate, caused thick marine sedimentation. The tectonic pulses that appear from Geohistory diagrams (figure 8.25 A-G), caused unconformities (SBP1 and SBP 2) which delineate different sedimentary cycles during Lllerdian time. The occurrence of major unconformity e.g SBP 3 during Upper Cuisian is controlled both by tectonics and eustacy. The timing of the tectonic uplift and major eustatic cycles (Haq et al., 1987) is the same, therefore it is inferred that both tectonics and eustacy played an important role in the closure of the basin. The mean Geohistory diagram (figure 8.25 G) indicates that rapid uplift did not allow renewed phase of Middle Lutetian 1 marine sedimentation in the in the Potwar Basin and the TIR to etablish.

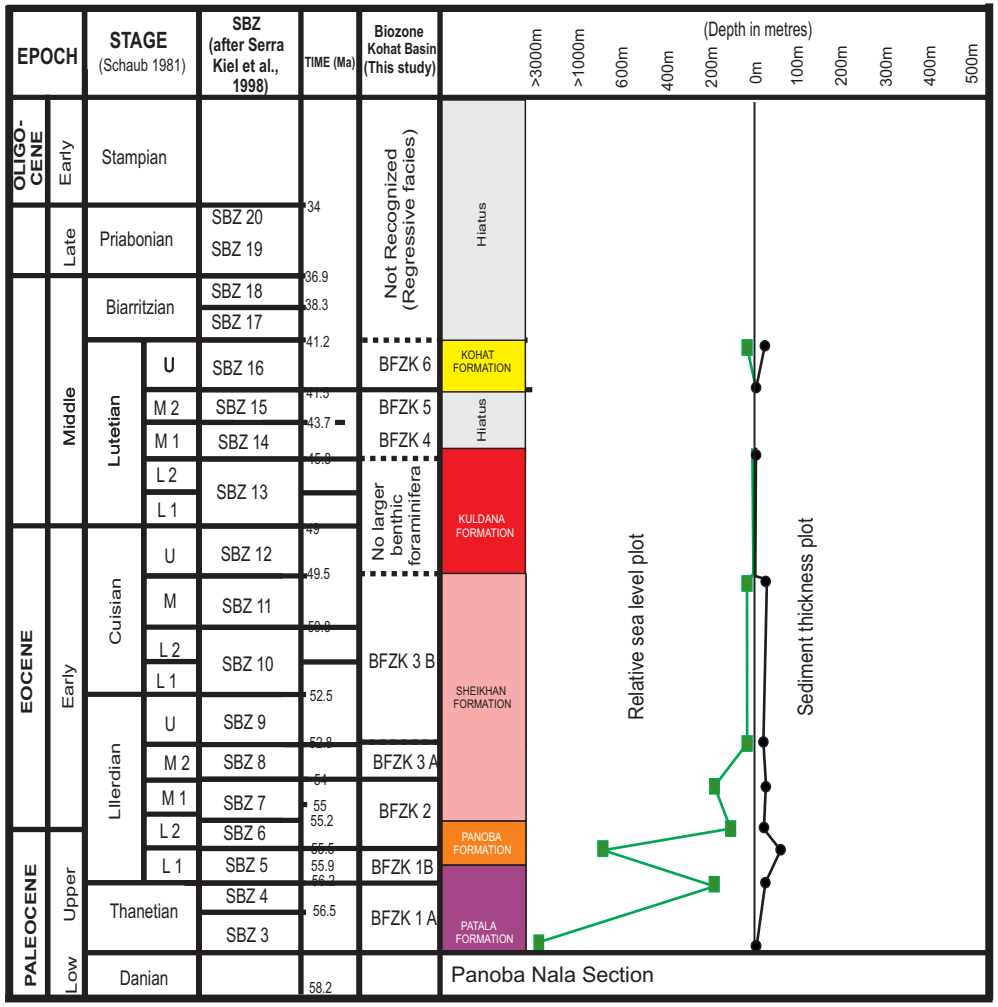


**Figure 8.24 A:** Geohistory diagram of the Panoba Nala Section

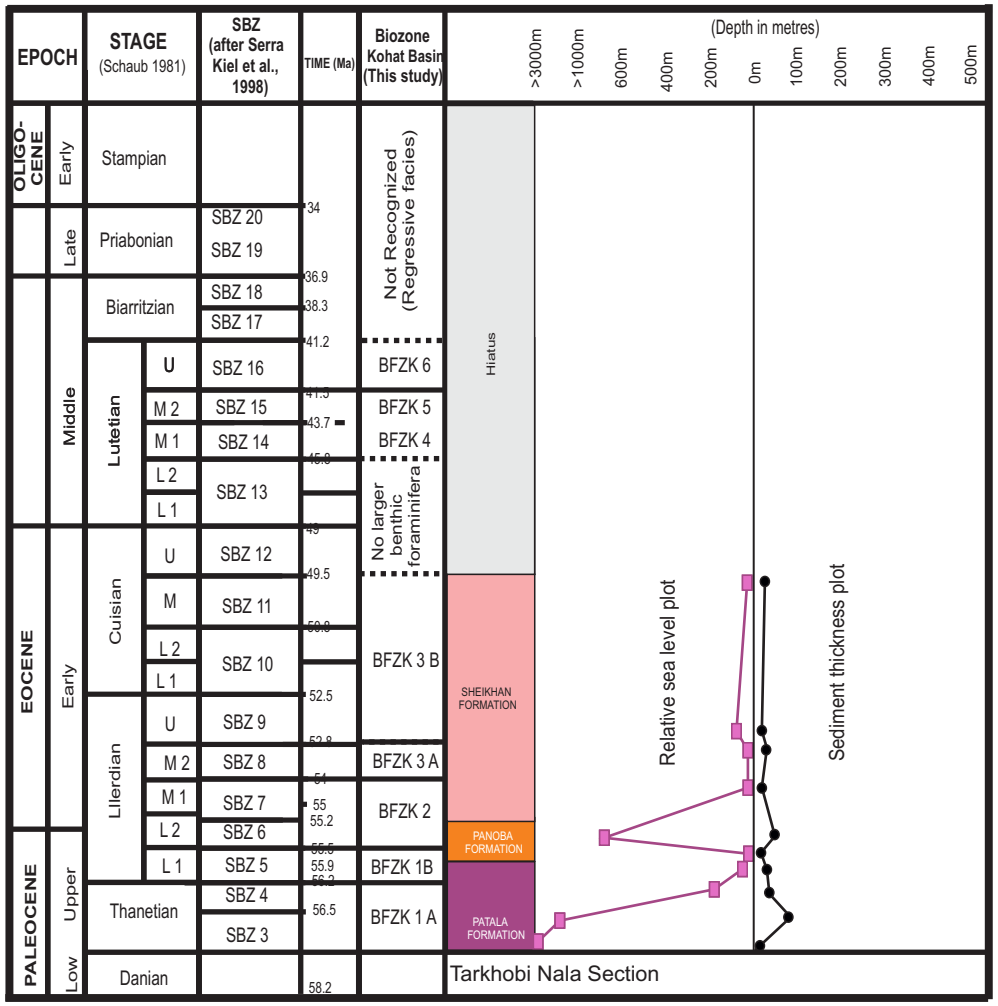


Figure 8.24**B:** Geohistory diagram of the Tarkhobi Nala Section

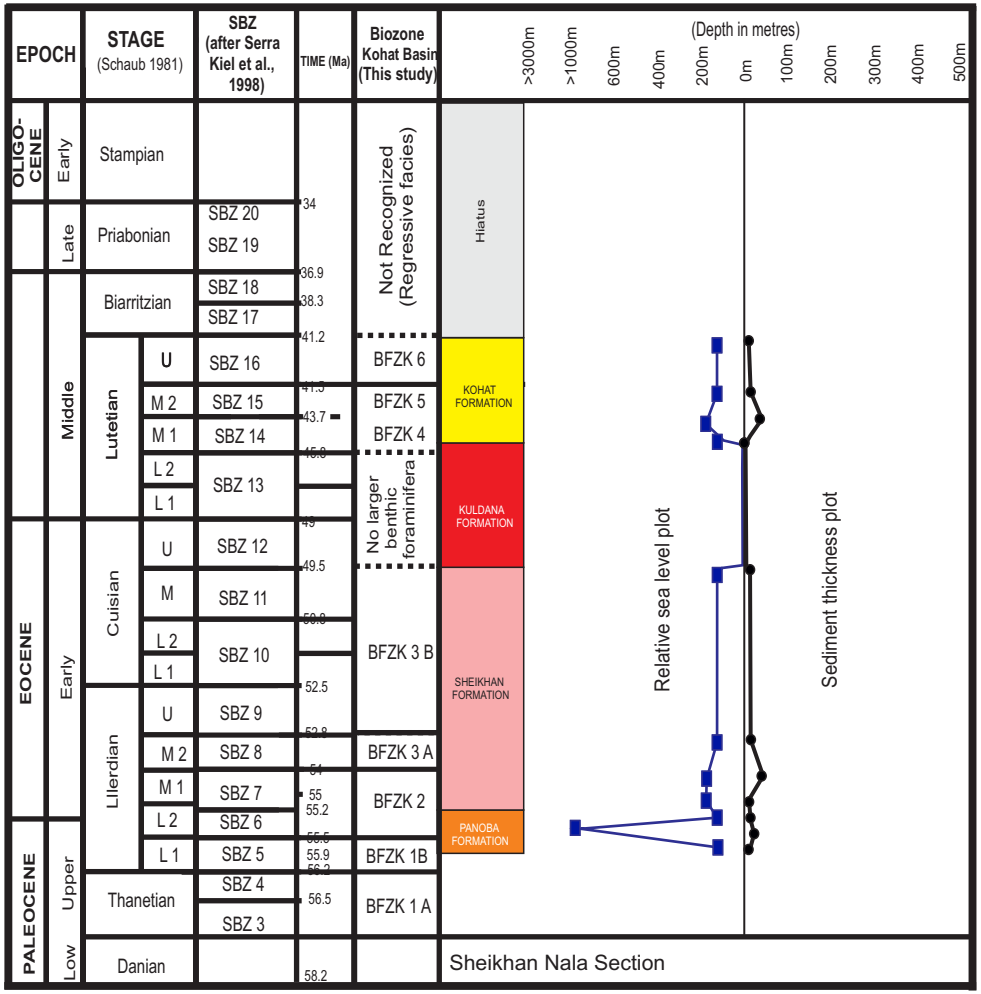


**Figure 8.24 C:** Geohistory diagram of the Sheikhan Nala Section

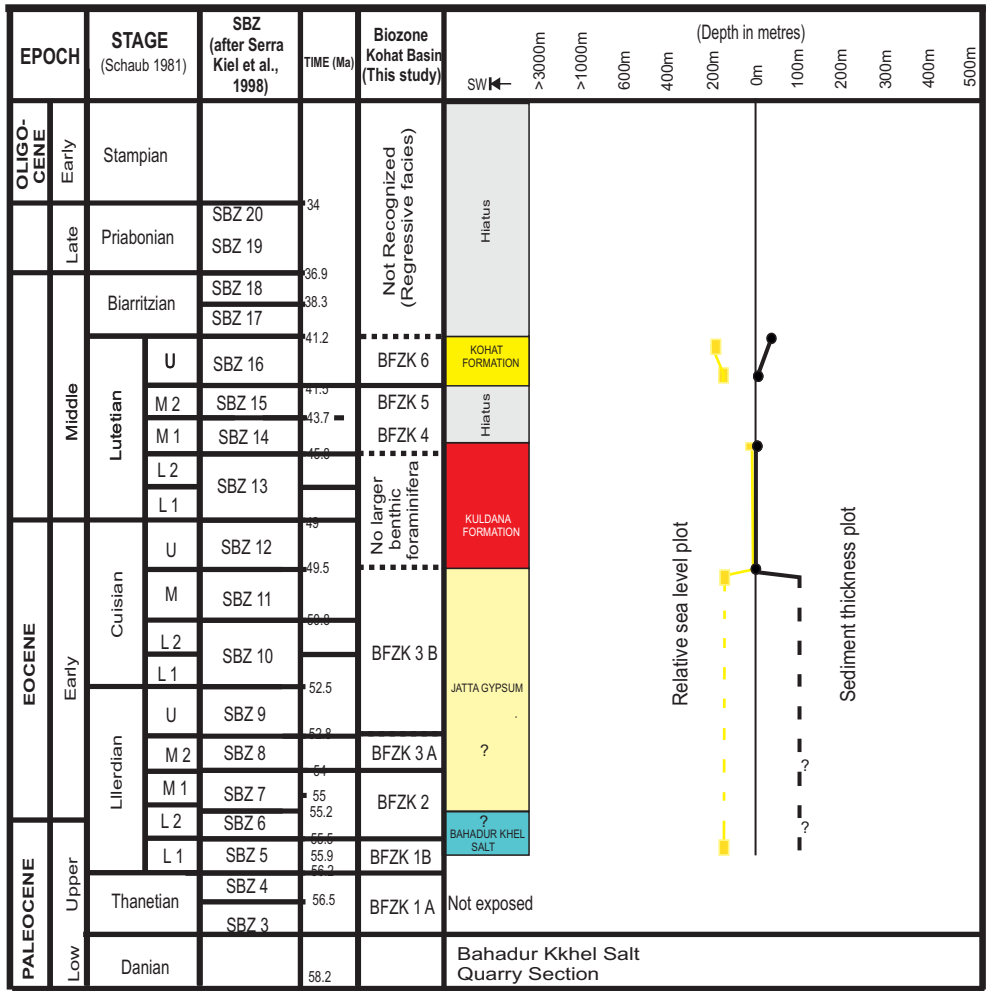


**Figure 8.24 D:** Geohistory diagram of the Bahadur Khel Salt Quarry Section.

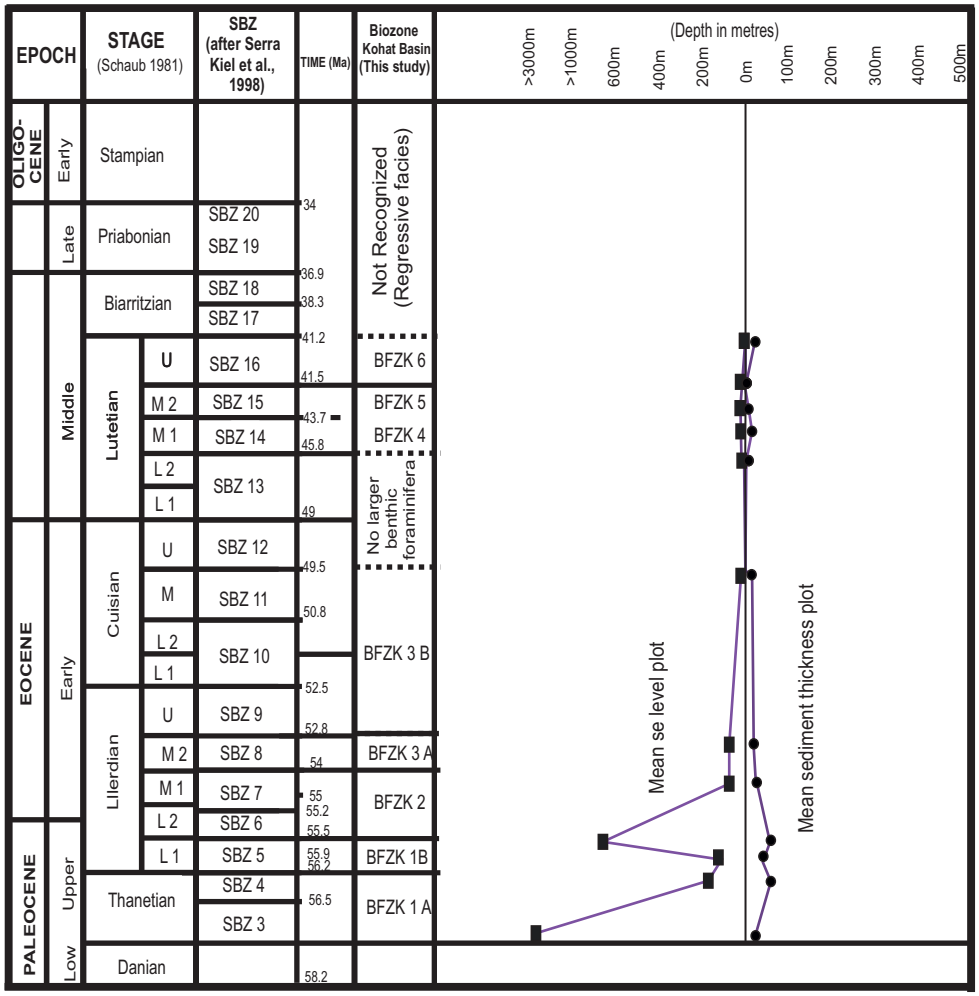


**Figure 8.24 E:** Mean Geohistory diagram of the Kohat Basin

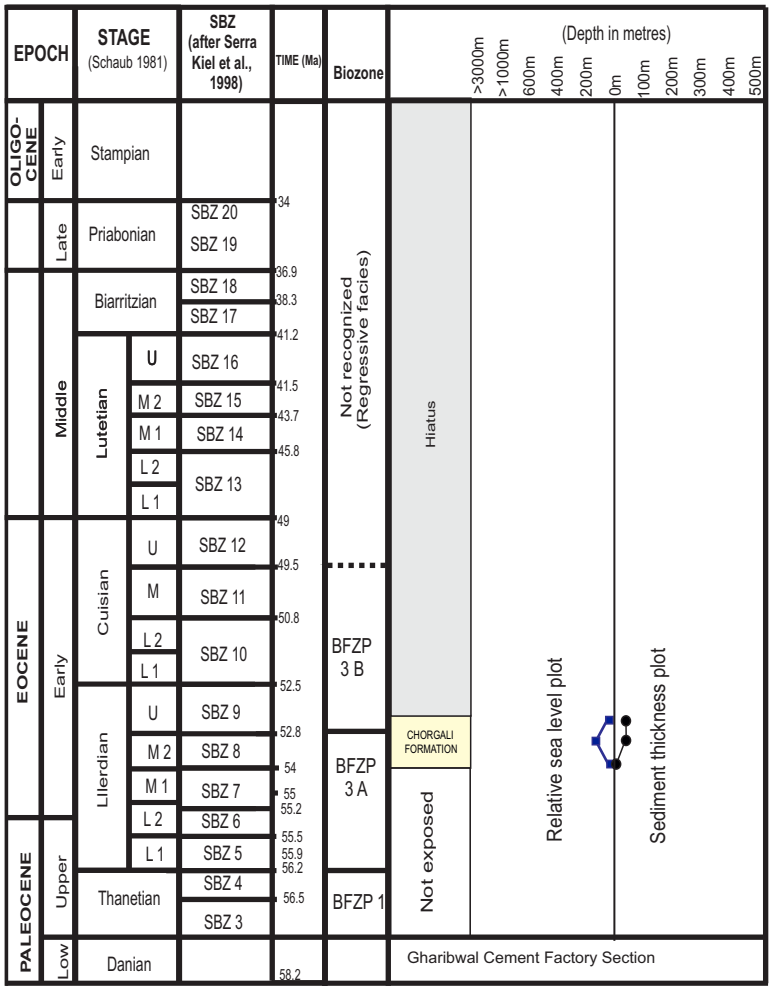


**Figure 8.25 A:** Geohistory diagram of the Gharibwal Cement Factory Section.

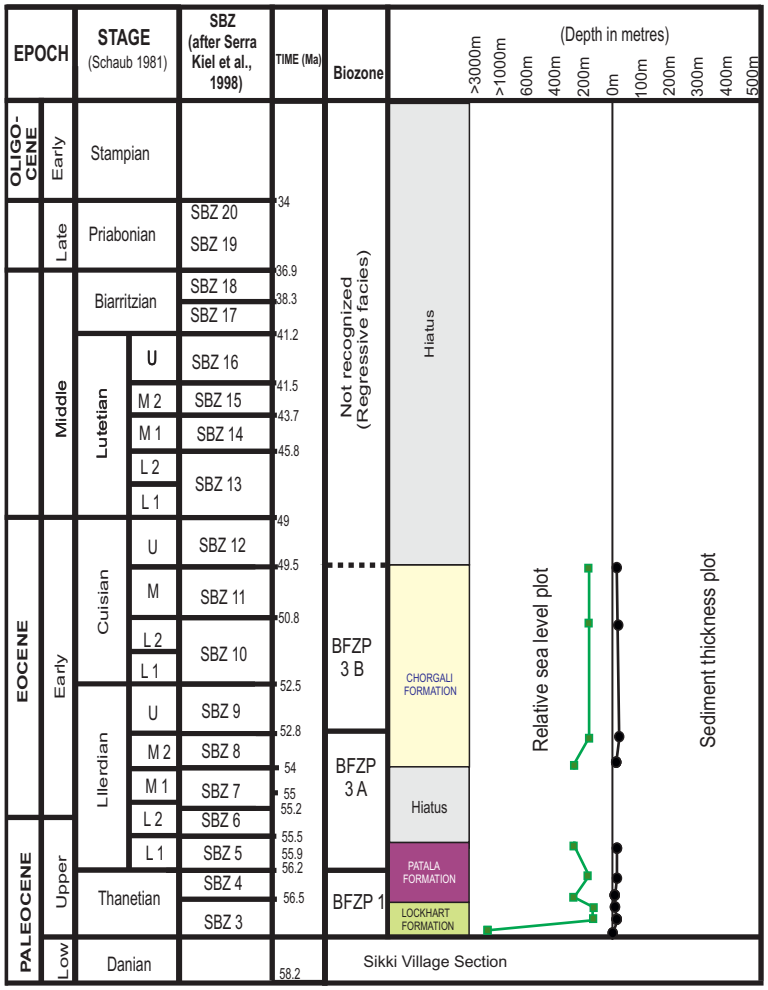


**Figure 8.25 B:** Geohistory diagram of the Sikki Village Section.

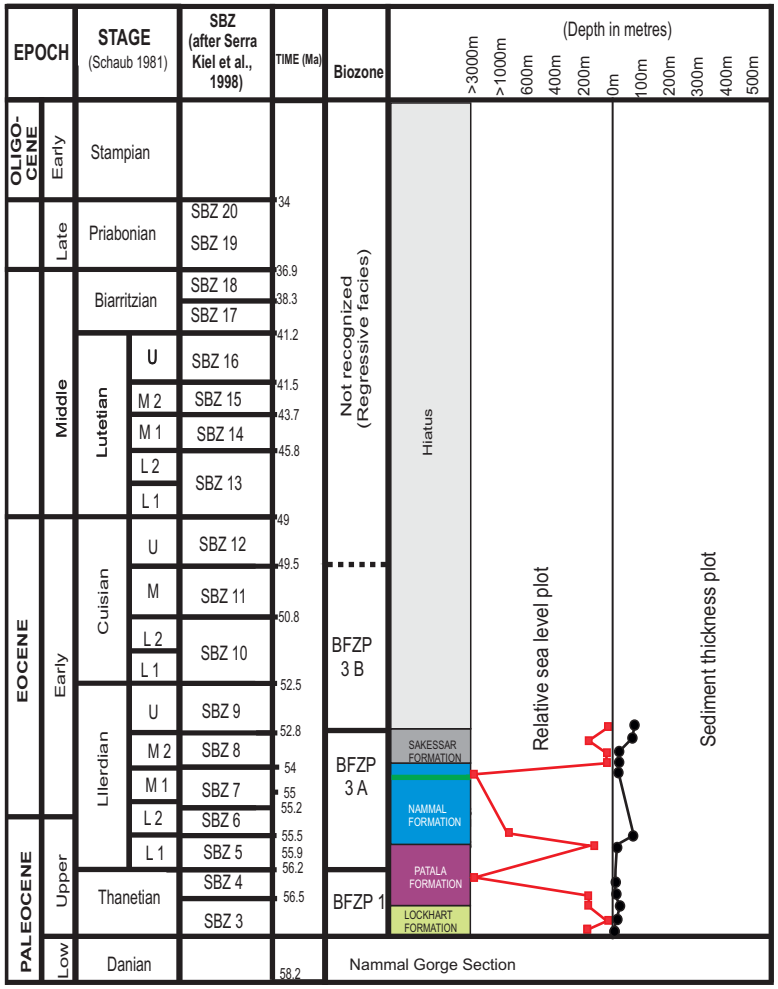


**Figure 8.25 C:** Geohistory diagram of the Nammal Gorge Section.

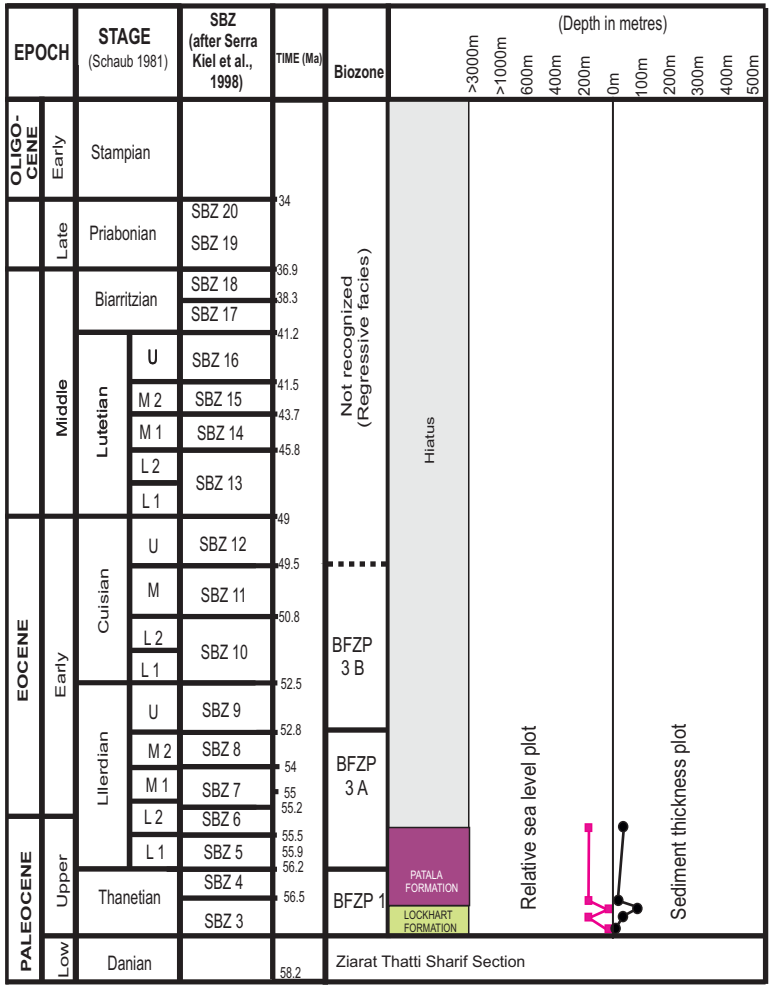


**Figure 8.25 D:** Geohistory diagram of the Ziarat Thatti Sharif Section.

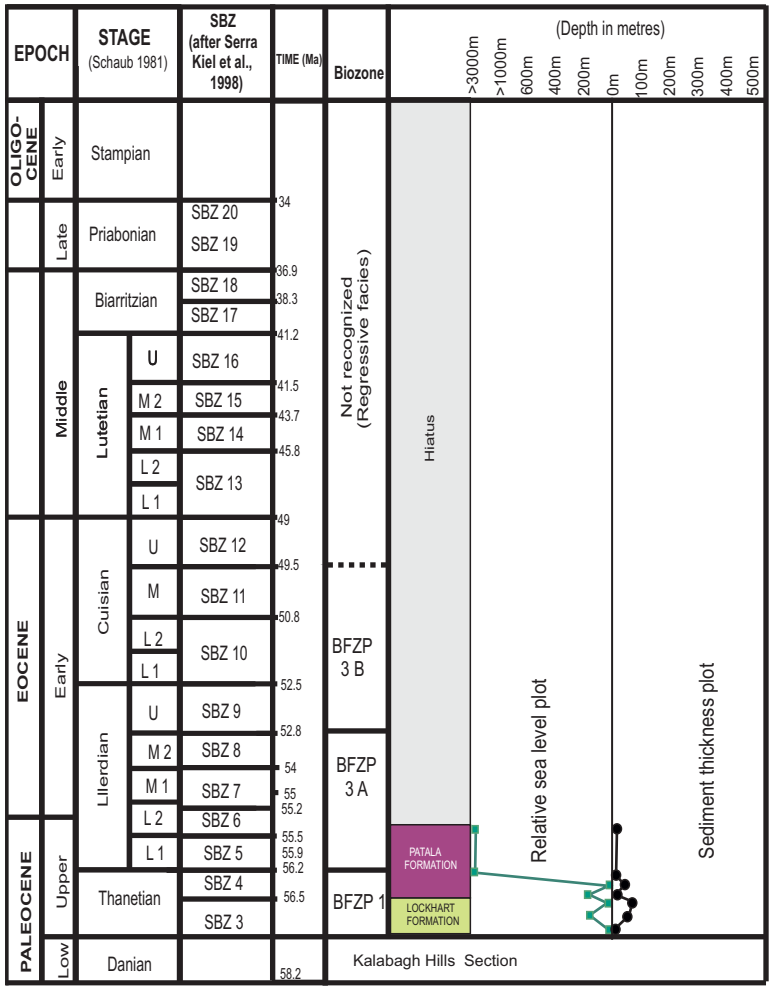


**Figure 8.25 E:** Geohistory diagram of the Kalabagh Hills Section.

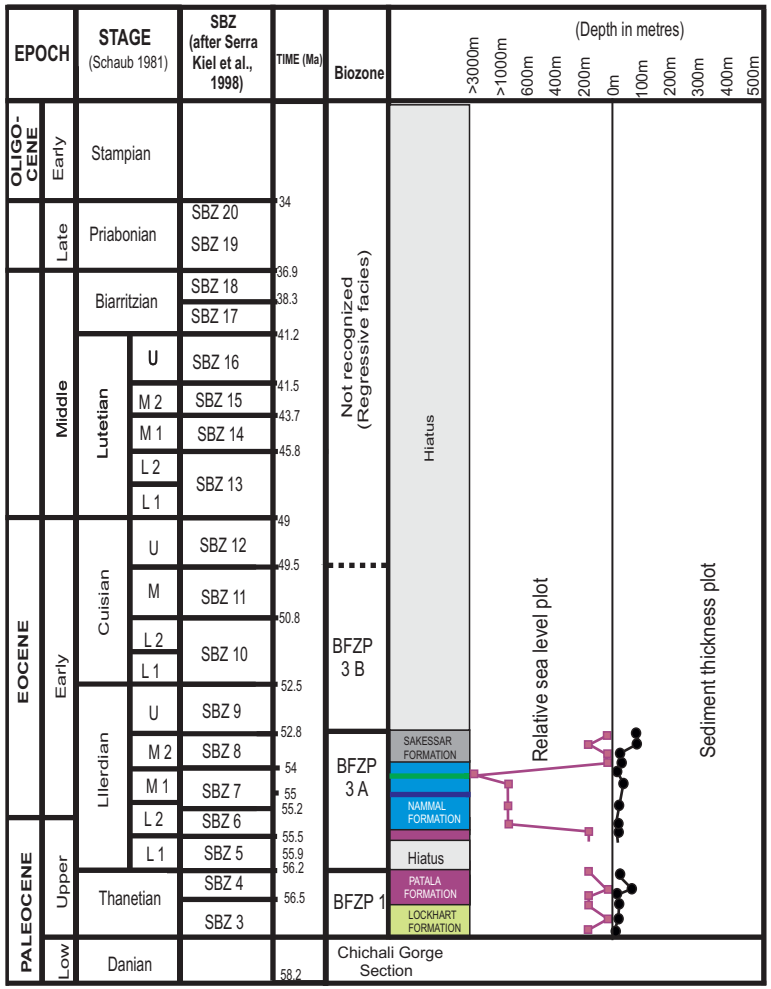


**Figure 8.25 F:** Geohistory diagram of the Chichali Gorge Factory Section.

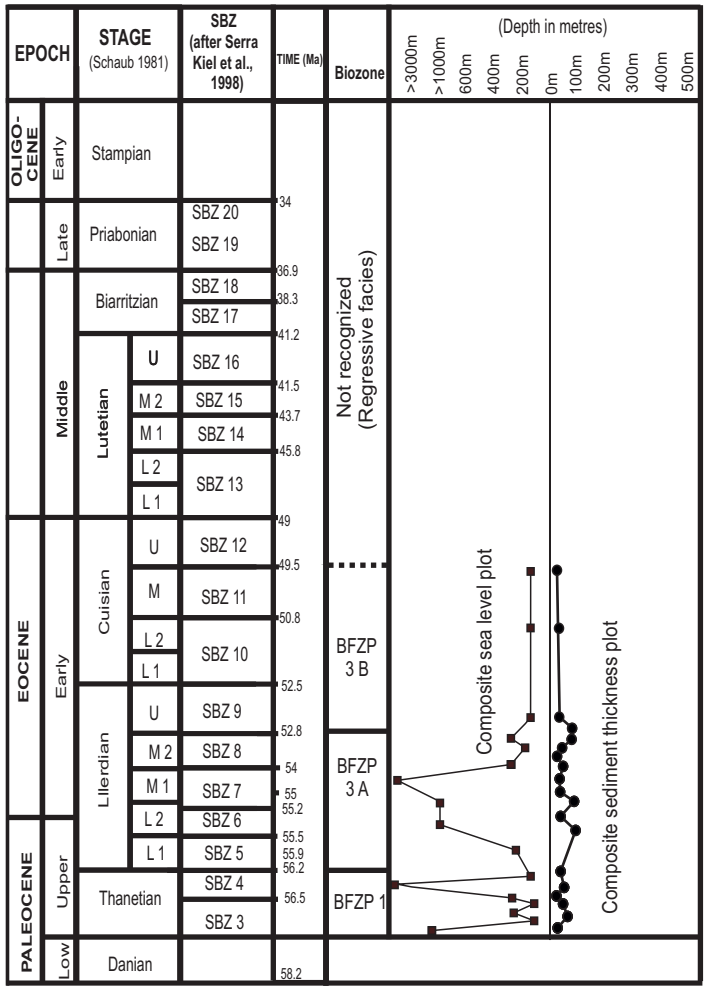


**Figure 8.25 G:** Mean Geohistory diagram of the Potwar Basin and the Trans Indus Ranges (TIR).

## 8.7 Conclusions

The study of the Paleogene tectono-stratigraphic evolution of depositional sequences in the Kohat Basin, Potwar Basin (including the Trans Indus Ranges) in north-west Pakistan evidences major episodes of transgression and regression of the sea. Timing of these major episodes is constrained by using larger benthic foraminiferal biostratigraphy. An insight into the tectono-stratigraphic evolution of the depositional sequences is based on the detailed facies and paleoenvironmental interpretation of the stratigraphic units. The following conclusions can be drawn from this study.

- The Kohat Basin witnesses two cycles of Transgression-Regression and are termed as TRK 1-TRK 2.
- The timing of the TRK 1 cycle is constrained by the BFZK 1-BFZK 3 B Biozones representing Thanitian to Middle Cuisian time. The TRK 1 cycle is characterized by the sequence SK 1 which consists of the Patala Formation, the Panoba Formation, the Sheikhan Formation, the Bahadur Khel Salt and the Jatta Gypsum, deposited in the transgressive phase of the TRK 1 cycle during the TSTK 1 followed by the HSTK 1. There is a gradual shallowing upward facies trend in the SK 1 sequence. The maximum flooding surface MFSK 1 during transgressive phase of the TRC 1 cycle correlates with the eustatic sea level rise at 56.5 Ma in the global sea level charts of Haq et al. (1987).
- The forced regressive phase of the TRK 1 cycle in the Kohat Basin began with the eustatic sea level fall at 49.5 Ma in the global sea level charts of Haq et al. (1987). The regressive phase continues from the Middle Cuisian to Upper Cuisian resulting in the lowstand systems tract (LST) deposits of the Lower Kuldana Formation. The age of the mammal bones bearing Kuldana Formation is constrained (Upper Cuisian to Lower Lutetian 2) by the underlying BFZK 3 (B) Biozone in the Sheikhan Formation and the BFZK 4 Biozone in the overlying Kohat Formation. The deposition was controlled by interplay of eustatic sea-level fall and by the synorogenic sedimentation from the northwest of the study area.

- The TRK 2 cycle began with a eustatic sea-level rise in the Middle Lutetian 1, and can be correlated with the eustatic sea level rise at 45.8 Ma in the global sea level charts of Haq et al. (1987). The upper part of the Kuldana Formation and thick carbonates of the Kohat Formation comprise Sequence SK 2 which was deposited in TSTK 2 and the HSTK 2. The BFZK 4-BFZK 6 Biozones constrain the timing of the transgressive phase of the TRK 2 cycle that is spanning from Middle Lutetian 1 to Upper Lutetian.
- The regressive phase began with the complete exposure of the platform carbonates of the Kohat Formation. The timing of closure of the Kohat Basin is constrained by the BFZK 6 Biozone, representing Upper Lutetian. The final closure of Tethys Ocean in the Kohat Basin occurred at 41.2 Ma.
- The depositional sequences in the Potwar Basin and the TIR are influenced by three Transgressive–Regressive cycles termed as TRP 1-TRP 3.
- The timing of the TRP 1 cycle is constrained by the BFZP 1 Biozone representing Thanitian age. In the transgressive phase of the TRP 1 cycle the sequence SP 1 was deposited which consists of the upper part of the Lockhart Formation and lower middle part of the Patala Formation. These were deposited in TSTP 1 followed by the HSTP 2. The maximum flooding surface MFSP 1 is synchronous with the MFSK 1 in the Kohat Basin and both correlate with the 56.5 Ma eustatic sea level rise in the global sea level charts of Haq et al (1987).
- The regressive phase of the TRP 1 Cycle is represented by the sequence boundary SBP 1 (56.2 Ma), demarcated in the upper part of the Patala Formation and is shown by an exposure surface.
- The timing of the TRP 2 Cycle is constrained by the BFZK 2 Biozone and is spanning from Lower Lllerdian to Upper Lllerdian time. The transgressive phase of the TRP 2 cycle resulted in the deposition of sequence SP2 which comprises the upper part of the Patala Formation and lower part of the

Nammal Formation and shows deposition in the TSTP 2 and subsequent HSTP 2.

- The regressive phase of the TRP 2 cycle is represented by the exposure of the Nammal Formation and is marked by the sequence boundary SBP 2 (55 Ma).
- The timing of the TRP 3 cycle is constrained by the BFZP3 (A) and BFZP 3 (B) Biozones which shows Middle Lllerdian 2 to Middle Cuisian deposition. SP 3 sequence was deposited during the transgressive phase of the TRP 3 cycle. The upper part of the Nammal Formation shows deposition in TSTP 3 followed by deposition of HSTP 3, depositing thick ramp carbonates of the Sakessar and Chorgali Formations.
- In the Potwar Basin and the TIR, the biostratigraphic data suggest that marine conditions vanished in Middle Cuisian time. The combined effects of the collisional tectonics and the eustatic sea level fall at 49.5 Ma as shown in the global sea level charts of Haq et al. (1987) caused closure of the marine basin. This is represented by the sequence boundary SBP 3 which correlates with the SBK 1 sequence boundary in the Kohat Basin.
- The exposure-flooding events associated with the TRP 1-TRP 2 cycles in the Potwar Basin and the TIR are controlled by local tectonics while exposure of the platform at 49.5 Ma links with the global eustatic fall in sea level (Haq et al., 1987).
- The reestablishment of the marine conditions in the Middle Eocene is not recorded in the Potwar Basin. There exists a disconformity spanning from Middle Eocene to Oligocene in the Potwar Basin including the Trans Indus Ranges, whilst this disconformity spans from Upper Eocene to Oligocene in the Kohat Basin.
- The Kohat Basin, Potwar Basin including the TIR became part of the Himalayan foreland basin and received thick fluvial molasses deposits during Miocene to Pliocene time.

## 8.7 Future work

In this thesis I have described the tectono-stratigraphic evolution of the Kohat and Potwar Basins (including the Trans Indus Basin). In order to test and further refine our understanding of the ideas proposed in this thesis, if the following areas of investigation are given priority.

- To better understand and refine the zonal distribution of larger benthic foraminiferal species, more stratigraphic sections in the study should be studied.
- The condensed section which represents Upper Lllerdian-Middle Cuisaian strata in the study area needs further investigation in other parts of the basins to better describe the synchronous distribution of *Alveolina rotundata, Assilina laxispira* and *Orbitolites complanatus* species.
- The calibration of proposed larger benthic foraminiferal biozonation with the planktonic foraminiferal biozonation will test the validity and profitability of these biozones.
- To understand the role of foraminiferal response to the development of facies, the paleoecological analysis of different foraminiferal species must be given priority.
- To test the validity of a distally steepened carbonate ramp model for the study area further work needs to be done on various facies developments that that occurs along ramp slope profile.
- The understanding of reservoir characterization (e.g. porosity) of different microfacies can be increased by looking at the diagenetic fabric, various types of cement and timing of cementation.
- The genetic stratigraphy of proposed depositional sequences at $4^{th}$ & $5^{th}$ order scale of cyclicity can potentially increase our understanding of the role played by eustacy and tectonics in the development of various depositional cycles in the study area.
- The bio-chrostratigraphic framework of the depositional sequences can be improved by integrating further data from the planktonic foraminiferal, dinoflagellates nanoplanktonic and stable isotope dating of the units.

- Future investigations related to the provenance and isotopic analysis of clastic facies of the Patala, Panoba, Nammal and Kuldana Formations will reveal the role of tectonics at the time of deposition of different depositional sequences and can provide another data set for the comparison of the proposed timing of the closure of Tethys Ocean due to India-Asia collision, presented in this thesis.
- Any suggestions related to the improvement and refinements of this thesis are welcomed.

# BIBLIOGRAPHY

Abbasi, I. A., & McElroy, R., 1991: Thrust kinematics of the Kohat Plateau, Trans Indus Salt Range, Pakistan: *Journal of Structural Geology*, v. 13, pp. 319–327.

Adams, C.G., Lee, D.E., Rosen, B.R., 1990: Conflicting isotopic & biotic evidence for tropical sea-surface temperatures during the Tertiary. *Palaeogeography, Palaeoclimatology, Palaeoecology,* 77, pp. 289–313.

Afzal, J., 1996: Late Cretaceous to Early Eocene foraminiferal biostratigraphy of the Rakhi Nala area, Sulaiman Range, Pakistan. *Pakistan Journal of Hydrocarbon Research*, 8: pp. 1–24.

Afzal, J., 1997: Foraminiferal biostratigraphy & paleoenvironments of the Patala & Nammal Formations at the Paleoecene/Eocene boundary in Salt Range & Surghar Range, Pakistan (*unpublished PhD dessert*), University of Punjab, Pakistan, pp. 155.

Ahmad, S., 2010: Himalayan-induced deformation & Kinematics of the arcuate Nature of the Trans-Indus Salt Range, north-west Himalayas, Pakistan**,** *AAPG Convention*, New Orleans, Louisiana.

Aigner, T., 1983: Facies & origin of nummulitic buildups: an example from the Giza Pyramids Plateau (Middle Eocene, Egypt). Neues Jahrbuch fu¨ r Geologie und Palal¨ontologie. Abh & lungen 166, pp. 347– 368.

Aigner, T., 1984: Dynamic stratigraphy of epicontinental carbonates Upper Muschelkalk (M. Triassic), South-German Basin. - N. Jb. *Geol. Paläont*. Abh., 169/2, pp. 127-159, 14 figs., Stuttgart.

Anadón, P., 1978a: El Paleógeno continental anterior a la transgression biarritziense (Eoceno medio) entre los ríos Gaià y Ripoll (Provs. de Tarragona y Barcelona). (*Doctoral Thesis*) University of Barcelona. pp. 1-257.

Anadón, P., Feist, M., 1981: Charophytes et biostratigraphie du Paléogène Inférieur du bassin de l'Èbre oriental. *Palaeontographica,* 178(4-6), pp. 143-168.

Anderton, R., 1985: Sedimentation & tectonics in the Scottish Dalradian. *Scottish Journal of Geology*, 21, pp. 407-436

Anketell, J.M., Mriheel, I.Y., 2000: Depositional environment & diagenesis of the Eocene Jdeir Formation, Gabes–Tripoli Basin, western offshore Libya. *Journal of Petroleum Geology,* 23, pp. 425–447.

Arni, P., Lanterno, E., 1972: Conside´rations pale´oe´cologiques et interpre´tation des calcaires de l'E´ oce`ne du Ve´ronais. *Archives de Sciences* (Gene`ve) 25, pp. 251– 283 (in French).

Aubry, M.P., 1985: North-western European Paleogene magnetostratigraphy, biostratigraphy, & paleogeography: calcareous nannofossil evidence. *Geology*, 13: pp. 198–202.

Bacelle, L., Bosellini, A., 1965: Diagrammi per la stima visiva della composizione percentuale nelle rocce sedimentarie. - Ann. Univ. Ferrara, N.S., Sez. IX, Sci. *Geol. Paleont*., 1/3, pp. 59-62, 24 Pls., Ferrara.

Bain, Rj., & Kindler, P., 1994: Irregular fenestrae in Bahamianeolianites: a rainstorminducedorigin: *Journal of Sedimentary Petrology*, v. A64, pp. 140-146.

Baker, D.M., Lillie, R.J., Yeats, R., Johnson, G.D., Yousaf, M. & Zamin, A.S.H., 1988: Development of the Himalayan Frontal Thrust Zone: Salt Range Pakistan: *Geology*, 16, pp. 3-7.

Bannert., D., 1986: Stress release in the Himalayan forel& areas northern Pakistan as inferred from l& sat images, Fed. Inst. Geosci. & natural Res., 56. *Unpublished Rep*. BGR/HDIP; Hannover / Islamabad.

Barattolo., F. 1991: Mesozoic & Cenozoic marine benthic calcareous algae with particular regard to Mesozoic Dasycladaleans. - In: *Riding, R*.: Calcareous algae & stromatolites. – pp. 504-540, 6 Figs., Berlin (Springer).

Bard., J.P, 1983: Metamorphism of the obducted island arc: Example of the Kohistan Sequence. In Pakistan Himalaya Collided Range, *Earth & Planetry Science letters*, pp. 65.

Bassi, D., 1998: Coralline algal facies & their palaeoenvironments in the late Eocene of northern Italy (Calcare di Nago Trento). *Facies* 39, pp.179– 202.

Beaumont, C., 1981: Foreland basins, *Geophysical Journal of the Royal Astronomical Society*, v. 65, pp. 291–329.

Beck, R. A., & others, 1995: Stratigraphic evidence for an early collision between north-west India & Asia: *Nature*, v. 373, pp. 55–58.

Beck, R. A., Burbank, D.W., Sercombe,W. J., Khan, A. M., & Lawrence, R. D., 1996: Late Cretaceous ophiolite obduction & Paleocene India-Asia collision in the westernmost Himalaya, *in Proceedings* of the 10th Himalayan-Karakoram-Tibet Workshop, Monte Verita, Switzerland: Geodinamica Acta, Special Volume.

Berger, S., Kaever, M.J. 1992: Dasycladales, an illustrated monograph of a fascinating algal order. – pp. 274, Stuttgart (Thieme).

Berggren, W.A., Kent, D.V., Swisher III, C.C., Aubry, M.-P., 1995a. A revised Cenozoic geochronology and chronostratigraphy. In: Berggren,W.A., Kent, D.V., Aubry, M.-P., Hardenbol, J. (Eds.), Geochronology, Time Scales and Global

Stratigraphic Correlation. *Special Publication No. 54. SEPM (Society for Sedimentary Geology)*, pp.129–212.

Blanford., W.T. 1879: The geology of western Sind. *Memoir of the Geological Survey of India*, 17(1): pp. 1–197.

Blondeau., A, 1966: Les nummulites de l'Eoc6ne de Belgique. Bulletin de la *Socitte gtologique de France*, 8: pp. 909-919.

Blondeau., A, 1972a: Les nummulites. De l'enseignement a la recherche des *scitnces de la terre,* Paris: Vuibert, pp. 1-254.

Blondeau., A, 1980: Le calcaire *B Nummulites* en Tunisie. Annales des Mines et de Gtologie de Tunisie, Tunis, 28, 111: pp. 183-191.

Blondeau., A. 1981: Lutetian. – *Bull. Inf. Geol. Basin de* Paris, 2: pp.167–180.

Blondeau., A., Bassoullet., J.P., Colchen, M., Han, T.L., Marcoux, J., Mascle, G., & Van Haver,T. 1986: Disparition des FormationsMarines aL'Eocene Inferieur enHimalaya. *Sci Terre,*Mem, 47, pp. 103-111

Bolli., H.M., Beckmann, J.P., Saunders, J.B., 1994: Benthic foraminiferal biostratigraphy of the south Caribbean region. Cambridge University Press, Cambridge, pp. 408.

Bosellini., A., 1989: Dynamics of Tethyan carbonate platforms, *in* Crevello, P. D.,Wilson, J. L., Sarg, J. F., & Read, J. F., eds., Controls on carbonate platform & basin development: Society of Economic Paleontologists & Mineralogists Special Publication 44, pp. 3–13

Bosence, D.W. 1983: Description & classification of rhodoliths (rhodoids, rhodoliths). - In: Peryt, T.M. (ed.): Coated grains. - 217-224, 4 Figs., Berlin (Springer).

Bosence, D.W. 1983: The occurrence & ecology of recent rhodoliths.- A review. - In: Peryt, T.M. (ed.): Coated grains. – pp. 225-242, 5 Figs., 1 Tab., Berlin (Springer).

Bossart, P., Ottiger, R., & Heller, F., 1989: Paleomagnetism in the Hazara-Kashmir Syntaxis, NE Pakistan: Eclogae Geologicae Helvetiae, v. 82, pp. 585–601.

Boussac, J., 1911: Etudes paltontologiques sur le Nummulitique alpin. Memoires Explique Carte gtologique dtt. France, pp.1439.

Brasier, M.D., 1980: Microfossils. George Allen & Unwin, UK.
Brown. J.S, (1943): Suggested use of the word moicrofacies. Economic Geology 38: pp. 325.

Burbank, D.W., 1983: The chronology of intermountain basin development in the Northwestern Himalaya & the evolution of the northwest syntaxis. Earth & planetary science letter, 64, pp. 77-92.

Burchette, T.P. & Wright, V.P., 1992: Carbonate ramp depositional systems. Sediment. Geol., 79. pp. 3-57.

Burchette, T.P., Wright, V.P., 1992: Carbonate ramp depositional systems. - *Sed. Geol., 79*, pp. 3-57, 18 Figs., 3 Tabs., Amsterdam.

Buxton, M.W.N., Pedley, H.M., 1989: A st&ardized model for Tethyan Tertiary carbonate ramps. - *Journal of the Geological Society London, 146*, pp.746-748.

Calvet, F., Tucker, M., 1988: Outer ramp carbonate cycles in the Upper Muschelkalk, Catalan basin, N.E. Spain. - Sed. Geol., 57, pp.185-198.

Calvet, F., Tucker, M.E., Henton, J.M., 1990: Middle Triassic carbonate ramp systems in the Catalan Basin, northeast Spain: facies, system tracts, sequences & controls. - In: Tucker, M.E., Wilson, J.L., Crevello, P.D., Sarg, J.R. & Read, J.F.: Carbonate platforms. Facies, sequences & evolution. - *Spec. Publ. Int. Ass. Sedimentol., 9,* pp. 79-108, 25 Figs., Oxford (Blackwell).

Cuvillier, J., 1930. Revision du Nummulitique tgyptien. *Memoire deI'Institute Egypte,* 16: pp. l-371.

Chassefiere, B., Lundhardt, O., Levy, A., 1969: Donne´es nouvelles sur les cadoules (e´difices coquilliers) de la lagune de Thau (He´rault.). Compte Rendu Sommaire Des Se´ances De La Socie´te´ Ge´ologique De France 5, pp. 140– 142 (in French).

Cole, W.S., 1960: The genus Camerina.- *Bulletins of American Paleontology, Ithaca*, *v. 41*, pp. 189-205, 4 Pls.

Cole, W. S., 1964: American mid-Tertiary Miogypsinid foraminifera: classification & zonation. *Cushman Found. Foram. Res., Contrib., 15*: pp.138-150.

Coward, M.P., Windley, B.F., Broughton, R., Luff, I.W., Peterson, M., Pudsey, C.J., & Khan, M., 1986: Collision tectonics in the NW Himalayas. In: Coward, M. P., & reistectonics. *Special publication of the Geol. Soc. London, v. 19*, pp. 203-219.

Critelli, S., Garzanti, E., 1994: Provenance of the Lower Tertiary Murree redbeds (Hazara–Kashmir Syntaxis, Pakistan) & initial rising of the Himalayas. *Sedimentary Geology 89*, pp. 265– 284.

Cushman, J. A., 1948: Foraminifera—their Classification & Economic Use: Harvard University Press, Cambridge, Massachusetts, 588 p.

D'Archiac, V.E.J.A.D., & Haime., J. 1853: Description des Animaux fossiles du Groupe nummulitique de l'Inde. Précédé d'un résumégéologique et d'une monographie des Nummulites, Paris, 2: pp.1–373.

Danialchik, W., & Shah, S. M. I., 1967: Stratigraphic nomenclature of formations in Trans Indus Mountains, Mianwali District, west Pakistan, U.S Geol. Surv. Proj. Report (IR) Pk-33:45p.

Danilchik, W. & Shah, S.M.I., 1987: Stratigraphy & coal resources of the Makarwal area, Trans-Indus Mountains, Mianwali District, Pakistan. United States Geological Survey *Professional Paper*, pp. 1341: 1–38.

Davies, L. M., 1940: The upper Kirthar beds of northwest India. Geol. Soc. London, *Quarterly Journal of the Geological Society of London, v. 96*, pt. 2, pp. 199-230, pls. 9-12, 1 table.

Davies, L.M., & Pinfold, E.S., 1937: The Eocene beds of the Punjab Salt Range. *Memoir of the Geological Survey of India, 24*: pp. 1–79.

Davies, L.M., 1927: The Ranikot beds at Thal (North-West Frontier Ranges of India). *Quarterly Journal of the Geological Society of London, 83*: pp. 260–290.

Davies, L.M., 1930: The fossil fauna of the Samana Range & some neighbouring areas, the Paleocene foraminifera. *Memoir of the Geological Survey of India, Paleontologia Indica, 15:* pp. 67–79.

Davies, L.M., & E.S. Pinfold., 1937: The Eocene Beds of the Punjab Salt Range. *Memoir of the Geological Survey of India, Paleontologia Indica, 1:* pp. 1–79.

De Castro, P., 1997: Introduzione allo studio in sezioni sottili delle Dasicladali fossili (An approach to thin-section study of fossil Dasycladales. - Quaderni dell'Accademia Pontaniana Napoli.

De Sigoyer, J., Chavagnac, V., Blichert-Toft, J., Villa, I., Luais, B., Guillot, S., Cosca, M., Mascle, G., 2000: Dating the Indian continental subduction & collisional thickening in the northwest Himalaya: multichronology of the Tso Morari eclogites. *Geology 28*, pp. 487– 490.

DeCelles, P.G., Gehrels, G.E., Quade, J., & Ojha, T.P., 1998a: Eocene early Miocene foreland basin development & the history of Himalayan thrusting, western & central Nepal: *Tectonics*, v. 17, pp. 741–765.

DeCellesa P.G, Gehrelsa G.E., Najman. Y., Martina A. J, Carterc. Garzanti. E., 2004: Detrital geochronology & geochemistry of Cretaceous–Early Miocene strata of Nepal: implications for timing & diachroneity of initial Himalayan orogenesis: *Earth & Planetary Science Letters 227,* pp. 313– 330.

Demicco, R.V., & Hardie, L.A., 1994: Sedimentary Structures & Early Diagenetic features of shallow marine carbonate deposits. Atlas Ser. 1, Society of Economic Paleontologists & Mineralogists, Tulsa, OK, pp.265.

Douville, H., 1919: l'hcene inferieur en Aquitaine et dans le Pyrenes. Memoires pour servir a I'Explication de la Carte Gtologique dttaillee de la France,Paris, pp.1-84.

Dunham, R.J., 1962: Classification of carbonate rocks according to depositional texture. - *Amer. Ass. Petrol. Geol. Mem., 1*, pp. 108-121, 7 Pls.

Eames, E. E., 1952a: A contribution to the study of the Eocene in western Pakistan & western India: The geology of standard sections in the western Punjab & in the Kohat District. *Quarterly Journal of the Geological Society of London 107:* pp.159-171.

Eames, E E., 1952b: A contribution to the study of the Eocene in western Pakistan & western India: D. Discussion of the faunas of certain standard sections, & their bearing on the classification & corrrelation of the Eocene in western Pakistan & western India. *Quarterly Journal of the Geological Society of London 107:* pp.173-196.

Eames. F. E., 1950: Eocene in western Pakistan & western India; bearing on the classification & correlation of the faunas of the certain standard sections in Pakistan & western India: contribution to the study of the Eocene *Quarterly Journal of the Geological Society 1951; v. 107*; pp. 173-200.

Embry, AF., & Klovan, JE., 1971: A Late Devonian reef tract on North-eastern Banks Island, NWT: *Canadian Petroleum Geology Bulletin*, *v. 19*, pp. 730-78.

Emery, D., & K.J. Myers, 1996: *Sequence stratigraphy*: Oxford, Blackwell Science, 297 p.

Fadel, M. K. B., 2008: Evolution and geological significance of larger benthic foraminifera. Published by Elsevier B.V. ISBN: 978-0-444-52956-5, 515 p.

Fatmi, A.N., 1973: Lithostraitigraphic units of the Kohat-Potwar province, Indus Basin, Pakistan .*Geological survey of Pakistan: Memoir, 16*.

Ferrer, J., 1971: El Paleoceno y Eoceno del borde suroriental de la Depresión del Ebro (Cataluña). *Mémoires suisses de Paléontologie*, *90*, pp.70.

Flügel, E., 1972: Microproblematika in Dünnschliffen von Trias-Kalken. - Mitt. Ges. Geol. Bergbaustud. Österr., 21, pp.957-988, 5 Pls., 2 Tab., Innsbruck.

Flügel, E., 1982: Microfacies analysis of limestones. – pp. 633, 78 Figs., 53 Pls., 58 Tabs. Berlin (Springer).

Flügel, E., 1985: Diversity & environments of Permian & Triassic dasycladacean algae. In: Toomey, D.F. & Nitecki, M.H. (eds.): *Paleoalgology*.

Flügel, E., 1991: Triassic & Jurassic marine calcareous algae: a critical review. In: Riding, R: Calcareous algae & stromatolites. pp. 481-503, 8 Figs., Berlin (Springer).

Folk, R.L., 1962: Spectral subdivision of limestone types, in Ham, W.E., ed., classification of carbonate rocks- A Symposium: *American Association of Petroleum Geologists Memoir 1*, pp. 62-84.

Gannser, A., 1964: Geology of Himalayas. *Inter-Science*, London, p. 289.

Gallala, N., Zaghbib T.D., M.M. Turki., I. Arenillas., J.A. Arz., & Molina. E: 2009: Upper Cretaceous & lower Paleogene benthic foraminiferal paleoecology from north-eastern Tunisia: El Melah section*: Geophysical Research Abstracts, v. 11*, EGU2009-3700.

Garzanti, E., Critelli, S., & Ingersoll, R. V., 1996: Paleogeographic & paleotectonic evolution of the Himalayan Range as reflected by detrital models of Tertiary sandstones & modern sandstones (Indus transect, India & Pakistan): *Geological Society of America Bulletin*, *v. 108*, pp. 631–642.

Gee, E. R., 1945: The age of the Saline series of the Punjab & of Kohat: National Academy of Sciences of India, Proceedings, section B, v. 14, pt. 6, pp. 269–310.

Gee, E.R., 1935: The saline series (Early Eocene) of north-western India (abs) Proc. 22nd Indian, Sci. Cong., Calcuta, pp. 207.

Geel, T., 2000: Recognition of stratigraphic sequences in carbonate platform & slope deposits: empirical models based on moicrofacies analysis of Palaeogene deposits in south-eastern Spain. *Palaeogeography, Palaeoclimatology, Palaeoecology 155*, pp. 211 –238.

Gerlach, S.A., 1972: Substratum: general introduction. In: Kinne, O. (Ed.), *Marine Ecology*. Wiley, New York, pp. 1245–1250.

Ghose, B.K., 1977: Paleoecology of the Cenozoic reefal foraminifers & algae—a brief review. *Palaeogeography, Palaeoclimatology, Palaeoecology 22*, pp. 231–256.

Gilham, R.F., Bristow, C.S., 1998: Facies architecture & geometry of a prograding carbonate ramp during the early stages of foreland basin evolution: lower Eocene sequences, Sierra del Cadı, SE Pyrenees, Spain. In: Wright, V.P., Burchette, T.P. (Eds.), Carbonate Ramps. *Geological Society of London Special Publication.*

Gill, W.D., 1953: The genus *Assilina* in the Laki (Lower Eocene) of the Kohat-Potwar Basin, north-west Pakistan. Contributions of the Cushman Foundation for *Foraminiferal Research 4:* pp.76-86.

Gingerich, P D., 2003: Stratigraphic & micropaleontological constraints on the Middle Eocene age of the mammal-Bearing Kuldana Formation of Pakistan; *Journal of Vertebrate Paleontology*, *v. 23,* No. 3, pp. 643-651

Gingerich, P D., 1977: A small collection of fossil vertebrates from the Middle Eocene Kuldana & Kohat Formations of Punjab (Pakistan). Contributions from the Museum of Paleontology, University of Michigan 24: pp. 190-203.

Gorsel, J.T. Van., 1988: Biostratigraphy in Indonesia: methods, pitfalls & new directions. Proceedings of the Indonesian Petroleum Association, 16th Annual Convention. IPA, Jakarta: pp.275-300.

Gregory, W.A., & Hart, G.F., 1992: Towards a predictive model for the palynologic response to sea-level changes. *Palaios, 7,* pp. 3-33.

Hallock, P., 1981a: Algal symbiosis: a mathematical analysis. *Marine Biology, 62*, pp. 249– 255.

Hallock, P., 1981b: Light dependence in Amphistegina. *Journal of Foraminiferal Research 11*, pp. 40–46.

Hallock, P., 1985: Why are larger foraminifera large? *Paleobiology 11*, pp.195– 208.

Hallock, P., Hansen, H.J., 1979: Depth adaptation in Amphistegina: change in lamellar thickness. *Bulletin of the Geological Society of Denmark 27*, pp. 99–104.

Hallock, P., Schlager, W., 1986: Nutrient excess & the demise of coral reefs & carbonate platforms. *Palaios 1*, pp. 389–398.

Hansen, H.J., Buchardt, B., 1977: Depth distribution of Amphistegina in the Gulf of Elat, Israel. Utrecht *Micropaleontological Bulletins* 15, pp.205– 224.

Hansen, H.J., Dalberg, P., 1979: Symbiotic algae in milioline foraminfera: CO2 uptake & shell adaptations. *Bulletin of the Geological Society of Denmark 28,* pp. 47–55.

Hansen, H.J., Reiss, Z., 1972: Scanning electron microscopy of some asteriginid foraminifera. *Journal of Foraminiferal Research 2*, pp. 191– 199.

Haq, B. ul., J. A. Hardenbol., & P. R. Vail., 1987. Chronology of fluctuating sea levels since the Triassic. *Science 235*: pp.1156-1167.

Haque, A.F.M.M., 1956: The Foraminifera of the Ranikot & the Laki of the Nammal Gorge, Salt Range. Pakistan. *Paleontologia Pakistanica, 1*: pp. 1–300.

Harpe De La. P., 1877: Notes sur les nummulites des Alpes occidentals. Actes Societe Helvetique Sciences naturelles, Paris, 60: pp. 227-323.

Harland, W.B., R.L. Armstrong, A.V. Cox, L.E. Craig; A.G. Smith, and D.G. Smith 1989: "*A Geologic Time Scale 1989*," Cambridge University Press, Cambridge

Hayens J. R., 1981: Foraminifera. London: Macmillan, pp.433.
Special Pub-Cushman Foundation for *Foraminiferal Research* 16, pp.40– 43.

Heckel, P.H., 1972: Possible inorganic origin for Stromatactis in calcilutite mounds in the Tully Limestone, Devnonian of New York. - *J. Sed. Petrol., 42/1*, pp. 7-18, 6 Figs.

Hens on, F.R.S., 1950: Cretaceous & Tertiary reef formations & associated sediments in Middle East. *American Association of Petroleum Geologists Bulletin 34*, pp. 215– 238.

Herb, R., 1988: Evolution of diversity, paleoenvironments & extinction in large nummulitids. *Revue Pale´obiologie 2, Benthos '86*, Symposium sur les Foraminife`res Benthinque, Gene`ve pp. 663.

Hohenegger, J., Yordanova, E., Hatta, A., 2000: Remarks on west Pacific Nummulitidae (Foraminifera). *Journal of Foraminiferal Research 30*, pp.3–28.

Hohenegger, J., Yordanova, E., Nakano, Y., Tatzreiter, F., 1999. Habitats of larger foraminifera on the reef slope of Sesoko Island, Okinawa, Japan. *Marine Micropaleontology 36*, pp.109–168.

Holland, C. H. et al., 1978: A guide to stratigraphical procedure, *Geological Society of London Special Report*, 10: pp. 1-18.

Hottinger, L. & H. Schaub 1960: Zur Stufeneinteilung des Paleocans und des Eocans. Einfuhrung der Stufen Ilerdien und Biarritzien. *Eclogae geol. Helvet., 53*: pp.453–480.

Hottinger, L., 1960: Recherches sur les Alvéolines du Paléocène et de l'Eocène. Schweizerische Palaeontologische Abh & lungen 75-76: pp. 1-243.

Hottinger, L., 1973: Selected Palaeogene larger foraminifera. In: Hallam, A. (Ed.), *Atlas of Palaeobiogeography*. Elsevier, Amsterdam, pp. 443– 452.

Hottinger, L., 1977a: Distribution of larger Peneroplidae, Borelis & Nummulitidae in the Gulf of Elat, Red Sea. *Utrecht Micropaleontological Bulletins 15,* pp. 35–109.

Hottinger, L., 1983: Processes determining the distribution of larger foraminifera in space & time. *Utrecht Micropaleontological Bulletins 30*, pp. 239– 253.

Hottinger, L., Dreher, D., 1974: Differentiation of protoplasm in Nummulitidae (Foraminifera) from Elat, Red Sea. *Marine Biology 25*, pp.41–61.

Hunt, D., Tucker, M.E., 1993: Sequence stratigraphy & carbonate shelves with an example from the mid-Cretaceous (Urgonian) of southeast France. In: Posamentier, H.W., Summerhayes, C.P., Haq, B.U. & Allen, G.P. (eds.): *Sequence stratigraphy & facies associations*. - Spec. Publ. Int. Ass. Sedimentol., 18, pp. 307-341, 23 Figs., Oxford.

Jan, M.Q., 1980: Petrology of the obducted mafic metamorphics from the southern part of the Kohistan Island Arc sequence. *Geol. Bull. Univ. Pesh, 13*, pp. 95-107.

Johnson, H.M., J. Stix, L.Tauxe., P. F. Cerveny, & R. A. K. Tahirkheli., 1985: Paleomagnetic chronology, fluvial processes & tectonic implications of the Siwalik deposits near Chinji Village, Pakistan. *Journal of Geology 93*: pp.27-40.

Jones, R.W., 1999: Marine invertebrate (chiefly foraminiferal) evidence for the palaeogeography of the Oligocene–Miocene of western Eurasia, & consequences for terrestrial vertebrate migration. In: Agusti, J., & rews, P., Rook, L. (Eds.), Hominoid Evolution & Climatic Change in Europe. The Evolution of Neogene Terrestrial Systems in Europe, v. 1. Cambridge Univ. Press, UK, pp. 274–308.

Kapellos, C. and Schaub, H., 1975. L'Ilerdien dans les Alpes, dans les PyrCnees et en Crimee. Correlation des zones a grand foraminiferes eta Nannoplancton. *Bulletin de la SociCtC geologique de France*, 17: pp.148-161.

Kazmi, A. H., & Abassi, I.A., 2008: *Stratigraphy & Historical Geology of Pakistan* Published by National Centre of Excellence in Geology, University of Peshawar, Peshawar, Pakistan ISBN: 978-969-9119. 524.p.

Kazmi, A.H., & Jan, M. Q., 1997: *Geology & tectonics of Pakistan*. Graphic Publishers, 5C, 6/10, Nazimabad, Karachi, Pakistan, 500.p.

Kazmi, A.H., 1984a: Petrology of the Bibai volcanics, NE Baluchistan. *Geol. Bull.* Univ. Peshawar, 17: pp. 43-51.

Kazmi, A.H., & Rana, R.A., 1982: Tectonic map of Pakistan: Geological Survey of Pakistan, scale: 1:2,000,000.

Khan, M.A., Turi, K.A., Abbasi, I.A., 1990: The structures in the hanging wall of the Main Boundary Thrust (MBT), late post folding thrusts & normal faults from the Kohat Hill Range, N. Pakistan *Geol. Bull*. Univ. Pesh, v. 23, pp. 175-186.

Klootwijk, C.T., Gee, J.S., Peirce, J.W., Smith, G.M., McFadden, P.L., 1992: An early India–Asia contact: paleomagnetic constraints from Ninetyeast Ridge, ODP Leg 121. *Geology 20*, pp.395–398.

Köthe, A., Khan, A.A., & Ashraf, M., 1988: Biostratigraphy of the Surghar Range, Salt Range, Sulaiman Range & the Kohat area, Pakistan, according to Jurassic through Paleogene calcareous nannofossils & Paleogene dinoflagellates. Geologisches Jahrbuch, B71: pp.1–87.

Kureshi, A. A., 1975: Texonomic Studies of Tertiary larger formaminifera of Pakistan. Rec. G.S.P. v. 38, pp. 44-47, pl. 1-11.

Langer, M.R., Hottinger, L., 2000: Biogeography of selected ‘‘larger’’ foraminifera. *Micropaleontology 46 (Supplement 1),* pp.105–126.

Larsen, A.R., 1976: Studies of recent Amphistegina: taxonomy & some ecological aspects. Israel *Journal of Earth-Sciences 25,* pp.1– 26.

Larsen, A.R., Drooger, C.W., 1977: Relative thickness of the test in Amphistegina species from the Gulf of Elat. *Utrecht Micropaleontological Bulletins 15*, pp.225–239.

Latif, M. A., 1970a: Explanatory notes on the geology of South-eastern Hazara, to accompany the revised Geological Map: *Wein Jb. Geol.* B. A., Sonderb. 15. pp. 5-20

Le Fort, P., 1975: Himalayas: The collided range present knowledge of the continental arc. *Am. Jour. Sci., v. 75*-A, pp. 1-44.

Lillie, R., Johnson. D., Yousaf, M., Zamin, A.S.H., & Yeats., 1987: Structural development with in the Himalayan foreland fold & thrust belt of Pakistan. In c. Beaument, & A.J. Tankard, eds. Sedimentary basin & basin forming mechanics, Canadian Soc. Petrol. Geol: memoir, v.12, pp. 379-392.

Loeblich, A. R. & Tappan, H., 1964: Protista 2. Sarcodina chiefly Thecamoebians & Foraminiferida, Part C: In: *Treatise on Invertebrate Palaeontology* Moore, R. C. (ed). 2 v. Geological Society of America & University of Kansas Press, pp.1-900.

Loucks, R.G., Moody, R.T.J., Bellis, J.K., Brown, A.A., 1998: Regional depositional setting & pore network systems of the El Garia Formation (Metlaoui Group, lower Eocene), offshore Tunisia. In: MacGregor, D.S., Moody, R.T.J., Clark-Lowes, D.D. (Eds.), Petroleum Geology of North Africa. Geological Society of London, Special Publication, v. 132, pp. 355–374.

Luterbacher, H., 1998: Sequence stratigraphy & the limitations of biostratigraphy in the marine Paleogene strata of the Tremp Basin (central part of the southern Pyrenean foreland basin, Spain). In: De Graciansky, P.C., Hardenbol, J., Jacquin, T., Vail, P.R. (Eds.), *Mesozoic & Cenozoic Sequence Stratigraphy of European Basins. Society for Sedimentary Geology Special Publication*, v. 60, pp. 303–309.

Malcolm, B.H., 2000: Foraminifera, sequence stratigraphy & regional correlation; an example from the uppermost Albian of Southern England *Reveu de Micropaleontology v. 43*, Issue 1, pp.27-45.

Malecki. J 1973: Bathysiphons from the Eocene of The Carpathian Flysch, Poland *Palantologia Polnica No 2*, v. XVIII.

Markello, J.R., Read, J.F., 1981: Carbonate ramp to deeper shale shelf transitions of an Upper Cambrian intrashelf basin, Nolichucky Formation, southwest Virginia Appalachians. - *Sedimentology, 28*, pp.573-597, Oxford.

Mathur, N.S. 1977: Age of the Subathu formations in the Garhwal region, Uttar Pradesh, India. *Bull. Indian Geol. Assoc., 10(2)*, pp. 21-27.

Maxwell, W.G.H., Day, R.W., Fleming, P.J.G., 1961: Carbonate sedimentation on the Heron Island reef, Great Barrier Reef. *Journal of Sedimentary Petrology 31*, pp. 215–230.

McDougall, J.W., & Hussain, A., 1991: Fold & thrust propagation in the western Himalaya based on a balanced cross section of the Surghar Range & Kohat Plateau, Pakistan: *American Association of Petroleum Geologists Bulletin*, v. 75, pp. 463–478.

McEnery, M.E., Lee, J.J., 1981: Cytological & fine structural studies of three species of symbiont-bearing larger foraminifera from the Red Sea. *Micropaleontology 27*, pp.71– 83.

Meischner, D.,1964: Allodapische Kalke, Turbidite in riffnahen Sedimentations-Becken. - In: Bouma, A.H. & Brouwer, A. (eds.): *Turbidites. - Dev. Sedimentol., 3*, pp.156-191, 5 Figs., 3 Pls., Amsterdam.

Meissner, C. R., & Rahman, H., 1973: Distribution, thickness & lithology of Paleocene rocks in Pakistan: *U.S. Geological Survey Professional Paper 716-E*, pp.6.

Meissner, C. R., Hussain, M., Rashid, M. A., & Sethi, U. B., 1975: Geology of the Kohat-Potwar depression, Pakistan. *AAPG Bull. v. 70*, pp. 396-414.

Meissner, C.R., Master, J.M., Rashid, M.A. & Hussain, M. 1968: Stratigraphy of the Kohat quadrangle. *United States Geological Survey, Project Report, PK-20*: pp.1–86.

Meissner, C.R., J.M. Master., M.A. Rashid., & M. Hussain., 1974: Stratigraphy of the Kohat quadrangle, Pakistan: *United States Geological Survey Professional paper 716-D*, pp.1-30.

Metcalfe, R. P., 1993: Pressure, temperature & time constraints on metamorphism across the Main Central thrust zone & High Himalayan Slab in the Garhwal Himalaya, in Treloar, P. J., & Searle,M. P., eds., *Himalayan tectonics*.

Middlemiss, C. S., 1896: the Geology of Hazara & the Black Mountains: *India. Geol. Surv., Mem., v. 26*, pp. 302.

Middleton, G.V., 1978: Facies. In: Fairbridge, R.W., Bourgeois, J. (Eds.), Encyclopedia of Sedimentology. Dowden, Hutchinson & Ross, Stroudsburg, PA, pp. 323–325.

Miller, K.G., Rufolo, S., Sugarman, P.J., Pekar, S.F., Browning, J.V., & Gwynn, D.W., 1997: Early to middle Miocene sequences, systems tracts, & benthic foraminiferal biofacies: *Proceedings of the Ocean Drilling Program, Scientific Results, v. 150X,* pp. 169–186.

Mitchum, R.M. Jr., 1977: Seismic stratigraphy & global changes of sea-level, Part II Glossary of terms used in seismic stratigraphy. in C.E. Clayton ed., Seismic stratigraphy -application to hydrocarbon exploration: AAPG Memoir 26, pp. 49.

Molina, E., Gonzalvo, C., Mancheno, M.A., Ortiz, S., Schmitz, B., Thomas, E., & Salis, K.V., 2006: Integrated stratigraphy & chronostratigraphy across the Ypresian-Lutetian transition in the Fortuna Section (Betic Cordillera, Spain) *Newsl. Stratigr. 42 (1),* pp. 1–19 6, fig. Berlin, Stuttgart, 22. 11.

Murray, J.W., 1987: Benthic foraminiferal assemblages: criteria for the distinction of temperate & subtropical carbonate environments. In: Hart, M.B. (Ed.), Micropalaeontology of Carbonate Environments. Ellis Horwood, UK, pp. 9–20.

Nagappa, Y., 1959: Foraminiferal biostratigraphy of the Cretaceous–Eocene succession in the India–Pakistan, Burma region. *Micropaleontology, 5*: pp.145–192.

Najman, Y., Garzanti, E., 2000: Reconstructing early Himalayan tectonic evolution & paleogeography from Tertiary foreland basin sedimentary rocks, northern India. *Geological Society of America Bulletin 112*, pp.435– 449.

Najman, Y., Johnson, C., White, N.M., & Oliver, G., 2004: Evolution of the Himalayan foreland basin, NW India: *Basin Research, v. 16*, pp. 1–24.

Nakata, T., 1989: Active faults of the Himalaya of India & Nepal. In: Malinconico, L.L.& Lillie, R.J. (eds). Tectonics of the western Himalayas. *Geol. Soc. Amer., Spec. Paper 232*, pp. 243-264.

Newell, N.D., 1956: Geological reconnaisance of Raroia (Kon Tiki) Atoll, Tumotu Archipelago. *Bulletin of the American Museum of Natural History 109*, pp.317– 372.

Noetling, F., 1903: Ubergang Zwosorchen Kredi and Eocan in Baluchistan. *Central B. I Miner. Geol., Paleon.* Jahrb 6: pp.129-137 & pp. 161-172.

Nuttall, W.L.F., 1926: The larger foraminifera of the Upper Ranikot Series (Lower Eocene) of Sind, India. *Geological Magazine, 63*: pp.112–121.

Pascoe, E.H., 1963: *A manual of the geology of India & Burma.* Government of India Press, Calcutta, 3: pp.2073–2079.

Pfender, J., 1938: Contribution a la paleontologie des couches crttacCes et Cocenes du versant sud de 1'Atlas de Marrakech (Maroc). In Moret, L., Ed., Notes et

Mtmoires de la Service Mineralogique et de la Carte giologique Maroc, 49, pp.1-77, pls. 12.

Pia, J., 1920: Die Siphoneae verticillatae vom Karbon bis zur Kreide. - Abh. zool.-botan. Ges., pp.1-262, 27 Figs., 8 Pls., Wien.

Pivnik, D. A., & N. A. Wells., 1996: The transition from Tethys to the Himalaya as recorded in northwest Pakistan. *Geological Society of America Bulletin 108*: pp. 1295-1313.

Pognante, U., & D. A. Spencer., 1991: First report of eclogites from the Himalayan belt, Kaghan valley (northern Pakistan), *Eur. J. Mineral., 3*, pp. 613 – 618.

Powell, C. M., 1979: A Speculative tectonic history of Pakistan & surroundings: some constraints from the Indian Ocean. In: Farah, A. & DeJong, K.A. (eds) *Geodynamics of Pakistan*. Geol. Surv. Pakistan, Quetta, pp.5-24.

Racey, A., 1992a: An assessment of the relative taxonomic value of morphological characters in the genus Nummulites. *Journal Micropalaeontology, 1 l (2)*: pp.197-209.

Racey, A., 1994: Biostratigraphy & palaeobiogeographic significance of Tertiary nummulitids (foraminifera) from northern Oman. In: Simmons, M.D. (Ed.), Micropalaeontology & Hy- drocarbon Exploration in the Middle East. Chapman & Hall, London, pp. 343–370.

Racey, A., 1995: Lithostratigraphy & larger foraminiferal (nummulitid) Biostratigraphy of the Tertiary of Norhthern Oman. *Micropaleontology, v. 41,* supplement, pp.123, txt figs 1-93, Pls 1-11, appendix 1.

Racey, A., 2001: A review of Eocene nummulite accumulations: structure, formation & reservoir potential. *Journal of Petroleum Geology 24*, pp.79–100.

Read, J.F., 1982: Carbonate platforms of passive (extensional) continental margins: types, characteristics & evolution. *Tectonophysics, 81*: pp.195-212.

Read, J.F., 1985: Carbonate platform facies models. *Bull. Am. Assoc. Pet. Geol., 69*: pp. 1-21.

Reading, H.G., 1986: *Sedimentary Environments & Facies*. Second Edition, Blackwell Scientific Publications, Oxford.

Reichel, M., 1964: Alveolinidae. In: Moore, R.C. (Ed), Treatise on Invertebrate Paleontology, Part C. Protista, v. 2. University of Kansas Press, Lawrence, KA, pp. pp.503– 510.

Reiss, Z., 1977. Foraminiferal research in the Gulf of Elat—Aqaba.

Renema, W., 2002: Larger foraminifera as marine environmental indicators. *Scripta Geologica 124,* pp.1–260.

Renema, W., Troelstra, S.R., 2001: Larger foraminifera distribution on a mesotrophic carbonate shelf in SW Sulawesi (Indonesia). *Palaeogeography, Palaeoclimatology, Palaeoecology 175*, pp.125– 146.

Richter F, M., Rowley D.B., and DePaolo D.J, 1992. Sr Isotope evolution in sea water: the role of tectonics *Earth Planet Sci. Lett*. 109 11-23.

Roohi & Baqri R.S.H., 2004:.The importance of *Nummulites* & *Assilina* in the correlation of middle & upper Eocene rocks of Pakistan, 19th Himalaya-Karakoram-Tibet Workshop, Niseko, Japan.

Rosen, R. N., & W. A. Hill., 1990: Biostratigraphic application to Pliocene–Miocene sequence stratigraphy of the western & central Gulf of Mexico & its integration to lithostratigraphy: *Gulf Coast Association of Geological Societies Transactions, v. 40*, pp. 737–743.

Ross, C.A., 1974: Evolutionary & ecological significance of large, calcareous Foraminiferida (Protozoa), Great Barrier Reef. *Proceedings of the 2nd International Coral Reef Symposium, Brisbane, Australia, v. 1*, pp. 327–333.

Ross, C.A., Ross, J.R.P., 1978: Adaptive evolution in the soritids Marginopora & Amphisorus (Foraminiferida). *Scanning Electron Microscopy 2*, pp.53– 60.

Rowley, D.B., 1996: Age of initiation of collision between India & Asia: a review of stratigraphic data. *Earth & Planetary Science Letters 145*, pp.1– 13.

Rowley, D.B., 1998: Minimum age of initiation of collision between India & Asia north of Everest based on the subsidence history of the Zhepure mountain section. *Journal of Geology 106*, pp.229–235.

Sakai, H., 1989: Rifting of the Gondwanaland & uplifting of the Himalayas recorded in Mesozoic & Tertiary fluvial sediments in the Nepal Himalayas, in *Sedimentary Facies in the Active Plate Margin*, edited by A. Taira & F. Masuda, pp. 723–732, Terra Sci., Tokyo.

Sarkar, S.S., & Wadia D.N., 1968: The Lutetian Transgression, v. 35, pp. 763-770

Sakai, H., Hamamoto, R., & Arita, K., 1992: Radiometric ages of alkaline volcanic rocks from the upper Gondwana of the Lesser Himalayas, western Central Nepal & their tectonic significance: Kathmandu, Nepal, Tribhuvan University *Department of Geology Bulletin, v. 2*, pp. 65–74.

Samanta, B.K., 1968: Nummulites (foraminifera) from the upper Eocene Kopili Formation of Assam, India. *Palaeontology 11(5):* pp. 669-682.

Sameeni, 1998: "Alveolinid Biostratigraphy of the Kohat Formation, Northern Pakistan", "Foram 98" Monterry, Mexico, Soci. Mexicana de Pal. A.C. *sp. publ.p.95. Geological Society of America Bulletin 74*, pp. 93–114.

Sarg, J.F., 1988: Carbonate sequence stratigraphy, in Wilgus, C.K., Hastings, B.S., Kendall, C.G.S.C., Posamentier, H.W., Ross, C.A., & Van Wagoner, J.C., eds., Sea-Level Changes: An Integrated Approach: Tulsa, OK, SEPM Special Publication No. 42, pp. 155-182.

Sartorio, D., Venturini, S., 1988: Southern Tethys Biofacies. AGIP, Milan.
Schlanger, S.O., 1963. Subsurface geology of Enewetak Atoll. *U.S. Geological Survey Professional Paper 260bb*, pp. 991– 1066.

Searle, M. P., & 10 others., 1987: the closing of Tethys & the tectonics of the Himalaya: *Geological Society of America Bulletin, v. 98*, pp. 678–701.

Searle, M. P., & Rex, A. J., 1989: Thermal model for the Zanskar Himalaya: *Journal of Metamorphic Geology, v. 7*, pp. 127–134.

Searle, M.P. & Treloar, P.J., 1993: Himalayan Tectonics as introduction. Geol. Soc. Lond. Spec. 74: pp. 1-7.

Searle, M.P., Corfield, R.I., Stephenson, B., McCarron, J., 1997: Structure of the north Indian continental margin in the Ladakh–Zanskar Himalayas: implications for the timing of obduction of the Spontang ophiolite, India–Asia collision & deformation events in the Himalaya. *Geological Magazine 134*, pp.297–316.

Seeber, L., & Armbruster, J., 1979: Seismicity of the Hazara arc in northern Pakistan: decollement versus basement faulting. In: Farah, A. & DeJong. K. A. (eds). Geodynamics of Pakistan. Geol. Surv. Pakistan, Quetta, 131-142.

Sercombe, W. J., Pivnik, D. A., Wilson, W. P., Albertin, L. M., Beck, R. A., Stratton, M. A., 1998: Wrench faulting in the northern Pakistan foreland. *AAPG. Bull., v.82,* Num. 11. pp. 2003-2030.

Serra-Kiel, J., Hottinger, L., Caus, E., Drobne, K., Fern&ez, C., Jauhri, A.K., Less, G., Pavlovec, R., Pignatti, J., Samso, J.M., Schaub, H., Sirel, E., Strougo, A., Tambareau, Y., Tosquella, Y. & Zakrevskaya, E., 1998: Larger foraminiferal biostratigraphy of the Tethyan Paleocene & Eocene.*Bulletin de la Société Géologique de France 169*: pp. 281-299.

Serra-Kiel, J., Reguant, S., 1984. Paleoecological conditions & morphological variation in monospecific banks of Nummulites: an example. Bulletin des Centres de Recherches Exploration-Production Elf-Aquitaine. *Memoire 6*, pp. 557–563.

Serra-Kiel. J. Travé E. Mató E. Saula C., Ferràndez-Cañadell P., Busquets ,Tosquella. J., & J. Vergés., 2003: Marine & Transitional Middle/Upper Eocene Units of the Southeastern Pyrenean Forel& Basin (NE Spain), *Geologica Acta*, *v.1,* pp.177-200.

Severin, K.P., Lipps, J.H., 1989: The weight–volume relationship of the test of Alveolinella quoyi: implications for the taphonomy of large fusiform foraminifera. *Lethaia 22*, pp. 1 –12.

Shah, S.M. I., 1977: *Stratigraphy of Pakistan*: Geological Survey of Pakistan, Memoirs, v. 12, pp. 1-137.

Sibley, D.F., & Gregg, J.M., 1987: Classification of dolomite rock textures: *Journal of Sedimentary Petrology, v. 57*, pp. 967-975.

Sinclair, H.D., Sayer, Z.R., Tucker, M.E., 1998. Carbonate sedimentation during early foreland basin subsidence: the Eocene succession of the French Alps. In: Wright, V.P., Burchette, T.P. (Eds.), Carbonate Ramps. *Geological Society of London Special Publication*, v. 149, pp. 205– 227

Smale. D., Nelson. C. S., Kamp, P. J. J., & Ricketts. B., 2005: An integrated sequence stratigraphic, palaeoenvironmental, & chronostratigraphic analysis of the Tangahoe Formation, southern Taranaki coast, with implications for mid-Pliocene (c. 3.4-3.0 Ma) glacio-eustatic sea-level changes: J*ournal of the Royal Society of New Zeal& Volume 35*, Numbers 1 & 2, March/June , pp. 151-196.

Somerville, I. D., & Strogen, P., 1992: Ramp sedimentation in the Dinantian limestone of the Shannon Trough, Co. Limerick, Irel&. In: B.W. Sellwood (Editor), *Ramps & Reefs. Sediment. Geol., 79*: pp. 59-75.

Staubli, A., 1989., Polyphase metamorphism & the development of the Main Central thrust: *Journal of Metamorphic Geology, v. 7*, pp. 73–93.

Tahirkheli, R. A. K., Mattauer, M., Proust, F., & Tapponnier, P., 1979: The India-Eurasia suture zone in the northern Pakistan: Synthesis & interpretation of recent data at plate scale, in Farah, A., & DeJong, K. A., eds., *Geodynamics of Pakistan:* Quetta, Geological Survey of Pakistan, pp. 125–130.

Tahirkheli, R.A.K., 1982: Geology of the Himalaya, Karakoram & Hindukush in Pakistan. *Geol. Bull.* Univ. Peshawar, v. 15, pp. 1-15.

Tahirkheli, R.A.K., 1983: Geological Evolution of Kohistan Island Arc on the southern flank of Karakoram-Hindukush in Pakistan. *Gefis. Teorica applicatta 25 (99-100)*, pp. 351-364.

Tanoli.S.K., Abbasi, I. A., Riaz. M., Rehman. O., Iqbal. H. & Akhtar, M. K., 1993a: Sedimentology of the Eocene sequence in the Kohat Basin. Unpublished report*, collaborative research project* of NCE in Geology & OGDC, Islamabad.

Tanoli.S.K. Abbasi, I. A., Riaz. M., Rehman. O., Iqbal. H. & Akhtar, M. K., 1993b. Chashmai Formation: A new early Eocene Formation in the Kohat Basin. Pakistan *Journal of Petroleum Technology, 2*, pp. 37-41.

Tim R. Naish, Florian Wehland, Gary S. Wilson Greg H. Browne1, Tonarini, S., I. Villa, F. Oberli, M. Meier, D. Spencer, U. Pognante, & J. Ramsay., 1993:Eocene age of eclogite metamorphism in Pakistan Himalaya: Implications for India-Eurasia collision, *Terra Nova, 5*, pp.13 – 20.

Treloar, P. J., & Izatt, C. N., 1993: Tectonics of the Himalayan collision between the Indian plate & the Afghan block: A synthesis, in Searle, M. P., & Treloar, P. J., eds., Himalayan tectonics: *Geological Society of London Special Publication 74*, p. 69–87.v. 9, pp. 116–144

Tucker, M. E., & V. P. Wright., 1990: *Carbonate Sedimentology*: Cambridge, Blackwell Science, pp. 482.

Tucker, M.E., Calvet, F., Hunt, D., 1993: Sequence stratigraphy of carbonate ramps: systems tracts, models & application to the Muschelkalk carbonate platform of eastern Spain. - In: Posamentier, H.W., Summerhayes, C.P., Haq, B.U. & Allen, G.P. (eds.): Sequence stratigraphy & facies associations. - *Spec. Publ. Int. Ass. Sedimentol., 18*, pp. 397-415, 16 Figs., 1 Tab., Oxford.

Uddin, A., & Lundberg, N., 1998: Cenozoic history of the Himalayan-Bengal system & composition in the Bengal basin, Bangladesh: *Geological Society of America Bulletin,v. 110*, pp. 497–511. *Utrecht Micropaleontological Bulletins 15, 7 – 26. v. 149*, pp. 181–203.

Vredenburg, E.W., 1906: Nummulites douvillei, an undescribed species from Kachh with remarks on the zonal distribution of Indian Nummulites. *Records of the Geological Survey of India*, *34*: pp.79–95.

Warwick, P. D., & Wardlaw, B. R., 1992: Paleocene–Eocene stratigraphy in northern Pakistan: Depositional & structural implications: 7th Annual Himalaya-Karakoram-Tibet Workshop Programme & Abstracts, Oxford, pp. 97.

Weiss, W., 1988: Larger & Planktonic Foraminiferal Biostratigraphy of Cretaceous & Palaeogene in the Salt Range, the Kohat area & the Sulaiman Range, Pakistan, Hannover, *HDIP-BGR*, pp. 57.

Weiss, W. 1993: Age assignments of larger foraminiferal assemblages of Maastrichtian to Eocene age in northern Pakistan. *Zitteliana, 20*: pp. 223–252.

Wells, N. A., 1983: Transient streams in sand-poor red beds: Early–middle Eocene Kuldana Formation of northern Pakistan, in Collinson, J. D., & Lewin, J., eds., Modern & ancient fluvial systems: *International Association of Sedimentologists Special Publication 6*, pp. 393–403.

Wells, N. A., 1984: Marine & continental sedimentation in the early Cenozoic Kohat basin & north-western Indo-Pakistan [Ph.D. dissert.]: Ann Arbor, University of Michigan, 465 pp.

Wescott, W. A., & Ethridge, F. G., 1980: Fan-delta sedimentology & tectonic setting—Yallahs fan delta,southeast Jamaica: *American Association of Petroleum Geologists Bulletin*, *v. 64,* pp. 374–399.

Wilson, J.L., 1975: *Carbonate facies in geologic history* - 471 pp., 183 Figs., 30 Pls., New York (Springer).

Yeats, R. S., & Hussain, A., 1987: Timing of structural events in the Himalayan foothills of northern Pakistan: *Geological Society of America Bulletin, v. 99*, pp. 161–176.

Zeitler, P.K., Tahirkheli, R.A.K., Naeser, C.W., Johnson, N.M., 1982: Unroofing history of a suture zone in the Himalaya of Pakistan by means of fission-track annealing ages. *Earth & Planetary Science Letters 57 (1),* pp. 227–240.

**Appendix 1.** Taxonomic list and original references of the larger benthic foraminiferal species. For the determinations at the generic and species level, I largely followed the taxonomy presented in Nuttal (1926), Gills (1953), Racey (1995) and Renema (2002). After comparison of the available synonymy list of the recorded species I selected widely used species name in the following list.

### *Nummulites pinfoldi* Davies (1940)
**Synonymy**
**1924** *Nummulites cf, ramondi* Defrance--------- Davies, p.211; 1926b, p 199.
**1940** *Nummulites pinfoldi* Davies---------Davies, p. 230, pl. X, figs. 1-6, 8.

### *Nummulites atacicus* Leymerie (1919)
**Synonymy**
**1846** *Nummulites atacica* ----- Leymerie, p. 358, pl. 13, figs. 13a-e.
**1919** *Nummulites atacicus* Leymerie ------ Douville, p. 41-43, pl. 5, fig. 21.
**1981** *Nummulites atacicus* Leymerie---------Schaub, p. 119, table 14, fig. I ; pl. 25, figs. 1-51.

### *Nummulites subatacicus* (1919)
**Synonymy**
**1919** *Nummulites subatacicus* -------- Douville, p. 41-43, pl. 3, figs. 7-8.

### *Nummulites globulus* Leymerie (1846)
**Synonymy**
**1846** *Nummulites globulus* -------- Leymerie, p. 7, pl. 13, figs. 140a-d.
**1919** *Nummulites globulus* Leymerie ---- Douville, p. 54, pl. 1, figs. 12-17.
**1937** *Nummulites globulus* Leymerie ----Davies and Pinfold, p. 22, pl. 3, fig. 3.
**1978** *Nummulites mamilla* (Fichtel and Moll)—Kureshy, p.54, pl. 6, fig. 3.

### *Nummulites mamilla* Fichtel and Moll (1925)
**Synonymy**
**1925** *Nummulites mamilla* (Fichtel and Moll) ---Nuttall, p. 445, pl. 27, figs. 1-3.
**1978** *Nummulites mamilla* (Fichtel and Moll)—Kureshy, p.54, pl.6, fig. 3,

### *Nummulites beaumonti* d' Archiac & Haime (1853)
**Synonymy**
**1853** *Nummulites beaumonti* ------ d' Archiac & Haime, p. 133-134, pl. 8, figs.1-3; 1881.
**1871** *Nummulites pengaroensis* ------- Verbeek, p. 3- 6, pl. 1, figs. la-k.
**1874** *Nummulites birritzensis* d, Archaic & Haime 1853----Verbeek, p. 155
**1912a** *Nummulites Kelatensis* Carter------- Douville, p.262.
**1926** *Nummulites stemineus* ---Nuttall, p. 130- 131, pl. 1, figs. 4, 5.
**1959** *Nummulites beaumonti* d' Archiac & Haime-----Nagappa, p. 180, pl. 8, figs. 5-17, pl. 9, figs.1, 2.

### *Nummulites acutus* Sowerby (1840)
**Synonymy**
**1840** *Nummularia acuta* ------Sowerby, p. 329, pl. 24, figs. 13,13a.
**1881** *Nummulina djokdjokartae* ------Martin, p. 109,110, pl. 5, figs. 8-11.
**1906** *Nummulites douvillei*------ Vredenburgh, 6, p. 79-84, pl. 8, figs. 1-13
**1908** *Nummulites vrendenbergi*------- Prever p. 239.
**1926** *Nummulites djokdjokartae* (Martin) -------Nuttal, p. 134.
**1934** *Camerina diokdiokartae* (Martin) ----- Caudri, pl. 67, 72. fig19.
**1959** *Nummulites acutus* (Sowerby) -- Nagappa, p. 180,181, pl. 9, figs. 8,9, pl. 10, figs.1, 2.

### *Nummulites djokdjokartae* Martin (1881)
**Synonymy**
**1881** *Nummulina djokdjokartae* -----Martin, p. 109,110, pl. 5, figs. 8-11.
**1912** *Nummulites djokdjokartae* (Martin) ----Douville, p. 283, pl. 22, figs. 8, 9.

### *Nummulites pengaroensis* Verbeek (1871)

**Synonymy**

**1871** *Nummulites pengaroensis*----Verbeek p. 3-6, pl. 1, figs. la-k.
**1931** *Camerina pengaroensis* Verbeek---Umbgrove, p. 50.
**1932** *Camerina pustulosa* Douville--- Doornik, p.286.
**1981b** *Nummulites pengaroensis* Verbeek---- Hashimoto & Matsumaru, p 68.
**2002** *Nummulites pengaroensis* Verbeek----Renema, p.257. pl. 10, fig A-E.

### *Nummulites perforatus* De Montfort (1972)

**Synonymy**

**1808** *Eogeon perforatus* ------De Montfort, p. 166-167.
**1972a** *Nummulites perforatus* (de Montfort) ------Blondeau, p. 238; pl. 34, figs 6-11.
**1981** *Nummulites perforatus* (de Montfort) -------- Schaub, p. 88; table2, fig. m; pl. 17; pl. 18; pl. 19, figs 1-8.
**1995** *Nummulites perforatus* (de Montfort) ------ Racey. A, Pl 3, figs 1-7.

### *Assilina dandotica* Davies & Pinfold (1937)

**Synonymy**

**1937** *Assilina dandotica*---- Davies and Pinfold, p. 28, pl. 4, figs. 1-3, 6-8.
**1981** *Assilina dandotica*---- Schaub p. 206, pl. 84, figs. 1-16.

### *Assilina granulosa* d'Archiac (1906)

**Synonymy**

**1847** *Nummulina granulosa*. sp. nov. (Pars)------- d, Archaic, *Bull. Soc. Geol. France*, (2) Vol.IV, p. 1010.
**1853** *Nummulites granulosa*. d,Archiac (pars) ----d, Archaic & Haime Descr. An. Foss. Gr. Numm. Inde, pp 151-153, 181; Pl. X, figs. 11-12, 16-17.
**1906** *Assilina granulosa* (d'Archiac) (pars)-----Vredenburgh, Rec. Geol. Surv.Ind. XXXIV, pp. 86-87, 94, 173-199.
**1953** *Assilina granulosa* (d'Archiac) -----Gill, p. 82, pl. 4, figs. 8-15.
**1972** *Assilina laxispira* de la Harpe ---Blondeau. p. 71, pl. 38, figs. 5-7.

### *Assilina leymerie* d, Archaic & Haime (1896)

**Synonymy**

**1896** *Assilina spira* de Roissy— Verbeek & Fennnema, p. 1102-1103.
**1896** *Nummulites (Assilina) leymeriei* d'Archiac & Haime----Verbeek & Fennema, p. 1103-1104.
**1932** *Assilina granulosa* d'Archiac---- Doornink, p. 301-303.
**1934** *Assilina* spec. *granulosa-exponens* (pars) ----Caudri, p. 34-39.
**1953** *Assilina leymerie* (d, Archaic & Haime) ---Gill, p. 83, pl.14, figs.17
**2002** *Planocamerinoides* sp--- Renema, fig. 6.20; Pl. 12, figs. G-K.

### *Assilina pappilata* Nuttal (1926a)

**Synonymy**

**1879** *Nummulites granulosa* d, Archaic (pars) -----Fedden, p. 199.
**1926a** *Assilina papillata* Nuttal.----- Nuttal, p. 44, pl. 6, figs. 5-7.
**1981** *Assilina papillata* Nuttal ---------Schaub, p. 205, pl. 96, figs. 26-39; pl. 97, figs. 1 4, 8-12. *cum syn.*

### *Assilina subpappilata* Nuttal (1926a)

**Synonymy**

**1926a** *Assilina sub papillata*------- Nuttal. p. 44, pl. 6, figs. 5-7.

### *Assilina davisie* de Cizancourt (1938)

**Synonymy**

**1938** *Assilina davisie* de Cizancourt------ Mem. Soc. Geol. France, n.s. 17. fasc.1. Mem. 39, pl. 3, fig 24.
**1924** *Assilina granulosa* (d, Archiac) ----Davies, Jour. Asiat. Soc. Bengal, (n.s.), vol. 20, p. 213.
**1925** *Assilina granulosa* (d, Archiac) (part) ---Nuttal, Ouart. Tour. Geol. Soc. London, vol. 81, pl. 26,-fig. 2.
**1937** *Assilina* cf. *A. pustulosa* Doncieux -------Davies and Pinfold, vol 24, Mem. 1, pl. 4, figs. 13-15, 18, 22.

### *Assilina subdavisie* de Cizancourt (1938)

**Synonymy**

**1938** *Assilina subdavisie* de Cizancourt, Mem. Soc. Geol. France, n.s. 17. Mem. 39. pI. 23, fig 24.

### *Assilina spinosa* Davies (1937)

**Synonymy**

**1937** *Assilina spinosa*------ Davies p.31, pl. 4, fig. 11,12
**1953** *Assilina spinosa* Davies-------- Gill p. 82, pl.14, figs.3-7.

### *Assilina subspinosa* Davies (1937)

**Synonymy**

**1879** *Nummulites granulosa*. d, Arch (pars)----Fedden, Mem. Geol. Surv. Ind., XVII, p. 199.
**1906** *Assilina miscella* (d, Arch. & Haime) ----Vredenburgh, Rec. Geol. Surv. Ind., XXXIV, pp. 86, 94, 187-188.
**1926** *Assilina ranikoti,* sp. Nov. (pars) ----Nuttal, *Geol. Mag. Lond., Vol.* LXVIII, p. 117; Pl. X, figs. 7-8.
**1926** *Assilina ranikotensis,* Nuttal; Nuttal rec. Geol. Surv. Ind., LXV, pp. 307.
**1937** *Assilina subspinosa*------ Davies, p.31.

### *Assilina pustulosa* Doncieux (1926)

**Synonymy**

**1924** *Assilina granulosa* (d, Archiac) ------ Davies, Jour. Asiat. Soc. Bengal, (n.s.), vol. 20, p. 213.
**1926** *Assilina pustulosa*--------- Doncieux, p. 52, pl. 5, figs. 3643; pl. 6, fig. 1.
**1953** *Assilina davisie de Cizancourt var nammalensis var. nov.* ----- Gill, p.81, pl. 13, fig 1-5.

### *Assilina laminosa* Gill (1953)

**Synonymy**

**1912b** *Assilina orientalis*---- Douvillé, p. 263.
**1953** *Assilina laminosa*---- Gill, p. 76-86.
***2002*** *Planocamerinoides orientalis* (Douvillé, 1912b)---Renema, fig. 6.19; pl. 12, fig. F.

### *Assilina sublaminosa* Gill (1953)

**Synonymy**

**1953** *Assilina sublaminosa* ----Gill, p. 83, pl.13, figs.18-19

### *Assilina suteri* Schaub (1981)

**Synonymy**

**1960** *Assilina reicheli* ----Ziegler, p. 225, fig. 9, pl. 3, figs. 6, 7.

**1981** *Assilina suteri* ---------Schaub, p**.** 216, pl. 95, figs. 1-9.
**1995** *Assilina suteri* Schaub ----- Racey, pl. 8, figure 12, 13-19.

### *Assilina exponense* Sowerby (1840)

**Synonymy**
**1840** *Nummulites exponense*----- Sowerby , p. 719, pl. 41, figs. 14 a-e.
**1861** *Assilina exponens* (Sowerby) –Carter, p. 373-376, pl. 15, figs.6a-d.
**1861** *Assilina obesa* -------Carter, p. 368, pl. 15, figs. 2a-d.
**1915** *Nummulina mamillata* (d'Archiac) -------Danielli, p. 191-193, pl. 22, figs.15-23; pl. 24, figs. 4,
8, 9; pl. 25, fig. 6.
**1995** *Assilina exponens* (Sowerby 1840) ------ Racey. pl. 9, figures 6-10.

### *Assilina cancellata* Nuttal (1926a)

**Synonymy**
**1926a** *Assilina cancellata*----------Nuttal, p. 141, pl. 5, figs. 1-13.

### *Assilina subcancellata* Nuttal

**Synonymy**
**1926** *Assilina Subcancellata*------- Nuttal, p. 14.

**Appendix 2.** Taxonomic list and original references of recorded smaller benthic foraminiferal species. The determinations at the generic and species level, I largely followed the taxonomy presented in Davies (1940), Loblich and Tappan, (1988) and Bolli et al., (1994). After comparison of the available synonymy list of the recorded species I selected widely used species name in the following list.

***Textularia dibollensis var humblei* Cushman and Applin (1926)**
**Synonymy**
**1926** *Textularia dibollensis var humblei*. p. 165, pl. 5, figs. 12-19.
**1941** *Textularia dibollensis var humblei* (Cushman and Applin) p. 144-152, pl. 24, figs 7a, 7b.

***Textularia hannai* Davies (1941)**
**Synonymy**
**1941** *Textularia hannai*------- Davies pl. 24, figs 11-13, 19a, 19b.

***Textularia martini* pijpers (1933)**
**Synonymy**
**1933** *Textularia martini*------- Pijpers, p. 57, figs. 6-10.

***Textularia grahamensis* Cushman and Waters (1959)**
**Synonymy**
**1959** *Textularia grahamensis* ---Cushman and Waters, p. 492, pl. 7, fig 5a.

***Textularia barrettii* Jones and Parker (1863)**
**Synonymy**
**1863** *Textularia barrettii*-----Jones and Parker, p. 80-105.
**1922** *Textularia trochus*----- d 'Orbigny, p. 20, pl. 3, figs. 3-6.

***Textularia losangica* Loblich and Tappan (1951)**
**Synonymy**
**1943** *Textularia washitensis Carsey*--- Tappan, p. 486, pl. 78. figs. 5-9.
**1951** *Textulaia losangica* ----Loblich and Tappan p. 82, pl.21, figs 4-5.
**1994** *Textulaia losangica* Loblich and Tappan --- Bolli et al., p. 84, fig 22.9.

***Conotrochammina cf dispersa* Finlay (1994)**
**Synonymy**
1994 *Conotrochammina cf dispersa Finlay*---- Bolli et al., fig 22.38.

***Bathysiphon eocenicus* Cushman & Hanna (1927)**
**Synonymy**
**1927** *Bathysiphon eocenica*------ Cushman & Hanna, p. 210, p1. 13, figs 2, 3.
**1951** *Bathysiphon eocenica* Cushman & Hanna-----Cushman & Stainforth, p. 142, p1. 25, fig. 4.
**1994** *Bathysiphon eocenicus* Cushman & Hanna --- Bolli et al., p. 65, fig. 18.3.

***Arenobulimina truncata* Reuss (1845)**
**Synonymy**
**1845** *Bulimina truncanata*------Reuss, p.37, pl. 8, fig. 73.
**1988** *Arenobulimina truncanata* (Reuss) --- Kaminski et al., 1988, p. 194, pl. 8, fig. 10
**1994** *Arenobulimina truncanata* (Reuss) -------Bolli et al., p. 91, figs 24.19-20.

***Dendrophyra excelsa* Grzybowski (1898)**
**Synonymy**
**1898** *Dendrophyra excelsa* -----Grzybowski p. 16, pl. 10, fig 2-4.
**1994** *Dendrophyra excelsa Grzybowski*---- Bolli et al., fig 18.8.

***Burmudezina cubensis,* Palmer and Bermudez (1959)**
**Synonymy**
**1959** *Burmudezina cubensis*----- Palmer and Bermudez. p. 564, pl.43, fig 23.

***Gaudryina leveagata* Frank (1914)**
**Synonymy**
**1914** *Gaudryina leveagata* -----Frank, p. 431, pl.27, figs 1-2.

***Hyperammina elongata* Brady (1878)**
**Synonymy**
**1878** *Hyperammina elongata*---- Brady, p. 433, pl. 20, fig. 2.
**1928** *Hyperammina elongata* H.B. Brady, ----Cushman and Renz, p. 86, pl.12, fig. 1.
**1994** *Hyperammina elongata* Brady----Bolli et al., fig.18.19.

***Guadryinella pussilla* Magneiz-Jannin (1975)**
**Synonymy**
**1975** *Guadryinella pussilla* -----Magneiz-Jannin, p. 68, pl. 5, fig. 15-22.
**1994** *Guadryinella pussilla* Magneiz-Jannin--- Bolli et al., p. 181, fig. 24.14.

***Gaudryina pyramidata* Cushman (1946)**
**Synonymy**
**1946** *Gaudryina pyramidata* ----Cushman, p. 21, pl. 2, fig 21.
**1951** *Pyramidata* Cushman var tumiyensis ----Israelsky p. 18, pl. 8, fig. 7.

***Cibicides cf simplex* Brotzen (1948)**
**Synonymy**
**1948** *Cibicides cf simplex*------- Brotzen, p.83, pl. 13, figs.4, 5.
**1994** *Cibicides cf simplex*---------Bolli, p .149, figs 40.15-17.

***Cibicides alleni* Plummer (1926)**
**Synonymy**
**1926** *Truncatulina alleni*----Plumer, H. J: UTB 2644, p. 144, pl. 10, fig. 4.
**1951** *Cibicides alleni* (Plumer) ---Cushman, J.A: USGSPP 232, p. 166, pl. 18.
**1956** *Cibicides alleni* (Plumer) --- Haq, p. 207, pl. 16, fig 1a-c, pl. 33, figs. 3a-c

***Cibicides mensilla* (Schwager) *var. nammalensis* (1956)**
**Synonymy**
**1956** *Cibicides mensilla* (Schwager) *var. nammalensis*---- Haq, p. 206, pl 20, fig. 10.

***Cibicicoides tuxpamensis laxispiralis* Beckmann (1991)**
**Synonymy**
**1991** *Cibicidoides tuxpamensis laxispiralis* -----Beckmann, p. 827, pl.2, figs 10, 14, 15.
**1994** *Cibicidoides tuxpamensis laxispiralis* Beckmann ---------Bolli et al, p .148, figs. 40.4-6.

***Cibicidoides tuxpamensis tuxpamensis* Cole (1928)**
**Synonymy**
**1928** *Cibicidoides tuxpamensis tuxpamensis*----- Cole, Bull. Am. Paleontol, 14/53, p.219, pl. 1 figs 2, 3; pl. 3, figs. 5, 6.
**1994** *Cibicidoides tuxpamensis tuxpamensis* Cole------Bolli, p .148, figs 40.1-3.

***Gavelinella dakotensis* Fox (1954)**
**Synonymy**
**1954** *Planulina dakotensis* -----Fox, Prof. pap. U.S. Geol. Survey, 254-E, p. 119, pl. 26.
**1994** *Gavelinella dakotensis* (Fox) ---------Bolli et al, p .162, figs. 46.14-16.

***Gavelinella aracajuensis* Petri**
**Synonymy**
**1954** *Eponoides aracajuensis* Petri-----Bol. Fac. Filosofia, Ciencias, Letras, Univ. Sao Paulo,

***Gavelinella schloenbachi* Reuss (1863)**

**Synonymy**

**1863** *Rotalia schlonbachi*----- Reuss, p. 84, pl. 10, fig. 5.

**1994** *Gavelinella schloenbachi* (Reuss) -------Bolli, p .164, figs. 46.33-34, 40-41.

***Bulimina stokesi* Cushman and Renz (1946)**

**Synonymy**

**1946** *Bulimina stokesi* Cushman and Renz-------p. 37, pl. 6, fig. 14.

**1994** *Bulimina stokesi* Cushman and Renz------- Bolli et al., p. 136, figs. 36.24-26.

***Uvigerina gallowayi basicordata* Cushman and Renz (1945)**

**Plate 14; figure 9**

**Synonymy**

**1945** *Uvigerina gallowayi* ----Cushman and Renz, pl. 07, fig. 14.

**1994** *Uvigerina gallowayi basicordata* Cushman and Renz—p. 239, fig. 5.13.

***Uvigerina spinicostata* Cushman and Jarvis (1994)**

**Synonymy**

**1945** *Uvigerina spinicostata* ----Cushman and Stainforth, pl. 7, fig. 16.

**1994** *Uvigerina spinicostata* Cushman and Jarvis--- Bolli et al., p. 239, fig. 54.25-26

***Bollivinoides decoratus decoratus* Jones (1886)**

**Synonymy**

**1886** *Bollivina decoratus*----- Jones, Porc. Belfast. Nat. Field Club, n. ser., 1, appendix 9, p. 330, pl. 27, figs. 7, 8.

**1964** *Bollivinoides decoratus decoratus* (Jones 1886) --- Beckmann & Koch, p.43, pl. 6, fig.10.

**1994** *Bollivinoides decoratus decoratus* Jones------Bolli et al., p. 129, fig. 34.35.

***Bollivinoides delicatulus curtus* Reiss (1954)**

**Synonymy**

**1954** *Bollivinoides curta*--- Reiss, Contrib. Cushman Found. Foramin. Res., 5, p. 58, pl. 30, figs. 15- 16.

**1964** *Bollivinoides delicatulus curtus* (Reiss 1954) --- Beckmann & Koch, p.43, pl. 6, fig. 2-3.

**1994** *Buliminella grata* Parker and Bermudez------Bolli et al., p. 137, fig. 37.3.

**Appendix 3**

| PATALA FORMATION | | |
|---|---|---|
| PANOBA NALA SECTION | **Sample No** | **Petrographic features** |
| | **PTP 1-PTP6** | **Panktonic wackestone microfacies (PTK 1)**<br>**Allochems:** Planktonic foraminifera (10-30 % with an average of 15%)<br>**Matrix:** Allomicritic matrix dominates (60-90 % with an average of 75 %) |
| | **PTP 7-PTP12** | ***Nummuiltic* wackestone microfacies (PTK 2)**<br>**Allochems:** Larger benthic foraminifera dominated by *Nummulites sp*. (15-20 % with an average of 17%) and algae (5-10 % with an average of 8 %)<br>**Matrix:** Allomicritic matrix dominates (50-90 % with an average of 70 %) |
| | **PTP13-PTP16** | **Mixed faunal wackestone to Packstone microfacies (PTK 3)**<br>**Allochems:** Larger benthic foraminifera dominated by *Nummulites sp*. , *Assilina sp, Alveolina sp., Orbitolites complanata, Milliliolids,* Ostracodes, bivalves (60-80% with an average of 65%).<br>**Matrix:** Allomicritic matrix dominates (20-40 % with an average of 30 %) |
| | **PTP17-PTP 21** | **Diverse foraminiferal Packstone microfacies (PTK 4)**<br>**Allochems:** Larger benthic foraminifera dominated by *Nummulites sp*. , *Assilina sp, Discocyclina sp.,* (70-90% with an average of 80%).<br>**Matrix:** Allomicritic matrix ranges in abundance from 20-30% with an averge of 22%. |

| PATALA FORMATION | | |
|---|---|---|
| TARKHOBI NALA SECTION | **Sample No** | **Petrographic features** |
| | **PTT 1-PTT 5** | **Panktonic wackestone microfacies (PTK 1)**<br>**Allochems:** Planktonic foraminifera (10-30 % with an average of 15%)<br>**Matrix:** Allomicritic matrix dominates (60-90 % with an average of 75 %) |
| | **PTT 7-PTT12** | ***Nummuiltic* wackestone microfacies (PTK 2)**<br>**Allochems:** Larger benthic foraminifera dominated by *Nummulites sp*. (15-20 % with an average of 17%) and algae (5-10 % with an average of 8 %)<br>**Matrix:** Allomicritic matrix dominates (50-90 % with an average of 70 %) |
| | **PTT 13-PTT16** | **Mixed faunal wackestone to Packstone microfacies (PTK 3)**<br>**Allochems:** Larger benthic foraminifera dominated by *Nummulites sp*. , *Assilina sp, Alveolina sp., Orbitolites complanata, Milliliolids,* Ostracodes, bivalves (60-80% with an average of 65%).<br>**Matrix:** Allomicritic matrix dominates (20-40 % with an average of 30 %) |
| | **PTT17-PTT 21** | **Diverse foraminiferal Packstone microfacies (PTK 4)**<br>**Allochems:** Larger benthic foraminifera dominated by *Nummulites sp*. , *Assilina sp, Discocyclina sp.,* (70-90% with an average of 80%).<br>**Matrix:** Allomicritic matrix ranges in abundance from 20-30% with an averge of 22%. |

| PANOBA FORMATION | | |
|---|---|---|
| PANOBA NALA SECTION | **Sample No** | **Biofacies** |
| | **PTT 1-PTT 5** | ***Bulimina* biofacies**<br>**Fauna:** mostly smaller benthic foraminifera (*Bulimina gracilis, Bulimina tuxpamensis,Taxtularia cuyleri Taxtularia hannai* )<br>**Preservation:** good (foraminiferal tests are identifiable)<br>**Diversity:** low to high |
| | **PTT 7-PTT12** | ***Uvigerina* biofacies**<br>**Fauna:** mostly smaller benthic foraminifera (*Uvigerina rustica, Uvigerina gallowwayi basicordata*, *cibicides cf. simplex, Cibicides alleni, Cibicides mensilla, Cibicidoides tuxpamensis, Loxostomum applinae, Vulvulanaria patalensis, Praebulimina cf seebensis, Bulimina strokesi, Bolivinoides decoratus*)<br>**Preservation:**very good<br>**Diversity:** High |
| | **PTT 13-PTT16** | ***Bathysiphon/Gaudryina* biofacies**<br>**Fauna:** mostly agglutinated smaller benthic foraminifera (*Bathsiphon robustus, Bathysiphon eocenicus, Gaudryina leveagata, Guadryinella pussilla, Guadryina pyramidata, Haplophragmoides concavus, Haplophragmoides porrectus, Cibicides sp,Bolivinoides sp., cibicidoides sp*.)<br>**Preservation: good**<br>**Diversity:** moderate to high |

| PANOBA FORMATION | | |
|---|---|---|
| SHEIKAH NALA SECTION | **Sample No** | **Biofacies** |
| | **PTT 1-PTT 5** | ***Bulimina* biofacies**<br>**Fauna:** mostly smaller benthic foraminifera (*Bulimina gracilis, Bulimina tuxpamensis, Praeglobobulimina ovata, Taxtularia cuyleriTaxtularia hannai, Taxtularia barreti, Taxtularia getrudeana, Taxtularia martinin, Taxtularia dibolensis*)<br>**Preservation:** good<br>**Diversity:** low to high |
| | **PTT 7-PTT12** | ***Uvigerina* biofacies**<br>**Fauna:** mostly smaller benthic foraminifera (*Uvigerina rustica, Uvigerina spinicostata, Uvigerina gallowwayi basicordata*, *Cibicidoides tuxpamensis laxispiralus, millliliods,Gavlinella dakotensis, Gavlinella schloenbachi, Stensioeina excolata,cibicides cf. simplex, Cibicides alleni, Cibicides mensilla, Cibicidoides tuxpamensis, Loxostomum applinae, Vulvulanaria patalensis, Praebulimina cf. seebensis, Bulimina strokesi, Bolivinoides decoratus*)<br>**Preservation:**very good<br>**Diversity:** High |
| | **PTT 13-PTT16** | ***Bathysiphon/Gaudryina* biofacies**<br>**Fauna:** mostly agglutinated smaller benthic foraminifera (*Bathsiphon robustus, Bathysiphon eocenicus, Gaudryina leveagata, Guadryinella pussilla, Guadryina pyramidata, Haplophragmoides concavus, Haplophragmoides porrectus, Bolivinoides sp., Gavlinella schloenbachi, Stensioeina excolata, Cibicides cf. simplex, Cibicides alleni, Cibicides mensilla,Cibicidoides tuxpamensis, Loxostomum applinae, Vulvulanaria patalensis, Praebulimina cf. seebensis, Bulimina strokesi, Bolivinoides decoratus, Bulimina gracilis, Bulimina tuxpamensis, Praeglobobulimina ovata, Taxtularia sp.*)<br>**Preservation:** good<br>**Diversity:** moderate to high |

| PANOBA FORMATION | | |
|---|---|---|
| TARKHOBI NALA SECTION | **Sample No** | **Biofacies** |
| | **PTT 1-PTT 5** | ***Bulimina* biofacies**<br>**Fauna:** mostly smaller benthic foraminifera (*Bulimina gracilis, Bulimina tuxpamensis,Praeglobobulimina ovata, Taxtularia hannai, Taxtularia barreti, Taxtularia getrudeana, Taxtularia martinin,Taxtularia dibolensis* and *milliolids*)<br>**Preservation:** good<br>**Diversity:** high |
| | **PTT 7-PTT12** | ***Uvigerina* biofacies**<br>**Fauna:** mostly smaller benthic foraminifera (*Uvigerina rustica, Uvigerina spinicostata, Uvigerina gallowwayi basicordata*, *Cibicides mensilla,Cibicidoides tuxpamensis, Loxostomum applinae, Vulvulanaria patalensis, Praebulimina cf. seebensis,Cibicidoides tuxpamensis laxispiralus, milliliods, Gavlinella dakotensis,Gavlinellaschloenbachi, Stensioeina excolata,cibicides cf. simplex, Cibicides alleni, Bulimina strokesi, Bolivinoides decoratus*)<br>**Preservation:**very good<br>**Diversity:** High |
| | **PTT 13-PTT16** | ***Bathysiphon/Gaudryina* biofacies**<br>**Fauna:** mostly agglutinated smaller benthic foraminifera (*Bathsiphon robustus, Bathysiphon eocenicus, Gaudryina leveagata, Guadryinella pussilla, Guadryina pyramidata, Haplophragmoides concavus, Haplophragmoides porrectus, Loxostomum applinae, Vulvulanaria patalensis, Praebulimina cf. seebensis, Bulimina strokesi, Bolivinoides decoratus, Bolivinoides sp., cibicidoides sp*. *Gavlinella schloenbachi, Stensioeina excolata,cibicides cf. simplex, Cibicides alleni, Cibicides mensilla, Cibicidoides tuxpamensis*<br>**Preservation:** good<br>**Diversity:** moderate to high |

| SHEIKHAN FORMATION | | |
|---|---|---|
| | **Sample No** | **Petrographic features** |
| **TARKHOBI NALA SECTION** | **SNT 1-SNT 7** | **The peloidal – *Alveolina* rich bioclastic wackestone to packstone microfacies (SHF 3)**<br>The nonskeletal constituents include about 20 - 25 % peloids of varying sizes and shapes. Peloids are found in irregular, rounded, and random shapes, associated with bioturbation of algae and echinoids. The allomicrite matrix abundance ranges from 40-60 %, with an average of 40 %. |
| | **SNT 8-SNT 9 & SNT 11-12** | The dominant allochems are bioclasts of *Assilina* sp., and subordinate *Lockhartia* sp., echinoid clasts, small brachiopods are found. The allochemic abundance ranges from 40 to 80 %, with an average of 65 %. *Assilina* sp. bioclasts dominate and have a size range from 1 mm to 4 mm. The echinoid clasts are scattered in inhomogeneous allomicritic matrix which ranges in abundance from 40 to 50 %, with an average of 35 % . |
| | **SNT 10** | In thin section the SHF 7 microfacies shows the wackestone depositional texture which is dominated by a rich large benthic foraminiferal assemblage of *Discocyclina* sp. associated with *Nummulites* sp. and *Assilina* sp. The *Discocylina* sp. tests are completely preserved and scattered bioclasts are also common. Matrix is inhomogeneous allomicrite that ranges in abundance from 50 to 80 %, with an average of 75 %. |

| SHEIKHAN FORMATION | | |
|---|---|---|
| | **Sample No** | **Petrographic features** |
| **SHEIKHAN NALA SECTION** | **SNS 1-SNS 3** | ***Diverse bioturbated/burrowed wackestone - packstone microfacies (SHF 1)***<br>In thin section, the SHF 1 microfacies is characterized by a rich allochemic constituent of gastropods, echinoids, small brachiopods, *Nummulites* sp., and sparse ostracode shells. The matrix is grey coloured allomicrite, thoroughly bioturbated, ranges in abundance from 40-60 %, with an average of 50%. |
| | **SNS 4-SNS 9** | ***Bioclastic wackestone microfacies (SHF 2)***<br>The allochemic abundance in the SHF 2 microfacies ranges from 60–80 %, with an average of 65 %. Small gastropods, brachiopods, milliolids, *Nummulites* sp., distorted echinoid spines and algal peloids constitute the main allochemic constituents. |
| | **SNS 10- SNS11** | **The peloidal – *Alveolina* rich bioclastic wackestone to packstone microfacies (SHF 3)**<br>The allomicrite matrix abundance ranges from 30-60 %, with an average of 35 %. The nonskeletal constituents include about 10 - 25 % peloids of varying sizes and shapes. Peloids are found in rounded and random shapes. |
| | **SNS 12-SNS 13** | ***Diverse bioclastic/burrowed mudstone - wackestone microfacies (SHF 4)***<br>SHF 4 microfacies is characterized by diverse allochems that include *Alveolina* sp., *Nummulites* sp., *Assilina* sp., milliolids, brachiopods, gastropods, ostracodes, and minor green algae.The allomicrite matrix dominates and its abundance ranges from 20-60 %, with an average of 45 %. |

| SHEIKHAN FORMATION | | |
|---|---|---|
| | **Sample No** | **Petrographic features** |
| **SHEIKHAN NALA SECTION** | **SNS 14-SNS 22** | ***Milliolid rich packstone-grainstone microfacies (SHF 6)***<br><br>The SHF 6 microfacies shows the milliolid rich packstone to wackestone depositional textures. Allochems range in abundance from 40-80 %, with an average of 60 %. The allochems show dominance of foraminifera i.e. milliolids, *Alveolina* sp., *Nummulites* sp., *Operculina* sp. and *Lockhartia* sp. |

| SHEIKHAN FORMATION | | |
|---|---|---|
| PANOBA NALA SECTION | **Sample No** | **Petrographic features** |
| | **SNP 1-SNP 16** | ***Assilina rich bioclastic wackestone - packstone microfacies (SHF 8)***<br>The dominant allochems are bioclasts of *Assilina* sp., and subordinate *Lockhartia* sp., echinoid clasts, small brachiopods are found. The allochemic abundance ranges from 40 to 80 %, with an average of 65 %. *Assilina* sp. The echinoid clasts are scattered in inhomogeneous allomicritic matrix which ranges in abundance from 40 to 50 %, with an average of 35 %. . |
| | **SNP 17** | ***Discocyclina rich wackestone microfacies (SHF 7)***<br>The SHF 7 microfacies shows a rich large benthic foraminiferal assemblage of *Discocyclina* sp. associated with *Nummulites* sp. and *Assilina* sp. Matrix is inhomogeneous allomicrite that ranges in abundance from 60 to 75 %, with an average of 65 %. |
| | **SNP 18-SNP 28** | ***Poorly fossiliferous lime mudstone/dolomicrite microfacies (SHF 9)***<br>The SHF 9 microfacies shows poorly preserved biogenic content dominated by foraminifera and algal peloids. Micritic matrix ranges from 70-90 %, with an average of 85 %. |

| KOHAT FORMATION | | |
|---|---|---|
| SHEIKHAN NALA SECTION | **Sample No** | **Petrographic features** |
| | **KTS 1-KTS 9** | ***Foraminiferal packstone microfacies (KTF 1)***<br>In thin section the KTF 1 microfacies is characterized by the packstone depositional texture. Predominance of *Assilina* sp. bioclasts is noted with good biogenic preservation. The size of *Assilina* sp. bioclasts is ranging from 2 mm to 6 mm *Nummulites* sp. tests are also seen having spar filled chambers. Packing of the bioclasts is lose to moderate and they have poor sorting.The micritic matrix and scattered biodebris of *Assilina* sp. snd *Nummulites* sp. filled the intergranular space. |
| | **KTS 10-KTS 15** | ***Nummulitic packstone -grainstone microfacies (KTF 2)***<br>In thin section the KTF 2 microfacies is characterized by the packstone to grainstone depositional fabrics with dominant allochemic component of *Nummulites* sp. and subordinate *Assilina* sp. Brachiopod spines are also found.The biogenic content in mostly benthic and shows good preservation. |
| | **KTS 16-KTS 20** | ***Operculina rich mudstone-wackestone microfacies (KTF 3)***<br>In thin section the KTF 3 microfacies is characterized by the mudstone to wackestone depositional fabric. The biogenic content is well preserved and includes bioclastic assemblages of *Operculina* sp., rare small *Nummulites* sp., *Assilina* sp. |
| | **KTS 17-KTS 32** | ***Alveolina rich wackestone microfacies (KTF 4)***<br>In thin section the KTF 4 microfacies is characterized by dominance of monospecific assemblage of *Alveolina* sp. scattered in a micritic matrix which ranges from 25-55 %, with an average of 35 %. Sparse biodebris of *Nummulites* sp., *Assilina* sp., echinoids and small gastropods are also found. |

| KOHAT FORMATION | | |
|---|---|---|
| PANOBA NALA SECTION | **Sample No** | **Petrographic features** |
| | **KTP 1-KTP 3** | ***Nummulitic wackestone microfacies (KTF 5)***<br>In thin section the KTF 5 microfacies is characterized by the mudstone to wackestone depositional fabrics. The bioclasts include *Nummulites* sp., *Assilina* sp. and rare small boring gastropods. from 30 to 50 %, with an average of 35 %. The allomicrite matrix is dominant and it is enriched with scattered bioclastic fragments of foraminifera. The matrix is ranging from 40 - 80 %, with an average of 45 %. Microspar is 10-30%, with an average of 22 %. |
| | **KTP 4-KTP 7** | ***Gastropodal mudstone- wackestone microfacies (KTF 6)***<br>In thin section the KTF 6 microfacies is characterized by mudstone to wackestone depositional textures. Bioclastic constituents include dominance of small gastropods and rare *Nummulites* sp. Scattered small articulated brachiopods having <2 mm size and few >5mm size brachiopod spines are also observed. Echinoid spines are scattered. Allomicritic matrix is common and its abundance is ranging from 40-60 %, with an average of 45 %. Spar constitutes 20-40 %. |
| | **KTP 8 -KTP 15** | ***Intraclastic-bivalve rich wackestone microfacies (KTF 7)***<br>In thin section the KTF 7 microfacies is characterized by the wackestone depositional texture. The bioclasts abundance ranges between 10 - 20 %, with an average of 14 %. Intraclasts abundance is ranging from 30-50 %, with an average of 40 %.Small gastropods are seen scattered in an allomicritic matrix. Very rare detrital quartz grains are found |

| KOHAT FORMATION | | |
|---|---|---|
| BAHADUR KHEL TUNNEL SECTION | **Sample No** | **Petrographic features** |
| | **KTB 1-KTB 4** | ***Nummulitic wackestone microfacies (KTF 5)***<br>The KTF 5 microfacies show the mudstone to wackestone depositional fabric. The bioclasts include *Nummulites* sp., and rare small gastropods from 20 to 40 %, with an average of 25 %. The allomicrite matrix is ranging from 40 - 80 %, with an average of 55 %. |
| | **KTB 5-KTB 18** | ***Gastropodal mudstone- wackestone microfacies (KTF 6)***<br>The KTF 6 microfacies is characterized by mudstone to wackestone depositional textures. Allochemic constituents include small gastropods and *Nummulites* sp. Allomicritic matrix is ranging from 30-60 %, with an average of 40 %. Spar constitutes 20-40 % with an average of 25 %. |
| | **KTB 19 -KTB 23** | ***Intraclastic-bivalve rich wackestone microfacies (KTF 7)***<br>The KTF 7 microfacies show wackestone depositional texture. The bioclasts abundance ranges between 5 - 20 %, with an average of 12 %. Intraclasts abundance is ranging from 40-60 %, with an average of 45 %. Very rare detrital quartz grains are found. |

| LOCKHART FORMATION | | |
|---|---|---|
| SIKKI VILLAGE SECTION | **Sample No** | **Petrographic features** |
| | **LOKS 1 (2m thick)** | ***Diverse benthic foraminiferal wackestone-packstone microfacies (LKF 3)***<br>The biogenic content is well preserved having a rich allochemic constituent of larger benthic foraminifera ranging in abundance from 50-70%, with an average of 55%. The identified foraminiferal species are *Discocyclina ranikotensis*, *Miscellanea miscella, Operculina salsa, Lockhartia haime, Nummulites pinfoldi, Ranikothalia sindensis, Assilina spinosa* and *Alveolina globula.* The micritic matrix abundance ranges from 30–60 %, with an average of 45%. |
| | **LOKS 2-LOKS 3 (2.2m thick)** | ***Planktonic-benthic mixed foraminiferal lime mudstone - wackestone microfacies (LKF 4)***<br>The LKF 4 microfacies is characterized by the lime mudstone-wackestone depositional textures.The abundance of the allochems ranges from 10 –30 %, with an average of 18 %. Species of the larger benthic foraminifera include *Ranikothalia sahini* (figure 7.4 B)*, Operculina salsa*, *Miscellanea miscella* and *Discocyclina ranikotensis* having an abundance range of 30-45% of the total allochems .The micritic matrix dominates and ranges in abundance from 60-90 %, with an average of 75 %. Less than 5 % scattered quartz is also present in the allomicritic matrix. |
| | **LOKS 4-LOKS 8 (8m thick)** | ***Algal foraminiferal wackestone-packstone microfacies (LKF 1)***<br>The allochemic constituent ranges from 40-80 %, with an average of 60%. The microfloral components are dominated by calcareous green algae with an abundance that ranges from 40-60 % of the total allochems. The micritic matrix dominates and its abundance ranges from 25-45 % with an average of 30 %. |

| LOCKHART FORMATION | | |
|---|---|---|
| NAMMAL GORGE SECTION | **Sample No** | **Petrographic features** |
| | **LOKN 1, LOKN 4-7 (17m thick)** | ***Diverse benthic foraminiferal wackestone-packstone microfacies (LKF 3)***<br>The allochemic constituent of larger benthic foraminifera ranging in abundance from 40-70%, with an average of 50%. The species of *Discocyclina ranikotensis*, *Miscellanea miscella, Operculina salsa, Lockhartia haime, Ranikothalia sindensis, Assilina spinosa* and *Alveolina globula.* The micritic matrix abundance ranges from 25–60 %, with an average of 40%. |
| | **LOKN 2-LOKN 5 (13m thick)** | ***Alveolina rich bioclastic wackestone-packstone microfacies (LKF 2)***<br>The LKF 2 microfacies is characterized by the wackestone-packstone depositional texture having abundant allochems ranging from 40-70 %, with an average of 55%. Among the allochems alveolinid foraminifera dominate with good biogenic preservation. |
| | **LOKN 8 (8m thick)** | ***Algal foraminiferal wackestone-packstone microfacies (LKF 1)***<br>The allochemic constituent ranges from 40-80 %, with an average of 60%. The microfloral components are dominated by calcareous green algae with an abundance that ranges from 40-60 % of the total allochems. The micritic matrix dominates and its abundance ranges from 25-45 % with an average of 30 %. |

| LOCKHART FORMATION | | |
|---|---|---|
| NAMMAL GORGE SECTION | **Sample No** | **Petrographic features** |
| | **LOKT 1, LOKT 6 (29m thick)** | ***Alveolina rich bioclastic wackestone-packstone microfacies (LKF 2)***<br>The LKF 2 microfacies is characterized by the wackestone-packstone depositional texture. The allochems abundance ranging from 30-60 %, with an average of 45%. The micritic matrix ranges in abundance from 20–50 %, with an average of 30 %. Sparry cement fills the intergranular spaces. |
| | **LOKT 7-LOKT 9 (20m thick)** | ***Diverse benthic foraminiferal wackestone-packstone microfacies (LKF 3)***<br>The allochemic constituent of larger benthic foraminifera ranging in abundance from 40-60%, with an average of 40%. The micritic matrix abundance ranges from 20–60 %, with an average of 30%. The matrix has shown evidence of bioturbation and burrowing of small gastropods, ostracodes, algal thali and bivalves. Some terrestrial influx is seen in the form of scattered quartz grains. |
| | **LOKT 10-LOKT 22 (82m thick)** | ***Algal foraminiferal wackestone-packstone microfacies (LKF 1)***<br>The allochemic constituent ranges from 40-80 %, with an average of 60%. The microfloral components are dominated by calcareous green algae with an abundance that ranges from 40-60 % of the total allochems. The micritic matrix dominates and its abundance ranges from 25-45 % with an average of 30 %. Larger benthic foraminifera are commonly scattered through the allomicritic matrix. Well preserved foraminiferal species of *Miscellanea miscella, Alveolina vredenburgi*, *Nummulites deserti, Assilina spinosa, Alveolina globula,* and *Lockharti haime* are identified. Subordinate occurrence of bioclastic invertebrate fauna includes brachiopods (1mm - 3mm size range), ostracodes (2mm – 3mm size range), and small boring gastropods (less than 2 mm size). |

| LOCKHART FORMATION | | |
|---|---|---|
| KALABAGH HILLS SECTION | **Sample No** | **Petrographic features** |
| | **LOKK 1, LOKK 10 (50m thick)** | ***Alveolina rich bioclastic wackestone-packstone microfacies (LKF 2)***<br>The LKF 2 microfacies is characterized by the wackestone-packstone depositional texture. The allochems abundance ranging from 30-70 %, with an average of 48%. The micritic matrix ranges in abundance from 35–50 %, with an average of 40 %. After larger benthic foraminifera (mostly alveolinids), gastropods are the second most abundant allochems ranging in size from 0.5 mm to 2 mm with burrowing and boring modes. |
| | **LOKK 11-LOKK 12 (12m thick)** | ***Diverse benthic foraminiferal wackestone-packstone microfacies (LKF 3)***<br>The allochemic constituent of larger benthic foraminifera ranging in abundance from 30-60%, with an average of 42%. The micritic matrix abundance ranges from 30–60 %, with an average of 40%. Gastropods, bivalves and ostracodes are common. |
| | **LOKK 13-LOKK 22 (62m thick)** | ***Algal foraminiferal wackestone-packstone microfacies (LKF 1)***<br>The micritic matrix dominates and its abundance ranges from 30-45 % with an average of 32 %. The allochemic constituent ranges from 45-70 %, with an average of 55%. Calcareous green algae is common with an abundance that ranges from 40-50 % of the total allochems. Larger benthic foraminifera species of *Miscellanea miscella, Alveolina vredenburgi*, *Nummulites deserti, Assilina spinosa, Alveolina globula,* and *Lockharti haime* are present. Bracheopods, gastropods and ostracodes are also present. |

| LOCKHART FORMATION | | |
|---|---|---|
| CHICHALI NALA SECTION | **Sample No** | **Petrographic features** |
| | **LOKC 1, LOKC 7-8 (12m thick)** | ***Diverse benthic foraminiferal wackestone-packstone microfacies (LKF 3)***<br>The allochemic constituent of larger benthic foraminifera ranging in abundance from 30-60%, with an average of 42%. The micritic matrix abundance ranges from 30–60 %, with an average of 40%. Gastropods, bivalves and ostracodes are common. |
| | **LOKC 2-LOKC 6 (24m thick)** | ***Algal foraminiferal wackestone-packstone microfacies (LKF 1)***<br>The micritic matrix dominates and its abundance ranges from 25-45 % with an average of 35 %. The allochemic constituent ranges from 50-70 %, with an average of 57%. Calcareous green algae is common with an abundance that ranges from 30-60 % of the total allochems. Larger benthic foraminifera species of *Miscellanea miscella, Alveolina globula,* are present. |

| PATALA FORMATION | | |
|---|---|---|
| | **Sample No** | **Petrographic features** |
| **SIKKI VILLAGE SECTION** | **PTSV 1-2, PTSV 4-6 (6.9m thick)** | ***Algal-milliolid rich bioclastic wackestone-packstone microfacies (PTF 1)***<br>In thin section, the PTF 1 microfacies is characterized by wackestone-packstone depositional texture. The biogenic content is moderately preserved. The allochems are dominated by algae and milliolid foraminifera, that range in abundance from 40-60 %, with an average of 50 %. Ostracodes, bivalves and small gastropods are also present with an abundance range from 5-20 %, with an average of 12 %. The micrite matrix ranges in abundance from 50-70%, with an average of 45 %. |
| | **PTSV 3 (2.2m thick)** | ***Diverse foraminiferal wackestone-packstone microfacies (PTF 5)***<br>In thin section, the PTF 5 microfacies is characterized by the wackestone-packstone depositional textureThe allochems are diverse and ranging in abundance from 25–60 %, with an average of 40 %. Allomicritic matrix dominates and its abundance ranges from 35 – 60 %, with an average of 38 %. Sparry calcite is also found as cement, filling the large fractures and intergranular spaces. The matrix is allomicritic in nature and related to the breakdown of the skeletal material. These allochems mainly include larger benthic foraminifera (i.e. *Ranikothalia sindensis, Ranikothalia sahini, Miscellanea miscella, Dictyoconiodes cooki, Nummulites lahiri, Operculina salsa, Lockhartia pustulosa* and *Lockhartia haime*), Bivalves, brachiopods, ostracodes and scattered echinoid clasts are also present. |

| PATALA FORMATION | | |
|---|---|---|
| NAMMAL GORGE SECTION | **Sample No** | **Petrographic features** |
| | **PTN 14, PTN 51-60 (6m thick)** | ***Diverse foraminiferal wackestone-packstone microfacies (PTF 5)***<br>In thin section, the PTF 5 microfacies is characterized by the wackestone-packstone depositional texture. Allomicritic matrix dominates and its abundance ranges from 30 – 50 %, with an average of 40 %. The allochems ranging in abundance from 28–50 %, with an average of 42 %. These allochems include larger benthic foraminifera, and bivalves. |
| | **PTN 16-17 (3m thick)** | ***Algal-milliolid rich bioclastic wackestone-packstone microfacies (PTF 1)***<br>PTF 1 microfacies is characterized by wackestone-packstone depositional texture. The allochems are dominated by milliolid foraminifera and algae that range in abundance from 30-80 %, with an average of 50 %. Ostracodes, bivalves and small gastropods are also present with an abundance range from 10-20 %, with an average of 12 %. The micrite matrix ranges in abundance from 50-70%, with an average of 40 %. |

| PATALA FORMATION | | |
|---|---|---|
| ZIARAT THATTI SHARIF SECTION | **Sample No** | **Petrographic features** |
| | **PTTS 1-PTTS 11 (50m thick)** | ***Diverse foraminiferal wackestone-packstone microfacies (PTF 5)***<br>In thin section, the PTF 5 microfacies is characterized by the wackestone-packstone depositional texture. PTF 5 is characterized by stylolaminated, stylobrecciated and stylonodular fabrics. The matrix abundance ranges from 20 – 50 %, with an average of 35 %. The allochems ranging in abundance from 25–60 %, with an average of 45 %. |
| | | |

| PATALA FORMATION | | |
|---|---|---|
| KALABAGH HILLS SECTION | **Sample No** | **Petrographic features** |
| | **PTK 1-PTK 7 (33m thick)** | ***Diverse foraminiferal wackestone-packstone microfacies (PTF 5)***<br>The PTF 5 microfacies is characterized by the wackestone-packstone depositional texture. The allochems are ranging in abundance from 20–55 %, with an average of 35 %. Matrix abundance ranges from 30–60 %, with an average of 40 %. The matrix is allomicritic in nature.These allochems mainly include larger benthic foraminifera (i.e. *Ranikothalia sindensis, Miscellanea miscella, Nummulites lahiri, Operculina salsa,* and *Lockhartia haime*), and ostracodes are also present. |
| | **PTK 8 PTK 11 (14m thick)** | ***Algal-milliolid rich bioclastic wackestone-packstone microfacies (PTF 1)***<br>PTF 1 microfacies is characterized by wackestone-packstone depositional texture. The allochems are dominated by milliolid foraminifera and algae that range in abundance from 40-80 %, with an average of 60 %. Ostracodes and small gastropods has abundance range from 12-20 %, with an average of 14 %. The micrite matrix ranges in abundance from 60-70%, with an average of 45 %. |
| | **PTK 12 (3m thick)** | ***Peloidal mudstone microfacies (PTF 4)***<br>The PTF 4 microfacies is characterized by mudstone to wackestone depositional textures. The biogenic content is poorly preserved and rare planktonic and larger benthic foraminiferal bioclasts are found scattered in the micritic matrix. The micritic matrix ranges in abundance from 70 to 90 %, with an average of 85 %.<br>Peloids are very common ranging in size from 0.1 to 0.3mm, and found in nets, scattered and isolated forms. The diagenetic fabric is characterized by chemical compaction forming stylolites, internal micritization and pyritization of the bioclasts. |

| PATALA FORMATION | | |
|---|---|---|
| CHICHALLI NALA SECTION | **Sample No** | **Petrographic features** |
| | **PTC 6 (4m thick)** | ***Coralline red algal-stromatolite mudstone- wackestone microfacies (PTF 6)***<br>In thin section, the PTF 6 Microfacies is characterized by the mudstone to wackestone depositional textures. The PTF 6 microfacies show presence of red coralline algae forming stromatolites. The stromatolites are having spaced hemispheroids which are laterally linked (LLH) with each other and stacked hemispheroids (domes) which are not linked (SH) with each other. Occasional planktonic foraminifera are also present. The micritic matrix dominates and its abundance ranges from 70 to 90 %, with an average of 85 %. |
| | **PTK 16, 19,36 (11m)** | ***Fenestral bioclastic mudstone-wackestone microfacies (PTF 2)***<br>PTF 2 microfacies is characterized by the mudstone to wackestone depositional texture. The allochems are dominated by algae and benthic foraminifera. The abundance of bioclasts ranges from 5 to 40 % with an average of 25 %. These bioclasts are poorly preserved, have poor sorting and lack any preferred orientation. The sparry matrix dominates and ranges in abundance from 50–75 %, with an average of 60 %. The fenestral fabric is a prominent feature of the PTF 2 microfacies. The fenestral openings are synsedimentary in origin, filled with calcite and are ranging in size from 0.2mm to 2mm. |
| | **PTC 17 (3m thick)** | ***Algal-milliolid rich bioclastic wackestone-packstone microfacies (PTF 1)***<br>PTF 1 microfacies shows wackestone-packstone depositional texture. The allochems are dominated by milliolids, green algae (abundance ranges from 50-70 %, with an average of 55 %). Gastropos ranges in abundance from 5-25 %, with an average of 10%. The micrite matrix ranges in abundance from 50-70%, with an average of 55 %. |

| PATALA FORMATION | | |
|---|---|---|
| CHICHALLI NALA SECTION | **Sample No** | **Petrographic features** |
| | **PTC 37 (3m thick)** | ***Diverse foraminiferal wackestone-packstone microfacies (PTF 5)***<br>The PTF 5 microfacies is characterized by the wackestone-packstone depositional texture. The allochems abundance ranges from 30–65 %, with an average of 40 %. Matrix abundance ranges from 20–60 %, with an average of 35 %. These allochems mainly include larger benthic foraminifera (i.e. *Ranikothalia sindensis, Miscellanea miscella, Operculina salsa,* and *Lockhartia haime*), echinoid spines and ostracodes are also present. |
| | **PTC 22-23, 27, PTC 31-35 (3m thick)** | ***Peloidal mudstone microfacies (PTF 4)***<br>The PTF 4 microfacies is characterized by mudstone to wackestone depositional textures. The biogenic content is poorly preserved and rare planktonic and larger benthic foraminiferal bioclasts are found scattered in the micritic matrix. The micritic matrix ranges in abundance from 70 to 90 %, with an average of 85 %.<br>Peloids are very common ranging in size from 0.1 to 0.3mm, and found in nets, scattered and isolated forms. The diagenetic fabric is characterized by chemical compaction forming stylolites, internal micritization and pyritization of the bioclasts. |
| | **PTC 38-41 (3m thick)** | ***Foraminiferal packstone microfacies (PTF 3)***<br>In thin section, the PTF 3 microfacies is characterized by packstone depositional texture. The biogenic content is well preserved, with good sorting, preferred orientation and graded bedding fabric of the bioclasts. The allochems are dominated by foraminiferal bioclasts that range in abundance from 60–90 %, with an average of 80 %. |

| NAMMAL FORMATION | | |
|---|---|---|
| NAMMAL GORGE SECTION | **Sample No** | **Petrographic features** |
| | **NN 1-9, NN 21-22 (25m thick)** | ***Nummulites- Discocyclina rich packstone microfacies (NMF 1)***<br>In thin section, the NMF 1 microfacies is characterized by the packstone-grainstone depositional textures having a rich allochemical constituent of larger benthic foraminifera (dominated by > 50 % - <80 % , with an average of 70%, allochems of *the Assilina, Nummulites, Discocyclina, Ranikothalia* and *Operculina*). In spite the presence of broken bioclasts of *Discocylina* the overall biogenic preservation is good. The grains shows a cross bedded fabric, sorting of the grains is moderate. The micritc matrix is ranging from 10% - 30 %, with an average of 15%. |
| | **NN10-17 (18m thick)** | ***Foraminiferal bioclastic wackestone microfacies (NMF 2)***<br>In thin section, the NMF 2 microfacies is characterized by wackestone-packstone depositional texture. The allochems are mainly larger benthic foraminifera (i.e. *Assilina spinosa*, *Ranikothalia sahini* and *Discocyclina*) ranging in abundance from 20-40%, with an average of 22 %. The sparry matrix ranges from 20-50 %, with an average of 30 %. |
| | **NN18-20 (45m thick)** | ***Pelagic mudstone to- wackestone microfaciesmicrofacies (NMF 4)***<br>In thin section, the NMF 4 Microfaciesmicrofacies is characterized by the mudstone to -wackestone depositional textures. Abundant planktonic foraminifera are found within the micritic matrix.The planktonic foraminiferal abundance ranges from 10 to 30 %, with an average of 18 %. The micritic matrix ranges from 60 to 80 %, with an average of 65 %. |

| NAMMAL FORMATION | | |
|---|---|---|
| NAMMAL GORGE SECTION | **Sample No** | **Petrographic features** |
| | **NN 23-24 (37m thick)** | ***Peloidal lime mudstone microfacies (NMF 6)***<br>In thin section, the NMF 6 microfacies is characterized by lime mudstone depositional texture. In thin section NMF 6 is characterized by an abundance of peloids and sparse larger benthic foraminifera i.e. *Ranikothalia sahini* rare gastropods and ostracodes. The micritic matrix is abundant and ranges from 50 to 70 %, with an average of 55 %. |
| | | |

| NAMMAL FORMATION | | |
|---|---|---|
| | **Sample No** | **Petrographic features** |
| **CHICHALI NALA SECTION** | **NC 1 (4m thick)** | ***Nummulites- Discocyclina rich packstone microfacies (NMF 1)***<br>In thin section, the NMF 1 microfacies show packstone depositional textures. Allochemical constituent of larger benthic foraminifera (dominated by benthic foramnifera > 50 % - <80 % , with an average of 60 %). Allochems of *the Assilina, Nummulites, Discocyclina, Ranikothalia* and *Operculina*). Size of the *Nummulites* test ranges from 2mm to 4mm, *Discocyclina* size ranges from 2mm to 5mm, *Ranikothalia* size ranges from 3mm to 7mm, *Operculina* size ranges from 1mm to 4mm, and *Assilina* size ranges from 1mm to 4mm. The micritc matrix is ranging from 15 - 30 %, with an average of 18%. |
| | **NC 2-3, NC 14-15 (28m thick)** | ***Foraminiferal bioclastic wackestone microfacies (NMF 2)***<br>In thin section, the NMF 2 microfacies is characterized by wackestone-packstone depositional texture. The allochems are dominated by larger benthic foraminifera, ranging in abundance from 20-40%, with an average of 22 %. The sparry matrix ranges from 20-50 %, with an average of 30 %. The brachiopod bioclasts of up to 3mm size show internal micritization) and rare *Assilina spinosa* and ostracode bioclasts are partially silicified The sparry matrix ranges from 20-50 %, with an average of 40 %. Some planktonic foraminifera are also found within the sparry matrix. The bioclasts show graded bedding fabrics (normal and reverse) and increased sorting upward. |

| NAMMAL FORMATION | | |
|---|---|---|
| CHICHALI NALA SECTION | **Sample No** | **Petrographic features** |
| | **NMC 5 (10m thick)** | ***Planktonic-Discocyclina rich wackestone-packstone microfacies (NMF 3)***<br>In thin section, the NMF 3 Microfacies is characterized by wackestone-packstone depositional texture.. The biogenic content is well preserved. The allochems are dominated by a mixture of planktonic and benthic forams, abundance of allochems ranges from 40-60 %, with an average of 50 %. The planktonic foraminifera include globorotaliids while larger benthic foraminifera are dominated by species *Discocyclina sella* and *Discocyclina scalaris*. *Discocyclina* bioclasts range in size from 3mm to 6mm and are mostly found in small nests and sometime scattered in the micritic matrix. The abundance of the micritic matrix ranges from 40 – 60 %, with an average of 45. |
| | **NMC 6,8-13 (28m thick)** | ***Pelagic mudstone to- wackestone microfaciesmicrofacies (NMF 4)***<br>NMF 4 microfacies is characterized by the mudstone to -wackestone depositional textures. Planktonic foraminiferal abundance ranges from 20 to 30 %, with an average of 20 %. The micritic matrix ranges from 50 to 80 %, with an average of 70 %. |
| | **NMC 16-20 (60m thick)** | ***Peloidal lime mudstone microfacies (NMF 6)***<br>NMF 6 microfacies is characterized by lime mudstone depositional texture and is characterized by an abundance of peloids (20-30 %) and sparse larger benthic foraminifera and gastropods. The micritic matrix abundance ranges from 40 to 60 %, with an average of 50 %. |

| SAKESSAR FORMATION | | |
|---|---|---|
| NAMMAL GORGE SECTION | **Sample No** | **Petrographic features** |
| | **SKN 1-6 (55m thick)** | ***Algal–gastropod rich bioclastic wackestone-packstone microfacies (SKF 2)***<br>SKF 2 microfacies is characterized by wackestone-packstone depositional texture. The biogenic content is moderately preserved. The allochems are dominated by dasycladacean algae and small micritized boring gastropods while subordinate milliolid forams and brachiopods are also found. The algae abundance ranges from 30-50%, with an average of 45 % while gastropod abundance ranges from 5-10%, with an average of 4 %. The micritic matrix ranges in abundance from 40 – 60 %, with an average of 45 %. |
| | **SKN 7-10 (30m thick)** | ***Algal-peloidal lime mudstone to wackestone microfacies (SKF 1)***<br>In thin section, SKF 1 microfacies is characterized by the lime mudstone - wackestone depositional textures. The biogenic content is poorly preserved and grains are mostly micritized. Phylloid algal bioclasts are the dominant allochems, while few brachiopods and gastropods are also seen. The bioclasts abundance ranges from 30-60 %, with an average of 45 %. The micritic matrix ranges from 30 to 60 % with an average of 45 %. The subordinate spar presence is related to the breakdown of the algal biodebris. Abundant peloids are found in the sparry matrix. Mud peloids are very common, having rounded shape and less than 0.2 mm size. |

| SAKESSAR FORMATION | | |
|---|---|---|
| NAMMAL GORGE SECTION | **Sample No** | **Petrographic features** |
| | **SKN 11-20 (63m thick)** | ***Foraminiferal bioclastic wackestone-packstone microfacies (SKF 3)***<br>SKF3 microfacies is characterized by wackestone-packstone depositional texture. The allochems are dominated by the larger benthic foraminifera i.e. *Alveolina globula*, *Nummulites globulus* and subordinate algae. The abundance of foraminifera ranges from 40-50%, with an average of 45 %, while algae abundance ranges from 5-10%, with an average of 3 %. The spary matrix ranges from 40–60 %, with an average of 45. |
| | | |

| SAKESSAR FORMATION | | |
|---|---|---|
| CHICHALI NAL SECTION | **Sample No** | **Petrographic features** |
| | **SKC 1-12, 15 (97m thick)** | ***Algal–gastropod rich bioclastic wackestone-packstone microfacies (SKF 2)***<br>SKF 2 microfacies show wackestone-packstone depositional texture. Dasycladacean algae and small micritized boring gastropods while subordinate milliolid forams and brachiopods constitute the major allochems. The algae abundance ranges from 30-60%, with an average of 40 % while gastropod abundance ranges from2-10%, with an average of 6 %. The micritic matrix ranges in abundance from 30–60 %, with an average of 35 %. |
| | **SKC 13-14 (15m thick)** | ***Foraminiferal bioclastic wackestone-packstone microfacies (SKF 3)***<br>SKF3 microfacies is characterized by wackestone-packstone depositional texture. The allochems include foraminifera and subordinate algae. The abundance of foraminifera ranges from 30-50%, with an average of 40 %, while algae abundance ranges from 5-10%, with an average of 3 %. The spary matrix ranges from 30–60 %, with an average of 40. |
| | **SKC 16-26 (65m thick)** | ***Algal-peloidal lime mudstone to wackestone microfacies (SKF 1)***<br>SKF 1 microfacies is characterized by the lime mudstone - wackestone depositional textures. Phylloid algal bioclasts, brachiopods and gastropods constitute the major allochems with an abundance ranges from 40-60 %, with an average of 48 %. The micritic matrix ranges from 20 to 70 % with an average of 50 %. |

| CHORGALI FORMATION | | |
|---|---|---|
| GHARIBWAL CEMENT FACTORY SECTION | **Sample No** | **Petrographic features** |
| | **CGGW 1,3,6<br>CGGW 11-14<br>(8.5m thick)** | ***Diverse foraminiferal wackestone-packstone microfacies (CGF 1)***<br>In thin section, the CGF 1 microfacies is characterized by wackestone-packstone depositional textures. The biogenic content is well preserved and allochem abundance ranges from 30-60%, with an average of 45 %. The dominant allochems are larger benthic foraminifera i.e. *Nummulites atacicuc, Nummulites globulus, Nummulites mammilatus, Assilina granulosa, Assilina leymerie, Assilina pustulosa, Alveolina globula, Alveolina rotundata, Lockhartia pustulosa* and *Discocyclina fortisie.*. Overall the micritic matrix dominates and ranges in abundance from 40 to 70 %, with an average of 40 %. 5-10 % dolomite crystals are also found. 1-2 % pyrite is seen |
| | **CGGW 2,7-8<br>(3.2m thick)** | ***Dolomitized fenestral lime mudstone microfacies (CGF 3)***<br>In thin section, the CGF 3 microfacies is characterized by a dolomitized mudstone depositional texture. The bioclasts abundance ranges from 5-8 %, with an average of 4 %. The dolomite is fabric retentive, medium grained and crystalline. Crystals are euhedral to subhedral. Peloids are also seen, their abundance ranges from 5-10%, with an average of 2%. Spar abundance ranges from 10-20%, with an average of 12 %. Chert is also found and its abundance ranges from 1-3 %. |
| | **CGGW 4,5,9,10<br>CGGW 15-32<br>(28.2m thick)** | ***Algal-foraminiferal wackestone-packstone microfacies (CGF 2)***<br>CGF 2 microfacies is characterized by wackestone-packstone depositional texture. The bioclasts abundance ranges from 40-70%, with an average of 50 %. The dominant allochems are green algae and larger benthic foraminifera.The matrix is dominated by micrite associated with the biodebris of the foraminiferal and algal bioclasts and ranging in abundance from 20-40 %, with an average of 25 %. |

| CHORGALI FORMATION | | |
|---|---|---|
| SIKKI VILLAGE SECTION | **Sample No** | **Petrographic features** |
| | **CGSV 1-3 (5.3m thick)** | ***Assilina-Discocyclina rich bioclastic wackestone-packstone microfacies (CGF 5)***<br>In thin section, the CGF 5 microfacies is characterized by wackestone-packstone depositional texture. The biogenic content is well preserved having dominance of foraminiferal bioclasts with abundance ranges from 30-70%, with an average of 45 %. The foraminiferal assemblage is dominated by *Assilina laminosa, Assilina pustulosa, Assilina granulosa, Assilina laxispira, Assilina spinosa, Nummulites globulus, Nummulites mamillatus, Alveolina rotundata, Alveolina globula, Operculina salsa* and *Discocyclina fortisie* . Most of the foraminiferal bioclasts have a size range between 2mm to 5mm. The micritic matrix dominates and its abundance ranges from 40 to 70 %, with an average of 55 %. Some spar is related to the foraminiferal biodebris. |
| | **CGSV 4,7,11 (6.5m thick)** | ***Diverse foraminiferal wackestone-packstone microfacies (CGF 1)***<br>CGF 1 microfacies is characterized by wackestone-packstone depositional textures. Allochem abundance ranges from 40-60%, with an average of 40 %. The dominant allochems are larger benthic foraminifera. Overall the micritic matrix dominates and ranges in abundance from 50 to 70 %, with an average of 45 %. |
| | **CGSV 5,6,10 CGSV 12-20 (28.4m thick)** | ***Algal-foraminiferal wackestone-packstone microfacies (CGF 2)***<br>CGF 2 microfacies is characterized by wackestone-packstone depositional texture. The dominant allochems are green algae and larger benthic foraminifera with an abundance ranges from 50-80%, with an average of 55 %..The matrix is dominated by allomicrite and ranges in abundance from 30-50 %, with an average of 35 %. |

| CHORGALI FORMATION | | |
|---|---|---|
| GHARIBWAL CEMENT FACTORY SECTION | **Sample No** | **Petrographic features** |
| | **CGSV 8,9 (2.8m thick)** | ***Dolomitized fenestral lime mudstone microfacies (CGF 3)***<br>CGF 3 microfacies is characterized by a dolomitized mudstone depositional texture. The bioclasts abundance ranges from 2-8 %, with an average of 4 %. The dolomite is medium grained and crystalline. Peloids abundance ranges from 5-15%, with an average of 4%. Spar abundance ranges from 15-20%, with an average of 14 %. |
| | | |